

Vegetation Modeling of Holocene
Landscapes in the Southern Levant

by

Mariela Soto-Berelov

A Dissertation Presented in Partial Fulfillment
of the Requirements for the Degree
Doctor of Philosophy

Approved April 2011 by the
Graduate Supervisory Committee:

Patricia L. Fall, Chair
Soe Myint
Billie L. Turner
Steven Falconer

ARIZONA STATE UNIVERSITY

August 2011

ABSTRACT

This dissertation creates models of past potential vegetation in the Southern Levant during most of the Holocene, from the beginnings of farming through the rise of urbanized civilization (12 to 2.5 ka BP). The time scale encompasses the rise and collapse of the earliest agrarian civilizations in this region. The archaeological record suggests that increases in social complexity were linked to climatic episodes (e.g., favorable climatic conditions coincide with intervals of prosperity or marked social development such as the Neolithic Revolution ca. 11.5 ka BP, the Secondary Products Revolution ca. 6 ka BP, and the Middle Bronze Age ca. 4 ka BP). The opposite can be said about periods of climatic deterioration, when settled villages were abandoned as the inhabitants returned to nomadic or semi nomadic lifestyles (e.g., abandonment of the largest Neolithic farming towns after 8 ka BP and collapse of Bronze Age towns and cities after 3.5 ka BP during the Late Bronze Age).

This study develops chronologically refined models of past vegetation from 12 to 2.5 ka BP, at 500 year intervals, using GIS, remote sensing and statistical modeling tools (MAXENT) that derive from species distribution modeling. Plants are sensitive to alterations in their environment and respond accordingly. Because of this, they are valuable indicators of landscape change. An extensive database of historical and field gathered observations was created. Using this database as well as environmental variables that include temperature and precipitation surfaces for the whole study period (also at 500 year intervals), the potential vegetation of the region was modeled. Through this means, a continuous chronology of potential vegetation of the Southern Levant was built.

The produced paleo-vegetation models generally agree with the proxy records. They indicate a gradual decline of forests and expansion of steppe and desert throughout the Holocene, interrupted briefly during the Mid Holocene (ca. 4 ka BP, Middle Bronze

Age). They also suggest that during the Early Holocene, forest areas were extensive, spreading into the Northern Negev. The two remaining forested areas in the Northern and Southern Plateau Region in Jordan were also connected during this time. The models also show general agreement with the major cultural developments, with forested areas either expanding or remaining stable during prosperous periods (e.g., Pre Pottery Neolithic and Middle Bronze Age), and significantly contracting during moments of instability (e.g., Late Bronze Age).

DEDICATION

To Augie, Nico, and Ilya.

ACKNOWLEDGMENTS

I would first like to thank my advisor, Dr. Patricia L. Fall, for taking me on as her student and planting the seed of what would become this project. Her constant support and guidance show that I could not have found a better mentor and friend. I am also grateful to my other committee members, Dr. Steven Falconer, Dr. Soe Myint, and Dr. B.L. Turner II., who have inspired me through their works and enthusiasm. Dr. Falconer's archaeological investigations and knowledge of prehistory, Dr. Myint's passion and instruction of how to use tools to detect and map features on the Earth's surface, and Dr. Turner's invigorating research in land use and land cover change, have certainly influenced the way I view the world.

I express my deepest gratitude to Liz Ridder and Patricia Fall, who were excellent field assistants in Jordan. I am also grateful to the people at ACOR for allowing us to stay there and use their facilities (Dr. Barbara Porter, Dr. Christopher Tuttle, Carmen Ayoubi, Mohammed Adawi, Sa'id Adawi, Abed Adawi). Our stay at the Deir 'Alla dighouse was superb, thanks to the hospitality of Ahmed and his family who cooked wonderful food and made sure we had everything in hand. Sincere thanks to Dr. Gerrit and his crew, who allowed us to share the facilities at Deir 'Alla. Dr. Gerrit also provided us with useful maps and was generally great company. In Amman, Dr. Maysoon Al-Nahar took time from her busy schedule to make us feel welcome and provided many useful references.

I wish to thank the various sources that provided funding for my research project. Partial funding for this research was provided by the Mediterranean Landscape Dynamics Project (NSF Grant # 0410269). I sincerely appreciate the challenging and unique opportunity to have been a part of this exciting interdisciplinary project, which was responsible for the climate dataset used in this research to model plant distributions. From

this project, I thank Alexandra Miller, Isaac Ullah, Brett Hill, Michael Barton, Patricia Fall, Steven Falconer, Sidney Rempel, and Maysoon Al-Nahar. My first year and final semesters were funded by scholarships from the Graduate College (Doctoral Enrichment Fellowship and Dissertation Improvement Grant). Some travel money was also obtained through the Mathew G. Bailey Field Work Scholarship and an ASU travel grant. Without this financial support, the completion of my work would have been extremely difficult.

I am also grateful to the following people, who have provided support in different ways. Steven Savage, for kindly providing old historical maps from the Palestinian Exploration Fund; Elizabeth Ridder, for helping me obtain documents, always being available to help, and for being a friend; Jo Wallace, for offering great support and having the best disposition of anyone I have ever met; Tracy and Pat, for helping me with the mad rush of dissertation formatting.

I also wish to express my gratitude to my parents and my family. My passion for the processes that shape the earth started at an early age while tagging along with dad and his students in geology field trips. I thank him for being an inspiration. My parents in law (especially Benita who has helped me so much with the boys), and my aunt Karen have provided wonderful support. Nico and Augie have been incredibly patient, and I am grateful for that. And lastly, I wish to thank my loving husband Ilya, who shares many of my passions. His constant support and love made this journey quite bearable and fun.

TABLE OF CONTENTS

	Page
LIST OF TABLES	xi
LIST OF FIGURES.....	xiv
LIST OF MAPS.....	xx
CHAPTER	
1 INTRODUCTION	1
1.1 Rational	1
1.2 Where it Fits In.....	5
1.3 Summary	7
2 STUDY AREA AND GEOGRAPHICAL SETTING	9
2.1 Topography	9
2.2 Climate	14
2.3 Plant geographical regions.....	16
2.3.1 The Concept of Plant Geographical Region.....	16
2.3.1.1 Mediterranean Region	23
2.3.1.2 Irano Turanian Region	26
2.3.1.3 Saharo Arabian Region.....	27
2.3.1.4 Sudano Decanian Region.....	28
2.4 Vegetation	29
2.4.1 Vegetation of the mesic parts of the study area	35
2.4.1.1 Forests	36
2.4.1.2 Open Forests	41
2.4.1.3 Coastal Vegetation.....	44
2.4.1.4 Mediterranean Savannoid Vegetation	44

CHAPTER	Page
2.4.2 Steppe Vegetation	45
2.4.2.1 Semi Steppe Batha	45
2.4.2.2 Shrub Steppe Vegetation	45
2.4.3 Vegetation of the Xeric Parts of the Study Area.....	46
2.4.3.1 Desert Savannoid Vegetation	46
2.4.3.2 Desert Scrub Vegetation	47
2.4.3.3 Stony Desert Vegetation	48
2.4.4 Edaphically influenced Vegetation.....	49
2.4.4.1 Halophytic Vegetation	49
2.4.4.2 Riparian Vegetation	49
2.4.4.3 Tropical Sudanian Vegetation	51
2.4.4.4 Sand Dune Vegetation	51
2.5 Geology and soils.....	52
3 PALEOENVIRONMENTAL RECONSTRUCTION	61
3.1 Proxy records, indicators of past environments	62
3.1.1 Dead Sea Lake Level Changes	64
3.1.2 Paleobotanical Records.....	67
3.1.3 Other proxy records	79
3.1.4 Records from archaeological sites.....	85
3.2 Paleoenvironmental reconstruction and gaps	88
4 VEGETATION MODELING	92
4.1 Species Distribution Modeling	92
4.1.1 Modeling geographic distributions.....	92

CHAPTER	Page
4.1.2 Why do we need to map and model vegetation?	95
4.1.3 Evolution of species distribution modeling.....	96
4.1.4 Species distribution modeling approaches	97
4.1.5 Maxent, the approach chosen for this study	106
4.2 Environmental parameters selected in this research	109
4.2.1 Creation of an observation database	110
4.2.1.1 Selection of Indicator Species	117
4.2.2 Selection of environmental parameters	138
4.3 Modeling and mapping vegetation in this research	140
4.3.1 Climatically influenced vegetation.....	140
4.3.2 Edaphically influenced vegetation categories.....	147
4.3.2.1 Tropical Sudanian	148
4.3.2.2 Sand dune vegetation.....	149
4.3.2.3 Riparian Vegetation	150
4.3.2.4 Halophytic vegetation.....	150
4.4 MAXENT, the algorithm used in this research	152
4.4.1 Maxent, Model overview.....	152
4.4.2 Projecting to past environments	156
4.4.3 Parameters used in this study.....	158
4.4.4 Selecting a threshold.....	163
4.4.5 Combining model outputs into vegetation map	165
4.5 Model Validation	170
4.5.1 Statistical analyses	170

CHAPTER	Page
5.1.3.10 Desert savannoid.....	191
5.1.3.11 Desert Scrub.....	192
5.1.3.12 Stony Desert.....	193
5.1.4 Combined Maps	194
5.1.4.1 By plant geographic associations	194
5.1.4.2 By vegetation categories.....	197
5.2 Model evaluation	200
5.2.1 Threshold diagnostics	201
5.2.1 Area under the curve.....	203
5.2.1 Variable importance.....	206
6 PALEO VEGETATION MODELING.....	224
6.1 Model Outputs	226
6.1.1 Output for 12 ka BP	226
6.1.2 Output for 11.5 ka BP	232
6.1.3 Output for 11 ka BP	237
6.1.4 Output for 10.5 ka BP	242
6.1.5 Output for 10 ka BP	248
6.1.6 Output for 9.5 ka BP	254
6.1.7 Output for 9 ka BP	259
6.1.8 Output for 8.5 ka BP	264
6.1.9 Output for 8 ka BP	269
6.1.10 Output for 7.5 ka BP	274
6.1.11 Output for 7 ka BP	279

CHAPTER	Page
6.1.12 Output for 6.5 ka BP	284
6.1.13 Output for 6 ka BP	289
6.1.14 Output for 5.5 ka BP	294
6.1.15 Output for 5 ka BP	300
6.1.16 Output for 4.5 ka BP	303
6.1.17 Output for 4 ka BP	308
6.1.17 Output for 3.5 ka BP	313
6.1.18 Output for 3 ka BP	318
6.1.19 Output for 2.5 ka BP	323
6.2 Vegetation trends and comparison against proxy records	327
7 DISCUSSION.....	335
7.2 Environmental Reconstruction and Proxy Records	335
8 CONCLUSION.....	341
8.1 Summary and Findings	341
8.2 Paleo vegetation models and how they fit into the cultural context..	343
8.3 Potential areas of improvement and future work	345
REFERENCES	347

LIST OF TABLES

Table		Page
2.1.	General characteristics of the different plant geographical regions	17
2.2	Major soils of the Mediterranean Region	56
2.3.	Major soils of the Irano Turanian and Saharo Arabian Regions	58
3.1.	Lake Level Changes from the Late Pleistocene until the Late Holocene	66
3.2	Caveats that surround palynological reconstruction	68
3.3.	Palynological records of the region	69
3.4.	Additional proxy records	81
4.1.	Methods commonly used in Species Distribution Modeling	101
4.2.	Examples of published studies that have used MAXENT	107
4.3.	Indicator Species of the Mediterranean Zone	117
4.4.	Indicator Species of the Irano Turanian Zone	118
4.5.	Indicator Species of the Sudano Decanian Zone	118
4.6.	Indicator Species of the Saharo Arabian Zone.....	119
4.7.	Environmental Variables Commonly Used in SDM.....	139
4.8.	Environmental Variables Used in this Study	141
4.9.	Correlation Matrix for Independent Variables.....	144
4.10.	Variables Used Per Model.....	144
4.11.	Other studies that have used similar variables when projecting to other time periods.....	146
4.12.	Correlation Matrix of independent variables for the Tropical Sudanian Category.....	148
4.13.	Features used in MAXENT.....	154
4.14.	Parameters used to calibrate the models	159

Table	Page
4.15. Commonly Used Thresholds to Convert Continuous Maps to Presence/Absence Maps.....	164
4.16. Confusion Matrix.....	171
4.17. Indicator Species that are Present in the Pollen Record	163
5.1. Threshold Evaluation.....	203
5.2. Model parameters and model performance based on AUC.....	205
5.3. Variable contribution and jackknife test of variable importance for models by plant geographical region.....	210
5.4. Variable contribution and jackknife test of variable importance for models by forest categories.....	211
5.5. Variable contribution and jackknife test of variable importance for models only developed for the present.....	212
5.6. Variable contribution and jackknife test of variable importance for models that represent steppe vegetation	212
5.7. Variable contribution and jackknife test of variable importance for models that represent desert categories	213
5.8. Variable contribution and jackknife test of variable importance for models that represent the categories of coastal <i>Ziziphus</i> and Mediterranean Savannoid Vegetation	213
5.9. Response Curves for Models by Plant Geographical Region	214
5.10. Response Curves for Models by Forest Categories	215
5.11. Response Curves for Models Developed for the Present	218
5.12. Response Curves for Models that Represent Steppe Categories.....	220

Table	Page
5.13. Response Curves for Models that Represent Desert Categories and Mediterranean Savannoid Vegetation.....	221
6.1. Forest trends, according to model output.....	328
6.2. Proxy records in the region	329
6.3. Model comparison against proxy records	331

LIST OF FIGURES

Figure	Page
2.1. Distribution of plant geographical regions according to different authors	22
2.2. Vegetation map of Jordan created by Al-Eisawi	30
2.3. Vegetation map of Jordan and Palestinian territories, created by Kasapligil	31
2.4. Zohary's vegetation map of Western Palestine	32
2.5. Horowitz's map of major vegetation groups.....	33
2.6. Vegetation of the region created by Danin	34
2.7. Phytogeographical map of the region, created by Danin	35
2.8. <i>Quercus calliprinos</i> and <i>Pistacia palaestina</i> maquis at the Ajlun Woodland Reserve	39
2.9. <i>Quercus ithaburensis</i> maquis in Gilead	40
2.10. <i>Pinus halepensis</i> forests in Dibeen National Park	41
2.11. Forests of the Southern Plateau Region	43
2.12. Juniper on slopes near Petra	43
2.13. Stand rich in Mediterranean and Irano Turanian species overlooking Dana Canyon.....	44
2.14. Semi steppe batha vegetation near Shobek	45
2.15. Shrub steppe vegetation.....	46
2.16. Desert Savannoid Vegetation	47
2.17. Stony Desert Vegetation.....	48
2.18. Halophytic and Tropical Vegetation in the Dead Sea Valley.....	49
2.19. Wadi Bed Vegetation	50
2.20. <i>Calotropis procera</i> in the Southern Dead Sea Valley	51
2.21. <i>Haloxylon persicum</i> and <i>Hammada salicornia</i> in Wadi Rum	52

Figure	Page
2.22. Heavily eroded slope in Wadi Arava	54
4.1. Observations that fall into the pine forest subdivision.....	122
4.2. Observations that fall into the mixed evergreen oak forest subdivision	123
4.3. Observations that fall into the mixed deciduous oak forest subdivision.....	124
4.4. Observations that fall into the degraded forest subdivision.....	125
4.5. Observations that fall into the Mediterranean Savannoid Subdivision	126
4.6. Observations that fall into the Open forests of Carob and Pistacia	127
4.7. Observations that fall into the Open forests with Juniper.....	128
4.8. Observations that fall into the Semi Steppe Batha Subdivision	129
4.9. Observations that fall into the Shrub Steppe Subdivision	130
4.10. Observations that fall into the Desert Scrub Subdivision	131
4.11. Observations that fall into the Stony Desert Subdivision	132
4.12. Observations that fall into the Sand Vegetation Subdivision	133
4.13. Observations that fall into the Tropical Sudanian Subdivision	134
4.14. Observations that fall into the Halophytic Subdivision	135
4.15. Observations that fall into the Hydrophytic Subdivision.....	136
4.16. Observations that fall into the Desert Savannoid Subdivision	137
4.17. Mapping of Sand Vegetation.....	149
4.18. Combining the output into one vegetation map.....	167
4.19. Example of the Area Under the Curve (AUC).....	173
5.1. Resulting Modern Distribution of the Saharo Arabian Plant Geographical Region.....	166
5.2. Resulting Modern Distribution of the Irano Turanian Plant Geographical Region.....	168

Figure	Page
5.3. Resulting Modern Distribution of the Mediterranean Plant Geographical Region.....	169
5.4. Mapped Riparian Vegetation.....	172
5.5. Mapped Sand Vegetation.....	173
5.6. Resulting Modern Distribution of Halophytic Vegetation	174
5.7. Resulting Modern Distribution of Tripical Sudanian Vegetation	175
5.8. Resulting Modern Distribution of <i>Pinus halepensis</i> forests.....	178
5.9. Resulting Modern Distribution of Evergreen oak forests and maquis (<i>Quercus calliprinos</i>).....	180
5.10. Resulting Modern Distribution of Deciduous oak forests and maquis (<i>Quercus ithaburensis</i>).....	181
5.11. Resulting Modern Distribution of Open Forests of Carob (<i>Ceratonia siliqua</i>) and Pistacia (<i>Pistacia lentiscus</i>).....	183
5.12. Resulting Modern Distribution of Open Forests of Juniper, Cyprus, Oak, and Pistacia.....	185
5.13. Resulting Modern Distribution of Mediterranean Savannoid Vegetation .	186
5.14. Resulting Modern Distribution of Semi Steppe Batha Vegetation	187
5.15. Resulting Modern Distribution of Shrub Steppe Vegetation.....	189
5.16. Resulting Modern Distribution of Coastal <i>Ziziphus</i> Vegetation	190
5.17. Resulting Modern Distribution of Desert Savannoid Vegetation	192
5.18. Resulting Modern Distribution of Desert Scrub Vegetation	193
5.19. Resulting Modern Distribution of Stony Desert Vegetation	194
6.1. Summary of climatic conditions throughout the study period	226
6.2. Vegetation model for 12 ka BP, by plant geographical region	227

Figure	Page
6.3. Clamping and MESS during 12 ka BP.....	228
6.4. Suitability according to vegetation type for 12 ka BP	230
6.5. Vegetation model for 11.5 ka BP, by plant geographical association.....	233
6.6. Clamping and MESS during 11.5 ka BP.....	234
6.7. Suitability according to vegetation type for 11.5 ka BP	235
6.8. Vegetation model for 11 ka BP, by plant geographical association.....	238
6.9. Clamping and MESS during 11 ka BP.....	239
6.10. Suitability according to vegetation type for 11 ka BP	241
6.11. Vegetation model for 10.5 ka BP, by plant geographical association.....	243
6.12. Clamping and MESS during 10.5 ka BP.....	244
6.13. Suitability according to vegetation type for 10.5 ka BP	246
6.14. Vegetation model for 10 ka BP, by plant geographical association.....	249
6.15. Clamping and MESS during 10 ka BP.....	250
6.16. Suitability according to vegetation type for 10 ka BP	252
6.17. Vegetation model for 9.5 ka BP, by plant geographical association.....	255
6.18. Clamping and MESS during 9.5 ka BP.....	256
6.19. Suitability according to vegetation type for 9.5 ka BP	257
6.20. Vegetation model for 9 ka BP, by plant geographical association.....	260
6.21. Clamping and MESS during 9 ka BP.....	261
6.22. Suitability according to vegetation type for 9 ka BP	262
6.23. Vegetation model for 8.5 ka BP, by plant geographical association.....	265
6.24. Clamping and MESS during 8.5 ka BP.....	266
6.25. Suitability according to vegetation type for 8.5 ka BP	268
6.26. Vegetation model for 8 ka BP, by plant geographical association.....	270

Figure	Page
6.27. Clamping and MESS during 8 ka BP.....	271
6.28. Suitability according to vegetation type for 8 ka BP	273
6.29. Vegetation model for 7.5 ka BP, by plant geographical association.....	275
6.30. Clamping and MESS during 7.5 ka BP.....	276
6.31. Suitability according to vegetation type for 7.5 ka BP	277
6.32. Vegetation model for 7 ka BP, by plant geographical association.....	280
6.33. Clamping and MESS during 7 ka BP.....	281
6.34. Suitability according to vegetation type for 7 ka BP	283
6.35. Vegetation model for 6.5 ka BP, by plant geographical association.....	285
6.36. Clamping and MESS during 6.5 ka BP.....	286
6.37. Suitability according to vegetation type for 6.5 ka BP.....	287
6.38. Vegetation model for 6 ka BP, by plant geographical association.....	290
6.39. Clamping and MESS during 6 ka BP.....	291
6.40. Suitability according to vegetation type for 6 ka BP	293
6.41. Vegetation model for 5.5 ka BP, by plant geographical association.....	295
6.42. Clamping and MESS during 5.5 ka BP.....	296
6.43. Suitability according to vegetation type for 5.5 ka BP	298
6.44. Vegetation model for 5 ka BP, by plant geographical association.....	300
6.45. Clamping and MESS during 5 ka BP.....	301
6.46. Suitability according to vegetation type for 5 ka BP	302
6.47. Vegetation model for 4.5 ka BP, by plant geographical association.....	304
6.48. Clamping and MESS during 4.5 ka BP.....	315
6.49. Suitability according to vegetation type for 4.5 ka BP	306
6.50. Vegetation model for 4 ka BP, by plant geographical association.....	309

Figure	Page
6.51. Clamping and MESS during 4 ka BP.....	310
6.52. Suitability according to vegetation type for 4 ka BP	311
6.53. Vegetation model for 3.5 ka BP, by plant geographical association.....	314
6.54. Clamping and MESS during 3.5 ka BP.....	315
6.55 Suitability according to vegetation type for 3.5 ka BP	317
6.56. Vegetation model for 3 ka BP, by plant geographical association.....	319
6.57. Clamping and MESS during 3 ka BP.....	320
6.58. Suitability according to vegetation type for 3 ka BP	321
6.59. Vegetation model for 2.5 ka BP, by plant geographical association.....	324
6.60. Clamping and MESS during 2.5 ka BP.....	325
6.61. Suitability according to vegetation type for 2.5 ka BP.....	326

LIST OF MAPS

MAP		Page
2.1	Study Area	11
2.2	Map of elevation	12
2.3	Geographical subdivisions using biblical provinces	13
2.4	Map of precipitation and temperature	15
2.5	Plant geographical regions according to Zohary	19
2.6	Simplified Map of Geology	53
2.7	Map of Soils and Vegetation	55
3.1	Map of Proxy Records	63
4.1	Map of locations used to model vegetation in this study	112
4.2	Map of historical observations used in this study	115
4.3	Observations obtained through fieldwork	116
4.4	Observations subdivided into plant geographical territories	120
4.5	Area formerly Occupied by Lake Lisan and Lisan Formation.....	151
5.1	Modern Distribution of Plant Geographic Associations.....	197
5.2	Resulting Modern Vegetation Map.....	198
6.1	Vegetation model for 12 ka BP.	231
6.2	Vegetation model for 11.5 ka BP.	236
6.3	Vegetation model for 11 ka BP.	242
6.4	Vegetation model for 10.5 ka BP.	247
6.5	Vegetation model for 10 ka BP.	253
6.6	Vegetation model for 9.5 ka BP.	258
6.6	Vegetation model for 9 ka BP.	263
6.7	Vegetation model for 8.5 ka BP.	269

MAP	Page
6.8 Vegetation model for 8 ka BP.	274
6.9 Vegetation model for 7.5 ka BP.	278
6.10 Vegetation model for 7 ka BP.	284
6.11 Vegetation model for 6.5 ka BP.	288
6.12 Vegetation model for 6 ka BP.	294
6.13 Vegetation model for 5.5 ka BP.	299
6.14 Vegetation model for 5 ka BP.	303
6.15 Vegetation model for 4.5 ka BP.	307
6.16 Vegetation model for 4 ka BP.	312
6.17 Vegetation model for 3.5 ka BP.	318
6.18 Vegetation model for 3 ka BP.	322
6.19 Vegetation model for 2.5 ka BP.	327

Chapter 1

INTRODUCTION

This chapter introduces the aims, value and limitations of the dissertation. It also fits the research into the discipline of Geography. It concludes with a summary of the contents of each chapter.

1.1 Rationale

The primary goal of this work is to investigate how the natural environmental conditions have impacted the Southern Levantine landscape (modern Israel, Jordan and the Palestinian territories), which has supported complex human occupation for over twelve thousand years. This is done by creating models of past vegetation in the Southern Levant throughout most of the Holocene, from the beginnings of farming through the rise of urbanized civilization (12 to 2.5 ka BP).

The spatial and temporal contexts are important for several reasons. The Southern Levant is located in a zone of high topographic variability where the geographical territories of numerous plants of European, Asian and African origin meet, making this region sensitive to climate change, especially as related to changes in available moisture (precipitation). In other words, forests have been understood to contract and expand depending on the prevailing climate. Several major climatic fluctuations in precipitation and temperature have indeed been confirmed by proxy records during the Holocene. Given how close the different climatic belts and plant geographical regions are located within the study area, their boundaries are likely to be altered even when minor climatic events take place, with desert and steppe expanding during hot and dry periods and the opposite occurring during wet episodes. This study explores how vegetation has responded to climate change throughout the Holocene.

The time scale encompasses the rise and collapse of some of the earliest agrarian civilizations in this region. The archaeological record suggests a link between the prevailing climatic conditions and social development. For instance, favorable climatic conditions seem to coincide with intervals of prosperity or marked social development such as the transition between hunters and gatherers to the first semi-permanent settlements ca. 14 ka BP, the beginning of farming and first large villages ca. 11.5 ka BP, and the “secondary products revolution” 6 ka BP, when herd animals began to be exploited for their products (milk, wool, traction for cultivation). The opposite can be said about periods of climatic deterioration, when settled villages were abandoned as the inhabitants returned to hunter-gatherer and/or animal herding lifestyles. This was seen, for instance, during the abandonment of the largest Neolithic farming towns around 8 ka BP, as well as the pervasive collapse of Bronze Age towns and cities during the Late Bronze Age ca. 3.5 ka BP.

Without a doubt, the best way to reconstruct palaeoenvironments is through proxy records. However, these are not free of limitations, the most significant which include limited spatial and temporal resolutions. Furthermore, most records are biased to moister areas, leaving other marginal areas with very few records (in the more arid parts of the Southern Levant, most records for the early Holocene come from archaeological investigations). As a result, the ensuing paleoenvironmental history can be fragmented in terms of spatial and temporal resolution. It can also include conflicting interpretations, which many times result from dating inconsistencies.

This study provides an alternative method of landscape reconstruction through the application of plant distribution modeling. These are created at a high spatial resolution (1 km), with continuous coverage every 500 years throughout the Holocene from 12 to 2.5 ka BP. In this way, the models created provide a continuous, region wide

chronology, that suggest how vegetation has responded to climate change throughout the Holocene.

Granted, this rational (projecting vegetation models into the past) has its own limitations, the main of which lies in the hypothetical nature of the problem. A model is only a model, which is fundamentally created by an end user and has multiple considerations that can influence the final result. Furthermore, distribution models cannot capture the full complexity of the underlying processes that dictate how species are distributed. Nevertheless, models allow different scenarios and hypotheses to be explored. The vegetation models created in this study create a hypothetical reconstruction of the vegetation, which result from changes in temperature and precipitation. The exclusion of anthropogenic activities (as increasingly seen in the palinological record from the mid Holocene onwards) makes the potential reconstruction hypothetical. Although it does not reflect true conditions, it provides a platform that can be used to compare against records that capture the human footprint.

Species distribution modeling or SDM is a growing field that allows the distribution of species to be mapped across geographic space. It relies on numerical models that use environmental variables and a set of observations to map the distribution of a species across a landscape (Franklin 1995). Although species distribution modeling is a relatively new science, the last decade has seen it mature and become more robust (Franklin 2009). As a result of innovative and more accessible statistical and GIS tools as well as more available data from museums; herbarium collections; and online databases (for example, GBIF <http://data.gbif.org/>), SDM has been growing in popularity during recent years in fields like conservation science, planning, evolution biogeography, and ecology. During the last decade and especially during the last five years, many studies have begun to apply it towards the modeling of past and future environments (e.g.,

Carnaval and Moritz 2008; Fløjgaard et al. 2009; VanDerWal et al. 2009; Walker et al. 2009). The results of many of these studies show the potential in this line of research.

There are many steps involved in SDM, each of which involves decision making. These include designing a strategy to obtain samples or source these out from other references (e.g., museum collections), obtaining the appropriate predictor variables, determining if any variables are correlated, deciding on an algorithm with which to model the distribution, calibrating the algorithm, choosing a threshold if the output needs to be converted to a presence/absence map, and determining how the model will be evaluated. If appropriate consideration is given to all these steps, a model that can provide a strong prediction of a species' distributions can be built.

Ultimately, the success of the vegetation distribution model depends on the factors just mentioned. Two crucial ones are the observations (e.g., location of plant species and associations that are being modeled like pine forests, desert scrub, shrub steppe) and variables chosen to represent and characterize the vegetation. When projecting distribution models into different temporal scenarios, the greatest challenge is obtaining climatic information. For this region, there are several datasets developed by various interdisciplinary research projects that include a range of bioclimatic variables (e.g., Paleoclimate modeling intercomparison project <http://pmip.lscce.ipsl.fr/>).

Unfortunately, these are only available for limited dates and have a very coarse spatial resolution (ca. 50 km). An alternative is to create average yearly temperature and rainfall grids for specific years using the findings of some proxy records which are able to estimate these values (e.g., Bar-Mathews et al. 1997; Bar-Mathews et al. 2003; McGarry et al. 2004). However, this can only be done for limited areas within the study region. Instead, this study makes use of high resolution temperature and precipitation grids (1 km spatial resolution every 100 years) developed through the application of a macrophysical

climate model (Bryson and DeWall 2007) as part of the Mediterranean Landscape Dynamics Projects: Landuse and Landscape Socioecology in the Mediterranean Basin, a Natural Laboratory for the Study of the Long-Term Interaction of Human and Natural Systems (NSF Grant # 0410269). The model is described in Chapter 4.

An extensive database of historical and field-gathered observations was created by the author, which allowed vegetation to be characterized into meaningful associations that correspond to the different plant geographical territories of the region (e.g., deciduous oak forests, evergreen oak forests, desert savanna). Using this database as well as several environmental variables that include elevation, temperature and precipitation for the whole duration of the study period (also at 500 year intervals), the potential vegetation of the region was modeled and compared against paleoenvironmental records.

The produced paleo vegetation models indicate a gradual decline of forests and expansion of steppe and desert throughout the Holocene, interrupted briefly during the Pleistocene/Holocene transition and Mid Holocene. The models appear to agree with the major cultural developments, although they also highlight moments of environmental downturn that have not been accompanied by social unrest.

1.2 Where it Fits in

This research has been motivated by a profound interest in landscape change as a result of human and natural causes. It fits into Environmental Geography, with special emphasis on Land Use-Cover Change (LUCC) research, even though it does not investigate the human aspect of change. Instead, it focuses on land cover change (e.g., forest, desert, steppe), as a result of changes in climate. In a landscape that records human activities during the beginning of agriculture, orchard cultivation, pastoralism and birth of cities thousands of years ago, this limitation is acknowledged. Nevertheless, it

provides a basic framework that can be used to explore LUCC in the future, by incorporating different snapshots of the archaeological record that indicate how humans have used and impacted the land through time, and how they have responded to natural environmental changes.

Initially LUCC became a central theme of the sustainable development debate (Lambin et al. 2000) because of its direct application to studying changes in biodiversity, water quality, and land/air resources. LUCC enabled the association of such environmental changes with negative impacts of cumulative and increasing human activity (i.e. land use) on the land (i.e. land cover). Its broad relevance found many new applications among local and global research agendas (Rudel and Roper 1997; Turner et al. 1993). Geographers, anthropologists, sociologists and planners commonly adopt LUCC methods because of its utility for identifying and characterizing dynamic changes to environments.

During the 1990s some geographers began to focus their research on issues pertaining to global environmental change, particularly climate impacts and land-use practices (Liverman 1999). Many of the resultant pioneering studies came from environmental geography, an interface between the natural and social sciences, which provides the perfect milieu for studying human-environment dynamics such as LUCC. On account of these efforts, environmental geographers have assumed an important role in the exploration of human impact on global environmental change (Liverman 1999), and have increasingly utilized methods of LUCC, making it a key paradigm of the discipline (Turner 1997; Zimmerer 1996).

Revolutionary changes that occurred in the Levant during the Holocene paved the way to modern societies. These include the origin of agriculture, complex socio-political organization, domestication of animals, exploitation of animals for secondary

products (i.e., milk, wool, traction for cultivation). However, these progressive advances suffered periodic setbacks that appear to coincide with periods of climatic deterioration, when settled villages were abandoned as the inhabitants returned to hunter-gathering and/or agricultural and pastoral activities. A persistent subject that has interested archaeologists has to do with the way humans interacted and impacted their environment, and how sustainable and resilient they were when faced with environmental change. As modern societies cope with providing for growing population, lessening the impact on biotic as well as land, air, and water resources (caused by human activities), and face climate change, these questions resonate today and are the subject of investigation in LUCC research. This research offers a different means of reconstructing past environments at a fairly continuous resolution by applying species distribution modeling. The result can be compared against the more discontinuous human (archaeological) and environmental (paleoenvironmental) records. By doing this, it contributes to the broader topic of cultural-environmental relations.

1.3 Summary

This study is divided into eight chapters. After the Introduction, Chapter 2 introduces the reader to the environmental characteristics of the study area, including the topography, climate, and bedrock. The modern vegetation and plant geographical regions are also described.

Chapter 3 summarizes the main proxy records that have been used as indicators of paleoenvironmental conditions. Based on these, a summary of the paleoenvironmental history of the region is provided (from the late Pleistocene until the Late Holocene).

Chapter 4 is concerned with the methodology. Following a literature review of Species Distribution Modeling, the steps followed in this study to build and assess vegetation models are described.

Chapters 5 and 6 present the results of the vegetation models. Chapter 5 focuses on the vegetation models (both by detailed vegetation categories and plant geographic associations) for the present. These are also compared against published maps and anecdotal evidence. Chapter 6 presents the results of the paleovegetation models (by plant geographic association and vegetation type) from 12 to 2.5 ka BP.

Chapter 7 discusses how the paleovegetation models fit into the paleoenvironmental history of the region. In the final chapter, the models are fit into a broad overview of the cultural developments of the region from the Pleistocene/Holocene transition until the Late Holocene.

Chapter 2

STUDY AREA AND GEOGRAPHICAL SETTING

The goal of this chapter is to portray the environmental characteristics of the study area. It begins by first describing the major topographic units as well as the general climate. After this, the concept of plant geographical region or territory is introduced, followed by a summary of the regions present in the study area. This is important, given that these regions represent the classification adopted for the first series of models created in this study, and will later be referenced for comparison purposes against the modeled outputs throughout the Holocene. After this section, a more detailed description of the vegetation is given, according to the principal botanists of the region and making use of the same classification units that form the second series of more detailed models created in this study. The chapter finishes by describing various aspects of the geomorphology including the major bedrock and soils of the area and how these relate to vegetation.

2.1 Topography

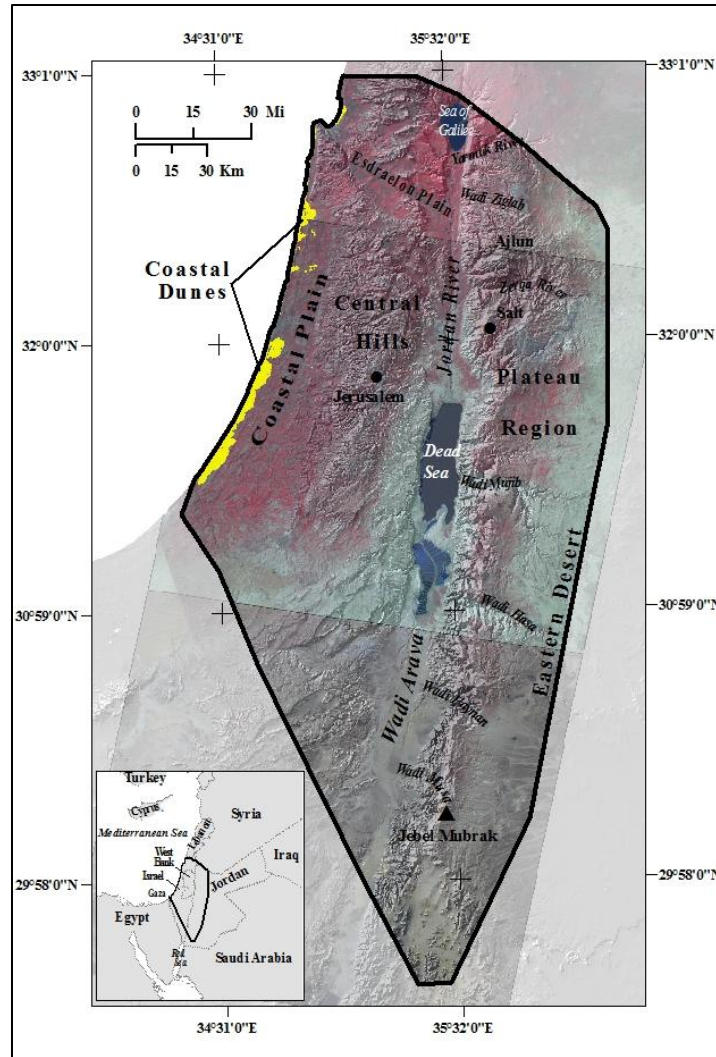
The study area coincides with most of the Southern Levant region between latitude 29°30' N to 33°N and longitude 34°17' E to 36°15'E (Map 2.1). This is where the modern states of Israel, Jordan, and the Palestinian Territories (West Bank and Gaza) are located and represents around 42,657 km². It is surrounded by the Sea of Galilee or Lake Kinneret in the north, the Negev Desert and the Red Sea in the south, the Jordan Plateau in the east and the Mediterranean Sea in the west.

The boundaries were chosen according to the extent of the climate grids, which were provided by the Mediterranean Landscape Dynamics Project (MedLand), an ongoing interdisciplinary investigation that studies long term social, environmental and ecological interactions in the Mediterranean Basin during the Holocene by reconstructing and

modeling past environments (Barton et al. 2004, 2011). Fortunately, this extent also suits the interests of the author for various reasons. The study area is located at the confluence of three continents. Consequently, plants of contrasting characteristics abruptly come together within this small area. As a result of climatic swings, their boundaries have shifted. In addition, early evidence of incipient agriculture and orchard cultivation as well as complex human occupation is also found within this region. Prevailing human occupation strategies have shifted throughout the Holocene, with some periods having records of sedentary populations and others of more transient, agro-pastoral communities. These natural and social characteristics make the study area a fascinating place in which to model plant distributions and vegetation change.

The topography is extremely diverse and can be divided into four major topographic units that follow a north-south gradient (Map 2.1). From west to east, the first is the Coastal Plains which stretch from the base of the mountains of Lebanon south towards the Sinai. Within the study area the Coastal Plains extend south to the Negev, where these plains reach their maximum width of about 50 km inland. This area includes a narrow strip of sand dunes adjacent to the coast, and reaches a maximum elevation of 200m. A series of rivers run across it and empty into the Mediterranean Sea, forming swamps wherever they intersect the sand dunes.

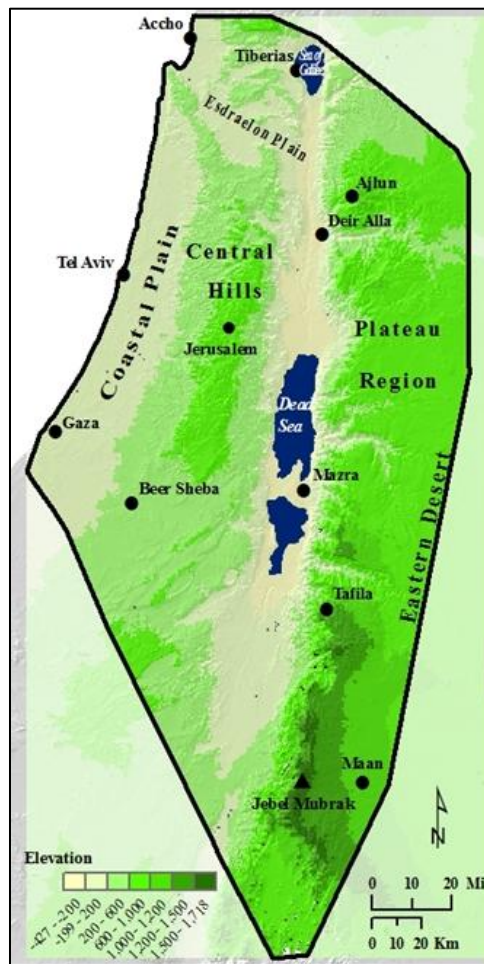
The Central Hills comprise the second unit. It ascends from the coastal plains as a chain of hills that reach 1200 m in the Upper Galilee and the Negev, and 1000 m in the Judean Mountains. These hills are traversed by several valleys, the largest of which are the Esdraelon and Beersheba Plains.



Map 2.1. Study area.

The third unit is the Rift Valley, which runs from Lake Kinneret in the north to the Red Sea or Gulf of Aqaba in the south (Map 2.2). It is part of the Afro-Syrian Rift Valley which extends from Africa to Turkey, and includes the lowest point on earth. It represents a dramatic change in elevation from its neighboring units, and in itself ranges in elevation from -410 m below sea level (bsl) at the Dead Sea to 200 m above sea level (asl). This valley is populated by saline swamps, sand dunes, tropical oases, desert, and grasslands. The Jordan River flows into the Dead Sea in the northern part of the Rift Valley, whereas the intermittent Wadi Arava is found south of the Dead Sea.

From the Rift Valley eastward, elevation dramatically changes once again as it ascends into the Jordanian Plateau (sometimes subdivided and referred to as the northern and southern highlands) which begins just south of the Yarmuk River and spreads south, intersected in several areas by deeply incised wadi valleys like that of Wadi Ziglab, Zerqa River, Wadi Mujib, Wadi Hasa and Wadi Musa. There are several mountains, and the tallest is Jebel Mubrak (1650 m asl) in the south. From here on to the east, the plateau flattens as it extends into the Eastern Desert (also known as the Syrian and Jordan Desert). Only the western fringe of this desert is captured within the study area.



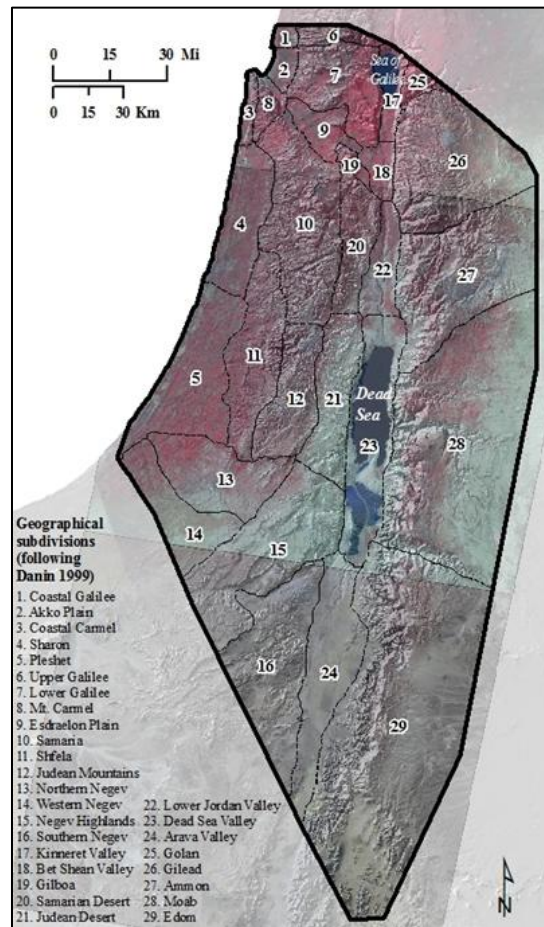
Map 2.2. Map of Elevation.

The drainage follows two main patterns. The rivers that run along the coastal plains drain into the Mediterranean Sea. The remaining rivers and wadis within the Dead

Sea basin drain into the Jordan River and Wadi Arava, and then into the Dead Sea.

Several perennial rivers are found in the northern portion whereas they are all intermittent in the south. As will be discussed in the following chapter, many of these intermittent wadis used to flow continuously during the Early Holocene.

This region has a long history of human habitation. Political boundaries have shifted and different names have been adopted to refer to regions and places through time. In this study, I refer to modern political divisions and territories only when describing conditions in the present. As many authors have done, I subdivided the study area (following Danin 1999) into biblical provinces and refer to these when describing different regions throughout the study area. These are shown in Map 2.3.



Map 2.3. Geographical subdivisions using biblical provinces.

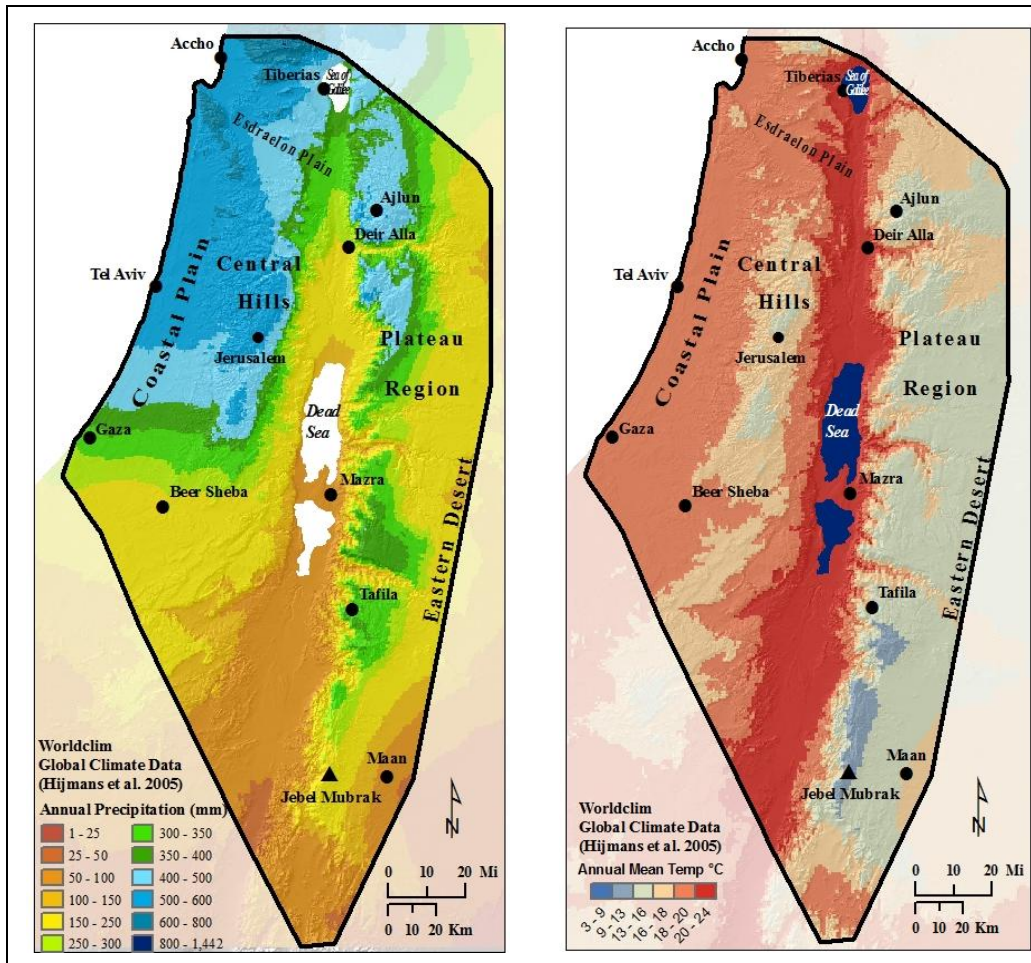
2.2 Climate

The climate of the region is Mediterranean, characterized by wet, cool winters and summers that tend to be long, hot, and dry. Precipitation concentrates around winter and spring (October to May), with most rain usually falling during January. However, seasonal rainfall patterns can fluctuate every year (Al-Eisawi 1996; Atkinson and Beaumont 1971). Summer rains, which are typically short but intense, arrive sporadically from Northeast Africa. They impact the drier areas that receive less than 100 mm/yr, causing the wadis to flow. An indicator of these events is the tree *Tamarix aphylla*, which is found on wadi beds and germinates during these times (Danin 1999).

Rainfall experiences both latitudinal and longitudinal gradients, with rain gradually decreasing from north to south and west to east (Map 2.4). The first is predominantly influenced by weather systems, and ranges from around 1,000 mm/yr in the Sea of Galilee region to less than 50 mm/yr south of the Dead Sea (Zohary 1973). The longitudinal gradient is driven by topography and orographic effects. As the air that comes from the Mediterranean encounters hills and mountains it rises and cools, causing increased precipitation on the windward side of the mountains, whereas the leeward side that descends into the Rift Valley is affected by a rain shadow. In a short distance forests then transition into steppes and desert. The Wadi Arava holds the lowest recorded precipitation in the area, with less than 50 mm/yr (Al-Eisawi 1996). As elevation ascends onto the mountains of the plateau east of the Rift Valley, temperature once again cools and precipitation increases and reaches the highest level around the Ajloun-Salt area (about 500 mm/yr). Further east, precipitation gradually drops once again.

Temperature is also influenced by elevation and latitude (Map 2.4). The hottest temperatures are found around the Wadi Arava with a mean annual maximum of 30°C, whereas the coldest temperatures are found in the southern highlands around the Ash-

Sharah mountains with a mean annual minimum of 5°C (according to data gathered by Al-Eisawi [1996] from 31 stations that represent the period 1966-1980). Temperature can also vary on a yearly basis (Al-Eisawi 1996). On the one end, cold and wet years can experience below zero temperatures resulting in snow accumulation on mountain tops (Danin 1999). At the other extreme, temperatures can reach 50°C in the Wadi Arava region (Al-Eisawi 1996).



Map 2.4. Average precipitation (left) and temperature (right) throughout the study area.

According to precipitation and temperature, the climate can be generally divided into Mediterranean, semi arid, arid, and dry tropical (Kasapliligil 1956). The Mediterranean climate is found in areas that receive precipitation over 350 mm/yr. This is also where the most productive soils and climax vegetation communities are found. The

semi arid climate surrounds the former, and receives between 100 to 350 mm/yr. In Jordan, the major agricultural crop found in these areas is wheat (Kasapligil 1956). As rainfall drops to less than 150 mm/yr, the climate becomes increasingly arid. This is characteristic of the desert areas, where the seasonal and daily temperature range is more extreme. The climate of the Rift Valley is considered to be a dry tropical climate, and precipitation drops significantly from north to south (400 to 35 mm/yr or less). These climatic categories have also been further subdivided by some authors (e.g., Al-Eisawi 1996; Long 1957).

2.3 Plant geographical regions

2.3.1 The concept of plant geographical territory

Biogeographers subdivided the world into chorological units ever since Alexander von Humboldt classified the landscape into vegetation zones through his plant geographical studies (1807). Instead of focusing on the individuals that constitute the flora (as was the common practice until then), he looked at the collective ensemble of species. By studying the growth forms of plants, their distribution, and relationship with their surrounding environment (Nicolson 1987), he was able to distinguish plant communities and associations (Whittaker 1962). From these ideas, Grisebach divided the world into formations that include the Irano Turanian and Mediterranean regions (later called phytogeographical regions), based on the physiognomy and species composition of groups of individuals (Whittaker 1962; Zohary 1973).

The Southern Levant region is a meeting place of three continents. Asia, Africa, and Europe intersect in this area, also known as the Levantine Landbridge (Por 1987) through which animals and plants have migrated and dispersed since the Miocene (Danin 1988; Horowitz 1979). Because of this extraordinary geographic coincidence, four major plant geographical regions converge here. Eig was the first to map these, after conducting

phytogeographical analyses of plant lists and assessing the physiognomic characteristics of the topography and geography of the region (1931/32, 1938). He distinguished four units within the study area: Mediterranean, Irano Turanian, Saharo Sindian and minor Sudano Decanian enclaves, each with distinct floristic and climatic characteristics (Table 2.1).

Table 2.1. General characteristics of the different plant geographical regions, and representative or indicator species according to Eig (1931/32) and Zohary (1962, 1966).

Region (Mean Annual Rainfall mm/yr)	Dominant soils	Description	Representative species
Mediterranean (400-1200)	Terra Rossa and rendzina on mountains. Hamra and sandy soils on the coastal plains. Alluvial and colluvial soils in valleys.	Areas that receive the most amount of rainfall. Includes most mountain ranges. Supports arboreal vegetation (e.g., pine forests, evergreen oak forest, deciduous oak forest) as well as garigue and batha vegetation, depending on the level of degradation.	Climax forest communities: <i>Pinus halepensis</i> ; <i>Quercus calliprinos</i> (evergreen oak), <i>Quercus ithaburensis</i> or tabor oak (deciduous oak), <i>Pistacia palaestina</i> , <i>Ceratonia siliqua</i> (carob tree) and <i>Crataegus aronia</i> (hawthorn), <i>Pistacia lentiscus</i> . Climax communities of lowland and warmer areas: <i>Hyparrhenia hirta</i> - <i>Ziziphus spina Christi</i> assoc.
Irano Turanian (200 – 350)	Many areas have low vegetation cover and suffer from high rates of erosion so soils tend to be of poor quality. Typically loess and calcareous soils are found.	Supports steppe vegetation. An abundance of small shrubs and bushes and lack of trees are the common features of this vegetation. Vegetation is accustomed to extreme temperatures (diurnal and annual) and low rainfall which causes many of the species to become dormant between summer and winter (Al-Eisawi 1985) (Davies and Fall, 2001).	Assoc. of <i>Anabasis Haussknechtii</i> - <i>Plantago Coronopus</i> , Assoc. of <i>Anabasis Haussknechtii</i> - <i>Poa sinaica</i> , <i>Anabasis syriaca</i> (Syrian anabasis), <i>Artemisia herba-alba</i> (white wormwood), <i>Ephedra</i> sp., Assoc. of <i>Haloxylon articulatum</i> - <i>Salsola villosa</i> , <i>Hammada scoparia</i> (black hammada); <i>H. salicornia</i> , <i>Juniperus phoenicia</i> , <i>Noaea mucronata</i> , <i>Ononis Natrix</i> , <i>Phlomidetum brachyodontis</i> , <i>Pistacia palaestina</i> , <i>Retama raetam</i> , <i>Retama Duriaei</i> - <i>Blepharis edulis</i> , <i>Retama Duriaei</i> - <i>Rhus oxyacanthoides</i> , <i>Salsola vermiculata</i> L. (saltwort)
Saharo-Arabian¹ (25 - 150)	Saline, sand and hammada soils. Loess found in marginal areas (Horowitz 1979).	Sparse vegetation which consists mainly of desert scrub and saline or halophytic vegetation, mainly of the <i>Chenopodiaceae</i> (goosefoot) family. Winters tend to be short and cool and summers long, hot, and dry.	<i>Anabasis articulata</i> (jointed anabasis); <i>Zygophyllum dumosi</i> (bean caper); <i>Gymnocarpetum fruticosi</i> , <i>Suaeda</i> L. sp. (sea blite), <i>Tamarix</i> L. spp. (tamarisk); <i>Salsola villosa</i> ; <i>Hammada salicornia</i> ; <i>Chenoleetum arabicae</i> ; <i>Suaedetum asphalticae</i>
Sudanian (Less than 50)		Enclaves of tropical vegetation surrounding springs.	<i>Ziziphus spina-christi</i> (Christ-thorn), <i>Hammada salicornia</i> (white hammada), <i>Acacia albida</i> Del., <i>Acacietum tortillidis</i> , <i>Zygophyllum dumosum</i> , <i>Suaeda palaestina</i> , <i>S. asphaltica</i> , <i>Salsola tetrandra</i> , <i>Populus euphratica</i>

The Mediterranean region holds climax forest communities and receives the most rain. Plants typical of this region were considered by Eig to belong to the east Mediterranean, west Mediterranean, north Mediterranean, south Mediterranean and

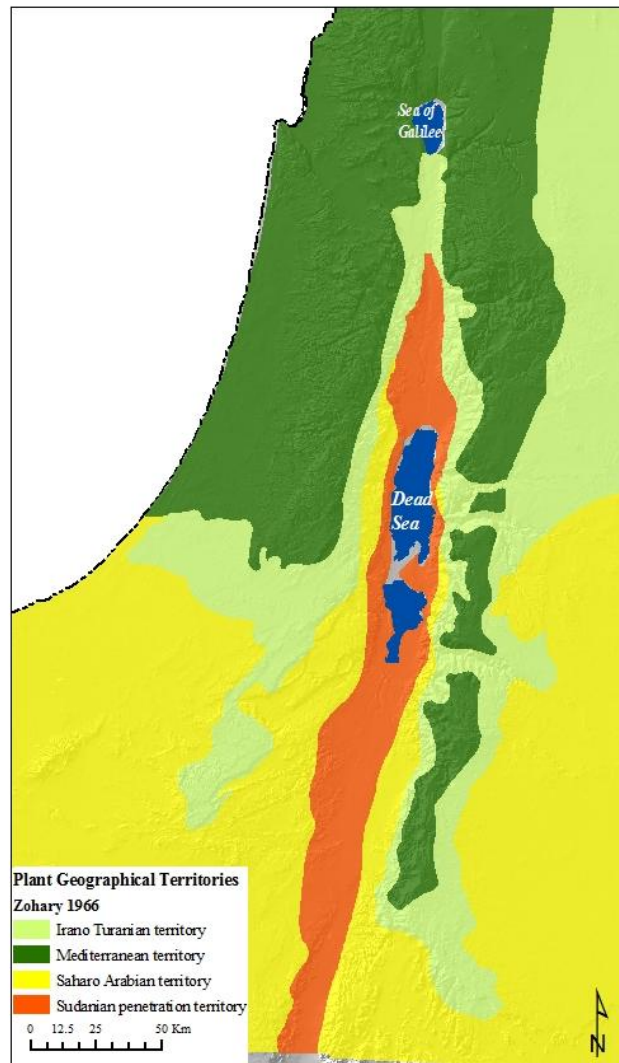
¹ In Jordan, the Saharo Arabian region is called Sudanian (Al-Eisawi 1996). The badias or hammadas of the plateau receive the name of Saharo Arabian.

omni-Mediterranean. The Irano Turanian region is characteristic of Iran and Central Anatolia and is predominantly populated by steppe vegetation. Eig further classified the species within this region as Mauritano steppe, Mesopotamian and Irano Anatolian species. The Saharo Sindian region, typical of the Saharan and Arabian deserts, is the driest and constitutes desert areas and species that originate from the west and middle Saharo-Sindian region.

Zohary updated Eig's map in 1962 and then altered it in 1966 (Map 2.5). He basically modified Eig's classification and renamed the Saharo-Sindian region "Saharo Arabian" and referred to the Sudano-Decanian enclaves around the Dead Sea Valley as territories of Sudanian penetration (Zohary 1966). Following Zohary (1973), Al-Eisawi also divided Jordan into plant geographical territories (1985) with some differences. He refers to the arid region of the Rift Valley and Southern Jordan as Sudanian whereas the Eastern Desert is referred to as Saharo Arabian or Badia.

Regardless of the methodology used, the task of subdividing the area into plant geographical territories will always be somewhat subjective. Even after determining the dominant taxa, distribution of plant communities, floristic characteristics, floral history, and endemics within climatic zones, there is always the consideration of how to treat species found across various regions. Eig found almost a third of the floristic species known at the time to be either bi- or plu-regional (1931). Furthermore, these inter regional species may display such distribution patterns for different reasons. Some may have a wide climatic tolerance, whereas others may be more characteristic of one region but may occur in other regions within small enclaves. For instance, particular soils or rocks in the desert may provide the necessary moisture requirements for species that are normally found in the wetter areas. Zohary and Feinbrun-Dothan (1966) found that about

50% of the deciduous trees or shrubs found in evergreen maquis and forest of the Mediterranean region are of Irano Turanian influence.



Map 2.5. Zohary's plant geographical territories, digitized from Zohary (1966).

When delimiting regions, there is also the challenge of placing boundaries. Zohary himself admits to how transition zones in particular are troublesome when it comes to delineating physical boundaries. Furthermore, he foresaw the possible alteration of boundaries in the future as more analytical tools become available (Zohary 1973).

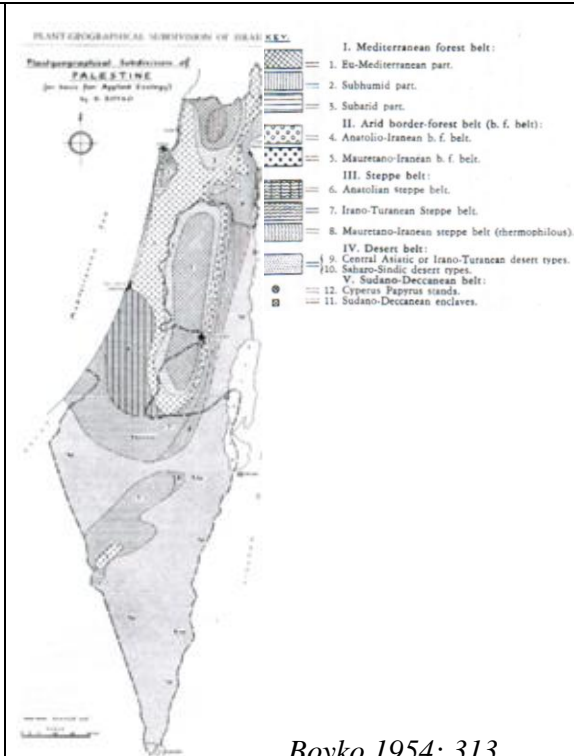
Several other authors have attempted to redefine some of these boundaries or further subdivide the plant geographical regions (e.g., Boyko 1954; Horowitz 1979; Whyte 1950). Boyko for instance subdivided the Mediterranean region into three categories according to the precipitation gradient and dominant forest vegetation, the Irano Turanian steppes into two categories (each with their own subdivisions), and the Saharo Arabian and Sudano Decanian regions each into two categories. As more floristic investigations were carried out in later decades (i.e., Danin 1970, 1983) and new statistical methods used to define biogeographical regions became available, more complex maps were created. In 1987, Danin and Plitmann used floristic parameters and vegetation distribution patterns to calculate the chorotype (group of species that has a similar geographic distribution, e.g., Mediterranean, Irano Turanian) frequency in 5 x 5 km² squares across Israel and the Palestinian territories. They then used quantitative methods to determine the chorotype frequency of the squares and classified these into plant geographical territories.

The resulting map shows these territories as well as pie graphs that indicate the chorotype frequency within each territory and is more in tune with the complex nature of these regions. For example, it shows how a particular chorotype increases or decreases according to latitude or longitude. In terms of the plant geographical boundaries, there is still some overlap with the earlier maps, at least when it comes to delineating some of the major boundaries like the Mediterranean region. Others were considered transition zones between different territories. For instance, Zohary's Irano Turanian territory became a transitional Irano Turanian-Mediterranean zone. Also, the Saharo Arabian boundary was shifted into the Irano Turanian region and subdivided into Saharo Arabian-Irano Turanian and Saharo Arabian-Sudanian transitional areas.

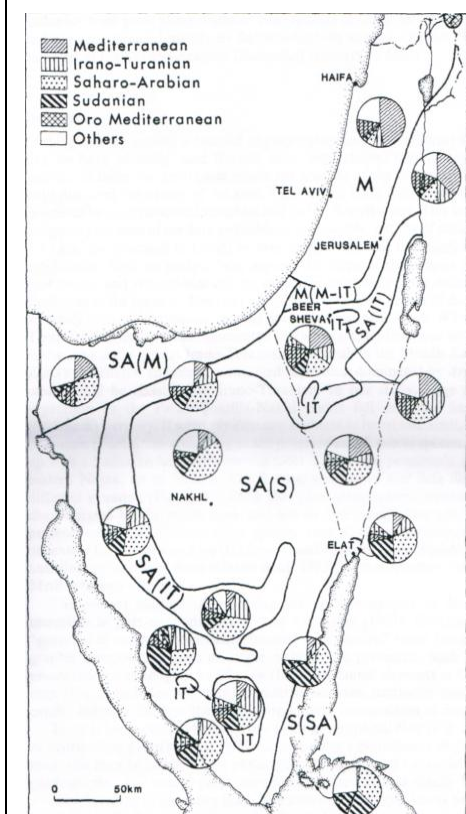
Different interpretations of plant geographical regions are shown in Figure 2.1. The most recent of these maps is also the most comprehensive (Danin and Plitmann 1987), since it is based on the analysis of 80,000 observations subdivided into a 5x5 km² grid. For the present study which also covers the region east of the Rift Valley, such data are not available. Furthermore, using this approach to generate maps at 500 year time intervals throughout most of the Holocene would be too convoluted. Because of this, Eig and Zohary's definition of plant geographical territories is used as the standard classification adopted in this study to generate the first set of models of plant geographical regions throughout the Holocene (Eig 1938; Zohary 1966). To counter the simplicity of these models, a second set of more detailed models (by vegetation) is also generated. Nevertheless, Eig and Zohary's delineation of regions should not be underestimated, since they both had a vast knowledge of the region that came from decades of field work and subdivided the regions according to multiple criteria, such as distribution of plant communities, dominant taxa (indicator species), floristic characteristics, floral history, endemics, etc. (Zohary and Feinbrun-Dothan 1966). The arid area of the plateau is distinguished from other arid areas in the more detailed vegetation models, where it is referred to as stony desert vegetation. Meanwhile, the desert vegetation of the Rift Valley is further subdivided into desert savannoid, desert scrub, halophytic and tropical Sudanian vegetation.



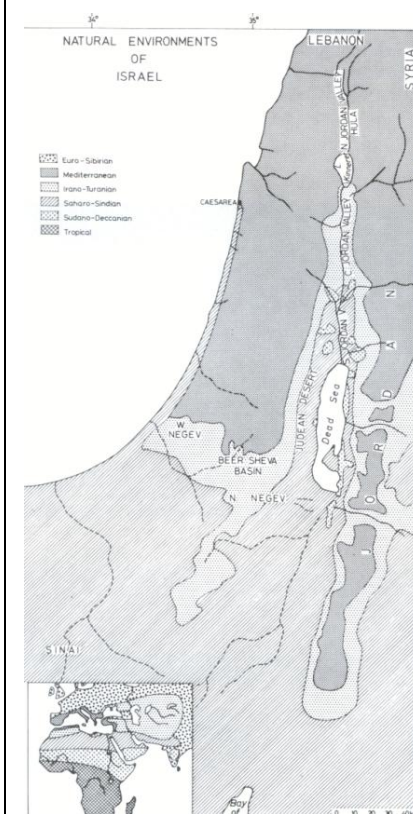
Al-Eisawi 1996: 48



Boyko 1954: 313



Danin and Plitmann 1987: 48



Horowitz 1979: 28

Figure 2.1. Distribution of plant geographical regions according to different authors.

2.3.1.1 Mediterranean region

Of all the regions, the Mediterranean seems to be the easiest to delineate. Rainfall ranges from 400 to 1200 mm/yr, 70 per cent of which falls during winter in short, intense bursts. Another 25 per cent falls between winter and spring (Akinson and Beaumont 1971). This region surrounds the Mediterranean Sea. It is the dominant region surrounding Lake Kinneret, and then spreads south on both sides of the Rift Valley via the mountainous regions, but is indented and missing in the lower elevations and hotter temperatures of the Rift Valley. In modern day Israel and the Palestinian territories, it covers an extensive area throughout the coastal plains and central hill region (except on the side facing the Rift Valley which is affected by rain shadow) and spreads south until around the Negev coastal plain and the Be'er Sheva Basin. To the east of the Rift Valley, the Mediterranean belt also trickles south along the plateau and reaches even further than its counterpart west of the Rift Valley. However, it is interrupted in several places by steep wadi valleys and narrows as it becomes bordered in the west by the Rift Valley and in the east by the Eastern Desert.

The longitudinal and latitudinal rain gradients affect the Mediterranean region in the following way (Horowitz 1979): west of the Rift Valley, rain gradually increases from around 400 to 1200 mm/yr from its southern extent and lowland areas (coastal plain) to the northernmost and higher elevation areas. East of the Rift Valley, it ranges from around 300 mm/yr in Ras En-Naqab in the south to around 650 mm/yr in the north. The impact of such a gradient is reflected on the vegetation, which becomes enriched the further north (Zohary and Feinbrun-Dothan 1966).

Across the elevation profile of the Mediterranean region (from the Mediterraneo-subtropical to the Eu-Mediterranean zone), plant communities differ in

terms of their tolerance to aridity. In the lowland areas of the Rift Valley and the coast, which are also the warmer and drier portions of this region (Kinneret and Bet Shean Valleys and the southern coastal plains), scattered patches of a type of savanna vegetation that is represented by the *Hyparrhenia hirta-Ziziphus spina-christii* association are found (Zohary and Feinbrun-Dothan 1966). This mainly consists of the grass *Hyparrhenia hirta* and scattered spiny trees like *Ziziphus spina-christi*, *Rhamnus palaestinus*, *Rhus tripartite*, and *Capparis spinosa*. Due to the increasing southward occurrence of desert plants along the coastal plains, some authors subdivide the Mediterranean region accordingly. Horowitz, for instance, classifies a narrow fringe along the coast from the Western Negev up to Caesarea that belongs to the Saharo Arabian category.

In between the Eu-Mediterranean and Mediterraneo-Subtropical zones are sub-arid climax communities like *Ceratonia siliqua* and *Pistacia lentiscus*. At the moister end of the spectrum are the Eu-Mediterranean arboreal communities which tend to reach heights of 1,200 m in the more mesic parts whereas in the more xeric areas (Edom) they reach up to 1,650 m (Zohary and Feinbrun-Dothan 1966). Zohary (1947a) characterizes this type of vegetation by the quercetea calliprini class. The climax forest vegetation consists of maquis and forest that include *Pinus halepensis*, *Hypericum serpyllifolium*, *Quercus calliprinos*, *Pistacia palaestina*, *P. lentiscus*, *Arbutus andrachne*, *Rhamnus alaternus*, *Q. ithaburensis*, *Juniperus phoenicea*, *P. atlantica*. As will be explained further on, these species occupy different areas within the Mediterranean region.

Some authors suggest that these forests once covered a greater extent, being compared in the past to the cedar forests of Lebanon (i.e., Baly 1957). But as a result

of thousands of years of pressure from animal grazing and human activities like farming, fuel wood collection, chopping of trees for construction purposes, and settlement expansion, the forests have been reduced substantially and become increasingly fragmented, except in a few areas where conservation efforts have protected them. Examples of these are the pine and oak forests of the Dibbin National Forest and Ajlun Nature Reserves. East of the Rift Valley, some authors (e.g., Horowitz 1992) entertain the idea that the forests of the northern highlands may have been connected to those of the southern highlands at some time in the past.

At present, the Mediterranean region resembles a mosaic of different vegetation formations (forest, maquis, garigue, batha) that intersect with one another throughout the landscape, reflecting the degree of degradation of the climax vegetation associations. The level below the climax forest is the maquis, represented by *Q.calliprinos-P.palaestina*. The most notable examples of this type of maquis and forest formations are found along the Judean Mountains, Galilee region, Gilead and Ammon. Other formations are the garigue and batha. The garigue is the intermediate form in the sucesional stage and consists of woody shrubs like *Sarcopoterium spinosum*, *Salvia fruticosa* and *Calycotome villosa*, *Cistus villosus*. If left undisturbed, an estimated 20 years is expected for forests to fully recover from the garigue stage (Kasapliligil 1956; Whyte 1950). The batha (term coined by Eig [1927]) or phrygana represents the most degraded stage, and consists of dwarf shrubs and herbs, the most notable of which is *Sarcopoterium spinosum*. Depending on the area, this leading plant can be accompanied by other species like *Teucrium polium*, *Salvia judaica*, *Helichrysum sanguineum*, on mountains and *Thymelaea hirsute* and *Scabiosa sp.* on kurkar hills of the coastal plains (Zohary 1973). When the batha is

further reduced due to grazing, vegetation is limited to thistles like *Urginea maritima*, *Ononis natrix*, *Asphodelus aestivus* and *Anchusa strigosa* (Kasapligil 1956).

2.3.1.2 Irano Turanian region

The Irano Turanian region sits between the Saharo Arabian and Mediterranean regions, and so can be seen as a transitional space between these two opposite regions distinguished by deserts and forests. The topography is quite varied, as it includes hills, plateaus, and plains, whereas the temperature is more uniform (Whyte 1950). It forms a rather narrow belt in some areas and receives between 150 to 350 mm/yr of rainfall. Temperature ranges are more intense than in the Mediterranean region. Summers are usually quite hot whereas the opposite occurs during winter. The mean annual minimal and maximum temperatures range from 5-20°C to 12-25°C, respectively (Al-Eisawi et al. 2000).

West of the Rift Valley, Eig delineated this region to a narrow strip on the Samarian and Judean hills that face the Rift Valley from Lake Kinneret to the Negev, where it occupies a more significant area. Along the narrow belt facing the Rift Valley, species from the adjacent territories are also frequently found (Eig 1938; Whyte 1950). The northern Negev is characterized by *Artemisia herba-alba* (Eig 1938), although *Pistacia atlantica* trees are found in the Negev Highlands. East of the Rift Valley, the Irano Turanian region is more extensive.

The climax vegetation is the steppe, which consists of grasses, small shrubs and bushes that sit over loess and calcareous soils (loess is the most productive of the two). This region suffers from extensive erosion due to a millennial history of grazing and ploughing (Boyko 1954). Being a transition zone, Mediterranean and Saharo Arabian species can be found intermixed with more typical Irano Turanian species that include *Noaea mucronata*, *Artemisia herba-alba*, *Retama raetam*, *Salsola vermiculata*, *Anabasis*

syriaca. Species that are sometimes common in Irano Turanian – Mediterranean transitional areas include *Amygdalus communis*, *Sarcopoterium spinosum* and *Crataegus azarolus*. Sometimes trees like *Ziziphus lotus* and *Pistacia atlantica* are also found surrounded by grasses, forming a savanna-like environment (Horowitz, 1979). As mentioned above, steppes also surround the juniper and oak forests of Edom and open forests with *Pistacia atlantica* in the Negev Highlands. Nevertheless, trees are not common in this type of environment, and these two areas are believed to be relics from a wetter climate.

2.3.1.3 Saharo Arabian region

The Saharo Arabian environment penetrates into the Southern Levant from Africa, the Sinai, and Arabia (Horowitz 1979). It is a desert-like environment that spreads along the Rift Valley from the Lower Jordan Valley (lowest point in earth) to the south and then wraps around the Irano Turanian region on both sides of the Rift Valley. Precipitation never exceeds 200 mm/yr, and usually falls during the winter months in short, intense episodes. The lowest amount is found in the Wadi Arava, where annual rainfall can be less than 50 mm. Evaporation rates exceed precipitation significantly (Horowitz 1979). Temperature differences are more extreme than in other environments. Summers are very hot and dry, although they occasionally experience intense short rain events that cause intermittent flowing wadis to flood. The diurnal temperature range is also more significant than in other regions. Mean annual minimum and maximum temperatures in the Rift Valley range from 10-20 to 20-35°C (Al-Eisawi et al. 2000). The substratum in the Rift Valley is mostly composed of sand dunes, and alluvial gravel and sand deposited from the surrounding upland regions, whereas the southern portion of Jordan consists of granite rocks, sand dunes and sand of aeolian origin. Along these areas there are also wide alluvial fans (Atallah 1977) and playas (also known as qas).

As mentioned before, in Jordan the Saharo Arabian region stretches east from its southernmost extent towards Wadi Rum and then spreads north surrounding the Irano Turanian region along the easternmost fringe of the study area (known as Badia by some authors in Jordan), marking the beginning of the Eastern Desert. Annual rainfall along this fringe is around 100 mm/yr, and plants are usually found on drainage areas (Al-Eisawi 1985). The surface, known as hammada, consists of sand, mud, gravel or pebbles.

Vegetation in the Saharo Arabian region is mainly determined by water availability, which in many instances translates to the location of wadis. The geology and soils present can also influence the vegetation. For instance, porous rocks that have high water infiltration rates can provide the necessary water for plants that would otherwise exist in areas that receive over 500 mm annual rainfall (Danin 1999). Vegetation can be found in contracted (along wadis) or diffused patterns (spread out and commonly found on slopes and depressions). According to Eig (1938), the Lower Jordan Valley includes a riparian forest characterized by *Populus euphratica*. The surrounding valleys and mountain slopes frequently include *Suaeda palaestina*, *Salsola tetrandra*, and *S. asphaltica*. The Negev region has low vegetation cover, and one of the most common species is *Zygophyllum dumosum*. In the southern parts of Jordan, some of the most frequently found species include *Haloxylon articulatum*, *Chenolea Arabica*, and *Salsola tetrandra*. On the plateau, indicator species of this environment include *Anabasis articulate*, *Anabasis syriaca*, *Artemisia herba-alba*, *Astragalus spinosus*, and *Achillea fragrantissima*.

2.3.1.4 Sudano Decanian region

Sudano Decanian areas consist of small enclaves that represent the northern extent of the African Palaeotropic flora (Davies and Fall 2001). The presence of continuous flowing springs and hot temperatures of the rift valley create the necessary microenvironment for

this type of vegetation which can be found in the Rift Valley from the Gulf of Aqaba to around Deir ‘Alla, but concentrates around the Dead Sea Valley. The most common species include *Acacia* sp., *Ziziphus spina-christi*, *Balanites aegyptica*, *Moringa aptera*, *Ocradenus baccata*, *Salvadora persica*, and *Calotropis procera*.

2.4 Vegetation

Because the study area is located at the confluence of three major plant belts and there is high climatic and topographic diversity, the flora is extremely rich (Zohary and Feinbrun-Dothan 1966, Zohary 1973, Horowitz 1979, Al-Eisawi 1996, Danin 2004). Within a short space, it ranges from Mediterranean maquis and forests to steppes, grasslands, deserts, extreme deserts, and tropical oasis. To an extent, vegetation is determined by edaphic factors, however it is mostly influenced by climatic parameters.

Several authors have mapped and described the vegetation of the region. Some of the earlier accounts transcended political boundaries before large scale modern development and agricultural enterprises radically transformed parts of the landscape (e.g., Post 1888, Eig 1927, 1931, 1938, Zohary 1973). Other more recent works have been constricted by political boundaries. A Jordanian vegetation map was created by Al-Eisawi (1996), one of the leading botanists of Jordan (Figure 2.2). He considered only the ‘natural’ remaining vegetation and vegetation regions. He subdivided the forests into evergreen oak, pine, deciduous oak, and juniper. He also included a fairly large longitudinal strip of *Mediterranean non-forest vegetation*, and states that some authors believe this region would eventually become forest, if left undisturbed. In the Irano Turanian region, he included the category *Steppe*. Along the Rift Valley he showed sand dune vegetation, saline (halophytic) vegetation, acacia and rocky sudanian vegetation, and tropical vegetation. He called the desert-like vegetation of the plateau *Hammada*

vegetation. He also classified the large wadis that drain into the Jordan River and Dead Sea as *Water (Hydrophytic) vegetation*.

An even earlier map of Jordanian vegetation was created by Kasapligil (1956), which also included the Palestinian territories of the West Bank (Figure 2.3). He was commissioned by FAO to conduct two years of in depth field work to assess the state of vegetation in Jordan and the West Bank, and to make recommendations regarding management and conservation practices. In addition to the forest categories which Al-Eisawi represents in his map, Kasapligil also included the description of *Secondary (degraded) forests, Pistacia atlantica*, and *Cupressus sempervirens*. He also included orchards and scattered *ziziphus* grasslands.

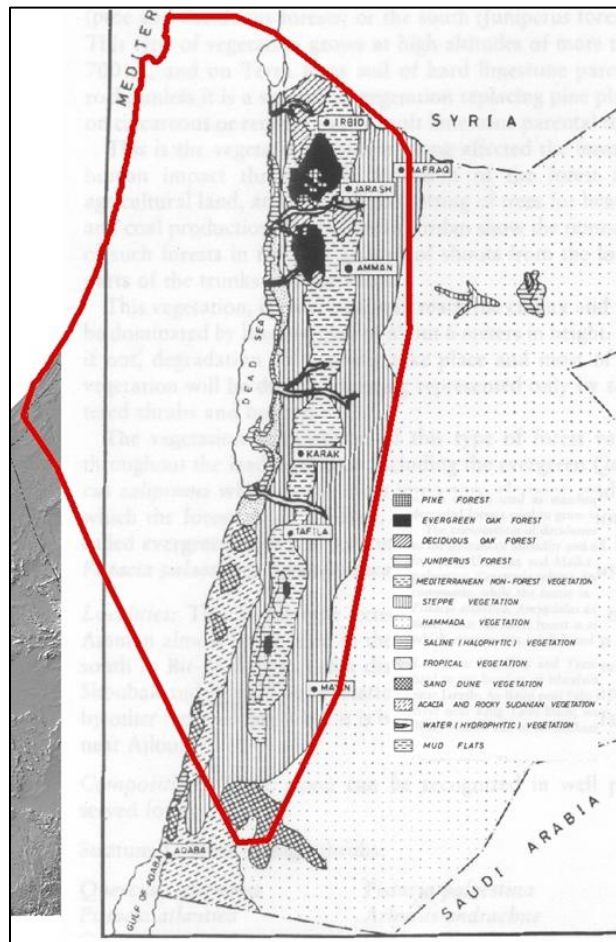


Figure 2.2. Vegetation map of Jordan, created by Al-Eisawi (1996: 48) and georeferenced by Soto-Berelov, showing study area extent.

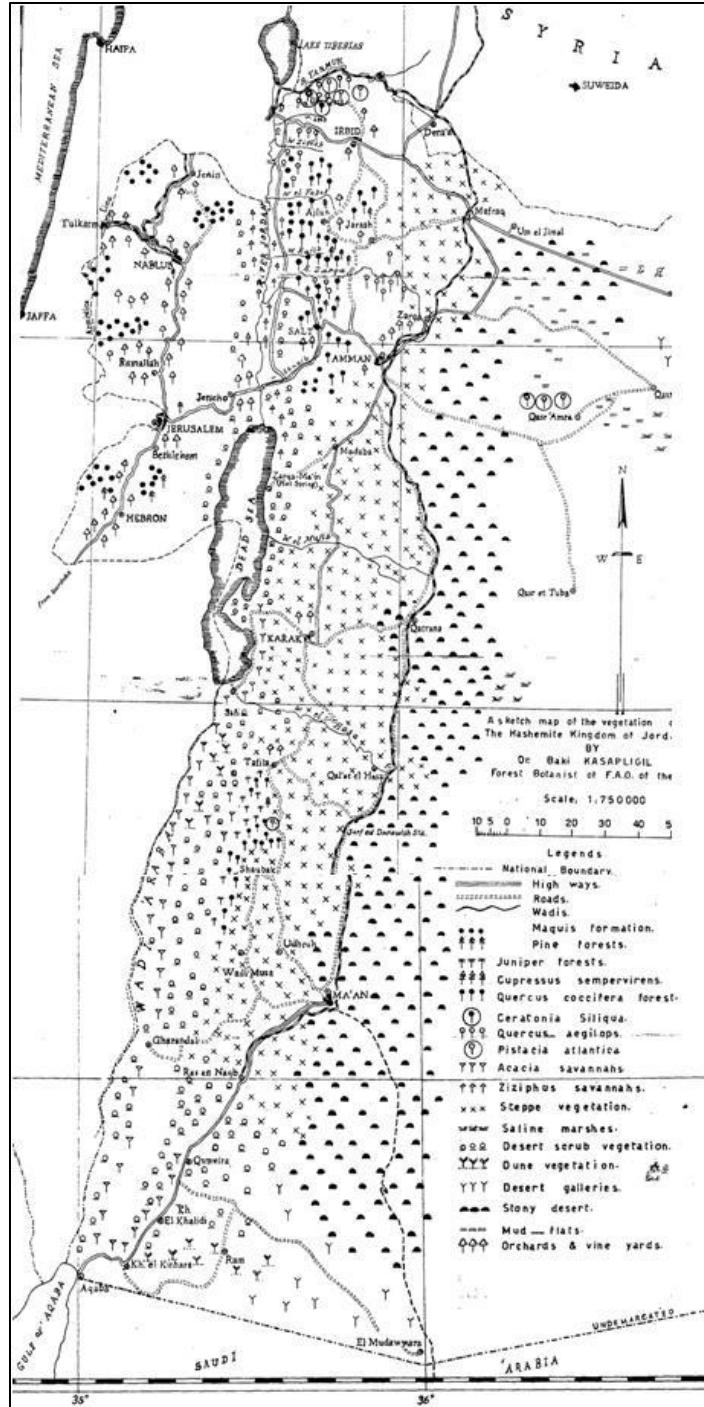


Figure 2.3. Vegetation map of Jordan and the Palestinian territories, created by Kasapliligil (1956).

Also based on extensive field work, floristic assessments and analysis of plant distributions, Jewish botanists have produced their share of information and vegetation maps. In 1947, Zohary presented what he called a vegetation map of western Palestine

(Figure 2.4.). It is a comprehensive map that includes information regarding both the vegetation found on the ground as well as the potential climax vegetation.

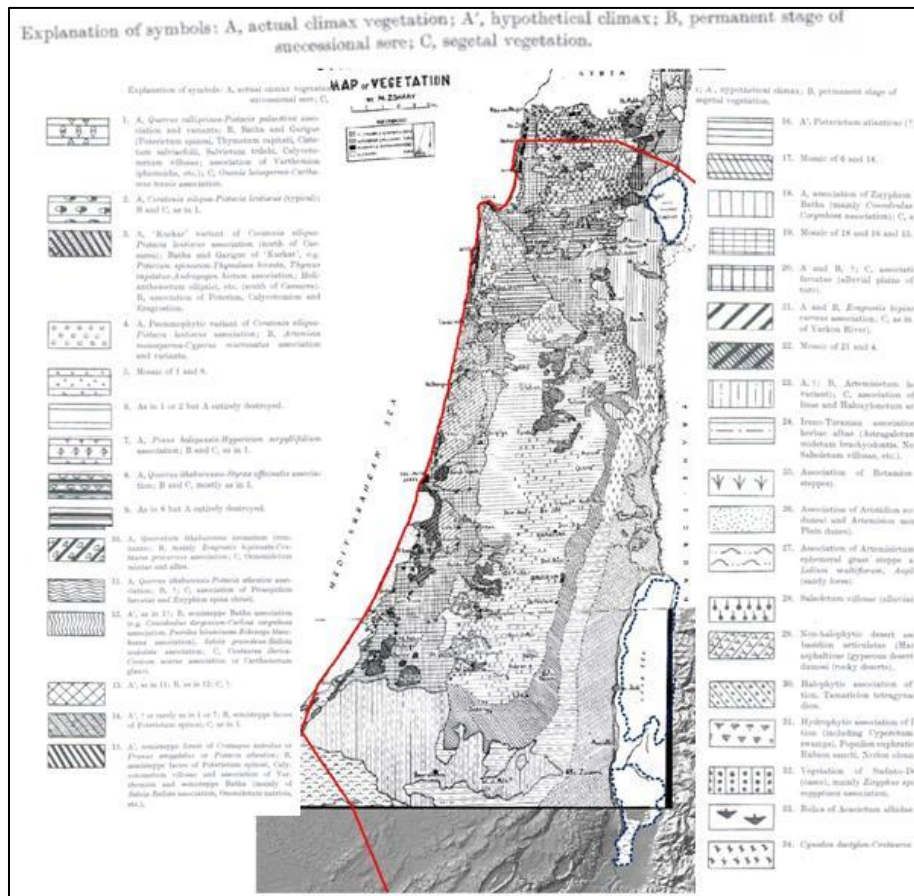


Figure 2.4. Zohary's vegetation map of Western Palestine (1947), georeferenced by Soto-Berelov. Also showing study area boundaries.

Additional maps have been created by Danin (1988, 1995) and Horowitz (1979) (Horowitz's interpretation is shown in Figure 2.5). A complete map of the region was assembled by Danin (1999), drawing from several sources including his own (Figure 2.6). Using data from Feinbrun-Dothan and Danin (1991), a more complex phytogeographical map was created by the same author (Danin 1995), following the same methodology of the most recent map of plant geographical territories previously discussed (Danin and Plitmann 1987). In it, the area was subdivided into 31 districts (shown here in Figure 2.7, to illustrate the patterns detected within this map). The flora

within each district was analyzed and attributed to a particular chorotype or phytogeographical region. Bar charts (per district) then indicate the percentage of each phytogeographical region within each district. This map allows broad patterns to be detected, such as the decline of Mediterranean species the further south one travels along the mountains west and east of the Rift Valley, as well as the closer one gets to the Rift Valley from the mountains on either side. The opposite can be said for Saharo Arabian species.

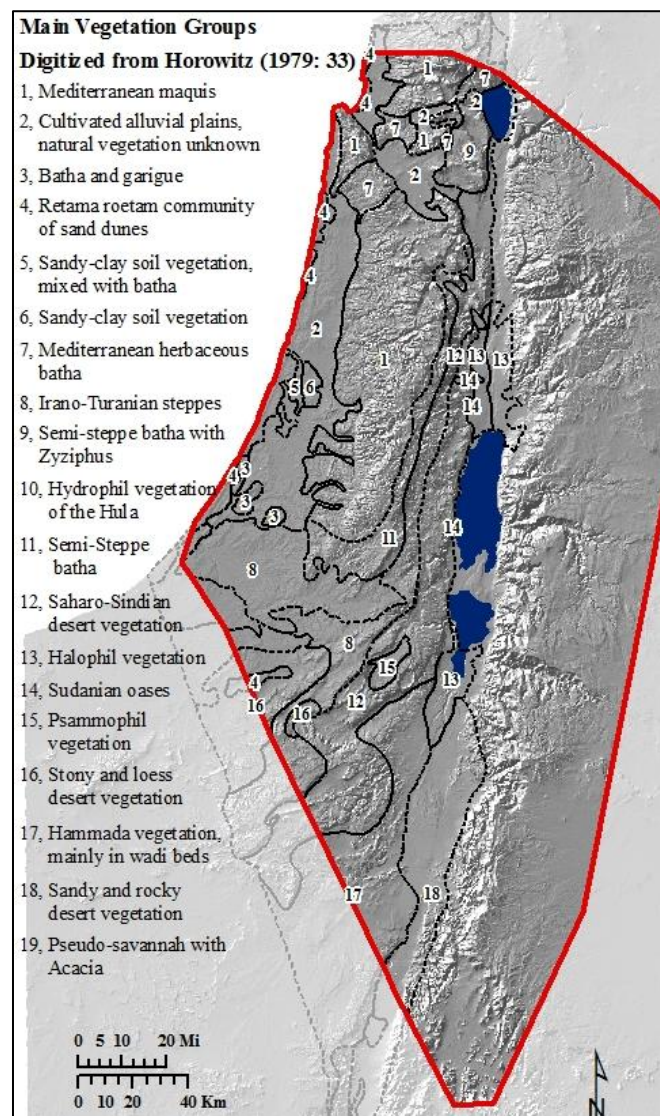


Figure 2.5. Map of major vegetation groups according to Horowitz (1979:33), georeferenced and digitized by Soto-Berelov. Also showing study area extent.

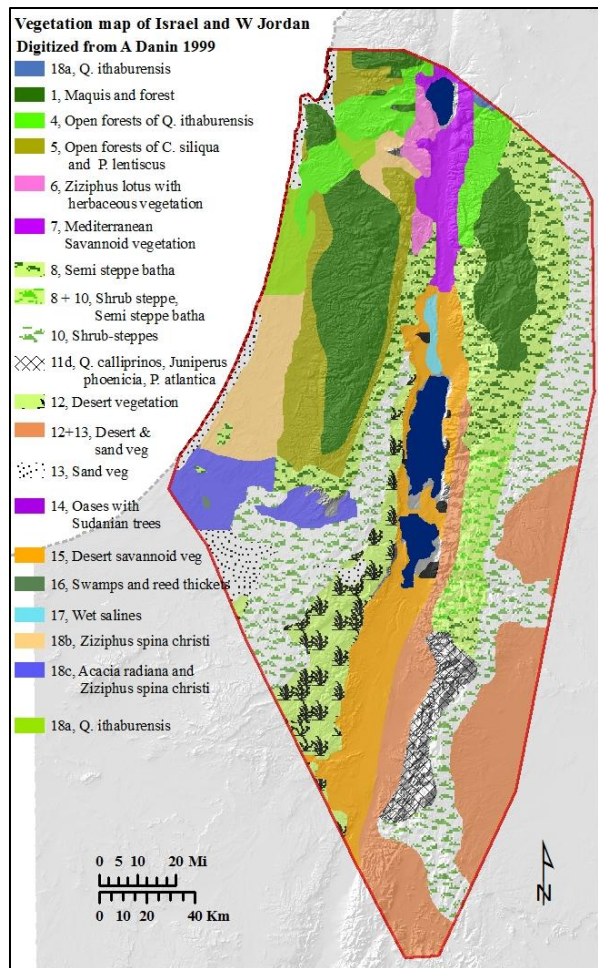


Figure 2.6. Danin's vegetation map of the region (1999: 107), georeferenced and digitized by Soto-Berelev, showing study area extent.

Because the goal of this study is to model potential vegetation at present and then throughout the Holocene, the vegetation must first be described by drawing from these works. Before doing so, it is important to point out that each of these maps was created by a different author who was driven by a particular purpose. The maps were also created at different dates, using different methodologies, classification schemes, and at different scales and resolutions. As a result, there will always be some differences amongst them. Nevertheless, they complement each other, and allow the reader to become informed about the distribution of the different types of vegetation present throughout the study

area, and the plant associations that dominate within each of these. In chapter 5, some of these maps and accompanying anecdotal evidence will again be referenced and used as comparison against the outputs from this study, when creating a present day map of potential vegetation of the region. For the most part, the breakdown of categories adheres to the classification scheme used in this study.

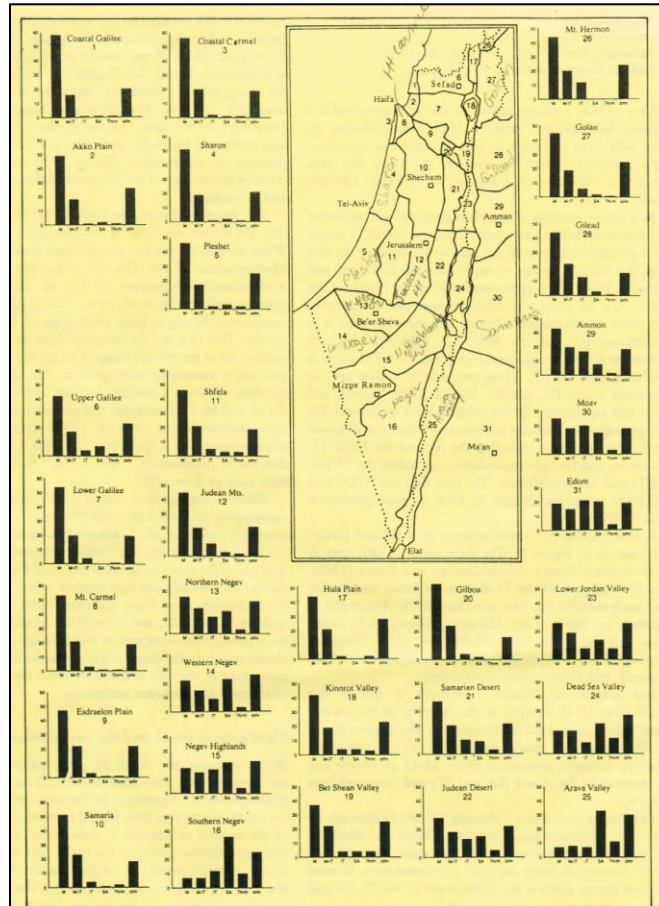


Figure 2.7. Phytogeographical map of the region (Danin 1995: 27). Full map and accompanying graphs shown to highlight the latitudinal and longitudinal impact on chorotypes.

2.4.1 Vegetation of the mesic parts of the study area

The naturally occurring vegetation throughout the study area has been impacted by human and animal activities for millennia. For thousands of years, man has been transforming the landscape through the use of tools like the plough, chopping of trees for

building or obtaining fuel wood, and by allowing domesticated animals to graze throughout the land. For the most part, these impacts can be reversed through succession, if given enough time to regenerate. In addition to these ancient practices, modern activities like mechanized irrigation and expansion of large urban centers has caused some of the original landscapes to become irreversibly converted into anthropogenic spaces. So the resulting landscape at present resembles a mismatched jigsaw puzzle, where forest patches can sit alongside orchards, roads, and urban areas. Nevertheless, a fair amount of studies have been done by botanists, archaeologists, ecologists, plant geographers and other specialists that allow a fairly comprehensive reconstruction of the natural vegetation, although some areas like the coastal plains have been so dramatically altered that the climax vegetation is only guessed.

2.4.1.1 Forests

The following associations are considered to represent climax Mediterranean maquis or forests: *Quercus calliprinos* or *Q. calliprinos-Pistacia palaestina* assoc. (evergreen oak forest), *Pinus halepensis-Hypericum serpyllifolium* association (pine forest), *Quercus ithaburensis* (deciduous oak forest), and *Ceratonia siliqua-Pistacia lentiscus* association (open forests of carob and pistacia). The first three are considered to represent the higher elevation and wetter areas. They are accompanied by *Q. ithaburensis*, *Ceratonia siliqua*, *P. lentiscus*, *P. atlantica*, and *Crataegus azarolus*. However, due to human and animal pressure, forests have been reduced dramatically.

The most representative association at present is that of *Q. calliprinos – P. palaestina*. West of the Rift Valley, it dominates throughout the main forest areas which constitute fragmented patches in the mountains of Samaria, Judea, Carmel, and the Galilee (Danin 1999). These are shown in Danin's 1999 and Horowitz's 1979 map as 'Maquis and forests' on the Judean mountains. They seem to occupy Terra Rossa soils

that derive from hard limestone and are frequently accompanied by *Crataegus azarolus*, *Styrax officinalis*, *Rhamnus palaestina*, *P. lentiscus*, *Ceratonia siliqua*, *Arbutus andrachne*, *Laurus nobilis* (Zohary 1973). Smaller stands are also found around Mt. Carmel, Gilead, Samaria, and Upper Galilee.

There is some debate regarding what constitutes the climax Mediterranean forests. Some authors believe it is the *Pinus halepensis* forests (Atkinson and Beaumont 197), whereas others argue that either pure stands of *Q. calliprinos* or mixed *Q. calliprinos* – *P. palaestina* represent the climax stage (Liphshitz and Biger 1990). Furthermore, most of the pollen proxy records (discussed in the next chapter) suggest that the *Q. ithaburensis*-*Pistacia atlantica* association was the most common association during the early Holocene.

The *P. halepensis* tree is known to have poor regenerative capacity if it is chopped or burned (Zohary 1973), so its distribution area may have been reduced significantly due to human activities thousands of years ago. At present, *P. halepensis* stands are less common than other climax forests. In 1973, Zohary reported a few remnant stands in Mount Carmel, around Yerka in the Galilee, Um Safah in Samaria, Hebron in the Judean Mountains, and in Gilead east of the Rift Valley. This last represents the largest stand and will be discussed below. Some of the species present in these stands include *Q. calliprinos*, *Arbutus andrachne*, *Phyllirea media*, *P. lentiscus*, and *P. palaestina* (Zohary 1973). They tend to be found on light Rendzina soils that derive from marly chalk.

At present, *Quercus ithaburensis* dominates in slightly lower elevations. Zohary (1947) identified three associations, each occurring in a different location: *Quercus ithaburensis*-*Styrax officinalis*, *Quercetum ithaburensis arenarium*, and *Quercus ithaburensis*-*Pistacia atlantica*. The first is found west of the Rift Valley, mainly around

the Ephraim Mountains in Samaria and western hills of the Lower Galilee. In the past, the extent was probably much greater, and included large parts of the Esdraelon Plain (Eig 1933). The second association, confined to the coastal plains, is believed to have inhabited large parts of the Sharon Plain (Eig 1933, Zohary 1947a, Zohary 1962, Danin 1999). The *Quercus ithaburensis-Pistacia atlantica* association is found in Transjordan, in the Golan and Gilead regions and will be discussed below.

Another forest category that is present in lower elevations but further south of the *Q. ithaburensis* maquis areas is the open forest of carob and pistacia. Curiously, it is only found west of the Rift Valley on Terra Rossa, Rendzina, and Kurkar soils. Zohary (1959: 285) described this alliance (Ceratonio-Pistacion alliance) as having a 'park-like' appearance with scattered carob trees and *Pistacia lentiscus* shrubs. He subdivided it into three categories, two of which (*Ceratonieto-Pistacietum lentisci typicum* and *Ceratonieto-Pistacietum lentisci orientale* associations) are found on the foothills of the Judean mountains from sea level up to around 300 m. They form a belt (see Danin's 1999 map, Figure 2.6) around these mountains in which *Quercus calliprinos* and *Pistacia palaestina* represent the climax Mediterranean association, although *P. halepensis* trees also occur in this area (oak and pistacia trees are sometimes found within the carob and pistacia maquis and vice versa). The first association is the most abundant. It is found along the hills that descend into the coastal plains (extending from around Duweima in the south into the frontier with Lebanon in the north). The second association penetrates into the Irano Turanian region and as a result, species like *Ziziphus lotus*, *Amygdalus communis*, and *Pistacia atlantica* can also be spotted. The third association (*Ceratonieto-Pistacia lentisci arenarium*) is found on the coastal plain in the Sharon region between Wadi Falik and Caesarea on sandy soils (Zohary and Orshan 1959). Remnants of this association further north and south suggest that it was more extensive in the past

(Zohary and Orshan 1959). This association is more drought and heat resistant than the *Q. calliprinos*. In Jordan, this category is not present, except for some scattered carob trees in the deciduous oak forest in Gilead and area where it transitions into the evergreen forest.

The remaining forests east of the Rift Valley are found on the plateau region in both the northern and southern highlands. In the northern plateau region which can be subdivided by the dissected Wadi Zarqa river valley, discontinuous forest areas extend about 80 km in length from around Wadi el-Arab to Wadi Kuffrein and reach their greatest width of about 25 km around Ajlun (Atkinson and Beaumont 1971). The maquis that occupies the greatest area is represented by *Quercus calliprinos* (Figure 2.8.), which is also accompanied by *Pistacia palaestina*, *P. lentiscus*, *Ceratonia siliqua*, *Arbutus andrachne*, and *Cistus villosus* (Al-Eisawi 1996). It is usually found on Terra Rossa soils and is considered to be a secondary forest to the climax *Quercus ithaburensis*-*Pinus halepensis* community (Atkinson and Beaumont 1971).



Figure 2.8. *Quercus calliprinos* maquis with intermixed *Pistacia palaestina* at the Ajlun Woodland Reserve (Soto-Berelev).

Slightly further north and at somewhat lower elevations are forest patches dominated by *Quercus ithaburensis* (Figure 2.9). These are usually found with *Pistacia atlantica*, *Ceratonia siliqua*, and *Styrax officinalis*. These forests are more fragmented than those of *Quercus calliprinos*, due to more human and animal pressure. Around the area where the *Quercus calliprinos* and *Q. ithaburensis* forests meet, both species can be found in tandem. Around Ajlun, there are also forests represented by *Pinus halepensis* (Figure 2.10). This category is usually found at elevations over 700 m in both calcareous and rendzina soils and in wetter areas (annual precipitation in these areas is between 500 to 700 mm). It is commonly found with *Quercus calliprinos* trees, which show secondary succession. The best preserved remnant patches are found around the Dibbin Forest reserve, and are accompanied by *Quercus calliprinos*, *Arbutus andrachne*, *Pistacia palaestina*, and *Pyrus syriaca*. There are also small patches of forests that mainly consist of *Quercus calliprinos* (85%) and wild olive (15%). These are found southwest of Jerash and are associated with *Ceratonia siliqua* (Atkinson and Beaumont 1971).



Figure 2.9. On the left, stand of *Quercus ithaburensis* maquis amidst houses near Umm Qays in Gilead (Soto-Berelov). On the right, *Q. ithaburensis* surrounding olive orchard southeast of Umm Qays (Soto-Berelov).



Figure 2.10. *Pinus halepensis* forest, Dibeen National Forest (Soto-Berelov).

2.4.1.2 Open forests

There are two main areas where open forests occur. The smaller of these is found in the Negev Highlands on smooth faced rocks (Danin 1999), within the Irano Turanian region. These are mostly composed of trees of *Pistacia atlantica*. In smaller quantities, *Amygdalus ramonensis* and *Rhamnus disperma* are also found. Danin shows this in his map (labeled as 11a, Figure 2.6), and considers them to be a refugium of relict Mediterranean species (Danin 1972, 1999).

The most significant open forests are located in the southern highlands or plateau region on sandstone, basalt, limestone, and chalk rocks. These seem a bit out of character, considering they are surrounded by steppe and desert. They are smaller, more fragmented, and have been subject to more human and animal pressure than those of the northern highlands. They occupy a tighter area (about 6km) that spreads for about 25 km from Wadi Dana to Wadi Musa, and they have several characteristics that distinguish them from other forests. For a start, they are surrounded by more extreme environmental conditions. Besides being more affected by the north-south and east-west rainfall gradient, they sit on an escarpment that is more deeply incised by wadi valleys that flow towards the Arava Valley (e.g. Wadi Hassa, Wadi Dana, Wadi Musa, Wadi Faynan, Wadi Saline). Also, the change in elevation is quite dramatic, ranging from below 300 m

bsl to 1700 m asl within a short distance. The mean temperature annual range is also greater in this area, as compared to the other mountainous regions. As a result, the resulting forests are found within a more steppe like environment that contains an Irano Turanian understory with shrubs like *Artemisia herba alba*, *Noaea mucronata*, and *Poa sinaica*.

These forests of the southern highlands also differ in composition from those of the north. The major species are *Quercus calliprinos* (these look smaller than those of the north – Figure 2.11) and *Juniperus Phoenicia*. Accompanying trees are *Cupressus sempervirens*, *Crataegus aronia*, and *Pistacia atlantica*. They are considered to represent a “refugium of Mediterranean flora in the transition between desert and shrub-steppe” (Danin 1999: 144). Kasapligil, Danin and Al-Eisawi show the distribution of these forest areas in their respective maps (Figures 2.3, 2.6, 2.2, respectively).

Quercus calliprinos stands are predominantly found on limestone bedrock between Tafila and Petra (Figure 2.11). They are sometimes found with *Juniperus phoenicia* on calcareous soils at elevations higher than 1300 m (e.g., AL-Illami, near Ad-Dabbaghat, and AL-Hisha south of Nijil, Shaubak). *Juniperus phoenicia* is most representative on Nubian sandstone bedrock along west-facing slopes between the environs of Dana and Ras en Naqab (Figure 2.12). This tree also occurs on pure stands or is accompanied by *Pistacia atlantica* in elevations between 500-1600 m and *Cupressus sempervirens*. *Pistacia atlantica* and *Cupressus sempervirens* stands are also found by themselves (Kasapligil 1956, Danin 1999) in this area.

Within this region, the richest assemblage of Mediterranean relict species throughout the Near East is considered to be in the Dana-Petra area (Danin 1999). It includes trees like *Quercus calliprinos*, *Pistacia atlantica*, *P. palaestina*, *P. khinjuk*, *Crataegus aronia*, *Juniperus phoenicea*, *Amygdalus korschinskii*, *Ceratonia siliqua*, *Olea*

europaea, *Arbutus andrachne*, *Rhamnus punctata*, *R. lycioides*, *R. disperma*, and *Ficus carica*. These are protected in the Dana Nature Reserve area. Figure 2.13 shows a stand rich in Mediterranean and Irano Turanian species overlooking Dana Canyon.

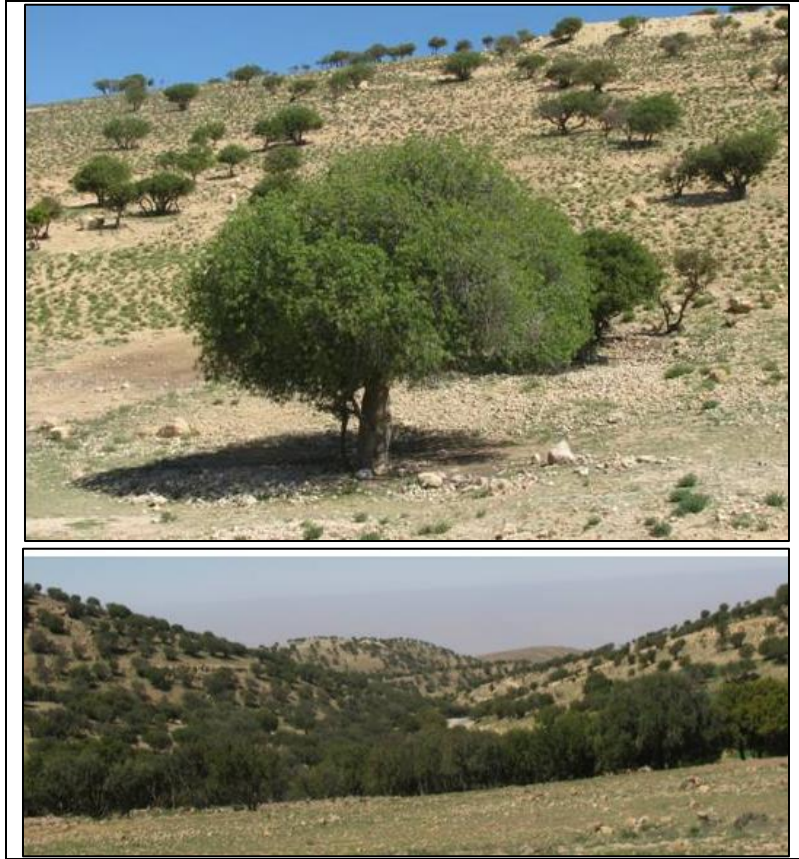


Figure 2.11. Forests of the Southern Highlands in the plateau region. On top, *Pistacia atlantica*, *Quercus calliprinos* and *Artemisia herba-alba* near Petra (Soto-Berelov). In the bottom, *Q. calliprinos* and *P. atlantica*, maquis near Petra (Soto-Berelov).



Figure 2.12. *Juniperus phoenicia* on slopes in Taybet Zan, near Petra (Soto-Berelov).



Figure 2.13. Stand rich in Mediterranean and Irano Turanian species overlooking Dana Canyon. Some of the species present include *Crataegus azarolus*, *Noaea mucronata*, *Euphorbia thamnoides*, *Rhamnus sp.*, *Calycotome villosa*, *Iris petrana* (Soto-Berelov).

2.4.1.3 Coastal vegetation

The coastal plains occupy a rather extensive area. They have some of the most fertile alluvial soils and because of this, and the fact that they can be easily accessed, they have been the most impacted by human activities. In Danin's map (Figure 2.6), he classified the whole region as *Synanthropic vegetation*. However, he subdivides this region into three areas that reflect the difference in aridity. The northernmost (18a), found in the Sharon plain, is likely to have been populated by *Quercus calliprinos* and *Q. ithaburensis* trees. The middle section is represented by *Ziziphus spina Christi* trees, whereas in the southernmost area (Negev) *Acacia radianna* trees are common.

2.4.1.4 Mediterranean savannoid vegetation

As previously mentioned, the northern portion of the Rift Valley receives significantly more rain than the rest of the Rift Valley. On phosphorous rich soils that lie over basalt rocks around the Sea of Galilee, a grassland environment is found. Cereal grasses like *Triticum dicoccoides* (wild wheat), *Hordeum spontaneum* (wild barley), and

Avena sterilis (wild oats) spread across the floor, amidst which stand scattered *Ziziphus spina Christi* and *Ziziphus lotus* trees. This grassland spills onto the sedimentary rocks of the Samarian desert, and the west facing slopes in Gilead below the *Q. ithaburensis* belt. They are also found on the steep topography surrounding the rift valley from the north of Jericho to the northern section of the Sea of Galilee.

2.4.2 Vegetation of the steppes

2.4.2.1 Semi steppe batha

Semi steppe batha refers to the areas populated by shrubs that surround Mediterranean climax communities. These areas generally receive around 350 mm/yr rainfall. Although *Sarcopoterium spinosum* is at the lower end of the spectrum within the Mediterranean forest succession stage, in this region it sometimes finds itself without competition from taller species and occupies considerable areas, along with other shrubs like *Ononis natrix*, *Echinops blancheana*, *Ballota undulata*, *Noaea mucronata*, and *Artemisia herba alba*. Figure 2.14 shows a photograph taken near Shobek (in the southern highlands) that is extensively populated by *Artemisia herba alba* and *Noaea mucronata*.



Figure 2.14. Semi steppe batha vegetation near Shobek (Soto-Berelov).

2.4.2.2 Shrub steppe vegetation

Within the precipitation-vegetation gradient where forests and desert savannoid vegetation sit at opposite extremes, shrub steppe is found in the middle. It refers to

shrubby areas that receive less precipitation than areas covered by semi steppe batha vegetation. Consequently, they are found surrounding and penetrating into the more arid Saharo Arabian region and include a mixture of Irano Turanian and Saharo Arabian species in places like the Negev Highlands, Judean Desert, Edom, Ammon, and Lower Jordan Valley (Figure 2.15). Depending on the location, the following species can be found in abundance: *Retama Duriaei*, *Phlomis brachyodon*, *Asphodelus microcarpus*, *Artemisia herba-alba*, *Noaea mucronata*, *Gymnocarpus fruticosi*, *Salsola jordanica*, *Anabasis articulate*, and *Retama raetam*.



Figure 2.15. Shrub steppe vegetation surrounding olive orchard SW of Heshbon in the Ammon region, 379m (Soto-Berelev).

2.4.3 Vegetation of the xeric parts of the study area

2.4.3.1 Desert savannoid vegetation

The southern portion of the Rift Valley is populated by a type of desert savanna that is mostly exemplified by Acacia trees that stand scattered amidst desolate gravelly plains, sand dunes, alluvial fans, and desert wadis (Figure 2.16). This is the hottest and driest portion of the region, and covers an area that is the lowest on the planet. Despite Acacia (*Acacia raddiana*, *A. tortilis*, *A. gerrardii*), other desert plants commonly spotted are *Ochradenus baccatus*, *Zygophyllum dumosum*, *Balanites aegyptiaca*, *Gymnocarpus*

fruticosi (*G. decander*), and *Haloxylon salicornicum* (on sand dunes). This vegetation category is shown in all of the maps. Al-Eisawi calls it *Acacia and rocky Sudanian vegetation*, Kasapligil refers to it as *Scattered Acacia grasslands*, Danin as *Desert savannoid vegetation*, and Horowitz as *Pseudo savannah with Acacia*.

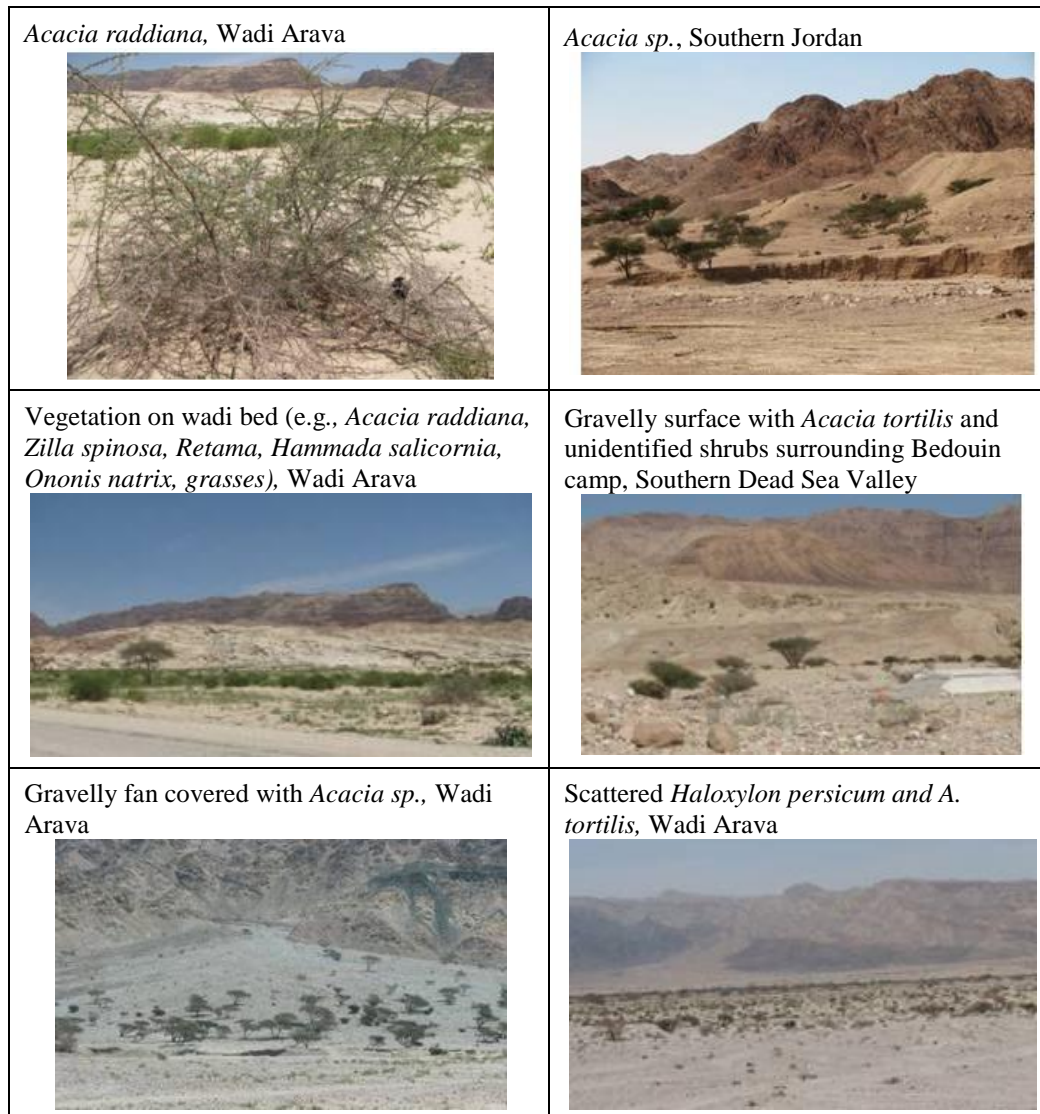


Figure 2.16. Desert savannoid vegetation (Soto-Berelov).

2.4.3.2 Desert scrub vegetation

In areas that receive less than 200 mm/yr precipitation, scrubby desert vegetation is found in diffused or contracted patterns (Danin 1999). Diffused refers to when the vegetation has a wide spread coverage on slopes and depressions, whereas contracted

means the plants are restricted to wadi beds. Zohary (1947) identified several major groups within these areas, which occur on the Saharo Arabian and Sudano Decanian regions. Although less representative, they can also be found in the Irano Turanian region, primarily in transition areas with the more arid zones.

In the Judean Desert and some plains of the Negev that are covered by gravelly soils, *Zygophyllum dumosum* is the leading species, accompanied by *Anabasis articulata*, *Gymnocarpus fruticosus*, *Stipa tortilis* and other species. On the soils that are rich in gypsum within the Judean Desert, *Suaeda asphaltica* is the most representative species, accompanied by *Poa eigii*, *Stipa tortilis* and others. Other plains covered by hammada in the Negev and drier areas east of the River Valley are mainly represented by *Anabasis articulata*, and to a lesser extent by *Zilla spinosa* and *Noaea mucronata*.

2.4.3.3 Stony desert vegetation

This type of desert vegetation is found along the eastern edge of the study area and represents the beginning of the Eastern Desert, which extends beyond the study area across a vast plain that is covered by volcanic and limestone gravel and pebbles. As shown in Kasapligil's vegetation map, the Hejaz railway more or less marks the area where steppe vegetation transitions into this category. The vegetation is very poor (Figure 2.17). Scattered desert shrubs of the chenopodiaceae family are found intermittently with a few patches of grasses and Irano Turanian shrubs, mostly on wadi beds.



Figure 2.17 Stony desert vegetation. Gravelly surface with roadside vegetation southwest of Qalat al Hasa in Edom, 1015m (Soto-Berelov).

2.4.4 Edaphically influenced vegetation

2.4.4.1 Halophytic vegetation

Halophytic vegetation predominates on the highly saline soils of the Lower Jordan and Dead Sea Valleys and along the Wadi Arava (Figure 2.18). Following the retreat of Lake Lisan (Map 4.5), saline deposits were exposed. Because rain decreases latitudinally, deposits around the Dead Sea and those found further south are not washed away by rains as they are further north, resulting in highly saline soils. In addition, this area contains springs and marshes that are permanently saline, due to a high groundwater table that is also saline. Some of the major constituents include *Atriplex halimus*, *Salsola tetrandrae*, *Suaeda sp.*, and *Nitraria retusa*.



Figure 2.18 Area with large concentration of halophytic and tropical plants (e.g., *Ochradenus baccatus*, *Nitraria retusa*, *Anabasis setifera*) on the eastern shore of the Dead Sea, 395 m bsl (Soto-Berelov).

2.4.4.2 Riparian vegetation

Riparian vegetation is found along rivers, wadis, and wetland areas. Perhaps the most significant area is the floodplain of the Jordan River. The area closest to the river (the *zor*) is populated by *Populetum euphraticae*. A second belt consists of *Tamaricetum*

jordanis, followed by the *Prosopis farcata- glabra* assoc. There are also a series of rivers that are tributaries of the Jordan River, which also contain riparian vegetation along their banks. Some of these are shown in Al-Eisawi's vegetation map. In addition, the coastal plain contains a series of rivers that flow from the Central Hills to the Mediterranean Sea, forming swamps whenever they intersect sand dunes adjacent to the sea. Some of the most popular species, besides the ones previously mentioned, include *Platanus orientalis*, *Phragmites communis*, and *Nerium oleander*.

In addition, the arid areas are crisscrossed by wadis that contain desert riparian vegetation along their banks. Most of these are within the Dead Sea basin, and eventually drain into the Wadi Arava in the Rift Valley. The vegetation on these wadi beds sometimes stands in contrast to their surroundings, which may be quite devoid of plant life (Figure 2.19). Species commonly found include *Tamarix sp.*, *Phragmites sp.*, *Salix sp.*, and *Nerium oleander*.



Figure 2.19. Vegetation on wadi bed (e.g., *Acacia sp.*, *Tamarisk sp.*, *Ziziphus spina christi*, *Hammada salicornia*, *Ochradenus baccatus*, *Calotropis procera*) in the Southern Dead Sea Valley, 272 m bsl (Soto-Berelov).

2.4.4.3 Tropical Sudanian vegetation

Enclaves of tropical Sudanian vegetation are found throughout the Rift Valley from Deir ‘Alla to Aqaba, but concentrate around the Dead Sea. The very hot temperatures found in this area coupled with permanently flowing springs allow this oasis-like vegetation to flourish, especially in places like Ghor Safi and Ghor Faifa (Al-Eisawi 1996). Trees and shrubs found in these environments include *Ziziphus spina Christi*, *Balanites aegyptiaca*, *Calotropis procera*, *Occradenus baccatus*, *Phoenix dactylifera*, *Acacia albida*, and *Moringa aptera*. Figure 2.20 shows a flowering *Calotropis procera* near the archaeological site ZAD 1 in the southern Dead Sea Valley.



Figure 2.20. *Calotropis procera* in the southern Dead Sea Valley (Soto-Berelev).

2.4.4.4 Sand dune vegetation

Extensive sand dunes are found inland, as well as along the coast. The coastal dunes form a narrow strip along the Mediterranean Sea which stretches from the Negev in the south to Caesarea in the north. These are formed from sediments that come from

the Nile River. After the dunes are formed, several stages of succession follow, which consist of an initial grass cover of *Ammophila arenaria*. Once the sand stabilises, it is succeeded by *Artemisia monosperma* and other *Artemisia* species. The final stage of succession is *Retama raetam* shrubs and in the northernmost area, *Pistacia lentiscus*, *Calicotome villosa*, and *Ceratonia siliqua*.

Inland sand dunes are found in the Negev, along the Rift Valley, and in southern Jordan. The Western Negev sands are initially dominated by the grass *Stipagrostis scoparia*, and eventually become populated by *Artemisia monosperma*, *Noaea mucronata* and *Panicum turgidum*. Along the Arava Valley, the sand originates from the weathering of Nubian Sandstone in the Plateau region and accumulates on the leeward side of these formations. The common species are *Haloxyton persicum*, *Hammada salicornia*, *Hammada salicornia*, and *Salsola cyclophylla*. The sands of the Wadi Rum region are dominated by *Haloxyton persicum*, *Hammada salicornia*, *Hammada salicornia*, and *Salsola cyclophylla* (Figure 2.21).

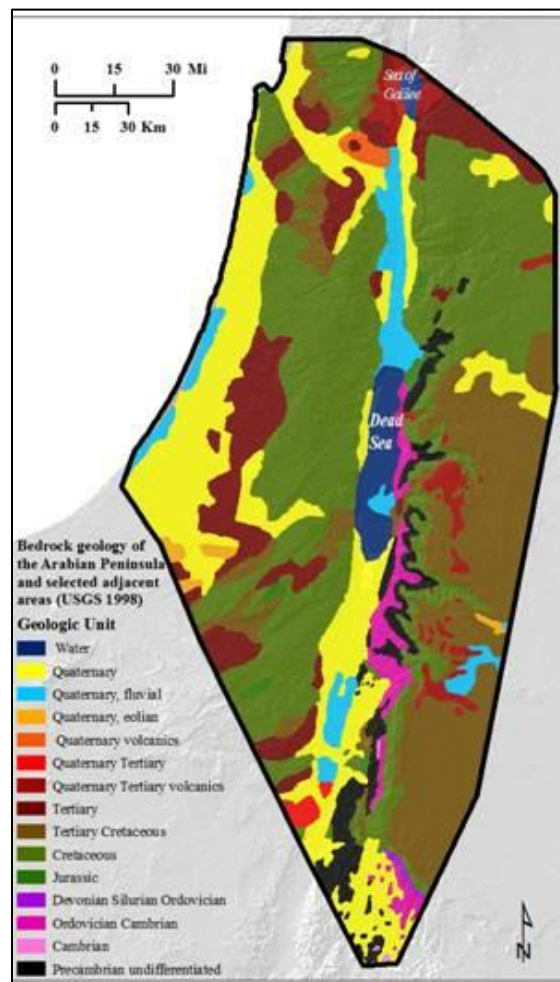


Figure 2.21. *Haloxyton persicum* and *Hammada salicornia* in Wadi Rum, (Soto-Berelev).

2.5 Geology and soils

The most common rocks in the northern part of the study area come from the Cretaceous and Tertiary periods and consist of limestone, dolomite, chalk and marl. In

the Mediterranean portions of this area, these consist of terrestrial and marine sediments deposited between the Tertiary (terrestrial and sandstone) and the Jurassic (marine and calcareous). The Golan and northeastern Galilee regions consist of basalt rocks. The valleys, on the other hand, have rocks from the Tertiary and Pleistocene period, while the Rift Valley consists of Cretaceous and older sandstones (Danin 2001). In the plateau region, the northern half of the bedrock is calcareous in origin, whereas the southern half is dominated by Nubian sandstone of the Lower Cretaceous (western slopes of the Tafila-Kerak region) and volcanic rocks like granites, basalts and dolomites (southernmost part). Both these types of rocks produce sandy soils that are also found in the Rift Valley. Map 2.6 shows a general map of geology.



Map 2.6. Simplified map of geology. Digitized from Pollastro et al. 1998.

The soils of the region, which have high amounts of calcium, are primarily influenced by the underlying bedrock as well as the climate (there are also a small number of soils that are eolic in origin). Most of the study area is impacted by severe erosion (Figure 2.22) and has low vegetation cover. As a result, soils tend to be of poor quality (Al-Eisawi 1996).

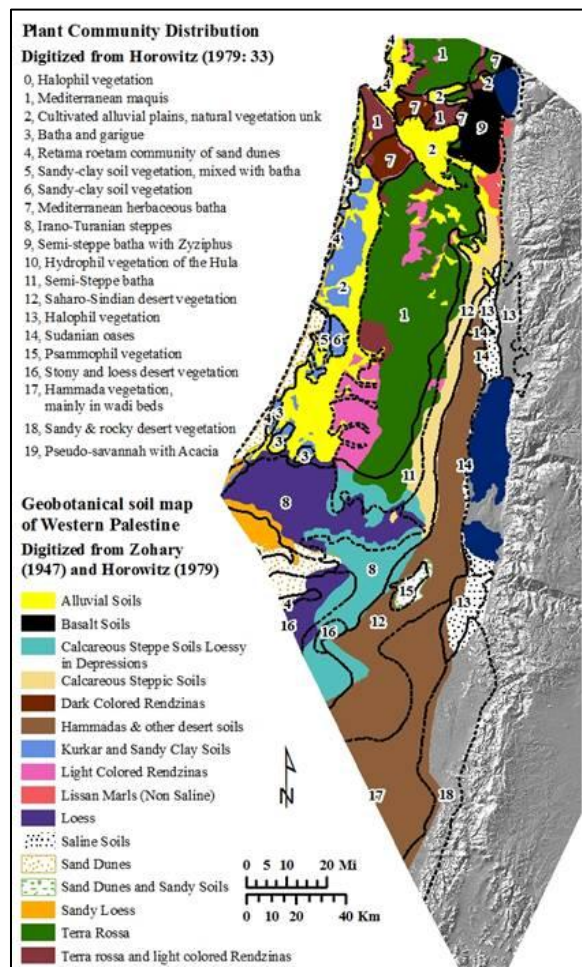


Figure 2.22. Heavily eroded slope in Wadi Arava (Soto-Berelev).

Areas that receive the largest amounts of rainfall and experience the least extreme temperatures have the most mature soils, which include a humiferous top layer (Terra Rosa and Rendzina). These are also the most fertile and support climax forest communities. As rainfall decreases, so does the quality of the soil. Loess and calcareous soils predominate in steppe areas whereas the drier areas mainly consist of saline and hammada soils. These originate from limestone, chalk, marl, chert, sandstone, magmatic, metamorphic rocks, and alluvium. Loess is found in some transitional areas between the wetter Mediterranean and Irano Turanian zones, such as the Northern Negev and Ammon regions (Danin 2001). The eastern boundary of the study area that marks the beginning of the Eastern Desert has lava and basalt pebbles and stones (Kasapligil 1956). Generally

speaking, sandy soils originate from older rocks, whereas Terra rossa soils develop on limestone.

Zohary in particular discussed how soils influence the different vegetation communities (1947a, 1947b). He distinguished six units that include calcareous soils, basalt soils, sandy and sandy-calcareous soils, loess, alluvial soils and saline soils. These can further be subdivided into soil types according to plant geographical region. They are summarized in Tables 2.2 and Table 2.3. To further illustrate the relationship between soils and vegetation, see Map 2.7, which shows the dominant soils of Israel and the Palestinian territories, as well as general vegetation according to Horowitz's vegetation map (1979).



Map 2.7. Soils and vegetation (digitized from Zohary 1947b and Horowitz 1979).

Table 2.2. Major soils of the Mediterranean region, summarized from Zohary (1947a, 1947b).

Soil units	Soil series within units	Varieties within soil series	Bedrock	Characteristics and distribution	Impact on vegetation
Calcareous soils in the Mediterranean region	Terra rossa soils	Transported to lowlands and valleys where it is altered by local conditions. Considered under the alluvial colluvial series.	Hard rocks, limestone and dolomites of the Upper Cretaceous (Cenomanian, Turonian, Santonian) and Eocene rocks	Considered to be the most fertile soil of the mountain regions. Include a thick hummiferous layer.	Areas densely covered by maquis and forests produce the most developed soil series throughout the region. In terms of vegetation, this series includes climax Mediterranean associations: <i>Quercus calliprinos</i> , and subclimax association <i>Q. calliprinos – Pistacia palaestina</i> . The destruction of these causes the removal of the humiferous layer. Batha and garigue replace the forest with the following associations: <i>Calycotometum villosae</i> , <i>Salvietum trilobae</i> , <i>Cistetum villosi</i> , <i>Poterietum spinosi (typicum)</i> , <i>Thymetum capitati (typicum)</i> , etc. After further degradation the soil becomes even more degraded and vegetation is replaced by associations of the <i>Varthemion iphionoidis</i> alliance. These soils are also found in the lower elevations of the hills that descend into the coastal plains and are represented by forests of <i>Ceratonia siliqua-P. Pistacia lentiscus</i> .
		Residual			
	Rendzina soils (Med. whitish grey soil)	Dark Rendzina	Soft rocks, highly calcareous marls, chalks & limestones of the Upper Cretaceous and Eocene formations. Found next to Terra rossa. Have a thick hummus layer but rarely found in this stage, due to the softness of the rock which makes this soil more accessible to cultivation than terra rossa.	Mainly occurs in NW Samaria and the SW Lower Galilee.	Climax vegetation is association of <i>Quercus ithaburensis – Styrax officinalis</i> .
		Light Rendzina		Most common in the northern and central part of the Mediterranean region west of the Rift Valley.	Climax vegetation has been preserved only in a few localities (Upper Galilee, Mt. Carmel, Samaria and Judean Mountains) – <i>Pinus halepensis – Hypericum serpyllifolium</i> association. In the western part of Upper Galilee the associations of <i>Quercus calliprinos – Pistacia palaestina</i> and <i>Ceratonia Siliqua – Pistacia Lentiscus</i> in various stages of degradation are found on this soil. Zohary speculates the possibility of a climax <i>Pinus halepensis</i> forest. When the soil is degraded the vegetation is replaced by <i>Sarcopoterium spinosum</i> .
		Rendzina derived from the Upper Eocene		SW Judean Mountains	Climax vegetation consists of <i>Q. calliprinos – P. palaestina</i> assoc. (higher elevations) and <i>Ceratonia siliqua – P. lentiscus</i> assoc. (lower elevations).
	Basalt soils	Basalt soils		Basalt from the Pliocene	Upper Jordan Valley, Eastern escarpment of Lower Galilee and north west Jordan, Golan plateau.

Table 2.2. (continued).

Soil units	Soil series within units	Varieties within soil series	Bedrock	Characteristics and distribution	Impact on vegetation
Alluvial soils	Alluvial soils		Includes soils transported from higher elevations by erosional processes.	Found in plains and valleys (Esdraelon Plain, Acre Plain), low terraces and in Upper, Middle, Lower Jordan Valley.	<p>The transported Terra Rossa falls into this category.</p> <p>On river banks and swamps riparian vegetation is found. Along the Jordan River the climax arboreal vegetation is represented by <i>Populion euphraticae</i>.</p> <p>The soils on oasis in the Lower and Middle Jordan Valley mainly come from adjacent mountains and differ from the surrounding desert and salt soils. Given the surrounding water availability that originates from springs and high temperatures of the Rift Valley, they support a climax tropical vegetation represented by the <i>Zizyphus spina-Christi</i> – <i>Balanites aegyptiaca</i> association.</p>
Sandy and Sandy-Calcareous soils	Coastal sand dunes		Eolian (consist of silica, hornblende, mica, feldspar)	Form a narrow strip along the coast	<p>Most dunes have poor vegetation cover and are continuously shifting.</p> <p>In flat areas, the dunes are split into two sections. The first includes the area affected by ocean spray. It mainly consists of the <i>Cakile maritima</i> – <i>Salsola Kali</i> association. The second is represented by <i>Ammophila arenaria</i> – <i>Cyperus conglomeratus</i> and <i>Artemisia monosperma</i> – <i>Cyperus mucronatus</i> association.</p>
	Kurkar soils		Calcareous sandstone hills	Parallel to the coastal sand dunes. These are older dunes that have been calcified.	<p>Climax veget is made up of various associations varying from North to South according to the precipitation gradient. Around Caesarea, the arboreal Mediterranean climax association <i>Ceratonia siliqua-Pistacia lentiscus</i> is found. Further south, climax vegetation is characterized by <i>Helianthemum elliptici</i></p> <p><i>Calycotometum villosae</i> and the <i>Poterium spinosum</i> – <i>Thymelaea hirsuta</i> assoc.</p>
	Red sand (sandy clay) or hamra		Derived from loam that is over or under the kurkar.	Occupies large areas of the coastal plains (Sharon and Pleshet coastal plains) and is considered the most productive soil of this area.	<p>Soil found throughout citrus groves of the coastal plains. Climax vegetation is a type of <i>Quercetum ithaburensis</i> (from the Yarkon River northwards). When the successional stage is batha, <i>Sarcopoterium spinosum</i> is found whereas <i>Calycotometum villosa</i> and other species are found under the garigue stage. Zohary noted that even further degradation has resulted in the area being occupied by the non-Mediterranean <i>Eragrostis bipinnata</i> – <i>Centaurea procurrens</i> association and its varieties.</p>

Table 2.3. Major soils of the Irano Turanian and Saharo Arabian regions, summarized from Zohary (1947a, 1947b).

Soil units	Soil series within units	Varieties within soil series	Bedrock	Characteristics and distribution	Impact on vegetation
Calcareous soils	Grey calcareous steppe soil		Soft chalk and limestone of Senonian and Eocenian formations	Present on the Irano Turanian regions of the Judean Desert and Negev.	Lacks a humiferous layer and is rich in calcium carbonate. Climax vegetation includes open and dwarf shrubs like <i>Artemisia herba-alba</i> , <i>Noaea mucronata</i> , <i>Salsola villosa</i> .
	Calcareous steppe soils, loessy in depressions			Present in the S & SE Judean desert & areas of the Negev.	The grey calcareous steppe soils become intermixed with loess in depressions and wadis. Usually used for cultivation.
	Lissan Marls	Lissan marl soils	Rich in gypsum.	Sediment deposits of the bottom of former Lake Lisan. Extends from Wadi Arava to the Sea of Galilee.	The greatest part of this soil is at present under cultivation (Beisan Valley) and its segetal vegetation is represented by a particular association of the <i>Prosopidion farcatae</i> . The climax vegetation consists of <i>Zizyphus Lotus</i> (in the North) and <i>Salsolium villosae</i> (in the South). Soils in the north are not as rich in salt content as those of the south, due to the increased precipitation of the north.
Hammadas	Gravelly desert soils (Hammada)	Haline-gypseous hammada	These are soils that have been impacted by the climatic conditions of their surroundings. They tend to be gravelly or stony.	Present along the Negev, Wadi Arava, southern and eastern Jordan.	Common in the Negev and Wadi Arava. Found on plains. Mostly consist of flint. Often devoid of vegetation. Sometimes populated by <i>Reaumurietum palaestinae</i> . Zohary mentions that these soils can be found intermixed with wadis or sandy soils. The effect is a mosaic of patterns and vegetation compositions (wadis and sandy soils can be densely covered by plants like <i>Haloxylon sp.</i> and <i>Anabasis articulata</i> – <i>Zilla spinosa</i> assoc.).
		Non-haline hammada			Common in Southern Jordan. Resembles haline-gypseous hammada in appearance but in contrast to the former, it is not salty. In Southern Edom this hammada is sparsely covered by vegetation (mainly <i>Anabasis articulata</i>). Further north vegetation grows denser and the <i>Anabasis</i> – <i>Hausknechtii</i> – <i>Poa sinaica</i> association becomes frequent on the plains that sit between the Irano Turanian and Saharo Arabian regions (Eastern Desert) covered by this type of hammada.
		Other hammada soils		On rocky desert and steppe hills.	Most typical plant is <i>Zygophyllum dumosi</i> .
				Common in eastern part of Judean Desert.	Characterized by <i>Suaedetum asphalticae</i> and <i>Chenoleetum arabicae</i> .

Table 2.3. (continued).

Soil units	Soil series within units	Varieties within soil series	Bedrock	Characteristics and distribution	Impact on vegetation
Sandy soils	Desert sand dunes and sand plains		In the Negev, eolian origin. In interior, Neogene and Nubian sandstone of the Lower Cretaceous and igneous rocks of Edom and Wadi Arava.	South of Gaza the coastal sand dunes expand into the Negev. There are also sand dune areas in the interior around Wadi Arava and southern Jordan.	The dunes of the Negev are characterized by <i>Ammophila</i> and <i>Artemisia</i> associations as well as by <i>Aristidetum scoparie</i> . The sand dunes of the interior are represented by several species. <i>Haloxylonetum persici</i> covers the slightly shifting dunes of Wadi Arava; <i>Haloxylonetum salicornici</i> is most characteristic of the sand areas of Kurnub, Turreibe and S. Wadi Arava. Other areas covered with sands derived from the Nubian Sandstone in the higher plains of Edom are inhabited by the <i>Anabasis articulata</i> – <i>Zilla spinosa</i> association.
Loess	Loess soils		Eolian origin (desert dust and sand). Texture consists of fine grained soil particles with clay and silt.	Most productive soil in steppe areas. Mainly found in the Irano-Turanian parts of the Negev (predominates around the Beersheba-Gaza region) and Edom and Moab regions in Jordan.	Found on plains and mountain valleys. Transported from southern and eastern desert areas by storms. Due to its porosity and mineral content, it can trap moisture. Considered the most fertile soil of steppes and deserts. Zohary subdivided it into two categories: <i>Archilleion Santolinae</i> . Fluvial loess in depressions in the S Negev [S of Asluj], characterized by <i>Haloxylonetum articulate</i> . <i>Loess sand (Sandy Loess)</i> . Found in the south as the loess transitions and blends into desert sands.
Saline soils	Automorphous salines		These saline soils are sodium chloride salines. Found on various types of soils like sands, alluvium, Lisan Marls in the Wadi Arava, Acre Plain, coastal plains, and Jordan Valley. However, they concentrate along the Lower Jordan Valley.	Lissan Marls north of the Dead Sea and Mount Sedom	Formed by the local environmental conditions. These include the saline hammadads. Scarcely covered by vegetation. One of the most common species are <i>Salsolium tetrandrae</i> .
	Hydromorphous salines	Flooded salines		Wadi Arava, Dead Sea shores and coastal plain.	These become flooded during the wet season. Have a very high salt content. Common species in these areas include <i>Suada monoica</i> , <i>Nitrarietum retusa</i> , <i>Arthrocnemum glaucum-Tamarix tetragyna</i> assoc.
		Groundwater salines		Lower Jordan Valley.	Marshes throughout the Lower Jordan Valley that have high salinity content due to the high ground water table (highly saline). Common association is <i>Atripliceto-Suaedion palaestinae</i> .

This chapter introduced the environmental context of the study area. Besides setting the scene, this is important given the objective of this study which is to map the distribution of plants using a series of environmental indicators. The climatic, topographic, and geomorphic characteristics were discussed. An overview of the botanists and specialists who have characterized vegetation in this region was also presented, followed by a detailed description of the main vegetation units.

Chapter 3

PALEOENVIRONMENTAL RECONSTRUCTION

Glacial (massive ice buildup) and interglacial (ice decay) episodes have ensued on a semi periodic basis throughout the late Quaternary (Bradley 1985), causing dramatic shifts in temperature and precipitation. The most recent glacial episode was at its peak during the Last Glacial Maximum around 20 thousand years ago, a time when lower temperatures and precipitation resulted in cooler and more arid conditions than present. The Bølling-Allerød interstadial (ca. 15-13 ka BP) brought warmer and wetter conditions, before cooling continued again during the Younger Dryas (ca. 12.7 – 11.5 cal ka BP), a period generally interpreted as having slightly colder and drier conditions, although probably not in the same magnitude as the LGM.

Ever since the end of the Pleistocene climatic shifts of such magnitude seem to have stopped. The Holocene has instead been impacted by minor events, whose duration, intensity and cyclical characteristics are in debate. Nevertheless, there is evidence that comes from multiple records that suggests that even minor climatic fluctuations have impacted vegetation distributions and human settlement patterns (e.g. Baruch 1986, 1990; Baruch and Bottema 1991, 1999; Horowitz 1971, 1979; Migowski et al. 2006).

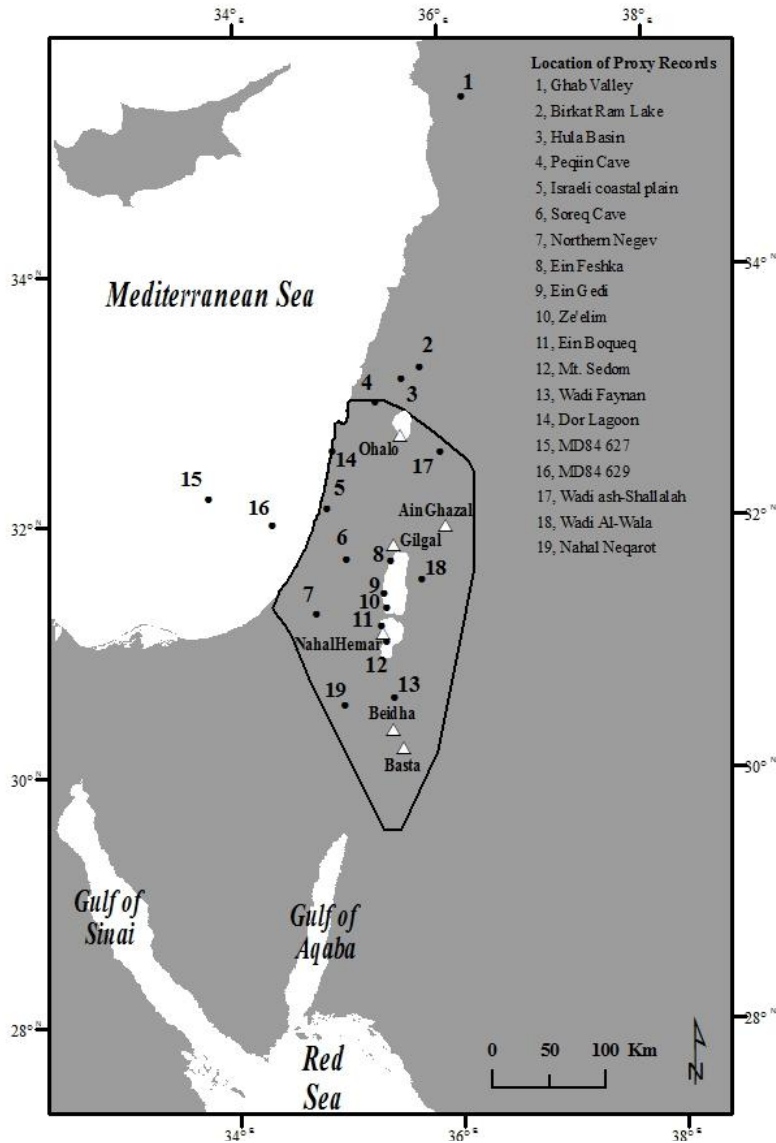
This chapter presents a review of the paleoenvironmental conditions of the study area. Regional proxies used as indicators of the dominant climatic and environmental conditions from the late Pleistocene until the late Holocene are discussed (e.g., pollen from several lakes, Dead Sea lake level fluctuations, cave speleothem records, sedimentary mineralogy). Lags or intervals marked by insufficient material for dating are also highlighted.

3.1 Proxy records, indicators of past environments

Some natural systems that may be inferred from glaciological (e.g., oxygen isotope analysis from ice cores), geological (e.g., marine organic and inorganic sediment deposits and terrestrial deposits like aeolian and glacial sediments), and biological sources (e.g., tree rings, pollen, plant macrofossils, insects) capture different climatic characteristics of the distant past. By providing a perspective on paleoclimates, they enable the reconstruction of paleoenvironments. However, paleoclimatic reconstruction is a science in itself, and there are many factors and challenges involved (Bradley 1985). For a start, climatic fluctuations occur on different time scales or frequencies, and can be caused by internal or external forces. For example, changes in the earth's orbital parameters have caused glacial and interglacial cycles during the late Quaternary, whereas volcanic eruptions have immediate climatic impacts that can last for centuries.

In addition, climatic indicators operate at different temporal and spatial scales, record climatic signals at different frequencies, and have different limits on the time range they can cover. For instance, tree rings are able to record climatic information on a yearly basis, but can only record a maximum of several thousand years. This makes them suitable for depicting high frequency or short term and abrupt climatic fluctuations like droughts. Ocean sediment cores on the other hand can provide low frequency continuous proxy records for millions of years, which makes them suitable for long term climatic trends (i.e., glacial episodes), but unsuitable for detecting abrupt climatic changes, since their temporal resolution is coarse. Furthermore, some records capture climatic signals at localized scales (e.g., cave speleothems, isotope analysis of mollusks) whereas others may provide more regional signatures (e.g., marine sediment cores).

In the Southern Levant and Near East, multiple proxy records have been used to reconstruct the paleoenvironmental history of the region (Map 3.1). In the following discussion, these are divided into the following categories: lake level changes, paleobotanical records, other proxy records (e.g., cave speleothems, isotope analysis, sedimentary analysis), and archaeobotanical evidence.



Map 3.1. Location of proxy records discussed in this study.

3.1.1 Dead Sea Lake Level Changes

The Dead Sea is a hypersaline lake that sits on a tectonic depression within the Rift Valley that is part of the Dead Sea Transform fault (Map 2.1). It is replenished by water that comes from the Jordan River, as well as groundwater and runoff from wadis and rivers on each side of the Rift Valley. Its catchment comprises an extensive area of 43,000 km² and its present surface level is 420 m bsl.

The Dead Sea was formerly known as Lake Lisan (name given to the lake when it covered a much greater area between ca. 70 to 14 ka BP). Records obtained from the Lisan formation (deposits of the former lake after it receded) indicate that the level of Lake Lisan went through multiple changes throughout its existence (Bartov et al. 2003; Haase-Schramm et al. 2004). Even before the existence of Lake Lisan, hypersaline lakes have occupied this depression (Stein 2001), whose levels have risen and fallen according to climatic fluctuations during the last 23 million years.

Changes in lake levels can help reconstruct paleoclimates at regional scales (Street and Grove 1979). During the late Pleistocene post glacial period, these changes were of great magnitude and seemed to occur abruptly. Evidence suggests that the lake rose and fell multiple times, reaching its greatest extent (at 180 m bsl, Map 4.5) around 17 cal ka BP, when it stretched from the Sea of Galilee or Lake Kinneret to about 30 km south of the present day southern extent of the Dead Sea (Niemi 1997). Shortly after, lake levels fell below 465 m bsl (some authors suggest 700 m bsl [Niemi 1997]) and then rose again, although it never reached its former extent (Stein et al. 2010). Following this ancient highstand of Lake Lisan, lower lake levels led to the formation of the much smaller Dead Sea (ca. 14 cal ka BP).

Lake level changes during the Holocene do not compare in magnitude to those experienced during the Pleistocene. Nevertheless, the Dead Sea has undergone several fluctuations due to the same factors that impacted lake level changes of former Lake Lisan. To a small extent, tectonic activity caused by the subsidence of the Dead Sea basin has resulted in a gradual drop in the level of the lake (Bartov et al. 2007). Operating simultaneously, variations in evaporation and precipitation throughout the Holocene have caused lake levels to oscillate. An understanding of this second factor has been used to build and enhance the paleoclimatic reconstruction of the region.

Lake level reconstructions and inferred paleoclimates can be derived from various sources. Historical records and the locations of archaeological sites have been used to determine the extent of the lake during different periods. Stein et al. (2010) built a Dead Sea lake level curve from the post glacial episode of the late Pleistocene until the beginning of the Holocene (17.4 – 10 cal ka BP), based on U-Th and radiocarbon dating from a series of cores located on the western shore of the Dead Sea. Frumkin (1997) summarized Dead Sea lake levels and estimated paleoclimates during the Holocene (classified into 10 stages), based on dated cave deposits in Mount Sedom, geomorphological analyses of terraces, sedimentologic studies of lake deposits, and the occupation history of various archeological sites. In addition, Migowski et al. (2006) analyzed three cores from the Northern Basin and obtained a continuous, fine scale record for the Holocene. They detected two major wet phases between 10-8.6 and 5.5-3.5 cal ka BP, and a series of abrupt arid events during 8.6, 8.2, 4.2, 3.5 cal ka BP. The findings from these authors are summarized in Table 3.1.

Table 3.1. Lake level changes from the late Pleistocene until the Late Holocene.

Source	Stage /Date	Lake changes / observations	Suggested Climate/cultural development
Bartov et al. 2003	17.4 to 16	Lake dropped from ca. 260 bmsl to 330 bmsl (Bartov et al. 2003)	Heinrich event 1 (H1) Warm
Stein et al. 2010	16 to 15	Level rise around 15 cal ka BC to 260 bmsl	
	14.6 to 13.2	Level dropped to below 465 bmsl	Warm – Natufian culture collapses towards the end this period.
	13 to 11	Lake rises above 400 bmsl	Cold and wet Coincides with Younger Dryas (12.7 to 11.5). Coincides with PPNA (12 – 10.7).
	11 to 10	Level drops. Salt unit is deposited	Dry. PPNB
Migowski et al. 2006	Ca. 10-8.2	Humid. Lake rose. But level was probably lower than -210 m contour between 12-8.8 cal ka BP, since this marks the PPN occupation of Jericho (Burleigh 1984, Bar-Yosef 1987).	Very wet
	8.1	Lowering of lake from ca. 412 to below 430 m bmsl. Possibly followed by a raise.	Dry
Neev & Emery 1995	7.5 to 5.5	Salt tongue deposit.	Very dry
Migowski et al. 2006	5.4 to 3.5	Wet, increased rainfall. However, two droughts that lasted a few centuries (ca. 300 years) were recorded.	Wet with sudden droughts (ca. 5.3-5.1 and 4.3-4.1)
	3.5 to 3.2	Lake drops to ca. 417m bmsl.	Dry
	From 3.2 to present	Lake has fluctuated around 370 to 400 m bmsl.	Fluctuations

Fluctuations in Dead Sea lake levels, some more dramatic than others, ranged between several periods of desiccation that resulted in the exposure of the southern basin to a rise in the lake up to the -280 m bsl elevation contour, which was the highest level recorded in the last 7,000 years (Frumkin 1997). Stein et al. (2010) interpreted a cold, wet Younger Dryas with increased freshwater runoff, based on their interpretation of a salt unit dated to ca. 10.8-10.2 cal ka BP, which was deposited after the Younger Dryas. The authors believe that the dramatic drop to 465 m bsl before 11 cal ka BP would have

resulted in extremely high salinity that was diminished during the wetter Younger Dryas and salt precipitation after 11 cal ka BP. During the Early Holocene, the region experienced a moist climate until about 8 cal ka BP, after which conditions became gradually more arid. This drying, coupled with tectonic forces operating on a minor scale, has caused the lake to drop gradually from the Mid Holocene until the present, although this trend was interrupted four about two millennia at around 5.5 cal ka BP (Migowski et al. 2006), with several arid intermissions (i.e., 4.2 cal ka BP).

3.1.2 Paleobotanical records

Some of the most relevant proxy records in this study come from pollen analysis. Pollen obtained from lake sediments is particularly useful, since it is usually found in continuous sequences and records vegetation trends over time. However, it is important to bear in mind a few considerations that affect the ensuing paleoenvironmental interpretations, such as prevailing wind direction (in this case westerly), limited temporal and spatial resolutions, etc. (Table 3.2).

Pollen sequences document vegetation changes that may result from environmental conditions or anthropogenic modification. After the Mid Holocene, pollen spectra tend to reflect a combination of anthropogenic and climatic influences, whereas pollen evidence from the Early Holocene is less likely to have been affected by human behavior, and more likely to indicate climatically induced change.

Table 3.2. Some caveats when reconstructing paeoenvironments from palynological analysis (summarized from Bradley 1985).

Consideration	Example
Not all pollen grains are equally preserved. Because of this, not all plants will be represented in the pollen record.	Pollen of <i>Populus</i> sp. may begin to disintegrate before other species.
The quantity of pollen produced by different plants is different.	Some plants are self fertilizing, so they produce less pollen than other species that depend on insects or other animals as a dispersal agent. The pollen produced in largest quantities is dispersed by wind (e.g., <i>Quercus</i> sp., <i>Pinus</i> sp.)
Pollen producing plants have different dispersal rates. Impacting on this is the size of the pollen grain (which also varies), and the synoptic conditions at the time it was produced.	Pollen produced by arboreal species is assumed to travel farther than pollen produced by shrubs and herbs because it is probably transported by stronger winds. At the same time, wind transported pollen is impacted by wind speed and precipitation.
The spatial extent is limited. Plants with lower dispersal rates will probably remain within close proximity of the source. Having said this, however, large lakes can allow greater vegetation reconstructions, since they capture run off from the whole basin.	The spatial extent is generally limited to the nearby surroundings. A pollen sample with high frequency of <i>graminea</i> may suggest that a grassland or open forest existed in the vicinity.
The temporal extent is limited.	Parts of the sequence need to be dated, in order to establish a chronology. When this is not possible, gaps will be found. The exact timing of climatic events can only be approximated and abrupt climatic fluctuations can be missed. In addition, dating errors can produce conflicting interpretations.

In the Southern Levant and Near East, pollen from various sources (including lakes) has been used to assemble vegetation chronologies. Several of these provide high resolution insight as to the prevailing climatic conditions and ensuing vegetation distributions (e.g., Ghab Valley in Syria, Hula Basin in northern Israel, Birkat Ram Crater lake in northern Israel). These are summarized in Table 3.3.

Table 3.3. Palynological records of the region.

Name, source and resolution	Description
<p>Hula Basin, Northern Israel, located within the Rift Valley</p> <p>Author: Horowitz 1971, 1979, Baruch and Bottema, 1991, 1999, Tsukada in van Zeist and Bottema, 1981, Van Zeist et al. 2009</p> <p>Temporal resolution: From Younger Dryas to Present</p>	<p>Description is summarized from van Zeist et al. (2009), since their interpretation addressed issues in the previously established chronologies. Only the pollen assemblage zones (PAZ) that relate to the time frame of this study are included.</p> <p>PAZ 1. Cultural period PPNA.11.3 – 10 cal ka BP – low arboreal pollen (mostly <i>Q. ithaburensis</i>) and slightly high herb pollen (mainly <i>Artemisia</i>, Poaceae (grasses), Chenopodiaceae). Ceralia pollen is also detected (wild barley, wild wheat and wild oats). Riparian vegetation is also represented, implying that the rivers and streams were flowing during this time (despite its arid character).</p> <p>PAZ 2. Cultural period PPNB. 10 – 8.42 cal ka BP – Rise in AP (mostly <i>Q. ithaburensis</i> and some <i>Q. calliprinos</i> and <i>Olea europaea</i>, <i>Pistacia</i>), drop in herb pollen, chenopodiaceae and <i>Artemisia</i>. Riparian trees continue to be well represented.</p> <p>PAZ 3. Cultural period PN. 8.4 – 7.9 cal ka BP – Drop in AP, mostly <i>Q. ithaburensis</i> (this trend actually began towards the end of PAZ 2) and rise in herb and ceralia pollen (which includes both wild and domestic cereals and grass). Riparian pollen also drops.</p> <p>PAZ 4. Cultural period mid PN to Chalcolithic. 7.9 – 5.9 cal ka BP – “AP/NAP ratios show moderate fluctuations, suggesting a relative stability of climate” (p. 56). Slight rise of <i>Q. ithaburensis</i>. Author interprets the <i>Q. ithaburensis</i>-<i>P. atlantica</i> to be the major ingredients of this more open woodland (compared to that seen during PAZ 2, which the authors believe to have been a more dense forest). Also some indicators of agriculture are detected (<i>Mercurialis annua</i>, weed that grows after fallow). Towards the end of this period, there is a slight increase in <i>Q. calliprinos</i>.</p> <p>Authors make the observation of abundant grasses naturally occurring since PAZ 3, which would have been suitable for grazing.</p> <p>PAZ 5. Cultural period mid Chalcolithic to EB. 5.9 – 4.1 cal ka BP – Drop in <i>Q. ithaburensis</i>, and rise in <i>Olea europaea</i> (the pollen curve of olive greatly increases during this period). The three are now equally represented in the record. The rise of olive is seen as the beginning of olive cultivation. There is also a slight increase in <i>Artemisia</i> pollen. The <i>Q. calliprinos</i> curve remains steady during half this period and then drops, recovering towards the end.</p> <p>PAZ 6. Cultural period MB to IA. 4.1 – 2.5 cal ka BP – Drop in the olive curve, and notable rise in deciduous and evergreen oak (the last of which is unprecedented in the record). Slight rise in <i>Pistacia</i>, <i>Pinus</i> and <i>Vitis</i>. <i>Mercurialis anna</i> pollen remains low.</p> <p>PAZ 7. Cultural period Persian to Hellenistic. 2.5 – 2.1 cal ka BP – Drop in <i>Q. ithaburensis</i> (nearly disappears from the record) and <i>Q. calliprinos</i> (not as dramatic as the evergreen oak). These drops are matched by an increase in <i>Olea europea</i>.</p> <p>Other observations: They also make the observation that pine occurs naturally within 20 km of the site in the Upper Galilee, so <i>Pinus halepensis</i> pollen present in the core suggests the existence of this tree within the surroundings of the Hula Valley. Whenever the values are missing, it indicates that there were no pines nearby. When values increase, so does the area occupied by these trees. Regarding pistacia (low pollen producer), it cannot be distinguished at the species level (e.g., <i>P. atlantica</i>, <i>P. terebinthus</i>, <i>P. palaestina</i>, <i>P. lentiscus</i>). If <i>Q. ithaburensis</i> is found with Pistacia, it probably represents <i>P. atlantica</i>. If <i>Q. calliprinos</i>, it probably refers to <i>P. palaestina</i>.</p> <p>They also find increasing levels of <i>Sarcopoterium</i> in the most recent deposits which suggest an increase in the degradation of maquis and forests by humans and/or animals.</p>

Table 3.3. (continued).

Name, source and resolution	Description
Birkat Ram Crater lake, northern Golan Heights, 33°15'N, 35°40'E, 940m asl Author: Schwab et al. 2004 Temporal resolution: Last 6.5 ka.	<p>Detected anthropogenic impact in the landscape during four periods: Chalcolithic to Early Bronze Age, Hellenistic to Byzantine, Crusader, Modern (the first two fall within this study's time frame). During the first period, they found high values for <i>Olea europaea</i> and low <i>Q. ithaburensis</i> values.</p> <p>From the Middle Bronze Age to the Iron Age, pollen from deciduous oak (<i>Q. ithaburensis</i>) increased and herb and olive pollen dropped.</p> <p>At around 2500 cal ka BP, the curve for oak abruptly declines to extremely low values (from 70 to 5%). Meanwhile, olive pollen is on the rise.</p> <p>These findings are consistent with the Hula pollen record (van Zeist et al. 2009).</p>
Sea of Galilee or Lake Kinneret Author: Baruch 1986, 1990 Temporal resolution: Second half of the Holocene	<p>Shows that during the Early Bronze Age and throughout this cultural time period, oak forests declined while olive orchards increased. This trend stopped temporarily and was in fact, reversed, during the EBIV urban collapse (Baruch, 1990). <i>Sarcopoterium</i> and <i>Plantago</i> pollen is first documented in the spectra during the Late Bronze and Iron Ages, indicating human disturbance.</p> <p>During the Iron Age, olive frequencies take off and peak at the Hellenistic period. Then they begin their decline, most dramatic during the Roman/Byzantine period. At the time of the olive peak, oak is almost invisible. After the peak, values of <i>Plantago</i> and <i>Sarcopoterium</i> increase.</p>
Dead Sea Author: Neumann et al. 2010 Temporal resolution: Late Bronze Age to present	<p>Cover six cores across the latitudinal extent of the lake.</p> <p>The Late Bronze Age is marked by low arboreal pollen (e.g., pine, oak), low pollen from cultivated plants (e.g., olive), high herb pollen. Lake also drops to -417 m bsl leaving the southern basin exposed, which suggests arid conditions. Cores further south show increased chenopodiacea values, also suggesting increasing aridity. Possibly a period of prolonged drought.</p>
Dead Sea Author: Heim et al., 1997 Temporal resolution: Late Holocene	<p>Shows how after the collapse of the Byzantine Empire, orchards are abandoned (olive) and pine (<i>Pinus</i>) and evergreen oak (<i>Q. ilex</i>) regenerate. There is also an expansion of more arid steppe vegetation.</p>
Ein Gedi, Dead Sea Author: Baruch, 1990 Temporal resolution: First 9,000 years of the Holocene.	<p>PrePottery Neolithic is dominated by deciduous oak (<i>Q. boissierii</i>) and modest amounts of pistachio. This continues until the Chalcolithic and Bronze Age. High frequencies of <i>Artemisia</i> are present throughout the PPN and Pottery Neolithic. Fall et al. (2002: 465) suggest it could be an early Holocene remnant of Pleistocene steppe vegetation or an outcome of grazing activities following the beginning of pastoralism.</p>
Ghab Valley, NW Syria, 35°39'N, 36°15'E, 240m asl Original authors: Niklewski and Van Zeist 1970, Van Zeist and Woldring 1980, van Zeist and Bottema 1982 Other authors: Yasuda et al. 2000 Temporal resolution: High Resolution Last 20 ka yr	<p>There were issues with the dating in the original interpretations.</p> <p>Captures the transition from steppe to forest during the final stages of the last glacial episode.</p> <p>At ca. 13 cal ka BP (Younger Dryas), pollen from grasses appears suggesting incipient agriculture. During this period (ca. 13-11.5), chenopodiacea values also increase.</p> <p>May depict earliest anthropogenic signature of forest clearing in the Levant (ca. 10 cal ka BP). A drop in deciduous oak forest is followed by increase in evergreen oak and pine (secondary forest?).</p> <p>From 10-8.4 cal ka BP, forests are replaced by cultivated orchards. At around 7.4 cal ka BP, a reversal is seen (drop in orchards and rise in arboreal pollen indicating forest regeneration). At around 5.1 cal ka BP, arboreal pollen drops and is replaced by high olive values.</p>

Table 3.3. (continued).

Name, source and resolution	Description
<p>Dead Sea</p> <p>Author: Neumann et al. 2007</p> <p>Temporal resolution: Ze'elim - Pottery Neolithic to Middle Ages</p> <p>Ein Feshka – Late Bronze Age to Middle Ages</p>	<p>Derived from two erosion gullies in the western shore: Ze'elim, which is located at the desert margin and Ein Feshka, located closer to the more moist Judean Mountains.</p> <p>Ze'elim only records sequences dated from the late Pottery Neolithic to the Middle Bronze Age (the middle and late Chalcolithic and Early Bronze Age are missing). High chenopodiaceae and low arboreal values indicate arid conditions towards the transition between the PN and the Chalcolithic (6500 cal ka BP). The Middle Bronze Age sees an improvement of climate conditions (decrease in chenopods, increase in olive orchards. Oak values are low, probably because of anthropogenic factors. See author's references for towns in the Judean mountains that are flourishing during this time. Later on during this period, oak, pine, and pistacia increases while chenopod values decrease, suggesting a return to more humid conditions. Towards the end of the MBA (period goes from ca. 4030 – 3630 cal ka BP), oaks and olives drop again, suggesting arid conditions. The level of the lake also drops at this time.</p> <p>Ein Feshka captures the LBA, which shows low arboreal pollen values. Pollen from cultivated vegetation is also low whereas herb values are the highest recorded. This suggests arid conditions, which seems to continue throughout the Iron Age.</p>
<p>Wadi Faynan catchment area, S. Jordan</p> <p>Author: Hunt et al. 2004</p> <p>Temporal resolution: Holocene, low Resolution</p>	<p>These pollen sequences were derived from fluvial sediments.</p> <p>Analyzed small pollen assemblages, mollusks and plant macrofossils from river sediments. Found evidence of a steppe like environment along with riparian vegetation occurring in this area that is now extremely arid during the Early Holocene. The type of steppe believed to have thrived here is now found in the rift margin at 800m. The steppe was believed to be near the margin of a Mediterranean forest that included oak, pine, juniper, cypress, olive, elm, hop-hornbeam during the early Holocene. Rainfall is believed to have started to decline after 8.1. This pattern was interrupted in 7.4 ka, however trees did not regenerate maybe due to grazing pressure. Trees were completely absent by the Chalcolithic. Evidence of perennial rivers is found until about 6 cal ka BP.</p>
<p>Dor Lagoon, Carmel coastal plain</p> <p>Author: Kadosh et al. 2004</p> <p>Temporal resolution: Early Holocene</p>	<p>Increased precipitation detected between 10.3-9.5 cal ka BP allowed formation of marsh. Most AP belongs to <i>Quercus calliprinos</i> and some <i>Q. ithaburensis</i>, so this coastal area was probably forested.</p> <p>Between 9.4-8.5 the marsh dried. Non AP increases (<i>Chenopodiaceae/Amaranthaceae</i>), suggesting increased aridity.</p>
<p>Dead Sea</p> <p>Author: Rambeau 2010</p> <p>Temporal resolution: Holocene after 8 cal ka BP</p>	<p>Peat deposit close to the Dead Sea (northeast).</p> <p>The arboreal pollen curve has fluctuated throughout the sequence, however an increase in arboreal and shrub pollen is detected during the last five thousand years. In the most recent layers, the shrub <i>Atriplex halimus</i> appears frequently.</p> <p>The arboreal pollen includes trees from Saharo Arabian and Mediterranean plant geographical regions (<i>Acacia</i> and <i>Arbutus andrachne</i>). The author mentions the presence of <i>Acacia</i> throughout the whole sequence, however <i>Arbutus</i> seems to fluctuate (i.e., 2.5 – 2 cal ka BP). Unfortunately, the author doesn't provide any more information.</p>
<p>Eastern Mediterranean region</p> <p>Author: Rossignol-Strick 1999</p> <p>Temporal resolution: Ca. 10-6.8 cal ka BP</p>	<p>Interpretation derived from 18 marine pollen cores from early Holocene sapropel in the eastern Mediterranean Sea and linked to terrestrial pollen records from the Ghab Valley.</p> <p>The early Holocene was the wettest/warmest period High pistacia values detected at the beginning of the Holocene. Deciduous oak values also reach their highest peak ca. 8.8 cal ka BP. According to this, she estimates the mean annual rainfall between 300 – 1200 m asl to be in the range of 800 – 1200 mm. The area below the forest belt is populated by a savanna dominated by Pistacia trees with estimated average annual temperature of 15°C and winter temperatures higher than 5°C.</p>

Most palaeovegetation reconstructions have relied on the sequences from the Ghab and Hula cores (e.g. Baruch and Bottema 1999; Niklewski and Van Zeist 1970; Van Zeist and Bottema 1991; Van Zeist and Woldring 1980). According to early interpretations based on radiocarbon dating only (for the Hula Basin: Horowitz 1971, 1979; Tsukada in van Zeist and Bottema 1981, for the Ghab Valley: Niklewski and Van Zeist 1970), the Pleistocene-Holocene transition displayed localized climatic and vegetation characteristics for northern Israel and northwest Syria. The Younger Dryas period caused arid conditions in northern Israel and increased arboreal pollen in southwest Syria.

Rosignol-Strick (1995) contested this when she analyzed pollen from marine cores from the Mediterranean and Arabian Sea and found that the impact of the Younger Dryas was regional. An overall trend of increased *Chenopodiaceae* pollen was detected, which suggested arid conditions. In addition, Rosignol-Strick identified a phase of high *Pistacia* values between 10.2-6.7 cal ka BP, with a suggested mean annual precipitation between 300 and 500 mm/yr. Furthermore, she identified both these phases in the Hula and Ghab cores, thus providing an alternative chronostatigraphy (Robinson et al. 2006). According to her and other authors (Meadows 2005), the discrepancies are the result of chronologies being derived exclusively from radiocarbon dates which provided overestimated sample ages.

The same author analyzed a series of pollen records from the early Holocene throughout the Eastern Mediterranean and compared these to high resolution terrestrial pollen records from the Ghab and Hula basins (Rosignol-Strick 1999). She found that during the early Holocene, *Chenopodiaceae* pollen values were always higher in the

marine pollen cores, suggesting a large representation of this family along the coast. However, during the Younger Dryas, Chenopodiaceae values are greater in the terrestrial records. The view that the Early Holocene represents the wettest period is confirmed by corresponding high peaks in pistacia and deciduous oak (ca. 8.8 cal ka BP) in marine pollen cores throughout the Eastern Mediterranean Sea, and in the Hula and Ghab terrestrial pollen records (Rossignol-Strick 1995, 1999).

The Ghab Valley and Lake Hula pollen cores show similar stratigraphies and vegetation trends that relate to those observed from marine pollen cores (Rossignol-Strick 1995, 1999). These form a picture of a treeless open landscape suggested by high Chenopodiaceae and *Artemisia* values until around 17 cal ka BP. During the next 3000 years a reversal occurred. Arboreal pollen started to rise and replace Chenopodiaceae and *Artemisia*, a trend that accelerated after ca. 14.5 cal ka BP.

Van Zeist et al. (2009) further clarified the paleoenvironmental developments derived from the Hula by analyzing a different core from the basin and comparing it to the Ghab core through biostratigraphic correlation (instead of using the ¹⁴C chronology that was earlier proposed). Their chronology encompasses the duration of this study period, roughly between the Natufian and Persian cultural periods. Within these, they found seven pollen assemblage zones (PAZ), which are described below.

During the first pollen assemblage zone (PAZ 1; ca. 11.3 – 10 cal ka BP), the surrounding vegetation was interpreted to consist of an open forest of deciduous oak and *Pistacia atlantica* (the latter underrepresented in the pollen record, and found in charcoal remains from the nearby archaeological site Ohalo II [Nadel et al. 2004]). The understory likely consisted of grasses. Some minor *Artemisia* and chenopodiaceae pollen was

detected (shrubs), which the authors believe to have originated from nearby areas.

Interestingly, despite the suggested arid conditions of the Younger Dryas, pollen from riparian vegetation was well represented within this zone, implying that rivers and streams were flowing.

PAZ 2 (ca. 10 – 8.42 cal ka BP) shows an expansion of the *Quercus ithaburensis* – *P. atlantica* forest. The pollen values for *Quercus calliprinos* and *Olea europaea* also increased. During PAZ 3 (ca. 8.4 – 7.9 cal ka BP), a drop in arboreal and riparian pollen and rises in herb and cereal pollen are interpreted to indicate a dry episode. PAZ 4 (ca. 7.9 – 5.9 cal ka BP) appears to have been a stable period, since the arboreal and non arboreal pollen ratios remained fairly constant. Nevertheless, climate appears to have somewhat ameliorated, since there is a slight rise in *Quercus ithaburensis* and *Quercus calliprinos*. The authors also detect signs of agricultural activity in the pollen record, through the appearance of weeds that grow after fields are fallowed (i.e., *Mercurialis annua*).

The next phase (PAZ 5, 5.9 – 4.1 cal ka BP) shows a drop in *Quercus ithaburensis* and a rise in *Quercus calliprinos*. Perhaps the most significant change observed during this phase is a dramatic increase in *Olea europaea*, providing an obvious sign of orchard cultivation. All of these fluctuations in the pollen record indicate increasing human pressure from grazing and agricultural activities, the last of which is mainly in the form of orchard cultivation, given the decline in *Mercurialis annua* pollen (a commonly occurring weed in cultivated and fallow fields).

PAZ 6 (ca. 4.1 – 2.5 cal ka BP) shows a drop in the olive curve and rise in pine, pistacio and evergreen oak, which the authors interpret as signs of succession after the

abandonment of olive orchards. The next zone (PAZ 7; ca. 2.5 – 2.1 cal ka BP) shows a significant decline in *Quercus ithaburensis* and a moderate drop in *Quercus calliprinos*, with an accompanying increase in *Olea europaea*, suggesting the renewed enterprise of orchard cultivation.

Based on a pollen sequence from the Birkat Ram Crater Lake in the northern Golan Heights, Schwab et al. (2004) reached a similar interpretation from the Mid Holocene to the present. They also detected significant anthropogenic impact from the Chalcolithic to the Early Bronze Age (high olive and low *Quercus ithaburensis* arboreal pollen [AP], corresponding to PAZ 5 of Hula), and from the Hellenistic to the Byzantine cultural period (an abrupt drop in oak and rise of olive, corresponding to PAZ 7 of the Hula record). On the other hand, from the Middle Bronze Age to the Iron Age, this trend was reversed (PAZ 6 of Hula). Over this interval, the olive pollen curve drops, while deciduous oak rises.

In another pollen core that comes from the Sea of Galilee (Baruch 1986, 1990) and covers the second half of the Holocene, the author found evidence of olive expansion and oak reduction during the Early Bronze Age. He also detected a deterioration of climatic conditions towards the end of the Early Bronze Age, and a reversal of this trend in the subsequent Middle Bronze Age. These trends were not detected in the Hula or Birkat Ram Crater lake pollen cores. Baruch also detected renewed olive expansion that began during the Iron Age and peaked during the Hellenistic period.

Unfortunately, the records just discussed are geographically biased toward areas that receive the largest amounts of rainfall. The resulting reconstruction is therefore reflective of the Mediterranean region, whereas the Irano Turanian and Saharo Arabian

regions are seriously underrepresented. Although the time frame does not extend as far back as some of the records just discussed, there are a few palynological sequences obtained from the more arid parts of the study area which help overcome this bias. These can be grouped into two categories: records extracted from the Dead Sea (the catchment of the lake expands across multiple plant geographical regions) and records derived from fluvial sediments in South Jordan.

The Dead Sea records have been summarized by Neumann et al. (2007, 2010), who also compared vegetation trends to lake level changes (the location of these is shown in Map 3.1). Two records were obtained from erosion gullies (Ze'elim, located at the desert margin and Ein Feshka, located close to the Judean Mountains) on the western shore of the Dead Sea (Neumann et al. 2007). Although these records come from the Dead Sea, they mainly reflect the conditions of the western portion of the Rift Valley (Judean mountains, Judean Desert, and the Negev), since the winds are predominantly westerlies. To a lesser extent, pollen is also collected from the north via the Jordan River, and from the wadis and rivers that drain into the Dead Sea from the east. Wind-blown pollen can also make its way into the Dead Sea. Because the local arid vegetation produces low amounts of arboreal pollen, it can be underrepresented in the record, as opposed to more distant mesic vegetation. Consequently, the record closer to the Judean mountains (Ein Feshka) mainly reflects changes in Mediterranean vegetation distribution, whereas the Ze'elim record, which is located in the desert fringe, reflects more arid vegetation.

The Ze'elim pollen stratigraphy extends from the Pottery Neolithic (7.2 – 6.5 cal ka BP) until the Middle Bronze Age (4 – 3.5 cal ka BP). However, the Middle and Late

Chalcolithic periods are missing. They detected high Chenopodiaceae and low AP values towards the end of the Pottery Neolithic, thus suggesting arid conditions. On the other hand, the Middle Bronze Age shows an improvement in environmental conditions, with a decrease in Chenopodiaceae and an increase in olive. The authors interpret the latter trends to result from the expansion of olive orchards in the Judean Mountains. Pollen from the date palm (which grows naturally in the nearby oases) and *Tamarix* (a riparian taxon) are also detected. Later in this period, oak, pine, and pistacio increase while Chenopodiaceae values drop, suggesting even more humid conditions. Towards the end of the Middle Bronze Age and beginning of the Late Bronze Age, oaks and olive decline at the same time as the level of the Dead Sea experiences a drop (Migowski et al. 2006), suggesting a return to arid conditions.

The chronology from the Ze'elim pollen sequence continues in the Ein Feshka one, which also shows low AP values for the Late Bronze Age. Pollen from cultivated vegetation is also low, whereas herb values reach the highest recorded values in the sequence. This evidence also suggests arid conditions during the Late Bronze Age, which seem to extend into the Iron Age.

Paleoenvironmental reconstructions were further expanded through palynological analyses of six cores (from Ein Gedi [2], Ein Feshka, Ze'elim, Ein Boqueq and Mount Sedom) and two erosional outcrops across the latitudinal extent of the Dead Sea (Neumann et al. 2010). All of these are located on the western shore, so they mainly reflect conditions from the moister Judean and Samarian mountains in the north to the drier Negev and Judean deserts in the south. Only four cores were successfully dated, so the chronologies of the remaining two were inferred by matching pollen characteristics

reflected in different pollen zones. These reflect vegetation trends from the late Bronze Age until the present. During the Bronze Age, they found low AP (both from cultivated species and expected Mediterranean species) and high values for herb species. Concurrently, the southern Dead Sea Basin became exposed as the level of the lake dropped to -417 m bsl. The Iron Age provides more contradictory results, with some cores suggesting an increase in humidity and agricultural activity towards the end of this period, whereas others suggest arid conditions during part of the Iron Age.

Unfortunately, the records for Southern Jordan are few (Hunt et al. 2004; Rambeau 2010), although some studies that appear promising will soon be published (Rambeau et al. in press; Smith et al. in press). Hunt et al. (2004) analyzed pollen assemblages, mollusks and plant macrofossils derived from fluvial sediments in the Wadi Faynan drainage (Map 3.1). They found evidence that suggests significantly more rainfall during the Early Holocene. The surrounding area, which now ranges from desert to steppe, is believed to have ranged from steppe to open forests. The type of steppe believed to have thrived here is now found along the rift margin at 800m asl. The steppe was believed to be near the margin of a Mediterranean open forest that included oak, pine, juniper, cypress, olive, elm, and hop-hornbeam during the early Holocene. The authors found that after 8 ka BP, rainfall started to decline. This pattern was interrupted at 7.4 ka, but trees did not regenerate, and were completely absent by the Chalcolithic period (although the authors report other evidence that suggests streams were perennial before 6 cal ka BP).

An analysis of peat deposits close to the northeastern Dead Sea shore covers the last eight thousand years (Rambeau 2010). Unfortunately, the resolution is poor and the

author's findings are generalized. Throughout the sequence, the arboreal pollen curve fluctuates, although a steady increase is seen during the last five thousand years. The arboreal pollen includes tree taxa from the Saharo Arabian and Mediterranean plant geographical regions (*Acacia sp.* and *Arbutus andrachne*). The author mentions the presence of *Acacia* throughout the whole sequence, however *Arbutus* seems to fluctuate (i.e., 2.5 – 2 cal ka BP).

3.1.3 Other proxy records

Several other proxy records derived from palaeosols, fluvial sediments, stable isotope analysis, speleothems and lacustrine sediments also contribute to the paleoenvironmental reconstruction of the region, by indicating climatic as well as vegetation trends through time (Table 3.4). These records mostly come from the coastal plains, Judean Mountains, Rift Valley and the Negev, while records from the Jordanian Plateau are sparse (although see Cordova 2007).

In the coastal plains, Gvirtzman and Wieder (2001) analyzed palaeosol and sand dune sequences that cover the last 53 thousand years. They detected a total of 13 climatic events, the bulk of which occurred during the Holocene (these are summarized in Table 3.4). Relatively wet conditions before 12.5 cal ka BP and from 10 to 7.5 cal ka BP were detected. The record also shows a series of minor climatic events that suggest arid conditions during the Mid and Late Holocene.

In the mountainous region west of the Rift Valley, several studies have analyzed $\delta^{18}\text{O}$ variations in speleothems (e.g., Bar-Mathews et al. 1997, 2003; McGarry et al. 2004), which record changes in temperature and precipitation and allow estimates of these rates to be determined. Goodfriend also reconstructed paleorainfall values

(Holocene) for the Negev region from the fossil record of ^{18}O found in the shells of land snails (1991) and correlated these to ^{18}O rainfall values. These indicate the source and trajectory of rain bearing systems. He found that values for the Early Holocene are similar to those for the present, thus suggesting a similarity in terms of the prevailing atmospheric circulation pattern of the region. However, between 7.4 and 6.8 cal ka BP, ^{18}O values were depleted by 2%, which the author interprets to result from shifts in the trajectory or frequency of storms that come from northeast Africa and are associated with large amounts of rainfall, perhaps resulting in increased flooding during this time.

In the Northern Negev region, Goodfriend also investigated how the distribution of C_4 plants (which predominate in arid environments) has changed since the Mid Holocene, by analyzing the organic matter ($^{13}\text{C}/^{12}\text{C}$) found in the shells of land snails. He then used this information to derive paleorainfall values across the Negev. According to field work conducted by this author to determine the distribution of C^3 and C^4 plants in the Northern Negev, the 260 mm isohyet represents a transition zone between C^3 and C^4 plants. His findings indicate that between 7.4 and 3.2 cal ka BP, the 260 mm isohyet was found where the present 150 mm isohyet stands, which is 20 km further to the south of its modern location. In other words, the findings suggest that this area used to receive significantly more rainfall than it does at present. Furthermore, between ca. 11-7.8 cal ka BP, C_3 plants are believed to have occupied considerable parts of the Negev, suggesting that Early Holocene mean annual rainfall north of the present day 100 isohyets was over 290 mm (Goodfriend 1990, 1991). Several other studies done in the Negev and the Sinai further substantiate this view (see next section).

Table 3.4. Additional proxy records.

Proxy record	Location	Reference Method	Time period	Method output	Authors interpretations		
					Approx. date ka BP	Overall climate	Approx. time of peak cal ka BP
Palaeosol , Gvirtzman and Wieder 2001	Palaeosol and sand dune sequences on the central coastal plain of Israel	Luminiscence and radiocarbon dating. Classified sequences of palaeosols, aeolianites, dunes by examining soil characteristics.	Last 53 k ya	Soils were classified from wet to dry.	12.5 – 11.5	Dry	12±0.5
					11.5 – 10.5	Wet	11±0.5
					10.5 – 10	Dry	10.25±0.5
					10 – 7.5	Wet	8.75±0.5
					7.5 – 7	Dry	7.25±0.5
					7 – 6.5	Wet	6.75±0.5
					6.5 – 5	Dry	5.75±0.5
					5 – 4.6	Wet	4.8
					4.6 – 4	Dry	4.3
					4 – 1.3	Wet	2.7
1.3 – 0	Dry	?					
Fluvial , McLaren et al. 2004	Fluvial sediments in Wadi Faynan, Wadi Dana, S. Jordan.	¹⁴ C and OSL dating of stratigraphy (fluvial terraces, alluvial fans, Aeolian sediments)		Broad conclusions as to prevailing climate.	Date of Aeolian deposit to 13.7 cal ka BP suggests dry climatic phase. Followed by deposits of perennial streams suggest climate was wet during 9.5-8 cal ya BP. Followed by aeolian deposits that suggest climate was becoming progressively arid after 7400 cal ka BP.		
Stable isotope in tree ring , Frumkin 2009	Mt. Sedom, SW shore of Dead Sea	Radiocarbon dating and isotope analysis. Variations in carbon and nitrogen isotopes within tree rings of subfossil <i>Tamarix</i> tree trunk.	Ca. 4265-3930 BP.		There was a progressive increase of ¹³ C and ¹⁵ N isotopic enrichment which culminated with a spike in these. This suggests a prolonged drought during this time that culminated with the tree's death. The southern Dead Sea Basin was dry during this time.		
Speleothem record , Bar-Matthews et al. 2003	Soreq Cave, Central Israel Pequin Cave, Northern Israel	Uranium series dating of stalagmite.	Last 250 ka	Estimated paleo rainfall values and compared cave records with marine records and found that climatic changes occurring throughout the Eastern Mediterranean were synchronous.	Decreased precipitation and increased aridity was found during YD, 5.1 ka (estimated 220 mm/yr), after 2.5 ka. Early Holocene (11-7.5 ka) and 4.7 ka suggest wetter, warmer conditions. At around 7.5-8 ka they estimate around 600 mm/yr. Rainfall during 4.7 ka peaked, followed by decreasing precipitation.		

Table 3.4. (continued).

Proxy record	Location	Reference Method	Time period	Method output	Authors interpretations					
					Age BP	Projecte dTemp (°C)	Projected Mean Ann Rainfall mm/yr	Vegetation nearby	Changes in $\delta^{18}\text{O}$ and $\delta^{13}\text{C}$	
Speleothem record , Bar-Matthews et al. 1997	Soreq Cave, Judean Hills	Detect differences in $\delta^{18}\text{O}$ and $\delta^{13}\text{C}$ in successive equilibrium growth layers of stalagmites. Uranium series dating.	Last 25 ka	Construct paleoclimatic records with broad conclusions about rainfall and vegetation patterns						
					15 - 12	14.5 - 18	550 - 750	C3	Drop of $\delta^{18}\text{O}$ and $\delta^{13}\text{C}$. Spike of $\delta^{18}\text{O}$ ca. 14.5 ka	
					12 - 10	14.5 - 18	680 - 850	C3	$\delta^{18}\text{O}$ reaches lowest level and $\delta^{13}\text{C}$ starts to increase. Spike of $\delta^{18}\text{O}$ and $\delta^{13}\text{C}$ ca. 11.5 BP.	
					10 - 7	14.5 - 19	675 - 950	C3	Few speleothems recorded during this time	
					7 - 1	18-22	450-580	C3	$\delta^{18}\text{O}$ spike ca. 6-5 ka and spike of $\delta^{18}\text{O}$ and $\delta^{13}\text{C}$ at ca. 3 ka	
					Present	18-22	500	C3	Isotopic equilibrium	
Speleothem , McGarry et al. 2004	Soreq, Peqin, Ma'ale Efrayin Caves	Fluid inclusion measurements of speleothems	Last 25 ka	Estimates the temp. range during which speleothems formed	Temperature ranges are estimated at: Between 8 to 10 cal ka BP = 14 to 17°C. Between 0.8 to 1.2 cal ka BP = 20 to 22°C.					
Speleothem record , Bar-Matthews and Ayalon 2011	Soreq Cave, Judean Hills	Uranium series dating of stalagmite.	Mid Holocene (7-4 ka BP)	Identified several wet and dry events at a high resolution and associated these with transitions between cultural periods.	Wet event	Dry event	Cultural period shift			
					6700-6680					
						6650-6600				
					6550-6450		Mid Chalc-Late Chalc			
						6250-6180				
					6170-6100					
					5760-5740					
						5700-5600	Late Chalc-EBI			
					5500-5450					
						5250-5170				
4800-4700		EBII - EBIII								
	4200-4050	EBIV, collapse of empire (Egypt & Mesop.)								

Table 3.4. (continued).

Proxy record	Location	Reference Method	Time period	Method output	Authors interpretations
Lacustrine sediments, Magaritz et al. 1991	Dead Sea shore	Measured the $\delta^{13}\text{O}$ of organic sediments from Dead Sea sediment core		Broad conclusions as to prevailing climate	After ca. 9.4 cal ka BP, conditions were relatively arid. After ca. 5.7 cal ka BP, conditions became relatively moist.
Molluscs, Goodfriend 1990	Southern Israel (Northern Negev)	Analyze the $\delta^{13}\text{C}$ concentration of organic matter in gastropod shells over time to estimate the composition or abundance of C_3/C_4 plants in the Negev Desert.	Last 12 k ya	Broad conclusions as to distribution of C_3/C_4 plants and precipitation trends.	Between ca. 7.4-3.2 cal ka BP, the C_3/C_4 transition area was about 20 km further south than where it is at present. So during this time, rainfall values were higher than present day ones.
Molluscs, Goodfriend 1991	Southern Israel (Northern Negev)	Estimate paleorainfall isotopic values for the Negev derived from the fossil record of ^{18}O in snails. Dates were obtained through radiocarbon analysis.	Holocene		Detected shifts in the atmospheric circulation patterns of rain systems which come from northeast Africa (these bring large amounts of rain). Between 7.4 – 6.8 cal ka BP, these became more frequent, probably resulting in increased rainfall and floods in this region.
Several Rambeau et al. In press.	Beidha, southern Jordan plateau	Combined several lines of evidence to reconstruct the environment during its human occupation including U-series dating of carbonate concretions surrounding the archaeological site, geomorphological reconstructions and carbon and oxygen stable isotope analyses of carbonate precipitations from a nearby fossil spring.	Reconstruct climatic variation between ca. 16.5-8.4 BP.		Favorable climatic conditions were found for the times when the site was occupied. Onset of arid conditions during 8.5 BP, when spring dried up. Wet conditions prior to PPNB.

Climatic shifts during the Mid Holocene were recently analyzed at a high temporal resolution using a speleothem record from Soreq Cave in the Judean Hills (Bar-Matthews and Ayalon 2011). Several wet and dry events were identified (Table 3.4), and some were related to cultural shifts. The transition from the Mid to Late Chalcolithic and Early Bronze II to Early Bronze III correspond to wet periods. On the other hand, droughts prevailed during the transitions from the Late Chalcolithic to Early Bronze I and during the collapse of the empires in Mesopotamia and Egypt (Early Bronze IV).

In Southern Jordan, fluvial sediments in the Wadi Faynan basin were analyzed by McLaren et al. (2004), revealing several changes from the Late Pleistocene until the Mid Holocene. Aeolian deposits dated to 13.7 cal ka BP show signs of an arid period. These were covered by deposits of perennial flowing streams which suggest wetter conditions from 9.5 to 8 cal ka BP. Additional aeolian deposits dated to ca. 7.4 cal ka BP show signs of climatic deterioration.

Contradictory evidence to most studies which suggest a wet Early Holocene was presented by Magaritz et al. (1991), who measured the $\delta^{13}\text{O}$ in organic sediments of the Dead Sea shore and detected a period of drought after 9.4 cal ka BP, which shifted towards a wetter period after 5.7 cal ka BP. Robinson et al. (2006) note that these findings are contrary to most others discussed in their comprehensive review, and that the dating of this material is limited.

At nearby Mt. Sedom (on the southwestern shore of the Dead Sea), Frumkin (2009) analyzed a fossilized *Tamarix* tree that clearly reflects the prolonged drought that occurred towards the end of the Early Bronze Age (Early Bronze IV ca. 4300 – 4 ka BP). During 4265 – 3930 BP, ^{13}C and ^{15}N isotopic enrichment was observed (indicating

prolonged drought), which ended in a spike in $\delta^{13}\text{C}$ and $\delta^{15}\text{N}$ values at the end of the record (time of the tree's death).

Cordova (2008) reconstructed Mid Holocene climatic and landscape characteristics northeast of the Dead Sea through the geomorphological and palynological analysis of two wadis (Wadi ash-Shallalah and Wadi Al-Wala) located in the transition between the Mediterranean and Irano Turanian regions (Cordova 2008). He also related the fluctuating stream and floodplain history to settlement patterns observed during the Early Bronze Age (EB) period, which is further subdivided into EBI (5.5 – 5 ka BP), EBII (5 – 4.7 ka BP), EBIII (4.7 – 4.3 ka BP), and EBIV (4.3 – 3.9 ka BP). These subdivisions are based on several stylistic characteristics as well as prevailing settlement and population patterns (Philip 2001), which range from a steady increase during the first two stages, followed by a slow and significant decline during EBIII and EBIV, respectively. Cordova found evidence of stream aggradation between 7 – 6 ka BP, stream stability between 4.6 – 4 ka BP, and stream incision around 4 ka BP was found. These were associated with periods of high rainfall (when high amounts of olive and some cereal pollen were obtained, suggesting orchard cultivation on the slopes and agricultural activity on floodplains), fluctuating rainfall, and rainfall decline, respectively.

3.1.1 Records from archaeological sites

The analysis of plant remains from archaeological sites (archaeobotany) complements other proxy records. Although the spatial resolution is usually limited to the catchment of the site, it enhances the pollen record (Hunt et al. 2004; Miller 1998). Furthermore, it provides insight into the human environment relationship, since it

facilitates an understanding of how humans and animals were impacting the landscape. For example, what people were using for fuel (dung or wood) can suggest the density of nearby vegetation and whether it was denuded. It can also help answer how domestic animals were impacting the landscape and what constituted the inhabitants diet.

Miller used both microbotanical (pollen from lakes) and macrobotanical (e.g. charcoal from archaeological sites) evidence to reconstruct the vegetation history of the Levant (Miller 1998). Naturally, the cumulative archaeobotanical record is more limited than the pollen record. The best documented periods are between the Aceramic Neolithic and the Bronze Age (Miller 1991).

Some of the earliest evidence comes from Ohalo I in the northern Rift Valley (ca. 19 BP, Kebaran period). The microremains point towards the existence of shrubby vegetation growing near the site which includes *Ziziphus sp.* (*Ziziphus spina Christi* and *Ziziphus lotus* presently grows in the area). Another site located in the more arid Jordanian Plateau (Jilat 6) has an assemblage dominated by chenopodiacea (ca. 16 BP) which are characteristic of the modern steppe vegetation of the area (Rossignol-Strick 1993).

Gilgal is a site located in the Jordan Valley that was occupied during the Natufian (ca. 11.3BP) and then during the PPNA around ca. 7.8 BP. It seems it wasn't occupied during the Younger Dryas. During both periods of occupation, macrobotanical remains are similar to the contemporary vegetation of the area: riparian species like *Tamarix* and *Populus*, other woody species, and pistacia (which grew in nearby slopes).

Some of the early agricultural sites of the PPNA and PPNB like Basta and Nahal Hemar that are nowadays located in steppe were probably occupied by forest-steppe

during their occupation. Willcox (1991: 121) draws this conclusion given the presence of pistacia, almond, hackberry and hawthorn (suggesting more moist conditions). In another study that looks at the occupation of a site during the PPNA and PPNB periods in the north Syrian Euphrates region, the same author finds charcoal samples of *Pistacia atlantica*, *Rhamnus* and *Amygdalus*, whereas at present the steppe has been degraded and no longer supports these species (Willcox 1996: 149). A similar pattern is found in the very arid steppe of southern Jordan where precipitation at present is about 100 mm/yr. Sites like Jilat 6 (ca. 9.5 – 8.5 BP), Azraq 31 and Dhuweila (both 8.5 – 8 BP) appear to have been farming barley, emmer and eikorn (Garrard et al. 1996).

Rambeau et al. (in press) used multiple lines of evidence from environmental and archaeological records to investigate climate change at the archaeological site of Beidha located in the southern plateau region (near Petra) during the Natufian and PPNB periods. They found that environmental conditions were favorable during the periods when it was occupied. The site was abandoned around 8.5 ka BP, coinciding with the drying of a fossil spring. Their findings also suggest that conditions were wetter during the preceding PPNA (12-10.6 cal ka BP).

In another study that looked at macrobotanical remains in the Central Negev during the Epipaleolithic, Goring-Morris et al. (1998) made a surprising discovery at Nahal Neqarot, when they uncovered a significant proportion (316 out of the 387) of charred wood remains dated to the Middle Epipaleolithic (ca. 18,800 – 13, ka BP) that were found to be *Juniperus sp.* (probably *Juniperus phoenicia*). The three dated samples belong to C₃ plants, which require much more moisture than the present day C₄ plants that predominate in the region.

3.2 Paleoenvironmental reconstruction and gaps

Proxy records from ice and marine cores record long term climatic information, which shows fluctuating glacial and interglacial cycles. The climatic response throughout the Near East to glacial episodes has been reduced temperature and rainfall (although the magnitude is still in debate), resulting in an expansion of steppe vegetation and a retreat of forests or a transition from dense to open forests. On the other hand, interglacials have predominately been warmer and more humid, causing a reversal in the vegetation trend of glacial periods.

The latest glacial episode occurred towards the end of the Pleistocene, which transitioned into an interglacial at the beginning of the Holocene. However, operating at the same time are shorter climatic events which appear to cause temporary interruptions to the glacial cycles, such as Heinrich events and the Younger Dryas. At the same time, there appear to be episodes of even shorter duration (centennial or decadal) such as the dry and wet periods detected by Bar-Matthews and Ayalon (2011).

To a certain extent, landscape characteristics change according to climatic shifts. Different vegetation communities prefer certain climatic conditions. At the same time, erosion rates can accelerate depending on precipitation, as can the recurrence of floods. Lake levels can raise or drop, and forest and desert belts can expand and contract. An example of how substantial these changes can be is the final retreat of Lake Lisan towards the end of the Pleistocene, which allowed humans to settle in the Rift Valley.

Many of these climatic events have been recorded by proxy records, but these sometimes disagree when it comes to detecting the magnitude, timing, or duration of climatic events. For example, the effects produced by the Younger Dryas (ca. 12.7 – 11.5

cal ka BP) remain contested, especially regarding its environmental effects. According to most palynological and speleothem records, temperatures and precipitation declined. In Gvirtzman and Wieder's analysis of soils (2001), they found that during this time, a layer of dust accumulated, signaling long term arid conditions. However, Stein et al. (2010) provide evidence of a wetter Younger Dryas that allowed the level of the Dead Sea to rise, which was followed by a dry spell from 11 to 10 cal ka BP, during which a large salt layer was deposited while the level of the lake dropped. In the Hula Basin pollen record, Van Zeist et al. (2009) identified the Younger Dryas in PAZ 1, which they dated to 11.3 – 10 cal ka BP (the period which Stein et al. [2010] identify as arid). Despite low *Quercus ithaburensis* and high grass pollen values, van Zeist et al. inferred that streams were flowing, due to the high pollen values obtained for riparian vegetation.

The marine and lake pollen records suggest that climatic conditions underwent an abrupt change following the Younger Dryas (within a thousand years) from pervasive dry conditions to the wettest climate that has been recorded so far during the Holocene (Rossignol-Strick 1995, 1999; Van Zeist et al. 2009; Yasuda et al. 2000). Most records agree that the early Holocene has been the wettest and warmest period since the Late Pleistocene (e.g., Bar-Matthews et al. 1997, 2003; Roberts et al. 2011; Robinson et al. 2006; Rossignol-Strick 1995, 1999). As a consequence, there were large tracts of mixed evergreen and deciduous woodland (Wilkinson 2003). Speleothem analysis also suggests that the period of 10-7 cal ka BP was particularly wet and marked by significant flooding events (Bar-Matthews et al. 1997), even though the Dor Lagoon in the Carmel coastal plain appears to have dried sometime between 9.4 – 8.5 cal ka BP (Kadosh et al. 2004).

The southern, more arid portion of the study area also experienced wetter conditions during the Early Holocene (Fish 1989; Goodfriend 1990, 1991; Henry 1986), apparently as a result of monsoonal rains and a more northerly belt of convectional rain, which resulted in an expansion of grassland into the Saharan desert (Gasse 2000). Between 11.5 and 8.8 cal ka BP, the northern Negev is believed to have been densely populated by C₃ plants (unpublished and referenced in Goodfriend 1991: 423). In Southern Jordan, Hunt et al. (2004) found evidence which suggests that before 8 ka BP, there was more moisture which caused areas that are now desert to be steppe.

After the Early Holocene wet period, conditions began to resemble those of today, with rainfall declining and temperatures rising slightly. The exact timing of this shift is still debated. Pollen analyses done in Israel, Jordan and Saudi Arabia found that a drying trend began 6 to 5 ka BP (e.g., Baruch and Bottem 1991; Fish 1989; Horowitz, 1979; Van Zeist and Bottema 1991). In Southern Jordan, Hunt et al. (2004) detected a decline in precipitation after 8000 cal ka BP, which was interrupted at 7.4 and 6 cal ka BP. In the eastern desert in Jordan, archaeological and geomorphological evidence suggests the drying phase began between 7-5 cal ka BP (Allison 1997).

A drought that lasted a few hundred years appears to have occurred during the Early Bronze Age IV period (ca. 4300 – 3900 BP), part of which is interpreted by Frumkin (2009) based on the rings of a *Tamarix* tree from Sedom Cave (2009) dated to ca. 4265 – 3930 BP as well as a high resolution speleothem record in the Judean Hills dated by Bar-Matthews and Ayalon 2011. Various studies that looked at lake level changes also agree that at ca. 4 ka BP, the level of the Dead Sea dropped, causing the southern Dead Sea Basin to become exposed (Enzel et al. 2003; Frumkin et al. 2001). An

earlier study done by Fumkin et al. (2001) that analyzed fossilized oak, also from the Sedom Cave, found that at around ca. 4 ka BP, conditions were extremely dry.

Climatic conditions appear to have improved during the Middle Bronze Age (4 - 3.5 cal ka BP) (Leroy 2010; Neumann et al. 2007, 2010), which again worsened during the Late Bronze Age. Neumann et al. (2010) found evidence of a pervasive drought during this cultural period in six sedimentary sequences collected from the western shore of the Dead Sea. The records that trace the Iron Age are less conclusive as to the overall climatic conditions and vegetation characteristics, although it appears that the deterioration of the climate during the Late Bronze Age continued into the first half of the Iron Age (Rambeau 2011).

What appears to be missing from the literature is the response of vegetation to these changes (mostly after the Mid Holocene, when it becomes hard to dissociate the human footprint from the pollen records), especially in marginal areas (Rambeau 2011). Marginal areas located between two or more plant geographical regions are more likely to be affected by even minor climatic variations, leading to the expansion or contraction of their boundaries (Goodfriend 1990, 1991, 1999; Gvirtzman and Wieder 2001; Hunt et al. 2004).

A summary of the prevailing paleoenvironmental conditions according to various proxy records has been provided in this chapter. As can be seen, broad climatic shifts have been detected throughout the Holocene. A very wet early Holocene seems to have been followed by a drying trend. At the same time, these 'trends' appear to have been interrupted by wet and dry episodes of shorter duration.

Chapter 4

VEGETATION MODELING

The purpose of this chapter is to present, explain, and justify the methodological steps used in this research. An overview of species distribution modeling, the theory behind it, and the most commonly used methods available for ecological modeling are first presented. This is followed by a summary of the steps needed to build a robust ecological model, with particular reference to the steps implemented in this study to model and map vegetation distributions at present and in the past. These include obtaining suitable data, selecting an appropriate algorithm, and assessing the predictive performance of the results.

4.1 Species distribution modeling

4.1.1 Modeling geographic distributions

Species distribution modeling or SDM is a growing field that allows the distribution of species to be predicted across geographic space. In the literature, SDM is also sometimes referred to as bioclimatic models, climate envelopes, ecological niche models or ENM, habitat models, resource selection functions or RSF, range maps, and ecological models (Elith and Leathwick 2009). SDM relies on numerical models that use environmental variables and a set of occurrences to map the distribution of a species across a landscape (Franklin 1995). As a result of innovative and more accessible statistical and GIS tools as well as more available data from museums, herbarium collections and online databases (for example, GBIF <http://data.gbif.org/>), SDM has been growing in popularity during recent years in fields like conservation science, planning, evolution biogeography, and ecology (Corsi et al. 2000; Elith et al. 2003; Guisan and

Zimmermann 2000; Kremen et al. 2007; Peterson and Robins 2003; Scott et al. 1996; Welk et al. 2002; Wheeler, 1993).

Ecological modeling combines statistical and mathematical algorithms with ecological niche theory, which implies that for a population to maintain equilibrium, it relies on a set of environmental parameters (Grinnell 1924) that need to be held more or less constant. If a sample of occurrences of this species is obtained, one may be able to determine the species' distributional environmental parameters and use this information to derive its theoretical fundamental ecological niche (Peterson and Cohoon 1999). Assuming a species is in equilibrium with its environment, species distribution models can characterize the relationship between observations and environmental parameters and reflect this on their potential geographic distributions which could or could not coincide with the fundamental niche of the species (all the hypothetical areas that meet the environmental parameters necessary for a species) or with its realized niche (usually a subset of the fundamental niche that represents the geographical area actually occupied by a species). Although these types of models are believed to be less robust than mechanistic models which are based on the actual physiological characteristics of a species instead of the environmental parameters that constitute its habitat (but are harder to implement since they require information that is harder to obtain, Malanson et al. 1992; Prentice et al. 1992; Woodward and Rochefort 1991), they can also produce very similar results (Hijmans and Graham 2006).

There are many steps involved in SDM, each of which requires decision making. These include designing a strategy to obtain samples or source these out from other references (*e.g.*, museum collections); obtaining the appropriate predictor variables;

determining if any variables are correlated; deciding on an algorithm with which to model the distribution; calibrating the algorithm; choosing a threshold if the output needs to be converted to a presence/absence map; and determining how the model will be evaluated. If appropriate consideration is given to all these steps, a model that can provide a strong prediction of species distributions can be built.

Species distribution models can provide valuable ecological insight and be applied to multiple purposes. For example, they can be used to determine the distribution of a species in an area that has not been entirely sampled, due to logistical constraints. This has resonance in the area of conservation planning and management when, for instance, suitable habitats for rare and endangered species need to be identified (Araújo and Williams 2000) or areas that have a high extinction risk need to be found (Araújo et al. 2002). At the same time, they can be used to extrapolate predictions into other geographic domains and time periods. Among other applications, this can assist in determining the distribution of species at a global level, studying the dynamics of invasive species (Peterson 2003), assessing how invasive species could disperse under different scenarios (Thuiller et al. 2005), or understanding how climatic shifts like global warming can impact the distribution of a species (Pearson and Dawson 2003). SDM can also offer insight into debates regarding refugial areas during glacial episodes (Svenning et al. 2008) and help explain genetic variation amongst species in different areas. Some studies have also used SDM to see how different climate scenarios may have influenced the distribution of different species that have become extinct due to reasons that are not clear. Nogués-Bravo et al. (2008), for instance, played out different scenarios using a climate envelope model as well as population models to investigate whether the

extinction of the woolly mammoth was due to climate change or intensified human hunting.

4.1.2 Why do we need to map and model vegetation?

Vegetation is constantly being influenced by human activities and/or natural disturbance events such as fires, droughts, floods, landslides, grazing, agriculture, and growth of urban areas. Without these disturbances, plant populations and communities are gradually replaced by others through succession and eventually arrive at a semi stable state, called climax. Although of course, an absolutely stable state is hardly reached or maintained due to some of the disturbances just mentioned as well as the ongoing development of soils, landforms and microclimate (to name a few), most vegetation ecologists accept the idea of a relatively stable, terminal stage in vegetation development. This terminal stage is often termed 'natural vegetation' and is considered to be in a dynamic equilibrium with the actual set of environmental conditions of a place at a given point in time (Mueller-Dombois and Ellenberg 1974).

In this study, the long history of human and animal disturbance has undoubtedly altered the original vegetation, as argued by Fall et al. (2002). Nevertheless, a series of climax populations can be expected whenever an area experiences relative stability. In other words, the plant cover can then be in equilibrium with the environmental conditions of the area. The present day terminal stage of vegetation succession which would develop under actual environmental conditions is referred to by Tuxen (1956) as present day potential natural vegetation (because it represents the potential and not necessarily the existing one). So, in other words, the potential natural vegetation is a hypothetical vegetation that can sometimes also be inferred from the existing vegetation (Mueller-

Dombois and Ellenberg 1974).

In the Mediterranean, where human cultivation and grazing activities have had profound effects on the vegetation since the Neolithic, the natural vegetation has been replaced by vegetation types which differ in degree of artificiality. But even after thousands of years, while humans have influenced, modified, and sometimes radically altered the landscape, pockets of natural vegetation still exist. The plants found in these pockets, termed “indicators” in this study (discussed in the next section), can be used to characterize the natural vegetation. These can be used to create maps of potential vegetation of the study area across multiple time scales using the theory and tools embedded in predictive habitat distribution modeling. Once this is achieved, the models can be compared against proxy records as well as archaeological evidence. Whilst a comparison against proxy records, especially pollen, allows the models to be validated, a comparison against archaeological footprints (i.e. charcoal and macrobotanical remains) theoretically allows the researcher to disentangle the natural from the anthropogenic landscapes that existed at different points in time.

4.1.3 Evolution of species distribution modeling

Before the development of modern quantitative methods with which to characterize and model the relationship between a species and its environment, earlier studies applied the ecological knowledge behind this relationship to map or describe the geographical range occupied by a species or a community (Grinnell 1904; Murray 1866; Schimper 1903; Whittaker 1956). Later on, statistical methods, such as linear regression and discriminant analysis, began to be employed (Elith and Leathwick 2009). In the case of a simple regression, one predictor or independent variable is capable of predicting the

distribution of the response or dependent variable. In multiple regression, a series of independent variables are used to explain the distribution of the response variable, which can be used for determining presence/absence areas of a species (Guisan et.al 1999).

This line of research advanced substantially during the 1970s, following the application of generalized linear models (GLM). These were better able to grasp the species-environment relationship and therefore model it in a way that is more realistic (Austin 1985) using presence-absence information. Another advance is that these methods can also provide insight as to the relative contributions of the different variables (Guisan et al. 2002).

The logic behind these regression modeling methods was instrumental in advancing the field and was later on applied to newer modeling methods (Elith and Leathwick 2009). At the same time, tools that process and store spatial information like geographic information systems (GIS) have evolved, as have instruments that capture and process spatial information (e.g., satellites, global positioning systems or GPS). Whereas 30 years ago spatial data was difficult to obtain in digital format, there is at present a plethora of information that can be accessed easily. The marriage between these technological and quantitative advancements allowed this field to really blossom during the 1990s.

4.1.4 Species distribution modeling approaches

‘Presence only’ information also has increased substantially as museums and herbarium collections become accessible through the world wide web. Consequently, a group of algorithms that only consider presence information have become quite popular (e.g., MAXENT, GARP, Bioclim) in recent years. Overall, a number of algorithms and

tools that can predict the distribution of a species based on its dependency with certain environmental variables have been developed during recent decades (see Table 4.1 for a summary of some of the most commonly used). They can generally be divided into statistical methods, machine learning techniques and artificial neural networks.

The output produced by different SDM methods can be quite different (Pearson et al. 2006; Randin et al. 2006). The main reason is because different methods may use different algorithms to characterize the relationship between a species and a set of predictors, and then apply different methods to perform the prediction. There are also a series of parameters that can have an impact on the result. For instance, the relationship between the dependent and the independent variables can be treated as simply linear (as in linear regression), or in more complex ways (for example, when linear variables are transformed into functions like step or complex curves). Also, different weights can be assigned to the different predictor variables. Once the relationship has been established, the suitability of a cell can be determined in several ways, like adding the responses of the different variables used in the prediction, selecting the variable that most impacted or restricted the species distribution, or choosing a combination of these. The output can then be presented as a continuous suitability surface or a binary prediction (presence/absence).

Another important distinction between the different methods available has to do with the type of information they use to build the model. Some methods (e.g., GAM, GLM) use presence and absence information, whereas others only use presence information. Furthermore, some algorithms use presence and background information. In this case, presence observations are considered to be part of the background. The

methods then concentrate on determining how the environmental conditions at the presence locations relate to the environment throughout the rest of the study area (the background).

SDM is being increasingly used to investigate theoretical questions and applied to practical considerations. Some government agencies are adopting SDM for management and conservation purposes as well as to research the impact of climate change on species distributions (e.g., Point Reyes Bird Observatory online application, Atlas of Living Australia, Israel Biodiversity Information System [BioGIS]). Fortunately, model comparison represents an area that has received considerable attention in the literature (Elith and Burgman 2003; Elith and Leathwick 2009; Elith et al. 2006; Fielding and Bell 1997; Franklin 1995, 2009; Guisan and Zimmerman 2000). One of the most comprehensive studies that compares models that use presence only data was carried out by Elith et al. (2006). They compared 16 modelling methods by modeling the distribution of 226 species across six regions in the world. These included an envelope method (BIOCLIM); distance based methods (DOMAIN and LIVES); regression based methods (GLM, GAM, BRUTO, MARS, GARP); machine learning methods (MAXENT and BRT) and generalised dissimilarity models (GDM). They trained the models using presence only information, and then used an independent dataset containing presence-absence to validate the models. They found that the more recently developed methods (MAXENT, BRT, GDM and MARS) generally outperformed the more established ones.

In a recent study (Phillips et al. 2009), the performance of the more robust methods (BRT, MAXENT, MARS, GAM) was compared in terms of sampling bias, by comparing the outputs of the algorithms when using random background as opposed to

target background. They found that the same bias shown in the sample should be reflected in the background sample, as this considerably improves the performance of the models.

Other studies have applied different SDM models for different purposes, meanwhile comparing which models perform better. Benito et al. (2009), for instance, compared five different models (Bioclim, Domain, GARP, MAXENT, ENFA) for conservation purposes. They wanted to investigate the extinction risk of an endemic plant species with regards to the spread of greenhouse gasses in the Mediterranean. After assessing the results produced by the different models using a modified Receiver operating characteristics (ROC) – Area under the curve (AUC) approach, they found that Maxent and Domain performed better than GARP and ENFA (as will be described later in this chapter, the AUC is one of several measures used to assess the models).

One study in particular investigated how four SDM methods (GAM, MAXENT, BIOCLIM, DOMAIN) perform when predicting species into novel climates (Hijmans and Graham 2006), when comparing them to a mechanistic model (considered to produce better results). MAXENT and GAM performed the best and produced results that were comparable to those produced by the mechanistic model. Nevertheless, MAXENT was found to slightly overpredict (predict a slightly greater area than what was expected) whereas the opposite was found with BIOCLIM.

Table 4.1. Methods commonly used in Species Distribution Modeling (summarized from Pearson 2007 and Phillips et al. 2006).

Software / Model, Reference	Method / Principle	Information used	Description
<p>DOMAIN</p> <p>Carpenter et al. 1993, http://www.cifor.cgiar.org/online-library/research-tools/domain.html, http://diva-gis.org/</p>	Gower distance metric	Presence	Domain uses the Gower distance metric to calculate suitable space. Environmental space is represented as a rectilinear region with n dimensions (n refers to the environmental variables used to predict). A Domain suitability index is then created using the Gower distance metric which, for any two points for each predictor variable, is the sum of the standardized distance (the standardized distance between two points is the absolute difference of these points divided by the range of values across all cells between the two points). The Domain similarity metric is then calculated by subtracting the Gower distance from 1 (Hernandez, et al. 2006). The maximum value is 100, which implies cells where observations are found.
<p>BIOMAPPER/ ENFA</p> <p>Hirzel et al., 2002, http://www2.unil.ch/biomapper/</p>	Ecological niche factor analysis (ENFA)	Presence and background	Based on multivariate ordination. The model produces uncorrelated factors of biological significance. As Phillips et al. put it (2006: 235), environmental space is linearly transformed into “orthogonal <i>marginality</i> and <i>specialization</i> factors” and “environmental suitability is then modeled as a Manhattan distance in the transformed space.”
<p>MAXENT</p> <p>(machine learning method)</p> <p>Elith et al. 2011 Phillips et al. 2004, 2006 http://www.cs.princeton.edu/~schapire/maxent/</p>	Maximum entropy	Presence and background	MAXENT is a general purpose software that allows species distribution modeling using presence only data. Instead of absence, it uses background information. It uses the underlying information of environmental variables at each of the ‘presence’ locations to determine the target probability distribution of a species by finding the probability distribution of maximum entropy (most spread out, or closest to uniform) (Phillips et al, 2006). It makes use of what can be inferred about the environmental conditions at the presence locations and makes sure the suitable distribution agrees with this. It can use both continuous and categorical variables. The output is a continuous suitability surface that ranges from 0 to 1.
<p>Bayesian</p> <p>Aspinal 1992 McCarthy 2007</p>	Bayesian	Presence and absence/ Presence	It is a machine learning method that is based on a combination of the probability of observing species (nominal – categorical data) with their probabilities of being found depending on the value of each predictor.

Table 4.1. (continued).

Software / Model, Reference	Method / Principle	Information used	Description
<p>GARP (machine learning method) Stockwell and Noble 1992, Stockwell and Peters 1999, http://www.nhm.ku.edu/desktopgarp/</p>	Genetic algorithm (GA)	Presence and absence/ Presence and pseudo absence	Based on a genetic algorithm to combine a series of decision rules. It uses a subset of background (to be treated as absence) and presence pixels and the relationship of these with the predictor variables to create rules that output the potential space in binary format.
<p>GRASP Implemented in R www.r-project.org/ Lehman et al. 2002, Elith et al. 2006, Leathwick et al. 2006</p>	Regression: Generalized linear model (GLM), Generalized additive model (GAM), Boosted regression trees (BRT), Multivariate adaptive regression splines (MARS)	Presence and absence/ Presence and pseudo absence	<p>GLM are a family of statistical methods (e.g. multiple linear regression and logistic multiple regression) that predict the distribution of species using the species' response to a linear combination of predictor variables. They are more flexible than other techniques because they allow the response variable to be one of several distributions (e.g. Poisson, Gaussian, Binomial, normal, gamma).</p> <p>GAM are semi-parametric extensions of GLM (Hastie and Tibshirani, 1986). Their strength lies in their ability to handle non linear relationships between the response and predictor variables (Guisan et al. 2002). Both these methods are normally applied to presence-absence data however they have recently been applied to presence-only data. This is done by taking a random sample of pixels from the study region and using these instead of 'absence' records (Ferrier and Watson, 1997; Ferrier et al., 2002).</p> <p>MARS are a non linear regression method (Leathwick et al. 2006) which can also model the complex relationships between a species and a set of predictor variables (Franklin 2009). When compared to GAMs, it has been proven to perform faster and is capable of handling larger datasets and larger numbers of predictor variables (Franklin 2009).</p>
<p>OpenModeller</p>	Multiple methods (e.g., GARP, Bioclim, GAM, GLM, Neural Networks)	Presence	This is a software that allows different modelling methods to be implemented to perform SDM. The software reads presence observations and environmental variables and then, depending on the method algorithm selected by the user, projects its distribution.

Table 4.1. (continued).

<p style="text-align: center;">BIOCLIM</p> <p>Busby 1986, Nix 1986 Implemented through DIVA-GIS</p>	Envelope	Presence	<p>Uses a bioclimatic envelope to predict potential species distribution areas, which are those with values that are within the range derived from the occurrence dataset (Busby, 1986; Nix, 1986). Environmental space is represented as a rectilinear region with n dimensions (n refers to the environmental variables used to predict). A percentile distribution is calculated for each variable used in the prediction. The values are then assessed for each grid cell and outliers are omitted by using only the 5 to 95 percentile limits of each variable distribution (Carpenter et al., 1993). The results range from zero to 50 (low to high).</p>
<p>Rule based algorithm</p>	Applied through a macro	Presence and absence/ Presence only	<p>Rules that describe the relationship between the predictor variables and the response variable can be developed for a GIS in Arc Macro Language (AML) or other scripting language (e.g. Avenue, VBA) using conditional statements (Guisan and Zimmermann 2000). The script or macro can then be run using overlay methods.</p>
<p>Classification tree</p>	GIS or Remote Sensing software	Presence	<p>Classification methods include classification and regression trees, rule-based classification and maximum likelihood classification which in some GIS and remote sensing packages are known as supervised and unsupervised classification.</p>
<p>Random forests (machine learning method) Implemented in R Breiman 2001</p>		Presence and pseudo absence	<p>Random forests is related to CART. Based on the environmental variables and observations, it builds a series of trees (based on classification methods instead of regression) by randomly choosing subsets. Then it takes the averages of all the trees to make a final one.</p>

Another study examined the effect of sample size (ranging from five to 100 observations) on model accuracy, by using four modeling methods: GARP, BIOCLIM, MAXENT, DOMAIN (Hernandez et al. 2006). Maxent was found to provide some of the most favorable results. As Phillips et al. pointed out (2006), this could be because MAXENT is a generative method (versus discriminative), which is known to perform better with small sample sizes (Ng and Jordan 2001).

Dormann et al. (2008) investigated how much uncertainty is introduced in a model during the different steps of its development (e.g., data selection, modeling algorithm chosen, variable selection) by building a framework that allowed them to quantify the uncertainty introduced during each step of the modeling process while projecting a bird species to different climate change scenarios. They found that data quality (concerning both the observations and environmental variables used) and model type were responsible for the most uncertainty. Nevertheless, when it comes to data quality, they found collinearity (when variables are highly correlated) to be less of a problem than the quality of the observations per se. Of the methods tested (machine learning methods were not included in this study), GLM and GAM outperformed neural networks. Other methods that have been found to handle correlated variables well are ENFA and Maxent (Hirzel et al. 2001; Phillips et al. 2006).

Barry and Elith (2006) remind us that there are limitations when modeling species distribution, due to the complexity of the problem. They found that five of the most common sources of errors in SDM were produced by omitting environmental variables, small sample size, bias in the sample, lack of absence records, and errors within the variables. In terms of environmental variables, they mention how it is common

to omit variables that may be the most relevant and use others that may be more accessible instead. For instance, although variables that reflect growing days and extreme maximum and minimum temperatures may be more relevant to map the distribution of a plant, they may be hard to obtain and average temperature could be used instead. Also, a small sample size can hinder the complexity of the model's fit, since more samples are required to derive more complex features. Nevertheless, some models have been shown to perform better than others when using small sample sizes. Observation bias can also cause the resulting distribution to predominate along the sampled areas. Furthermore, unsuitable areas are harder to identify and validate when there is lack of absence information. Nevertheless and as described above, some algorithms (e.g., GAM, MARS, BRT, and MAXENT) have in built mechanisms that help overcome many of these issues.

Because SDM involves multiple steps and has many facets that require decision making, there is no step by step manual. Instead, there are recommended best practices while many other aspects continue to be investigated (Elith and Graham 2009). For conservation purposes, Elith and Leathwick (2009) recommend using MAXENT or one of the regression methods (e.g., GAM, GLM, MARS, BRT) which are often used by ecologists working with SDM. This last group has been around for a few decades and is fairly robust when it comes to SDM, since it can incorporate and process the complexity of the relationship between a series of observations and ecological variables.

The most suitable method will ultimately depend on the individual context (Elith and Leathwick 2009): accessibility to the tool (i.e., does it have a graphical user interface), the type of information used as observation, number of observations (some methods outperform others when working with small numbers of observations),

ecological and statistical knowledge of the modeler, time available for modeling and for becoming acquainted with the method, computational capacity, quality of the method in the particular area in which it wants to be used (e.g., for extrapolating to new regions or places, for identifying suitable areas for an endangered species). Also, it is important to remember that the application of a method involves only one part of the SDM modeling process. The data preparation steps and evaluation of the output also need to be interpreted with care, and with reference to the method used.

4.1.5 Maxent, the approach chosen for this study

MAXENT is a software tool that was developed with species distribution modeling in mind using presence only data and pseudo absences or background information generated from within the study boundary, (Phillips et al. 2006; Phillips and Dudik 2008). This program comes from the machine learning discipline and has a probabilistic framework. It transforms variables (environmental predictors or covariates) into functions, and estimates the suitability of each cell according to what it can infer about the environmental conditions at the presence locations. To ensure that suitable areas across the surface agree with what is found at the presence locations, it sets constraints. In other words, MAXENT is based on the assumption that a close approximation of a species potential geographic distribution can be obtained by estimating a probability distribution of maximum entropy subject to the constraints imposed by the relationship between a series of observations and a set of environmental variables. Values range from 0 to 1, with higher values indicating higher likelihood of suitable conditions.

Out of all the methods available to model the distribution of a species in geographic space, MAXENT was chosen because it has proven to perform as well, or better than other methods when modeling distributions in the present (Elith et al 2006; Hernandez *et al.* 2006, Hijmans and Graham 2006; Phillips *et al.* 2006). It is also capable of extrapolating into past and future scenarios and has internal mechanisms that estimate uncertainty produced by conditions that are different to those used for training the model (Hernandez *et al.* 2006; Hijmans and Graham 2006; VanDerWal *et al.* 2009; Elith et al. 2010; Elith et al. 2011). Since it was launched in 2004, it has been used extensively in SDM studies within multiple contexts (see Table 4.2. for some examples). Furthermore, government agencies and non-government organizations have adopted this software for biodiversity mapping purposes (e.g., <http://www.prbo.org/>, <http://www.ala.org.au/>).

Table 4.2. Examples of published studies that have used MAXENT.

Source	Application	Location	Purpose/Description
Buermann et al. 2008	Methodological and conservation biogeography	South America	Explore how remotely sensed data (MODIS and QSCAT) can be used in SDM by modeling the potential distribution of 8 species across South America using MAXENT. They found that these sources of data are quite useful for SDM at regional and continental scales and can also be applied in predicting range shifts of species.
Carnaval and Moritz 2008	Biogeography, forest refugia, palaeoclimate modeling	Brazil	Modeled the distribution of the Brazilian Atlantic forest at present and under two past climates (6 and 21 kyr BP) using BIOCLIM and MAXENT to determine refugial areas and investigate areas with high species diversity. Both models were successful, although BIOCLIM slightly overpredicted the results for the present and MAXENT for 21 kyr BP. They believe in combining different modeling methods when predicting distributions.
Fløjgaard et al. 2009	Biogeography, forest refugia, palaeoclimate modeling	Eurasia	Used MAXENT to develop distribution models of seven rodents during the LGM, to test the northern refuge hypothesis (temperate and boreal species were distributed further north of the Mediterranean region during the cold and dry LGM period). Also developed the models with BIOCLIM and applied the threshold that maximizes sensitivity and specificity. For the present, the predicted distributions were successful although slightly better with MAXENT (using only two predictor variables). For the LGM, predicted areas from both algorithms agree. These support the northern refuge hypothesis.
Hernandez et al. 2008	Methodological and conservation biogeography		Examined the effect of sample size (ranging from 5 to 100) on model accuracy, by using four modeling methods: GARP, BIOCLIM, MAXENT, DOMAIN (Hernandez et al. 2006). Maxent was found to provide some of the most favorable results.

Table 4.2. (continued).

Source	Application	Location	Purpose/Description
Hijmans and Graham 2006	Species distribution model comparison		Given the known superiority of mechanistic models when predicting species distributions, the authors first predicted the potential distribution of 100 plant species for the present, a warmer future scenario, and a colder past scenario and then compared the output to those produced by four different SDM methods (GAM, MAXENT, BIOCLIM, DOMAIN) to evaluate their respective ability in predicting species distributions under different climates. MAXENT and GAM performed the best and produced results that were comparable to those produced by the mechanistic model. Nevertheless, MAXENT was found to slightly overpredict whereas the opposite was found with BIOCLIM.
Lizier et al. 2009	Species distribution modeling, Data quality	North America	Authors want to bring awareness to the fact that increasing data availability through museum, herbarium collections, and other sources needs to be handled with caution before using as observations in SDM since they can result in inaccurate distributions of species. They compare the distribution of the sasquatch to the black bear as an example using MAXENT.
Parolo et al. 2008	Conservation biology	Alps, Europe	Used MAXENT to model a threatened plant species for conservation management.
Penman et al. 2010	Conservation, climate change	New South Wales, Australia	Used BIOCLIM and MAXENT to predict the distribution of an endangered snake under future climate scenarios. Both methods predict that their distribution range will become quite reduced under the tested scenarios and identified current areas for conservation. This study provides evidence that climate plays a big role on the distribution of some species.
Phillips et al. 2006	Methodology of MAXENT	Global	The authors explain MAXENT, and compare it to GARP. Both algorithms were found to perform better than random and visually produced reasonable results, although MAXENT performed better in most tests.
Tittensor et al. 2009	Conservation biogeography, SDM in ocean (remote environments)	Global	Used MAXENT and ENFA to model the global distribution of suitable habitat of stony corals on seamounts. Although both distributions show similar distribution in geographic space, MAXENT outperformed ENFA in terms of AUC performance. Predicted distributions agree with current biogeographical knowledge.
Walker et al. 2009	Biogeography, phylogeography, refugia, palaeoclimate modeling	North America	Used MAXENT to model the potential distribution of a millipede to investigate refugial areas during the LGM suggested by genetic information. The present day distribution according to MAXENT was deemed satisfactory. For the LGM, the distribution suggested refugial areas that match the hypothesized refugial areas and results of the phylogenetic analyses. Contrary to the findings of Carnaval and Moritz (2008), MAXENT did not overpredict and if anything, underpredicted slightly.
VanDerWal et al. 2009	Historical refugia, palaeoclimate modeling, and biogeography	Northern Australia	Investigated how climatic fluctuations during the late Quaternary (Last glacial maximum or LGM at 18kyr BP, Pleistocene/Holocene transition or PHT at 7.5 kyr BP, Holocene climatic optimum or HCO AT 5 kyr BP) impacted the distribution of rain forests in the Australian Wet Tropics using SDM (MAXENT).

Other aspects that make it attractive include the following: It only requires ‘presence’ data (replaces absence with background information). It performs well when modeling low numbers of occurrence records (Hernandez et al. 2006). It is capable of incorporating and modeling the complex ways in which species relate to the environment by transforming variables into features (e.g., linear, quadratic, hinge, product, threshold). Because it is based on the principle of maximum entropy, the output consists of the optimal distribution (subject of course to the observations and variables implemented). It can use both continuous and categorical variables. It has a series of internal validation methods. The default parameters used to calibrate the model have been tested with large datasets and perform well (Phillips and Dudík 2008). Finally, it is relatively straightforward and can be implemented through a software tool that is free and available via the *world wide web* (<http://www.cs.princeton.edu/~schapire/MaxEnt>). There is also a growing community who uses this approach, so there are help files (MAXENT_help_v3.3.3.doc), a tutorial (Phillips 2010, MAXENT_tutorial_2010.doc), and a user group (<http://groups.google.com/group/MAXENT>) that can offer support.

4.2 Environmental parameters selected in this research

The predicted distribution area of a species is not a true representation of the species niche but rather a hypothetical space that the species could potentially inhabit. As mentioned above, it is affected by the modeling parameters (method applied, environmental parameters, information used as observations). Depending on the selection and quality of these parameters, the model can approximate the species’ distribution space in a more or less realistic way. It is crucial that careful consideration is given to the observations and environmental parameters chosen to run a model (Lozier et al. 2009).

As the old saying goes, *garbage in, garbage out*. The observations selected need to be carefully scrutinized, and an understanding of how the variables were derived is also important, as these will influence the output. This section describes the observations and variables used to create models of past vegetation in this research.

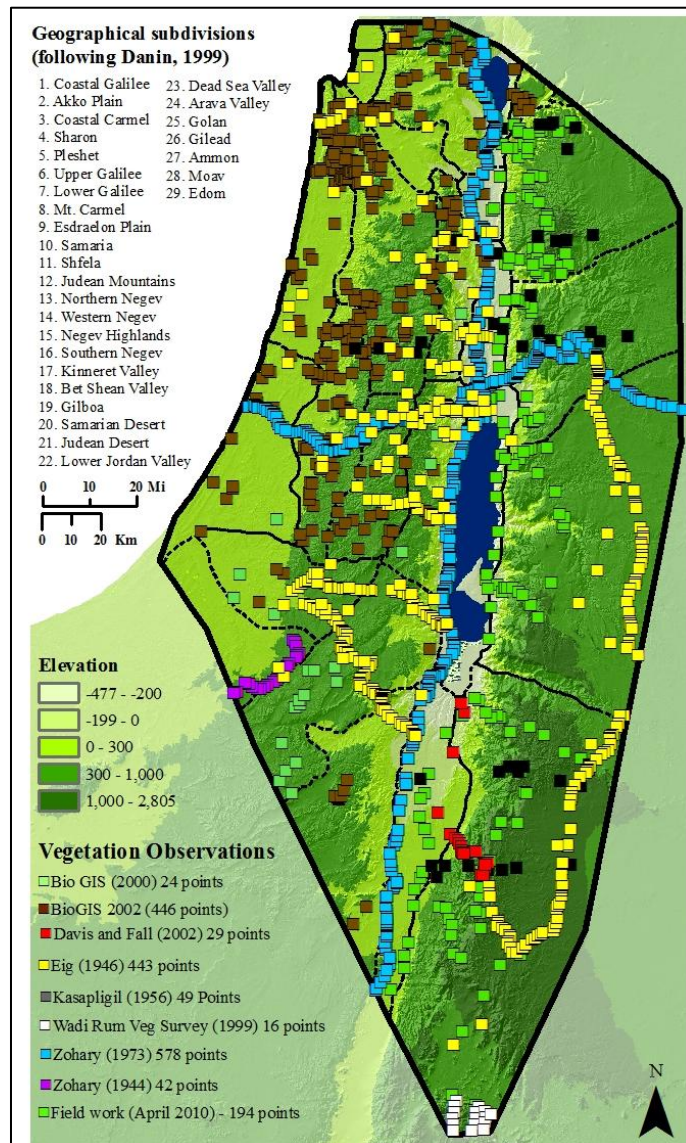
4.2.1 Creation of an observation database

As described in Chapter 2, the study area is located in a meeting zone of various plant geographical zones or territories (Table 2.1.). The more humid Mediterranean maquis and forests transition into Irano Turanian steppes and semi steppes, which in turn transition into the very dry and hot Saharo Arabian region that also contains pockets of tropical Sudanian vegetation. For the most part, the plants within these zones can be delineated by considering the major topographic and climatic factors that characterize the region. Each of these regions would have responded to climate changes by either expanding or contracting the geographic range they occupy at present.

A database of 1804 observations throughout the four plant geographical regions was created by conducting field work and compiling information from several sources (Map 4.1). Vegetation transects created at different times during the last 125 years were digitized (Davies and Fall 2001; Eig 1946; Kasapligil 1956; Post 1888; Qishawi et al. 1999; Zohary 1944; Zohary 1973). The oldest of these was carried out by Post, who spent three weeks collecting botanical samples and describing the flora of Moab, Gilead, and Hauran during the spring of 1886. Although he describes the general state of the vegetation and provides insightful comments in his daily reports, most locations proved difficult to locate with the precision needed for this study. Primary sources included the vegetation transects and intensive botanical surveys done by Michael Zohary in Palestine

(including the modern state of Israel and Jordan as well as the Palestinian territories) over a 45 year period starting in the 1920s (Zohary 1944, 1973). These cross much of the Middle East from the Black and Caspian Seas to Egypt and the Arabian Sea at a time when international borders were permeable in the 1920s and 1930s prior to the beginning of World War II. As such, they offer irreplaceable catalogs of the mosaic of natural and cultural landscapes prior to the widespread intensification and industrialization of irrigation agriculture and the energy intensive green revolution technology that characterizes the modern landscape of the region. Most of Zohary's research was undertaken in the lands of modern Israel, Jordan, Sinai and Lebanon which coincides with the research area.

In Jordan and the West Bank, botanical surveys done by Baki Kasapligil were also of primary importance (Kasapligil 1956). From 1954 to 1956, Kasapligil was assigned by the FAO to survey the state of the vegetation in Jordan and the West Bank, and make recommendations regarding management and conservation practices. As a result, the author produced several publications that include the locations of plants observed whilst surveying or conducting transects. In these transects (which he called profiles), he names the major vegetation types as well as provides information on the geology, elevation, and climate. In the present study, data from five of his east-west transects were digitized.



Map 4.1. Observations database.

The vegetation information in these transects was reported in one of two ways: vegetation reported at a specific place or vegetation found along a road section. They were digitized by identifying the places mentioned in the transect and retracing the route traveled. In this case, two digital files were used as reference: shapefiles of roads and

digital gazetteers of ‘place-names,’ which include comprehensive inventories of geographic locations along with their respective coordinates (<http://earth-info.nga.mil/gns/html/namefiles.htm>). First, the place mentioned was located and digitized as a point shapefile². The transect would then be completed by digitizing the road that connected the places identified in the transect³. Accompanying information found in the text would be used to ensure the transects were being digitized in the correct place. This information includes elevation and distances between places. For instance, the distance from point ‘a’ to ‘b’ would be measured and the elevation would be extracted from a 30m ASTER DEM. The transects that did not match these parameters were not included.

The observations included in the two most recent studies provided coordinates and were easily entered into the database (Davies and Fall 2001; Qishawi et al. 1999). Davies and Fall (2001) collected surface pollen and described the vegetation found along an elevation gradient (1700 to -300 m) that started near Petra in the plateau region and ended in the Wadi Araba. These observations were taken at 100 meter elevation intervals and include plants from all of the vegetation zones as they transition from species representative of juniper and oak forests into desert savannoid species (i.e., *Acacia tortilis*). In the Wadi Rum region, a floral survey was undertaken by Qishawi et al. (1999) for conservation purposes. Although the observations all fall within the Saharo Arabian Region, they are important because they provide additional points in the southern

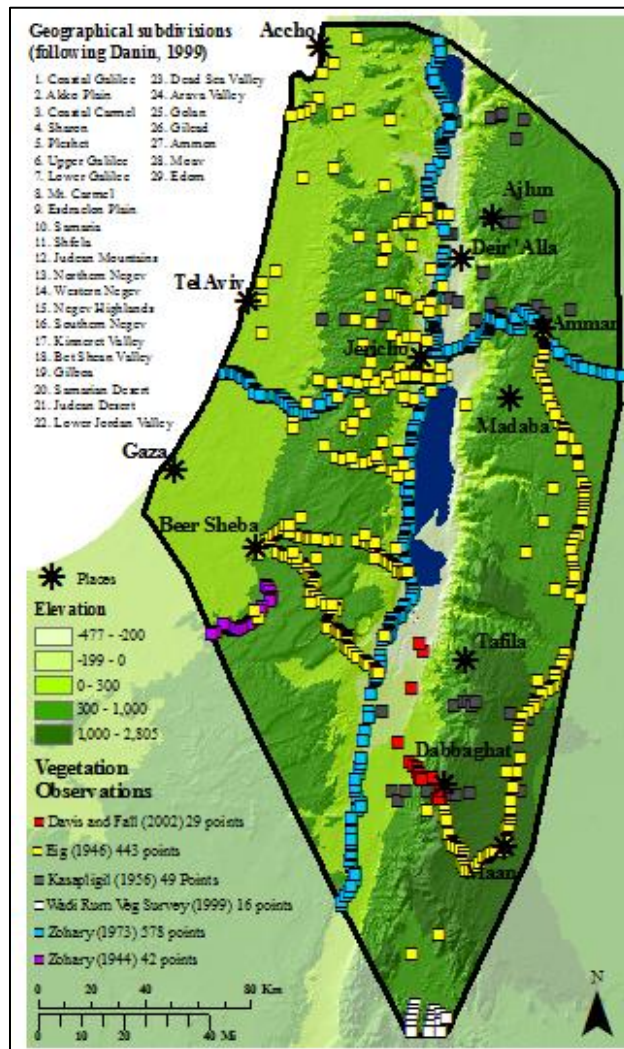
2 These received the name *VegTransects_pt*_LETTER The letter referred to a specific transect so for example *VegTransects_pt_d* refers to the transects done by Zohary in 1944 along the Sinai Peninsula.

3 These received the name *VegTransects_ln*_LETTER

portions of the study area and show the effect that latitude has on vegetation (precipitation declines and temperatures increase the further south you go).

Each location in the shapefile would then be attributed with a unique identifier which links to a look up table (LUT) that includes information regarding the vegetation found in these transects. In some cases, additional information was also provided such as substrate, slope, and condition of vegetation (anthropogenic influence). This data was also entered into the LUT. In total, a database with over 1,200 observations was created from these sources, with information of dozens of plant species (e.g., *Ziziphus spina-cristii*) and species associations (e.g., association of *Quercus calliprinos-Pistacia palestina*). Map 4.2 shows all the historical observations.

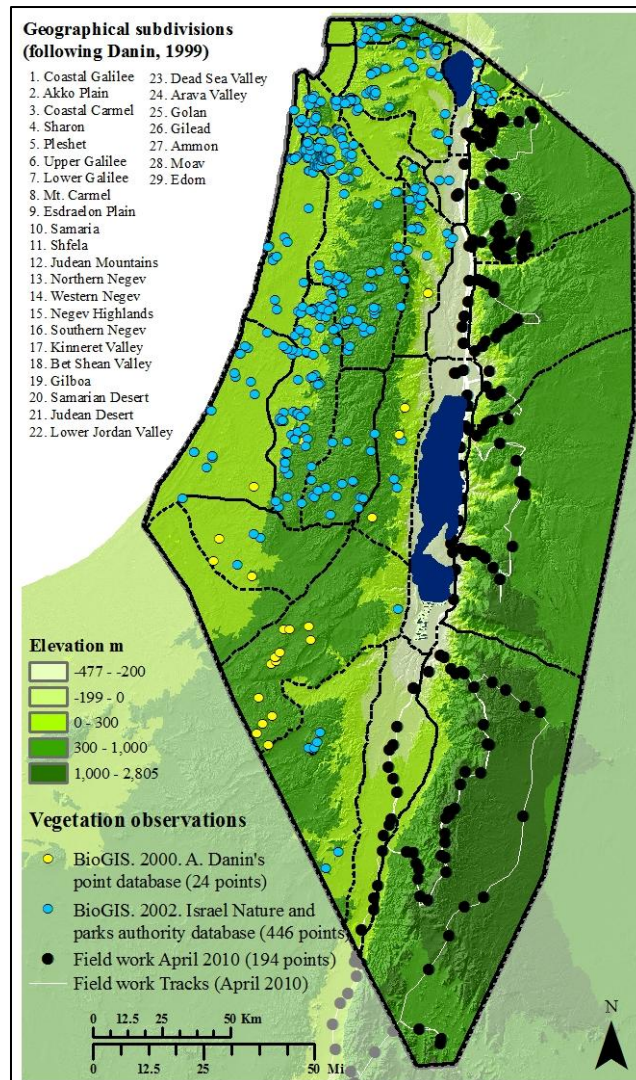
Nevertheless, after visually reviewing the observations, there were still a few areas that had large gaps (i.e., coastal plain). To counter this, about 470 observations that originate from the Israel Biodiversity Information System were incorporated (BioGIS 2000 and BioGIS 2002). This database includes thousands of records of plants and animals in Israel and the West Bank obtained from museum and herbarium collections, as well as from surveys done by academic institutions, governments, and non government organizations (BioGIS, the Israel Biodiversity Information System). The database can be accessed online (<http://www.biogis.huji.ac.il/>) and allows users to query different species and obtain information like coordinates, date of collection, and database source.



Map 4.2. Historical observations.

To complement the historical observations, fill in remaining gaps, and assess the accuracy of some of the digitized historical observations, field work was conducted during the Spring of 2010 by this researcher, her advisor Patricia L. Fall, and an assistant and colleague Elizabeth Ridder. During four weeks, a series of latitudinal transects from the Rift Valley to the plateau were conducted. Some time was also spent in the forested areas of the northern and southern highlands, delimiting the boundaries of the existing

forest areas and obtaining additional observation points. Overall, 194 additional observations were collected in Jordan (Map 4.3). This allowed valuable information regarding the extent and transition areas of the different plant geographical territories to be obtained. In addition, some of the historical transects and observations done by Zohary and Eig in areas that had not been converted to other uses were verified.



Map 4.3. Observations gathered from field work and the BioGIS 2000; 2002 database.

4.2.1.1 Selection of indicator species

To model plant geographical territories (from here on referred to as plant geographic associations) at present and throughout the Holocene, indicator species for each of the plant geographical territories were sourced from the literature (Al-Eisawi 1996; Danin 1988, 1999; Eig 1931/32, 1938, 1946; Kasapligil 1956; Zohary 1973). Tables 4.3 to 4.7 list the species/associations/alliances that are indicative of the major phytogeographical or plant geographical territories. Furthermore, Map 4.4 shows how the observations fall into these categories.

Table 4.3. Indicator species of the Mediterranean Zone.

Region or Zone	Species /Association/Alliance	Description
MEDITERRANEAN This territory has been the most affected by human disturbance. The best preserved remnants are found in the northern highlands in the Golan and Gilead regions.	Association of <i>Pinus halepensis</i> - <i>Hypericum serpyllifolium</i> Association of <i>Quercus callirpinos</i> - <i>Pistacia palaestina</i> Association of <i>Ceratonia Siliqua</i> - <i>Pistacia Lentiscus</i>	Forest and Maqui Represents climax vegetation that consists of pine and oak forests (as well as a few other species like pistacia and juniper).
	Association of <i>Quercus ithaburensis</i> – <i>Pistacia atlantica</i> Association of <i>Pistacia atlantica</i> - <i>Crataegus azarolus</i>	
	Association of <i>Cistus villosus</i> & <i>Cistus salvifolius</i> , <i>Calycotome villosa</i>	Garigue Shrub and dwarf shrub associations.
	<i>Echinopetum Blancheani</i> (also known as <i>Echinops polyceras</i> ; <i>E. spinosus</i> ; <i>E. blancheanus</i>) <i>Sarcopoterium spinosi</i> <i>Thymetum capitati</i> or <i>Coridothymus capitatus</i> <i>Ononidetum Natricis</i> Assoc. of <i>Carthamus tenuis</i> - <i>Ononis leiosperma</i> <i>Thymelaea hirsute</i>	Batha Represents the most degraded level of Mediterranean vegetation

Table 4.4. Indicator species of the Irano Turanian Zone.

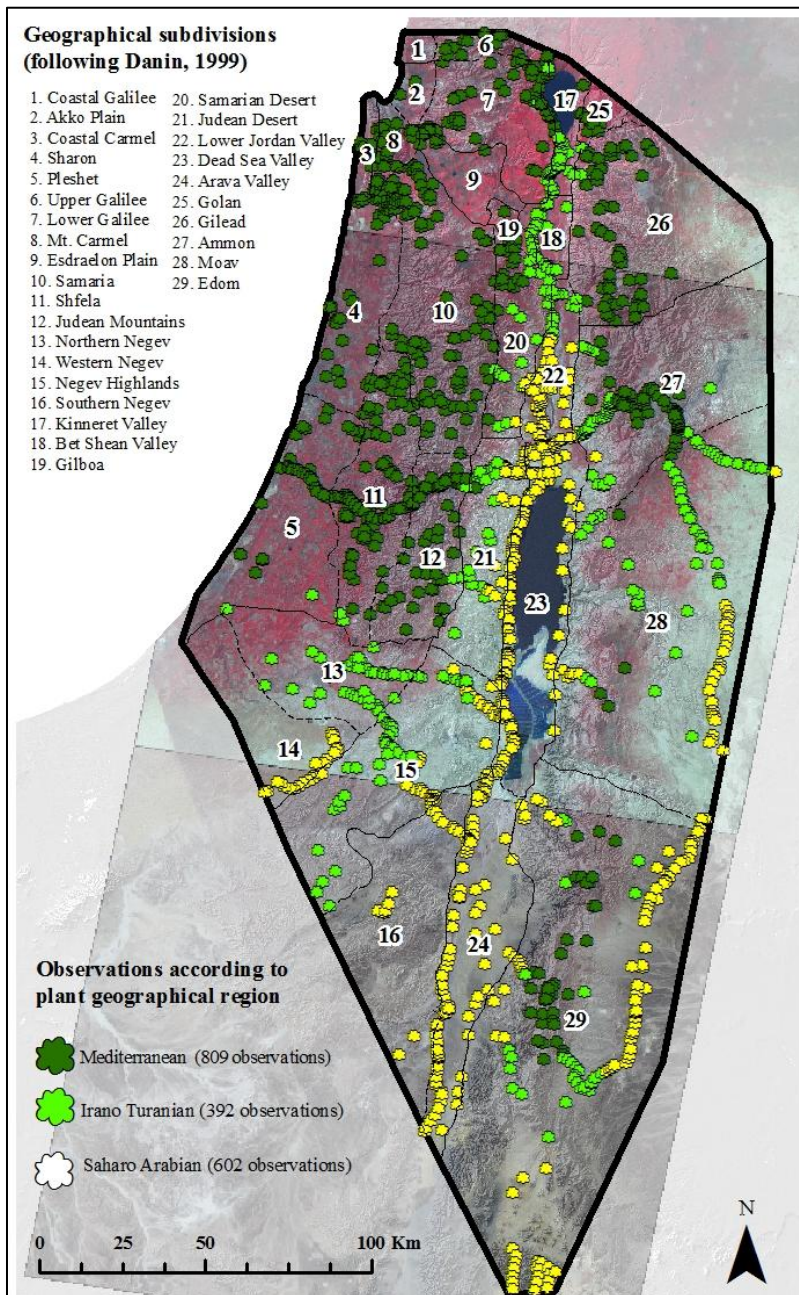
Region or Zone	Species /Association/Alliance	Description
<p>IRANO TURANIAN</p> <p>This territory forms a sort of belt in between the Mediterranean and Saharo Arabian territories. As you approach either of these, transition zones are found were species from various regions are found intermixed.</p>	<p>Artemision Herbae albae alliance <i>Artemisia sieberi</i> (Syn. <i>Artemisia Herbae alba</i>)</p> <p>Haloxylonion articulate alliance Assoc. of <i>Anabasis Haussknechtii-Poa sinaica</i> Assoc. of <i>Haloxylon articulatum</i> (Syn. <i>Haloxylon scoparium</i> and <i>Hammada scoparia</i>) - <i>Salsola villosa</i> Assoc. of <i>Anabasis Haussknechtii-Plantago Coronopus</i></p> <p>Association of <i>Salsola vermiculata-Hammada scoparia</i> (<i>Hammada scoparia</i> is also known as <i>Haloxylon articulatum</i> and <i>Haloxylon scoparium</i>)</p> <p><i>Ziziphus lotus</i>, <i>Astragalus spinosum</i></p>	<p><i>Artemisia herba alba</i> is one of the most common shrubs of the Irano Turanian steppes.</p>
	<p>Noeion mucronatae alliance <i>Noaea mucronata</i></p>	
	<p>Retamo-Phlomion brachyodontis alliance <i>Phlomidetum brachyodontis</i>, Assoc. of <i>Phlomis brachyodon-Blepharis edulis</i>, <i>Retama Duriaei-Blepharis edulis</i>, <i>Retama Duriaei-Rhus oxyacanthoides</i></p>	<p>Found in the transition zones into Saharo Arabian territories and depending on the location.</p>
	<p><i>Noeion mucronatae</i>, <i>Haloxylon articulatae</i>, and <i>Artemision Herba albae</i>; <i>Suaedion asphalticae</i>, <i>Chenoleion arabicae</i>, <i>Gymnocarpion fruticosi</i>, and <i>Zygophylletum dumosi</i>; <i>Salsoletum villosae</i>; <i>Anabasis articulate-Zilla myagroides</i>; <i>Reaumurietum palaestinae</i>; <i>Atriplicetum palaestinae</i>.</p>	
	<p><i>Artemisia herba-alba</i>, <i>Sarcopoterium spinosum</i>, <i>Retamo-Phlomion brachyodontis</i></p>	

Table 4.5. Indicator species of the Sudano Decanian Zone.

Region or Zone	Species /Association/Alliance
<p>TROPICAL SUDANO DECANIAN</p>	<p>Acacion tortilidis palaestinae alliance Acacietum tortilidis palaestinum Association Anabasetosum articulate subassociation Haloxylonetosum salicornici subassociation <i>Zizyphus spina-Christi-Balanites aegyptiaca</i> Association <i>Ziziphus spina-Christi-Moringa aptera</i> Association <i>Tamarix nilotica</i>, <i>Ochradenus baccatus</i>, <i>Ziziphus spina Christi</i>, <i>Balanites aegyptiaca</i>, <i>Calotropis procera</i>, <i>Fagonia mollis</i>, <i>Retametosum Roetami</i></p>

Table 4.6. Indicator species of the Saharo Arabian Zone.

Region or Zone	Species /Association/Alliance	Description
<p>SAHARO ARABIAN</p> <p>Along its northern extent, this region is mainly found in the Rift Valley (Lower Jordan Valley). Also mixes with riparian vegetation from the Jordan River and adjacent wadis and rivers as well as saline vegetation. South of the Dead Sea, the Saharo Arabian region expands longitudinally. There is also sand dune vegetation as well as tropical Sudanian vegetation surrounding springs.</p>	<p>Zygophyllion dumosi alliance <i>Zygophyllion dumosi</i></p>	<p>According to Eig (1946), this represents the main alliance of the Saharo-Sindian territory. It is found on several surface types: gravel, compact and soft soil.</p>
	<p>Gymnocarpion fruticosi alliance <i>Gymnocarpetum fruticosi</i> (<i>G. decander</i>) <i>Gymnocarpus fruticosus-Zilla spinosa</i> assoc.</p>	<p><i>Gymnocarpus fruticosi</i>, <i>Suaeda asphaltica</i>, and <i>Chenoleion arabicae</i> dominate in the mountains of the Lower Jordan Valley</p>
	<p>Chenoleion arabicae alliance <i>Erodium glaucophyllum-Herniaria hemistemon</i> assoc. <i>Chenoleetum arabicae</i> <i>Chenolea arabica-Salsola villosa</i> assoc.</p>	
	<p>Suaedion asphalticae alliance <i>Suaedetum asphalticae</i></p>	<p>Eig subdivided this association into two: <i>sub-irano-turanicum</i> and <i>saharo-sindicum</i>. The first is found in the transition zone into Irano Turanian territory. In the second, it is usually found amongst dwarf shrubs like <i>Salsola vermiculata</i> spp. <i>villosa</i>, <i>Zygophyllum dumosum</i>.</p>
	<p>Anabasion articulata alliance (<i>Anabasis articulata-Zilla spinosa</i> assoc.) <i>Altriplicetum palestinae</i> <i>Reaumurietum palaestinae</i> <i>Halogetonetum alopecuroidis</i> <i>Haloxylon articulatum</i> <i>Anabasis articulata - Noea mucronata</i> Association <i>Suaeda asphaltica</i></p>	
	<p>Salsolion villosae alliance <i>Salsoletum villosae</i> <i>Salsola villosa-Gymnocarpus fruticosus</i> assoc. <i>Salsola villosa-Stipa tortilis</i> assoc. <i>Anabasis articulata-Notoceras bicornis</i> assoc.</p>	<p>Abundant in the Judean Desert, Lower Jordan Valley (northwards from the mid section) and the Negev. Can also be found in transition into Irano Turanian territory.</p>



Map 4.4 Observations shown by plant geographical regions.

In addition to assigning the observations to plant geographic associations, they were also subdivided into vegetation categories according to the dominant plant association. For the Mediterranean association the categories include pine forests; mixed evergreen oak maquis and forest; mixed deciduous oak maquis and forest; open forests of carob and pistacia; coastal vegetation; and forests with juniper, cyprus, oak, and pistacia. The Irano Turanian association mainly includes the categories Mediterranean savannoid, semi steppe batha, and shrub steppe. The Saharo Arabian association includes the categories stony desert vegetation, desert savannoid, and desert scrub. Figures 4.1 to 4.16 provide a description of each of these categories, a breakdown of the indicator species and sub-associations within each, and a map showing the observations that fall into each category. The description is informed by several sources including Al-Eisawi 1996, 1998; Danin 1988, 1999; Eig 1946; Kasapligil 1956; Zohary 1944, 1973, as well as the Flora of Israel Online website (Danin 2006). <http://flora.huji.ac.il>).

Description

This category represents the climax Mediterranean vegetation. It is commonly found with *Q. calliprinos* trees, which show secondary succession.

It is found at elevations usually over 700 m in both calcareous and rendzina soils and in wetter areas (annual precipitation in these areas is between 500 to 700 mm). East of the Jordan River it is found in the Gilead and Ammon regions.

Pure stands of *Pinus halepensis* are very few (Dibbin forest near Jerash). Mixed stands with *Q. calliprinos* are found between Salt and Ajlun, although Kasapliligil (1956) reported some further south around Fuheis. West of the Jordan River it is found in the wetter parts. This type of forest is highly susceptible to disturbance occurring from fires and heavy snow.

High trees

Pinus halepensis

Low trees/shrubs

Arbutus andrachne, *Quercus calliprinos*,

Pistacia palaestina

Low shrubs/bushes

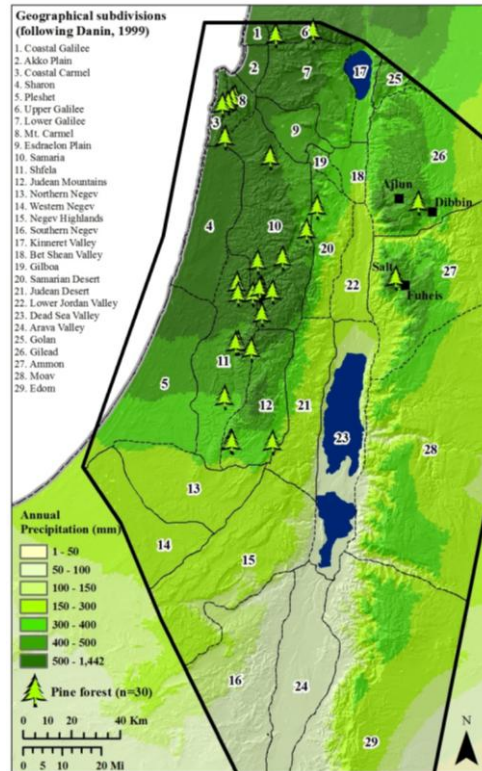
Calycotome villosa, *Cistus villosus*,

Cistus salvifolius



Pinus halepensis, *Quercus calliprinos*, *Arbutus andrachne* in Dibeen National Forest. Photo taken by Soto-Berelov.

Observations



Edge of Dibeen National Forest. *P. halepensis* mixed with *Q. calliprinos* and *P. palaestina*. Photo taken by Soto-Berelov.

Figure 4.1. Distribution of observations that fall into the pine forest subdivision.

Description

The evergreen *Quercus calliprinos* is the main constituent of this group. A frequent companion in the north is *Pistacia palaestina*.

This category is usually found at elevations higher than 500 m on calcareous rocks (hard limestone or dolomite) with terra rossa soil. West of the Jordan River it is found in the Upper Galilee, on the mountains of Judea, Carmel, Galilee, at the foot of Mt. Hermon.

East of the Jordan River, it is found in two latitudinal belts. In the northernmost extension it is found between 600 to 1,250 m and 500 to 700 mm annual precipitation (Amman-Salt-Jerash-Ajlun area). Interrupted stands stretch from Wadi Es-Sir (near Amman) until Deir Abu Said. It is also found on volcanic rocks (basalt with soils of high phosphorous content) and cones in the Golan region.

In the southern highlands, *Q. calliprinos* is found at higher elevations and dryer conditions (1,100 to 1,700 m and 200 to 300 mm respectively) in the western slopes of the mountains between Shaubak and Tafila. Stands of this tree are also found further south around Dabbagat. These represent the southernmost extent of *Q. calliprinos* maquis.

Dominant species:

Assoc. *Quercus calliprinos*-*Pistacia palaestina*, *Pyrus syriaca*, *Crataegus azarolus*, *Ceratonia siliqua*, *Pnus halepensis*

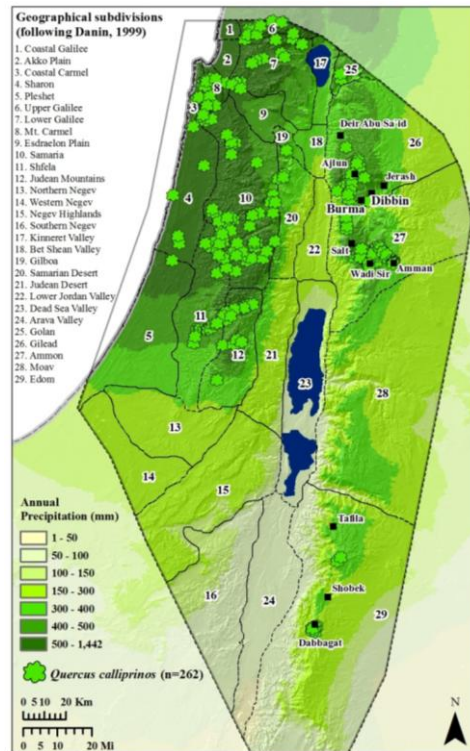
Additional species:

Rhamnus lycioides (Found on drier stands)



Quercus calliprinos forest in the Aljun woodland reserve. Photo taken by Soto-Berelev.

Observations



Open *Q. calliprinos* stand near Dabbagat. Foto taken by Soto-Berelev.

Figure 4.2. Distribution of observations that fall into the mixed evergreen oak maquis and forest subdivision.

Description

This category is represented by the deciduous *Quercus ithaburensis* oak. It is found on calcareous rocks with chalky ground (hard limestone with red or brown soils) in the Lower Galilee, Golan, and Gilead regions at elevations lower than 700 m and in areas that receive between 400-500 mm annual precipitation.

Dominant species:

Quercus ithaburensis, *Styrax officinalis*
There are also large stands in the Hula and Dan Valleys. In the past, this type of forest dominated the Sharon Plain. Zohary mentions remnants of *Q. ithaburensis* and *Pistacia atlantica* in this area. This is reflected in a few observations that fall within this coastal plain.

Kasaplilgil (1956) reports that in Jordan, the area covered by this type of vegetation extends from around El-Bahhatb to the Yarmouk valley in the north. Between the Wadi Ziglab and its southernmost extent, it is intermixed with *Q. calliprinos*. South of the Zerqa River, there is a stand that extends between El-Aluk and Sukhner. The last represents the easternmost extent of this type of forest.

In the Golan region around Um Qeis it is found at elevations lower than 500 m on volcanic rocks (basalt).

The accompanying species are dictated by temperature and moisture (rainfall).

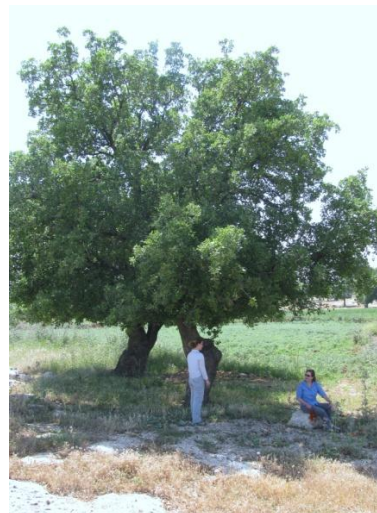
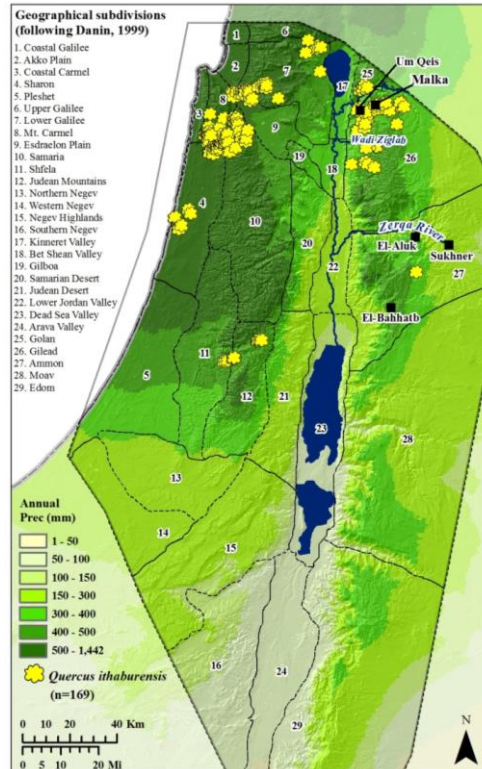
Accompanying species in more moist places (forests in Um-Qeis and Malka)

Pistacia palaestina, *Styrax officinalis*,
Amygdalus communis, *Ceratonia siliqua*
(Found on the transition belt of the *Q. ithaburensis* and *Q. calliprinos* forests)

Accompanying species in more xeric regions (forests in El-Aluk near Jerash and near transition zone Medit-IT)

Amygdalus communis, *Pistacia atlantica*,
Ramnus palaestinus, *Retama raetam*

Observations



Resting under the shade of a *Q. ithaburensis* tree, near Um-Qeis. Photo taken by Soto-Berelov.

Figure 4.3. Distribution of observations that fall into the mixed deciduous oak maquis and forest subdivision.

Description

This division refers to degraded Mediterranean forests (batha and garigue). If left undisturbed, they would presumably regenerate to maquis and forest. These observations were used when modeling the Mediterranean plant geographical association.

Dominant species:

Rhamnus palaestinus

Carthamus tenuis

Sarcopoterium spinosum

Ononis natrix

Ballota undulata

Noea mucronata

Calycotome villosa

Varthemia iphionoidea (syn.

Chiliadenus iphionoides)

Artemisia herba-alba

Poa bulbosa

Tymus capitatus



Ononis natrix. Photo taken by Soto-Berelov.

Observations

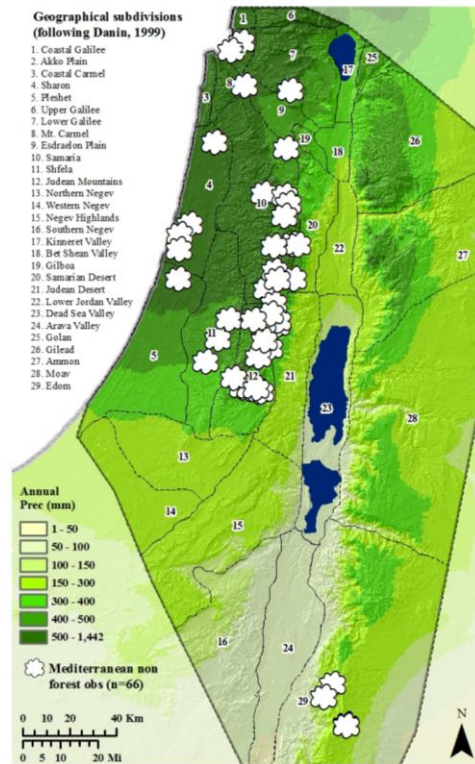


Figure 4.4. Distribution of observations that fall into the degraded forest (Mediterranean non-forest) subdivision.

Description

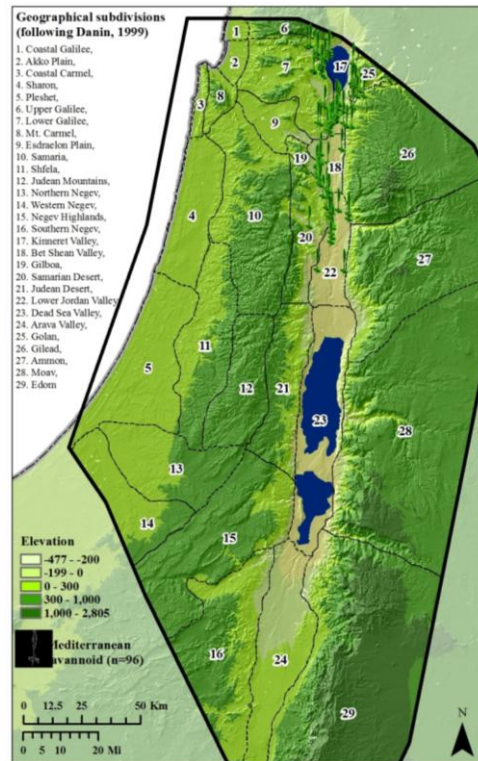
In the Rift Valley about halfway between the Dead Sea and the Sea of Galilee, there is a wet savannoid type vegetation dominated by *Ziziphus spina Christi* and *Ziziphus lotus*. Grasses like wild wheat, wild barley, and wild oats are also common.

This type of vegetation is commonly found on basalt rocks with phosphorous rich soils in southeastern Galilee and on slopes near the Sea of Galilee. It extends onto the sedimentary rocks of the Samarian desert.

East of the rift valley, it is found on west facing slopes in Gilead below the *Q. ithaburensis* belt and on the steep topography surrounding the rift valley from the north of Jericho onto the northern section of the Sea of Galilee.

Because the Mediterranean savannoid vegetation is found on the moist floodplain of the Jordan River and immediate surroundings, it has been heavily impacted by agricultural land use. During our field work, the main indicators we saw of this vegetation type in the Bet Shean and Lower Jordan Valleys were spread out *Ziziphus spina Christi* and *Ziziphus lotus* trees. The area immediately south of Lake Kinneret is surrounded by these grasses. Unfortunately, we could not take photographs due to heavy surveillance in the region.

Observations



Dominant grasses:

Triticum dicoccoides (wild wheat)
Avena sterilis (wild oat)
Hordeum spontaneum (wild barley)

Stipa capensis, *Ziziphus lotus*
Ziziphus spina Christi (scattered)

Z. spina-christi trees are also found in the coastal plains of the Pleshet region. Although these alluvial coastal plains are used intensively for irrigated agriculture, there are still scattered remnant trees.

Figure 4.5. Distribution of observations that fall into the Mediterranean savannoid (grasslands) subdivision.

Description

Zohary (1959: 285) described the Ceratonio-Pistacion alliance as having a ‘park-like’ appearance with scattered carob trees and *Pistacia lentiscus* shrubs. He subdivided it into three categories, all of which are found west of the Jordan Rift Valley. Two of these (*Ceratonieto-Pistacietum lentisci typicum* and *Ceratonieto-Pistacietum lentisci orientale* associations) are found on the foothills of the Judean mountains from sea level up to around 300 m. They form a belt (see map below) around these mountains in which *Quercus calliprinos* and *Pistacia palaestina* represent the climax Mediterranean association (these trees are sometimes found within the carob and pistacia maquis and vice versa). The first association is the most abundant. It is found along the slopes that descend into the alluvial valleys (extending from around Duweima in the south into the frontier with Lebanon in the north). The second association penetrates into the Irano Turanian region and as a result, species like *Ziziphus lotus*, *Amygdalus communis*, and *Pistacia atlantica* are also found.

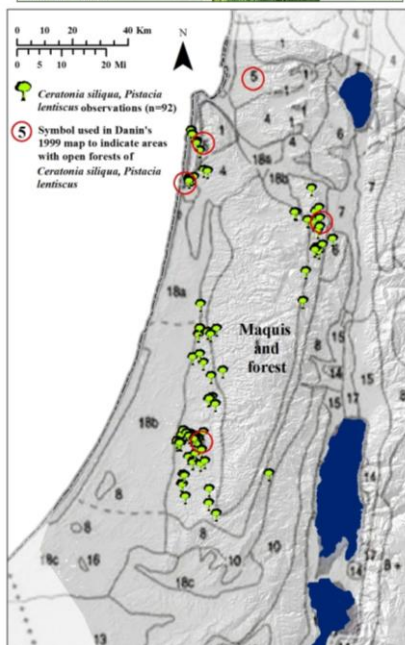
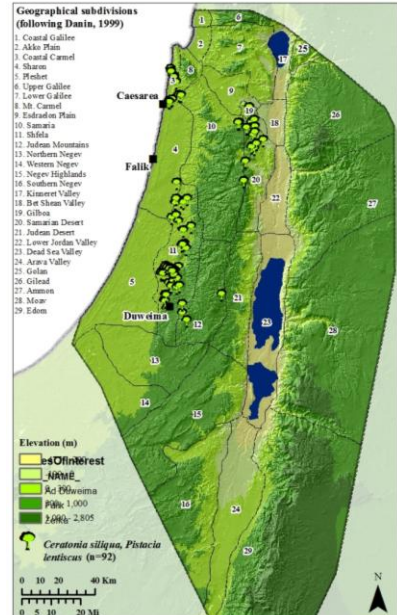
The third association (*Ceratonia siliqua-Pistacia lentisci arenarium*) is found on the coastal plain in the Sharon region between **Wadi Falik and Caesarea** on sandy soils (Zohary and Orshan 1959). Remnants of this association further north and south indicate that it was more extensive in the past (Zohary and Orshan 1959).

This association is more drought and heat resistant than the *Q. calliprinos*. The environmental requirements include the following:

elevations between 0 to 300 m, annual rainfall between 400 to 1,000 mm, relatively high winter temperatures, and various soils like terra rossa, rendzina, and kurkar (calcareous sandstone in the hills around Mt. Carmel between Athlit and Kefar Zerka) (Zohary and Orshan 1959).

This category is missing in Jordan, except for some scattered carob trees in the deciduous forest in Gilead and area where it transitions into the evergreen forest.

Observations



Danin's 1999 vegetation map of Israel, Sinai and Jordan showing area classified as open forests of *Ceratonia siliqua* and *Pistacia lentiscus*. Study observations are overlain on the map. The map was georeferenced by Soto-Berelov.

Figure 4.6. Distribution of observations that fall into the open forests of carob and pistacia.

Description

In the Edom region of the southern highlands, there are open forests dominated by *Juniperus phoenicea*. These are sometimes accompanied by oak, cyprus, and pistachio. They stretch from Tafila to Ras An-Naqab, and predominate along the western slopes at elevations that range between 850 to 1,500 m (although scattered trees have been found in wind protected areas at elevations as low as 600 m and higher than 1,500 m). Despite the presence of these Mediterranean trees, the understory is typically Irano Turanian (*Artemisia herba alba*, *Noaea mucronata*).

Trees that accompany juniper or are also found in this area:

Q. calliprinos, *Pistacia atlantica*, *Cupressus sempervirens*, *P. khinjuk*, *Ceratonia siliqua*, *Olea europaea*, *Arbutus andrachne*, *Ficus carica*, *F. pseudosycamoros*

Shrubs:

Artemisia sieberi, *Crataegus azarolus*, *Noaea mucronata*, *Astragalus*, *Rhamnus palaestinus*, *R. lycioides*, *R. disperma*, *Thymelaea hirsute*, *Amygdalus korschinskii*
On sandstone, juniper can be found by itself or accompanied by *P. atlantica*.

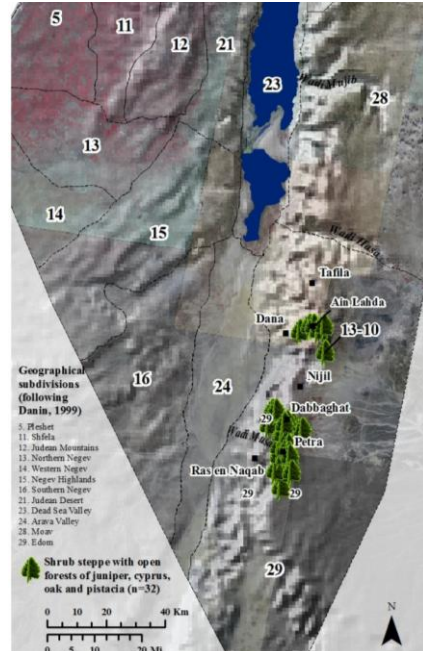
There is a stand of juniper and cyprus near Ain Lahda that is believed to be over 1,000 years of age.

In the Dana-Petra region, juniper stands are found on fissured limestone, chalk, basalt and on smooth sandstone formations. This region also contains the richest assemblage of relict Mediterranean species in all of the Near East, a **refugium that would have expanded during wetter times**.

Q. calliprinos is sometimes found with juniper on calcareous soils at elevations higher than 1300 m (e.g., AL-Illami, near Ad-Dabbaghat, and AL-Hisha south of Nijil, Shaubak).

Pistacia atlantica is found in elevations between 500-1600 m. There is a stand near Ad-Dabbaghat that is estimated to be 500 years old.

Observations



View of Dana Canyon with stand of juniper trees, taken at point 13-10 by Soto-Berelov.



Juniperus phoenicea trees near Petra. Photo taken by Soto-Berelov.

Figure 4.7. Distribution of observations that fall into the open forests with juniper.

Description

This subdivision stretches along the boundary of the Mediterranean zone where annual rainfall is 300-400 mm.

Sarcopoterium spinosum is unable to compete with taller plants during succession (due to lack of shade). However, in semi steppes it has no competition.

Artemisia sieberi or *Artemisia herba-alba* and *Noaea mucronata* dominate steppe areas in the Negev, Sinai, and Jordan.

Artemisia herba-alba, *Sarcopoterium spinosum*, and the *Retamo-Phlomis brachyodontis* associations are present in transition zones into the Mediterranean territory.

Dominant species:

Artemisia sieberi or *Artemisia herba-alba* (see description)

Noaea mucronata (see description)

Calycotome villosa

Euphorbia hierosolymitana Boiss

Ononis natrix

Rhamnus palaestinus

Capparis spinosa

Retama raetam (see transition)

Ziziphus spina christi

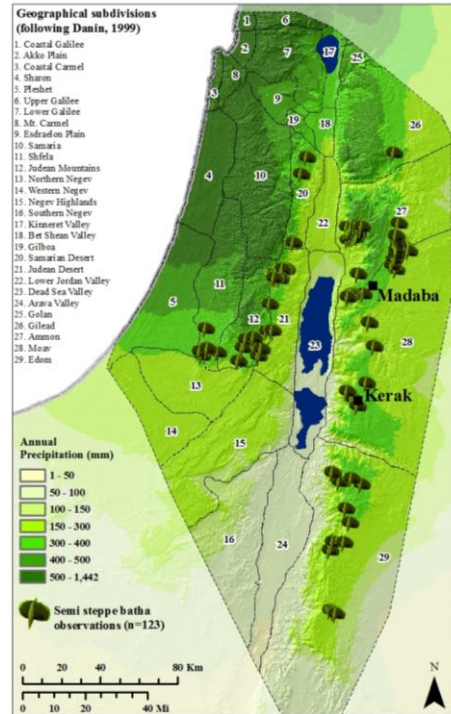
Sarcopoterium spinosum (see description)

Rhus tripartita



Stand of *Sarcopoterium spinosum* and *Noaea mucronata* outside of Madaba. Photo taken by Soto-Berelov.

Observations



Orchards and grasses amidst semi steppe batha with *Crataegus azarolus*, *Sarcopoterium spinosum*; *Euphorbia hierosolymitana*. Photo taken near Kerak by Soto-Berelov.

Figure 4.8. Distribution of observations that fall into the semi steppe batha subdivision.

Description

Semi shrubs predominate in areas that receive annual rainfall between 100-300 mm (parts of the Negev Highlands, Judean Desert, Edom, Amon, Lower Jordan Valley, Bet Shean Valley).

Dominant species:

Retama Duriaei, *Phlomis brachyodon*, *Asphodelus microcarpus*, *Artemisia sieberi* or *Artemisia herba-alba*, *Noaea mucronata*, *Gymnocarpus fruticosi*, *Salsola jordanica*, *Anabasis articulate*, *Halogeton alopecuroides* (syn. *Agathopora alopecuroides*), *Poa sinaica*

The following broad patterns can be inferred in this category:

Species common in lower elevations include *Acacia raddiana*, *A. Pachyceras*, *Tamarix nilotica*, *T. aphylla*

Some species appear in a contracted way on springs (limestone hills in western Sinai and sandstone hills in southwestern Jordan):

Phoenix dactylifera, *Nitraria retusa*, *Juncus arabicus*, *Phragmites australis*, *Cressa cretica*

Can also find Mediterranean plants like *Sarcopoterium spinosum* in the Negev.

On chalk and marl derived soils: *Salsola vermiculata*, *Bassia (Chenolea) Arabica*

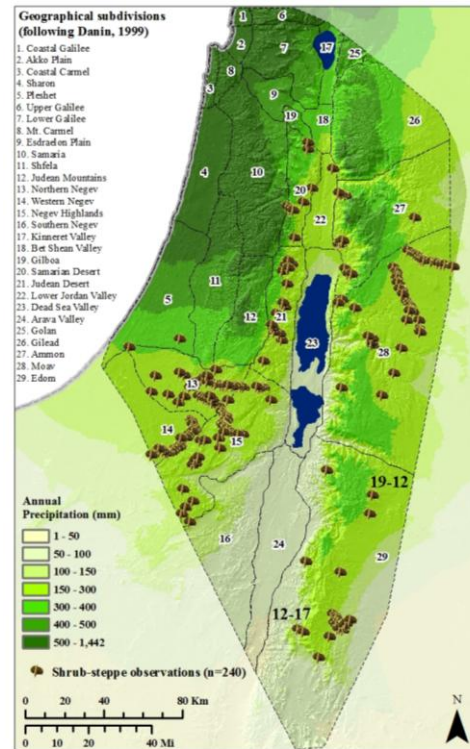
On loess derived soils *Anabasis syriaca* (syn. *Anabasis haussknechtii*), *Haloxylon scoparium* (syn. *Hammada scoparia*)

In wadis on limestones: *Retama raetam*, *Achillea fragrantissima*, *Atriplex halimus*



Artemisia herba alba, *Noaea mucronata*, *Anabasis articulate*. Photo taken near observation 19-12 by Soto-Berelov.

Observations



Bedouin camp amidst extensively grazed shrub steppe landscape. Photo taken at observation 12-17 by Soto-Berelov

Figure 4.9. Distribution of observations that fall into the shrub steppe subdivision.

Description

Desert is defined as those areas that receive less than 200 mm annual precipitation. It essentially is found within the Saharo Arabian and Sudano Decanian zones, although it penetrates slightly into the Irano Turanian zone (shrub steppe subdivision).

Vegetation in these areas is mainly determined by water availability, which in many instances translates to the location of wadis. The geology and soils present can also influence the vegetation. For instance, porous rocks that have high water infiltration rates can provide the necessary water for plants that would otherwise exist in areas that receive over 500 mm annual rainfall (Danin 1999).

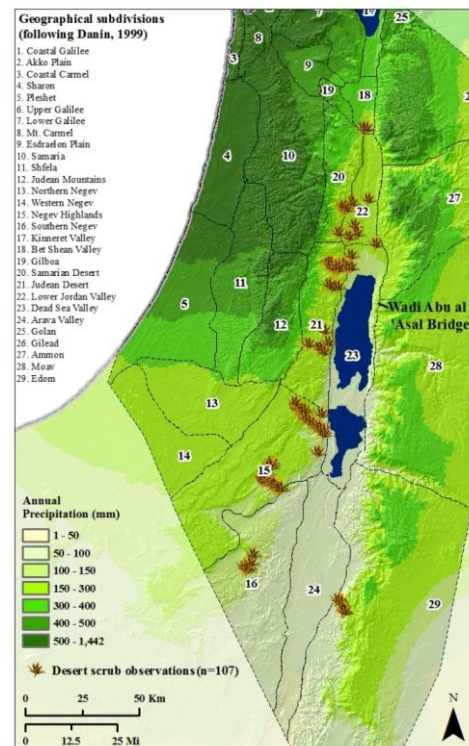
Vegetation is found in contracted (along wadis) or diffused patterns. Diffused means that plants are spread out and commonly found on slopes and depressions.

Anabasis articulata, *Zygophyllum dumosum*. In the transition zones into Irano Turanian territories and depending on the location, the following associations are also commonly found: *Noeion mucronatae*, *Haloxylon articulatae*, and *Artemision Herba albae*; *Suaedion asphalticae*, *Chenoleion arabicae*, *Gymnocarpion fruticosi*, and *Zygophylletum dumosi*; *Salsoletum villosae*; *Anabasis articulata-Zilla myagroides*; *Reaumurietum palaestinae*; *Atriplicetum palaestinae*.

On chalk and marl outcrops, diffused vegetation where *Suaeda asphaltica*, *Salsola tetrandia*, and *Haloxylon negevensis* can also be found. *Zygophyllum dumosa*. (Soto-Berelev)



Observations



Rocky landscape near Wadi Abu al 'Asal bridge. Very scarce vegetation, mostly along drainages. Species identified in the area include Tamarisk, *Phoenix dactylifera*, Oleander, *Salsola*, Plantago, *Lycium*. Photo taken by Soto-Berelev

Figure 4.10. Distribution of observations that fall into the desert scrub vegetation and desert wadi vegetation (Al-Eisawi refers to this as Run-off hammada) subdivisions.

Description

This category is an extension of the desert scrub and desert wadi vegetation. It was separated into a new category because it marks the beginning of the Eastern Desert where the surface is very gravelly. We adopted this term from Kasapligil, whereas Danin refers to it as desert/sand vegetation and Al-Eisawi as Hammada vegetation, which is in turn divided into run-off hammada, pebble and gravel hammada, sandy hammada.



Example of sandy hammada. Vegetation mostly in depressions and wadis. Photo taken on the Desert Highway at sample 19-10.



Example of pebbly hammada. Fairly barren landscape. Photo taken by Soto-Berelev just off the Desert Highway at sample 19-11.

Observations

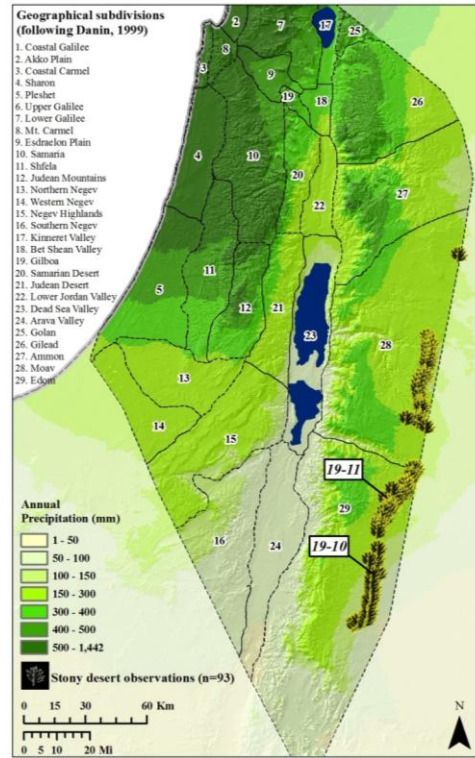


Figure 4.11. Distribution of observations that fall into the stony desert subdivision.

Description

This type of vegetation is found on inland and coastal dunes. The coastal dunes are found in Israel, where at present large parts have been transformed into irrigated agricultural use. There are inland dunes in the Western Negev, Arava Valley and in the Wadi Rum region. Although low amounts of rainfall occur in these areas, the water becomes trapped in the sand particles and creates favorable conditions for plant growth. The climatic and edaphic conditions are different in each of these areas, so the resulting vegetation (described below according to Al-Eisawi 1996 and Danin 1995) can vary.

The coastal sands originate from the Nile River. They are transported by currents to the coast and then blown further inland where they deposit. The first stage of succession involves the grass *Ammophila arenaria*. Once the sand stabilises, it is succeeded by *Artemisia monosperma* and other *Artemisia* species. The final stage of succession is *Retama raetam* shrubs and in the northernmost area, *Pistacia lentiscus*, *Calicotome villosa*, and *Ceratonia siliqua*.

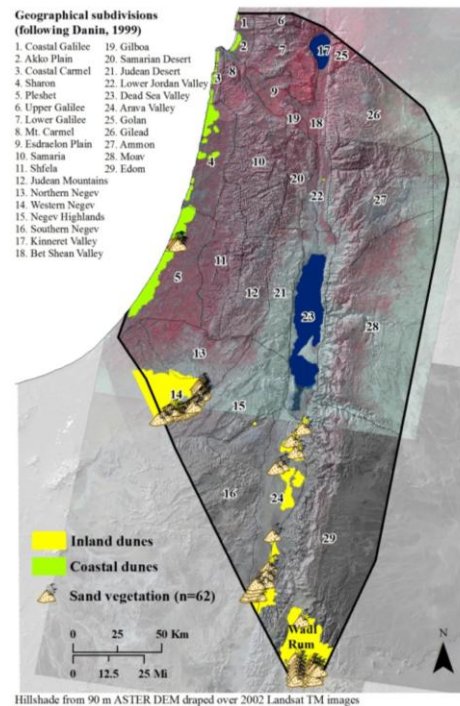
The Western Negev sands are dominated by the grass *Stipagrostis scoparia*. They eventually become populated by *Artemisia monosperma*, *Noaea mucronata* and *Panicum turgidum*.

Along the Arava Valley, the sand originates from the weathering of Nubian Sandstone in the Jordanian plateau and accumulates on the leeward side of these formations. The common species are *Haloxylon persicum*, *Hammada salicornia*, *Hammada salicornia*, and *Salsola cyclophylla*.

Dominant species:

Anabasis articulata
Artemisia monosperma
Haloxylon persicum (also known as *H. salicornium* or *Hammada salicornia*)
Retama rataem
Calligonum cummosum
Panicum turgidum
Hammada scopira
Plantago ovate
Silene villosa

Observations



Haloxylon salicornium predominates on sand dunes in the Arava valley. Photo taken by Soto-Berelov.

Productivity and uses of *Haloxylon*:

Haloxylon is one of the most useful desert plants, as it can be used for fuel, forage, and shelter.

Figure 4.12. Distribution of observations that fall within the sand vegetation subdivision.

Description

The combination of springs and high temperatures in the rift valley provide favorable conditions for Sudanian vegetation which extends along the Rift Valley from Aqaba in the south to around Deir ‘Alla in the north. It is found on alluvial soils. A lot of this area has been transformed into agriculture.

Dominant species:

- Acacia raddiana*
- Ziziphus spina christi*
- Acacia tortilis*
- Balanites aegyptiaca*
- Calotropis procera*
- Cordia sinensis*,
- Fagonia mollis Delile*,
- Maerua crassifolia*,
- Moringa perFegrine*
- Nerium oleander* (prominent in Jordan but absent in springs in Israel and the Sinai)
- Occradenus baccata*,
- Phoenix dactylifera* (date palm)
- Capparis deciduas* (in Jordan)
- Solanum incanum*
- Salvadora persica*

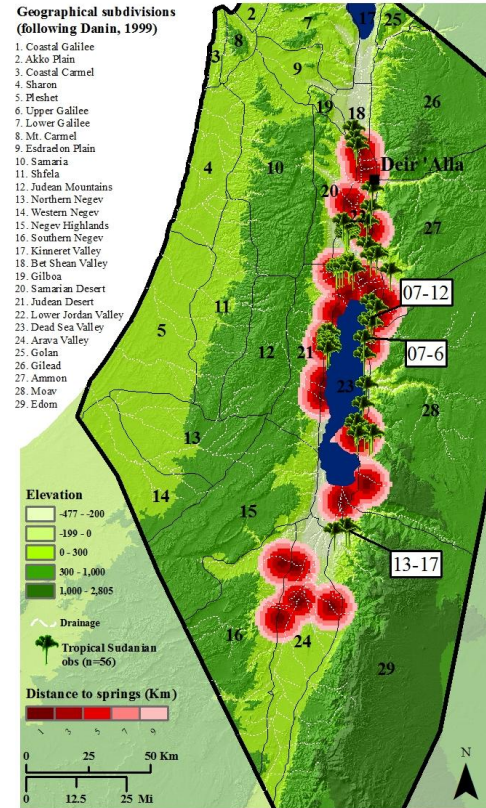


Phoenix dactylifera. Photo taken near Wadi Zarqa at 07-12 by Soto-Berelov.



Large *Ziziphus spina Christi* tree in a spring at location 07-6. Surrounding area used for irrigated agriculture. Photo taken by Soto-Berelov.

Observations



Wadi Fidan. Species present include *Acacia tortilis*, *Tamarisk sp.*, *Acacia sp.*, *Phoenix dactylifera*. Photo taken at 13-17 by Soto-Berelov

Figure 4.13. Distribution of observations that fall within the Tropical Sudanian vegetation subdivision.

Description

Occurs where the water table is close to the surface and where there are springs with high salt content. Also on the deposits of ancient salt lakes (i.e., Lake Lisan).

Rift Valley around the Dead Sea; Wadi Araba, around the Jordan River; Lower Jordan Valley

In the plains of the Lower Jordan Valley, the *Suaeda palaestina* and *Salsolion tetrandrae* associations predominate.

The assoc. of *Suaeda palaestina*-*Suaeda fruticosa* is found surrounding the Dead Sea in the Lower Jordan Valley.

Nitrarietum retusae is found near springs or marshes in soils that are not too saline.

Dominant species:

Altriplicetum Halimi, *Arthrocnemetum* spp., *Atriplex stylosa*, *Juncus littoralis*, *Limonium meyeri*, *Lycium* spp., *Nitrarietum retusae* (see description), *Phragmitetum communis* (*salinum*) *Prosopis farcata*, *Rhus tripartite*, Assoc. of *Salsola tetrandra*-*Halogeton alopecuroides*, *Salsolietum tetrandrae* (see description), *Suaedetum palaestinae* alliance: (see description), Assoc. of *Suaeda palaestina*-*Suaeda fruticosa* (see description), Assoc. of *Nitraria retusa*-*Suaeda palaestina*, Assoc. of *Atriplex Halimus*-*Suaeda fruticosa*, Assoc. of *Atriplex Halimus*-*Salsola villosa*, *Suaeda asphaltica* (common in the mountains of the Lower Jordan Valley), *Suaeda monoica*, *Suaeda vermiculata*, *Seidlitzia rosmarinus*, *Tamarisk* spp., *Prosopis farcata*-*Glycyrrhiza glabra* assoc. (see under Hydrophitic vegetation), *Tamarix nilotica* (also grows in non salty habitats)

Observations

Geographical subdivisions (following Danin, 1999)

1. Coastal Galilee
2. Akko Plain
3. Coastal Carmel
4. Sharon
5. Reshet
6. Upper Galilee
7. Lower Galilee
8. Mt. Carmel
9. Esdraon Plain
10. Samaria
11. Shfela
12. Judean Mountains
13. Northern Negev
14. Western Negev
15. Negev Highlands
16. Southern Negev
17. Kinneret Valley
18. Bet Shean Valley
19. Gilboa
20. Samaritan Desert
21. Judean Desert
22. Lower Jordan Valley
23. Dead Sea Valley
24. Arava Valley
25. Golan
26. Gilead
27. Ammon
28. Moab
29. Edom

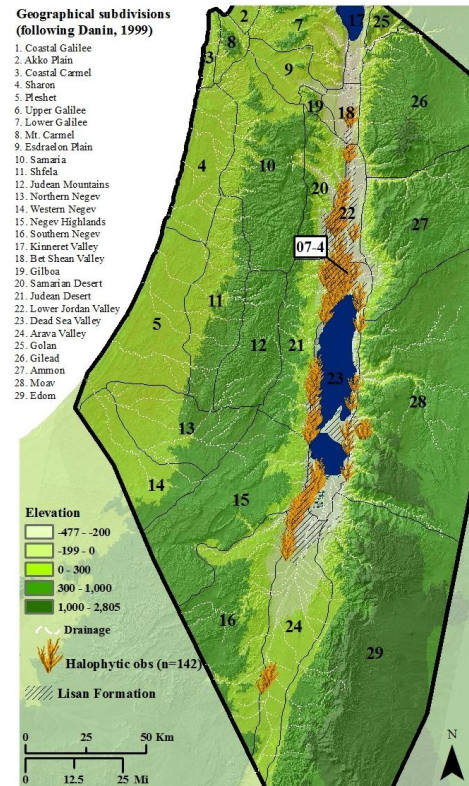


Photo showing Lisan Marl formation surrounded by riparian/halophytic vegetation. Taken at observation 07-4 by Soto-Berelov.

Figure 4.14. Distribution of observations that fall within the Saline halophytic plant subdivision.

Description

Riparian vegetation is most abundant along the Jordan River floodplain. The main association in this complex is the *Populion euphraticae* assoc. (Zohary 1973: 464). It includes the following species and associations:

Populetum euphraticae occupies the belt closest to the Jordan River. It is also found in the wadis that flow into the Jordan River and that are subject to periodic flooding.

Tamaricetum jordanis exists behind the belt of *Populetum euphraticae* and exists in almost pure stands. The soils are more saline than those of the *Populetum* belt (Eig 1946).

Prosopis farcata-Glycyrrhiza glabra assoc. forms the outermost belt of this complex. Also coincides at some locations with Mediterranean savannoid.

There are other rivers and several wetlands that drain into the Rift Valley from the eastern plateau region (e.g., Yarmouk River, Wadi Ziglab, Zarqa River, Wadi Mujib). In addition, there are a series of rivers that flow from the mountains into the coastal plain. Sometimes these intersect the sand dunes along the coast and form swamps (at present, many of these have been channelized but for the purpose of this study, the original trajectory of the rivers is shown). All these rivers and swamps are surrounded by aquatic vegetation. Some of the major constituents include the following:

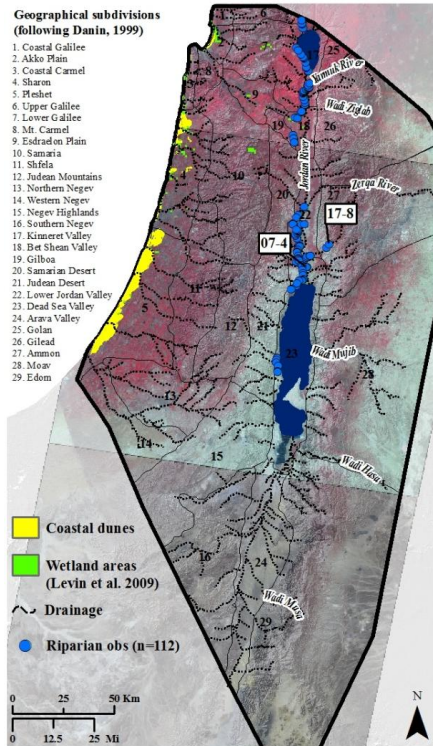
Populetum euphraticae, *Tamaricetum jordanis*, *Prosopis farcata-Glycyrrhiza glabra* assoc., *Platanus orientalis*, *Phragmites communis*, *Nerium oleander*

In addition, there are hundreds of dry waterbeds that are populated by desert wadi vegetation (restricted to the dry watercourse). Depending on where you stand on the elevation gradient, different species predominate. Upstream, small and short living semishrubs like *Pulicaria incisa* are found. These are followed by larger and longer living semishrubs such as *Anabasis articulata* and *Zygophyllum dumosum*. Further downstream, shrubs like *Retama raetam*, *Ochradenus baccatus*, *Lycium shawii* occur. At the bottom, larger trees like acacia and tamarisk can be seen.

Desert wadi vegetation

Retama rataem, *Atriplex halimus*, *Lycium europaeum*, *Artemisia sieberi* or *Artemisia herba-alba*, *Achillea fragrantissima*, *Phlomis brachyodon*, *Astragalus* spp., *Anabasis articulata*, *Tamarix* spp., *Peganum harmala*, *Acacia* sp., *Pulicaria incise*, *Zygophyllum dumosum*, *Ochradenus baccatus*, *Lycium shawii*

Observations



Tamaricetum jordanis bank close to the Jordan River at location 07-4. Photo taken by Soto-Berelov



Phragmites and *Oleander* at Wadi Shu'aib (location 17-08). Photo taken by Soto-Berelov

Figure 4.15. Distribution of observations that fall within the Hydrophytic/Riparian Hydrophytic Subdivision.

Description

This category occupies the very dry and hot portions of the Arava and Dead Sea valleys.

Al-Eisawi refers to it as Acacia and Sudanian rocky vegetation. Sporadic *Acacia* trees are found amongst desert semishrub.

Dominant species:

Acacia pachyceras (Syn. *Acacia gerrardii* Benth var. *nejdensis* Caudhary and *Acacia negevensis* [Zohary]). Dominates at high elevations: upper tributaries of Nahal Paran in Israel, Wadi Jirafi in Sinai, large gravel plains south of Ma'an in Jordan.

Acacia raddiana (less resistant to low temperatures) dominates in lower elevations

Acacia tortilis (Resists the highest temperatures) Grows in the southern Arava Valley and below sea level in the northern Arava and Dead Sea Valley.

Anabasis articulata

Hammada scopira (also known as *Haloxylon articulatum*, *Haloxylon scopirum*)

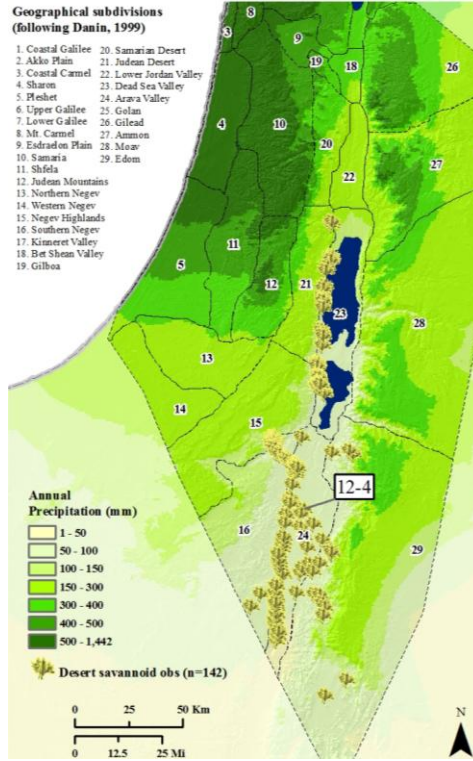
Zygophyllum dumosum

Fagonia spp.

Gymnocarpus fruticosi (*G. decander*)

Retama raetam

Haloxylon salicornicum



Alluvial fans in Arava Valley covered by *Acacia tortilis*. Photo taken by Soto-Berelov



Acacia sp. and small shrubs on this gravelly surface. Taken at location 12-4 by Soto-Berelov.

Figure 4.16. Distribution of observations that fall within the Desert Savannoid Ssubdivision.

4.2.2 Selection of environmental parameters

The success of a species distribution model depends on the degree to which biotic and abiotic factors are able to predict the distribution of a species as well as the availability and accuracy of these factors or environmental parameters. It is therefore crucial to consider the set of conditions that influence the geographic distribution of a species. These can be grouped into three categories: resource, direct and indirect factors. Resource conditions refer to those factors that are consumed by plants (i.e. nutrients, water, light). Direct conditions refer to physiological factors that are not consumed by plants, but that are important to them (i.e. temperature, pH). Indirect conditions then include those factors that have no physiological relationship with plants (i.e. slope, elevation, geology). It would be unrealistic to believe that this is a straightforward process and that these variables operate independent of one another. Nevertheless there are general rules that can be used as guidelines when choosing variables.

Guisan and Zimmermann (2000) argue that the scale of the study can determine the variables to be used. Relying on indirect variables only can be useful for small areas with complex topography whereas the other two groups of variables can minimize prediction errors over larger areas. For example, if a plant that has a wide geographical distribution is examined, it is more likely that factors such as the species' reliance on nutrients and temperature will remain constant than its occurrence at different elevations.

Another important consideration has to do with how accessible the variables are. Furthermore, when extrapolating distributions into past climates, variables for past conditions also need to be obtained (e.g., past soils, temperature, precipitation, location of

rivers, sea level changes). Knowledge on plant succession can also be useful, as well as information regarding how species may have competed in the past.

There are various sources from which the data necessary for mapping and/or modeling vegetation may be obtained. These include the following: field survey (e.g. measuring abiotic characteristics of plants), printed or digitized maps (e.g. maps showing soil type or geology), remote sensing data (e.g. to determine general vegetation types, rates of insolation), tabular data (e.g. climate related information derived from weather stations that can be interpolated across the study area), and high resolution digital elevation maps. Some of the most frequently used variables are included in Table 4.7.

Table 4.7. Environmental variables commonly used in SDM.

Substrate	This includes geology, soil type, soil pH, moisture content and texture. It can be extremely difficult to determine this information in the past. Nevertheless, a knowledge of bedrock types can assist in classifying soils into general levels.
Climate	Since the early nineteenth century, climate has been recognized as a crucial element in determining vegetation (Humboldt 1807). After physiological and biotic factors, it is probably the third most important contributing factor (Davis 1978). A number of elements aspects temperature, precipitation, moisture, incoming solar radiation and wind are included within this category. In addition, this information can be represented in different ways like annual precipitation, precipitation during spring (growing season for plants), temperature of the hottest month, snowfall during the coldest month, etc. Different studies have found particular combinations to be more useful than others. Arundel found that mean January and July temperatures as well as mean annual precipitation help to determine some eastern North American tree distributions (2005). Other studies that extrapolate into other time periods prefer to use annual averages instead of seasonal ones (Phillips 2010). In addition, it is important to verify that some of these variables are not correlated.
Topographic Factors	Many vegetation types are associated with certain elevation ranges which in turn also influence temperature and precipitation. This type of information can be derived from a digital elevation model or DEM, which tend to be fairly accurate and come at different resolutions (Guisan and Zimmermann 2000). Also from the DEM, a series of additional factors that may also influence vegetation can be derived. These include slope angle, northness, eastness, summer solstice insolation, spring equinox insolation (Guisan et al. 1999), aspect, and surface runoff.
High Impact Disturbance Events	Freak events that can cause notable impacts in the spatial distribution of the vegetation include fires, volcanic eruptions, droughts, earthquakes, avalanches, rockslides, severe storms and landslides.
Animal and Human Impact	Certain animals may influence the spatial distribution of some plant species. For instance, birds may be responsible for the spread of pollen, beavers can damn streams and hence promote river bank plants, grazing animals also impact the vegetation. Humans can also help shape the spatial distribution of vegetation types by either clearing trees or planting species.

4.3 Modeling and mapping vegetation in this research

4.3.1 Climatically influenced vegetation

Unless influenced by local edaphic factors (see next section), most plants in the study area are directly related to climate and topography. Because of this, the environmental variables listed in Table 4.8 were selected. All of these are commonly used to map species distributions (e.g., Austin et al. 1994; Brzeziecki et al. 1993; Cibula and Nyquist 1987; Palmer and Van Staden 1992). These variables were derived from several sources. Elevation was obtained from ASTER digital elevation models (DEM) at a 90 meter spatial resolution. From these, slope and aspect grids were also created. All of these were resampled to a 1km spatial resolution. Regional geology was digitized from a 1:200,000 geological map of Israel (Sneh et al. 1998) and a 1:750,000 geological photomap of Israel and adjacent areas (Bartov 1994). From these, a grid was derived showing the major rock types.

Springs and rivers are good indicators for some types of vegetation (i.e., tropical Sudanian). Accordingly, a shapefile of springs was created by querying 'springs' from the Geographic Names Server (GEOnet Names Server)⁴ for Israel, Jordan, and the West Bank. It is not expected that all existing springs are included in this shapefile, however it does represent most of them. These were then buffered and a grid file was created showing the area surrounding these springs at several distances (2, 4, 6, 8, greater than 8

⁴ The Geographic Names Database contains official standard names of foreign places (as well as information about the location) approved by the United States Board on Geographic Names and is maintained by the National Geospatial-Intelligence Agency (www.nga.mil). The National Geospatial-Intelligence Agency name, initials, and seal are protected by 10 United States Code §Section 445.

km, shown in Figure 4.15). The rivers were also buffered at 1, 2, 3, and 5 km (see below for a description of how this layer was created).

Table 4.8. Environmental variables used in study.

Variable	Level of measurement	Description	Source
Mask	Binary	A grid that shows areas where the model cannot be projected to. These include the Dead Sea, Sea of Galilee, and sand dune areas.	Soto-Berelov
Mean annual temperature (°C)	Continuous	Average annual temperature	MEDLANS
Mean Annual precipitation (mm)	Continuous	Total average annual precipitation (in mm)	MEDLANS
Mean summer temperature (°C)	Continuous	Average temperature for June, July, August	MEDLANS
Mean winter temperature (°C)	Continuous	Average temperature for December, January, February	MEDLANS
Mean summer precipitation (mm)	Continuous	Average summer precipitation during June, July, August	MEDLANS
Mean winter precipitation (mm)	Continuous	Average winter precipitation during December, January, February	MEDLANS
Elevation	Continuous	90m ASTER DEM that was resampled to 1km	ASTER
Geology/ Substrate	Categorical	Indicates major rock type (e.g., limestone, chalk, basalt, sandstone)	
Slope	Continuous	Derived from 90m ASTER DEM and resampled to 1km. Unit in degree signifying maximum rate of change in elevation from each pixel to its neighbor.	ASTER
Distance to rivers	Categorical	The wadis and Jordan River were buffered to 1, 2, 3, 4, greater than 5km distance.	Soto-Berelov
Distance to springs	Categorical	The springs were buffered to 1,3,5,7,and greater than 9 km.	GEOnet Names Server
Temperature for the hottest month	Continuous	Average temperature of the hottest month, which is July for the present.	MEDLANS

The climate variables were developed as part of the MedLand project, through the implementation of a Macrophysical Climate Model (MCM) developed by Bryson and McEnaney-DeWall (2007) at the Archaeoclimatology Laboratory (University of Wisconsin, <http://ccr.aos.wisc.edu/bryson/archaeoclim.html>). This MCM allows climatic variables like monthly temperature, precipitation, and evapotranspiration to be retrodicted (at a 100 year temporal resolution for the late Pleistocene and Holocene) in locations that have the standard 30 year climate information. These paleo climate values are derived by extrapolating modern climatic data with “centers of action” (Barry and Carleton 2001), derived from the global temperature gradient that results from incoming solar radiation (Milankovitch cycle). The centers of action include parameters like high and low pressure systems such as the North Pacific high, the jet stream, and the Intertropical Convergence Zone (ITCZ), and other atmospheric circulation parameters. These climate values are also calibrated with a database of over 2,000 volcanic events that have occurred in the past (Bryson 2007).

The team from the Archeoclimatology Laboratory has developed high resolution models to study climatic fluctuations during the Holocene in several places in Africa, the Near East, and the Americas (e.g., Arzt 2003, 2005; Bryson 1992, 1997; Bryson and Bryson 1997, 1998, 1999; Callaghan 2003; Kaplan et al. 2005; Lawler 2007; McDonald and Bryson 2010; McEnaney et al. 2006; Ruter et al. 2004). Their findings seem promising, since some of the climatic changes they capture are also documented in proxy and archaeological records. Contrary to Global Circulation Models (GCM) which generate low resolution paleoclimatic information that is useful for regional studies, the

MCM generates high resolution climate data (monthly and yearly precipitation and temperature averages and extremes), and so is more suited for this study⁵.

When applying the model to the southern Levant, the latitude of the Cyrenaican subtropical high axis was used (Bryson and DeWall 2007). Based on non-linear regression, these parameters were then used to calibrate modern weather station information from 39 stations spread throughout the region and projected into past climates. Continuous surfaces were then created by interpolating the results using multiple regression (Hill et al. 2008).

Before including all of the variables mentioned in Table 4.8, they were assessed for spatial autocorrelation since correlations between variables has been highlighted as an important factor that could produce variable results (e.g., Elith 2006, Guisan et al. 2006, Heikkinen et al. 2006, Graham et al. 2008). To calculate this, the ratio of the covariance between two layers (in this case environmental variables) was divided by the product of their standard deviations. The correlation coefficient is unitless and ranges from 1 to -1. A value of zero signifies that two layers are not dependent on each other. A positive value of 1 means that the layers are directly related (i.e., when the cell values of a layer increase, the cell values of the other probably increases) and the opposite is true for a negative correlation coefficient. This procedure was conducted in ArcGIS 9.3 using the

⁵ Other studies that map species distribution at present frequently rely on the very high resolution climate surfaces created by Hijmans et al. (2005). These are available through the WorldClim – Global Climate website at <http://www.worldclim.org>. The website also provides links to a series of GCM models generated for various time periods in the past (e.g., 6 ka BP). For comparison purposes, the present day vegetation SDM models were also created using the surfaces from WorldClim. They produced comparable results to those generated using the climate surfaces created through the implementation of the MCM. Unfortunately, the paleoclimatic surfaces in the WorldClim website could not be compared to those produced by the MCM because their resolution is too coarse (50 km spatial resolution).

MAKESTACK command which generates a stack of the different grids as well as statistics about the individual grids, a covariance matrix, and a correlation matrix that shows how the different variables correlate with one another (Table 4.9). Variables that were highly correlated (>0.85) were removed, resulting in the non-redundant variables listed in Table 4.10.

Table 4.9. Correlation matrix of independent variables.

LAYER	1-Elev	2-Annual Precip	3-Annual Temp	4-Mean Sum Prec	5-Mean Sum Temp	6-Mean Win Prec	7-Mean Win Temp
1-Elev	1	0.11361	-0.92047	0.54756	-0.90079	0.1694	-0.9205
2-Annual Precip	0.11361	1	-0.36036	-0.13153	-0.45151	0.99446	-0.28431
3-Annual Temp	-0.92047	-0.36036	1	-0.39284	0.99204	-0.41186	0.9942
4-Meansumprec	0.54756	-0.13153	-0.39284	1	-0.38597	-0.10954	-0.38645
5-Mean Summer Tem	-0.90079	-0.45151	0.99204	-0.38597	1	-0.49835	0.97286
6-Mean Winter Precip	0.1694	0.99446	-0.41186	-0.10954	-0.49835	1	-0.33889
7-Mean Winter Temp	-0.9205	-0.28431	0.9942	-0.38645	0.97286	-0.33889	1

Table 4.10. Variables used per model.

Model category	Variables used per model									
	Annual Prec	Geology	Annual Temp	Elevation	Aspect	Slope	Dist to rivers	July Temp	Dist to springs	Mask
Mediterranean	x	x	x	x						x
Saharo Arabian	x	x	x	x						x
Irano Turanian	x	x	x	x						x
Pine forest	x	x	x	x	x	x				x
Deciduous	x	x	x	x	x	x				x
Evergreen	x	x	x	x	x	x				x
Open forests carob and pistacia	x	x	x	x	x	x				x
Open forests juniper, cyprus, oak, pistacia	x	x	x	x	x	x				x
Semi steppe batha	x	x	x	x						x
Shrub steppe	x	x	x	x						x
Desert savannoid	x	x	x	x	x	x				x
Desert scrub	x	x	x	x	x	x				x
Stony desert	x	x	x	x	x	x				x
Halophytic	x	x	x	x			x	x		x
Tropical Sudanian	x		x	x			x	x	x	x
Mediterranean Savannoid	x	x	x	x	x	x				x
Coastal Ziziphus	x	x	x	x						x

Average annual precipitation and temperature were kept instead of the extreme values because they are more transferable when looking at long term distributions (Phillips 2010). Another study that used these variables was done by Martinez-Meyer et al. (2006), who modeled the distribution of 23 extinct mammals during the LGM and present. Furthermore, elevation, slope, aspect, and geology were also included because they have been shown to be useful when modeling in an area that has complex topography (Guisan and Zimmermann 2010).

Contrary to some algorithms which project distributions using bioclimatic models that are solely based on the relationship between a species and climatic parameters, Maxent allows other variables like elevation to be included. These were kept when projecting past vegetation distributions even though the surface is the same as the present day one because they help to distinguish areas populated by certain vegetation associations (given the resolution used in this study [1km], these topographic variables are assumed to remain as they are at present). For instance, deciduous oak and open forests of carob and pistacia occupy the lower elevation areas of the Judean and Samarian Hills and the Galilee region, whereas evergreen oak is mainly found in the higher elevation areas. Juniper concentrates on Nubian sandstone whereas the halophytic vegetation is predominantly found on the Lisan Formation. Other studies that have used similar variables when modeling past distributions are shown in Table 4.11.

Table 4.11. Examples of other studies that have used similar variables when projecting species distributions into other time periods.

Reference	Description	Variables used
Benito et al. 2007	Applied two GCM's (UGAMP and ECHAM3) to model the distribution of 19 tree species in the Iberian Peninsula during the LGM and Mid Holocene.	Used six climatic variables and two physiographic ones (slope and aspect , derived from a DEM).
Scheingross et al. 2007	Develop distribution models of two butterfly alpine species at present and under a climate change scenario.	Series of climatic and environmental variables including elevation .
Buisson et al. 2010	Evaluate the potential impacts of climate change on French stream fish species and assemblages. Quantify uncertainty that could come from the dataset, SDM applied, general circulation model, and gas emission scenario used for projection.	Used three climate variables (avg. ann. temp. , avg ann. precip. , annual air temp. range). Environmental variables: e.g., distance from headwater, elevation , mean stream width.
Phillips 2010	Variables remain constant except for 2 temperature variables. In other words, elevation and a few other environmental variables remain the same when projected to a new climate, only ones that change are temperature.	2 temperature variables (avg and max temp) and a series of environmental variables including elevation .
Hannah et al. 2005.	Built a bioclimatic model to look at how the distribution of 300 species may change under future climate scenario	Climate variables, elevation , soils , land-cover, protected areas
Barry et al. 2002	Modeled 54 species (plants and animals) in Ireland and Britain at present and future scenario.	5 environmental variables of temperature, precipitation, soil class.
Barrows et al. 2008	Estimate the historic distribution of two lizards to determine habitat loss and evaluate potential habitat for conservation purposes.	Included elevation along with precipitation, soils, and other topographic variables like slope. Elevation found useful. Best model included annual precipitation , elevation , soil .
Iverson et al. 2010.	Model the distribution of 134 trees under future climate change scenarios.	38 environmental variables: 7 climate, 9 soil classes 12 soil characteristics 5 landscape 5 elevation
Swenson 2006	Used SDM to assess the environmental factors (variables) responsible for the maintenance of suture zones in North America (there are many avian hybrid zones within this region).	Used elevation , slope , aspect , and other variables. Elevation found to be important.
Benito et al. 2009	Assess extinction risk of plant species in relation to the spread of greenhouses in a Mediterranean landscape	Topography variables (e.g., elevation , slope, direct radiation), climate variables (e.g., avg. ann. precip. , yearly temperature), distance variables (e.g., to dams, population centers)

Table 4.11. (continued).

Reference	Description	Variables used
Mahiny and Turner 2003	Compared neural networks to logistic regression when looking at changes in remnant vegetation patches.	Used a series of topographic (including elevation, geology, slope, aspect), landscape metrics (e.g., shape, size, fractal dimension) and image based variables derived from remote sensing (i.e., NDVI). Slope was found to be one of the most important.
Elith et al. 2010	Goal of the paper is to explain this tool for SDM. They present several case studies, one of which includes projecting the distribution of a plant under a future climate scenario.	Isothermality, Mean temp. wettest quarter, Mean temp. warmest quarter, avg. ann. precip. , precip. driest quarter, estimate of solum plant available water holding capacity (with the observation that more soils variables should be added). They specifically mention how the model is trained with these variables and the future projection only includes a change in the climatic variables, whereas the soils variable remains the same.
Graham et al. 2004	Evolutionary Biology (investigate speciation processes). When building their climate layers, they used latitude, longitude and elevation to interpolate the monthly climatic surfaces of precip and temp across the surface. They used elevation again when creating the SDM.	SDM was run with elevation , water budget, avg. ann. precip. , coefficient of variation of annual precipitation, precip of the driest quarter, avg. ann. temp. , coefficient of variation of mean annual temperature.

4.3.2 Edaphically influenced vegetation categories

Some of the vegetation subcategories are mainly influenced by local conditions and will minimally be affected by changes in climate. These include tropical Sudanian vegetation, halophytic vegetation, sand dune vegetation, and riparian vegetation. In this study, it is assumed that their current potential distribution will not have changed significantly throughout the past. Because of this, **they were only modeled for the**

present and overlain onto the past vegetation models⁶. This section describes the methods and variables used to model the distribution of these subcategories.

4.3.2.1 Tropical Sudanian

Supplemental literature indicates that this type of vegetation is mainly restricted to the Rift Valley. The extremely hot temperatures of this region coupled with pockets that are constantly flooded due to the presence of springs or wadis, provide the necessary conditions for this type of tropical vegetation, which originates in Africa. The variables used to model this category are distance to springs, average yearly temperature, temperature of the hottest month (July), elevation, and proximity to rivers/wadis. Initially, average summer temperature and average winter temperature also were included. However, these proved to be highly correlated with temperature of the warmest month (Table 4.12). Because the vegetation is mainly confined to the Rift Valley, the grids were clipped to the region surrounding the Arava Valley, and to the Lower Jordan Valley. The model was run using all of the observations to train the model. They were partitioned through a 10-fold cross validation.

Table 4.12. Correlation matrix of independent variables for the Tropical Sudanian category.

#	Layer	Elevation	Ann Prec	Ann Tem	July Tem	Sum Tem	Win Tem
#	-----						
	Elev	1.00000	0.30805	-0.04256	-0.89873	-0.91153	-0.94428
	Ann Prec	0.30805	1.00000	0.28725	-0.63967	-0.62451	-0.53545
	Ann Temp	-0.04256	0.28725	1.00000	0.04442	0.04470	0.04474
	July Temp	-0.89873	-0.63967	0.04442	1.00000	0.99640	0.98126
	Sum Temp	-0.91153	-0.62451	0.04470	0.99640	1.00000	0.98884
	Win Temp	-0.94428	-0.53545	0.04474	0.98126	0.98884	1.00000

⁶ Nevertheless, the author acknowledges that this is a limitation in the study. Riparian vegetation surrounding swamps would have shrunk or expanded depending on the prevailing climate. Springs may have dried during times of drought. At the resolution of this study, however, this limitation is acknowledged and the assumption that they have minimally changed is adopted.

4.3.2.2 Sand dune vegetation

Sand dune vegetation is found on sand dunes areas. Two types of sand dunes exist in the study area (coastal and inland dunes). Although there are 62 observations in the database (11 gathered through field work), this category was not modeled. Instead, sand dune areas were extracted from geological maps (Bartov 1994; Sneh *et al.* 1998) and verified with satellite imagery and field observations. While conducting field work, mapped sand dunes were also assessed (Figure 4.17).

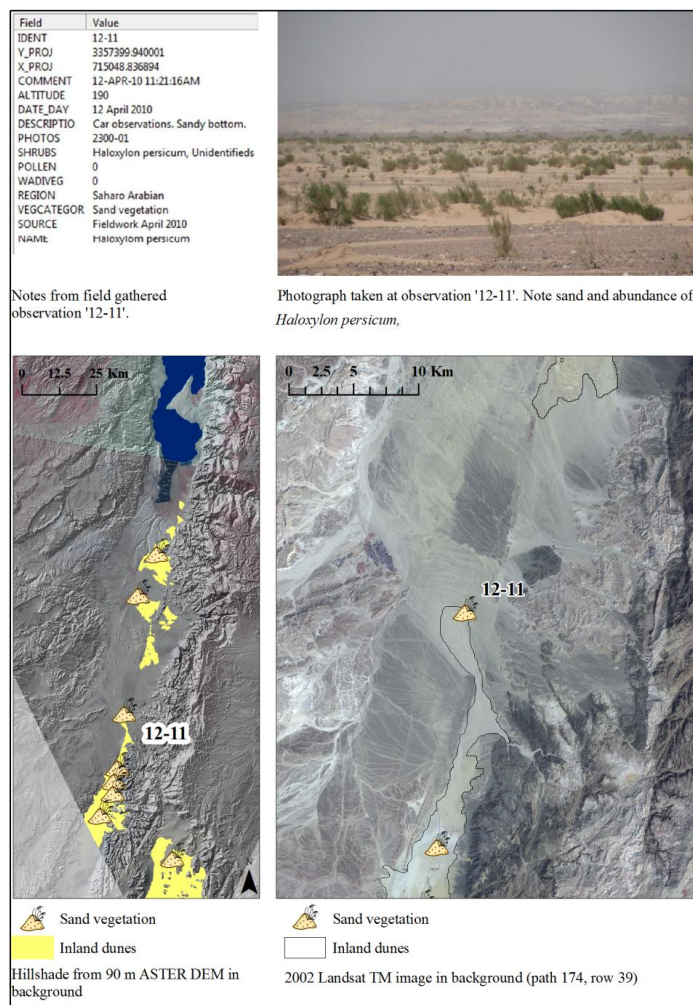


Figure 4.17. Mapping of Sand Vegetation.

4.3.2.3 Riparian vegetation

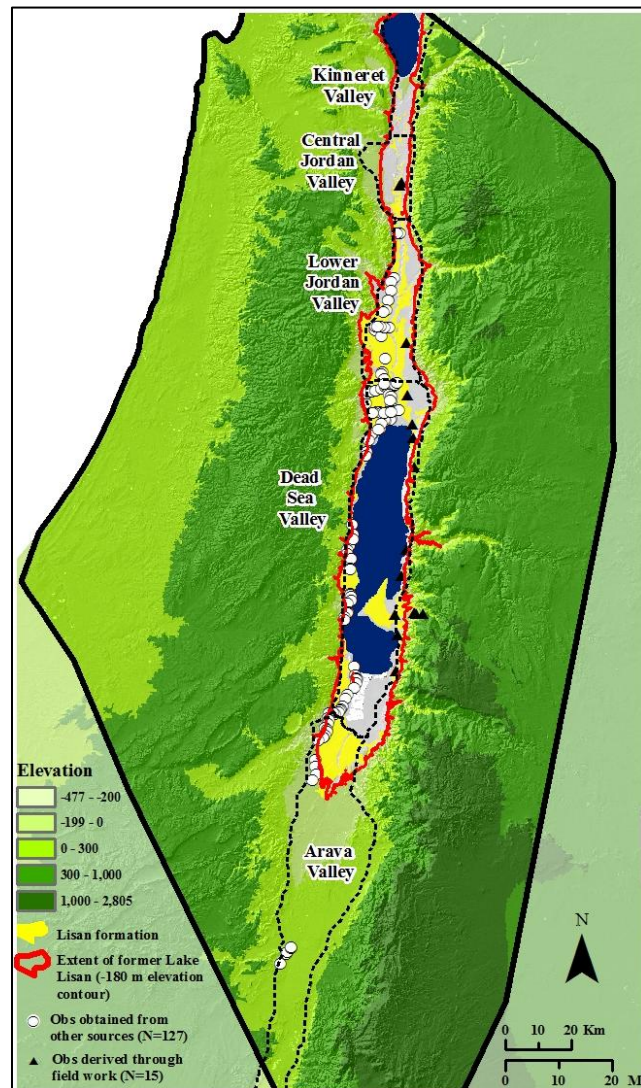
Riparian vegetation is essentially restricted to wetland areas and wadi and river banks. A belt of riparian forest surrounds the Jordan River and extends across its flood zone. The observations that fall within this category are in close proximity to the major rivers and wadis (Figure 4.15). To delineate this vegetation, the major streams, rivers, and wadis were first digitized. This was done by inspecting a shapefile of drainage lines obtained from GEOnet and overlaying it on satellite imagery. Although most major drainage features were captured in the shapefile, these appeared to be created at a fairly coarse scale. In addition, the course of some drainage features that drain into the Mediterranean Sea have been channelized. A new shapefile showing the major drainage features of the study was then created by on-screen digitizing, using satellite images of various resolutions (i.e., Corona, ASTER, Landsat, Spot), a high resolution DEM, and historical maps as reference sources.

The largest concentration of hydrophytic plants within the study area is found adjacent to the Jordan River. To map this vegetation, a 3 kilometer buffer was created along this river. All other drainage features (whether rivers or wadis) were buffered to 1 kilometer distances. In addition, wetland locations were obtained from Levin et al. (2009).

4.3.2.4 Halophytic vegetation

Halophytic plants are found on soils that have high concentrations of salt. Within the study area, the majority of these are found on the former Lake Lisan bed, from the Lower Jordan Valley southwards (Map 4.5). The combination of high temperature and low rainfall levels have caused these highly saline sediments to remain, causing favorable

conditions for these plants throughout this region. The variables used to model halophytic vegetation are geology (includes the Lisan formation), elevation, annual precipitation, annual temperature, July temperature, mask (see Table 4.10), and proximity to drainage features.



Map 4.5. Area formerly occupied by Lake Lisan and Lisan Formation.

To model this category, all the observations were used as training points. Several trials using the field obtained observations as ‘testing data’ were done. However, all of

the field data were gathered east of the Dead Sea, whereas the other observations were generated to the west (see Figure 4.14). This geographic division resulted in the area predicted for halophytic vegetation to occur predominantly west of the Dead Sea. Because of this apparent bias, all the observations were used for training the model, using a 10-fold cross validation method, which will be expanded in the next section.

4.4 Maxent, the algorithm used in this research

4.4.1 Maxent, Model overview

MaxEnt evolved from the disciplines of computer science and machine learning. It applies a machine learning technique that is based on the principle of maximum entropy (Jaynes 1957). This suggests that the best way to determine an unknown probability distribution is to make sure that it has met all the constraints posed to it (how species presence observations are associated with certain environmental data) and that it has maximum entropy (i.e., it has a nearly uniform distribution or is most spread out) (Jaynes 1957). The unknown probability distribution or π (Phillips et al. 2006) occurs in a defined geographical space with n pixels. There are a number of observations and a series of environmental variables that will provide the information needed to determine the species distribution. This is determined by examining the variables in a linear way, as well as by transforming the variables (also known as covariates, predictors, or inputs) into features: linear, quadratic, product, threshold, hinge, discrete or categorical.

The ability of the software to create features (Table 4.13) is one of its strengths since, by doing this, it is able to model complex relationships by incorporating the dependency that may exist between a species and a set of predictor variables (instead of just allowing the dependency between a variable and a species to be simply linear) by

constraining the optimal probability distribution based on this information. The probability distribution is characterized by the averages of the features which are close to the real observed means (Phillips et al. 2006). The features applied depend on the number of observations. If fewer than 10 observations are available, only linear features will be implemented, for up to 15 observations linear and quadratic are used, for up to 80 observations linear, quadratic and hinge features are used, and all features are used if there are over 80 observations. When more observations are available, the algorithm will find a distribution that fits a more complex dependency between the species being modeled and the environmental conditions. The relative contribution of each feature is determined by its weight (coefficient), which allows a certain deviation from the sample feature means so that the resulting distribution meets the constraints imposed by these empirical means (Elith et al. 2011).

MAXENT assumes that the observations form part of a random sample of the species real distribution. To offset selection bias, it randomly selects a sample from the sampling distribution. This way, both the observations and the background reflect the same bias (Phillips and Dudík 2008). Nevertheless, if the user has knowledge of the bias (for instance, if there was uneven sampling because of restricted access to some areas) a grid can be provided which indicates sampling bias (this was done for most categories that were modeled in this study).

The number of background points refers to how many cells are used to characterize the environmental conditions of the species, association or category being modeled. When the number of cells is larger than 10,000 (in this study its 44,755), the environmental conditions of the data are represented by 10,000 randomly selected cells,

unless otherwise specified. The predicted distribution is calculated across the background and presence observations, and then projected throughout the study area (Phillips and Dudík 2008).

Table 4.13. Features used in MAXENT (modified from Elith et al. 2011 and Maxent Help [v. 3.3.3e].

Feature Type	Used with the following number of observations	Description and constraint imposed on the estimated distribution
Linear (L)	Always used	This refers to the continuous variable itself. So the mean of this type of variable under the output distribution should be close to the mean of the observations.
Quadratic (Q)	At least 10	Refers to the square of an environmental variable and is used with L if at least 10 observations are available. The output distribution should reflect a similarity between the variance of a variable resulting from the distribution and what is observed in the sample observations.
Product (P)	At least 80	Product of two continuous variables. Used with L and Q when at least 80 observations are available. The output distribution should reflect the same covariance for each pair of variables as the observations.
Threshold (T)		This is a step function that is applied to continuous variables. At a given threshold, the feature will be either above or below. The purpose is to reflect how the proportion of the predicted distribution estimated above the threshold is close to that found in the observations.
Hinge (H)	At least 15	It is derived from continuous variables and is similar to T, except that it is linear. Replaces linear features when it is used.
Discrete or categorical(C)		Derived from categorical variables. The number of categories determines the number of features derived (per categorical variable). The purpose is to reflect a similarity between the proportion of cells that have a discrete value and what is seen in the observations.

In the beginning, MAXENT assumes a uniform distribution throughout the study area, following the concept of maximum entropy which assumes that if no sample is available, a species has a uniform distribution. In other words, it has the same chance of existing in any given place (or cell). MAXENT then performs a series of iterations during

which the weights of the features are adjusted (referred to as the training gain) to improve the fit of the data. Eventually, MAXENT will choose the distribution that has the highest entropy after the complexity between the species and predictor variables (features and constraints) has been accounted for. The degree to which the resulting distribution is spread out or smooth depends on the weights applied to the features through a parameter called regularization. The default regularization method has been shown to perform well (Elith et al. 2011; Hastie et al. 2009).

The estimated distribution is calculated across all the cells that have information for all of the environmental variables used. A non-negative probability value is assigned to each pixel and the sum of all the pixels equals 1. The value of a pixel is cumulative and ranges from 0 (low) to 1 (high) and represents the sum of the probability for that pixel and other pixels with lower or equal probability values, multiplied by 100 (Phillips et al. 2006). Pixels with higher values indicate areas that contain more suitable environmental conditions, so there is a higher chance of finding these species under the same conditions in which the observations were collected.

The default parameters for Maxent (e.g., combinations of features used depending on the number of samples, regularization parameters, amount of cells to be included in the background sample) were determined by testing different settings on a comprehensive dataset (Elith et al. 2006) that includes presence only data obtained from herbaria and natural history museums as well as presence-absence data obtained from surveys (Phillips and Dudík 2008). The first subset, composed of 226 species from 6 regions of the world and ranging from 2 to 5822 observations per species, was used to determine the features and regularization parameters that depend on the number of

observations. The presence-absence dataset, which includes 102 to 19,120 observations per species (presence and absence per species) was used to validate the results obtained from the presence-only data. The largely successful performance of MAXENT across dozens of contexts proves that the default settings are well suited to a broad range of presence-only datasets, even when small sample sizes are available.

4.4.2 Projecting to past environments

MAXENT is able to project a distribution into new geographic or temporal scenarios. It achieves this by training the model using the observation data and then extrapolating it into new spatial or temporal conditions. In this study, models of vegetation are trained on the present and projected into the past. Although only modern observations are needed, environmental variables of past conditions are necessary in order to extrapolate into different time scenarios. The variables that are assumed to drive vegetation distributions in this study are climatic ones, since the other variables (i.e., elevation, substrate) remain constant throughout the time period being reconstructed.

Predicting the distribution of a species under past climatic conditions is more precarious than doing so for the present climates (Elith et al. 2010), because a prediction is being made into the unknown (one is not able to obtain a sample of the conditions as one does for the present). Furthermore, environmental conditions might have been completely different. At least when predicting into past climates, one is likely to find alternative data with which to compare model outputs, which is not the case when projecting into the future. In this study, data for comparison comes from pollen records and other proxy data that are indicators of climatic conditions at different moments in the

past (discussed in Chapter 3). Nevertheless, it is important to show areas where model outputs are most uncertain, because the climatic conditions (according to the climate grids) were different to those of the present (which were used to train the models before they were projected and extrapolated into novel conditions). This is done by taking advantage of several tools built into the MAXENT software with this purpose in mind. These involve clamping, multivariate environmental similarity surface, and most dissimilar variable map.

Whenever a projection is being made, the most extreme environmental values in the training data (presence and background) are extrapolated in a straight line (Elith and Graham 2009). In other words, when a feature derived from a projected variable has a value that is greater or smaller than the feature used to train the model, it will be given the value that differs the most from that which was used to train the model (present day conditions). This is known as clamping. For each chronological interval being projected (e.g., 12 ka BP-11.5 ka BP, 11500-11 ka BP, and so on for each 500 year interval), MAXENT produces a surface which shows where clamping has occurred. Clamping identifies those cells that have values in the layers used for projecting the distribution that differ from those used for training. Simply said, it shows which cells have environmental conditions that are different to those of the present. It is important to show where clamping occurs since it indicates conditions that are different from those of the present, and implies greater uncertainty in model outputs. In this study, the clamping surface produced for each of the major plant geographical regions during each time period is shown in Chapter 6.

In addition to clamping, every time a projection is made, a multivariate environmental similarity surface (MESS) is created, which indicates how much the environmental conditions (in this case climate) deviate from those of the present (Elith et al. 2010). It does this by actually measuring the similarity of the predictor variables between a point (cell) and a group of reference points. The output is a continuous surface that ranges from -100 (red) to +100 (blue). Positive values (shown in blue) indicate that the environmental conditions were similar to those used to train the model (a cell with a value of 100 means that the environmental conditions at a particular time period are the same as the median environmental conditions at present). Negative values indicate decreasing similarity between the point and reference points. The variable(s) responsible for the greatest difference is shown in the most dissimilar variable map (MoD), which is also included for each time period in Chapter 6.

4.4.3 Parameters used in this study

This study uses Maxent version 3.3.3e from the graphical user interface (GUI) to generate the models. Each model was calibrated using the settings recommended by Phillips, the observations discussed in Figures 4.1 to 4.15 and the selected variables as shown in Table 4.10. They were trained with the observations and 10,000 randomly selected background points from a 1km grid across the study area, unless otherwise specified (bias grids were used for some models). Table 4.14. summarizes the settings used for each model.

Table 4.14. Parameters used in MAXENT to calibrate the models.

Category	Testing Method	# Training samples	# Test samples	Bias file used	# cells to determine distribution (background and Presence)	Settings and notes
Mediterranean	Data partition. Random 60% used for training, 40% used for testing.	351	234	No	Default background	Environmental layers used: annprec anntemp elev geol3(categorical) mask Regularization values: linear/quadratic/product: 0.050, categorical: 0.250, threshold: 1.000, hinge: 0.500 Feature types used: P L Q H T
Saharo Arabian	Data partition. Random 75% used for training, 25% used for testing.	294	98	Yes	1264	Environmental layers used: annprec anntemp elev geol3(categorical) mask Regularization values: linear/quadratic/product: 0.050, categorical: 0.250, threshold: 1.000, hinge: 0.500 Feature types used: P L Q H T
Irano Turanian	Data partition. Random 75% used for training, 25% used for testing.	225	74	Yes	1264	Environmental layers used: annprec anntemp elev geol3(categorical) mask Regularization values: linear/quadratic/product: 0.050, categorical: 0.250, threshold: 1.000, hinge: 0.500 Feature types used: P L Q H T
Forests with <i>P. halepensis</i>	Resampling, 10-fold crossvalidation	33	4	410	1264	Environmental layers used: annprec anntemp aspect elev geol3(categorical) mask slope Regularization values: linear/quadratic/product: 0.244, categorical: 0.250, threshold: 1.680, hinge: 0.500 Feature types used: L Q H
Mixed deciduous forests with <i>Q. ithaburensis</i>	Resampling, 10-fold crossvalidation	116	13	500	1264	Environmental layers used: annprec anntemp aspect elev geol3(categorical) mask slope Regularization values: linear/quadratic/product: 0.050, categorical: 0.250, threshold: 1.000, hinge: 0.500 Feature types used: P L Q H T

Table 4.14 (continued).

Category	Testing Method	# Training samples	# Test samples	Bias file used	# cells to determine distribution (background and Presence)	Settings and notes
Mixed evergreen forests with <i>Q. calliprinos</i>	Resampling, 10-fold crossvalidation	179	20	492	1264	Environmental layers used: annprec anntemp aspect elev geol3(categorical) mask slope Regularization values: linear/quadratic/product: 0.050, categorical: 0.250, threshold: 1.000, hinge: 0.500 Feature types used: P L Q H T
Open forests of carob and pistacia	Resampling, 10-fold crossvalidation	67	7	396	Default background	Environmental layers used: annprec anntemp aspect elev geol3(categorical) maskcarob1 slope Regularization values: linear/quadratic/product: 0.147, categorical: 0.250, threshold: 1.340, hinge: 0.500 Feature types used: L Q H
Open forests with juniper	Resampling, 10-fold crossvalidation	18	2	492	1014	Environmental layers used: annprec anntemp aspect elev geol3(categorical) mask slope Regularization values: linear/quadratic/product: 0.680, categorical: 0.250, threshold: 1.820, hinge: 0.500 Feature types used: H
Semi steppe batha	Resampling, 10-fold crossvalidation	77	8	488	1264	Environmental layers used: annprec anntemp elev geol3(categorical) mask Regularization values: linear/quadratic/product: 0.119, categorical: 0.250, threshold: 1.240, hinge: 0.500 Feature types used: L Q H
Shrub steppe	Resampling, 10-fold crossvalidation	178	20	500	1264	Environmental layers used: annprec anntemp elev geol3(categorical) mask Regularization values: linear/quadratic/product: 0.050, categorical: 0.250, threshold: 1.000, hinge: 0.500 Feature types used: P L Q H T

Table 4.14 (continued).

Category	Testing Method	# Training samples	# Test samples	Bias file used	# cells to determine distribution (background and Presence)	Settings and notes
Mediterranean Savannoid	Resampling, 10-fold crossvalidation	67	7	500	1264	Environmental layers used: annprec anntemp aspect elev geol3(categorical) mask slope Regularization values: linear/quadratic/product: 0.147, categorical: 0.250, threshold: 1.340, hinge: 0.500 Feature types used: L Q H
Desert savannoid*	Resampling, 10-fold crossvalidation	96	11	500	1264	Environmental layers used: annprec anntemp aspect elev geol3(categorical) mask slope Regularization values: linear/quadratic/product: 0.079, categorical: 0.250, threshold: 1.040, hinge: 0.500 Feature types used: P L Q H T
Desert scrub	Resampling, 10-fold crossvalidation	68	8	500	1264	Environmental layers used: annprec anntemp aspect elev geol3(categorical) mask slope Regularization values: linear/quadratic/product: 0.144, categorical: 0.250, threshold: 1.330, hinge: 0.500 Feature types used: L Q H
Stony desert	Resampling, 10-fold crossvalidation	67	7	486	1264	Environmental layers used: annprec anntemp aspect elev geol3(categorical) mask slope Regularization values: linear/quadratic/product: 0.147, categorical: 0.250, threshold: 1.340, hinge: 0.500 Feature types used: L Q H
Halophytic vegetation	Resampling, 10-fold crossvalidation	102	11	500	Default background	Environmental layers used: alt annprec anntemp geology(categorical) julytemp mask riversl(categorical) Regularization values: linear/quadratic/product: 0.050, categorical: 0.250, threshold: 1.000, hinge: 0.500 Feature types used: P L Q H T

Table 4.14 (continued).

Category	Testing Method	# Training samples	# Test samples	Bias file used	# cells to determine distribution (background and Presence)	Settings and notes
Tropical Sudanian vegetation	Resampling, 10-fold crossvalidation	43	5	490	1019	Environmental layers used: alt annprec anntemp julytemp mask rivers1(categorical) springs(categorical) Regularization values: linear/quadratic/product: 0.213, categorical: 0.250, threshold: 1.570, hinge: 0.500 Feature types used: L Q H
Coastal <i>Ziziphus</i> vegetation	Resampling, 10-fold crossvalidation	34	4	408	5392	Environmental layers used: annprec anntemp elev geol3(categorical) mask1 Regularization values: linear/quadratic/product: 0.239, categorical: 0.250, threshold: 1.660, hinge: 0.500 Feature types used: L Q H

4.4.4 Selecting a threshold

The Maxent outputs are given as a continuous surface, in which each cell has a value that is part of the distribution found by the model and indicates likelihood of presence. To create a binary map showing where the presence is most likely to occur, a threshold or cut-off value must be chosen. Depending on what value is chosen, the output can be extremely different, and impact the area predicted to be occupied by the species (prevalence, which can theoretically be calculated by dividing the cells in which the species is present by the total number of cells). This has obvious implications for the two types of errors that can be produced: errors of omission and errors of commission. A small omission error will be obtained with a small threshold value, but at the expense of greater commission error. In other words, as the threshold becomes bigger, errors of omission increase whilst those of commission decrease (Fielding and Bell 1997).

There is no straightforward rule, but the literature is full of suggestions that ultimately stress the importance of selecting a threshold that is best suited to the purpose of the model (Freeman and Moisen 2008; Liu et al. 2005). Table 4.15 summarizes some of the thresholds that are used most commonly. They all incorporate sensitivity and specificity, and many make use of the Area Under the Curve or AUC (read below for an explanation of the AUC). Sensitivity refers to the observations that are correctly classified (also known as the true positive fraction) and indicates the model's capacity of classifying true presence observations. On the other hand, specificity refers to how well the model can predict true absences.

Table 4.15. Commonly used thresholds to convert a continuous output to a presence / absence map.

Threshold	Description
Sensitivity = Specificity (Fielding and Bell 1997)	Both presences and absences have the same chance of being predicted.
Maximized sum of sensitivity and specificity	The point in the ROC plot in which the sum of sensitivity and specificity are maximized (Manel et al. 2001). The mean of the error rate of presences and absences are minimized (Freeman and Moisen 2008).
True skill statistic (TSS) (Allouche et al. 2006) This is equivalent to Max(sensitivity+specificity)	1 minus the sum of sensitivity and specificity or the true positive rate (presences correctly classified) minus the false positive rate (absences incorrectly predicted) (Freeman and Moisen 2008)
Select a threshold that will suit the purpose of the model Freeman and Moisen (2008) call this <i>ReqSens</i> and <i>ReqSpec</i>	For example, if there is a pre-required sensitivity of 0.90 there must be a 10 percent minimum error in the presence locations. If, on the other hand there is a specificity of 0.90, only 10 percent true absences can be misclassified (Fielding and Bell 1997).
Kappa statistic MaxKappa	Percentage of locations that are correctly classified after taking into account chance. MaxKappa is the threshold that results in the highest value of kappa (Freeman and Moisen 2008).
ROC plots	Although the ROC is a curve across all the thresholds, it can be used to select a cut-off point (Freeman and Moisen 2008). A recommended one is the one which minimizes the distance between the ROC plot and the upper left corner, (where sensitivity and specificity = 1).
Prevalence (Cramer 2003)	If the modeled prevalence is a reflection of the species' true prevalence.
Traditional threshold 0.5	Although commonly used, it can underestimate prevalence.
Minimum observed prevalence	The threshold is the lowest value obtained for a presence location. This threshold has been recommended when it comes to species that have low prevalence (Cramer).
Mean Probability	The mean probability of the model (Cramer).
Overall prediction success	Percent of correctly classified observations.

In this study, the results of each model for present day vegetation were first examined using different thresholds suggested by the literature. Viewing the whole probability surface is useful (Freeman and Moisen 2008), especially when the continuous

output distinguishes areas that have stronger predictions (Phillips et al. 2006). However, a threshold had to be chosen in order to combine the different classes into one vegetation model for each 500 year interval. While observing the continuous output produced by the different modeled categories, it was evident that selecting the threshold of minimum observed prevalence overestimated the area occupied by each of the categories. At the same time, selecting the traditional cut-off of 50 per cent suitability produced the opposite result. Different cut-off values that optimize the resulting distribution were then chosen for the different models by selecting the one that maximizes the sum of sensitivity and specificity. Determination of a threshold in this manner is highly recommended in the literature (Liu et al. 2005). The results section in the following chapter first shows a continuous probability surface for each of the models, followed by the binary presence-absence maps, based on the threshold chosen.

4.4.5 Combining model outputs into one vegetation map

After the vegetation zones are modeled for each time interval (between 12–2.5 ka BP), they are combined to produce one vegetation map as well as one plant geographical region map for each time period. This is done by combining the outputs of the different plant geographic associations into one map as well as by combining the different vegetation subcategories to produce one map.

For the most part the distributions of the different plant geographic associations don't overlap. However, whenever a particular cell does overlap it is assigned to both values. For example, if cell x is suitable to both the Mediterranean and Irano Turanian

zone, in the final summary map the cell will be assigned to the transition Irano Turanian-Mediterranean zone.

Combining the regions into one plant geographical map was fairly straightforward. However, for the more detailed map of vegetation subcategories, it was more complicated because they include a much larger number of categories, thereby increasing the possibility of having conflicting cells due to different combinations. As a result, a series of rules were developed and implemented through ArcGIS 9.2 (Figure 4.18). First, each category was classified into a number (Step 1). Then, the forest categories *Mixed deciduous oak*, *Mixed evergreen oak*, *Pine forest* were summed using cell statistics (Spatial Analyst, Local, Cell statistics, Sum) and then reclassified (Step 2). The same was done for the steppe (Step 3) and desert (Step 4) categories. Then, all the categories were combined (once again by using cell statistics) and reclassified (Step 5). If the resulting category was predicted for fewer than 50 cells (each cell is 1km; a cluster of 50 cells represents 50 km²; however these do not necessarily occur as a cluster), it was deleted. Finally, the categories Mediterranean savannoid, open forests of carob and pistacia, shrub steppe with open forests of juniper, and coastal *Ziziphus* vegetation⁷ were overlain on the resulting combined map to produce a final vegetation map. This was done because all of these categories can be found intermixed with others. If they had been combined with other categories, the resulting map would have had too many categories and been hard to understand.

⁷ This category was not included with the final past distribution maps because there were hardly any suitable areas when projecting in the past. It is interesting to note that this category, as discussed in Chapter 2, has been the most impacted by land use change and modern development.

Figure 4.18 Combining the output of vegetation subcategories into one vegetation map.

Step 1

Original Value	Description
0	Null
300	Mixed deciduous forest
350	Evergreen
375	Pine
77	Semi steppe batha
75	Shrub steppe
1	Desert savannoid
20	Desert scrub
50	Stony desert vegetation

Step 2

Value	Description	Reclassified
0	Null	Stays the same
300	Mixed deciduous oak forest	Stays the same
350	Mixed evergreen oak forest	Stays the same
375	Forest with <i>Pinus halepensis</i>	Stays the same
650	Mixed Evergreen-Deciduous forest	650 Mixed Evergreen-Deciduous forest
675	Forest with <i>Pinus halepensis</i> and mixed deciduous oak	3310 Forest with <i>Pinus halepensis</i> and mixed deciduous oak
725	Forest with <i>Pinus halepensis</i> and mixed evergreen oak	3330 Forest with <i>Pinus halepensis</i> and mixed evergreen oak
1,025	Evergr+Pine+Decid	3320 (Mixed Woodland)

Step 3

Value	Description	Reclassified	Comment
75	Shrub steppe	Stays the same	
77	Semi steppe batha	Stays the same	
152	Shrub Steppe-Semi Steppe Batha	152 Shrub Steppe-Semi Steppe Batha	These areas indicate transition between the shrub steppe – semi steppe batha categories.

Step 4

Value	Description	Reclassified	Comment
1	Desert savannoid	Stays the same	
20	Desert scrub	Stays the same	
21	Desert savannoid-Desert scrub	20 Desert scrub	The desert savannoid vegetation is mainly restricted to the Arava Valley and immediate surroundings. So when cells that are suitable to this category as well as desert scrub are found outside of this range, they are attributed to desert scrub which surrounds and penetrates into the desert savannoid vegetation.
50	Stony desert vegetation	50 Stony desert vegetation	
51	Desert Savannoid-Stony Desert	50 Stony desert vegetation	The stony desert vegetation is restricted to the dryer areas of the rift valley. If other of the desert categories are also found suitable in this area, the cell is attributed to the stony desert vegetation category.
70	Stony Desert-Desert Scrub	50 Stony Desert	
71	Stony Desert-Desert scrub-Desert Savannoid	50 Stony Desert	

Step 5

Value	Description	Reclassified	Comment
0	Null	Stays the same	
1	Desert Sav	Stays the same	
20	Desert scrub	Stays the same	
50	Stony Desert	Stays the same	
75	Shrub Steppe	Stays the same	
76	Shrub Steppe + DesertSavannoid	75 Shrub steppe	This category includes dryer plants that are found near dryer areas and moister plants near wetter areas (as it transitions to semi steppe batha vegetation).
77	Semi Steppe Batha	77	
78	Semi steppe batha + Desert Savannoid	75 Shrub steppe	
95	Shrub Steppe-Desert Scrub	95 Shrub Steppe-Desert Scrub	These areas indicate transition between the shrub steppe – desert scrub categories.
97	Semi Steppe Batha - Desert Scrub	75 Shrub steppe	
125	Shrub Steppe - Stony Desert	50 Stony desert	
127	Semi Steppe Batha - Stony Desert	50 Stony desert	
150	Shrub Steppe - Shrub Steppe	75 Shrub steppe	
152	Shrub Steppe-Semi Steppe Batha	152 Stays the same	
153	Shrub Steppe-Semi Steppe Batha-Desert Savannoid	75 Shrub steppe	
172	Shrub Steppe-Semi steppe batha-Desert Scrub	75 Shrub steppe	

202	Shrub Steppe-Semi steppe batha - Stony Desert	75 Shrub steppe	
300	Mixed deciduous oak forest	Stays the same	
320	Deciduous - Desert Scrub	75 Shrub steppe	
350	Mixed evergreen oak forest	Stays the same	
370	Evergreen - Desert Scrub	75 Shrub steppe	
375	Forest with <i>Pinus halepensis</i>	Stays the same	
377	Mixed deciduous oak forest-Semi Steppe Batha	300 Mixed deciduous oak forest	Because the upper range of annual precipitation that semi steppe batha vegetation requires is the same as the lower range of several of the forest categories, mixed cells are being assigned to the forest category.
425	Mixed evergreen oak forest - Shrub Steppe	77 Semi steppe batha	
427	Mixed evergreen oak forest - Semi Steppe Batha	350 Mixed evergreen oak forest	
450	Forest with <i>Pinus halepensis</i> - Shrub Steppe	77 Semi steppe batha	
452	Forest with <i>Pinus halepensis</i> - Semi Steppe Batha	375 Forest with <i>Pinus halepensis</i>	
475	Shrub Steppe-Semi steppe batha-Mixed deciduous oak forest	77 Semi steppe batha	
525	Mixed evergreen oak forest - Shrub Steppe-Semi steppe batha	77 Semi steppe batha	
527	Forest with <i>Pinus halepensis</i> - Shrub Steppe-Semi steppe batha	77 Semi steppe batha	
650	Mixed Evergreen/Deciduous forest	650 Mixed Evergreen/Deciduous forest	
727	Mixed Evergreen/Deciduous forest-Semi Steppe Batha	650 Mixed Evergreen/Deciduous forest	
802	Mixed Evergreen/Deciduous forest - Shrub Steppe/Semi steppe batha	77 Semi steppe batha	
675	Forest with <i>Pinus halepensis</i> and mixed deciduous oak	3310 Forest with <i>Pinus halepensis</i> and mixed deciduous oak	
725	Forest with <i>Pinus halepensis</i> and mixed evergreen oak	3330 Forest with <i>Pinus halepensis</i> and mixed evergreen oak	
1,025	Mixed evergreen oak forest - Forest with <i>Pinus halepensis</i> -Mixed deciduous oak forest	3320 (Mixed forest)	
3340	Mixed forest-desert scrub	75 Shrub steppe	
3393	Mixed forest-shrub steppe	77 Semi steppe batha	
3395	Mixed forest-semi steppe batha	3320 Mixed forest	
3472	Mixed forest - Shrub Steppe/Semi steppe batha	77 Semi steppe batha	

4.5 Model validation

To facilitate the evaluation of the different models, the data are divided into training and testing subsets. The output is then converted into binary maps to distinguish suitable versus unsuitable areas by selecting a threshold. Because there is no consensus in the literature regarding the best way to evaluate SDM models based only on presence information (Hirzel et al. 2006), the models were validated using various measures and statistics that evaluate different aspects of the model's performance. After a threshold has been applied, the results are compared qualitatively against known ranges for the different regions and vegetation categories or associations. The performance of the model is also tested through the *omission rate* and the *proportional predicted area* (Phillips et al. 2006), and based on whether the output is better than if it had been predicted by chance. The performance of the models across all thresholds was also examined using the area under the curve measure. In addition, variable performance is also characterized by several statistical tests generated by MAXENT. Finally, the projected models are qualitatively compared against palynological information and proxy records.

4.5.1 Statistical analyses

First of all, the datasets for each model were split into training and testing subsets. Because the models by plant geographic associations have large sample numbers, they were partitioned into distinct testing and training datasets (split sample approach, Fielding and Bell 1997). The models by vegetation subcategory have smaller sample sizes. The datasets were then split into samples using 10-fold cross validation, which is another effective way to evaluate the models' predictive output (Elith and Leathwick 2009). In this case, the data are split into several mutually exclusive training

and testing sets (Hastie et al. 2001; Kohavi 1995). When the model is run, the subsets are removed with each succession, and the model is re-estimated with the retained data and predicted to the omitted data. This option is recommended by many authors since it makes use of all the observations to train the model (Elith and Leathwick 2009).

Once the output is created, there are two types of errors that could occur: error of omission and error of commission. In the first, areas actually inhabited are omitted. The second involves predicting as part of a species' geographic distribution an area that is in reality uninhabited. Furthermore, it can be subdivided into real commission error and apparent commission error. In both cases a location has been misclassified, but the difference lies in that the misclassification could be due to the differences between realized and fundamental niche (Peterson et al. 1999). The traditional approach for assessing these errors consist of an error or confusion matrix (Table 4.16), from which various statistics can be derived like overall accuracy and Kappa.

Table 4.16. Confusion Matrix

	<i>Recorded present</i>	<i>Recorded absent</i>
<i>Predicted present</i>	a (true positive)	b (false positive)
<i>Predicted absent</i>	c (false negative)	d (true negative)

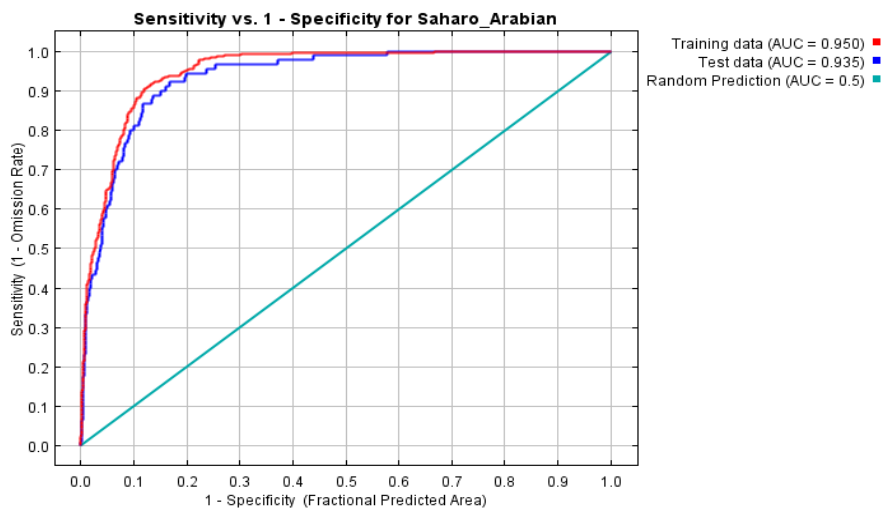
However, since the goal in this study is to estimate the potential distribution (which can never be fully validated due to the difference between the realized and fundamental niche) and there is no absence information, other measures derived from part of the confusion matrix can be used to indicate if the model is useful. For instance, we can investigate whether most observations predicted as part of the distribution are found in areas that appear reasonable and test if the prediction is better than if it had been done by chance.

Sensitivity or true positive fraction, which is the proportion of observations correctly predicted and represents omission error, can be estimated by $a/(a+c)$. You can also estimate the omission rate or false positive fraction, which represents errors of commission by $c/(a+c)$. Sensitivity and omission rate sum to 1, so if one has a high value, the other will be low. Although obtaining low omission rates are desired for a model (Anderson et al. 2003), further work is needed to determine if the model is useful since, for instance, you can achieve high sensitivity and low specificity by simply predicting a large fraction of the area as suitable (since all the observations will be correctly classified but so is most of the study area). So the results can be tested for their statistical significance by applying a one-tailed binomial or a chi-square test that assesses the statistical significance of obtaining the resulting omission rate by chance alone (Anderson et al. 2002). In other words it tests the null hypothesis that, given the fractional area predicted, the test points are predicted no better than if they had been predicted by chance (Elith 2008).

In addition, the widely used Area Under the Receiver Operating Characteristic curve (AUC) is estimated (Figure 4.19) internally by the software. This measure is derived from the receiver operating curve (ROC). The AUC is a statistic that evaluates the model's performance (regardless of threshold) by providing a measure of how well it is able to discriminate a location where a species is present (sensitivity) versus where it is absent (Fielding and Bell 1997; Hanley and McNeil 1982). Because Maxent has no information regarding absences, it uses randomly selected 'pseudo-absences' instead (Phillips et al. 2006). This curve is produced by plotting sensitivity on the y axis against 1 minus specificity across different thresholds on the x axis (1-specificity is also known as

the false positive rate and represents errors of commission, whereas specificity, also known as the true negative fraction, refers to the proportion of observed absence or pseudo absence records correctly predicted as absent). As mentioned in the section for selecting thresholds, the AUC curve is also used for selecting various thresholds (Pearson 2007). As the threshold increases, the proportional predicted area will decrease. As this happens, sensitivity decreases (observed presences correctly predicted), whereas specificity increases. This information is used to find some of the most commonly used thresholds like equal sensitivity and specificity or the maximized sum of sensitivity and specificity.

Figure 4.19 Example of the Area Under the Curve generated by MAXENT.



Basically, the closer the curve is to the upper left corner of the plot (Figure 4.19), the better the model's performance (Robertson et al. 1983). It ranges from 0 to 1 when presence/absence information is used. However when pseudo absences are used, the highest value is $1 - a/2$, with a referring to the portion of cells occupied by the species. Because a is unknown, it is not possible to determine the optimal value. The statistic can then be interpreted as meaning how well the model is able to distinguish a true presence

from a randomly chosen point. A value of one means the model was able to discriminate completely, a value of 0.5 means the model's discriminative performance was the same as a random guess, a value smaller than 0.5 means the model's discriminative performance was worse than a random guess (Elith et al. 2006). As a rule of thumb (Swets 1998), when the AUC is less than 0.5 it indicates the model was worse than chance, between 0.5 – 0.7 it indicates low accuracy, 0.7 – 0.8 suggests the model accuracy is fair, 0.8-0.9 is good, and values greater than 0.9 represent excellent model accuracy. Overall, AUC values above 0.75 are considered potentially useful (Pearce and Ferrier 2000). As Elith notes (2008), species with narrow distributions (with regard to the study area) are expected to have higher AUC values.

Maxent also has a series of internal validation methods that facilitate the interpretation of variable performance amongst models. There is a jackknife test that estimates the importance of the different variables. It also calculates response curves that show how the prediction relates to particular variables, as well as which variables were most important when training the model. All of these are reported in Chapter 5.

4.5.2 Proxy Records

As discussed in Chapter 3, proxy records that allow palaeoclimatic and paleoenvironmental reconstruction in the study area have been assembled at different space and time scales from various sources like ice cores, palaeobotanical records, lacustrine and fluvial sediments, cave speleothems, and palaeosols (Robinson et al. 2006).

Besides general information on when climatic shifts occurred, the palaeobotanical records are of special importance in this study since they allow vegetation reconstructions at different scales. Not all of the indicator species have equal representation in the pollen spectrum. Nevertheless, the presence and percentage of certain species provide valuable information that can be linked to the outputs of the models (by vegetation category). The predicted distributions are therefore qualitatively compared (Chapter 7) against vegetation inferred from pollen and other proxy records as discussed in Chapter 3. Table 4.17 lists the main species that are used for comparison.

Table 4.17. Indicator species present in the pollen record.

ARBOREAL POLEN	
<i>Quercus</i> (Woodland)	<i>Quercus</i> is a good indicator of rainy periods. The curve of <i>Quercus</i> pollen follows an increase in humidity and decrease of temperature (Horowitz 1971). A disadvantage is that it is usually hard to identify to the species level. Horowitz (1971: 262) found that peaks of <i>Quercus</i> indicate higher percentages of <i>Q. ithaburensis</i> grains. At present, <i>Quercus calliprinos</i> (evergreen) indicates the southern and eastern boundary of the Mediterranean maquis in Jordan. It is also a dominant tree in the forest-steppe of the southern Jordan highlands and is found alongside <i>P. palaestina</i> (Davies and Fall, 2001). <i>Quercus ithaburensis</i> (deciduous) grows today in the Golan, Israel and Jordan.
<i>Olea europaea</i>	Peaks of <i>Olea europaea</i> indicate warm climate. This is an insect-pollinated tree. Horowitz (1971: 262) indicates its pollen occurs in large quantities in the air. In his diagrams, he found spectra with 40 % <i>Olea</i> , which suggests warm climate. Its present distribution indicates the former extent of the evergreen maquis (Davies & Fall, 2001). It was domesticated in the sixth millennium BP (Neef 1990). Although it has been cultivated extensively throughout the region ever since, its peaks occurred during the Bronze Age and classical Roman and Byzantine occupations (Fall et al. 1998). In Jordan, <i>Olea europaea</i> defines the extent of late Holocene Mediterranean forests (Davies and Fall, 2001).
<i>Pistacia</i>	<i>Pistacia</i> is sometimes hard to identify to the species level. Its curve is similar to <i>Olea</i> , suggesting warm temperature during its peaks. It is an insect-pollinated tree. Because of this, it is usually underrepresented in pollen cores. Like almond, it is a drought tolerant tree.
<i>Pinus halapensis</i>	Like olive, its pollen has high dispersal capabilities. This is another indicator of warm and dry climatic conditions (Horowitz 1971). Nowadays it grows in areas drier and hotter than those where <i>Quercus</i> inhabits. The same was likely in the past (Horowitz 1971).
Bank trees like <i>Salix acmophylla</i>, <i>Populus euphratica</i>, <i>Acer</i>, <i>Ulmus</i>, <i>Tamarix jordanensis</i>	These indicate river bank vegetation which was not impacted by climate changes as much as other vegetation (they don't depend on humidity and temperature changes but on river flow). As Horowitz points out though, their curve reflects the percentage cover of surrounding maquis or forest indirectly, since an increase in the pollen production of forests is accompanied by a drop in the curve of bank trees. The opposite is also true, the pollen curve of forests drops when that of bank trees increases. Poplar (<i>Populus</i>) is found close to the Jordan River and behind it tamarisk (<i>Tamarix</i>) is found in almost pure stands (Zohary 1962).
NON ARBOREAL POLLEN	
<i>Centrospermae</i>, <i>Umbelliferae</i>, <i>Compositae</i>, <i>Cruciferae</i>, <i>Papilionaceae</i>	Peaks point to a humid and somewhat cool climate (Horowitz 1971). See Davies and Fall (2001) for a description of the Papilionaceae (legume) family and its major species.
<i>Artemisia</i> (steppe)	More frequent when it is dry, like today. Indicates steppe. At present, <i>Artemisia herba-alba</i> is found in abundance in the Syrian Desert, across the Negev Desert of Israel, upper Mesopotamia and the Iranian Plateau. In Jordan, its distribution indicates the SW boundary of the Irano Turanian steppe vegetation (Davies and Fall, 2001).
<i>Rubus sanctus</i>, <i>Lythrum salicaria</i>	Peaks under humid conditions.
<i>Chenopodiaceae</i> (goosefoot) (Desert & Semi Desert)	Most of its species are halophytes (live in saline habitats and desert conditions). Most common genera found in desert environments include <i>Haloxylon</i> Bunge., <i>Hammada</i> Iljin., <i>Anabasis</i> L., <i>Atriplex</i> L., <i>Noaea</i> Moq., <i>Salsola</i> L., <i>Suaeda</i> Forsk. Ex Scop. The pollen of this family is divided into four groups: <i>Noaea</i> ; <i>Suaeda</i> ; <i>Aellenia</i> ; other.
<i>Sarcopoterium Plantago</i>	These plants produce pollen in low quantities. They indicate disturbed forests.

The approach chosen to model the distribution of plant associations was presented in this chapter. After reviewing the evolution of the field of SDM and discussing the particular algorithm selected in this study, the different steps needed to run the models were outlined and discussed (e.g., observations used, variable selection, model calibration parameters, and evaluation metrics).

Chapter 5

RECONSTRUCTION OF MODERN VEGETATION

This chapter presents the results of the vegetation models for the present time period. Although the goal of this study is to model potential vegetation through the Holocene, the reconstruction of present day vegetation is crucial to this study because it is used to as the basis from which models are then extrapolated or projected into the past. The results are presented and discussed for each of the modeled categories, which include the more general models by plant geographic associations as well as the more detailed ones in which vegetation is subdivided into categories (both edaphically and climatically influenced vegetation groups). The continuous potential surface that was created by Maxent is shown with some commonly used thresholds. Once the threshold that maximizes the sum of sensitivity and specificity was applied, the resulting presence/absence map (per category) is also shown and discussed. In addition, the resulting suitable areas are also compared against other maps or anecdotal evidence selected from the literature. When comparing the results from this study to other maps it is important to remember that each of these was prepared at different scales and by different authors who may have had different classification schemes and objectives. Because of this, there will always be some informative disagreement amongst them.

Three of the detailed forest categories (*Quercus calliprinos*, *Q. ithaburensis*, *Pinus halepensis*) are also compared to another set of predictive models generated by the BioGIS project of the Hebrew University (BioGIS, the Israel Biodiversity Information System), which includes a national database of Israel's flora and fauna. Like the models being derived in this study, the models created in BioGIS also reflect the potential distribution range of the species, based on a series of observations derived from multiple sources. BioGIS relies on a different type of algorithm (bioclimatic model) than the one

used in this study (maximum entropy) to determine a suitable distribution (Kurtzman and Kadmon 1999). It also only makes use of climatic variables to determine the distribution range of the species being modeled. The suitable area includes all those cells that comply with the climatic values of the observations. These cells are ranked into minimum, 5th percentile, 95th percentile, maximum for each climatic variable. For example, for *Q. calliprinos* observations, the minimum mean annual rainfall according to the observations is 250 mm, the 5th percentile is 431 mm, the 95th 893 mm, and the maximum 1201 mm. The resulting distribution map is then subdivided into main and periphery areas (main including all the cells that meet the requirements of all the climatic variables used and are between the 5th and 95th percentile). It is important to remember that differences between model outputs can result from many factors, including differences between the observations used (spatial scale, locations used, collection methods) and variables implemented (how they were derived, which variables are used).

The last part of this chapter discusses the performance of the models, with regard to evaluation metrics. The receiver operating characteristics and area under the curve for the models created with Maxent are presented, as well as the statistical significance of the prediction once the threshold that maximizes the sum of sensitivity and specificity was applied. In addition, the contribution of the different variables with regard to the models created is discussed.

5.1 Model outputs

5.1.1 By plant geographical association

5.1.1.1 Saharo Arabian association

The Saharo Arabian association (Figure 5.1) represents the hottest and driest portions of the study area. A continuous surface of potentially suitable areas across various

thresholds shows that if the minimum training presence threshold is applied, most of the study area would fall under this category. Use of the selected threshold, on the other hand, shows most of the Rift Valley as belonging to this category. From the Arava Valley it stretches north to the Bet Shean Valley. Along the Arava Valley it also stretches into the Negev and lower elevations of the southern highlands of Moab and Edom. It also penetrates into the drainage basins of several wadis that drain into the Rift Valley. This is more obvious east of the Rift Valley where the larger basins are located (e.g., the Wadi Mujib). In the south eastern portion of the Wadi Arava in Jordan, it climbs towards the Jordanian highlands as it wraps around Irano Turanian and Mediterranean enclaves and then occupies the easternmost strip of the study area in the Moab and Edom subdivisions. This fringe, known as Badia in Jordan (Al-Eisawi 1996), represents the beginning of the eastern desert of Jordan or the North Arab Desert, which stretches into Iraq, Syria, and Saudi Arabia. Only the margin is captured in the study area.

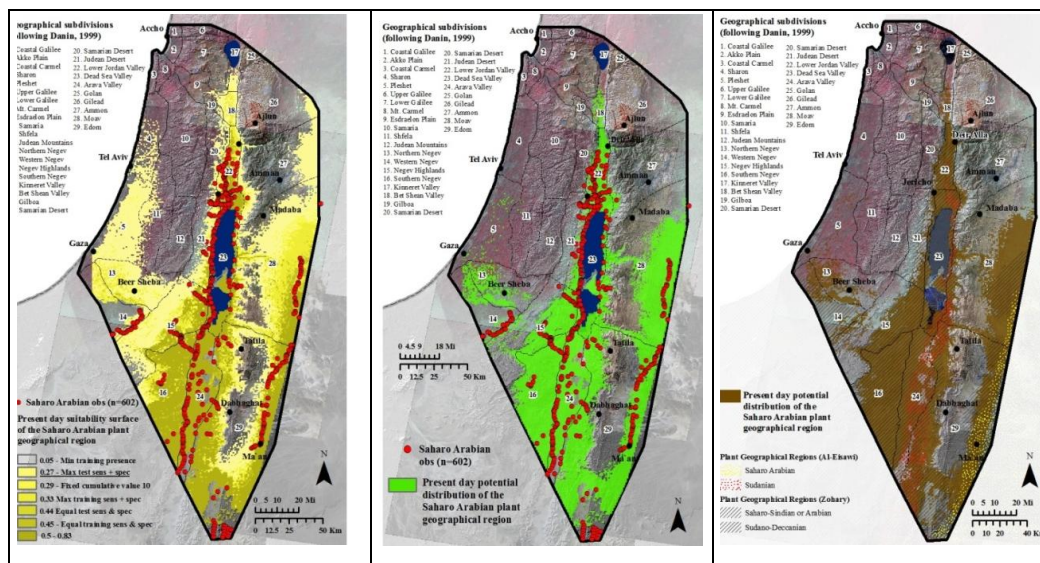


Figure 5.1. Resulting Modern Distribution of the Saharo Arabian plant association. Continuous suitability surface (left), presence/absence (middle), comparison against other sources (right)

In his map of plant geographical regions, Al-Eisawi (1985) actually divides the Saharo Arabian region, as defined in this study, into two categories: Sudanian and Saharo Arabian. The Sudanian area experiences the hottest temperatures and is below sea level. It extends in the Rift Valley from the Gulf of Aqaba to around Deir ‘Alla. The Saharo Arabian region then refers to the Eastern Desert.

The area found suitable by the model output for the Saharo Arabian plant geographical region is quite similar to the area delineated in other maps. For instance, Zohary (1962) shows almost the same extent in the Rift Valley and adjacent areas. Our model extends this region slightly farther north (Zohary’s stops at Deir ‘Alla whereas Al-Eisawi’s ends a few kilometers south of Deir ‘Alla) and penetrates into wadi valleys. Except for the Northern Negev, which Zohary classified as Irano Turanian, the remaining Negev subdivisions are almost identical with Zohary’s map. Southeast of the Rift Valley, Zohary shows the Saharo Arabian region expanding into the plateau (just north of Wadi Rum) exactly where the model produced here shows it. Al-Eisawi’s area in the Rift Valley is slightly tighter than ours. The largest discordance occurs on the plateau with regards to the fringe of desert vegetation that marks the beginning of the Eastern Desert. Except for the area around Ma’an, each reference map shows this region with varying widths and extents.

5.1.1.2 Irano Turanian association

The Irano Turanian association represents steppe vegetation, characterized by small shrubs and bushes and a lack of trees. The resulting distribution is shown in Figure 5.2. As the continuous surface shows, the threshold of minimum training presence would have resulted in a large chunk of the region being classified as Irano Turanian. Instead, the selected threshold is more exclusive and resembles the area delineated by Eig

(1931/32) and Zohary (1962; 1966). Except for the northern portion of the study area, it surrounds the Mediterranean region, forming a transition into the Saharo Arabian region. On the plateau, it interrupts the longitudinal Mediterranean belt in some of the wadi valleys like the Wadi Mujib, through which it penetrates into the lower elevations of the rift valley. In the northern Negev, it wraps around the Mediterranean region and then continues southward along the higher elevation areas of the Negev Highlands.

The Irano Turanian region is also present along the northern portion of the Rift Valley, from the Kinneret to the Lower Jordan Valley. This delineation differs from Zohary's interpretation. As with the Saharo Arabian region, most of the disagreement between the different sources is found in the plateau region. Basically the model produced by Maxent shows a larger suitable area than Zohary and Al-Eisawi show in Gilead and Ammon, whereas the opposite occurs in Moab and Edom (1962 and 1996, respectively).

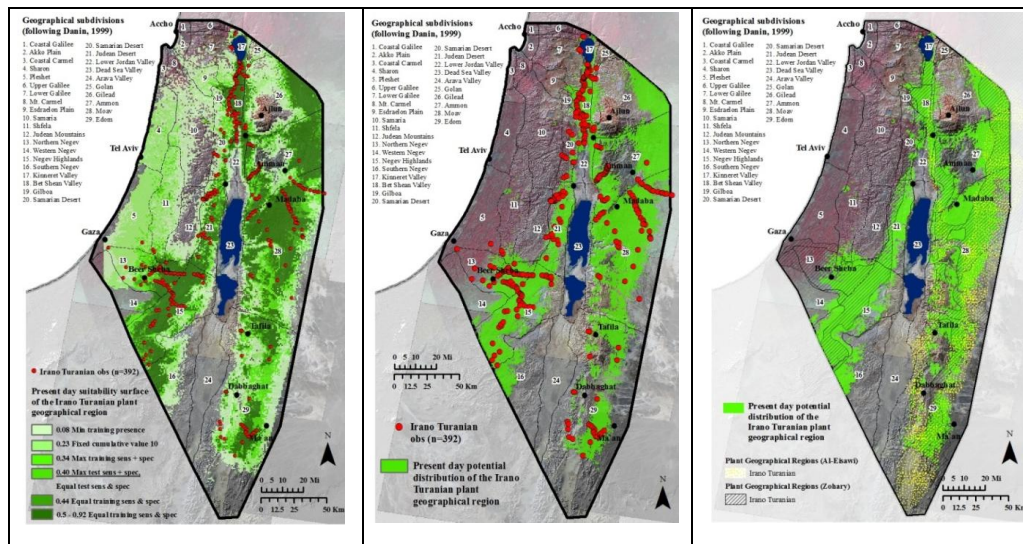


Figure 5.2. Resulting modern distribution of the Irano Turanian plant association. Continuous suitability surface (left), presence/absence (middle), comparison against other sources (right).

5.1.1.3 Mediterranean region

The Mediterranean association, shown in Figure 5.3, represents the vegetation of the moister portions of the study area, which are also the least impacted by extreme temperatures. Because of this, as well as the presence of fertile soils like Rendzinas and Terra Rossas, maquis and forests are able to develop. As was the case with Irano Turanian and Saharo Arabian model outputs, the threshold of minimum presence predicts an excessively large area as Mediterranean. In this case, this threshold appears to also incorporate the Irano Turanian region. Use of the chosen threshold, on the other hand, produces general agreement with Eig's (1931/32) and Zohary's (1962, 1966) delineation of this territory.

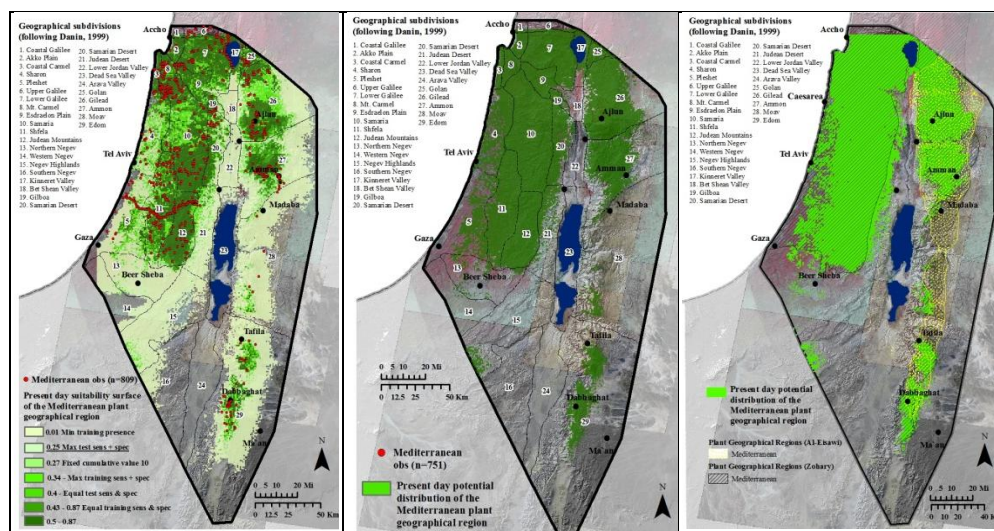


Figure 5.3. Resulting modern distribution of the Mediterranean plant association. Continuous suitability surface (left), presence/absence (middle), comparison against other sources (right).

Two large areas are found in the northern portion of the study area, on both sides of the rift valley. These meet in the northern part of the study area in the Kinneret Valley. As will be discussed below, these areas are potentially suitable to various climax forests such as evergreen oak, deciduous oak, pine, and the open forests of carob and pistacia.

On the western side of the rift valley, the Mediterranean region occupies a greater extent as it spreads south until it reaches the edge of the Northern Negev. East of the rift valley, the Mediterranean region is not as extensive as its coastal counterpart, although it is still the dominant region in both Gilead and Ammon. The area around Madaba marks a halt to this region. Further south still, a few patches are found in the plateau region of Moab and Edom.

The suitable Mediterranean area resembles that shown by other maps. Nevertheless there are several differences. For instance, Zohary depicts the whole coastal plain as belonging to the Mediterranean region, whereas the output from this model shows that only the coastal plain north of Sharon (including) is suitable. The suitability of the Mediterranean category for the remaining plains is fragmented, and becomes even more so farther south (the Pleshet plains are more fragmented than the Sharon). It is important to highlight that different authors have several interpretations regarding the coastal vegetation of Israel. In his map of natural environments, Horowitz shows a thin strip (about 5 km wide) adjacent to the coastal sand dunes which extends from the Western Negev all the way north to Cesarea as Saharo Arabian (Horowitz 1979: 28).

On the eastern slopes of the Judean Mountains Zohary draws the boundary of the Mediterranean region along the boundary with the Judean Desert, and the suitable areas according to the modeled output extend slightly into the Judean Desert (which Zohary classified as Irano Turanian). In the plateau region suitable areas according to Maxent occupy a smaller area than Zohary's interpretation, although there are still several suitable patches in Moab and Edom. Parts of these are presently populated by juniper, oak, cypress, and pistacio.

The Mediterranean region is also shown in Al-Eisawi's map, although it appears to be more general, since it shows Mediterranean areas as an uninterrupted strip of

varying widths that stretches from Gilead to Edom (around Dabbaghat). The southern extent of the Maxent output and Zohary's are slightly farther south (about 20 km).

5.1.2 Edaphically influenced vegetation types

5.1.2.1 Riparian vegetation

As described in Chapter 4 (Methods), the riparian vegetation category was delineated by buffering drainage networks throughout the study area (Figure 5.4). The most significant area influenced by riparian vegetation is found in the flood plain of the Jordan River in the Rift Valley. Consequently, the largest buffer was placed around this river (1.5 km on each side). This represents a belt of poplar (*Populus euphratica*) trees immediately adjacent to the river followed by one of tamarisk trees (*Tamarix jordanensis*).

The more arid portion of the study area contains hundreds of wadis, the largest of which were buffered 500 m on each side to represent riparian wadi vegetation. These include the series of wadis that dissect the highlands east of the Rift Valley, and are populated by species like *Nerium oleander*, *Tamarix sp.*, *Acacia sp.*, *Ochradenus baccatus*, *Phoenix dactylifera*, *Phragmites communis*, *Prosopis farcata*, and *Populus euphraticae*.

Along the coastal plain a series of rivers drain from the mountains to the coast. These have enabled the formation of swamps in the northern coastal plains, which developed where some of these rivers intersect the longitudinal sand dune belt adjacent to the Mediterranean Sea (Zohary 1947a). Riparian vegetation is found in these swamps and along the river banks. Recently, many of these rivers have been channelized, causing large swampy areas to shrink or dry completely. Nevertheless, the original course of these rivers was digitized and buffered 500 m on each side.

Although he didn't include it in his map, Zohary (1947) mentions the hydrophytic vegetation of the Coastal Plain (along rivers and wetlands) and along the Jordan River as the main areas where this type of vegetation is found. Besides the Jordan River, Al-Eisawi also mentioned the banks of other major rivers and wadis like the Yarmuk River, Zarka River, Wadi Shuaib, Wadi Al-Hasa, and Wadi Mujib (shown in his vegetation map which is included in Figure 5.4 for comparison purposes).

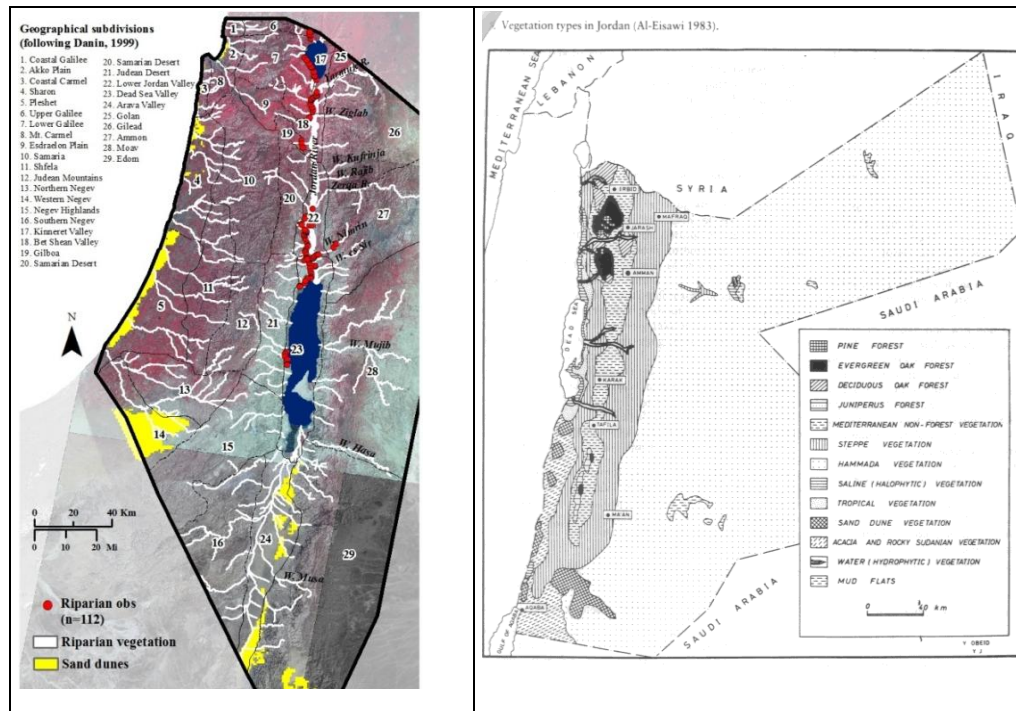


Figure 5.4. Mapped riparian vegetation.

5.1.2.2 Sand dune vegetation

Sand dune vegetation is essentially determined by the existence of sand dunes, which can be either along the coast or inland (Figure 5.5). Sand dune areas were delineated using a variety of sources like geology maps (Bartov 1994; Sneh *et al.* 1998), vegetation maps (Al-Eisawi 1996; Danin 1999), aerial photo interpretation, and field work conducted during the spring of 2010. As described in Chapter 4, sand dune species

can vary within these subsets, since each has different edaphic and climatic tolerances that influence plant growth in distinct ways.

To summarize, the coastal dunes originate from sediment that is transported from the Nile River to the Mediterranean Coast and then blown inland. The sands become stable through the establishment of the grass *Ammophila arenaria*, which is succeeded by *Artemisia monosperma* and other *Artemisia* species and finally by *Retama raetam* shrubs. In Sharon, succession actually reaches climax with the appearance of *Pistacia lentiscus*, *Calicotome villosa*, and *Ceratonia siliqua*. The Western Negev sands become populated by the grass *Stipagrostis scoparia* and eventually the species *Artemisia monosperma*, *Noaea mucronata* and *Panicum turgidum*. Farther east, sandy areas found in the Wadi Araba and Wadi Rum regions are dominated by *Haloxyton persicum*, *Hammada salicornia*, *Hammada salicornia*, and *Salsola cyclophylla*. In the classification used in this study, coastal dunes were differentiated from inland dunes.

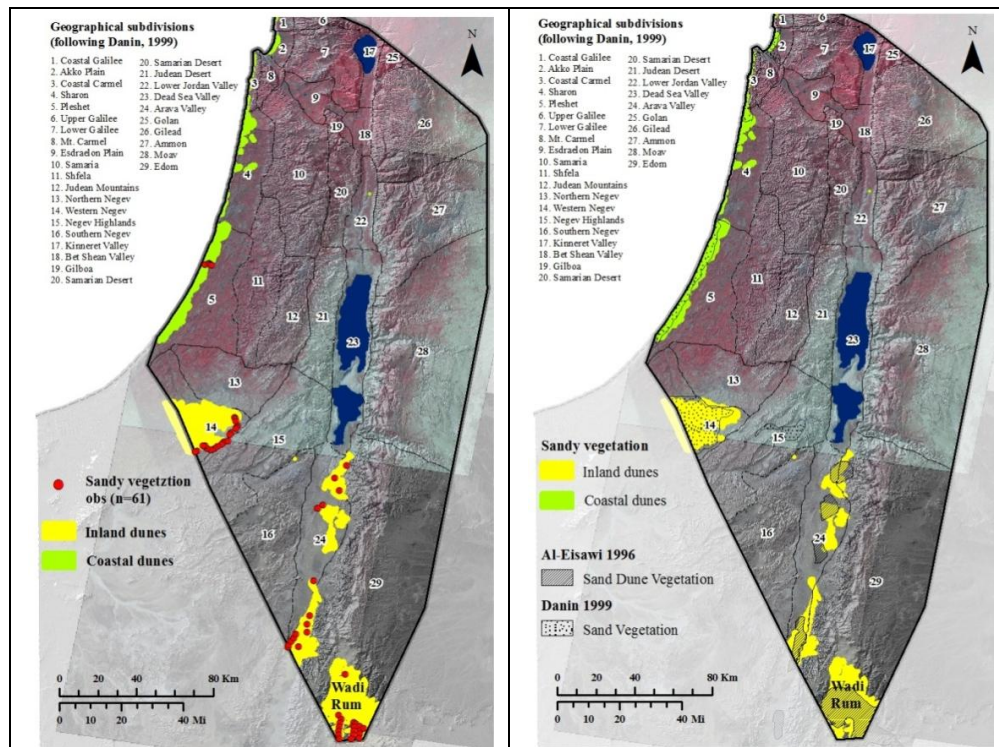


Figure 5.5. Mapped Sand Vegetation.

5.1.2.3 Halophytic vegetation

Halophytic vegetation concentrates on the highly saline soils of the Lower Jordan and Dead Sea Valleys and along the Wadi Arava. To delineate it more specifically, it was modeled with Maxent using 113 observations, as well as the environmental variable geology, annual precipitation, July average temperature, distance to rivers or wadis, elevation, and mean annual temperature. A mask was also used to constrain the output to the Rift Valley and immediately adjacent areas. The continuous surface across various thresholds shows its distribution to go from the Bet Shean Valley to the Arava Valley (Figure 5.6). Once the threshold was applied, the area found suitable slightly shrunk, and consists of the Dead Sea surroundings which stretch north to the Bet Shean Valley, where it concentrates on the flood plain. It stretches south a bit further than the Lisan Marls, which mark the edge of the ancient Lake Lisan.

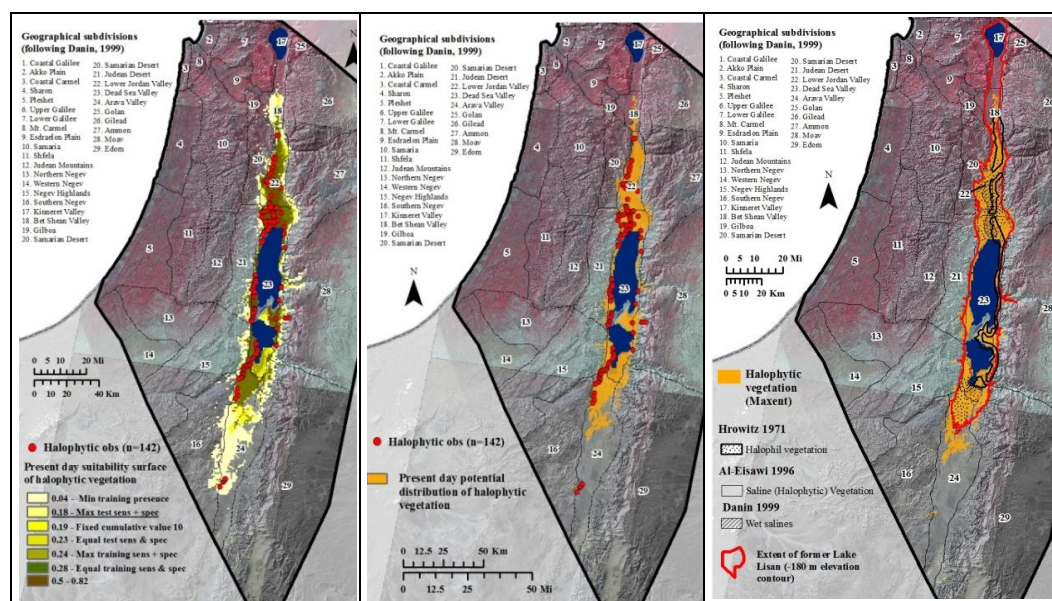


Figure 5.6. Resulting modern distribution of halophytic vegetation. Continuous suitability surface (left), presence/absence (middle), comparison against other sources (right).

According to Zohary (1947a), the vegetation would consist of the *Junceto-Phragmiton* association along the banks of saline or brackish springs or brooks;

Tamaricion tetragynae association on salines that are flooded during part of the year; *Salsolion tetrandra* association along the Lissan Marl formation (former Lake Lisan). Other authors classified this type of vegetation in their maps also around the Dead Sea area. The predicted suitable area according to Maxent is similar to these.

5.1.2.4 Tropical Sudanian vegetation

Within the study area, Tropical Sudanian vegetation is found in the Rift Valley. The high temperatures found in this area, existence of wadis and permanent flowing springs create the necessary tropical conditions for this vegetation. As a result, enclaves are found amidst the other xeric categories also present in this area (e.g., desert savannoid, halophytic, desert scrub, and Mediterranean savannoid grasslands of the far north). Suitable areas according to the model are found around the Dead Sea from the southern shore of the Dead Sea Basin to the Bet Shean Valley (Figure 5.7).

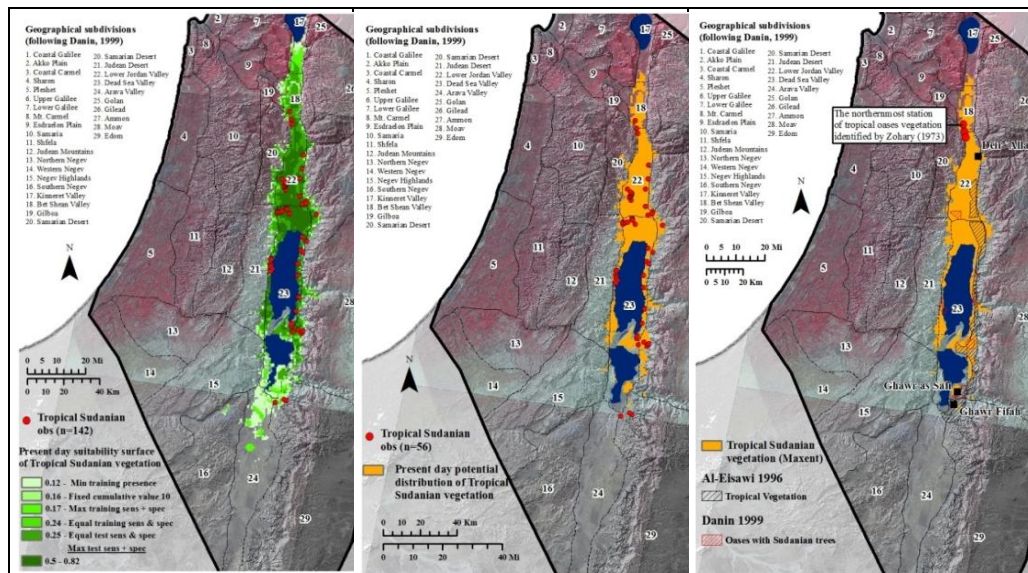


Figure 5.7. Resulting modern distribution of Tropical Sudanian vegetation. Continuous suitability surface (left), presence/absence (middle), comparison against other sources (right).

Tropical Sudanian enclaves identified by other authors also show this vegetation surrounding the Dead Sea and along the Lower Jordan Valley. Al-Eisawi mentions this

vegetation to be found between Aqaba and Deir ‘Alla, but adds that it is most prominent in the area surrounding the Dead Sea (hotspots include Ghor Safi and Ghor Faifa). In his map, Danin only attributes small areas to this category. Like Al-Eisawi, Zohary (1947) mentions the Dead Sea and Lower Jordan Valleys as the area where these oases are most prominent. In the northern distribution region, species like *Ziziphus spina Christi*, *Balanites aegyptica*, *Callotropis procera*, *Acacia tortilis* and *Acacia albida* are common. In addition to these, the southern part includes species like *Phoenix dactylifera*, *Salvadora persica*, *Moringa aptera*, *Occradenus baccata*, and *Nerium oleander*.

A few observations used in the model (shown in the figure 5.7, far right) represent the northernmost station of tropical oases vegetation (Zohary 1973). The modeled suitable area spreads about 20 km farther north of these. In another source (1947), Zohary also mentions remnants of *Acacia albidae* around a few places like Wadi Taiba, which suggests that this type of vegetation once spread over a greater area. Wadi Taiba matches with the northern extent of the suitable area according to the Maxent model.

5.1.3 Climatically influenced vegetation types

5.1.3.1 Pine forests

The type of forest represented by *Pinus halepensis* can be accompanied by several associates, including *Quercus calliprinos*, *Arbutus andrachne*, *Pistacia lentiscus*, and *Pistacia palaestina*. Along with *Hypericum serpyllifolium*, this pine forest represents one of the Mediterranean climax communities. During the time of their observations throughout the 1930s and early 40s, Eig and Zohary (1946; 1947) both mention that this category had been reduced to a few remnant stands, and presumably once occupied a much greater area. West of the Rift Valley, Eig mentions that the best preserved stands are found in the southwestern part of Mount Carmel. Zohary also reported these as well

as a few stands left in the Galilee (around Yerka), Samaria (around Safah), and the Judean Mountains (around Hebron). In general, these areas coincide with the areas classified as maquis and forest in Horowitz and Danin's maps, which are now dominated by the *Quercus calliprinos-Pistacia palaestina* association. East of the Rift Valley, *P. halepensis* stands are better preserved and can be found in Gilead and Ammon. Pure stands are found in the Dibbin Forest Reserve near Ajlun, where they are protected. This is reflected in Al-Eisawi's vegetation map. Like the Israeli botanists, the Jordanians also infer that the extent of pine forests was greater at some point. Kasapliligil notes that a few trees of *P. halepensis* scattered amongst *Q. calliprinos* dominated maquis around Fuheis shows evidence of this.

The continuous surface predicted by Maxent is shown in Figure 5.8, upper left hand corner. Once the threshold was applied, the area suitable to forests with *P. halepensis* appears to coincide with the observations mentioned above and, for the most part, resembles the output from BioGIS. The major difference lies in the patches around the Galilee which are missing in the BioGIS output. Also, the BioGIS model predicted a continuous stand stretching from Samaria to Mt. Carmel and a patch in the Esdraelon Plain which was not predicted in the Maxent output.

Pine forest is predicted in Jordan over areas much larger than present day observed distributions, but this greater predicted expanse seems to agree with anecdotal evidence. For instance, a large patch is found suitable in Gilead and Ammon, which is only interrupted by the Zerqa River. North of the river, it extends about 12 kilometers past Ajlun, which today marks its present day limit. In the south, it also expands about 12 kilometers past Fuheis. Beyond this, there are a few scattered isolated patches. The suitable predicted area thus seems to agree with that presented by other sources.

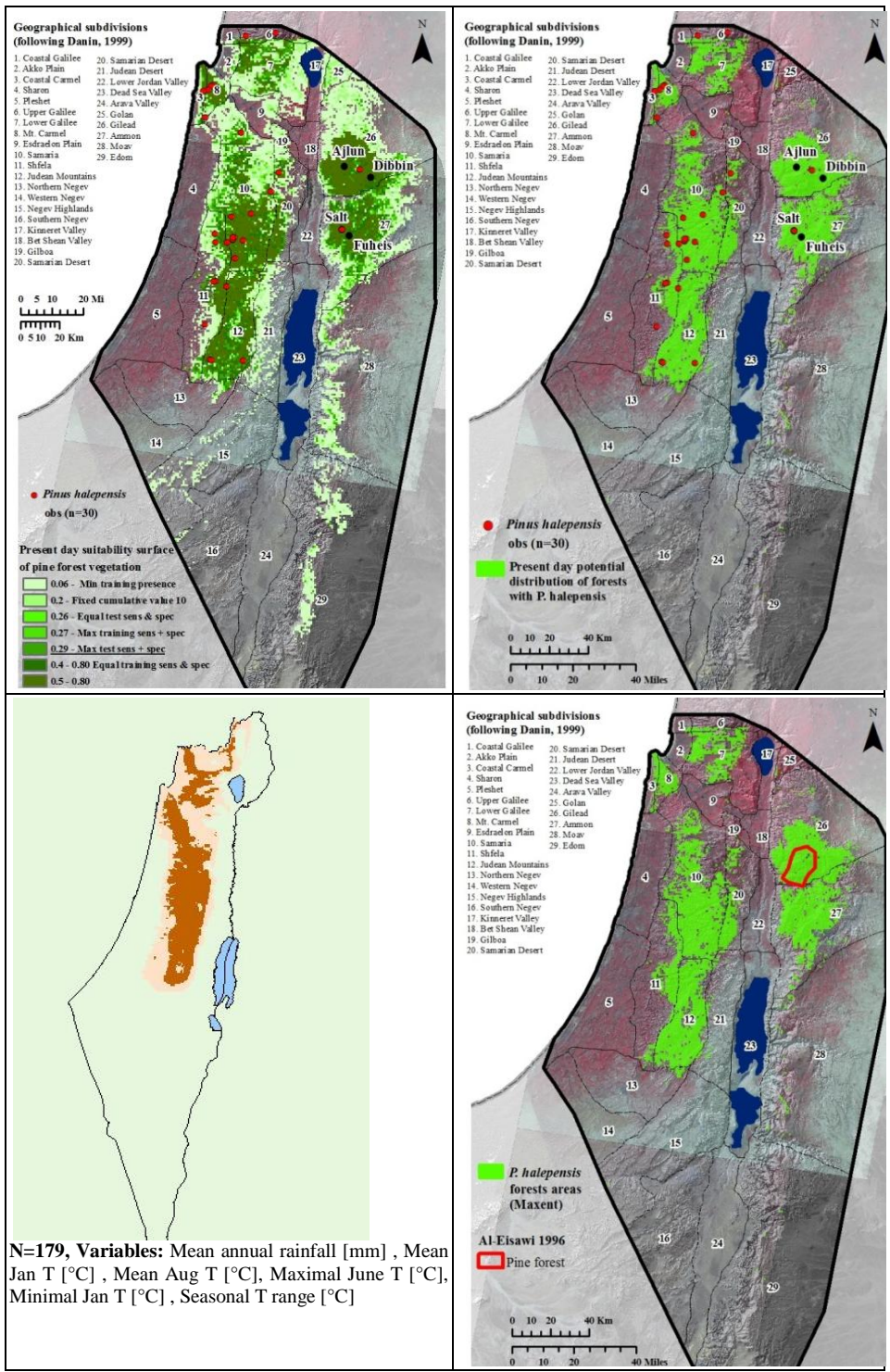


Figure 5.8. Resulting modern distribution of forests with *Pinus halepensis*. Continuous suitability surface (upper left), presence/absence (upper right), BioGIS potential distribution map (bottom left), comparison against other sources (bottom right).

5.1.3.2 Evergreen oak forests

According to Zohary, the *Quercus calliprini* association is “the most important group of arboreal associations within Mediterranean Palestine ... and constitutes the most characteristic type of the East Mediterranean Maquis” (Zohary 1947a: 8). There is no consensus about whether the *Quercus calliprinos* – *Pistacia palaestina* association (the most important association within this group) represents one of the climax Mediterranean associations or is a step down due to degradation. Regardless, this association is believed to have been the most prominent of the region (out of all the forest categories), and remains this way today. At present, it occupies significant (though fragmented) areas on both sides of the Rift Valley. West of the Jordan River, it is found in the Upper Galilee, on the mountains of Judea, Carmel and Galilee, and at the foot of Mt. Hermon. East of the Jordan River, it is found in the northern plateau districts of Gilead and Ammon around the Amman-Salt-Jerash-Ajlun area. In 1956, Kasapligil reported that this type of maquis extended from around Wadi Sir to Deir Abu Said. It is also found in the southern Plateau highlands in Edom, although accompanied by other constituents and exhibits a more dwarf like appearance.

The minimum training presence threshold classifies most of the forest area as being suitable for this category, whereas the selected threshold is more exclusive of areas that agree with the literature (Figure 5.9). The largest of these is found on the Judean Mountains, classified as *Maquis and forests* in Danin’s 1999 and Horowitz’s 1979 vegetation maps. This area is also shown in the potential distribution surface generated by BioGIS using a bioclimatic envelope model.

In addition to the areas indicated on other maps, suitable locations are also found in the Sharon coast and in the highlands of Moab. Liphshitz and Biger (1990) identify this coastal segment as being suited to this type of maquis. East of the Rift Valley in

Moab, a small suitable patch coincides with Al-Eisawi's non-forest Mediterranean vegetation category, which some authors believe would regenerate to a maqui or a forest of similar type if left undisturbed.

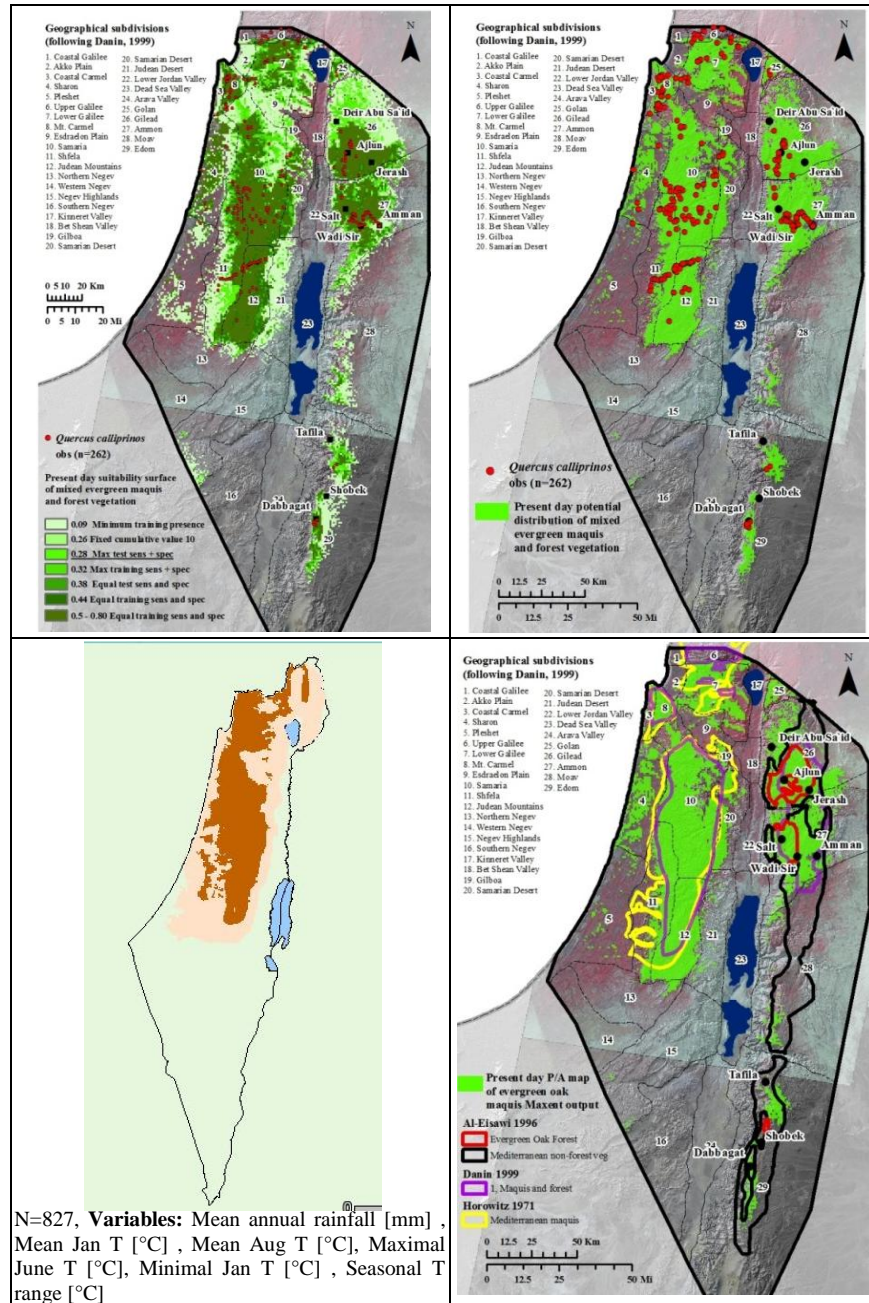


Figure 5.9. Resulting Modern Distribution of evergreen oak (*Quercus calliprinos*) forests and maquis. Continuous suitability surface (upper left), presence/absence (upper right), BioGIS potential distribution map (bottom left), comparison against other sources (bottom right).

5.1.3.3 Deciduous oak forests

The area predicted as suitable for deciduous oak forests is show in Figure 5.10.

There is some overlap with areas predicted as suitable for evergreen oak and pine forests, mainly along the Judean Mountains and the Galilee (and especially before the threshold was applied). But in general, this forest type is predicted to occur within the northernmost latitudes of the study area.

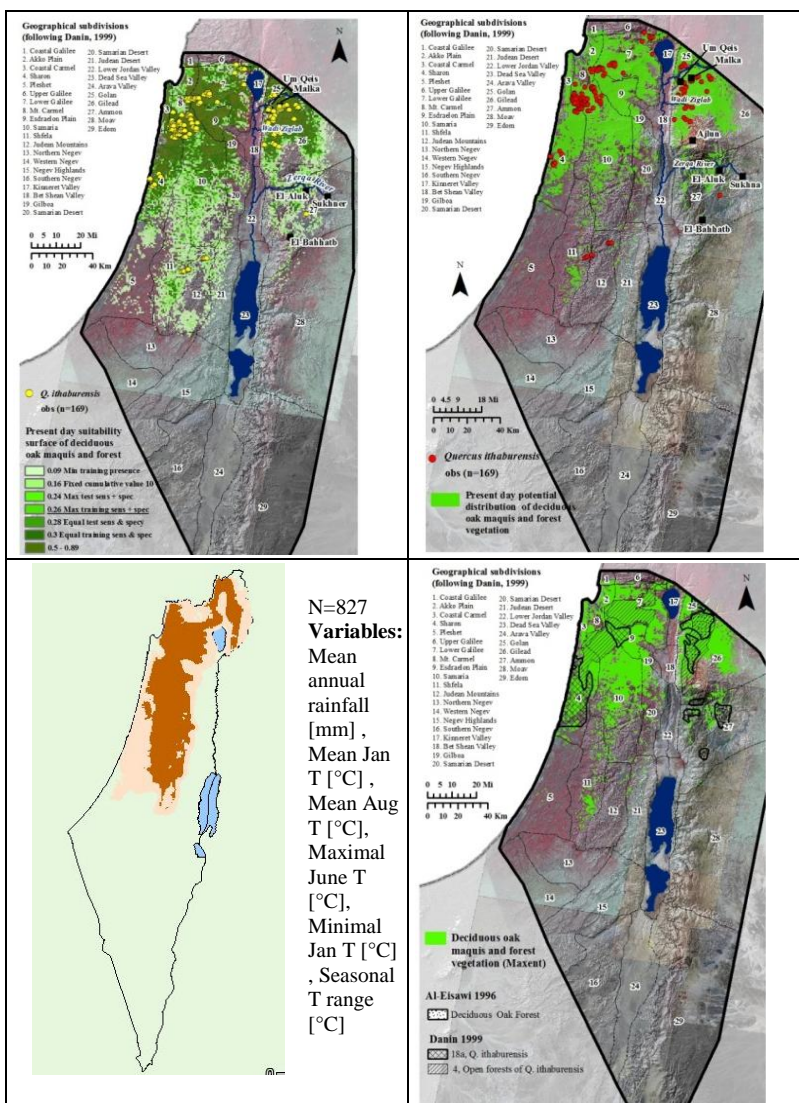


Figure 5.10. Resulting modern distribution of deciduous oak (*Quercus ithaburensis*) forests and maquis. Continuous suitability surface (upper left), presence/absence (upper right), BioGIS potential distribution map (bottom left), comparison against other sources (bottom right).

In Jordan, Kasaapligil (1956) reported that *Quercus Ithaburensis* is found intermixed with *Q. calliprinos* from El-Bahhatb to Wadi Ziglab, and becomes the dominant species from Wadi Ziglab to the Yarmouk Valley. He also mentioned a stand that extends between El-Aluk and Sukhner, which marks the easternmost extent of this type of maquis. These observations are captured by the model. From El-Bahhatb, scattered patches are seen which become denser around El-Aluk and the Zerqa River. There is a gap around Ajlun (this area is dominated by *Pinus halepensis* stands at present and also according to the model of *P. halepensis*), and then a continuous patch stretches all the way north to the Golan. The area predicted extends further east than it does at present, but this could be a result of degradation or these forests being transformed (i.e., urban areas, agriculture). Regardless, the extent does not go beyond Sukhna.

A visual inspection of the classification of this type of maquis by other authors shows some discrepancies. These are mainly because of differences in scale as well as what the authors were trying to capture. For instance, west of the Rift Valley, Danin assigned this category to a few remaining stands as well as to regions where it was present in the past but have been completely disturbed, such as part of the Esdraelon Plain and the Sharon coastal plain where this species is thought to have been the dominant tree (Danin 1999; Zohary 1947a; Zohary 1962). East of the Rift Valley, he assigned a continuous segment on the plateau in Gilead, whereas Al-Eisawi actually highlighted the areas where stands of *Q. ithaburensis* are present today. The model was able to capture all these areas.

5.1.3.4 Open forests of carob and pistacia

As mentioned before, the open forests of carob and pistacia (cerantonio-pistacion alliance) occur in three main locations (Zohary and Orshan 1959) west of the Rift Valley (Figure 5.11). The association Ceratonieto-Pistacietum typicum forms a continuous strip

along the lower elevation foothills of the mountainous region that extend from Duweima in the south into the border with Lebanon in the north. This association also includes the calcareous-sandstone hills opposite Mount Carmel. The second location is found facing the Rift Valley in the opposite side of the Samarian and Judean mountains (*Ceratonieto-Pistacietum lentisci orientale* association). It forms a much thinner belt that doesn't extend as far south and is most dense around Gilboa and the Samarian Desert (although Danin shows it in his map as almost completely encircling these mountains in the south). Around Gilboa, carob and pistacia come in contact with the *Ziziphus* grasslands of the Kinneret and Bet Shean Valleys. The third location, represented by the association *Ceratonieto-Pistacietum lentisci arenarium*, consists of stands found in the Sharon coastal plain between Falik and Nahariya, on top of consolidated dunes and on sandy soils. These stands have been significantly disturbed and only a few fragments remain (Zohary and Orshan 1959).

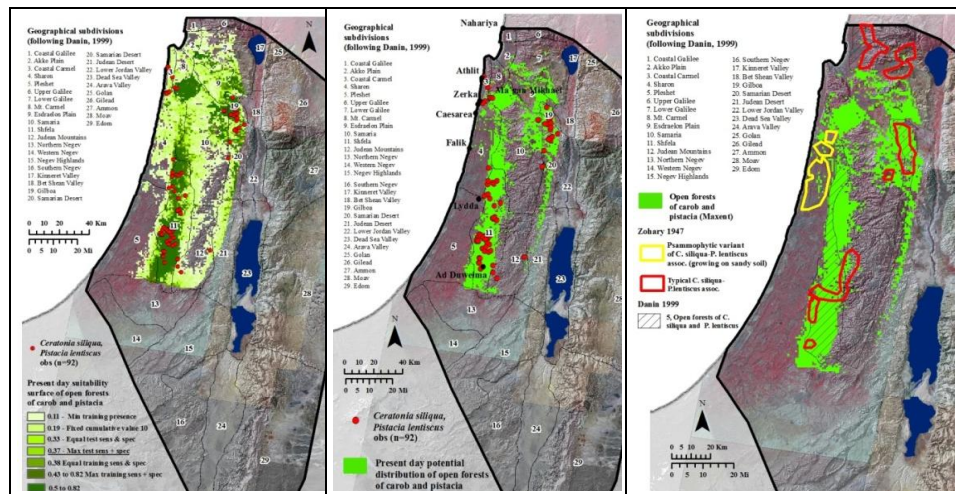


Figure 5.11. Resulting modern distribution of open forests with carob (*Ceratonia siliqua*) and pistacia (*Pistacia lentiscus*). Continuous suitability surface (left), presence/absence (middle), comparison against other sources (right).

Because this type of forest is only found west of the Rift Valley, a mask was applied when modeling the suitable distribution to limit the output to the northern half of

the area west of the Rift Valley. Once the threshold was applied, suitable areas basically agree with the literature (Figure 5.11). They essentially wrap around the mountains of Shfela, Samaria, and Judea, and form a thicker belt on the coastal side. Along the coast, isolated patches are also identified as suitable.

5.1.3.5 Shrub-steppe with open forests of juniper, cyprus, oak, pistacia

Although juniper, cyprus, oak, and pistacia trees are not always found together in this area, they were grouped into one category and represent the southernmost forests of the Jordan highlands or plateau region. Contrary to the rest of the forest categories, they are accompanied by understory species that are typical of steppe environments (e.g., *Artemisia herba alba*, *Noaea mucronata*). Once the threshold was applied, these forests are predicted to occupy a fairly continuous strip in the Highlands of Edom. A few fragmented pixels are also found just north of this strip in Moab, after it is intersected by Wadi Hasa. In its southern end, the suitable area veers slightly towards the southeast.

At present, open forests of this type which also include other typical Mediterranean trees like *Ceratonia siliqua*, *Olea europaea*, and *Arbutus andrachne*, stretch from Tafila to Ras An-Naqab and are found between 850 to 1,500 m, although scattered trees in wind protected areas can occur as low as 600 m and at elevations higher than 1,500 m. The Dana-Petra region has been found to contain the richest assemblage of relict Mediterranean species in all of the Near East, a refugium that would have presumably expanded during wetter times. Near Ad-Dabbaghat is a stand of *Pistacia atlantica* that is estimated to be 500 years old. In Khunnag AL-Arz near Tafila, there is a stand of *Juniperous phoenicea* and *Cupressus sempervirens* trees that is believed to be over 1,000 years.

When compared to the Juniper and Evergreen oak forests shown in Al-Eisawi's map, the area predicted as suitable represents a much wider distribution. This is in part due to the degradation of these forests which would otherwise occupy a greater extent (Figure 5.12). Nevertheless, the southeastern tip of the predicted strip is questionable, since areas occupied by this category are not indicated in any reference map to extend so far towards the southeast. It is worth mentioning, however, that further south in the Wadi Rum region, which is considered to be an extreme desert, Danin reports a few sightings of Mediterranean species which could be considered relics in this area. *Juniperus phoenicea* and *Ephedra foeminea* are amongst these (Danin 1991).

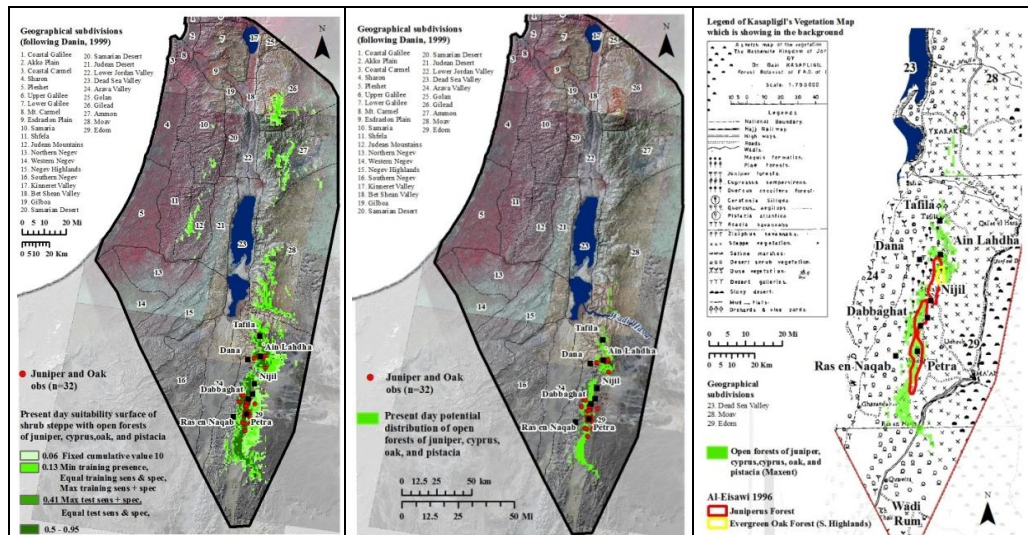


Figure 5.12. Resulting modern distribution of open forests of juniper, cyprus, oak and pistacia (left), presence/absence (middle), comparison against other sources (right).

5.1.3.6 Mediterranean savannoid

The Mediterranean savannoid vegetation is dominated by *Ziziphus spina Christi* and *Ziziphus lotus* as well as grasses like wild wheat, wild barley, and wild oats. Today, this region is found in the Rift Valley from the Lower Jordan Valley to the Sea of Galilee. It also expands into the Samarian desert. Similar climatic conditions to those present in this area occur along the coastal plains, where *Ziziphus spina Christi* is also common.

The continuous suitability surface across various thresholds shows that higher values were obtained throughout the northern portion of the Rift Valley, where it mainly occurs today (Figure 5.13). From here, the Mediterranean savannoid grasslands expand into wadi beds and valleys and connect with the coast via the Esdraelon Plain and the Galilee. The lowest values are found on the Pleshet coastal plains, which are in fact also suitable for *Ziziphus spina Christi* plants. Once the threshold was applied, suitable areas are mostly restricted to the Kinneret, Bet Shean, and Lower Jordan Valleys. Mediterranean savannoid vegetation then pushes into drainage systems and wadi valleys like the Yarmuk and Zerqa river valleys and the Esdraelon Plain. It is also found in the Akko Plain and immediately surrounding areas.

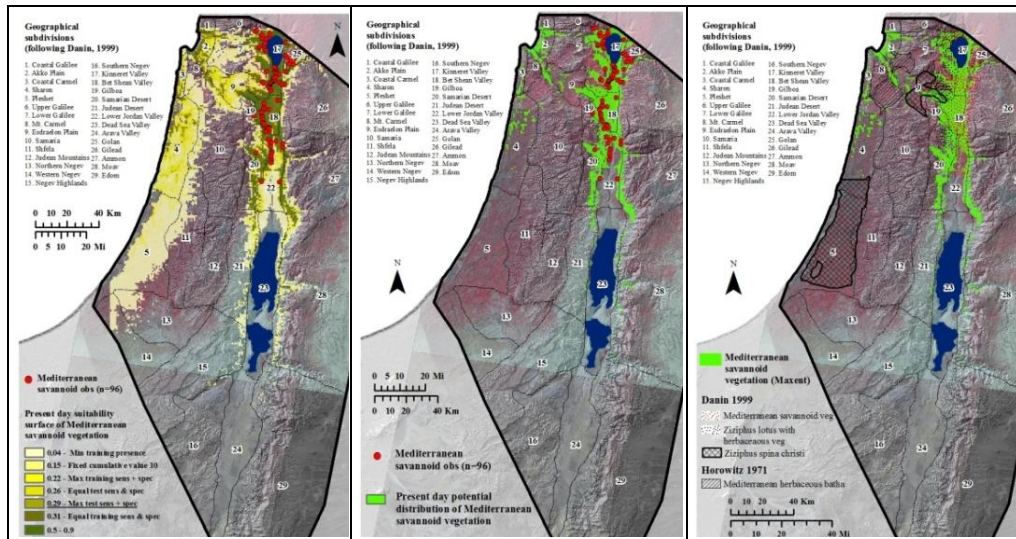


Figure 5.13. Resulting modern distribution of Mediterranean savannoid vegetation (left), presence/absence (middle), comparison against other sources (right).

5.1.3.7 Semi steppe batha

Along with shrub steppe, this category represents areas that mainly belong to the Irano Turanian plant geographical region (Figure 5.14). Both steppe categories lack trees, and are represented instead by small shrubs and bushes. Two of the most common species include *Artemisia herba alba* and *Noaea mucronata*. When compared to shrub

steppe, semi steppe batha occupies slightly moister areas. It essentially surrounds the forest categories, where mean rainfall is generally 300-400 mm/yr in the northern highlands and 100-300 mm/yr in the southern highlands. As a result, species also found in Mediterranean environments, like *Sarcopoterium spinosum*, *Calycotome villosa*, and *Euphorbia hierosolymitana* can occur alongside other Irano Turanian species, especially along transitional areas. This type of vegetation is more extensive east of the Rift Valley, where it can be found in all of the highland areas.

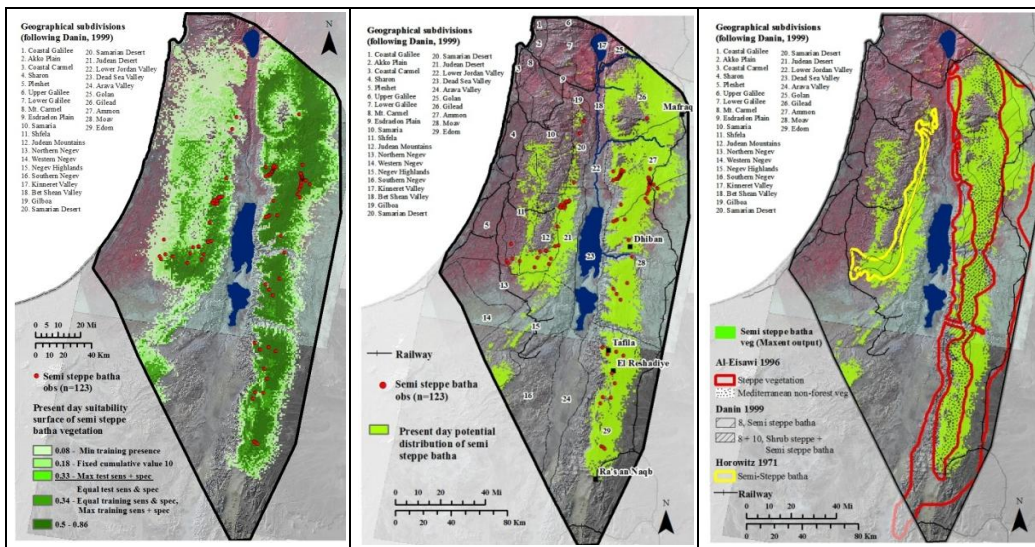


Figure 5.14. Resulting modern distribution of semi steppe batha vegetation. Continuous suitability surface (left), presence/absence (middle), comparison against other sources (right).

Al-Eisawi mapped this category under two classes: steppe vegetation and Mediterranean non-forest vegetation. His steppe category presumably also includes shrub steppe vegetation, which is more drought tolerant than semi steppe batha. Al-Eisawi's non forest category (at least parts of it) also may be populated by semi steppe batha vegetation.

Similarly to Al-Eisawi, Kasapliligil (1956) groups shrub steppe and semi steppe batha into one category. He plots this category's southernmost extent at Naqb, in agreement with the output of the Maxent model (see also Kasapliligil's description of

steppe under the Shrub steppe category below). Danin also shows semi steppe vegetation under two categories: semi steppe batha proper and a combined shrub steppe/semi steppe batha. As one would expect, suitable areas predicted by the model mostly overlap with all of these categories.

West of the Rift Valley, semi steppe vegetation is found mainly surrounding the Judean Mountains, especially on the slopes that face dryer areas (Negev and the Rift Valley). These areas agree with Danin and Horowitz's interpretation, and extend slightly further into the Judean Desert. Fragmented patches are also found in the foothills of these mountains that face the coastal plains, in areas similar to the open forests of carob and pistacia. At the same time, this category occurs in the Negev Highlands, an area which Danin classified as *Shrub steppe*. Danin notes that this region in the Negev Highlands also contains trees like *Pistacia atlantica* and *Rhamnus disperma* on smooth outcrops, as well as other Mediterranean relicts like *Ephedra foeminea* and *Prasium majus* (Danin 1999).

5.1.3.8 Shrub steppe

Shrub steppe vegetation is represented by grasses and dwarf shrubs like *Artemisia herba alba*, *Noaea mucronata*, *Anabasis articulate*, *Salsola vermiculata*, and *Bassia Arabica*. Once the threshold was applied, the shrub steppe category can be found surrounding the semi steppe batha vegetation on its xeric side (Figure 5.15). This is most clear west of the Rift Valley, where shrub steppe surrounds the more arid slopes of the Judean mountains. It occurs extensively in the Negev and Samarian deserts. These areas concur with Danin's distribution of shrub steppe vegetation.

East of the Rift Valley in Gilead and Ammon, suitable areas are found along the edge of the study area. Kasapligil notes that the steppe vegetation joins the Syrian Desert

just north of Mafraq. In other words, as one moves from west to east along this latitudinal segment, one would encounter the various maquis and forest categories followed by semi steppe batha, shrub steppe vegetation, and the Syrian Desert (just beyond the study area).

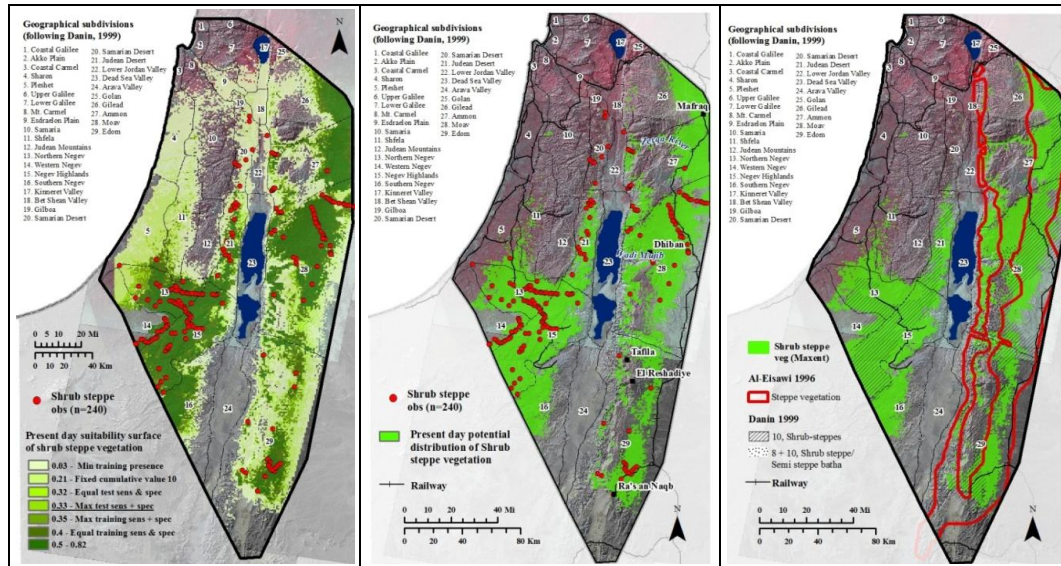


Figure 5.15. Resulting modern distribution of shrub steppe vegetation. Continuous suitability surface (left), presence/absence (middle), comparison against other sources (right).

A strip of shrub steppe vegetation continues southward, and as Kasaplilig noted, pushes into the drier stony desert vegetation and eastern desert as “pocket like intrusions through valleys and desert gullies” (Kasaplilig 1956: 27). As he also pointed out, the eastern limit is more or less marked by the railway. This category also penetrates into wadi and river valleys like the Zerqa River. It appears quite extensive in Moab, especially around Wadi Mujib. Overall, predicted areas agree closely with the descriptions and areas highlighted in other maps.

5.1.3.9 Coastal Ziziphus vegetation

A mask was applied when running the model to limit this vegetation type to the coast. The continuous surface across various thresholds shows all of the coastal area as suitable (Figure 5.16). Once the threshold was applied, most of the Pleshet plain is potentially suited to coastal Ziziphus vegetation, which extends north into the Sharon

Plain and around the foothills of the Judean mountains. A few isolated patches are also found in the Negev.

The coastal plains have been impacted by human activity extensively, to the point where the vegetation of the whole region is now classified as *Synanthropic vegetation* (anthropogenic). Nevertheless, Danin subdivides it into three main categories, which reflect the longitudinal effect of decreasing rainfall. In the northern coastal plains, the expected climax vegetation is formed by a maquis of *Quercus ithaburensis*. In the Pleshet coastal plain, the climax is *Ziziphus spina Christi*, which is accompanied by *Acacia Radianna* further south in the Negev coastal plain. The predicted distribution somewhat disagrees with this, since it shows suitable areas in the moister Sharon plain, with gaps in the Pleshet and Negev plains. When projecting this category into past periods, almost no suitable areas were found.

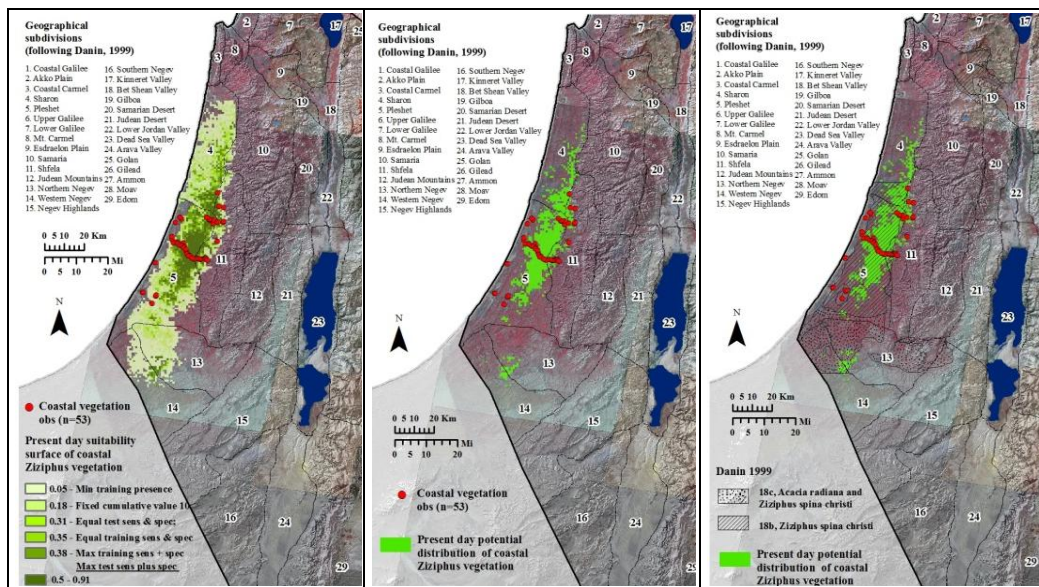


Figure 5.16. Resulting modern distribution of coastal *Ziziphus* vegetation. Continuous suitability surface (left), presence/absence (middle), comparison against other sources (right).

5.1.3.10 Desert savannoid

The continuous surface showing suitable areas across various thresholds captures all the categories that thrive under desert-like conditions (e.g., Desert scrub, Stony desert vegetation, Desert Savannoid, Saharo Arabian plant geographical association). Once the classification threshold was applied, the resulting area reflects desert savannoid vegetation more accurately (Figure 5.17). It is essentially found in the Rift Valley from the Dead Sea Valley southward, which is covered by gravel, sand dunes, and alluvial soils.

This type of vegetation is represented by sporadic *Acacia* species as well as other desert semi shrubs like *Anabasis articulata*, *Haloxylon salicornicum*, *Zygophyllum dumosum*, *Retama raetam*. Danin also refers to this vegetation as *Desert savannoid* whereas Al-Eisawi calls it *Acacia and Rocky Sudanian Vegetation*. All the maps show that this vegetation category is limited to the Rift Valley, but show slight variations in terms of its extent. Whereas Al-Eisawi limits it to the Wadi Arava, Danin extends it west into the Southern Negev and slightly north into the Lower Jordan Valley. In his work, Kasapligil refers to this category as *Acacia Grasslands* and found them to occupy the area along the Rift Valley from the Gulf of Aqaba to the southern Dead Sea Basin. He also reported that in the eastern slopes of the upper Wadi Araba, they penetrate wadi valleys but don't go beyond 600 m asl whereas they climb up to 750 m asl on the middle Wadi Araba eastern slopes, where they meet *Artemisia* shrubs and *Juniper* trees.

According to the current model, this vegetation type does not extend as far north as suggested by Danin, but it does expand into the lower elevations of the adjacent mountains and penetrates into the Wadi Mujib and Wadi Hassa (as Kasapligil described).

Fieldwork done in 2010 on the Jordanian side of the Jordan Rift showed that these predicted wadi distributions agree with observed vegetation patterns.

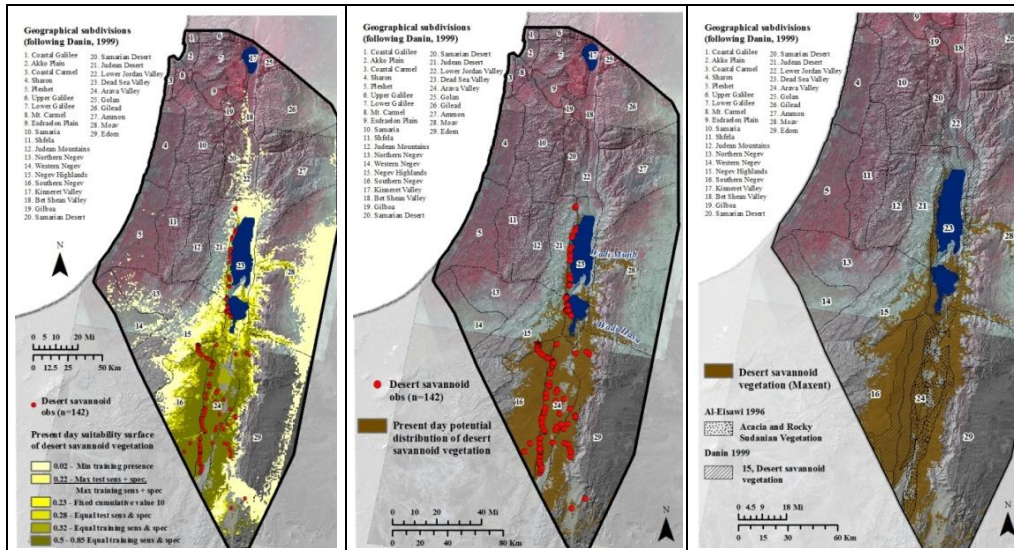


Figure 5.17. Resulting modern distribution of desert savannoid vegetation. Continuous suitability surface (left), presence/absence (middle), comparison against other sources (right).

5.1.3.11 Desert scrub

This category is represented by scrubby vegetation of the Chenopodiaceae (goosefoot) family. Like the desert savannoid vegetation, its distribution is found along areas that receive very low amounts of rainfall and is mainly dictated by water availability. Plants like *Salsola sp.*, *Anabasis articulata*, *Suaeda sp.* can be found in concentrated (along dry wadi beds) or dispersed patterns (Danin 1999).

Unlike the vegetation typical of the desert savannoid category, desert scrub is not limited by the very hot and humid conditions of the Rift Valley. As a result, it extends further than the area occupied by desert savannoid vegetation. In the Rift Valley, it spreads beyond the northernmost limit of desert savannoid vegetation and up the steep slopes of the Judean Desert and the ridges surrounding the Dead Sea Basin. It is also rampant across the Negev Highlands and the Southern Negev. These areas coincide with Danin's Desert vegetation category west of the Rift Valley, but do not coincide entirely

on the eastern side, where he combined the categories of desert vegetation and sand vegetation (Figure 5.18).

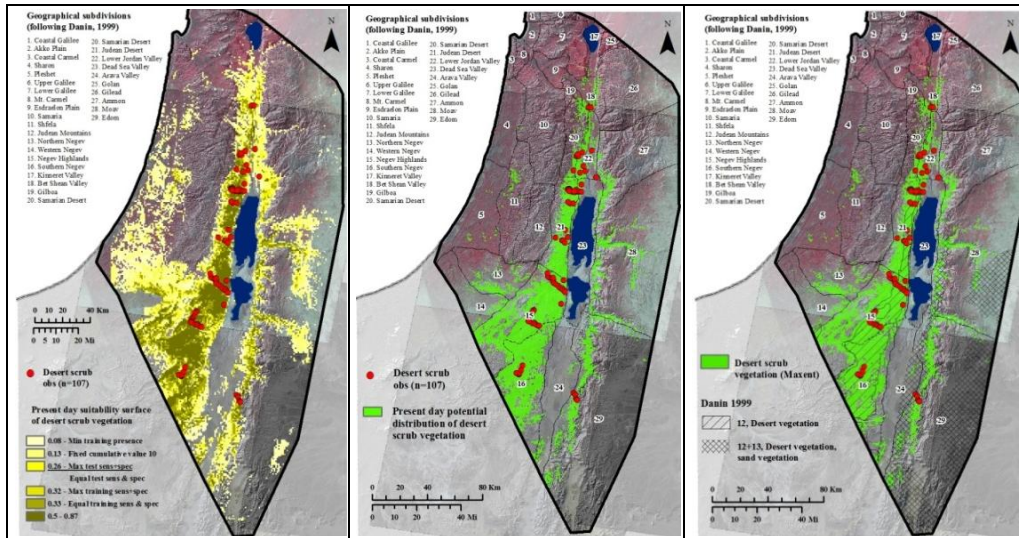


Figure 5.18. Resulting modern distribution of desert scrub vegetation. Continuous suitability surface (left), presence/absence (middle), comparison against other sources (right).

5.1.3.12 Stony desert

The continuous suitability surface based on multiple thresholds has a fairly compact distribution that was impacted minimally by the application of a classification threshold (Figure 5.19). Like desert scrub, this category is found in areas that are quite dry, have high evaporation rates, and experience extreme temperatures. The stony desert vegetation zone extends along the eastern edge of the study area, with an western limit that roughly coincides with that of shrub steppe vegetation at the edge of the Eastern Desert. The stony desert is known as *Badia* or *Hammada* by the botanists in Jordan and includes species that are common in the desert scrub regions. Irano Turanian species like *Artemisia herba alba* also are common, especially along dry wadi beds.

According to the model, suitable areas are predicted in Moab and Edom, including a few patches around Wadi Rum. Once again, the distributions proposed by

other authors overlap partially. Al-Eisawi classified this vegetation type as *Hammada*, whereas Danin lumped this category into the more general *Desert and Sand Vegetation* category. Consequently, Danin proposes a greater extent that includes areas in the Arava Valley (classified in this study as *Desert scrub*), whereas Al-Eisawi shows a narrower strip along the edge of the study area. The resulting classification adopted in this study lies somewhere in between.

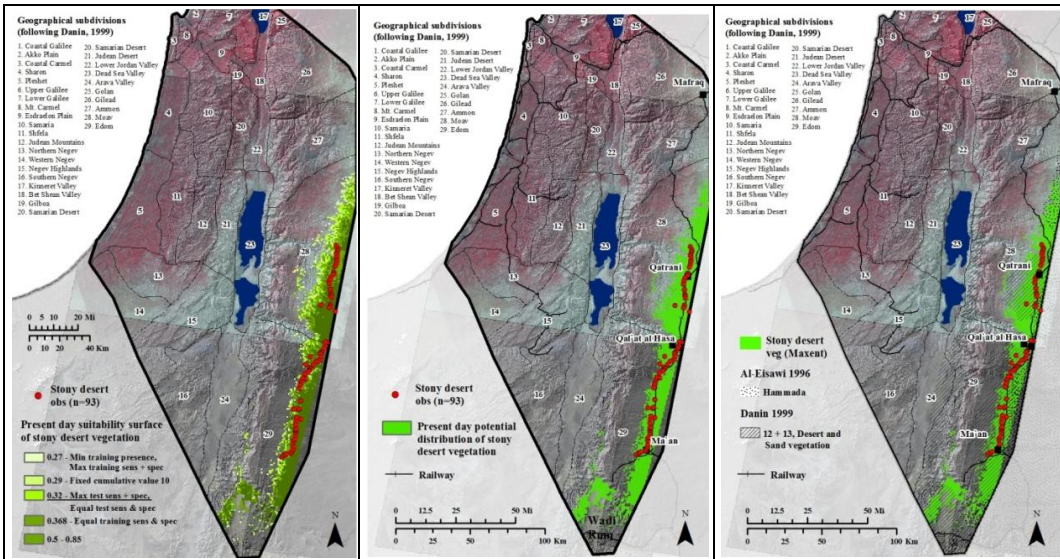


Figure 5.19. Resulting modern distribution of stony desert vegetation. Continuous suitability surface (left), presence/absence (middle), comparison against other sources (right).

5.1.4 Combined maps

5.1.4.1 By plant geographical regions

Several maps delineating plant geographical regions have been created by different authors. The first map of plant geographical regions was drawn by Eig (1931/32). After taking into account phytogeographical analyses of plant lists and the physiognomic characteristics of the main geographical units, he distinguished three main plant geographical units: Irano Turanian, Mediterranean, Saharo Sindian. After further

analysis, Zohary (1962; 1966) modified Eig's interpretation slightly. He called parts of Eig's Saharo Sindian region "Saharo Arabian," and referred to the Sudano-Decanian region as "Sudanian." These pockets located around the Dead Sea became a "territory of Sudanian penetration" (Zohary 1966). The boundaries between the three main regions more or less follow precipitation isohyets. Except in the southern highlands east of the Rift Valley, the Mediterranean boundary mainly follows the 350 mm/yr isohyet, the Irano Turanian follows the 250 mm/yr, and the Saharo Arabian follows the 100 mm/yr isohyet. East of the Rift Valley, Al-Eisawi shows a map of plant geographical regions that resembles Eig and Zohary's, except at a slightly coarser resolution.

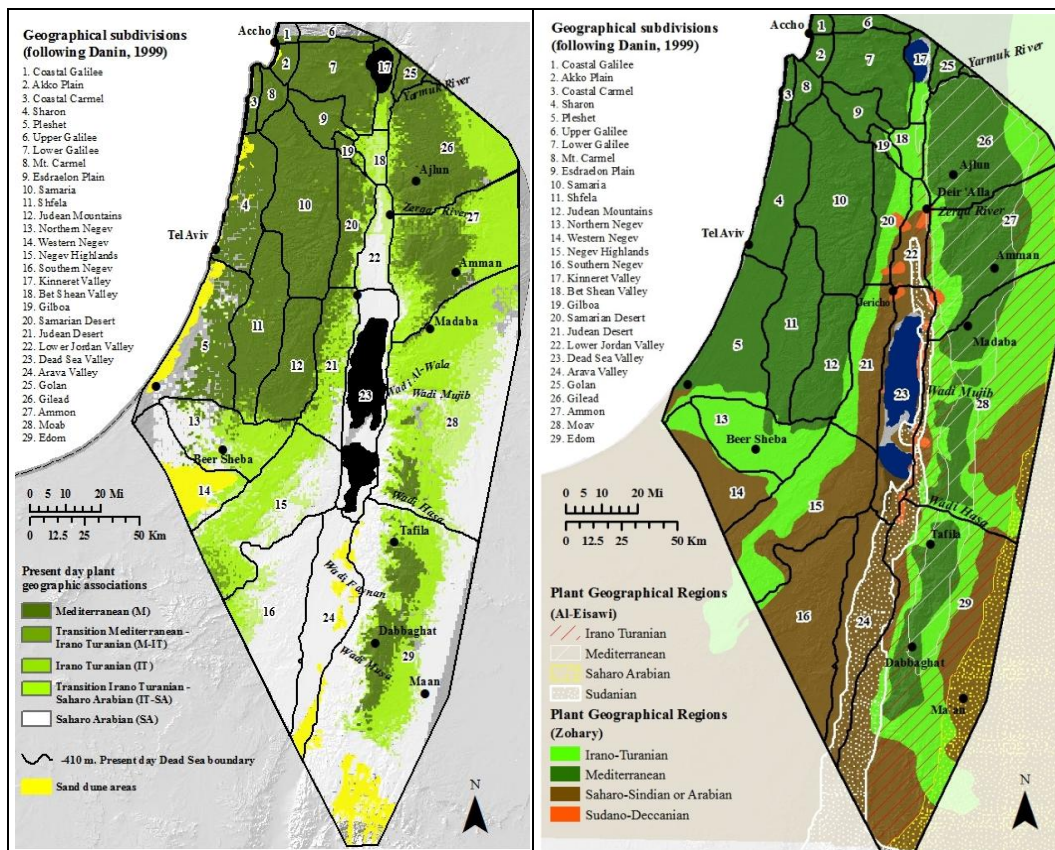
A few decades later, Danin and Plitmann (1987) revised this map using statistical methods designed to delineate biogeographical boundaries and over 80,000 observations across the whole region west of the Rift Valley and the Sinai which had been partitioned into 5x5 km² grid cells. Because many plants can be found in various regions, they also estimated the chorotype frequency for each region (e.g., in the Mediterranean region, 50% of the chorotypes are Mediterranean, 25% are Irano Turanian, 12% are Saharo Arabian). Except for the Mediterranean distribution, which resembles that of the earlier maps, they introduced categories and transition areas that result in the following differences from the earlier maps: most of the Irano Turanian region now became a transitional M-IT zone; the Saharo Arabian region was enlarged into the Irano Turanian region and subdivided into 3 categories: SA(M), SA(IT), SA(S) (where the region not in parenthesis is dominant); the Sudanian region now lies around the Red Sea and as a result does not fall within the study area.

The goal of this study is to recreate the vegetation of the study area at 500 year intervals from the Late Pleistocene until the Early Holocene, a task for which none of the previously used approaches is well suited. This study proposes and implements a new

method. Indicator species from each of the main regions were sourced from the literature. Hundreds of observations were acquired from vegetation transects surveyed during the last century and in new field work conducted in 2010. In addition, several climatic and topographic variables that characterize these indicator species also were determined. Species distribution modeling was then used to determine the distribution of the main plant geographical regions (in this study referred to as plant geographic associations), which were also broken down into vegetation types or subcategories.

Identification of the three main plant geographic associations also produced two additional transition zones (Map 5.1). These include a transition zone between the Mediterranean and Irano Turanian associations (M-IT), and between the Irano Turanian and Saharo Arabian (IT-SA) associations. As explained in Chapter 4, these zones are the result of two categories having suitable conditions in a particular cell. The M-IT zone occupies the smallest area. It is found alongside the larger Mediterranean region. There are also a few patches in the Negev Highlands, at the edge of the study area. The resulting IT-SA zone is larger. It is found in the Rift Valley between the Saharo Arabian and Irano Turanian associations, as well as on the plateau region in Moab, and in Wadi Mujib and Wadi Hasa. Some patches also occur in the Negev Highlands and Southern Negev.

When compared with Zohary's previously produced maps according to plant geographical regions, the main plant geographic associations produced by this study share similarities. In the Rift Valley, the Saharo Arabian region occupies a similar area. Zohary's Irano Turanian region occupies a larger area in the north, part of which is classified as IT-SA in the model presented here. Except for the coastal Negev, the extent of the Irano Turanian region also is very similar to Zohary's.

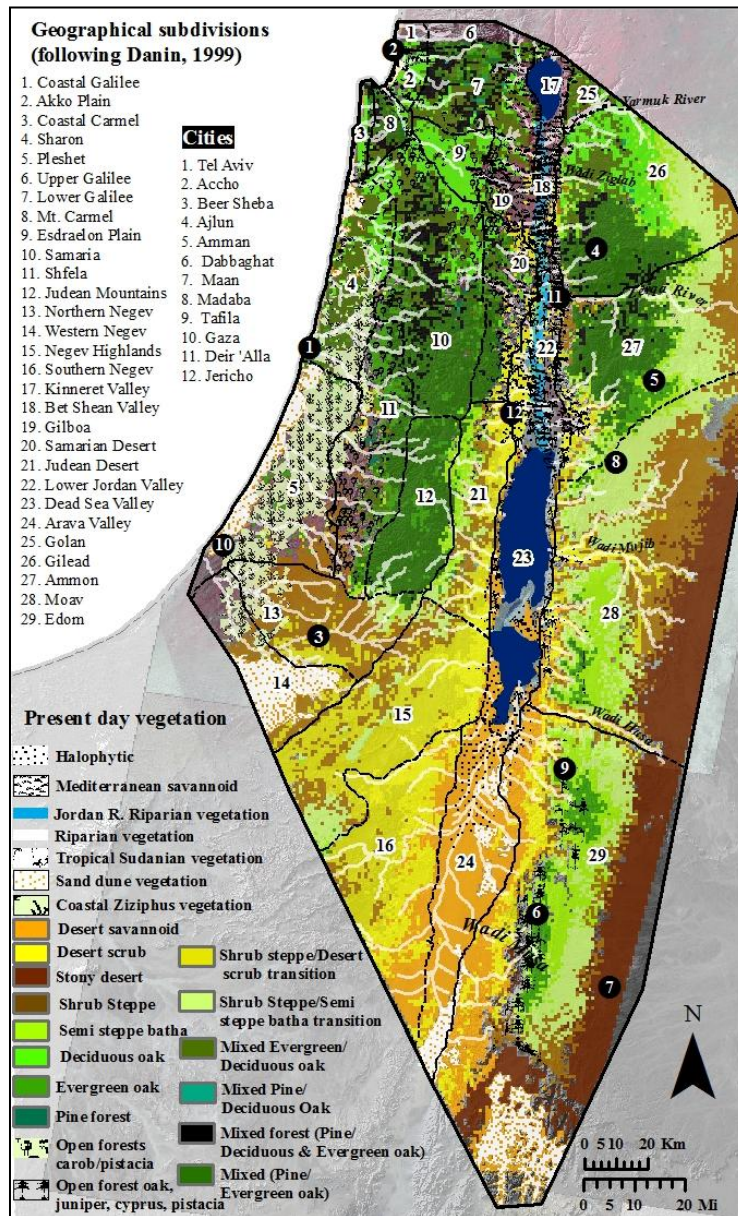


Map 5.1. Modern distribution of plant geographic associations. Map by plant geographic associations derived from Maxent model outputs (left) and map of plant geographical regions according to Al-Eisawi and Zohary.

5.1.4.2 By vegetation categories

The combined modern day vegetation map, according to vegetation subcategories, is shown in Map 5.2. As with plant geographic associations, vegetation categories were plotted on a common map, thereby revealing overlapping areas that indicate new transitional areas: Shrub steppe/Desert scrub transition vegetation; Shrub steppe/Semi steppe batha transition vegetation; Mixed evergreen/Deciduous oak forest; Mixed forest (pine, deciduous and evergreen oak). As discussed previously, these transitional zones are not surprising, since there are no hard boundaries dividing one category from another. For instance, desert scrub, shrub steppe and desert savannoid can all intersect, as can the forest categories with semi steppe batha vegetation. In addition,

there may be areas suitable to the same type of vegetation, as is the case with the open forests of juniper on the southern highlands east of the Rift Valley. Although these forests have Mediterranean species, the understory is made up of Irano Turanian species like *Artemisia herba alba* and *Noaea mucronata*. So, these forest areas intersect with areas suitable to steppe vegetation. *Artemisia herba alba* also appears in the more drought tolerant stony desert vegetation on dry wadi beds.



Map 5.2. Resulting modern vegetation map.

Observable modern vegetation is not expected to resemble this map, especially when it comes to the forest types, which have been impacted considerably by intensive land use activities, so that these forests have disappeared, diminished, and/or become highly fragmented. Nevertheless, this map suggests the most suitable areas for the different vegetation categories if all disturbance factors are removed. The higher precipitation forest categories predominate in the northern half of the study area, mainly in mountainous regions. The largest area is found in the Judean and Samarian mountains. It is represented by the mixed forest category of *Quercus calliprinos* and *Pinus halepensis*. *Quercus ithaburensis* appears in the northern half of this forest segment. As these mountains descend towards the coast, they become populated by open forests of carob and pistacia. The Sharon coastal plain is mainly suited to both evergreen and deciduous oak maquis. To a lesser extent, carob and pistacia, as well as riparian vegetation along streams and rivers, also are found in this area. The region around Mt. Carmel is also suited to the mixed pine/evergreen oak category, as is the northern half of the Lower Galilee region. A large patch of deciduous oak forest is found throughout the Esdraelon Plain. North and south of this patch are areas suitable to either the mixed oak category or all the forest categories in combination.

East of the Rift Valley, forests also make up a large area around Golan and Gilead. The Golan region may be suited to both types of oaks. South of this, there are large areas dominated by *Quercus ithaburensis*. Closer to the rift valley there appears to be a transition area in which both oaks are found (around Wadi Ziglab). Further south is a fairly large patch of mostly mixed forest with *P. halepensis* and *Q. calliprinos*, which is interrupted by the Zerqa River. The suitable forest areas even further south in the regions of Moab and Edom are much smaller in area. They are represented by the mixed oak, juniper, cyprus and pistacia category.

Surrounding the forests are various steppe categories. Semi steppe batha is found closest to the forests. It is surrounded by the shrub steppe/semi steppe batha transition area and then by shrub steppe vegetation. These categories are more distinct east of the Rift Valley, where a clear transition from forest to steppe and then to stony desert vegetation can be seen. However, on the mountain ridges that face the Rift Valley, the steppe categories are almost missing as forests transition to the desert categories more abruptly.

Desert savannoid vegetation represented by *Acacia sp.* is widespread in the Arava Valley. It is interrupted occasionally by sand dune and halophytic areas, and surrounded by desert scrub vegetation. East of the Rift Valley Desert savannoid vegetation penetrates into wadis, eventually intersecting the stony desert vegetation of the plateau. West of the Rift Valley, the desert scrub spreads into the Negev, where it transitions into the steppe categories.

The Rift Valley north of the Dead Sea is suited to several categories. The flood plain would be populated by several belts of riparian vegetation, as well as halophytic vegetation. Tropical Sudanian vegetation stretches into the Bet Shean Valley, where it is replaced by grasslands (Mediterranean Savannoid) that stretch into Gilboa and surround Lake Kinneret.

5.2 Model evaluation

The models were evaluated using various approaches. The first method consisted of visually evaluating how well the model predicted the area to be occupied by the species, after applying a threshold to convert the continuous suitability surface into a binary or presence/absence map. The second method makes use of the Receiver Operating Characteristics Area Under the Curve (AUC), which was calculated by Maxent

as an internal validation method. The third method assesses how the variables performed in the different models.

5.2.1 Threshold diagnostics

The goal of this study is to create generalized and detailed vegetation maps according to plant geographic associations and vegetation subcategories. For all of the categories that were modeled with Maxent, the threshold that maximizes the sum of sensitivity and specificity was used to convert the continuous suitability surface into a binary prediction that suggests suitable areas. This threshold is empirically inferred, and not simply arbitrary, since there is no standard optimal proposed threshold in the literature. This approach derives the threshold from the ROC plot, minimizes the mean of the error rate of presences and absences (or pseudo absences in the case of Maxent) (Freeman and Moisen 2008; Manel et al. 2001), and has proven superior to other methods for establishing modeling thresholds (Liu et al. 2005). The threshold derived for this study also produced results that are comparable, but not identical, to those proposed in the maps and descriptions of Israeli and Jordanian botanists, as well as consistent with field observations in 2010.

The application of any threshold will hold implications for the criteria that can be used to evaluate the model's accuracy. For instance, a threshold will dictate how much area is predicted as suitable, and this will impact the sensitivity (or fraction of observations correctly classified) and omission rates (observations that were not classified as suitable). Theoretically, you can achieve perfect sensitivity (1) and zero specificity (sensitivity plus omission rates always sum to one) by predicting the whole area as suitable, such that all observations may be considered correctly classified. To evaluate the statistical validity of a threshold value and avoid this potential pitfall,

Maxent performs a one-tailed binomial test or a chi square test (Zar 1996) that assesses the statistical significance of obtaining an observed omission rate due to random chance or sampling error (Anderson et al. 2002).

Table 5.1 summarizes a lot of this information. From left to right, it shows the logistic value at which the threshold was met, the fractional area that is predicted according to the threshold, omission error rates for the observations used for training, omission error rates for the observations set aside for testing, and the statistical significance of the prediction. For the purpose of this study which is to estimate the potential distribution of plant geographical regions and certain vegetation types, this is a valid way through which to assess the model since there is no way of testing if the model is correct but we can test whether it is useful (Pearson 2007). In other words, is it better than if it were predicted by chance alone?

For all of the categories, the P-value was significant ($P < 0.05$), which suggests that the models were better than if they had been generated by chance. When looking at the fractional predicted area of the categories by plant geographical association, the Mediterranean region predicted the largest area. In a similar way, the forest categories also obtained the largest fractional predicted area. This may seem somewhat surprising when seeing the actual condition of the forests which are fragmented and mostly represented by the early stages of succession (batha and garigue). Nevertheless, if they were left undisturbed, they would potentially occupy a significant part of the region. The steppe and desert categories also occupy considerable parts of the region, which is confirmed by the actual conditions on the ground.

Table 5.1 Threshold evaluation

Category	Logistic threshold*	Fractional predicted area	Training omission rate	Test omission rate	P-value
Irano Turanian	0.397	0.251	0.173	0.216	1.90E-26
Saharo Arabian	0.272	0.341	0.044	0.082	8.83E-34
Mediterranean	0.253	0.374	0.06	0.085	0.00E+00
Deciduous	0.2406	0.1842	0.1043	0.0698	6.88E-07
Desert Savannoid	0.2156	0.1418	0.0645	0.0373	8.97E-08
Desert Scrub	0.256	0.1712	0.0918	0.0536	8.56E-05
Evergreen	0.2836	0.2983	0.1	0.07	1.43E-07
Pine	0.2942	0.2203	0.1395	0.025	1.10E-02
Mediterranean Savannoid	0.2877	0.1056	0.099	0.0393	5.03E-06
Stony Desert	0.3162	0.0615	0.0496	0	3.35E-09
Open forests carob and pistacia	0.3719	0.2688	0.2551	0.2036	9.70E-03
Tropical Sudanian	0.2478	0.1028	0.13	0	1.20E-04
Open forests of juniper, oak, cyprus, pistacia	0.4002	0.0304	0.2611	0	1.96E-03
Semi steppe batha	0.3277	0.2302	0.1961	0.0972	3.18E-04
Shrub steppe	0.3303	0.22	0.1408	0.1216	1.95E-08
Coastal Ziziphus	0.3814	0.1784	0.2681	0.0833	9.50E-03

* When applying the threshold of Maximum sensitivity plus specificity

5.2.2 Area under the curve

The Area Under the Curve (AUC) is a measure used commonly in species distribution modeling to evaluate a model's predictive ability (Fielding and Bell 1997; Hanley and McNeil 1982), by indicating how well the model is able to discriminate where a species is present versus where it is absent. Because Maxent lacks information on absences, it randomly selects "pseudo absences." The AUC statistic, which ranges from 0 to 1, indicates how well a model is able to distinguish a true presence from a randomly chosen point. Swets (1998) recommends the following guideline: when the AUC is less than 0.5 it indicates the model was worse than chance, between 0.5 – 0.7 it

indicates low accuracy, 0.7 – 0.8 suggests the model accuracy is fair, 0.8-0.9 is good, and values greater than 0.9 represent excellent model accuracy.

Table 5.2 shows the AUC values for the different modeled categories (plant geographic associations and vegetation subcategories). All models indicate acceptable performance, with values over 0.75, a threshold suggested by Pearce and Ferrier 2000. These models produce scores ranging from 0.76 (open forests of carob and pistacia) to 0.789 (Irano-Turanian) to 0.98 (shrub steppe with open forests of juniper, Cyprus, oak, pistacia).

Table 5.2. Model parameters and model performance based on AUC

Category	Test AUC	SD	Performance	#Training samples	#Test samples	Regularized training gain	Unregularized training gain	Test Gain	Iterations	#Background points
Mediterranean	0.831	0.009	Good	351	234	0.8443	0.9358	0.8258	500	10265
Saharo Arabian	0.803	0.014	Good	294	98	0.8804	0.9266	0.7253	500	1264
Irano Turanian	0.789	0.02	Fair	225	74	0.7017	0.8604	0.5374	500	1264
Pine forest*	0.8673	0.0444	Good	33	4	1.2834	1.5713	0.9477	410	1264
Deciduous*	0.8938	0.0271	Good	116	13	1.4316	1.5925	1.2137	500	1264
Evergreen*	0.837	0.0256	Good	179	20	0.99	1.0972	0.8488	492	1264
Open forests carob and pistacia*	0.7612	0.0803	Fair	67	7	0.6776	0.8499	0.4416	396	10000
Open forests juniper, cyprus, oak, pistacia*	0.9816	0.0085	Excellent	18	2	2.898	3.4933	2.9518	492	1014
Semi steppe batha*	0.8654	0.0449	Good	77	8	1.0439	1.2268	0.9904	488	1264
Shrub steppe*	0.8604	0.0264	Good	178	20	1.0417	1.1973	0.9622	500	1264
Mediterranean Savannoid*	0.9352	0.0172	Excellent	67	7	1.7834	1.9486	1.6312	500	1264
Desert savannoid*	0.9215	0.0176	Excellent	96	11	1.7884	1.8879	1.5429	500	1264
Desert scrub*	0.9082	0.0296	Excellent	68	8	1.4375	1.7359	1.2887	500	1264
Stony desert*	0.964	0.0075	Excellent	67	7	2.5205	2.625	2.443	486	1264
Halophytic*	0.9489	0.0152	Excellent	102	11	2.0619	2.2438	1.9335	500	10038
Tropical Sudanian*	0.9522	0.016	Excellent	43	5	2.0983	2.3339	1.949	490	1019
Coastal Ziziphus*	0.881	0.066	Good	34	4	1.1626	1.455	1.1527	408	5392

* 10 fold cross validation

5.1.1 Variable importance

Depending on the category being modeled, different predictor variables were used. The models by plant geographical region were implemented with only 3 predictor variables, whereas the models by vegetation category included several other predictor variables. Other studies have used a much wider range of predictor variables. A limited set of predictor variables was adopted in this study for several reasons. Some variables were dropped after learning they were highly correlated with others. Also, not all variables found useful for this type of application were available for all the periods being modeled in this study. Models based on a small number of non-correlated variables that are expected to be more suited to projecting into other time periods because they are not as likely to overfit the species-climate relationship as more complex models would (Peterson et al. 2007). Finally, all the variables used are generally believed to be of importance when determining plant distributions (see Table 4.11).

The following tables summarize various outputs produced by Maxent that provide information regarding the importance of the different variables when generating suitable areas for the different models. The first set of tables contains two columns (Table 5.3 to 5.8). The first column includes information (in a subtable) regarding how each variable contributed to the model. The first field is called 'Percent Contribution.' Given that each feature derived from every environmental variable contributes to the gain of the model, the first column shows how each variable contributed to the model (the percent contribution is derived from the gain). However, Phillips states these are only heuristically defined (Phillips 2008). During a run, the Maxent algorithm will arrive at an optimal solution, and these are the variables it used to arrive at that optimum. However any model could have used a number of other paths, resulting in a different order of

importance, especially when variables are correlated. The next field titled ‘Permutation Importance’ also ranks variable importance, but this time it does so independent of the path taken by Maxent during a run. The training point values for each variable are generated randomly to assess the effect of randomization on the AUC. If the AUC significantly decreases, it means that the model is heavily dependent on the variable under consideration (Phillips 2008).

The second column consists of a jackknife plot of variable importance. This provides another way of assessing how variables impact a model. To obtain this graph, Maxent runs several models using different variable combinations. First, all the variables are used except for one (light blue bar). This shows what the gain would be if a particular variable was left out. Then a model is run using only one variable (dark blue bar), and finally a model is created using all variables (bottom bar in red). The second set of tables (5.7 to 5.13) shows the response curve of each variable. In other words, it shows how the suitability (logistic likelihood) of the species being modeled (y-axis) varies across the range of an environmental variable (x-axis), when all other variables are kept at their mean value (Elith 2008), and also when each variable is used in isolation to generate the model.

The variable that seems to be most important in determining suitable areas for all plant geographical regions is mean annual rainfall (Table 5.3). This variable is ranked at the top in percent contribution and permutation importance. The jackknife test of variable importance also shows that this variable allows a good fit to the training data when used alone. When omitted it decreases the gain for the Mediterranean and Saharo Arabian categories. The response curve plots (Table 5.9) show how this variable relates to each category. For the Mediterranean category, for instance, the gain starts to increase steadily above 300 mm/yr. For the Irano Turanian region, it peaks between 200 and 400 mm/yr.

For the Saharo Arabian region, on the other hand, suitability decreases dramatically as rainfall increases. The second most important variable, however, was different for each category. For the Mediterranean region the second most important variable was geologic substrate (limestone), which was followed closely by annual temperature. For the Irano Turanian and Saharo Arabian categories, the second most important variable is annual temperature, followed by elevation (Irano Turanian) and geology (Saharo Arabian).

Annual precipitation also was the most important contributing variable for the two forest categories represented by *Quercus calliprinos* and *Pinus halepensis* in terms of percent contribution, permutation importance, and the jackknife plot. For *Quercus ithaburensis*, annual precipitation is the most important variable in percent contribution, but is surpassed by elevation in terms of permutation importance. Nevertheless, the jackknife plot indicates that elevation and geology provide the second highest gain when used in isolation, whereas annual precipitation provides the highest gain. At the same time, it appears that elevation is an influential variable, since it provides the greatest effect on gain when omitted. For *Quercus calliprinos* and *Pinus halepensis*, annual precipitation and geology appear to diminish the gain the most when omitted.

Annual precipitation was not as significant for the other two forest categories. For carob and pistacia, the most important variable was geology, which lowered the gain substantially when omitted. This variable was trailed by mean annual temperature and precipitation. For juniper, elevation was the most influential variable, followed by slope, aspect, and geology.

For both steppe categories, annual precipitation was the most important variable. In both categories, this variable provided the greatest amount of information not captured by other variables, and significantly lowered the gain when omitted (light blue bar of jackknife plot). For shrub steppe vegetation, elevation appears to be second in

importance, followed by annual temperature and geology. For semi steppe batha, however, annual temperature appears to be of greater importance than elevation, as does geology.

Once again, annual precipitation was one of the most influential variables for the three xeric categories (desert scrub, desert savannoid, and stony desert vegetation). For desert scrub and desert savannoid vegetation, annual temperature and geology were also important, whereas for stony desert vegetation annual temperature and elevation contributed most substantially (after mean annual precipitation).

The Mediterranean savannoid category, which represents grasslands and scattered *Ziziphus spina Christi* and *Ziziphus lotus* trees, was most influenced by elevation, followed by annual precipitation and annual temperature. The coastal vegetation, which also has *Ziziphus spina Christi* as an indicator species, was also driven mainly by elevation, followed by geology and annual precipitation. Both elevation and geology reduce the gain substantially if they are omitted.

For the two categories that were only modeled for the present (halophytic and tropical sudanian), elevation was an important variable, which makes sense since they both thrive in the lower elevation areas of the Rift Valley. However, when omitting this variable, the gain of the model was reduced only modestly, suggesting that the information contributed by this variable is captured by other variables. Average annual temperature and distance to rivers and springs also were important variables.

Table 5.3. Variable contribution and jackknife test of variable importance for models by plant geographical association (derived from Maxent).

Category	Variable contribution			Jackknife test of variable importance		
	Variable	Percent contribution	Permutation importance	Without variable	With only variable	With all variables
Mediterranean	annprec	82.4	81.5			
	geol3	9.4	7.4			
	anntemp	5.6	7.6			
	elev	2.6	3.6			
	mask	0	0			
Irano Turanian	annprec	57.7	41.4			
	anntemp	21.5	36.7			
	elev	12.8	18.4			
	geol3	8.1	3.5			
	mask	0	0			
Saharo Arabian	annprec	90.9	57.5			
	anntemp	5.1	28.4			
	geol3	2.6	4.2			
	elev	1.4	9.9			
	mask	0	0			

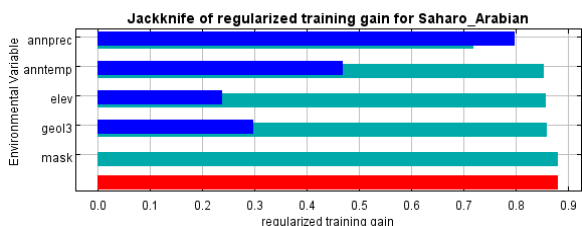
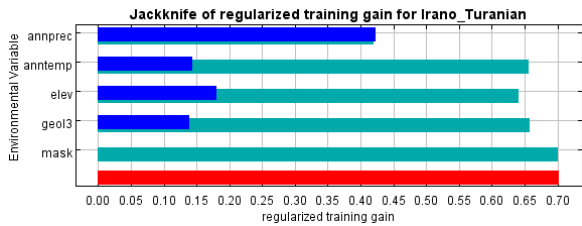
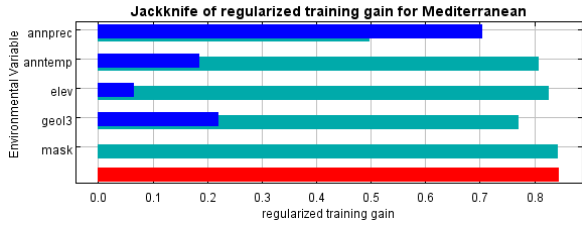


Table 5.4. Variable contribution and jackknife test of variable importance for models by forest categories (derived from Maxent).

Category	Variable contribution			Jackknife test of variable importance																					
				Without variable ■ With only variable ■ With all variables ■																					
Forests with <i>Pinus halepensis</i>	<table border="1"> <thead> <tr> <th>Variable</th> <th>Percent contribution</th> <th>Permutation importance</th> </tr> </thead> <tbody> <tr><td>annprec</td><td>45</td><td>61.1</td></tr> <tr><td>geol3</td><td>44.8</td><td>22.4</td></tr> <tr><td>slope</td><td>7.1</td><td>5.3</td></tr> <tr><td>elev</td><td>1.6</td><td>7.4</td></tr> <tr><td>aspect</td><td>1.2</td><td>0.8</td></tr> <tr><td>anntemp</td><td>0.3</td><td>3.1</td></tr> </tbody> </table>	Variable	Percent contribution	Permutation importance	annprec	45	61.1	geol3	44.8	22.4	slope	7.1	5.3	elev	1.6	7.4	aspect	1.2	0.8	anntemp	0.3	3.1			
Variable	Percent contribution	Permutation importance																							
annprec	45	61.1																							
geol3	44.8	22.4																							
slope	7.1	5.3																							
elev	1.6	7.4																							
aspect	1.2	0.8																							
anntemp	0.3	3.1																							
Forests with <i>Q. ithaburensis</i>	<table border="1"> <thead> <tr> <th>Variable</th> <th>Percent contribution</th> <th>Permutation importance</th> </tr> </thead> <tbody> <tr><td>annprec</td><td>56.8</td><td>33.4</td></tr> <tr><td>elev</td><td>19.1</td><td>39.9</td></tr> <tr><td>geol3</td><td>18.1</td><td>2.3</td></tr> <tr><td>anntemp</td><td>2.4</td><td>21.6</td></tr> <tr><td>slope</td><td>2.2</td><td>1.8</td></tr> <tr><td>aspect</td><td>1.5</td><td>1</td></tr> </tbody> </table>	Variable	Percent contribution	Permutation importance	annprec	56.8	33.4	elev	19.1	39.9	geol3	18.1	2.3	anntemp	2.4	21.6	slope	2.2	1.8	aspect	1.5	1			
Variable	Percent contribution	Permutation importance																							
annprec	56.8	33.4																							
elev	19.1	39.9																							
geol3	18.1	2.3																							
anntemp	2.4	21.6																							
slope	2.2	1.8																							
aspect	1.5	1																							
Forests with <i>Q. calliprinos</i>	<table border="1"> <thead> <tr> <th>Variable</th> <th>Percent contribution</th> <th>Permutation importance</th> </tr> </thead> <tbody> <tr><td>annprec</td><td>71.9</td><td>68.7</td></tr> <tr><td>geol3</td><td>21.4</td><td>13.5</td></tr> <tr><td>elev</td><td>3.1</td><td>8.2</td></tr> <tr><td>aspect</td><td>1.7</td><td>3.4</td></tr> <tr><td>anntemp</td><td>1.5</td><td>3.8</td></tr> <tr><td>slope</td><td>0.3</td><td>2.4</td></tr> </tbody> </table>	Variable	Percent contribution	Permutation importance	annprec	71.9	68.7	geol3	21.4	13.5	elev	3.1	8.2	aspect	1.7	3.4	anntemp	1.5	3.8	slope	0.3	2.4			
Variable	Percent contribution	Permutation importance																							
annprec	71.9	68.7																							
geol3	21.4	13.5																							
elev	3.1	8.2																							
aspect	1.7	3.4																							
anntemp	1.5	3.8																							
slope	0.3	2.4																							
Open forests with <i>Cerantonia siliqua</i> and <i>Pistacia lentiscus</i>	<table border="1"> <thead> <tr> <th>Variable</th> <th>Percent contribution</th> <th>Permutation importance</th> </tr> </thead> <tbody> <tr><td>geol3</td><td>55.2</td><td>40.4</td></tr> <tr><td>annprec</td><td>20.6</td><td>16.8</td></tr> <tr><td>anntemp</td><td>17.6</td><td>30.9</td></tr> <tr><td>slope</td><td>3.6</td><td>6.8</td></tr> <tr><td>elev</td><td>1.7</td><td>2.1</td></tr> <tr><td>aspect</td><td>1.5</td><td>3</td></tr> </tbody> </table>	Variable	Percent contribution	Permutation importance	geol3	55.2	40.4	annprec	20.6	16.8	anntemp	17.6	30.9	slope	3.6	6.8	elev	1.7	2.1	aspect	1.5	3			
Variable	Percent contribution	Permutation importance																							
geol3	55.2	40.4																							
annprec	20.6	16.8																							
anntemp	17.6	30.9																							
slope	3.6	6.8																							
elev	1.7	2.1																							
aspect	1.5	3																							
Open forests with juniper, pistacia, Cyprus, Oak	<table border="1"> <thead> <tr> <th>Variable</th> <th>Percent contribution</th> <th>Permutation importance</th> </tr> </thead> <tbody> <tr><td>elev</td><td>54</td><td>78.7</td></tr> <tr><td>slope</td><td>22.1</td><td>2.5</td></tr> <tr><td>aspect</td><td>11.8</td><td>9.3</td></tr> <tr><td>geol3</td><td>7.5</td><td>1.2</td></tr> <tr><td>annprec</td><td>4.6</td><td>8.3</td></tr> <tr><td>anntemp</td><td>0.1</td><td>0.1</td></tr> </tbody> </table>	Variable	Percent contribution	Permutation importance	elev	54	78.7	slope	22.1	2.5	aspect	11.8	9.3	geol3	7.5	1.2	annprec	4.6	8.3	anntemp	0.1	0.1			
Variable	Percent contribution	Permutation importance																							
elev	54	78.7																							
slope	22.1	2.5																							
aspect	11.8	9.3																							
geol3	7.5	1.2																							
annprec	4.6	8.3																							
anntemp	0.1	0.1																							

Table 5.5 Variable contribution and jackknife test of variable importance for models only developed for the present (derived from Maxent).

Category	Variable contribution			Jackknife test of variable importance
	Variable	Percent contribution	Permutation importance	Without variable ■ With only variable ■ With all variables ■
Halophytic	alt	39	2.5	
	anntemp	31.8	81.8	
	rivers1	11.3	2.8	
	geology	8.1	4.1	
	annprec	5.3	3.5	
	julytemp	4.5	5.2	
	mask	0	0	
	Tropical Sudanian	alt	58.3	
springs		17.7	0.5	
rivers1		8.4	0.3	
annprec		7.8	10.2	
julytemp		5.6	20.9	
wintemp		1.6	0.3	
anntemp		0.5	0	
summtem		0.1	0.1	
p				
mask		0	0	

Table 5.6. Variable contribution and jackknife test of variable importance for the models that represent steppe vegetation (derived from Maxent).

Category	Variable contribution			Jackknife test of variable importance
	Variable	Percent contribution	Permutation importance	Without variable ■ With only variable ■ With all variables ■
Shrub steppe	annprec	55.6	63.7	
	elev	28	30.9	
	anntemp	11.4	1.8	
	geol3	5	3.7	
	mask	0	0	
	Semi steppe batha	annprec	44.9	
elev		28	3.4	
geol3		18	11.7	
anntemp		9	37.7	
mask		0	0	

Table 5.7. Variable contribution and jackknife test of variable importance for the models that represent desert categories (derived from Maxent).

Category	Variable contribution			Jackknife test of variable importance
				Without variable ■ With only variable ■ With all variables ■
Desert scrub	Variable	Percent contribution	Permutation importance	
	annprec	38	36.6	
	geol3	27.2	11.4	
	anntemp	22.8	40.8	
	slope	5.7	4.5	
	elev	3.8	4.1	
	aspect	2.5	2.6	
	mask			
Desert savannoid	Variable	Percent contribution	Permutation importance	
	annprec	76.3	73	
	anntemp	15.9	18.5	
	geol3	2.7	1.4	
	elev	2.4	5.6	
	aspect	1.6	0.6	
	slope	1.1	0.9	
	mask			
Stony desert vegetation	Variable	Percent contribution	Permutation importance	
	annprec	42.5	59.7	
	elev	32.3	16.9	
	anntemp	19.7	11	
	slope	2.3	11.7	
	aspect	2	0.5	
	geol3	1.2	0.2	
	mask			

Table 5.8. Variable contribution and jackknife test of variable importance for the models that represent the categories coastal Ziziphus vegetation and Mediterranean savannoid (derived from Maxent).

Category	Variable contribution			Jackknife test of variable importance
				Without variable ■ With only variable ■ With all variables ■
Coastal Ziziphus	Variable	Percent contribution	Permutation importance	
	elev	55.5	67.7	
	geol3	25	12.5	
	annprec	10.7	9.8	
	anntemp	8.8	10	
Mediterranean Savannoid	Variable	Percent contribution	Permutation importance	
	elev	61.2	78.3	
	annprec	14.6	2.6	
	anntemp	12.4	16.9	
	geol3	5.9	1.3	
	slope	4.4	0.5	
	aspect	1.5	0.4	

Table 5.9. Response curves for models by plant geographical association (derived from Maxent).

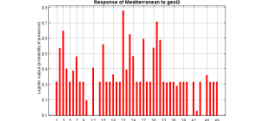
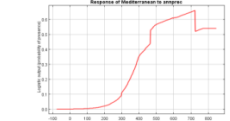

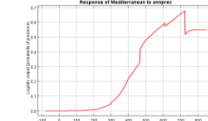
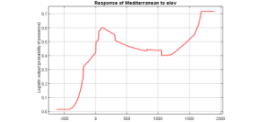
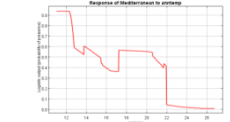

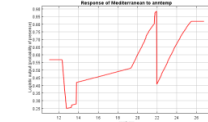
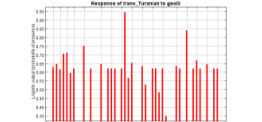

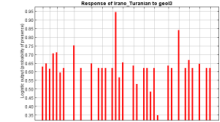
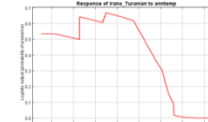



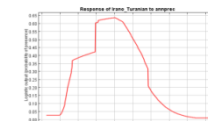
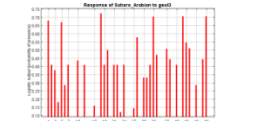

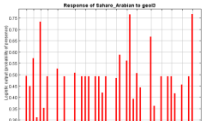
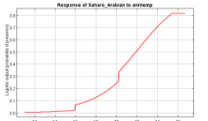
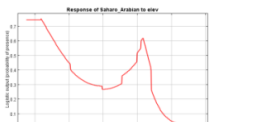

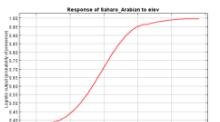

Category	Response curves using only one variable to generate the model		Response curves using one variable and holding other variables at their mean sample value	
Mediterranean				
				
Irano Turanian				
				
Saharo Arabian				
				

Table 5.10. Response curves for models by forest categories (derived from Maxent).

Category	Response curves using only one variable to generate the model		Response curves using one variable and holding other variables at their mean sample value	
<i>Pinus halepensis</i>				
<i>Q. ithaburensis</i>				

Table 5.10. (continued).

Category	Response curves using only one variable to generate the model		Response curves using one variable and holding other variables at their mean sample value	
Forests with <i>Q. calliprinos</i>				
Open forests with <i>Ceratonia siliqua</i> and <i>Pistacia lentiscus</i>				

Table 5.10 (continued).

Category	Response curves using only one variable to generate the model	Response curves using one variable and holding other variables at their mean sample value
<p>Open forests with juniper, pistacia, Cyprus, oak</p>	<p>Response of shrub_steppe_with_open_forests_of_Juniper,Cyprus_Pistacia to aspect</p> <p>Response of shrub_steppe_with_open_forests_of_Juniper,Cyprus_Pistacia to aspect2</p> <p>Response of shrub_steppe_with_open_forests_of_Juniper,Cyprus_Pistacia to aspect3</p> <p>Response of shrub_steppe_with_open_forests_of_Juniper,Cyprus_Pistacia to elev</p> <p>Response of shrub_steppe_with_open_forests_of_Juniper,Cyprus_Pistacia to elev2</p> <p>Response of shrub_steppe_with_open_forests_of_Juniper,Cyprus_Pistacia to slope</p>	<p>Response of shrub_steppe_with_open_forests_of_Juniper,Cyprus_Pistacia to aspect</p> <p>Response of shrub_steppe_with_open_forests_of_Juniper,Cyprus_Pistacia to aspect2</p> <p>Response of shrub_steppe_with_open_forests_of_Juniper,Cyprus_Pistacia to aspect3</p> <p>Response of shrub_steppe_with_open_forests_of_Juniper,Cyprus_Pistacia to elev</p> <p>Response of shrub_steppe_with_open_forests_of_Juniper,Cyprus_Pistacia to elev2</p> <p>Response of shrub_steppe_with_open_forests_of_Juniper,Cyprus_Pistacia to slope</p>

Table 5.11. Response curves for models only developed for the present time period (derived from Maxent).

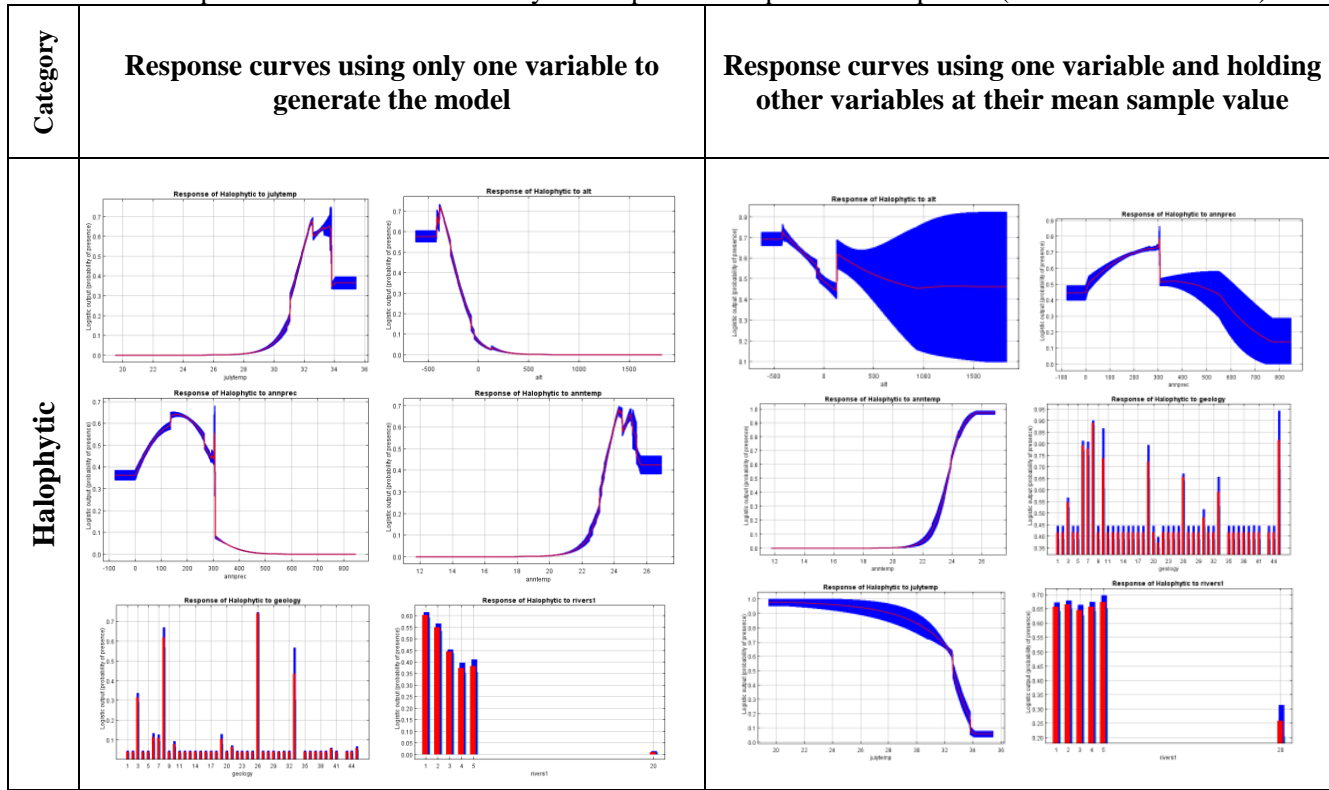


Table 5.11. (continued).

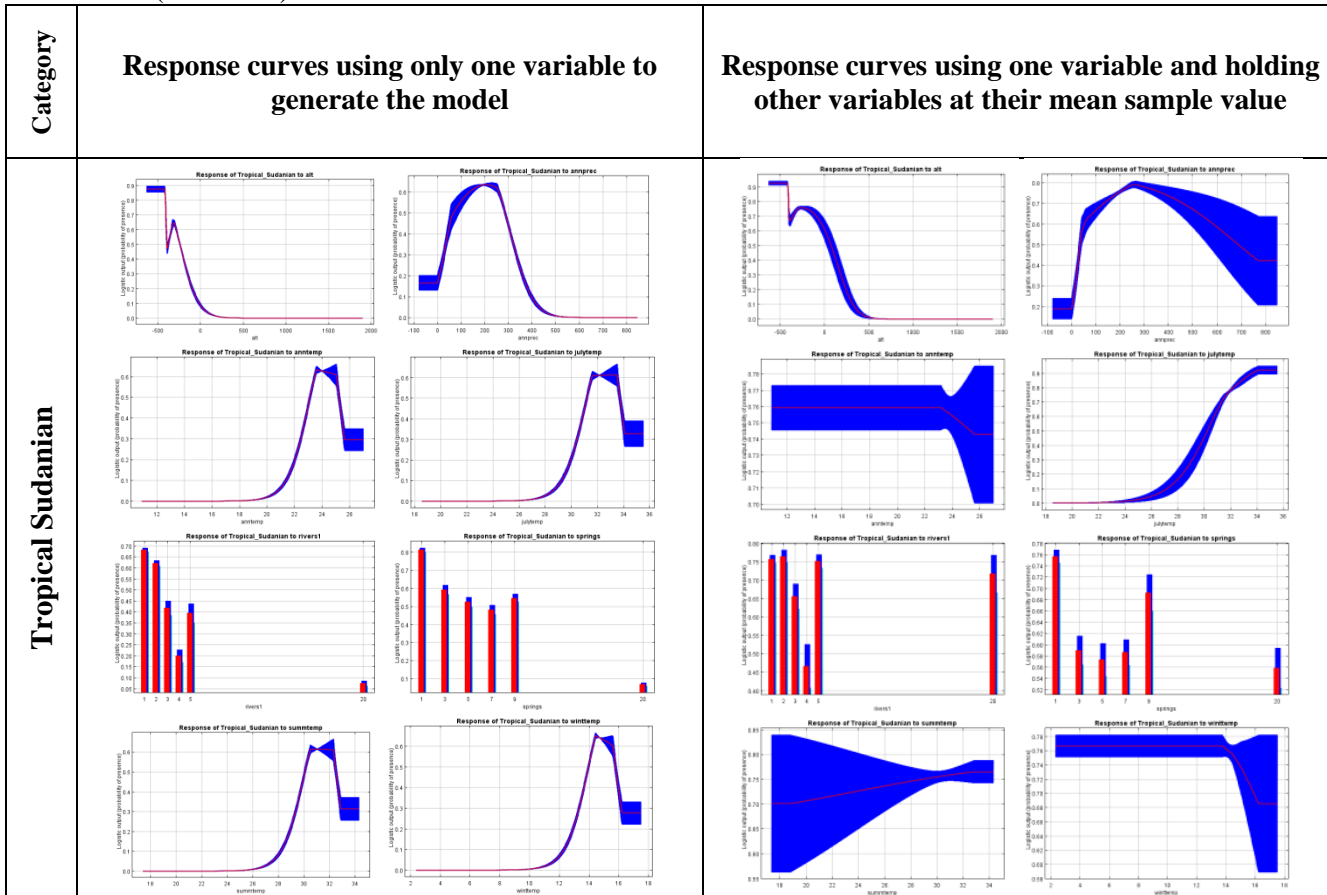


Table 5.12. Response curves for models that represent steppe categories (derived from Maxent).

Category	Response curves using only one variable to generate the model	Response curves using one variable and holding other variables at their mean sample value			
Shrub steppe					
	Semi steppe batha				

Table 5.13. Response curves for models that represent desert categories and Mediterranean savannoid vegetation (derived from Maxent).

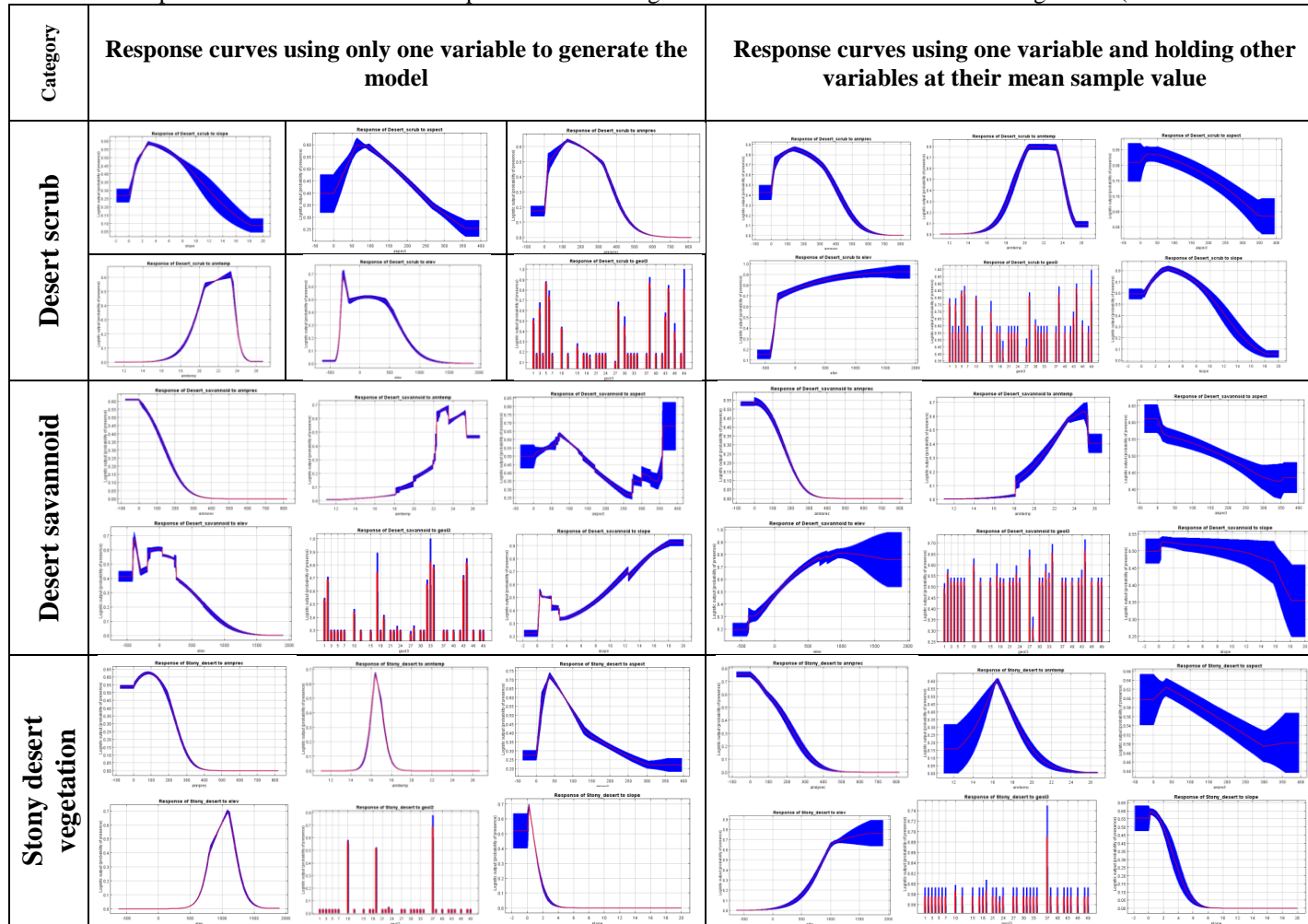


Table 5.13 (continued).

Category	Response curves using only one variable to generate the model	Response curves using one variable and holding other variables at their mean sample value
<p>Mediterranean Savannoid</p>		

The results of the present day vegetation models (according to the more generalized plant geographic association maps and the more detailed vegetation maps) were presented in this chapter. These were qualitatively evaluated by comparing them against published maps and ancillary references. The present day models of vegetation by detailed categories and plant geographic associations appear to significantly agree with other maps and anecdotal evidence, with the exception of the Shrub-steppe with open forests of juniper, cyprus, oak, pistachio in the southern Plateau region. The predicted distribution is much larger than what most maps depict it as. Although this could be a consequence of forest degradation, the southeastern tip of the predicted strip is questionable, since areas occupied by this category are not indicated in any reference map to extend so far towards the southeast. Nevertheless, further south in the Wadi Rum region Danin reports a few sightings of Mediterranean species which could be considered relics in this area and include *Juniperus phoenicea* and *Ephedra foeminea* (Danin 1991).

In addition to visually comparing the results against published maps and the literature, the models were evaluated according to the threshold selected, using the AUC, and assessing variable performance. All of these indicate good model performance. Nevertheless, when projecting the models into the past, the category of Coastal Ziziphus vegetation is missing in most of the models. It is possible that this category was not well represented.

Chapter 6

PALEOENVIRONMENTAL RECONSTRUCTION

In this chapter, the results from the paleo vegetation modeling are presented. The two types of models (by plant geographical association and vegetation type) are presented in 500 year blocks from the oldest to the most recent extrapolation (12000 to 2.5 ka BP). For each time period, the results from the models by plant geographic associations are first presented. This is followed by a description and figures showing how the climatic conditions differed to those of the present (see next paragraph). This is only done for the three plant geographic associations, with the understanding that the categories of the more detailed models would have been impacted in the same way. Then the results for the detailed models and summary maps are presented and discussed.

It is important to remember that projecting a model to conditions different to those under which the model was trained (different geographic space or time) increases uncertainty which becomes enhanced the greater the difference between the environmental conditions from the periods in question (i.e., if precipitation at one period is 5 times the precipitation at present or temperature is significantly higher or lower than the present conditions which were used to train the model). It is therefore crucial to highlight these areas, taking advantage of the clamping surface, multivariate environmental similarity surface (MESS), and most dissimilar variable map (MoD) produced by the Maxent software (Elith et al. 2010: Phillips, personal communication). Cells where clamping has occurred represent cells that are outside the training range, but have been constrained to the upper/lower boundary of the range used for training. The MESS surface differs from the clamping maps because here, the difference between present day conditions and those in another time period are quantified.

As explained by Elith et al. (2010), the units on the MESS which range from -100 to +100 indicate how much the value at a cell deviates from a set of reference points with regards to the predictor variables. These reference points can be drawn from the observations themselves or from any other sample within the study area. Models that were run at the same time (like that run for Irano Turanian and Saharo Arabian plant geographic associations) produce the same MESS map because they used the same reference points. On the other hand, the Mediterranean MESS differs slightly because it used another set of reference points. Increasing negative values show where extrapolation was greatest for the variable that was most dissimilar at a particular cell (darker shades of red), whereas positive values (displayed as blue) represent similar conditions. The MoD shows which variables were responsible for the extreme values in the MESS.

Figure 6.1 provides an overview of how the climatic conditions change throughout the duration of this study, according to the climate grids. It shows a handful of cities or places of interest spread throughout the study region, for which the average yearly temperature and rainfall values have been extracted (for each of the time periods of interest from 12 – 2.5 ka BP). Several things are obvious by looking at these graphs. During Pleistocene – Holocene transition, precipitation is significantly greater than at present. From this period until the Early Holocene, rainfall levels decrease. This trend is interrupted during 4 ka BP. Temperature during the Pleistocene – Holocene transition was lower than at present (was at its lowest at 10.5 ka BP), and then started to gradually increase until around 8.5 ka BP when it remains fairly stable (except for a drop during 4 ka BP).

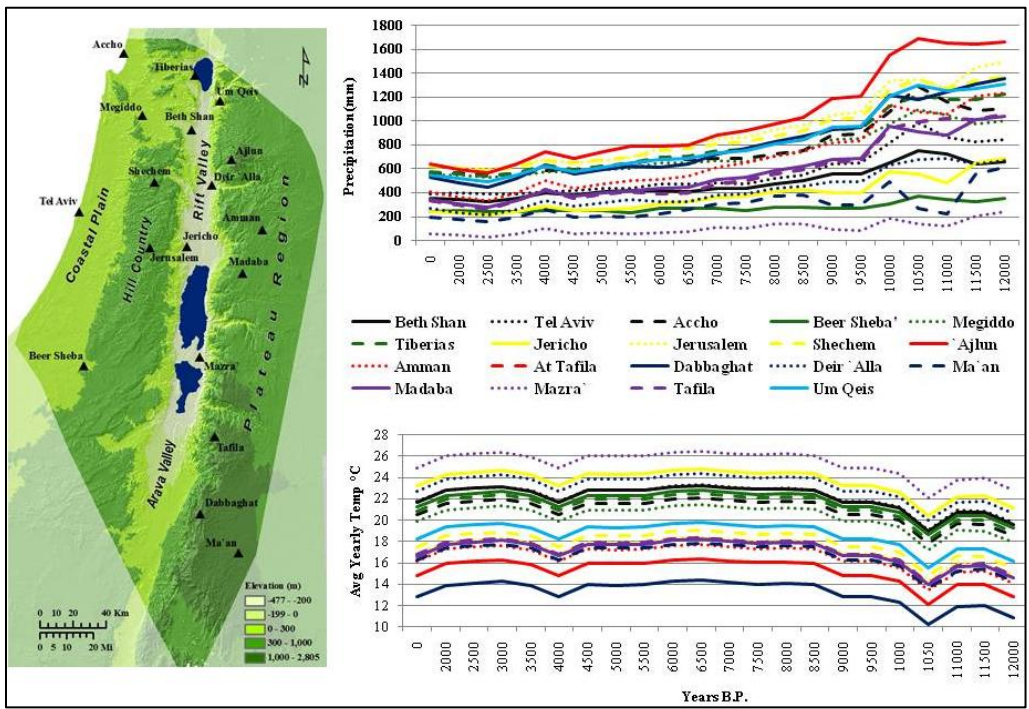


Figure 6.1. Summary of climatic conditions throughout the study period at locations mentioned in the text.

6.1 Model outputs (General description in 500 year blocks)

6.1.1 Model output for 12 ka BP

The following figure (Figure 6.2) presents the results for 12 ka BP by plant geographical association, after the threshold that maximizes the sum of sensitivity plus specificity was applied. The column on the left shows the area suitable for each of the plant geographic associations. These areas were combined to produce the map on the right, showing the extent of plant geographic associations in 12 ka BP.

The outputs of the models suggest that of the three plant geographic associations, the one that occupies the greatest area is the Mediterranean. West of the rift valley, it extends all the way south into the Negev Highlands. It also expands into the rift valley north of the Dead Sea and then towards the plateau region, where it occupies most of the area. The Sahara Arabian association is mainly confined to the Arava Valley and

surrounding areas. In the Negev, the Irano Turanian association appears as a belt between the Mediterranean and Saharo Arabian associations. East of the rift valley, it is mainly present on the plateau in Moab and actually makes its way into the rift valley via Wadi Mujib. Lake Lisan was supposed to reach its greatest extent at this time (shown through the -180m contour).

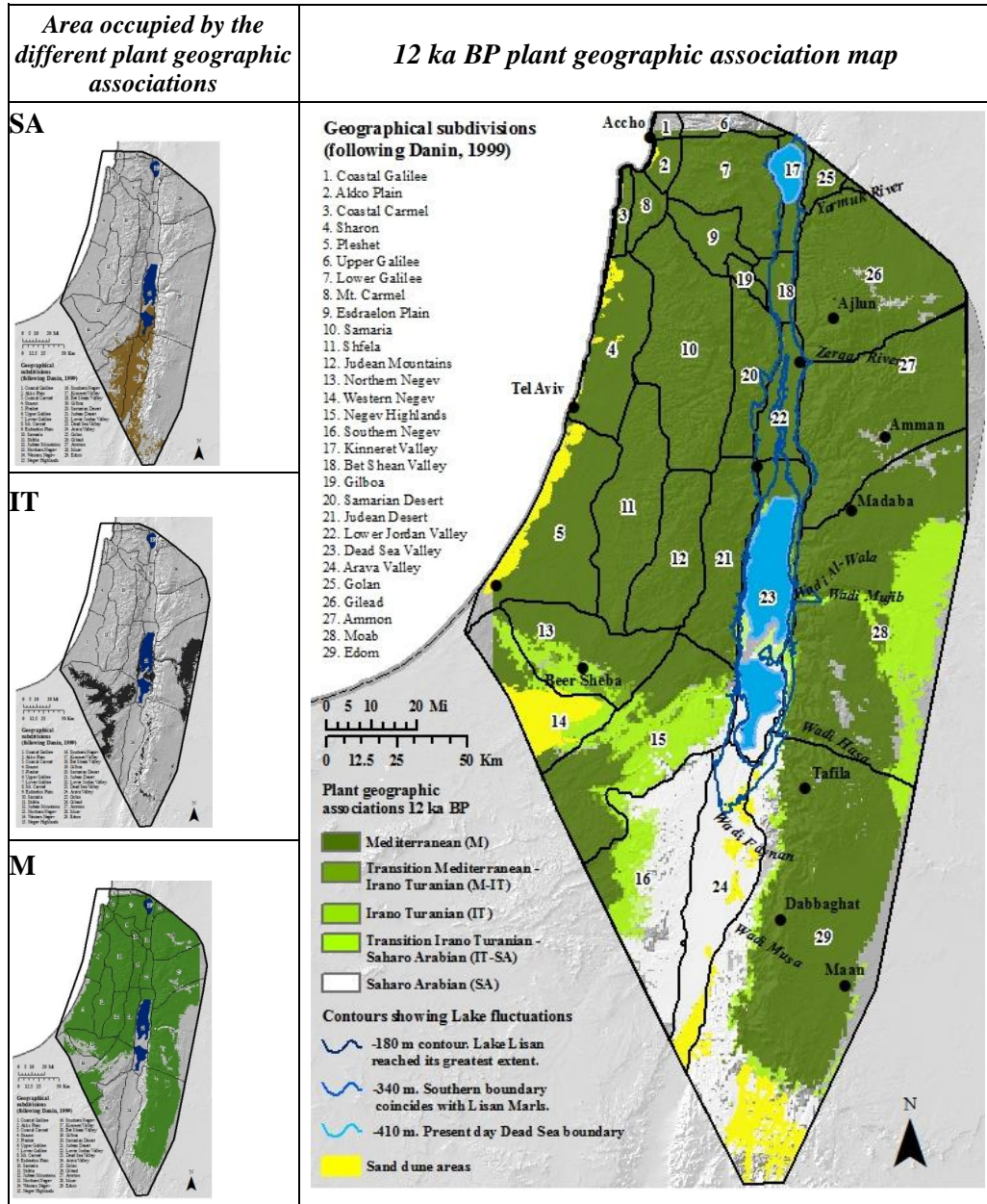


Figure 6.2. Vegetation model for 12 ka BP, by plant geographic association.

Figure 6.3 shows how the environmental conditions in 12 ka BP differed to those of the present. The first row shows where clamping has occurred. The second row shows the MESS maps. Increasing negative values show where extrapolation was greatest (darker shades of red). The figure on the right shows which variables were outside their training region in 12 ka BP (most dissimilar than those of the present), and responsible for extreme values seen in the MESS maps.

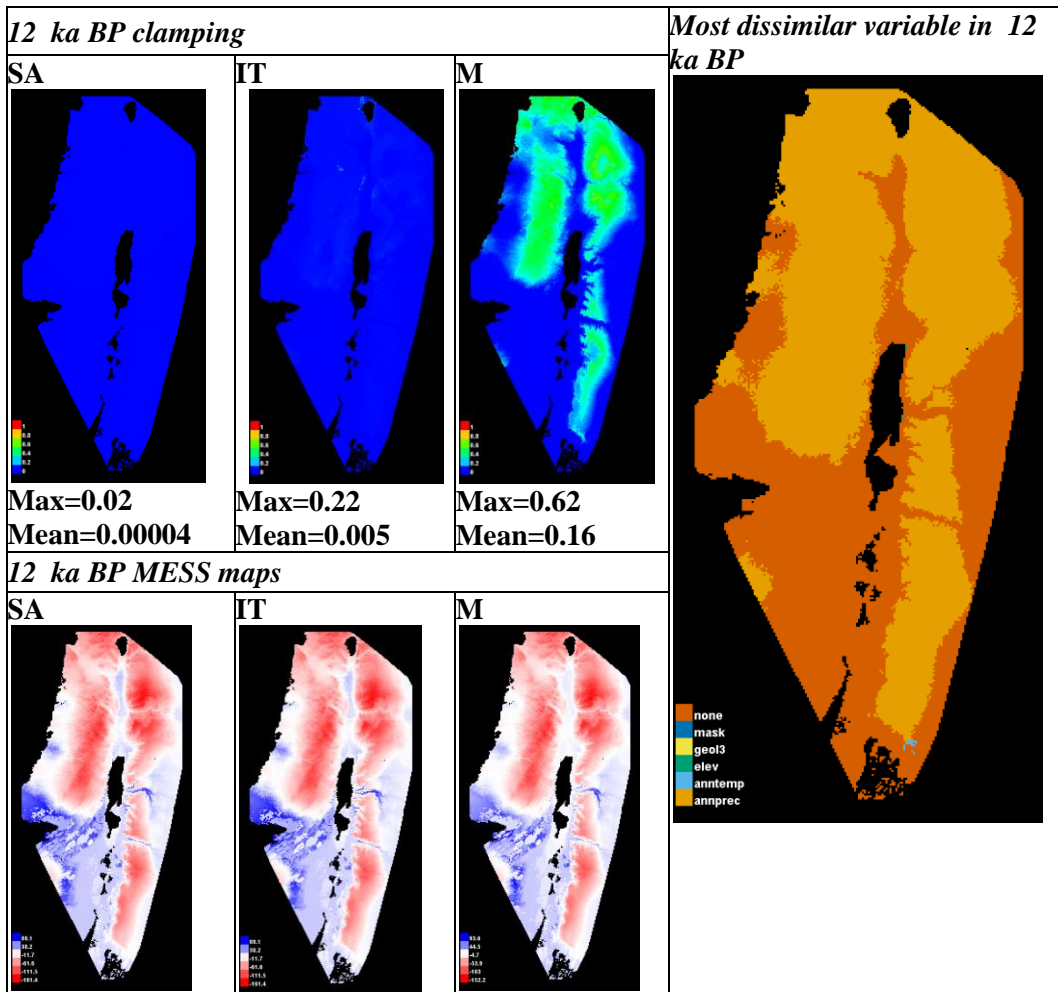


Figure 6.3. Clamping and MESS maps for 12 ka BP, taken from Maxent.

The MESS maps show that conditions in 12 ka BP were significantly different to those of today. As the figure on the right shows, this was essentially due to the

precipitation surface, which in some cells represents values that are around 3 times higher than present day ones. As a result, the Mediterranean category (and forest categories subsequently) was the most affected by clamping (highest value was 0.62). Clamping concentrates on the mountains west of the rift valley, along the plateau, and on the northern portion of the study area. In the more detailed models, the Mediterranean plant geographical association was broken into several forest categories which are affected by clamping in the same way.

Figure 6.4 shows the area occupied by the different vegetation subcategories in 12 ka BP, after the threshold that maximizes the sum of sensitivity plus specificity was applied. The categories were combined to produce a detailed vegetation map for 12 ka BP (Map 6.5)⁸.

Out of all the years for which models were created, this time period represents the second wettest, and the period when forests reached their greatest extent. The dominant forest category is the mixed evergreen oak forest (*Quercus calliprinos*) which is widespread throughout the study area. The mixed evergreen/deciduous oak forest category forms a belt around the northern half of the study area. The coastal plain is also completely populated by either deciduous *Quercus ithaburensis* forests or the mixed evergreen/deciduous category, which spread south into the Northern Negev.

⁸ The categories that were only modeled or mapped for the present are also included in the detailed vegetation map for all of the modeled time periods (e.g., Tropical Sudanian; riparian vegetation; halophytic vegetation; sand dune vegetation). It is expected that some of these categories would have been impacted by rainfall and lake level fluctuations and as a result the area they occupy may have been slightly different to that which is shown. For instance, during wet periods, the area occupied by riparian and Tropical Sudanian vegetation would have expanded.

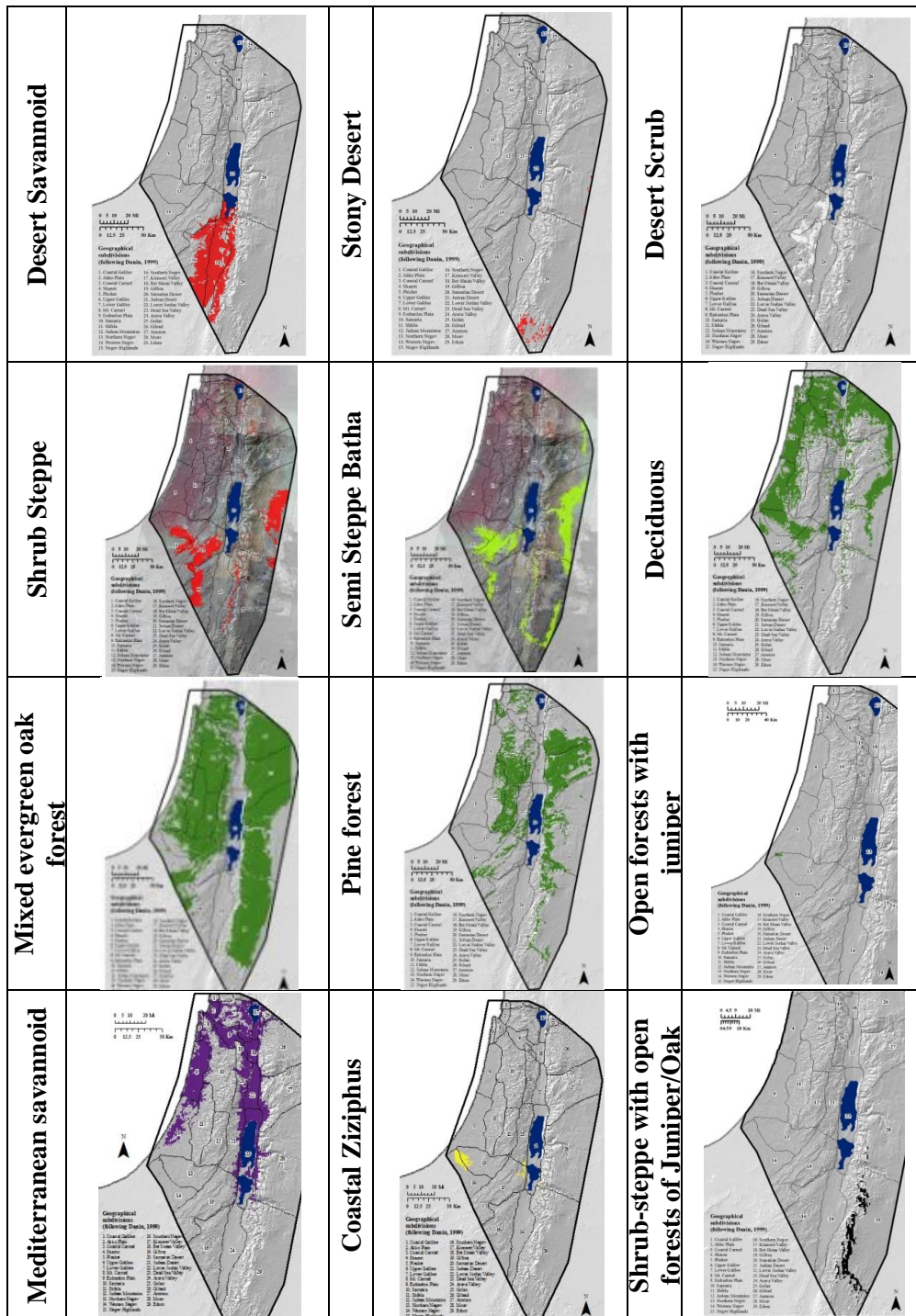
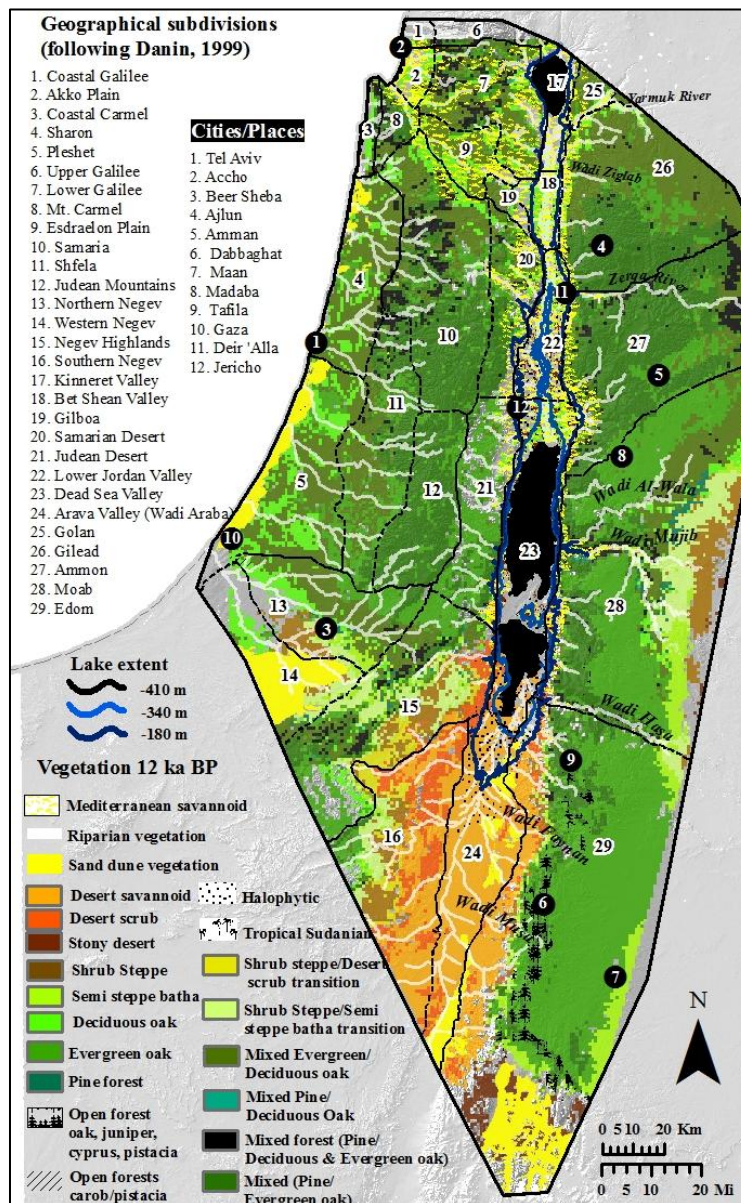


Figure 6.4. Suitable area in 12 ka BP per vegetation subcategory.

In the plateau region, forests cover the whole area except for the eastern edge of Moab and Edom, where steppe categories are found. The mixed pine/evergreen oak forest

category (*Pinus halepensis* and *Quercus calliprinos*) occupies a large area in the Judean and Samarian mountains. East of the Rift Valley, the largest patch of this type of forest occurs north and south of the Zerqa River. Smaller patches are found on the mountain ridges closest to the Rift Valley. *Pinus halepensis* occurs in tandem with *Quercus ithaburensis* along the lower elevation ridges of the Judean mountains, in the Lower Galilee, around Mt. Carmel, and eastern fringe of Gilead and Ammon.



The Mediterranean savannoid vegetation occupies an extensive area (significantly greater than at present) during this modeled period. It surrounds the Dead Sea from the Dead Sea Valley to the Kinneret Valley. It also occupies the Esdraelon Plain and extends into drainage basins that feed into Dead Sea.

The presence/absence maps show that some of the desert categories are almost missing. Stony desert vegetation has been replaced by the steppe categories and is only present in a few pixels in the eastern and southern boundary of Moab and Edom, respectively. The desert savannoid vegetation still dominates the Arava Valley and extends into the Southern Negev where it mixes with the desert scrub vegetation.

6.1.2 Model output for 11.5 ka BP

The following figure (Figure 6.5) presents the results for 11.5 ka BP by plant geographic association. The column on the left shows the area suitable for each of the associations. These areas were combined to produce the map on the right.

The extremely wet conditions of 12 ka BP continue in 11.5 ka BP. As a result, the Mediterranean category continues to occupy most of the study area. Nevertheless, a slight contraction from 12 ka BP is observed. The Irano Turanian association is now found on the edges of the Mediterranean association on the plateau and in the Negev. The Saharo Arabian association is mainly confined to the Arava Valley and its immediate surroundings. At the eastern edge of the study area, Irano Turanian – Saharo Arabian transition zones and the Saharo Arabian association is now present (absent in 12 ka BP).

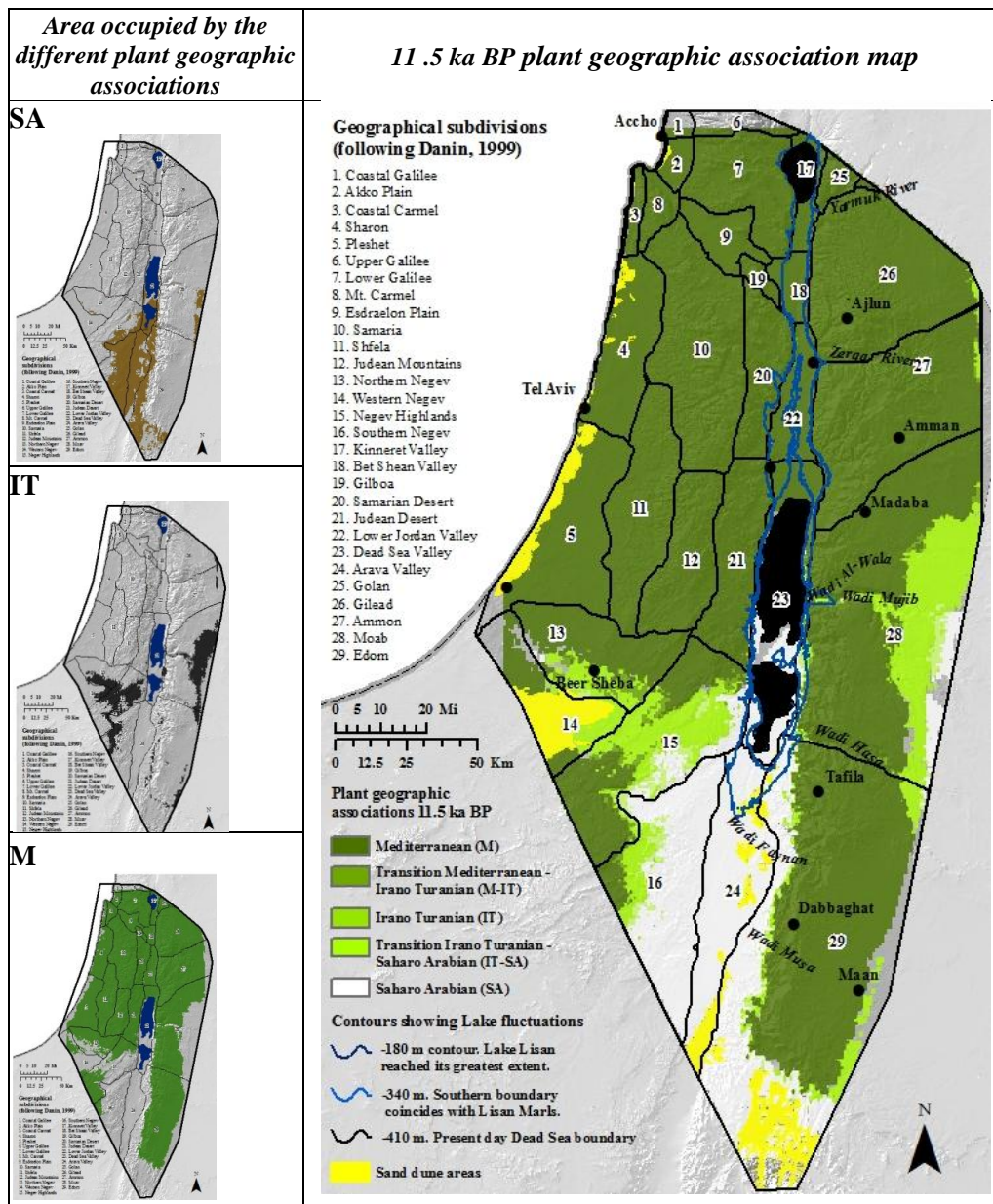


Figure 6.5. Vegetation model for 11.5 ka BP, by plant geographic association.

Figure 6.6 shows how the environmental conditions in 11.5 ka BP differed to those of the present. The first row shows where clamping has occurred. The second row shows the MESS maps. Increasing negative values show where extrapolation was greatest (darker shades of red). The figure on the right shows which variables were

outside their training region in 11.5 ka BP (most dissimilar than those of the present), and responsible for extreme values seen in the MESS maps.

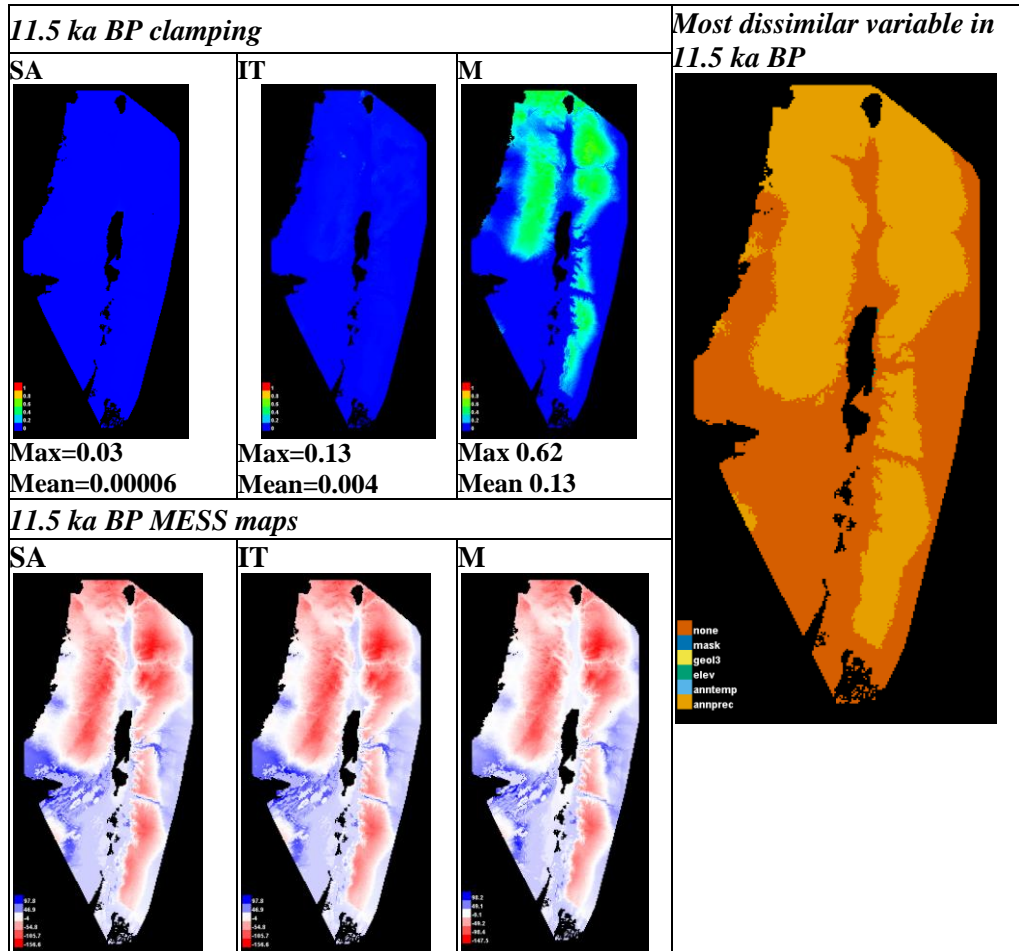


Figure 6.6. Clamping and MESS maps for 11.5 ka BP, taken from Maxent.

The clamping, MESS, and MoD for 11.5 ka BP indicate that conditions during this time period are extremely different to those of today. In some areas, precipitation remains at levels that are almost three times higher than present values. This results in high clamping values in the Mediterranean and forest categories. In fact, the only areas that are not impacted by novel conditions are the Negev and the eastern portion of the plateau in the Moab subdivision.

The following figure (Figure 6.7) shows the area occupied by the different vegetation types in 11.5 ka BP, after the threshold that maximizes the sum of sensitivity

plus specificity was applied. These categories were combined along with the outputs from the sand dune vegetation to produce a vegetation map for 11.5 ka BP (Map 6.2).

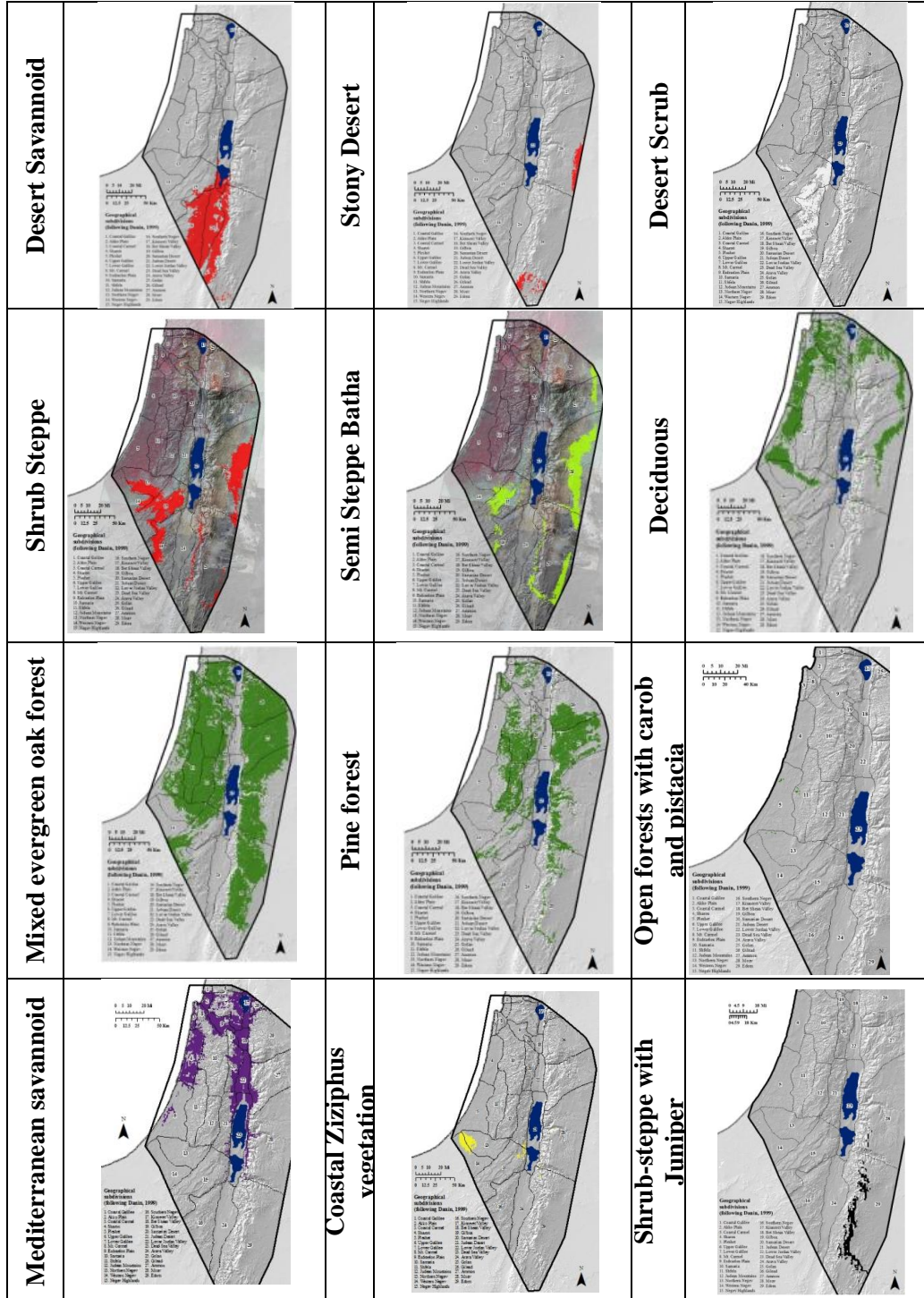
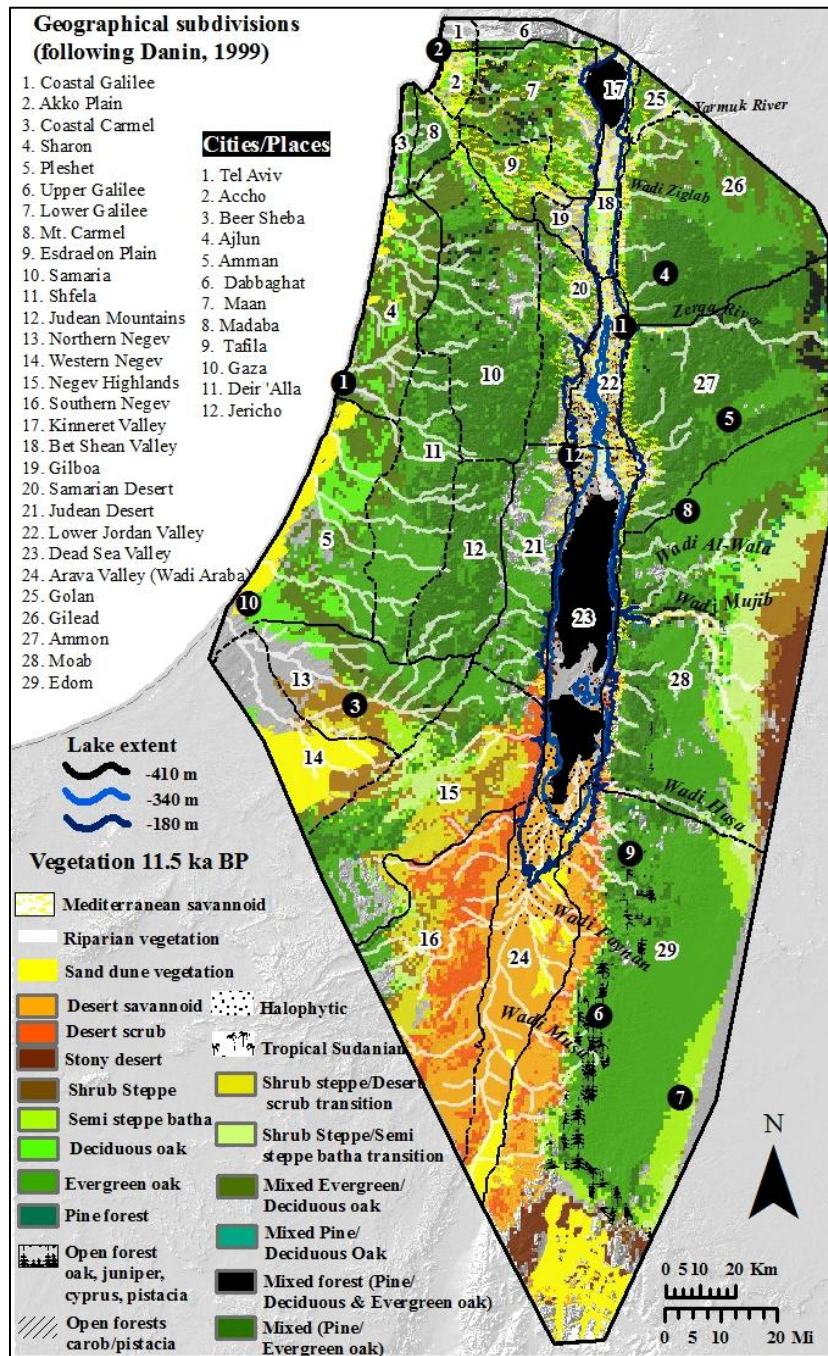


Figure 6.7. Suitable area in 11.5 ka BP per vegetation subcategory.



Map 6.2. Detailed vegetation map for 11.5 ka BP.

The forest categories continue to be far reaching and form an almost continuous longitudinal belt along the plateau region, mainly represented by the mixed evergreen (*Quercus calliprinos*) oak forest category. The coast is still dominated by both *Quercus calliprinos* and *Q. ithaburensis*. Nevertheless, when looking at the response of the

individual forest categories during this time period, a contraction is observed from 12 ka BP. This is most evident with regards to the deciduous oak forest category as well as the combined pine and deciduous oak, which have shrunk significantly. The evergreen oak forests have also contracted, being replaced along the edges by the various steppe categories. The Mediterranean savannoid category still surrounds the Jordan River. In the Kinneret valley, it wraps around Lake Kinneret. It also extends into the coast along the Esdraelon Plain and into river basins that discharge into the Jordan River (i.e., the Yarmuk River basin).

The desert categories continue to concentrate along the Arava Valley and the Negev. On the plateau, the stony desert vegetation is now present along the eastern edges, where it transitions into the steppe categories and then the forest categories.

6.1.3 Model output for 11 ka BP

The following figure presents the results for 11 ka BP by plant geographic association (Figure 6.8). The column on the left shows the area suitable for each of the modeled categories. These were combined to produce the map on the right, showing the extent of the plant geographic associations and transition areas in 11 ka BP.

Although the Mediterranean association continues to be the most abundant, the longitudinal strip east of the rift valley has slightly tightened and been replaced by the Irano Turanian association in the plateau as well as in parts of the Negev. The large Mediterranean patch in Moab is now surrounded by the Irano Turanian and Saharo Arabian plant geographic associations.

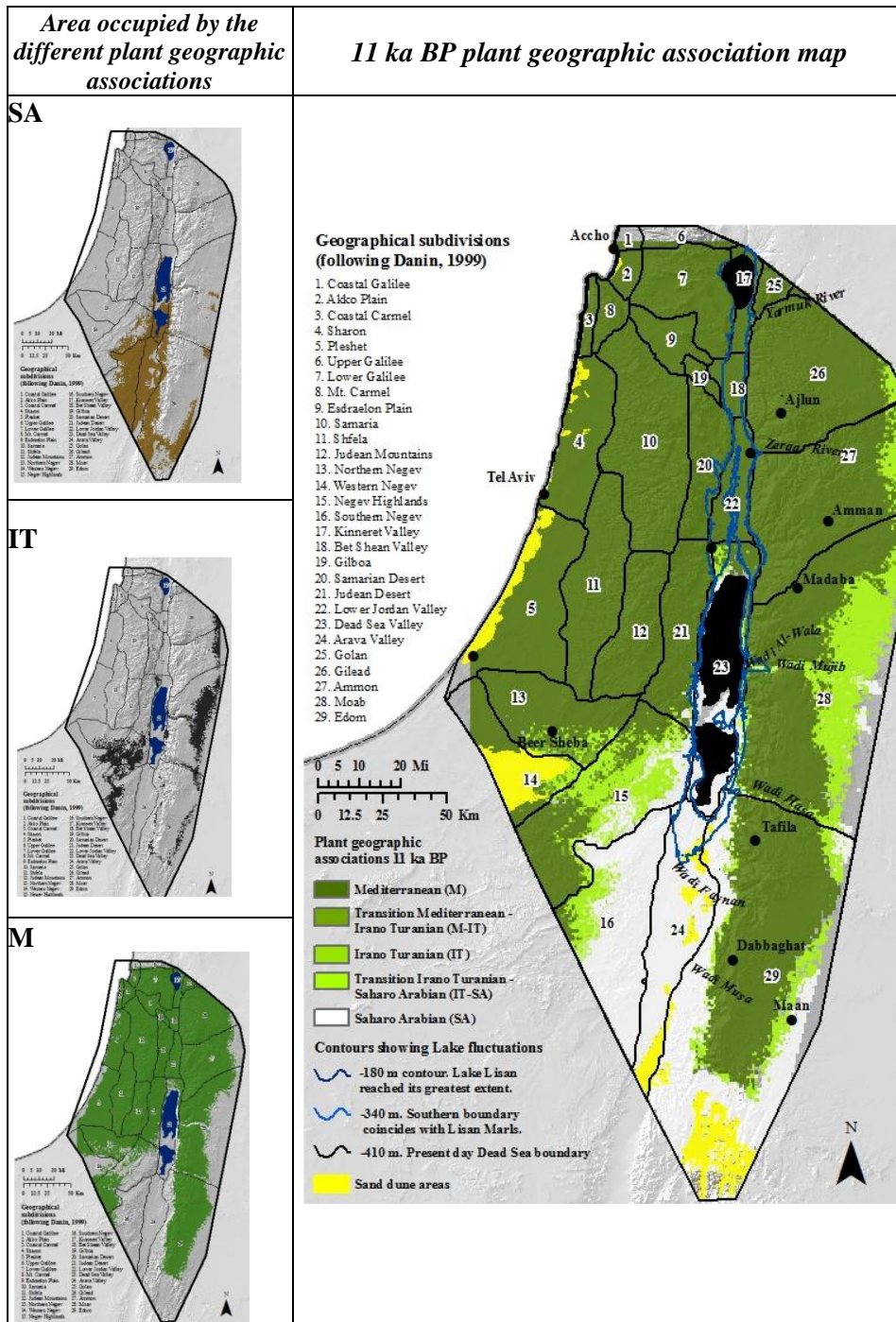


Figure 6.8. Vegetation model for 11 ka BP, by plant geographic association.

Figure 6.9 shows how the environmental conditions in 11 ka BP differed to those of the present. The first row shows where clamping has occurred. These figures were taken from the Maxent html output. The second row shows the MESS maps. Increasing

negative values show where extrapolation was greatest (darker shades of red). The figure on the right shows which variables were outside their training region in 11 ka BP (most dissimilar than those of the present), and responsible for extreme values seen in the MESS.

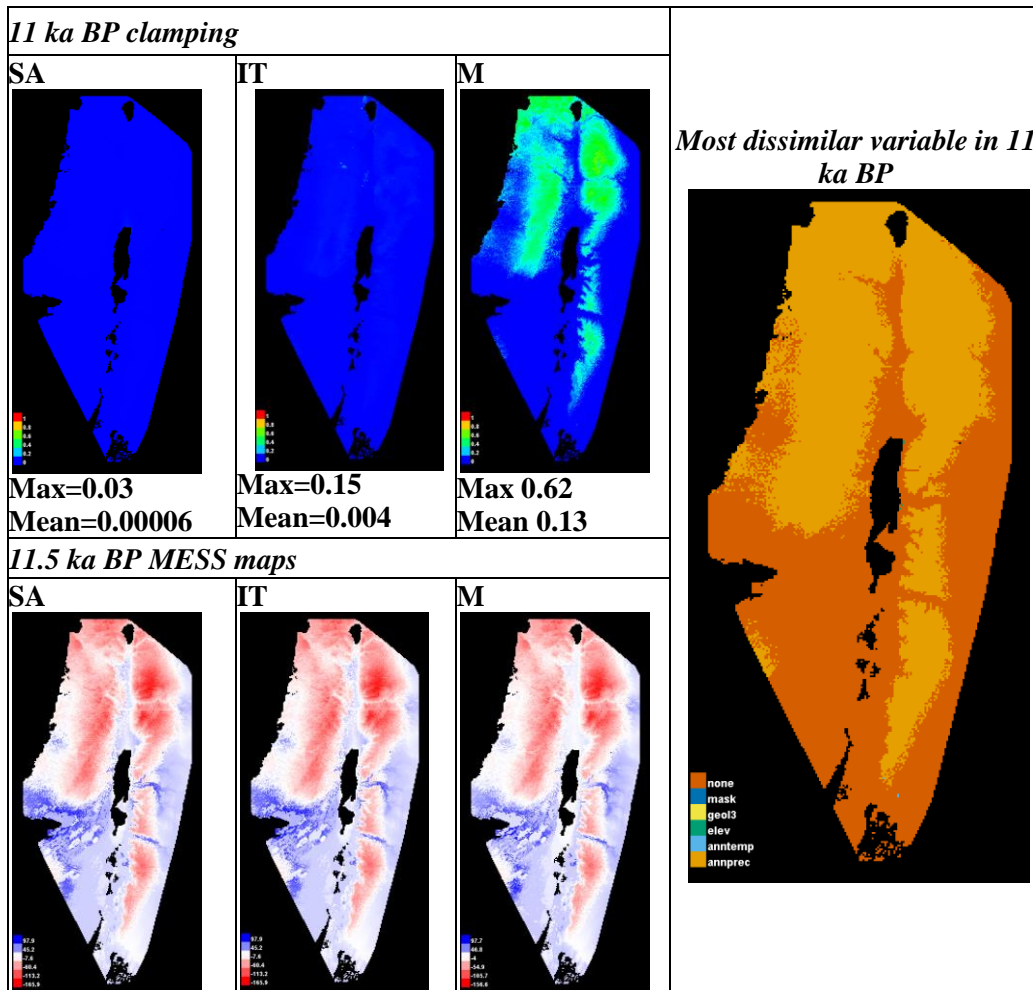


Figure 6.9. Clamping and MESS maps for 11 ka BP, taken from Maxent.

These sets of maps which show novel conditions in 11 ka BP indicate that conditions were like those experienced in the two earlier periods (11.5 and 12 ka BP). In some areas in the plateau, hill country and around the northern portion of the study area, precipitation is about three times its present day values. This causes the categories present

in these areas (Mediterranean, forest categories, some steppe, and Mediterranean savannoid) to remain affected by high clamping values.

The following figure (Figure 6.10) indicates the area occupied by the different vegetation types in 11 ka BP, after the threshold that maximizes the sum of sensitivity plus specificity was applied. These categories were combined with the area estimated to be populated by sand dune vegetation to produce the following detailed vegetation map (Map 6.3). This map provides more insight into the expansion of the Irano Turanian association (which includes the various steppe categories), as it encroaches upon the Mediterranean association (forest categories) along the plateau. Until 11 ka BP, forests had occupied most, if not all cells along the eastern boundary of the Gilead, Ammon, and Edom regions. In 11 ka BP, steppe categories appear along the eastern fringe as the forests contract. In Moab and Edom, the outer edge is now populated by a well defined strip of stony desert vegetation, indicating the beginning of the Eastern Desert which would stretch for thousands of kilometers beyond the study area.

The Negev highlands are represented by several categories which appear to intersect here. Along the lower elevations, the drier categories are found (i.e., desert scrub, desert savannoid, shrub steppe/desert scrub transition, and shrub steppe) whereas at higher elevations these transition into the three main forest categories. The coastal plains from the Negev to Carmel continue to be dominated by *Quercus calliprinos* and *Q. ithaburensis*. The presence/absence map of the open forests with carob/pistacia shows that this category is still virtually absent. The rift valley in the north continues to be occupied by Mediterranean savannoid vegetation which extends into the coast via the Esdraelon Plain.

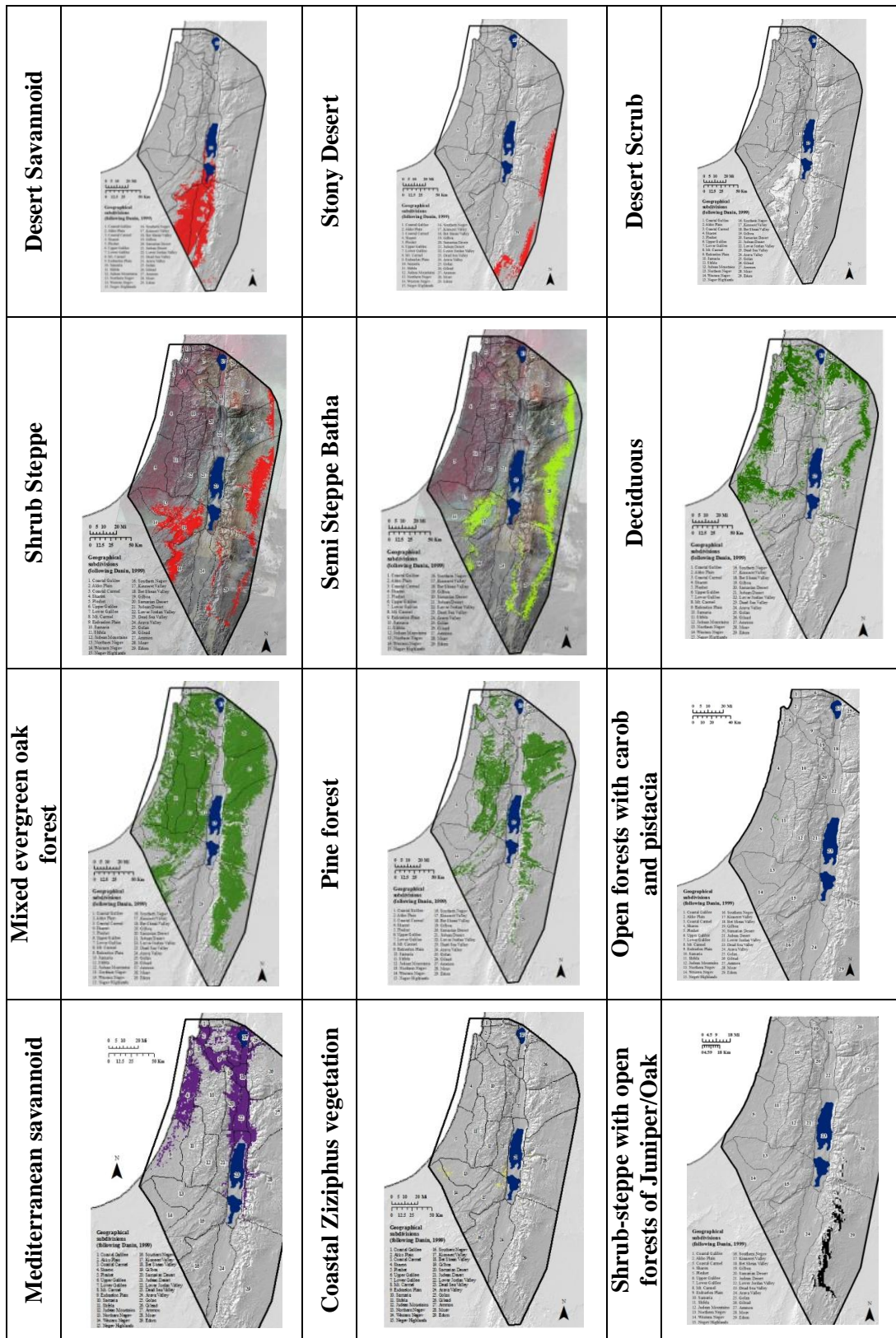
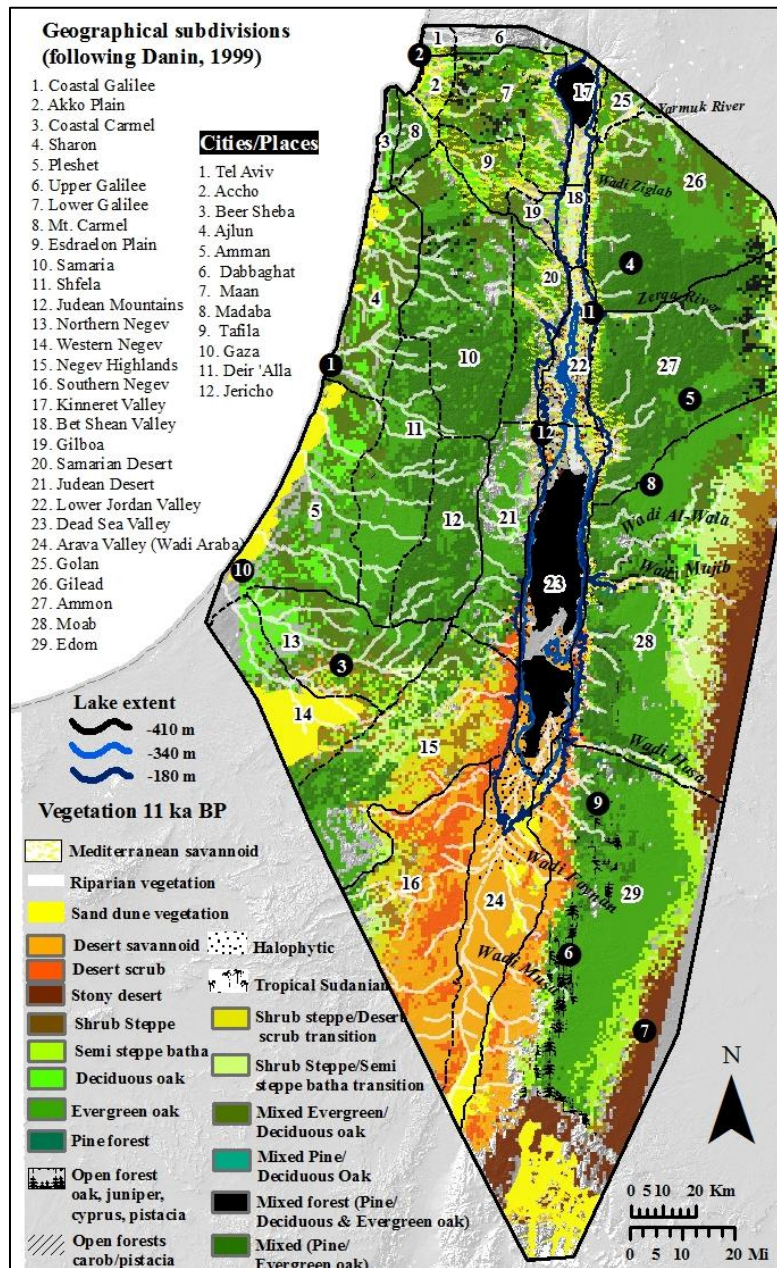


Figure 6.10. Suitable area in 11 ka BP per vegetation subcategory.



Map 6.3. Detailed vegetation map for 11 ka BP.

6.1.4 Model output for 10.5 ka BP

The following figure (Figure 6.11) presents the results for 10.5 ka BP by plant geographic association, after the threshold that maximizes the sum of sensitivity plus specificity was applied. The column on the left shows the area suitable for each of the

categories. These areas were combined to produce the map on the right, showing the extent of the plant geographic associations in 10.5 ka BP.

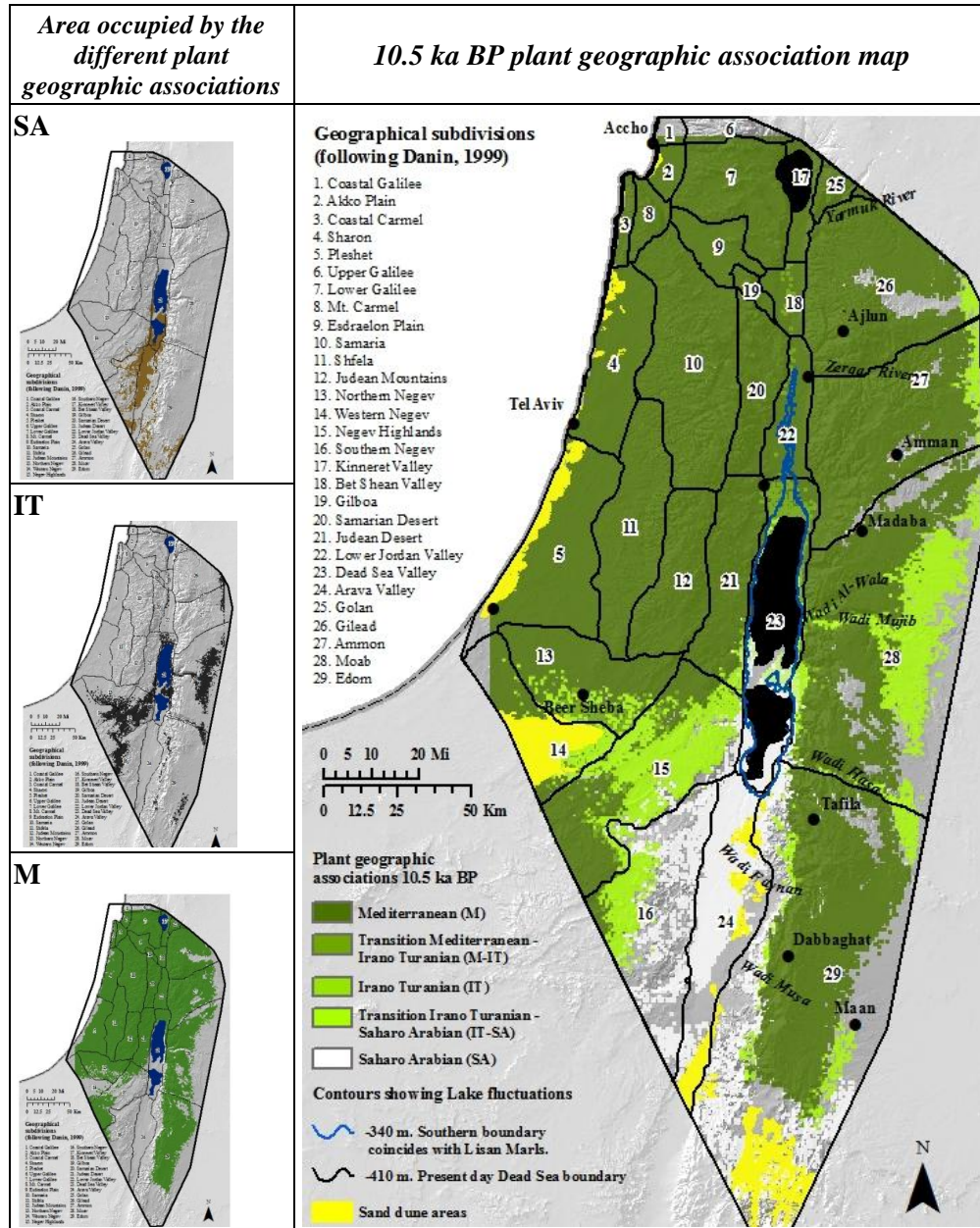


Figure 6.11. Vegetation model for 10.5 ka BP, by plant geographical association.

This period brings about a reversal of the so far observed trend of a shrinking Mediterranean association. From the previous period, areas populated by the Mediterranean association have slightly expanded. Even more pronounced is the

expansion of the Irano Turanian association into areas previously suitable to the Sahara Arabian association in the Negev and plateau region. In the plateau region and amidst the patch of the Mediterranean association, there are several gaps which coincide with areas that have about a 3°C average annual temperature difference from today's (lower).

Figure 6.12 shows how the environmental conditions in 10.5 ka BP differed to those of the present (taken from the Maxent output). The first row shows where clamping has occurred. The second row shows the MESS maps. Increasing negative values show where extrapolation was greatest (darker shades of red). The figure on the right shows which variables were outside their training region in 10.5 ka BP (most dissimilar than those of the present), and responsible for the extreme values seen in the MESS maps.

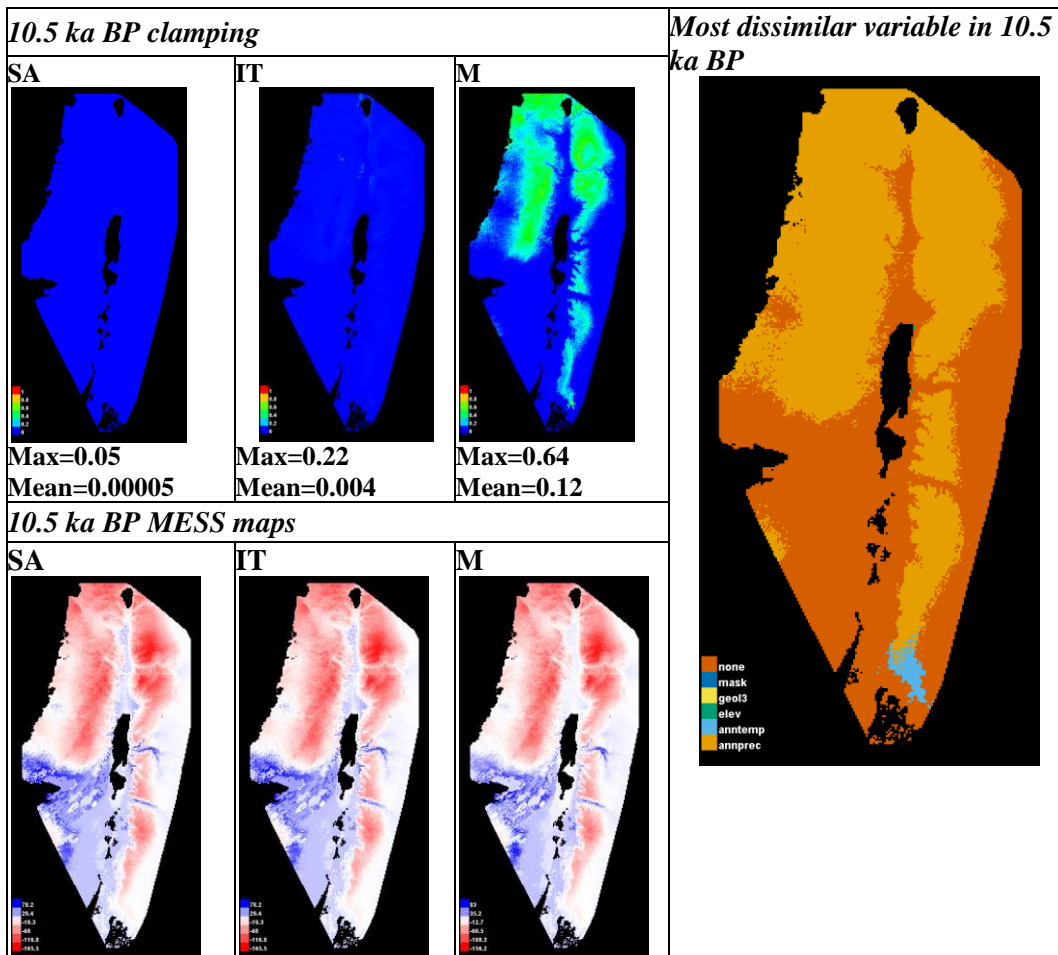


Figure 6.12. Clamping and MESS maps for 10.5 ka BP, taken from Maxent.

According to the environmental layers (average yearly temperature and precipitation), 10.5 ka BP was wetter than 12 ka BP and colder by about 1°C. Those areas that experience the highest amount of rainfall at present, in 10.5 ka BP have values that are up to three times higher than today's. Likewise, average yearly temperature is 2 to 3°C colder than at present. The maps above reflect these different conditions. The clamping map of the Mediterranean category shows moderate to high values throughout the Judean mountains, Lake Kinneret region, and the plateau region in Gilead and Ammon.

Figure 6.13 shows the area occupied by the different vegetation subcategories in 10.5 ka BP, after the threshold that maximizes the sum of sensitivity plus specificity was applied. These categories were combined to produce a more detailed vegetation map (Map 6.4). As just mentioned, 10.5 ka BP brings a halt to the trend of forest contraction seen so far. By 11 ka BP, the eastern boundary of the study area had become occupied by steppe and stony desert vegetation. In 10.5 ka BP, forests expand and push these categories to the edge of the study area. Most of this expansion is due to a dramatic increase (from 11 ka BP) in the mixed evergreen/deciduous oak forest category which represents the outermost belt of these forested areas (both in the coastal plains and throughout the plateau). Another category that increased from 11 ka BP is the mixed *Pinus halepensis*, *Quercus ithaburensis* category. In Gilead and Ammon, it is seen in the eastern edge of the study area whereas in Shfela and Samaria it is found on the lower elevation portions of the mountains.

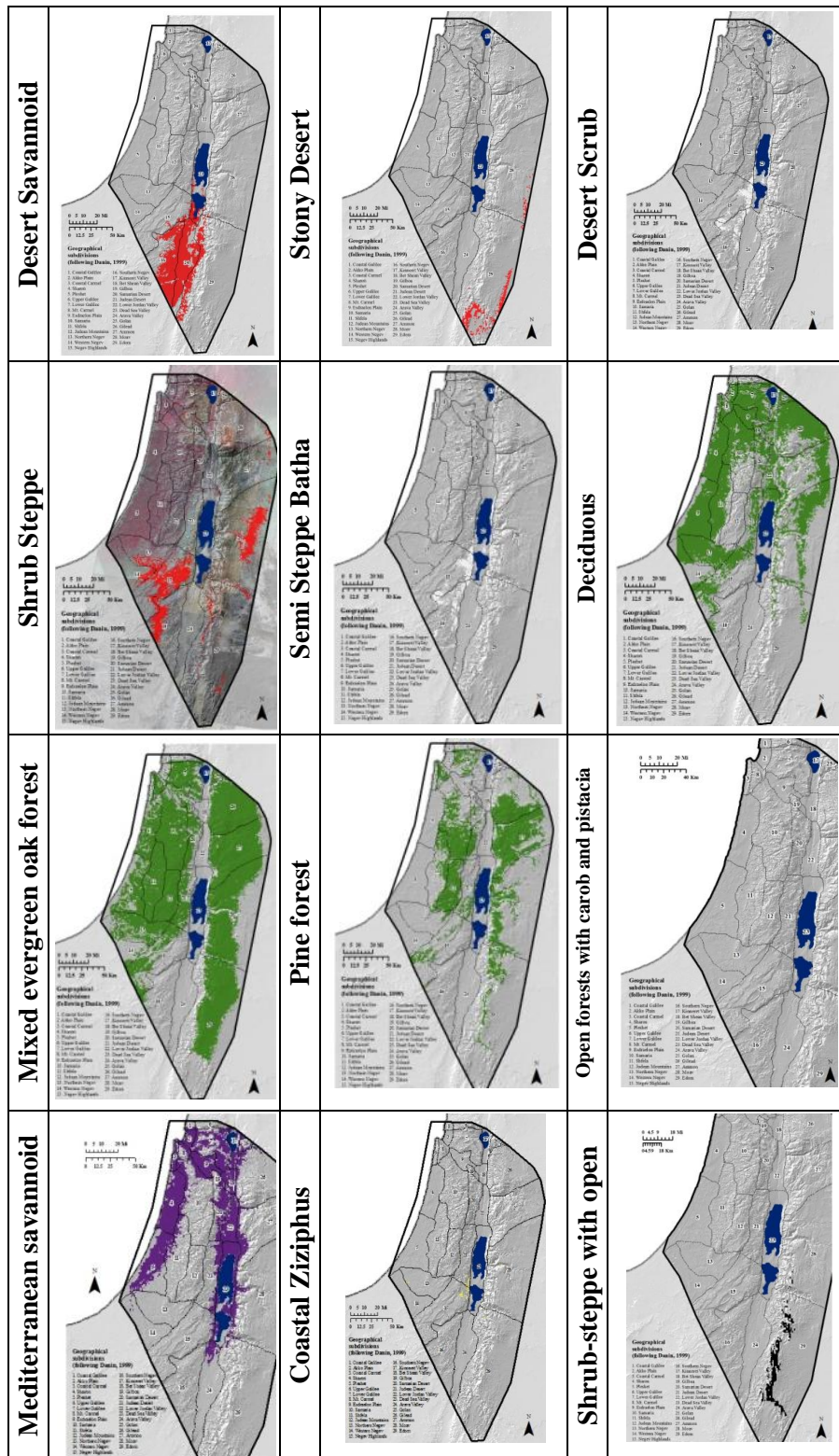
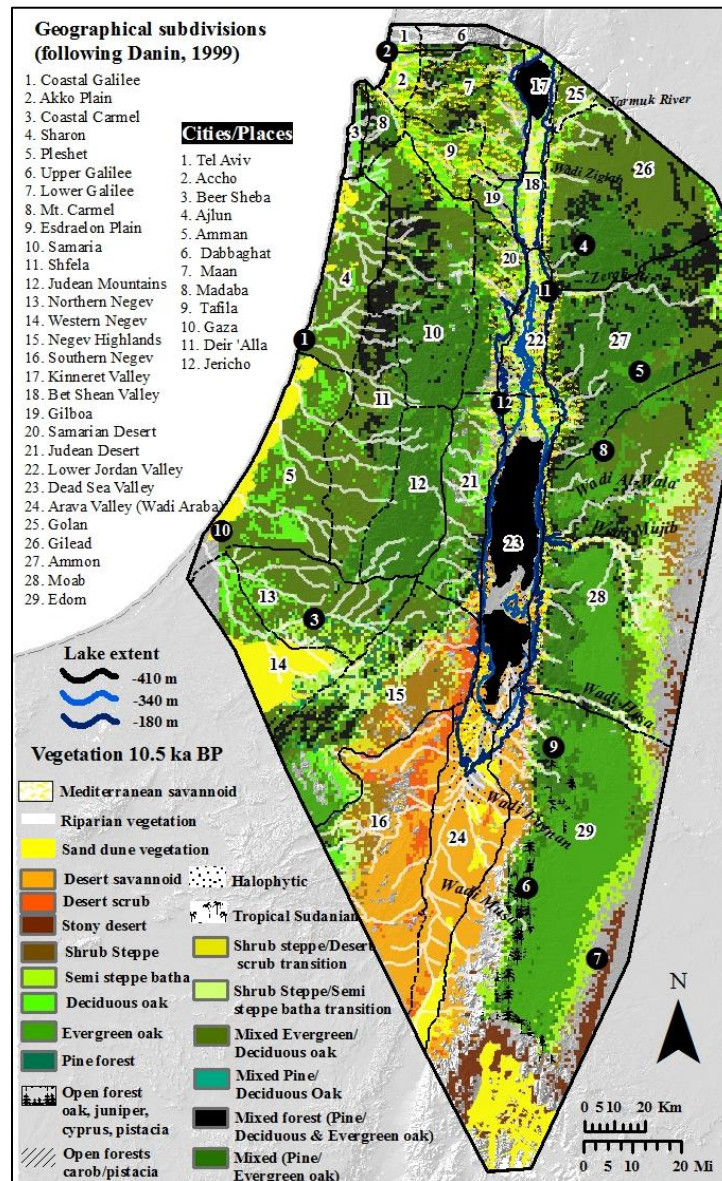


Figure 6.13. Suitable area in 10.5 ka BP per vegetation subcategory.



Map 6.4. Detailed vegetation map for 10.5 ka BP.

In the Negev, most of the shrub steppe/desert scrub transition vegetation has been replaced by shrub steppe vegetation, thus suggesting a return to more moist conditions from 11 ka BP. The areas in the Arava Valley and the Southern Negev that are occupied by the Saharo Arabian association (Figure 6.11), are shown in this more detailed map to mainly consist of the categories desert scrub; desert savannoid; and shrub steppe/desert

scrub transition area. Along its southernmost boundary with the Negev Highlands, there are steppe and forest patches.

The gaps present within the Mediterranean association in the map by plant geographic association are shown in the more detailed models to consist of the mixed evergreen forest category. Along the coastal plain, the mixed evergreen/deciduous oak forests have expanded into areas that were formerly occupied by evergreen oaks alone (in the Judean mountains). Another category that has expanded is the Mediterranean savannoid, which now reaches the southern Dead Sea Basin.

6.1.5 Model output for 10 ka BP

Figure 6.14 presents the results for 10 ka BP by plant geographic association, after the threshold that maximizes the sum of sensitivity plus specificity was applied. The column on the left shows the area suitable for each of the main categories. These areas were combined to produce a 10 ka BP map of plant geographic associations (shown on the right).

The produced map is similar to that of 10.5 ka BP. The Mediterranean association again expands (although not in the same magnitude as that seen from 11 to 10.5 ka BP). It now forms an almost continuous strip on the plateau, which is only intersected by the Irano Turanian association along the Wadi Mujib drainage basin. The Saharo Arabian association predominates in the Arava Valley, the Southern Negev and along the outermost edge of the study area in Edom. The Irano Turanian association forms a transitional belt between the Mediterranean and Saharo Arabian associations in the Negev region. In the plateau, it surrounds the Mediterranean category in Moab but is virtually absent in the Ammon subdivision.

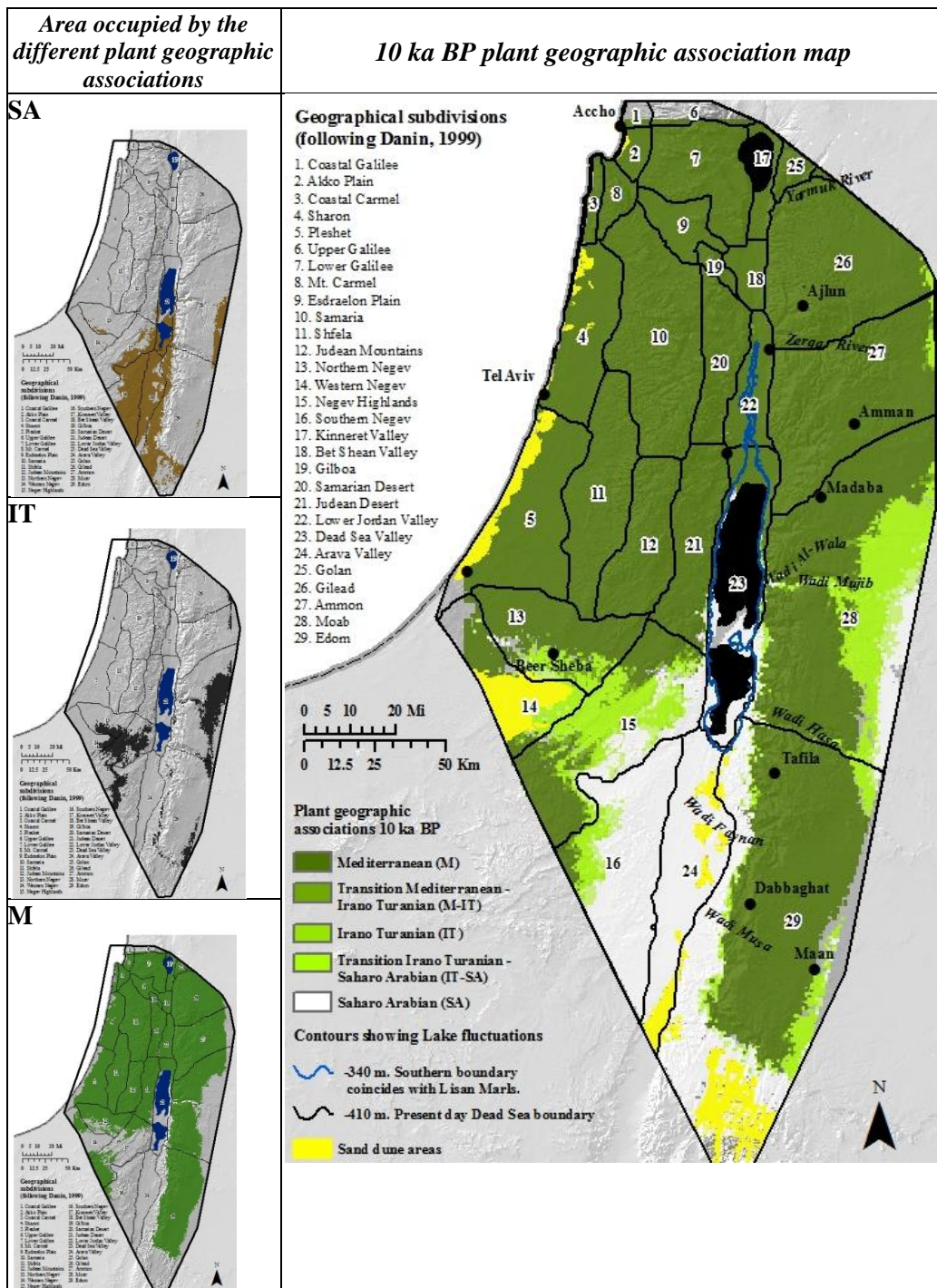


Figure 6.14. Vegetation model for 10 ka BP, by plant geographical association.

The following figure (Figure 6.15) shows how the environmental conditions in 10 ka BP differed to those of the present. The first row shows where clamping has

occurred. These figures were taken from the Maxent html output. The second row shows the MESS maps. Increasing negative values show where extrapolation was greatest (darker shades of red). The figure on the right shows which variables were outside their training region in 10 ka BP (most dissimilar than those of the present), and responsible for extreme values seen in the MESS maps.

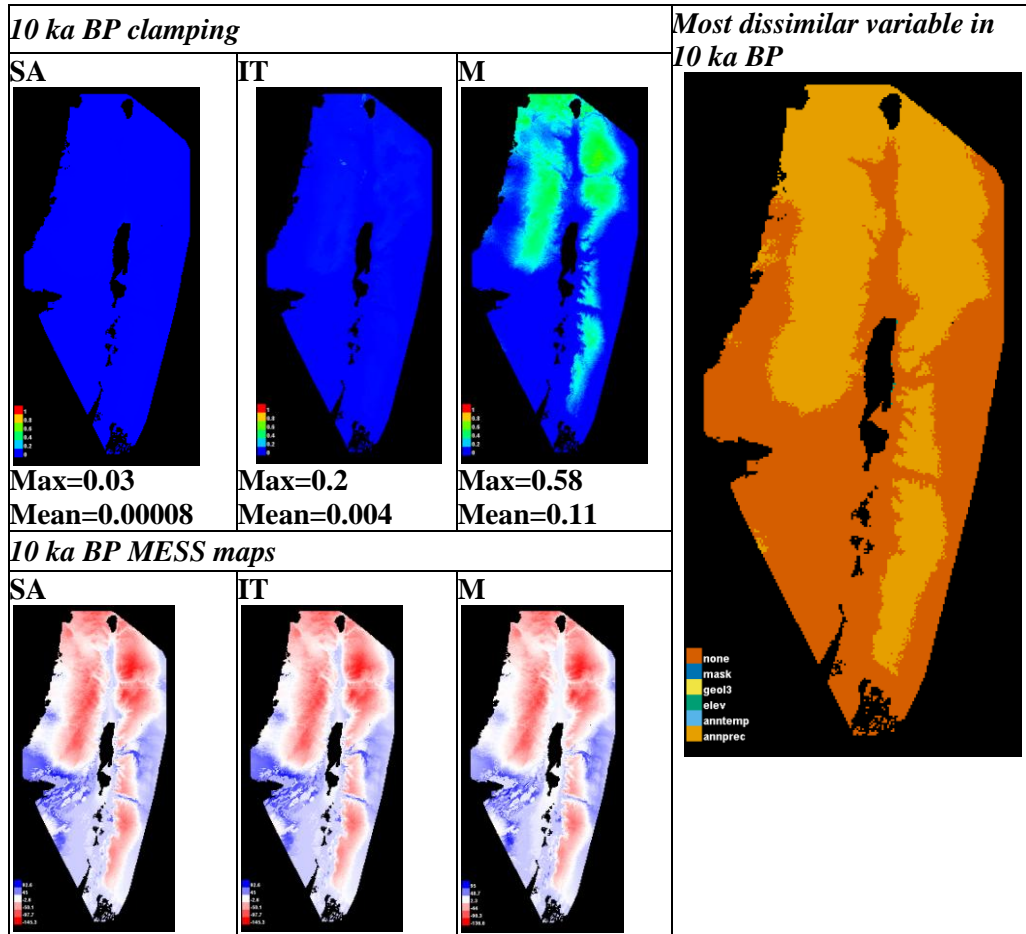


Figure 6.15. Clamping and MESS maps for 10 ka BP, taken from Maxent.

These maps indicate that climatic conditions in 10 ka BP are still quite different to those of today. In some regions, precipitation values remain over 2.5 times their present day values. Nonetheless, they are not as high as they were in 10.5 ka BP. The temperature surface is also not as cold as it was in 10.5 ka BP. The clamping map of the

Mediterranean category continues to show moderate to high values throughout the Judean mountains, Lake Kinneret region, and the plateau region in Gilead and Ammon.

Figure 6.16 shows the area occupied by the different vegetation types in 10 ka BP, after the threshold that maximizes the sum of sensitivity plus specificity was applied. These categories were combined to produce a detailed vegetation map for 10 ka BP (Map 6.5).

Although the map by plant geographic associations indicates that conditions were similar to 10.5 ka BP, the more detailed models show that several changes occurred. Forests are still widespread, however the constitution of these forests has shifted to a similar pattern observed in 11 ka BP. Pine and deciduous oak have substantially decreased and been replaced by the maquis represented by *Quercus calliprinos*. East of the Rift Valley, *Quercus ithaburensis* hardly appears on its own. By itself, it is most obvious in the Pleshet coastal plain which is also occupied by *Quercus calliprinos* and *Pinus halepensis*. The southern boundary of the large forested area west of the Rift Valley has contracted northward. In the previous date, the forest categories expanded past Gaza in the coast and occupied most of the Northern Negev. In 10 ka BP, steppe has moved into this area, pushing the forests slightly north of Beer Sheba. The grasslands of the northern part of the Rift Valley (Mediterranean savannoid) have also contracted.

The detailed map (Map 6.5) also shows that the Irano Turanian association in the Negev consists of the shrub steppe, shrub steppe/semi steppe batha transition, and shrub steppe/desert scrub transition categories. On the plateau, the Irano Turanian category consists of semi steppe batha, shrub steppe/semi steppe batha transition and shrub steppe categories and then becomes stony desert vegetation along the eastern fringe of the study area.

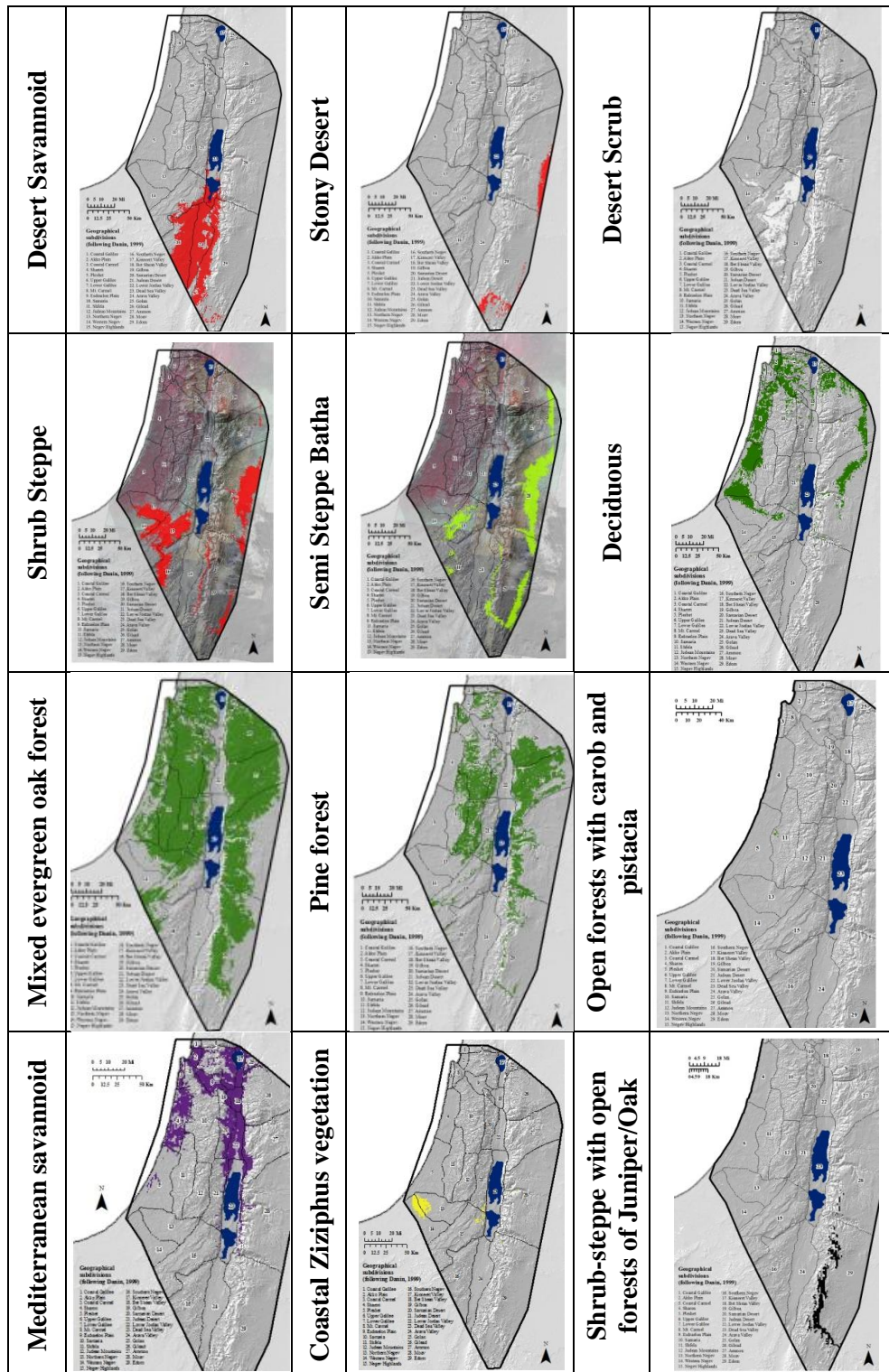
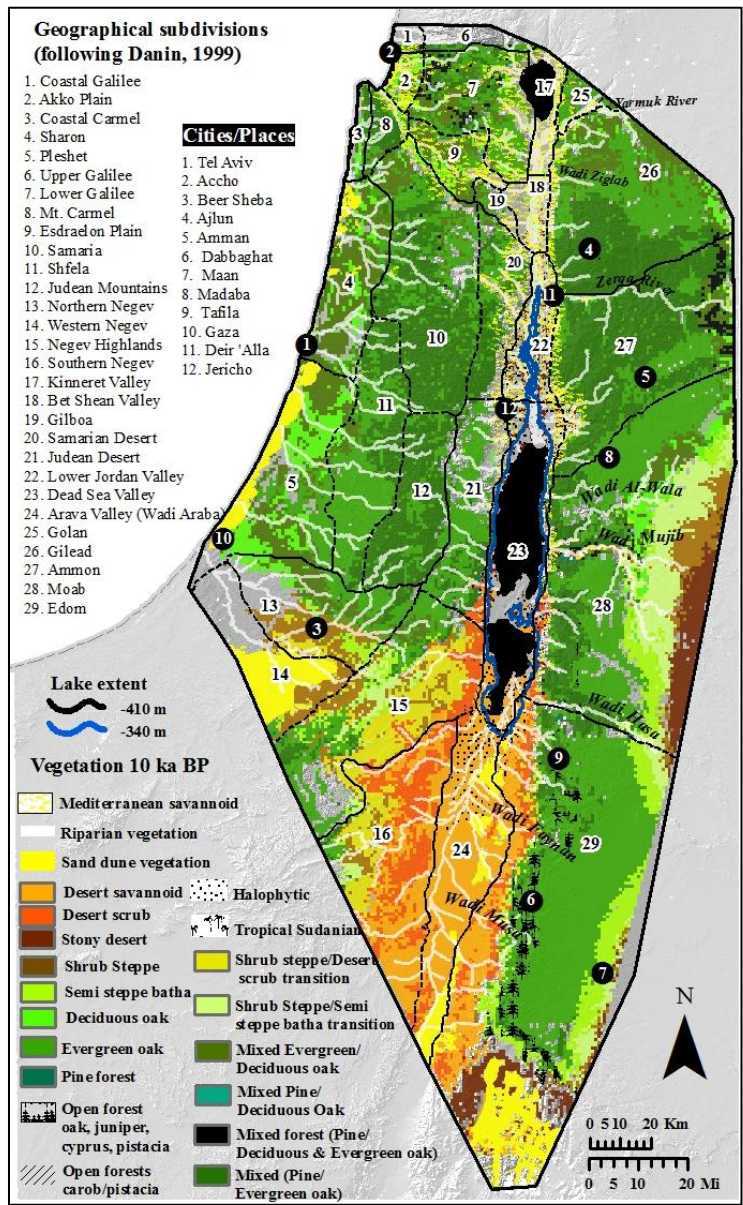


Figure 6.16. Suitable area in 10 ka BP per vegetation subcategory.



Map 6.5. Detailed vegetation map for 10 ka BP.

In the Edom region on the plateau, there were several obvious gaps adjacent to the mixed evergreen category which reoccur until 4 ka BP. This is because the logistic value obtained for the categories that would otherwise be expected in this region (forest or steppe) was below the selected threshold. In other words, it would be expected that these gaps belong to either the mixed evergreen or semi steppe batha categories, had they been above the selected threshold. To avoid having such large gaps, the cells were

assigned to whichever category (mixed evergreen oak or semi steppe batha) had the highest value in the suitability surface produced by Maxent.

6.1.6 Model output for 9.5 ka BP

The results for the modeled plant geographic associations for 9.5 ka BP are given in Figure 6.17. The column on the left shows the area suitable for each of the main categories. These areas were combined to produce a 9.5 ka BP map of plant geographic associations (shown on the right).

Although the Mediterranean category continues to be the most extensive, for the first time it appears to have contracted in all of the geographical subdivisions east of the rift valley (since 12 ka BP). Its southern extent in the Northern Negev and Negev Highlands has also contracted. This narrowing was replaced by the Irano Turanian plant geographic association region. Also, the Saharo Arabian association now occupies a greater area. It expanded to higher elevations from the Arava Valley, as well as into the northern portion of the Dead Sea Valley. It also occupies a greater extent on the plateau in Moab and Edom.

Figure 6.18 shows how the environmental conditions in 9.5 ka BP differed to those of the present. The first row shows where clamping has occurred. The second row shows the MESS maps. Increasing negative values show where extrapolation was greatest (darker shades of red). The figure on the right shows which variables were outside their training region in 9.5 ka BP (most dissimilar than those of the present), and responsible for extreme values seen in the MESS maps.

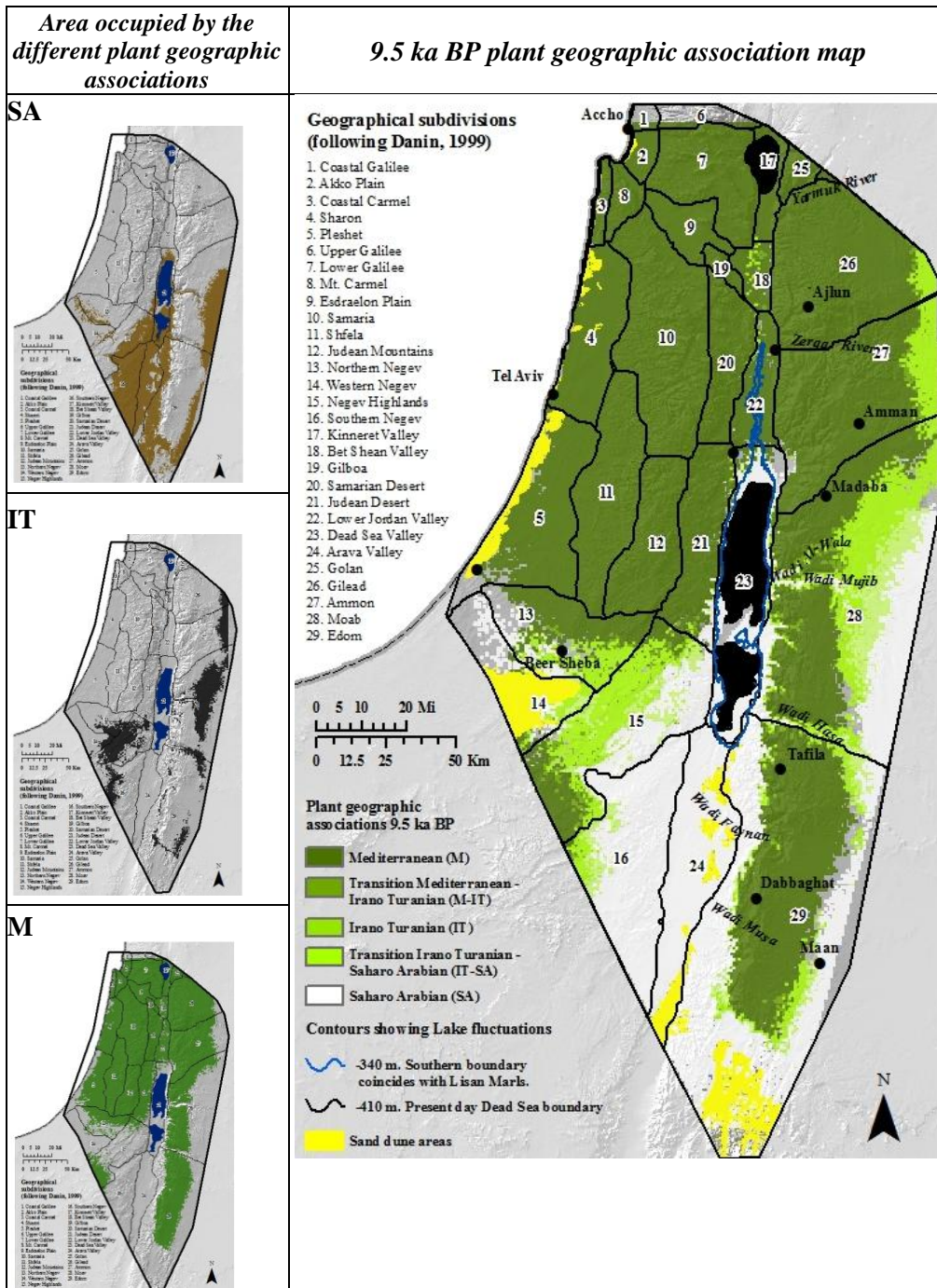


Figure 6.17. Vegetation model for 9.5 ka BP, by plant geographical association.

Although climatic conditions in 9.5 ka BP continue to be quite different than those of today (the Judean mountains and plateau region in Gilead and Ammon receive double present day precipitation levels), it is not in the same magnitude as that observed

in earlier time periods. As a result, the Mediterranean category has much lower clamping values than those observed prior to 9.5 ka BP.

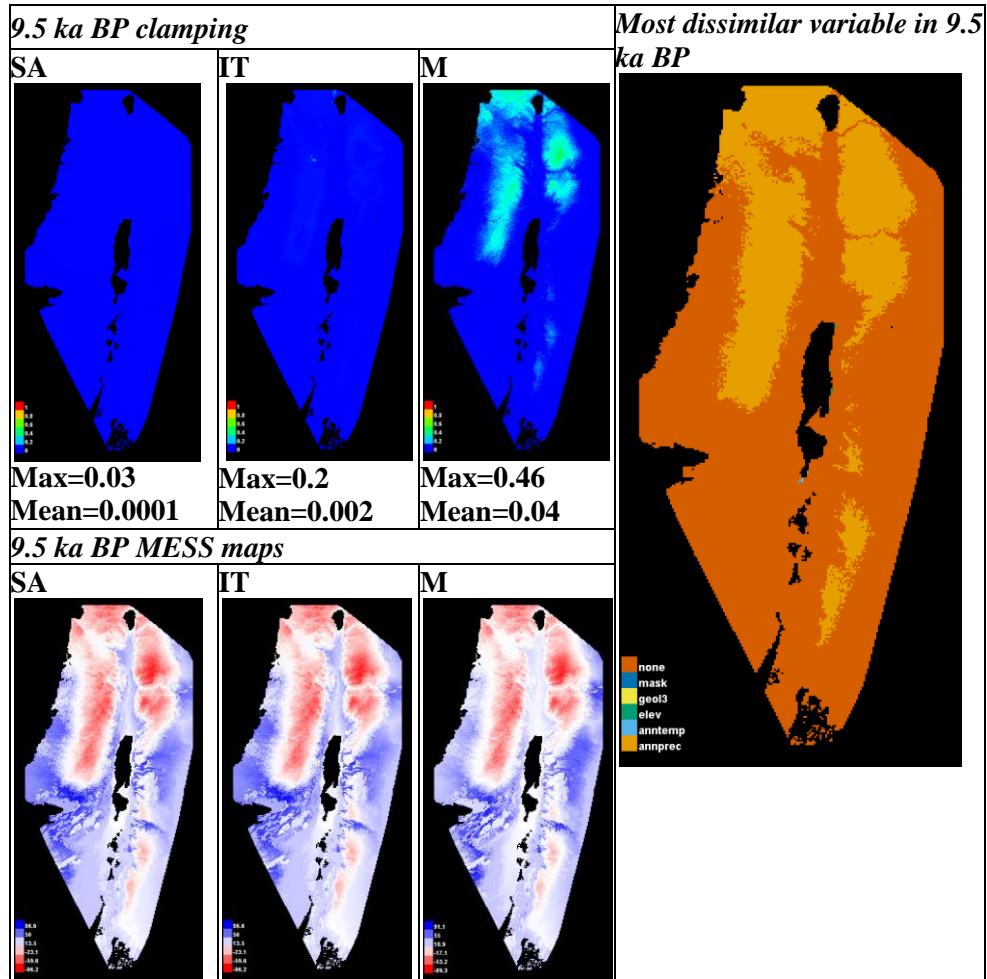


Figure 6.18. Clamping and MESS maps for 9.5 ka BP, taken from Maxent.

The following figure (Figure 6.19) shows the area occupied by the different vegetation subcategories in 9.5 ka BP, after the threshold that maximizes the sum of sensitivity plus specificity was applied. These categories were combined to produce the following detailed vegetation map for 9.5 ka BP (Map 6.6).

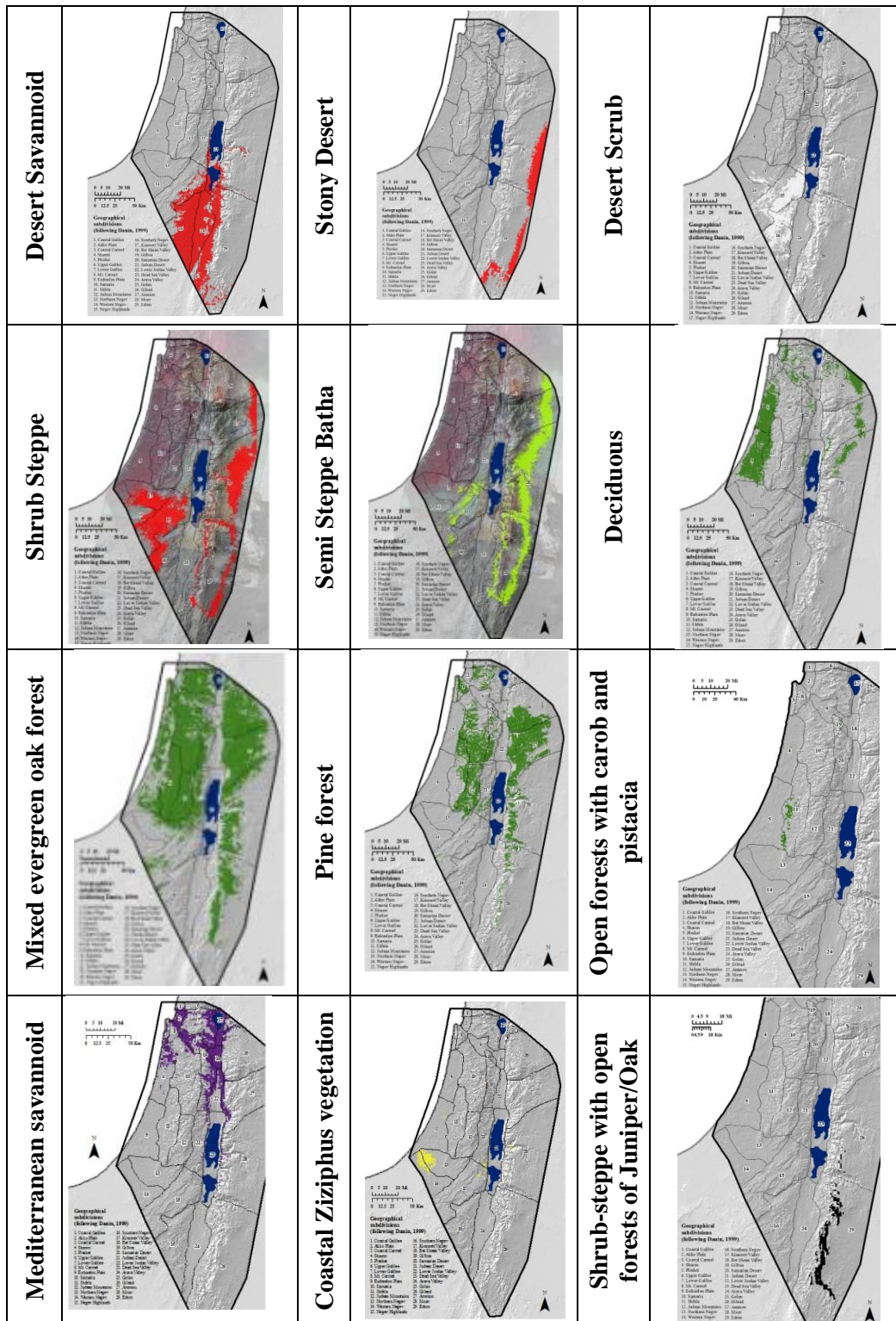
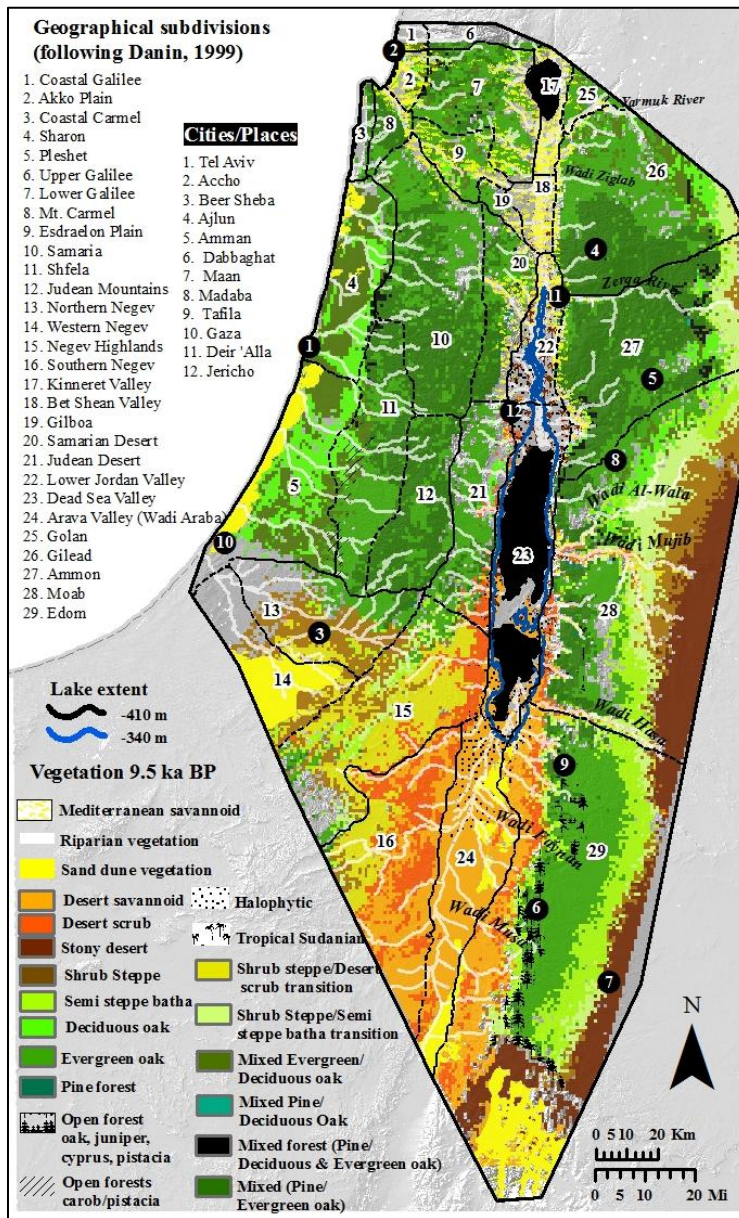


Figure 6.19. Suitable area in 9.5 ka BP per vegetation subcategory.



Map 6.6 Detailed vegetation map for 9.5 ka BP.

The 9.5 ka BP detailed vegetation map shows that areas formerly occupied by the mesic categories have contracted once again. The grasslands surrounding the Dead Sea and the Jordan River have slightly shrunk in width and latitude. However, a more obvious contraction is that experienced by all the forest categories that, until now, have been widespread throughout the region. All along the eastern boundary of the study area, the steppe categories and the stony desert vegetation have moved into formerly forested

areas. Throughout the coastal plains, conditions remain suitable for both oak categories, although its southernmost extent has shifted north about 10 km. On the other hand, the open forests of carob and pistacia which had been virtually absent throughout earlier periods, are now present on the foothills of the Judean mountains.

At the same time, the more xeric categories have expanded. Besides the stony desert vegetation and steppe categories which now form clearly defined strips along the eastern edge of the study area, shrub steppe and desert scrub have moved into the Negev Highlands, nearly replacing the evergreen oak maquis that was formerly present in this area. Also, desert savannoid, shrub steppe, and desert scrub vegetation is seen penetrating into Wadi Mujib and Wadi Hasa for the first time.

6.1.7 Model output for 9 ka BP

The results for the modeled plant geographic associations for 9 ka BP are given in Figure 6.20. The column on the left shows the area suitable for each of the main categories. These areas were combined to produce a 9 ka BP map of plant geographic associations (shown on the right).

This map suggests that conditions in 9 ka BP remain like those seen in 9.5 ka BP, with none of the categories undergoing significant changes. The Mediterranean association occupies most of the highland and coastal areas, whereas the Saharo Arabian association is found in the low lying areas of the Arava Valley, in parts of the Negev, and climbing up onto the plateau through the deep wadi valleys. It is also found along the eastern fringe of the study area. In between these two categories is the Irano Turanian association.

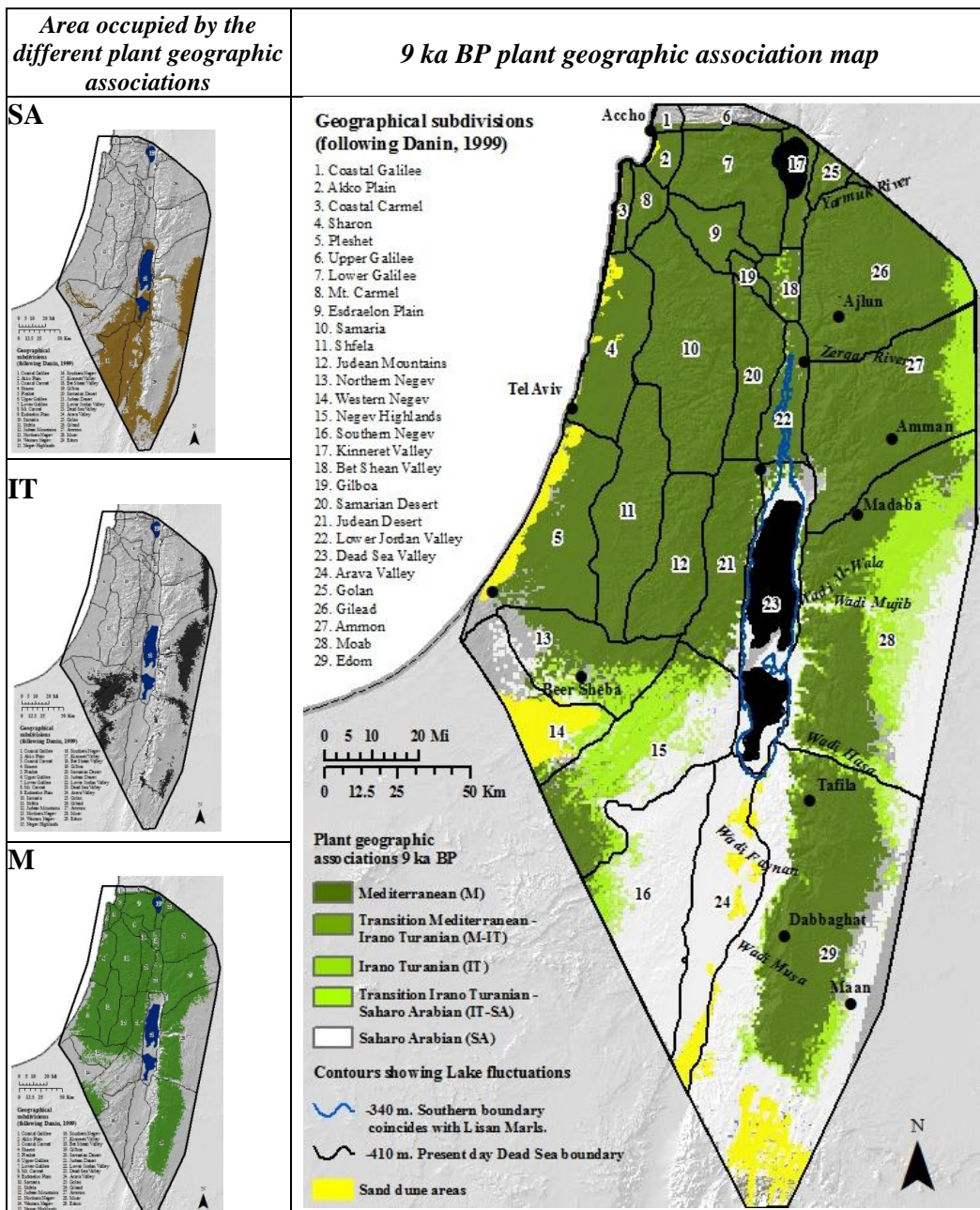


Figure 6.20. Vegetation model for 9 ka BP, by plant geographical association.

Figure 6.21 shows how the environmental conditions in 9 ka BP differed to those of the present. The first row shows where clamping has occurred. The second row shows the MESS maps. Increasing negative values show where extrapolation was greatest (darker shades of red). The figure on the right shows which variables were outside their

training region in 9 ka BP (most dissimilar than those of the present), and responsible for extreme values seen in the MESS maps.

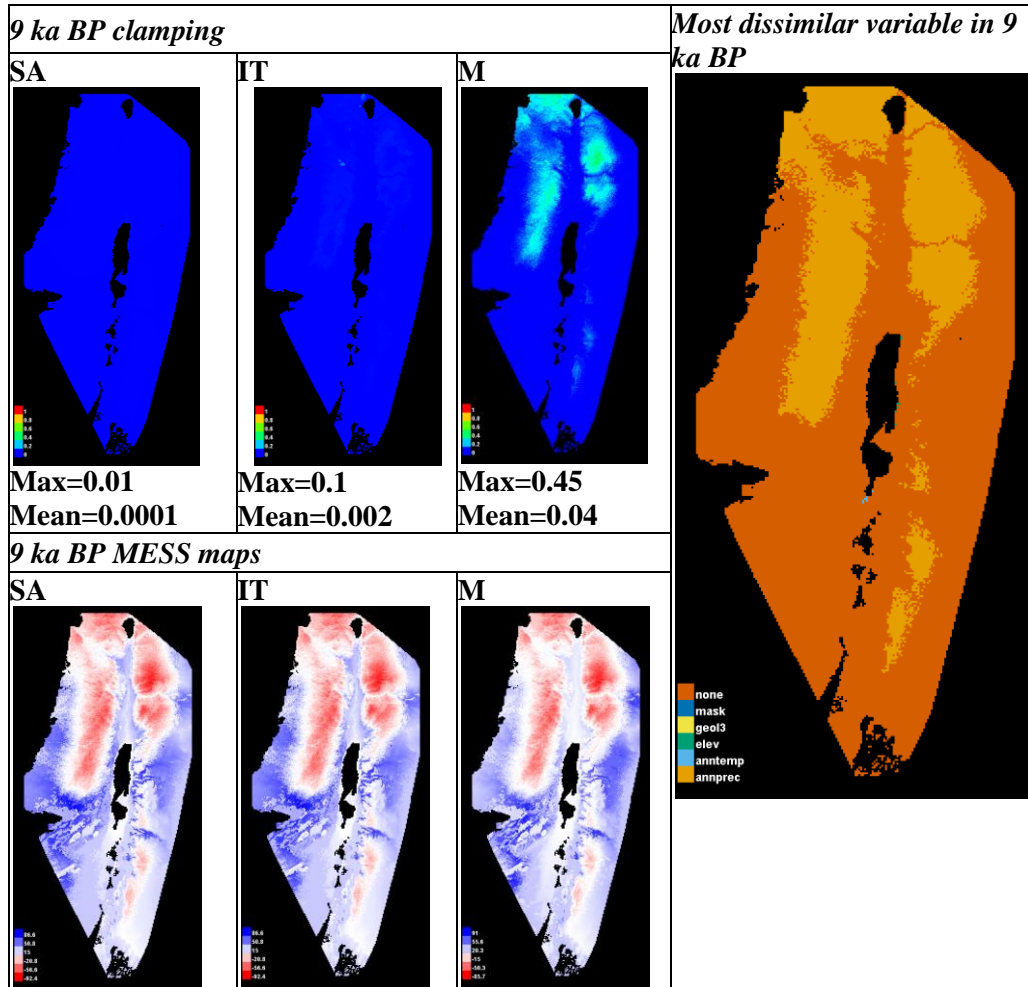


Figure 6.21. Clamping and MESS maps for 9 ka BP, taken from Maxent.

These plots show that the climatic conditions in 9 ka BP are very similar to those of 9.5 ka BP. Clamping values are much lower than in the earlier periods, although the mountains east and west of the Bet Shean and Lower Jordan Valleys continue to have high clamping values. This essentially impacts the Mediterranean and forest categories, where the highest values in the clamping surfaces are found.

The following figure (Figure 6.22) shows the area occupied by the different vegetation subcategories in 9 ka BP, after the threshold that maximizes the sum of sensitivity plus specificity was applied.

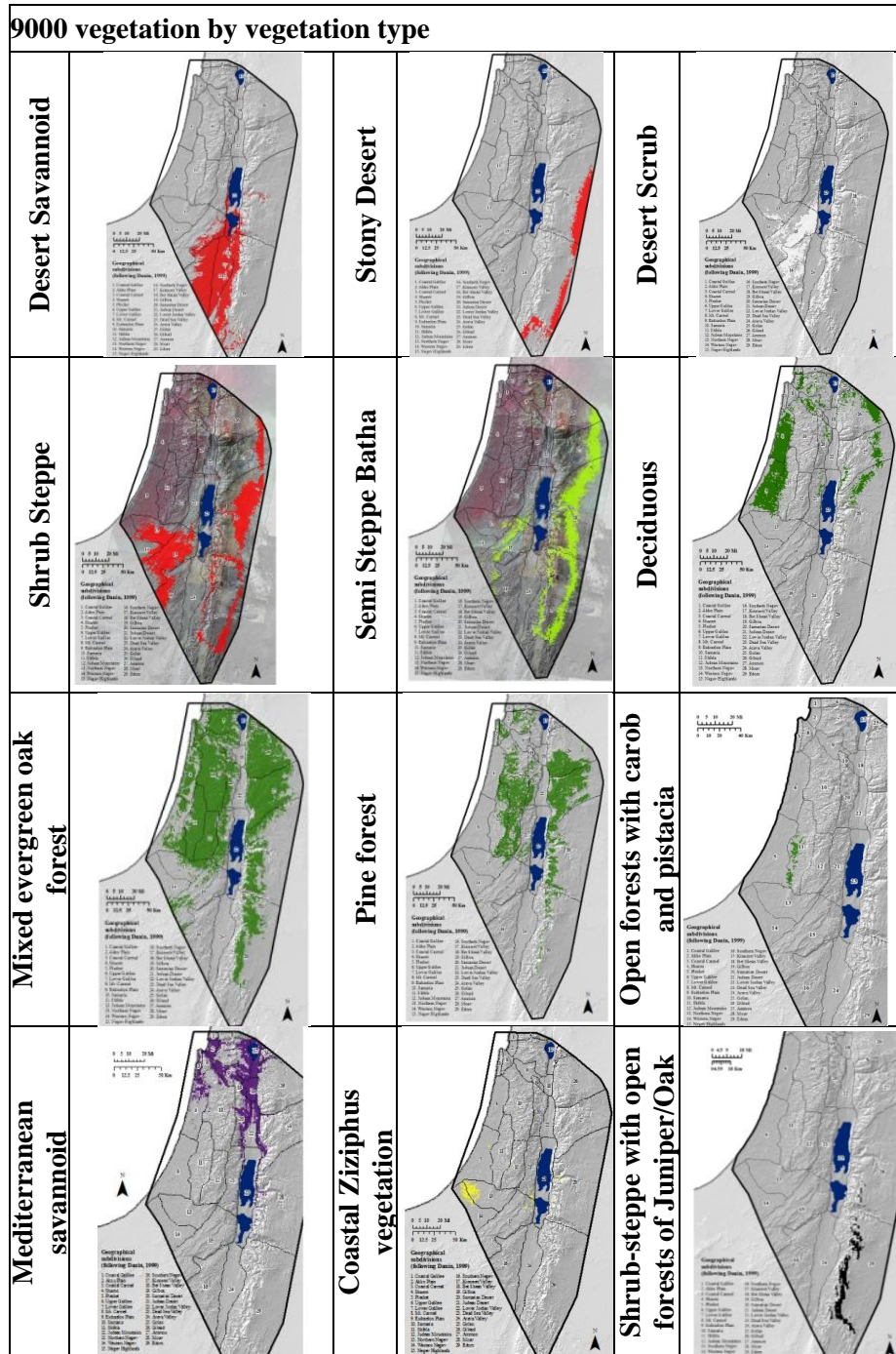
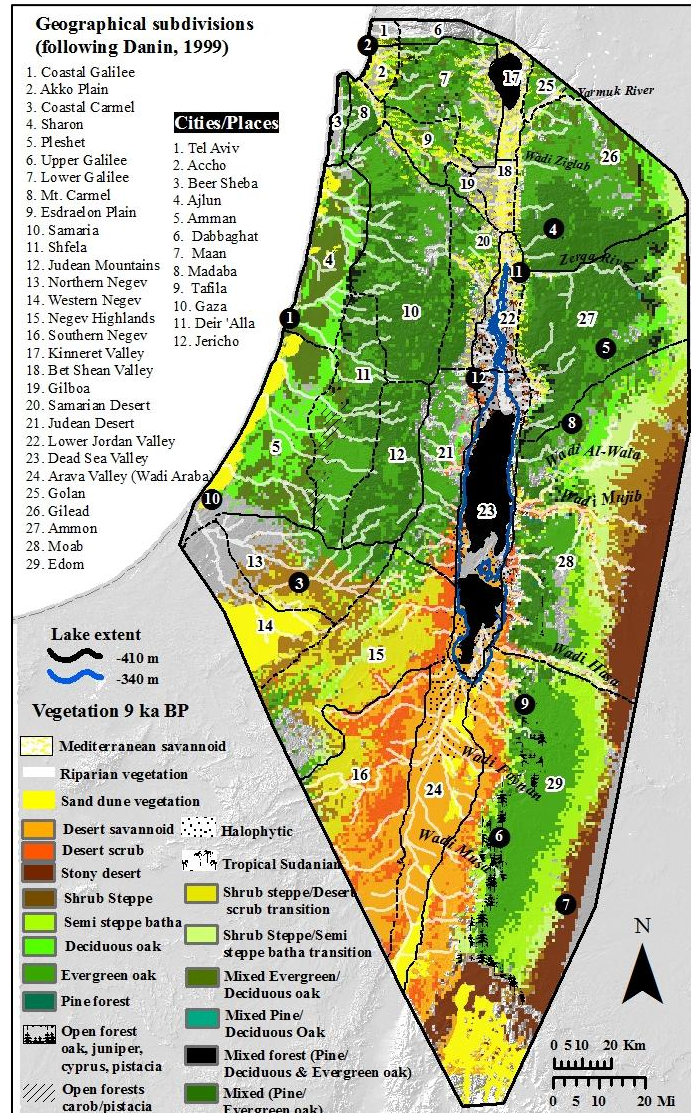


Figure 6.22. Suitable area in 9 ka BP per vegetation subcategory.

These categories were combined along with the outputs from the sand dune, halophytic, and tropical Sudian vegetation to produce the following detailed vegetation map (Map 6.6).



Map 6.6 Detailed vegetation map for 9 ka BP.

Both model outputs for 9 ka BP suggest that the vegetation during this time period was almost identical to 9.5 ka BP. None of the modeled categories experienced contractions or expansions of the same magnitude as those seen in earlier periods. Forests continue to occupy large parts of the mountainous areas east and west of the Rift Valley.

Beyond the sand dune belt, the coastal plains south of Mt. Carmel are populated by both *Quercus ithaburensis* and *Q. calliprinos*. The foothills of the Judean Mountains in Shfela are occupied by the open forests of carob and pistacia. The Carmel and Lower Galilee regions are populated by both oaks as well as *Pinus halepensis*. Lake Kinneret is surrounded by the grasslands of the Mediterranean Savannoid category. These penetrate into river and wadi basins that drain into the Jordan River in the Bet Shean Valley.

The forested areas in Gilead and Ammon are mainly represented by *Quercus calliprinos*. Around the Zerqa River, *Pinus halepensis* is also found whereas *Quercus ithaburensis* is present in the north. There is still an almost continuous belt of evergreen oak forests on the plateau which is only interrupted by the drier categories along some of the wadi valleys that intersect the highlands (*e.g.*, Wadi Mujib and Wadi Hasa). These forest areas are surrounded in the east by categories more suitable to drier conditions. Moving east from the forests, these are semi steppe batha, shrub steppe/semi steppe batha transition areas, shrub steppe, and stony desert vegetation.

6.1.8 Model output for 8.5 ka BP

The results for the modeled plant geographic associations for 8.5 ka BP are given in Figure 6.23. The column on the left shows the area suitable for each of the main categories. These areas were combined to produce an 8.5 ka BP map of plant geographic associations (shown on the right).

Two contrasting things seem to happen to the Mediterranean association from the previous period. The area it occupied in 9 ka BP contracts longitudinally (both in the coast and on the plateau) but expands southward about 5 km (this does not happen with the more detailed models). In the coast, the contracted area is not replaced by any other category (all of the categories had values that were below their respective thresholds). In

the plateau, however, it is replaced by the Irano Turanian association as well as an expanding Irano Turanian-Saharo Arabian transition zone.

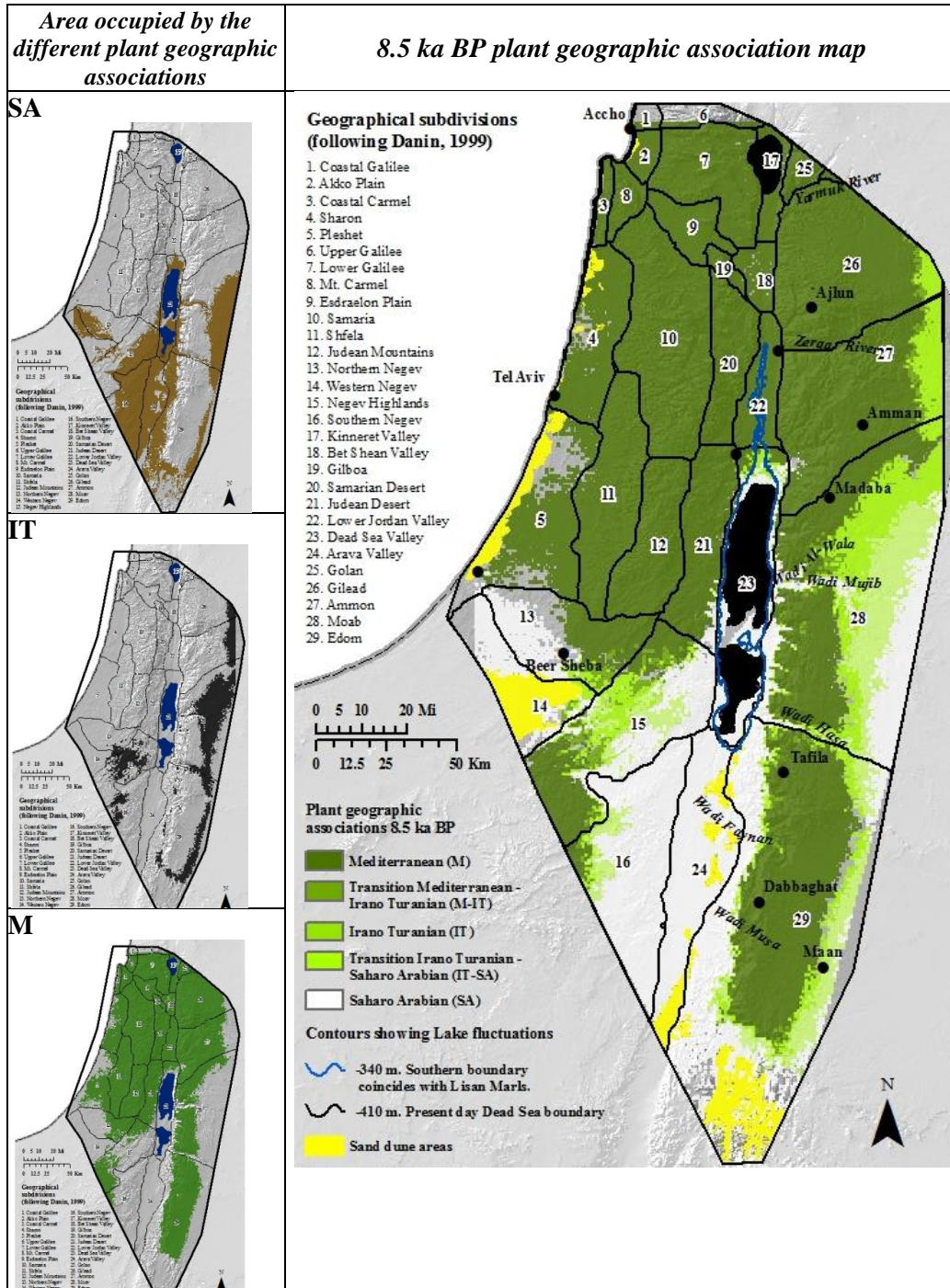


Figure 6.23. Vegetation model for 8.5 ka BP, by plant geographic association.

Figure 6.24 shows how the environmental conditions in 8.5 ka BP differed to those of the present. The first row shows where clamping has occurred. The second row shows the MESS maps. Increasing negative values show where extrapolation was greatest (darker shades of red). The figure on the right shows which variables were outside their training region in 8.5 ka BP (most dissimilar than those of the present), and responsible for extreme values seen in the MESS maps.

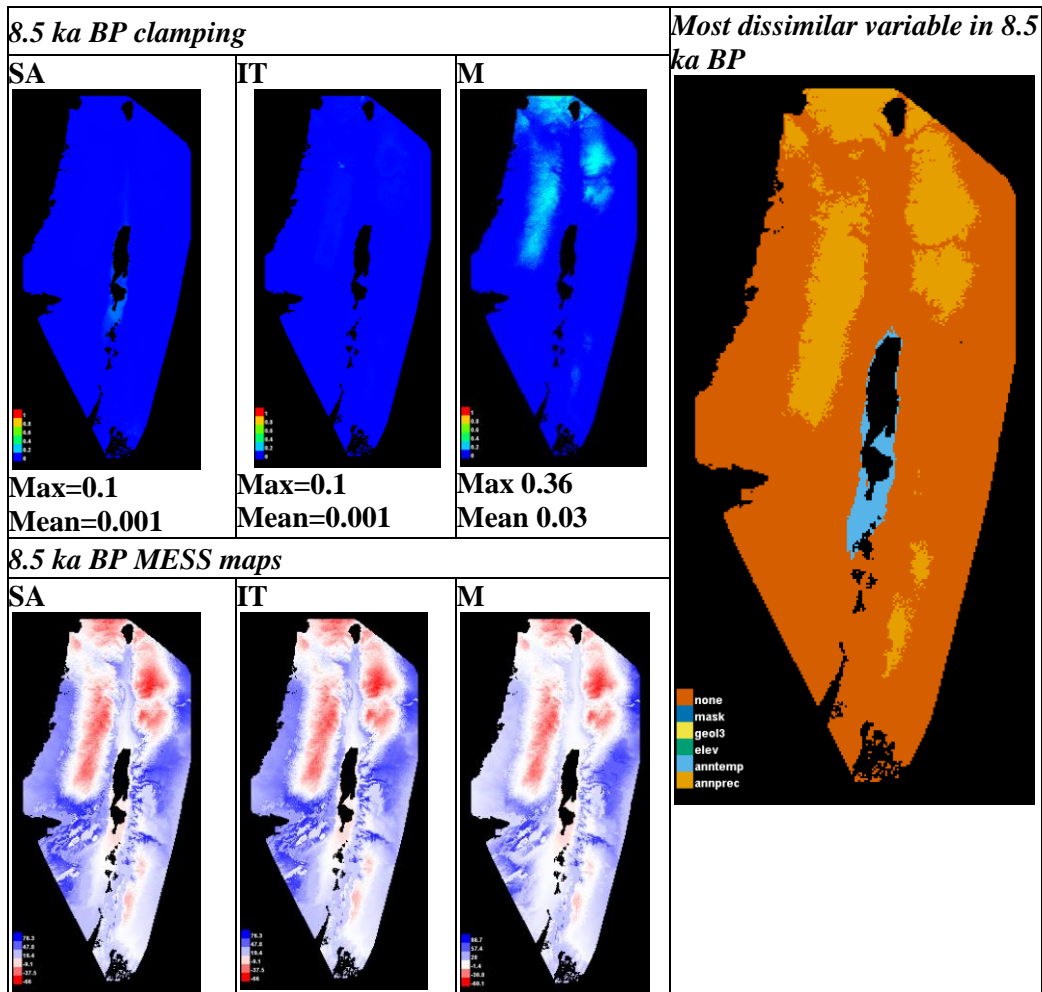


Figure 6.24. Clamping and MESS maps for 8.5 ka BP, taken from Maxent.

The clamping surface for the Mediterranean category indicates that although clamping values are lower than in 9 ka BP, precipitation in 8.5 ka BP continues to be more than at present. The MESS maps also show that hardly any extrapolation of

precipitation values occurs south of the Dead Sea (as had happened in previous years). At the same time, average annual temperature around the Dead Sea was slightly warmer than at present. In fact, figure 6.1 shows that average annual temperature in all of the climate stations throughout the study area was about 1°C warmer than at present.

The following figure (Figure 6.25) shows the area occupied by the different vegetation subcategories in 8.5 ka BP, after the threshold that maximizes the sum of sensitivity plus specificity was applied. These categories were combined to produce a detailed vegetation map for 8.5 ka BP (Map 6.7).

The most obvious change that has occurred from 9 ka BP is a significant contraction of the Mediterranean savannoid vegetation. For the first time since 12 ka BP, it is absent in the Bet Shean and Lower Jordan Valleys. It is also missing in the Esdraelon Plain, which formerly connected areas occupied by these grasslands in the Rift Valley and the Akko Plain. A few changes are also obvious amongst the forest categories. The deciduous oak forest, formerly abundant in Pleshet, is now only found in a few small patches accompanied by *Quercus calliprinos*. However, slightly further north in the Sharon plain, deciduous oak forests remain abundant. In the Judean Desert, the evergreen oak category is now fragmented. On the opposite side, the open forests of carob and pistacia now occupy a smaller area. The large forested strip found on the highlands east of the Rift Valley is now met by a wider belt of semi steppe batha vegetation along its eastern edge. Meanwhile in the Negev Highlands and the Southern Negev, the more drought tolerant categories have expanded.

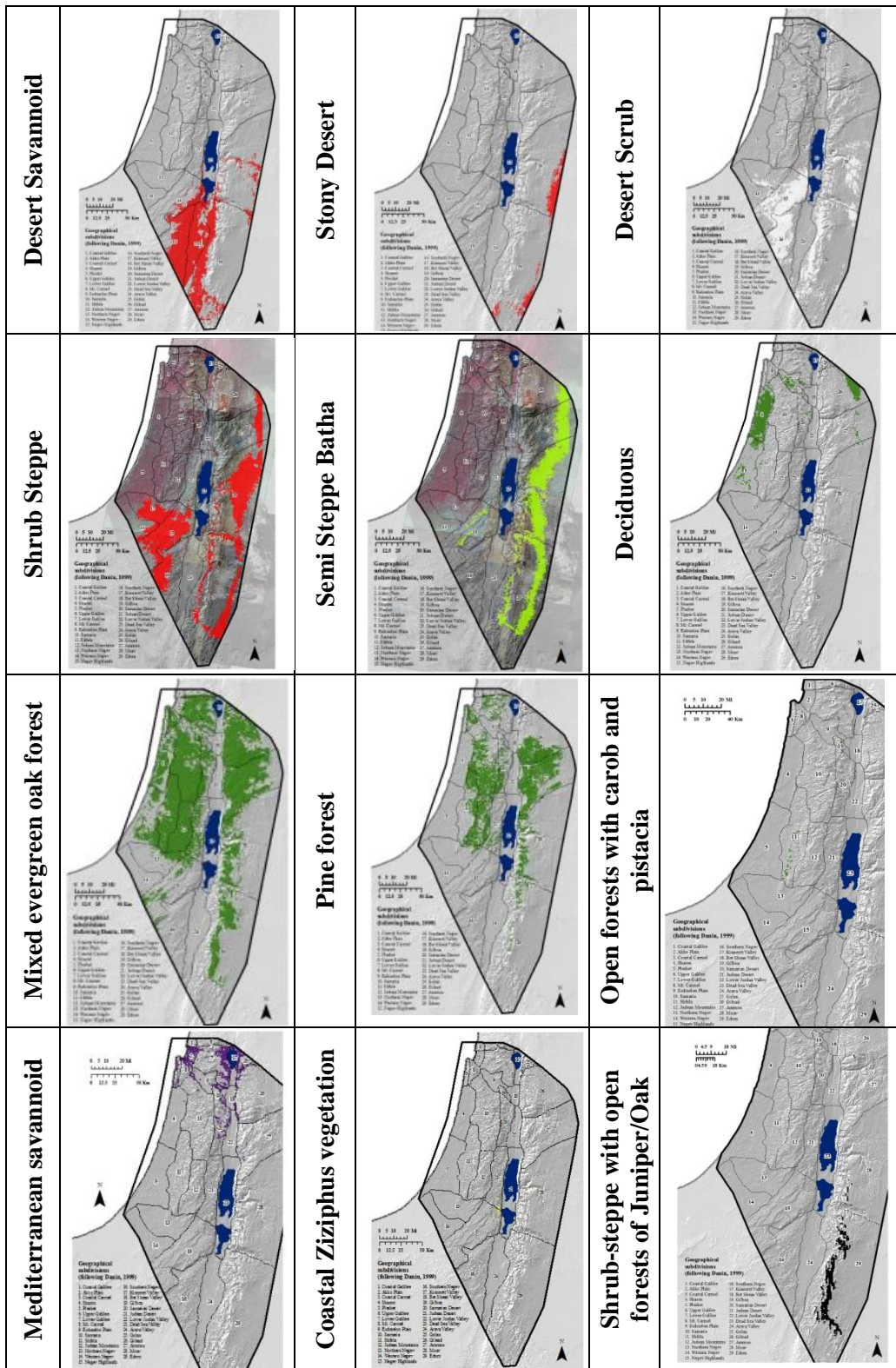
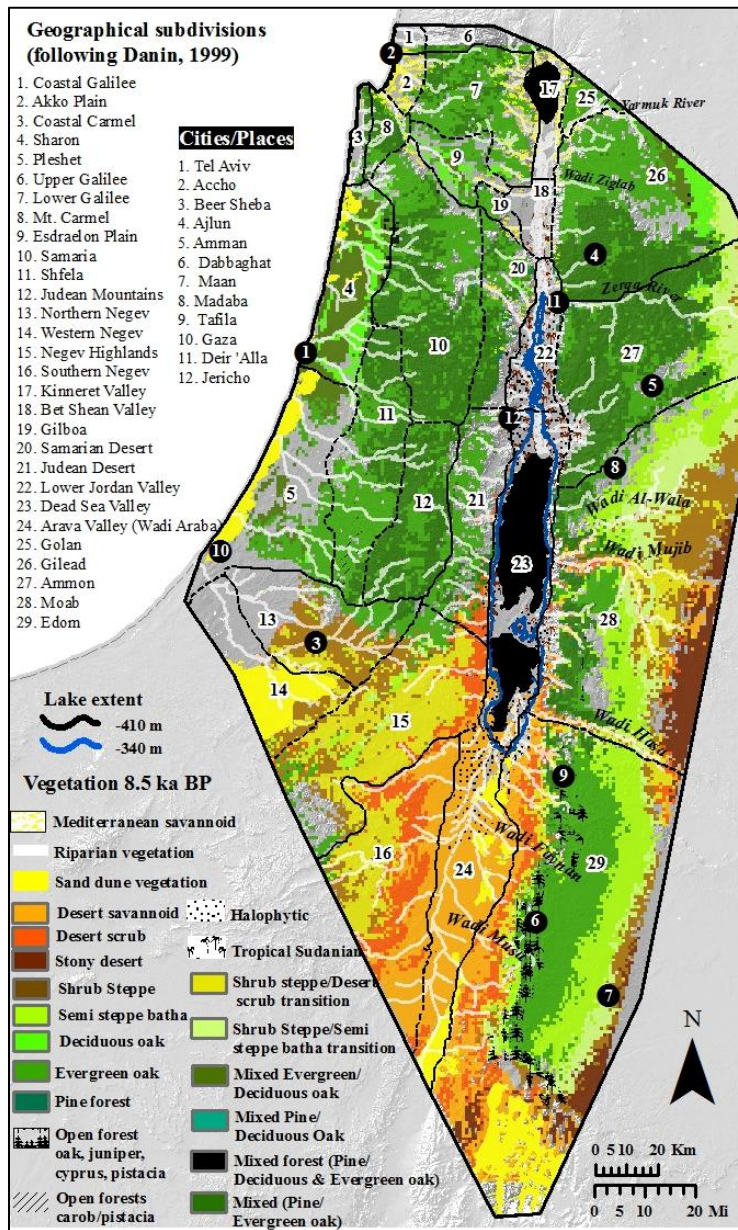


Figure 6.25. Suitability according to vegetation type for 8.5 ka BP.



Map 6.7 Detailed vegetation map for 8.5 ka BP.

6.1.9 Model output for 8 ka BP

The results for the modeled plant geographic associations for 8 ka BP are given in Figure 6.26. The column on the left shows the area suitable for each of the main categories. These areas were combined to produce an 8 ka BP map of plant geographic associations (shown on the right).

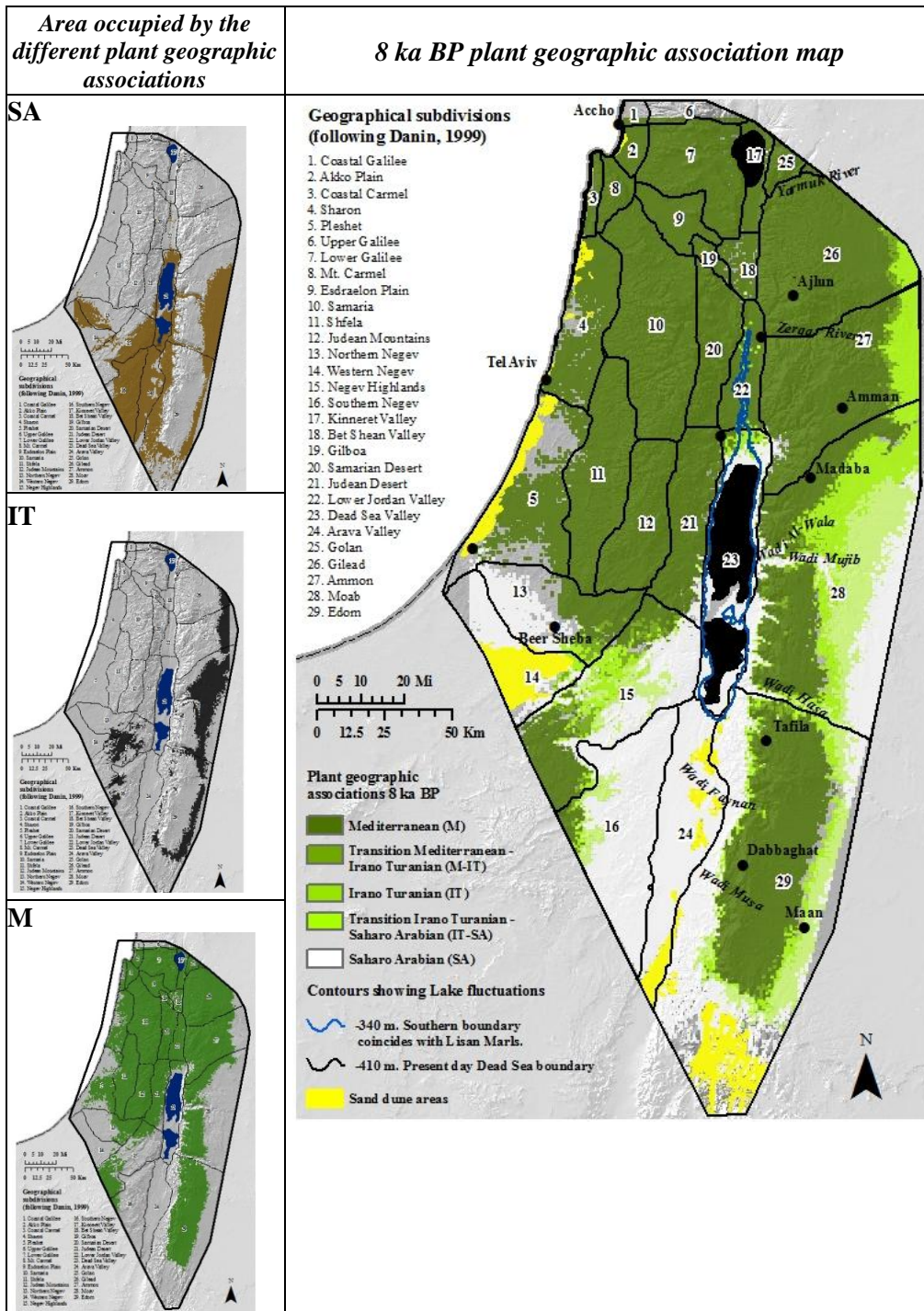


Figure 6.26. Vegetation model for 8 ka BP, by plant geographic association.

The most obvious change from 8.5 ka BP is the continued contraction of the Mediterranean association and slight expansion of the Irano Turanian association.

Nevertheless, the Mediterranean category continues to occupy most of the area, including the Negev Highlands.

Figure 6.27 shows how the environmental conditions in 8 ka BP differed to those of the present. The first row shows where clamping has occurred. The second row shows the MESS maps. Increasing negative values show where extrapolation was greatest (darker shades of red). The figure on the right shows which variables were outside their training region in 8 ka BP (most dissimilar than those of the present), and responsible for extreme values seen in the MESS maps.

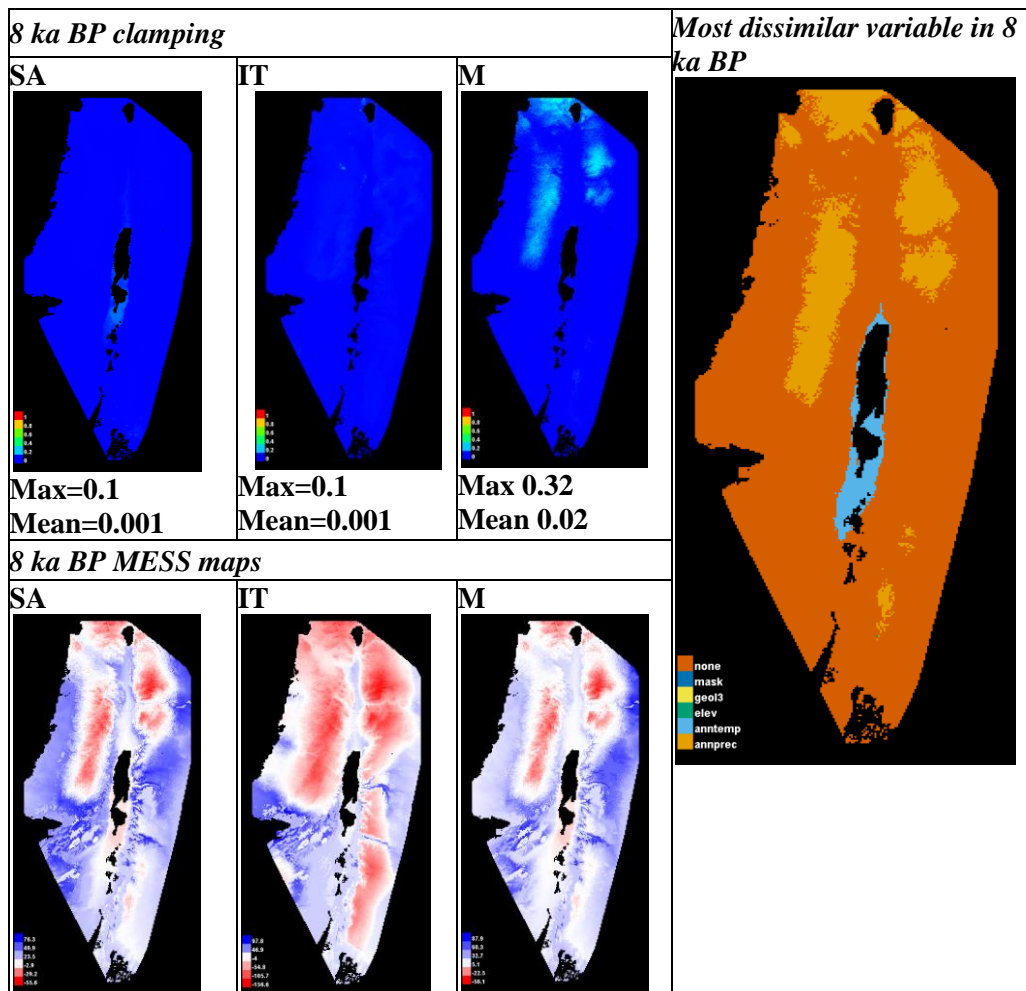


Figure 6.27. Clamping and MESS maps for 8 ka BP, taken from Maxent.

Figure 6.27 shows that the average yearly precipitation continues to decline from previous time periods, although it still remains higher than present day values in the mountains opposite the rift valley north of the Dead Sea. As a result, there continue to be some cells in these areas with moderate clamping values, which are nonetheless lower than the earlier periods. Like in 8.5 ka BP, temperature around the Dead Sea is slightly higher than at present.

Figure 6.28 shows the area occupied by the different vegetation subcategories in 8 ka BP, after the threshold that maximizes the sum of sensitivity plus specificity was applied. These categories were combined to produce the following detailed vegetation map (Map 6.8).

According to the modeled outputs, the vegetation in 8 ka BP is not that different to 8.5 ka BP. The categories representing the various forested areas have not changed. Nevertheless, one of the main differences is seen along the eastern edge of the forests located throughout the plateau region. The area they occupy is becoming thinner, especially in the south, as steppe vegetation continues to encroach upon them. A novel distribution pattern (from 12 ka BP) seen in this period regards the open forests of carob and pistacia, which appear in isolated cells around the Samaria mountains in Gilboa and near Mt. Carmel.

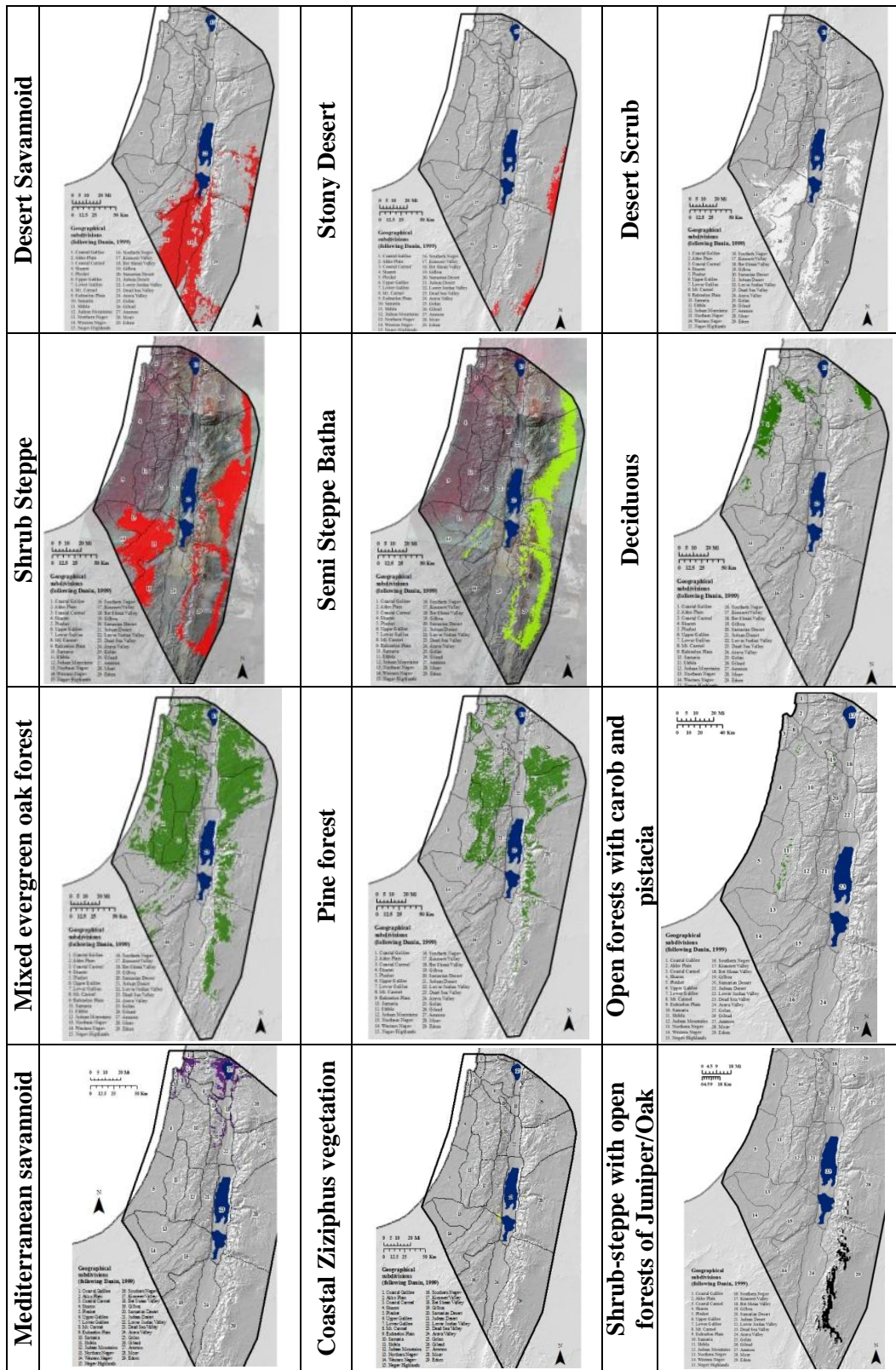
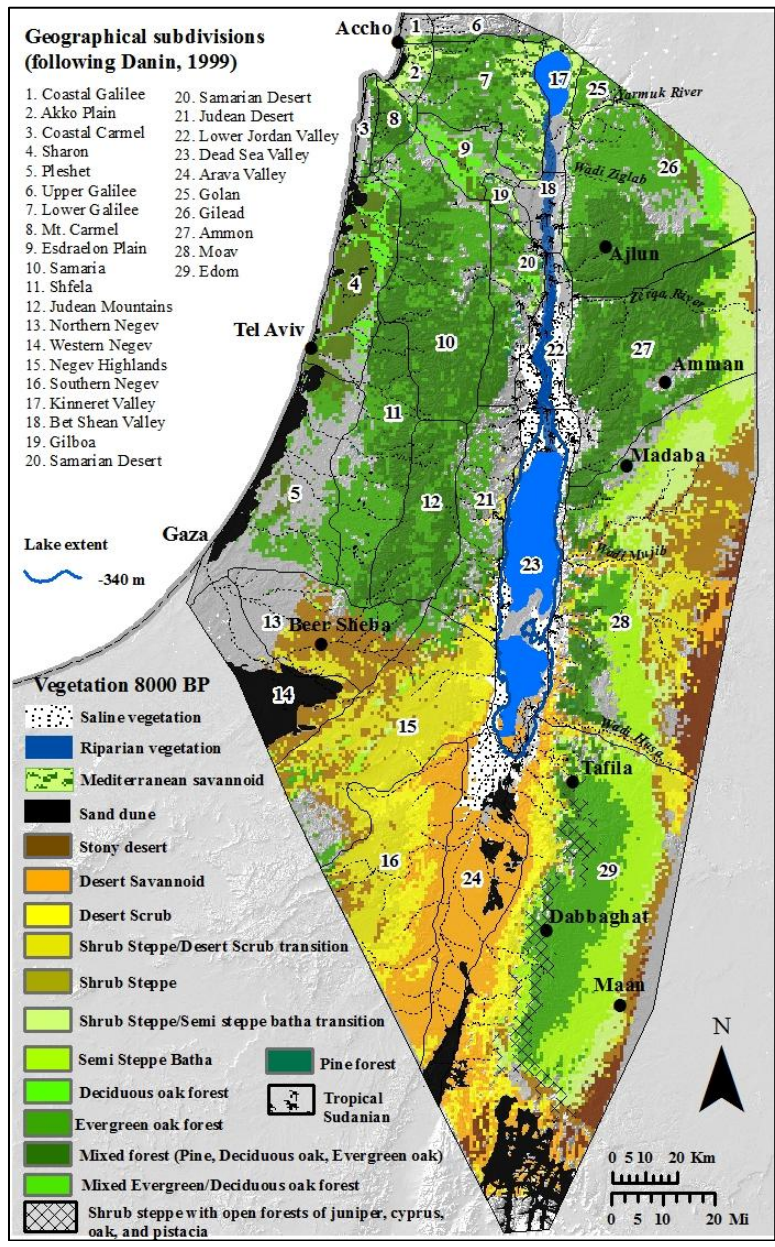


Figure 6.28. Suitable area in 8 ka BP per vegetation subcategory.



6.1.10 Model output for 7.5 ka BP

The results for the modeled plant geographic associations for 7.5 ka BP are given in Figure 6.29. The column on the left shows the area suitable for each of the main categories. These areas were combined to produce a 7.5 ka BP map of plant geographic associations (shown on the right).

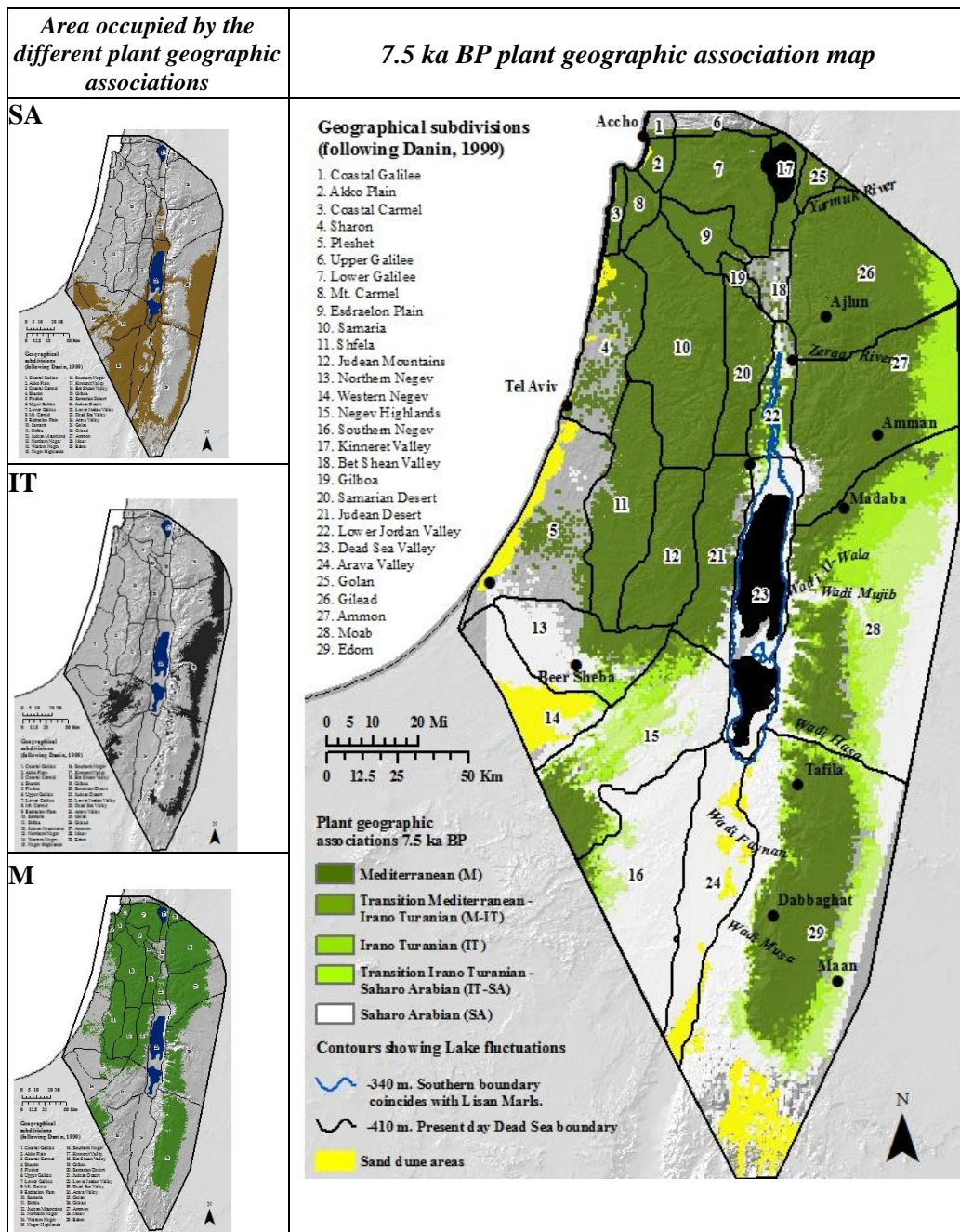


Figure 6.29. Vegetation model for 7.5 ka BP, by plant geographic association.

An obvious contraction of the Mediterranean association has once again occurred along both sides of the rift valley, as it is replaced by the Irano Turanian association. Just north of the Dead Sea in the Dead Sea Valley, the area occupied by the Saharo Arabian association has also expanded, reaching the Lower Jordan Valley for the first time.

The following figure (Figure 6.30) shows how the environmental conditions in 7.5 ka BP differed to those of the present. The first row shows where clamping has occurred. The second row shows the MESS maps. Increasing negative values show where extrapolation was greatest (darker shades of red). The figure on the right shows which variables were outside their training region in 7.5 ka BP (most dissimilar than those of the present), and responsible for extreme values seen in the MESS maps.

Clamping values that result from higher rainfall and impact the Mediterranean association along the mountainous areas continue to drop. Moderate clamping values are found around Lake Kinneret and along the mountains east and west of the Bet Shean and Lower Jordan Valley.

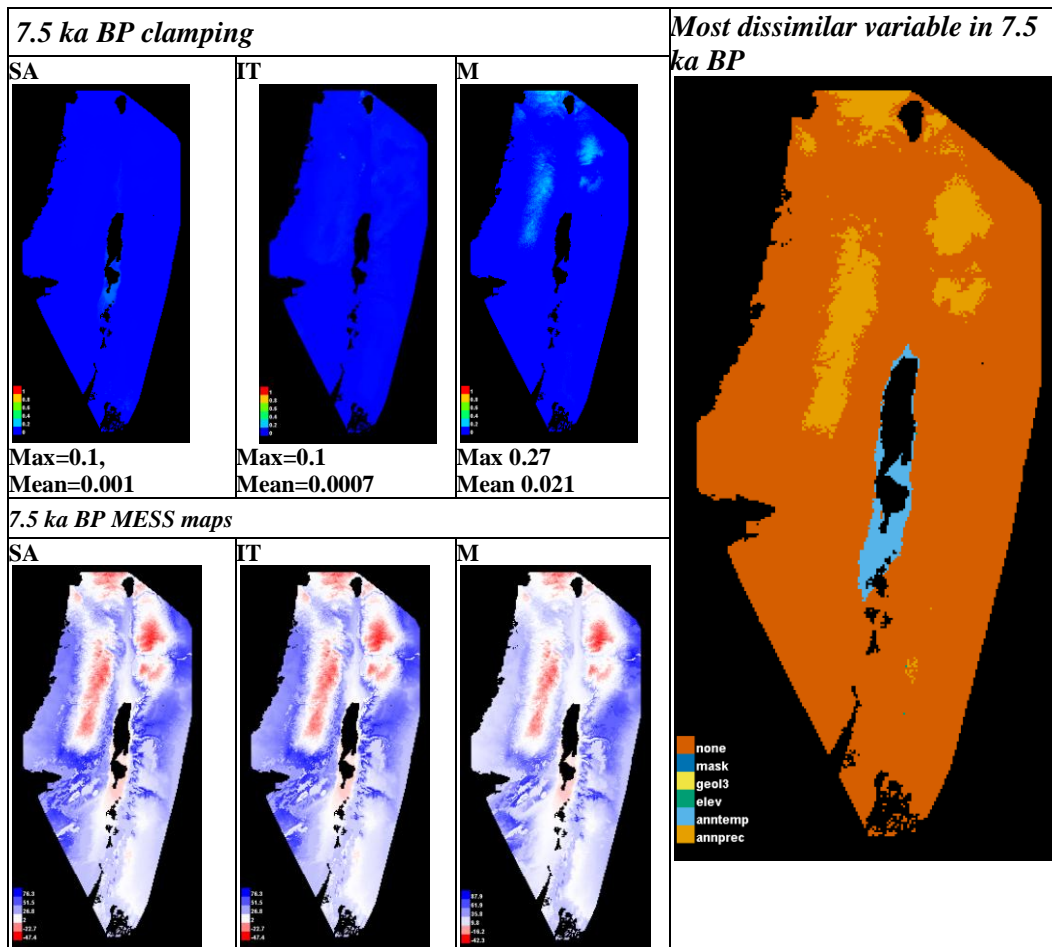


Figure 6.30. Clamping and MESS maps for 7.5 ka BP, taken from Maxent.

Figure 6.31 shows the area occupied by the different vegetation types in 7.5 ka BP. These categories were combined along to produce the following vegetation map (Map 6.9).

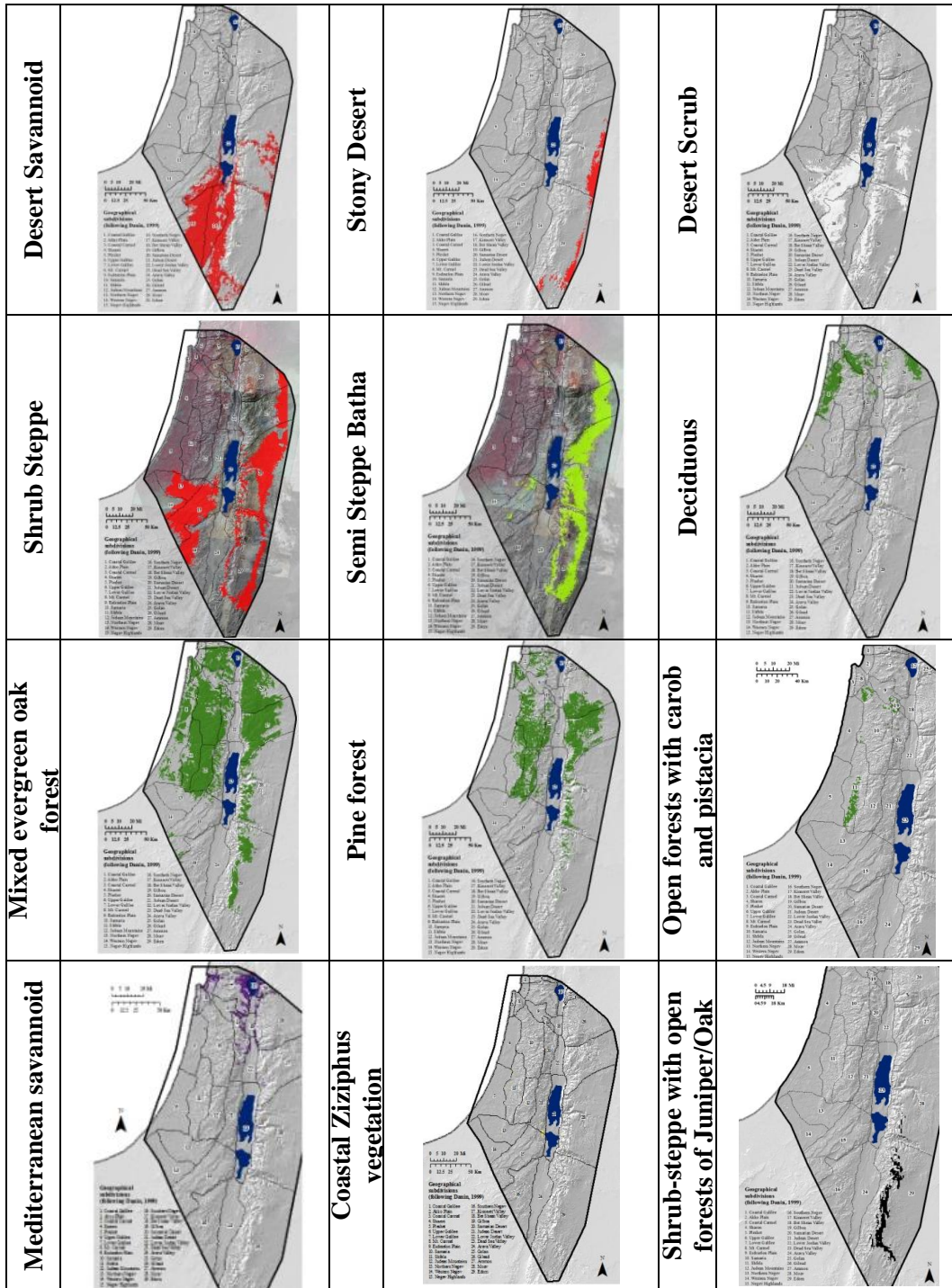
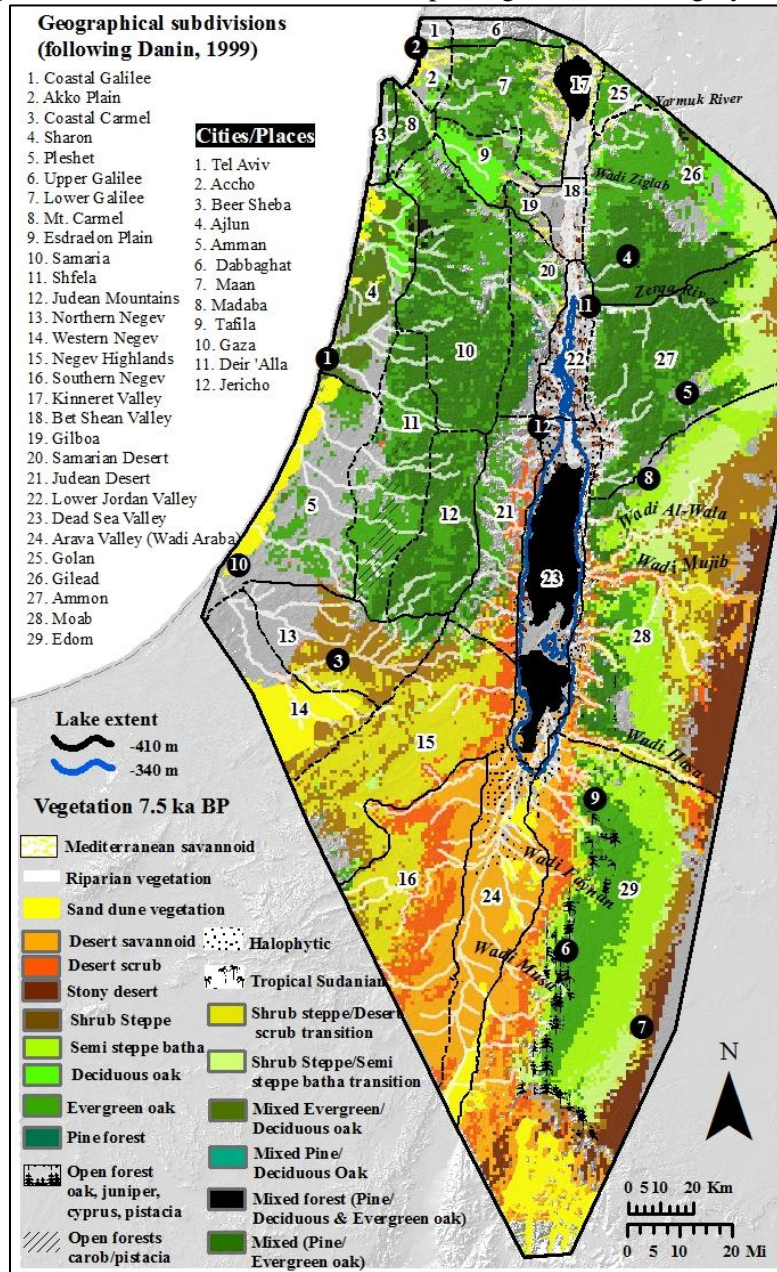


Figure 6.31. Suitable area in 7.5 ka BP per vegetation subcategory.



Map 6.9 Detailed vegetation map for 7.5 ka BP.

Like the map by plant geographic associations suggests, the more detailed vegetation map indicates that conditions suitable for forests were narrowing. The large areas occupied by forest patches on both sides of the rift valley have contracted yet again. West of the rift valley, the southernmost extent of the mixed evergreen oak forests

has retreated towards the Judean mountains about 5 kilometers. In addition, there are no longer patches of this type of forest in the Northern Negev and hardly any in the Negev Highlands.

On the plateau, forest areas are also becoming more fragmented and thinner in width. This is caused by an expansion of the more xeric categories on both sides. From the lower elevations of the Rift Valley, the desert savannoid, desert scrub, and shrub steppe vegetation are expanding. At the same time, the stony desert and steppe vegetation is expanding in the plateau. In the Ammon subdivision, the eastern fringe of the study area is entirely populated by the drier shrub steppe vegetation. Unlike the other forest categories, the open forests of carob and pistacia significantly expanded from the previous period, and now cover a wider area near Mt. Carmel and Gilboa. In the Esdraelon Plain in the north, a change in the constitution of the forest categories is seen. Whereas it had formerly been occupied by both oaks, it is now only represented by *Quercus ithaburensis*.

6.1.11 Model output for 7 ka BP

The results for the modeled plant geographic associations for 7 ka BP are given in Figure 6.32. The column on the left shows the area suitable for each of the main categories. These areas were combined to produce a 7 ka BP map of plant geographic associations (shown on the right).

Whilst the area suitable to the Saharo Arabian association has not changed (from 7.5 ka BP), the Mediterranean plant geographic association has again undergone a slight contraction east of the rift valley, where it is replaced by the Irano Turanian category.

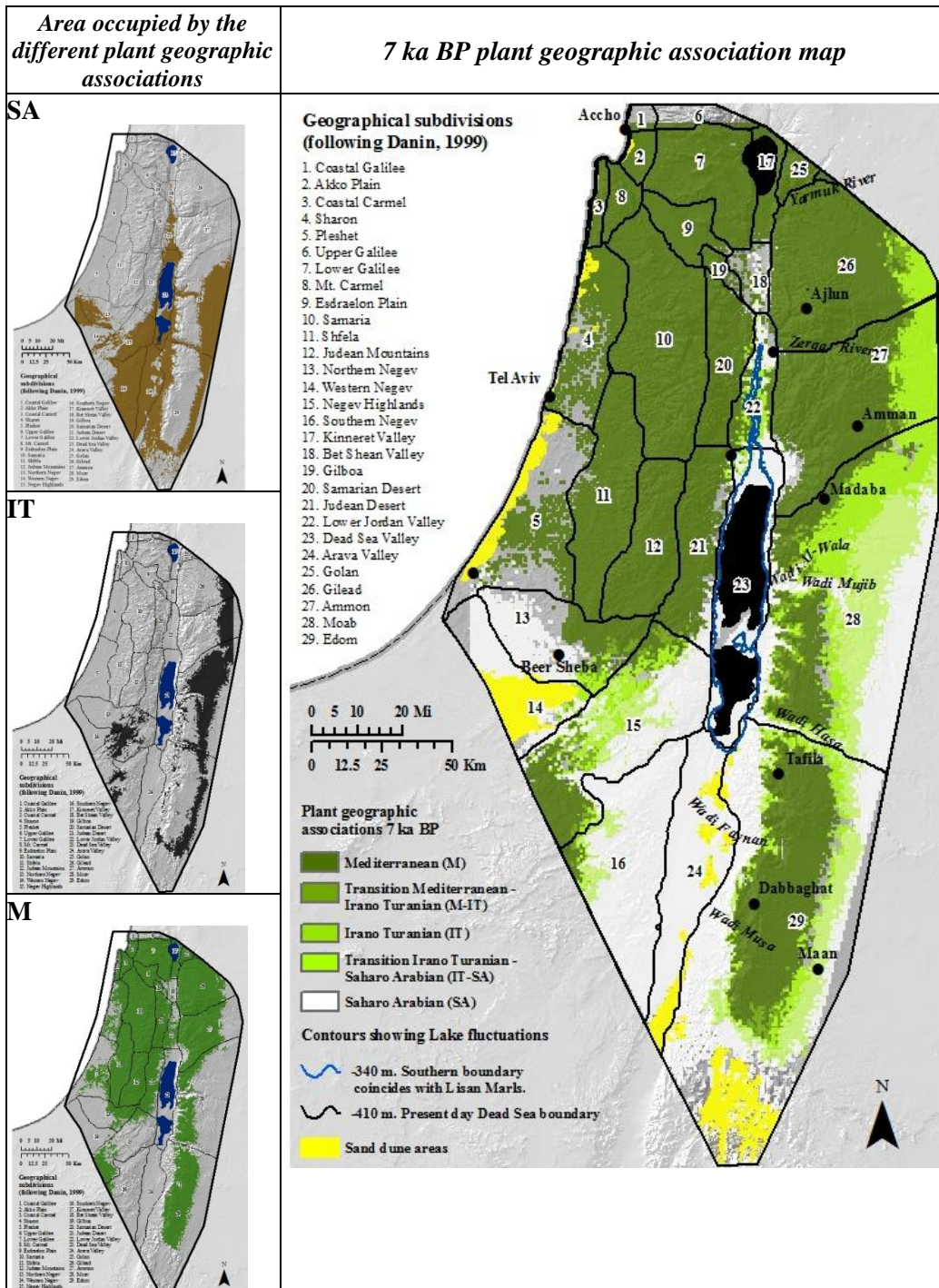


Figure 6.32. Vegetation model for 7 ka BP, by plant geographic association.

Figure 6.33 shows how the environmental conditions in 7 ka BP differed to those of the present. The first row shows where clamping has occurred. The second row shows

the MESS maps. Increasing negative values show where extrapolation was greatest (darker shades of red). The figure on the right shows which variables were outside their training region in 7 ka BP (most dissimilar than those of the present), and responsible for extreme values seen in the MESS maps.

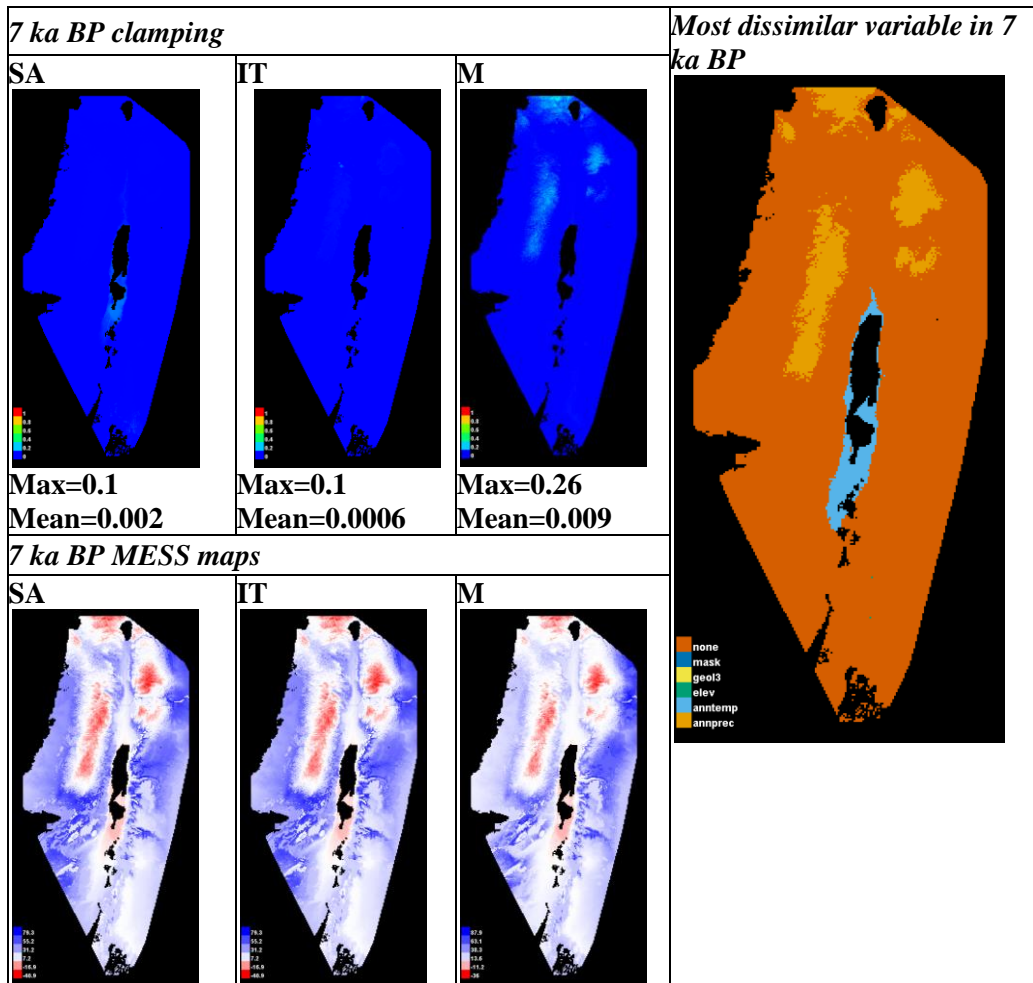


Figure 6.33. Clamping and MESS maps for 7 ka BP, taken from Maxent.

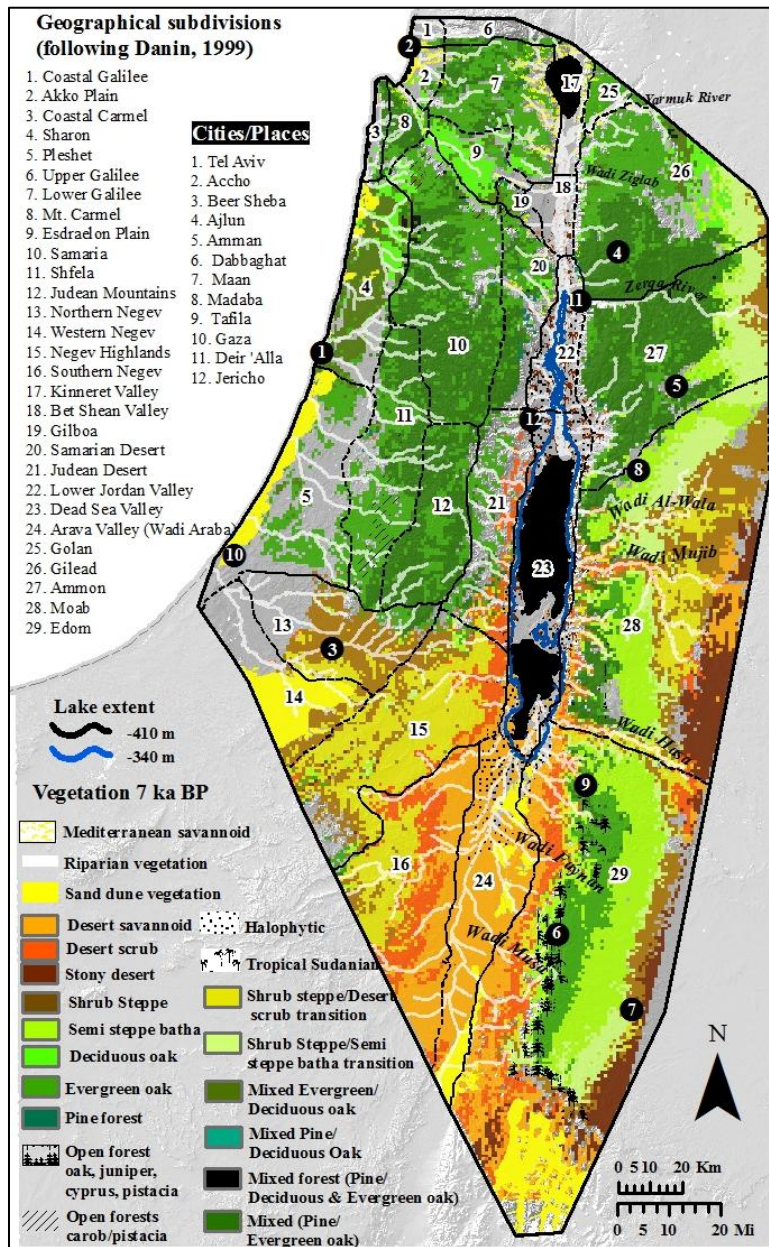
Clamping values continue to drop, as climatic conditions become less extreme when compared to the present. Still, precipitation levels remain higher than today's analogue, with areas along the hills opposite the Bet Shean and Lower Jordan Valley being the most affected. These plots also indicate that annual mean temperature surrounding the Dead Sea was slightly warmer than today's.

Figure 6.34 shows the area occupied by the different vegetation subcategories in 7 ka BP, after the threshold that maximizes the sum of sensitivity plus specificity was applied. These categories were combined to produce the following detailed vegetation map (Map 6.10).

Like the outputs produced by the plant geographic association models, this more detailed map shows that the forests east of the rift valley are becoming smaller in width (not in length) as they are replaced by semi steppe batha vegetation which continues to push in. West of the Rift Valley, however, the forests remain the same as they were in 7.5 ka BP. An exception is in the Judean Desert, where the patches of mixed evergreen oak forest become increasingly fragmented. Also, desert scrub appears along the lower elevations for the first time (since 12 ka BP) in this area. The composition of the forests does not seem to have changed from 7.5 ka BP.

One difference noticed from 7.5 ka BP is a slight reduction in the area occupied by the open forests of carob and pistacia. Nevertheless, these forests are still present in the three areas where they occur today (around the lower elevations of the mountains of Samaria, Gilboa, and Schfela).

Like the forest categories, the more drought tolerant vegetation categories have responded in different ways to the conditions of 7 ka BP. While the desert scrub and shrub steppe categories are expanding in the direction of the forests, the stony desert vegetation has slightly contracted.



6.1.12 Model output for 6.5 ka BP

The results for the modeled plant geographic associations for 6.5 ka BP are given in Figure 6.35. The column on the left shows the area suitable for each of the main categories. These areas were combined to produce a 6.5 ka BP map of plant geographic associations (shown on the right).

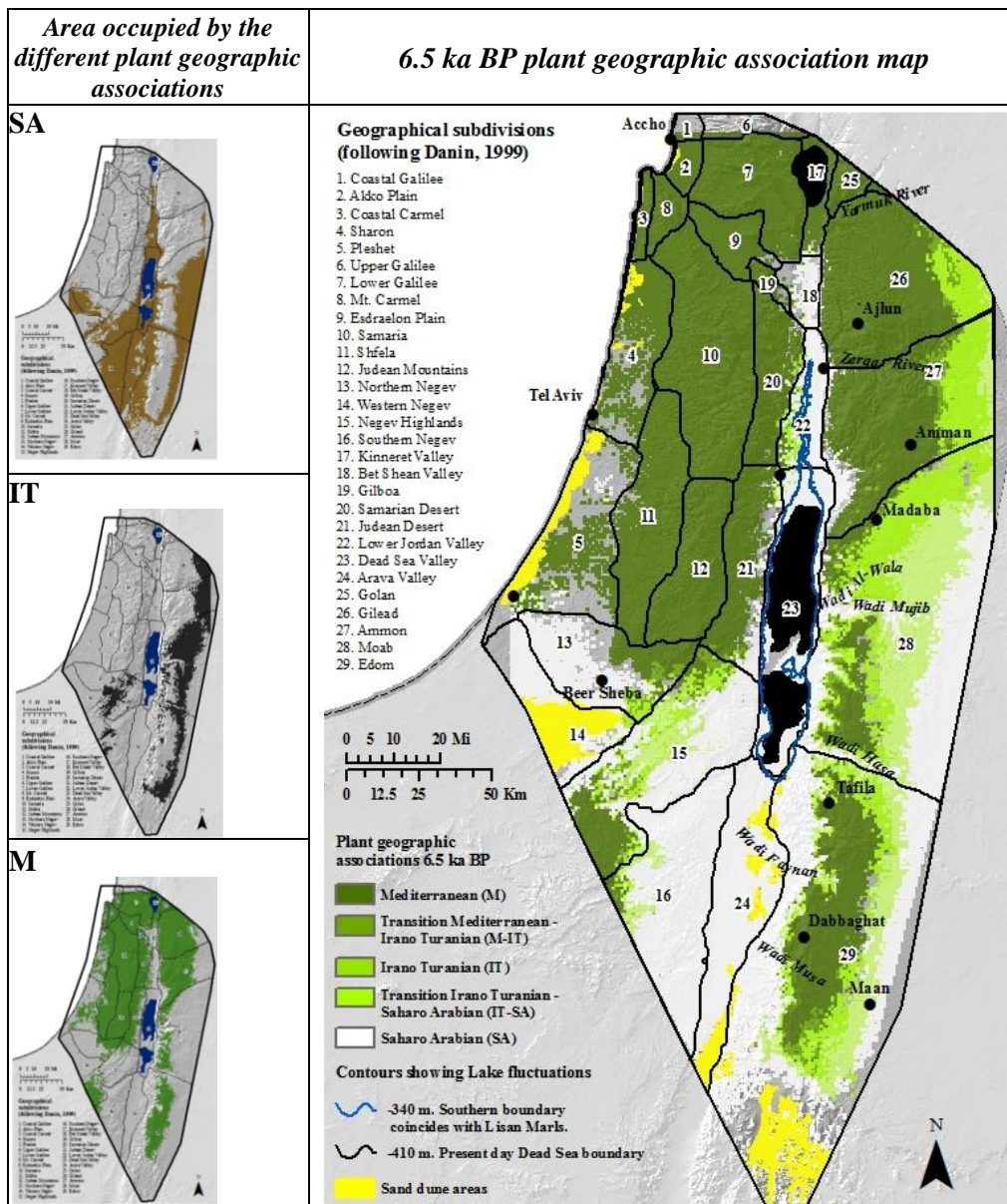


Figure 6.35. Vegetation model for 6.5 ka BP, by plant geographic association.

The outputs for 6.5 ka BP show that another contraction of the Mediterranean association has occurred east of the rift valley while it has slightly expanded along the coastal plains and Negev region. At the same time, the Saharo Arabian and Irano Turanian associations have expanded slightly. The first now stretches all the way into

Gilboa in the rift valley. The Irano Turanian association has expanded towards areas formerly occupied by the Mediterranean category.

Figure 6.36 shows how the environmental conditions in 6.5 ka BP differed to those of the present. The first row shows where clamping has occurred. The second row shows the MESS maps. Increasing negative values show where extrapolation was greatest (darker shades of red). The figure on the right shows which variables were outside their training region in 6.5 ka BP (most dissimilar than those of the present), and responsible for extreme values seen in the MESS maps.

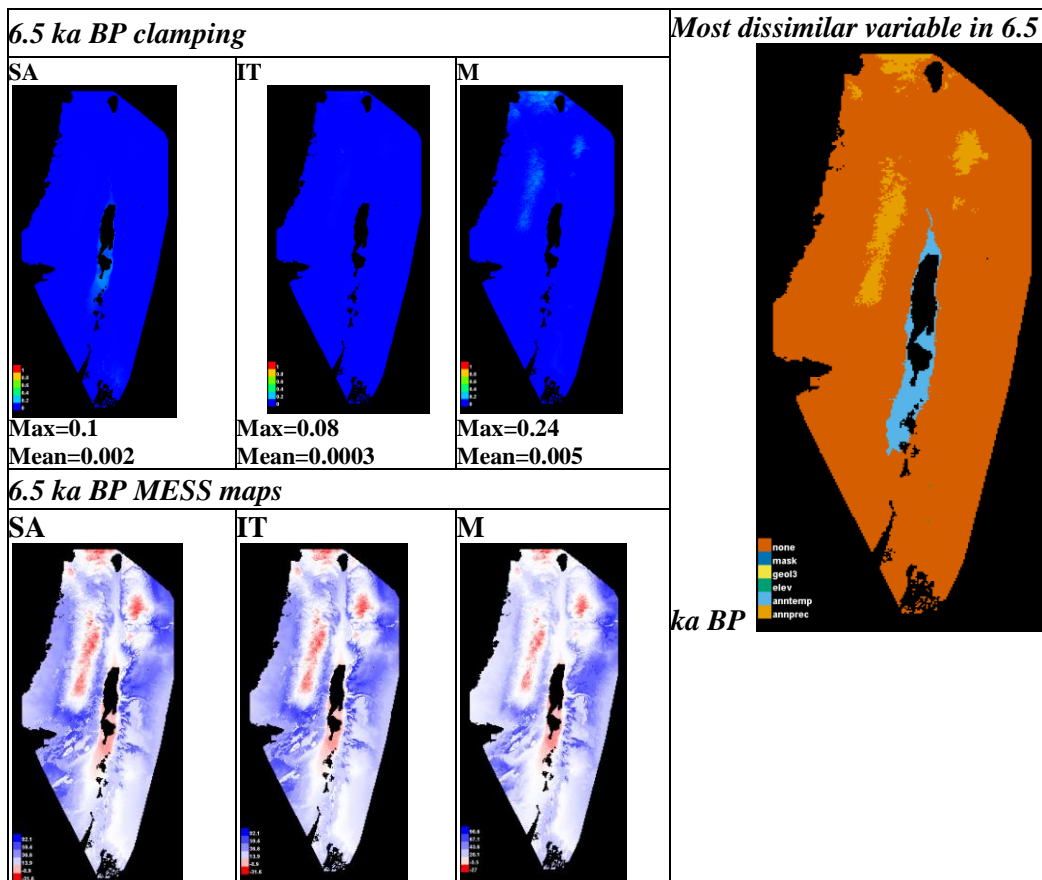


Figure 6.36. Clamping and MESS maps for 6.5 ka BP, taken from Maxent.

The extrapolation caused by precipitation values being higher than today's continues to decrease. Some clamping is still affecting the Mediterranean and forest categories, although the values are considerably smaller than in the earliest periods.

Figure 6.37 shows the area occupied by the different vegetation subcategories in 7 ka BP. These categories were combined to produce the following vegetation map (Map 6.11).

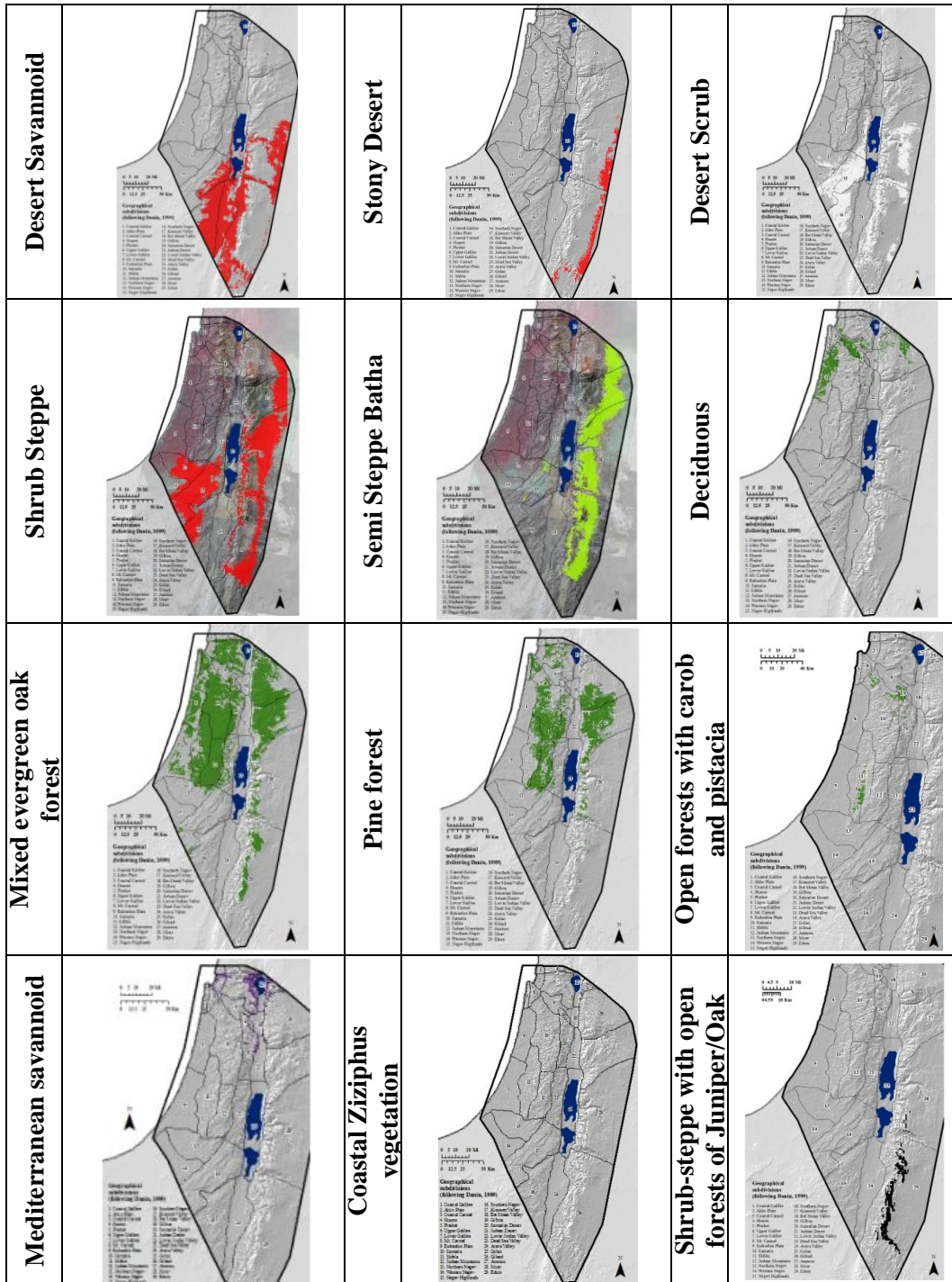
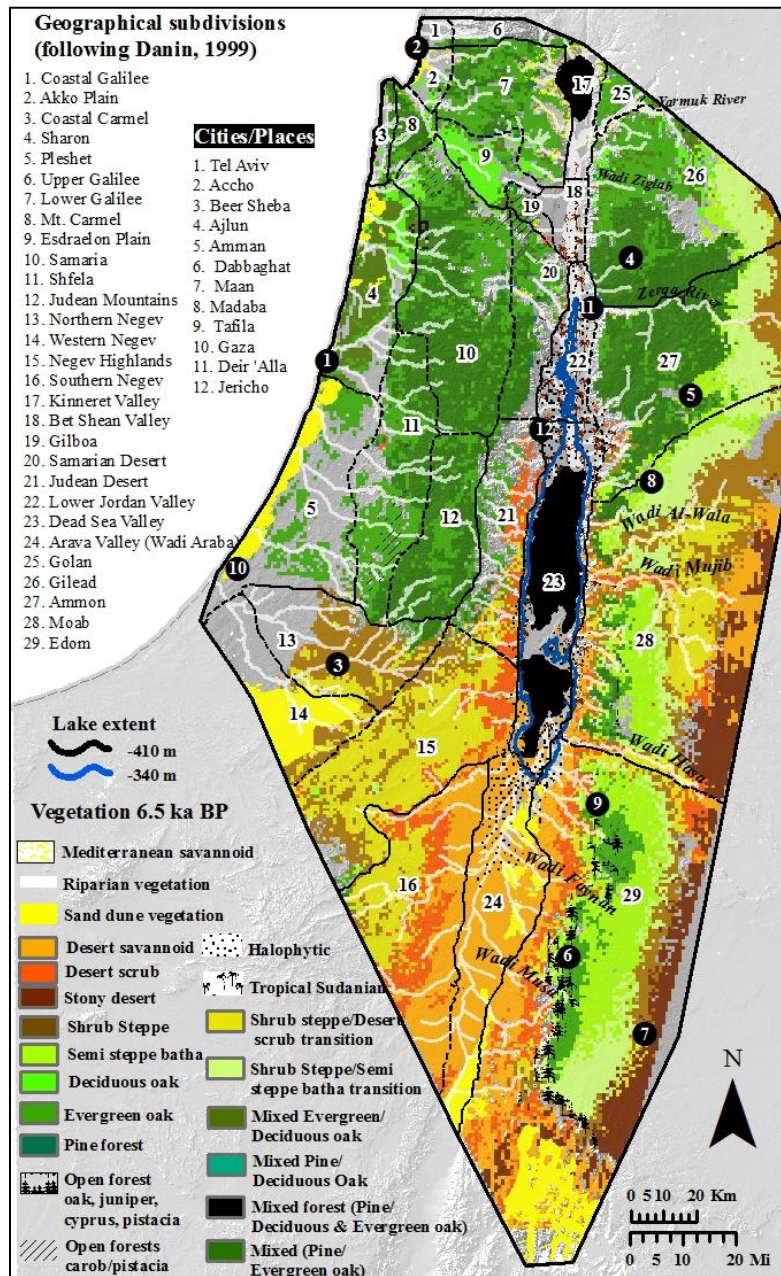


Figure 6.37. Suitable area in 6.5 ka BP per vegetation subcategory.



Once again, all of the forest categories have contracted from the previous date.

West of the Rift Valley, this is seen along the slopes that face the Rift Valley in the Judean Desert and the Northern Negev. The Judean Desert is increasingly becoming suitable to desert scrub vegetation as the forests with *Quercus calliprinos*, *Pistacia*

palaestina, and *Pinus halepensis* retreat. The three areas formerly occupied by carob and pistacia have also changed. While the patch in Gilboa increased, the other two (near Mt. Carmel and along the lower elevation foothills in Schfela) shrunk and also slightly shifted towards higher elevations. In the north, the Mediterranean savannoid vegetation has significantly contracted. It is now almost absent in the Akko Plain and occupies a tighter area around Lake Kinneret.

East of the Rift Valley, forested areas experience the most loss along the eastern border, as steppe vegetation pushes in. In the far north, the edge of the forest which was represented by *Quercus ithaburensis* in 7 ka BP has now been replaced by the semi steppe batha/shrub steppe transition category. Slightly to the south, the large forested area represented by *Quercus calliprinos* and *Pinus halepensis* has also contracted due to an encroaching semi steppe batha. There is also a slight contraction on the side facing the Rift Valley as desert scrub appears for the first time in the lower elevations of Ammon. This is also the case for the forested areas of Moab and Edom. Meanwhile, the desert scrub and shrub steppe vegetation has expanded in the Negev Highlands, the Southern Negev and the area surrounding Wadi Mujib and Wadi Hassa.

6.1.13 Model output for 6 ka BP

The results for the modeled plant geographic associations for 6 ka BP are given in Figure 6.38. The column on the left shows the area suitable for each of the main categories. These areas were combined to produce a 6 ka BP map of plant geographic associations (shown on the right).

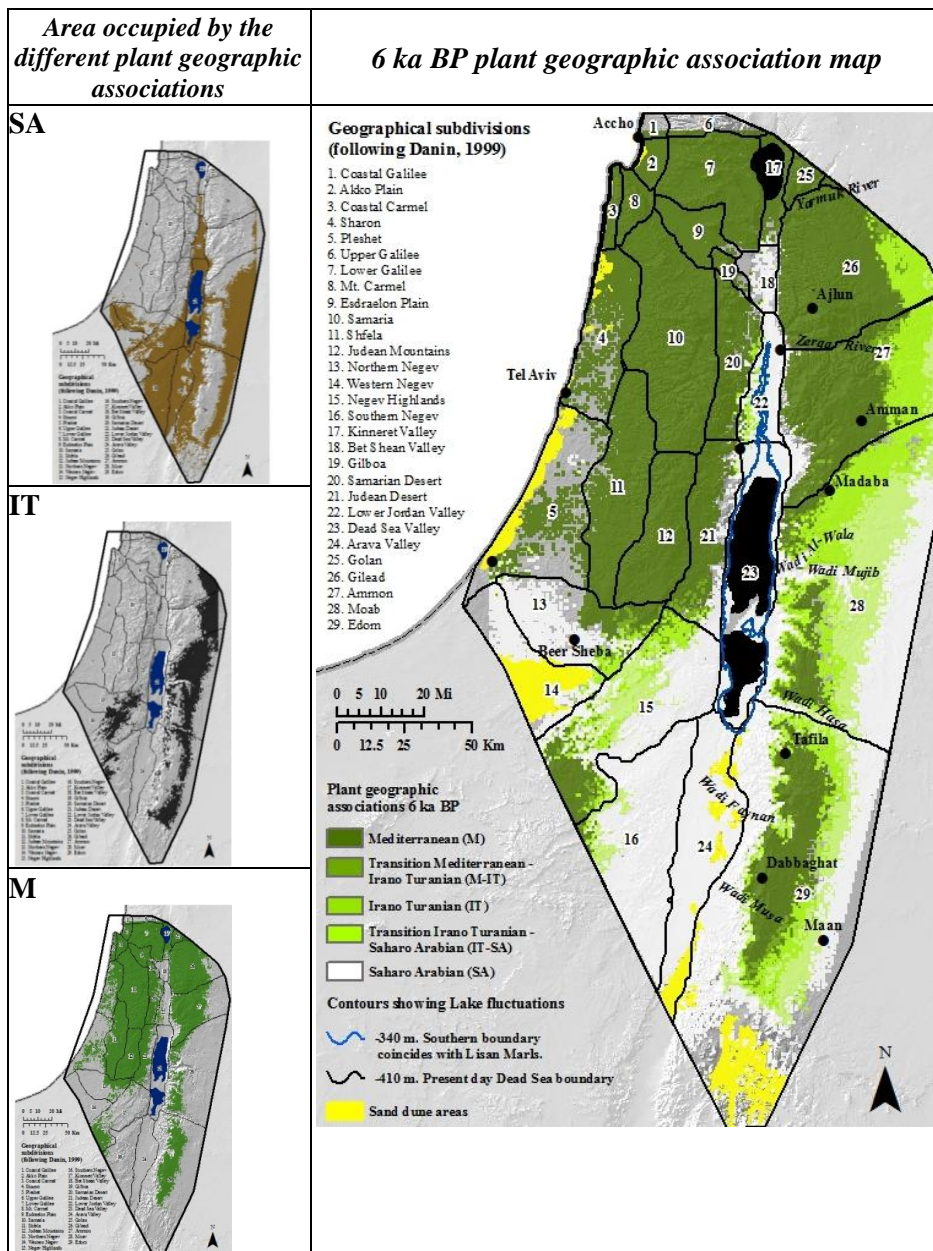


Figure 6.38. Vegetation model for 6 ka BP, by plant geographic association.

The gradual reduction of the Mediterranean association continues, as both the Saharo Arabian and Irano Turanian associations expand. This is especially obvious along the southernmost extent of the Mediterranean region on both sides of the rift valley, as it retreats in a northerly direction.

The following figure (6.39) shows how the environmental conditions in 6 ka BP differed to those of the present. The first row shows where clamping has occurred. The second row shows the MESS maps. Increasing negative values show where extrapolation was greatest (darker shades of red). The figure on the right shows which variables were outside their training region in 6 ka BP (most dissimilar than those of the present), and responsible for extreme values seen in the MESS maps.

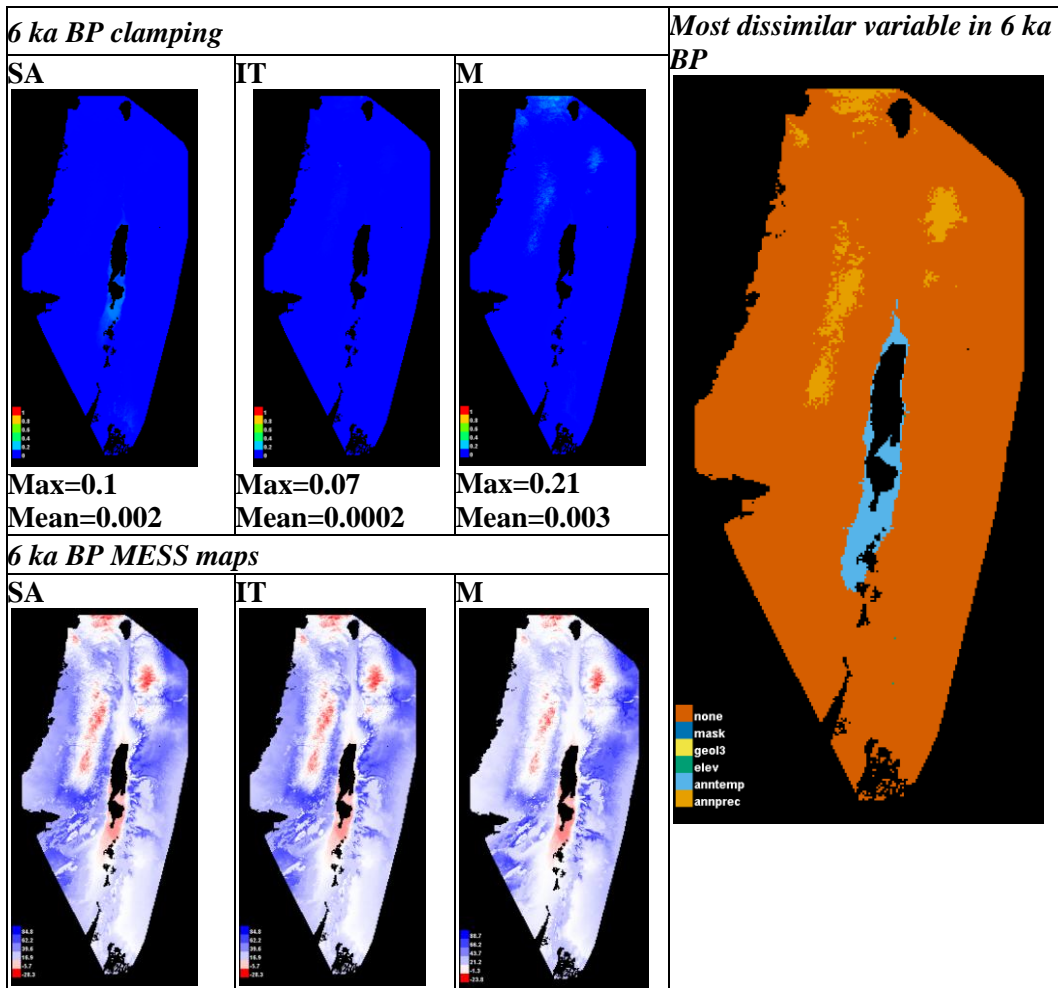


Figure 6.39. Clamping and MESS maps for 6 ka BP, taken from Maxent.

Once again, high clamping values found along the mountains on both sides of the Rift Valley continue to decline. These high clamping values are the result of wetter conditions in 6 ka BP, when compared to the present. Meanwhile, temperature around the

Dead Sea (mainly just south) is slightly higher than at present, causing minor clamping in the southern Dead Sea basin.

Figure 6.40 shows the area occupied by the different vegetation types in 6 ka BP, after the threshold that maximizes the sum of sensitivity plus specificity was applied. These categories were combined to produce the following detailed vegetation map (Map 6.12) for 6 ka BP.

The configuration of the different vegetation categories has minimally changed from 6.5 ka BP. Except for the open forests of carob and pistacia which have expanded, the other forested areas remain mostly unchanged. There is a slight contraction along the eastern edges of the mixed *Quercus callipronis*, *Pinus halepensis* forest segments in Gilead and Ammon as shrub steppe vegetation advances towards them. In the north, the Mediterranean Savannoid vegetation moderately expands.

The categories that have experienced the most obvious change from 6.5 ka BP are the xeric shrub steppe, stony desert vegetation, and desert scrub. These advance towards areas formerly occupied by the more moist categories. In the Judean Desert, shrub steppe and desert scrub continue to expand (desert scrub occupying areas along the lower elevations).

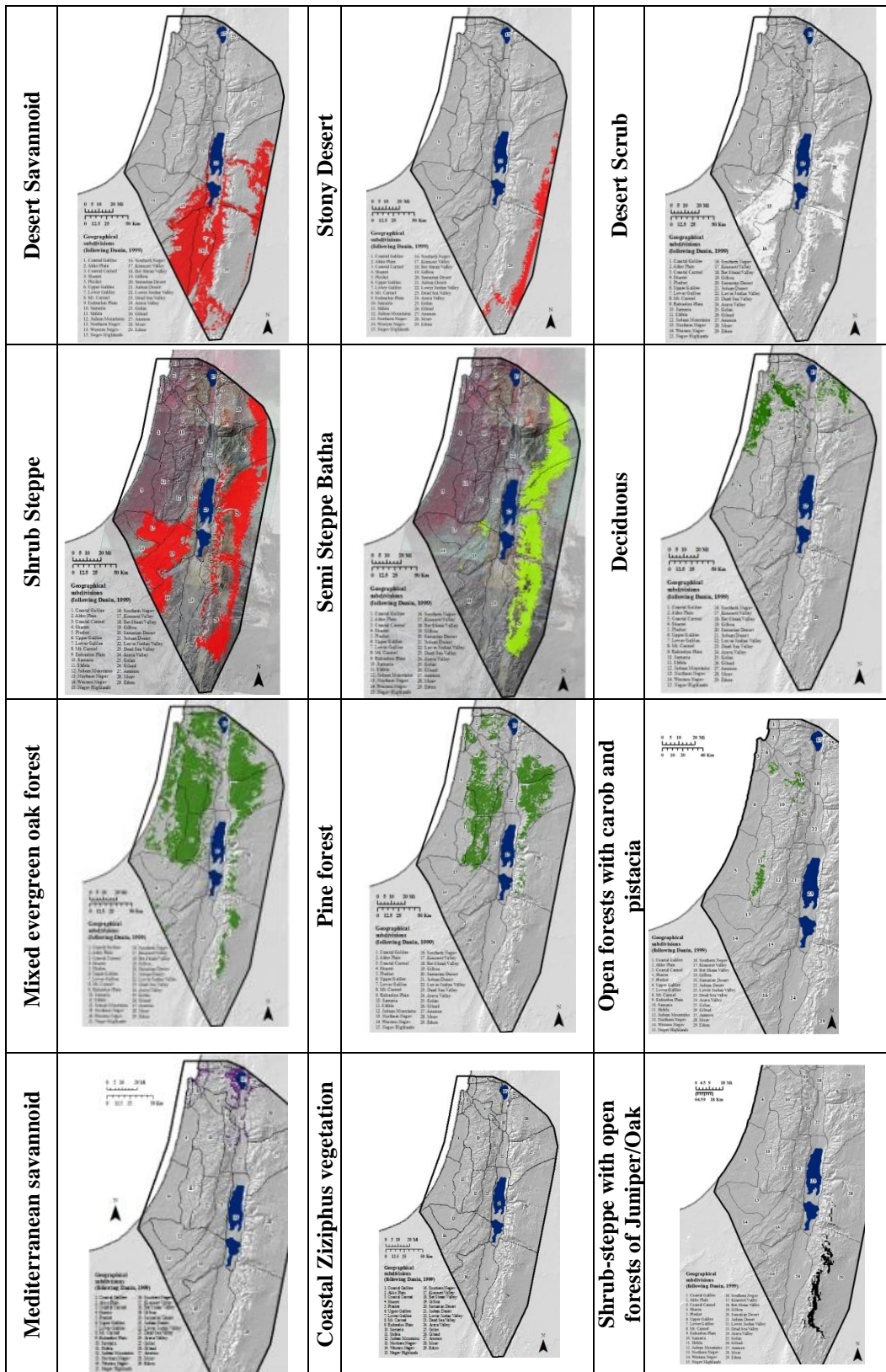
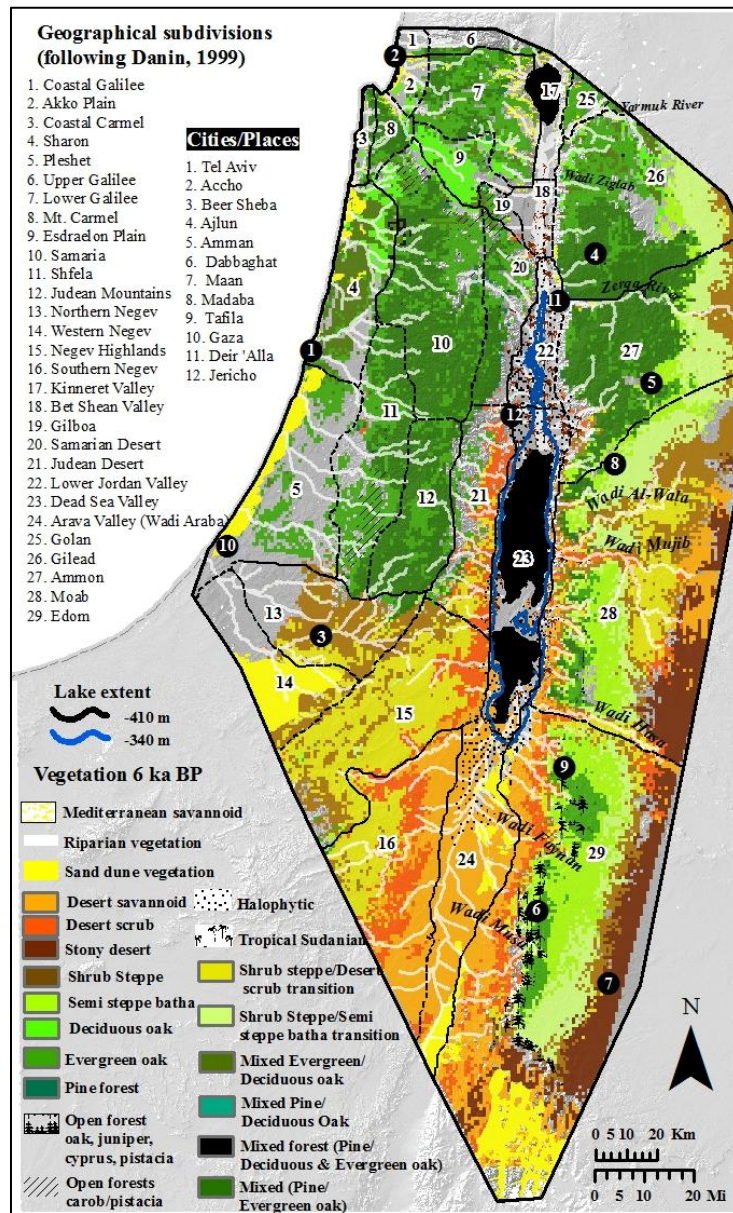


Figure 6.40. Suitable area in 6 ka BP per vegetation subcategory.



Map 6.12. Detailed vegetation map for 6 ka BP.

6.1.14 Model output for 5.5 ka BP

The results for the modeled plant geographic associations for 5.5 ka BP are given in Figure 6.41. The column on the left shows the area suitable for each of the main categories. These areas were combined to produce a 5.5 ka BP map of plant geographic associations (shown on the right).

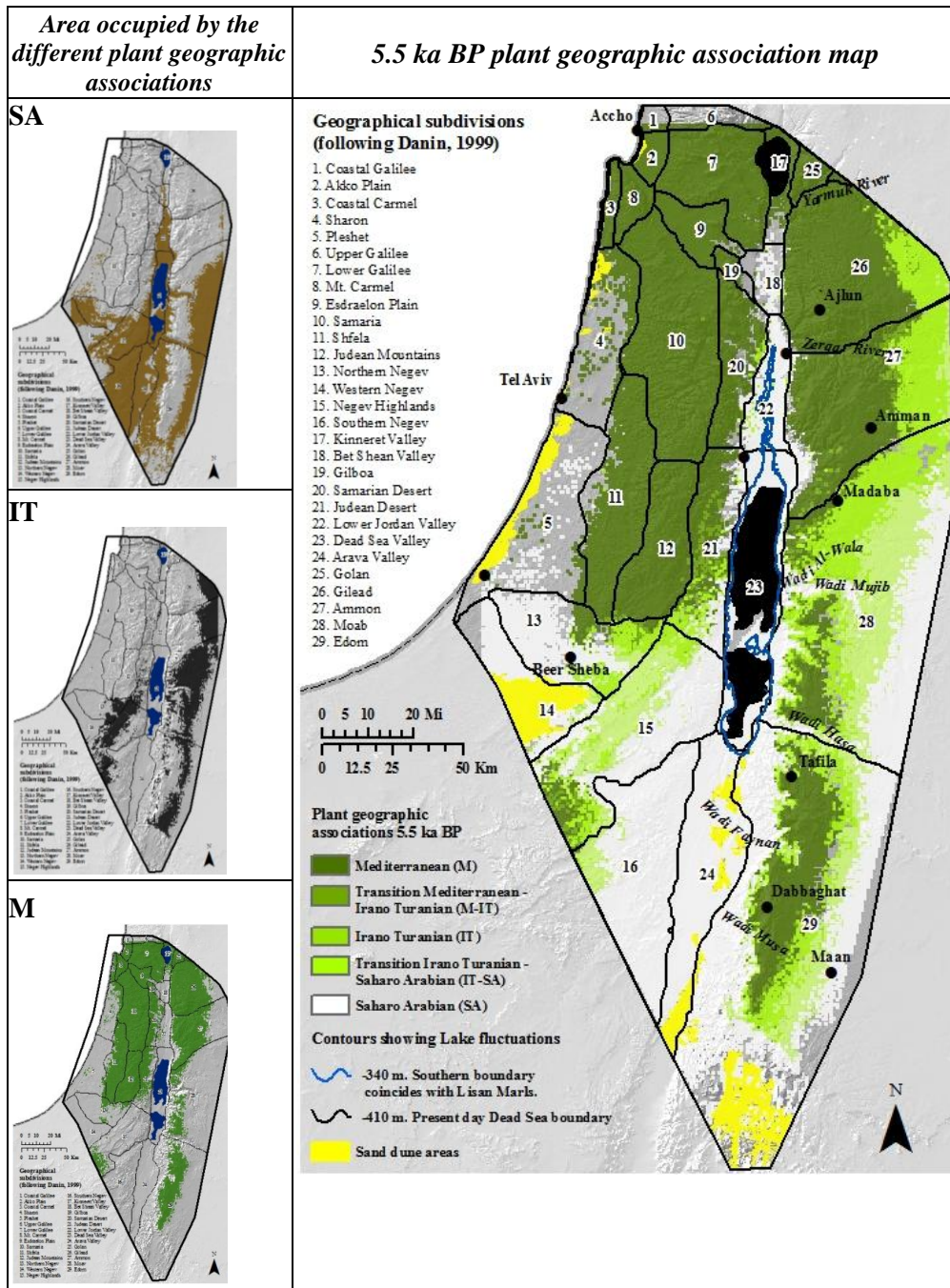


Figure 6.41. Vegetation model for 5.5 ka BP, by plant geographic association.

The Irano Turanian and Saharo Arabian associations continue to expand into areas formerly occupied by the Mediterranean category. North of the Dead Sea, the Mediterranean association retreats towards higher elevation areas.

Figure 6.42 shows how the environmental conditions in 5.5 ka BP differed to those of the present. The first row shows where clamping has occurred. The second row shows the MESS maps. Increasing negative values show where extrapolation was greatest (darker shades of red). The figure on the right shows which variables were outside their training region in 5.5 ka BP (most dissimilar than those of the present), and responsible for extreme values seen in the MESS maps.

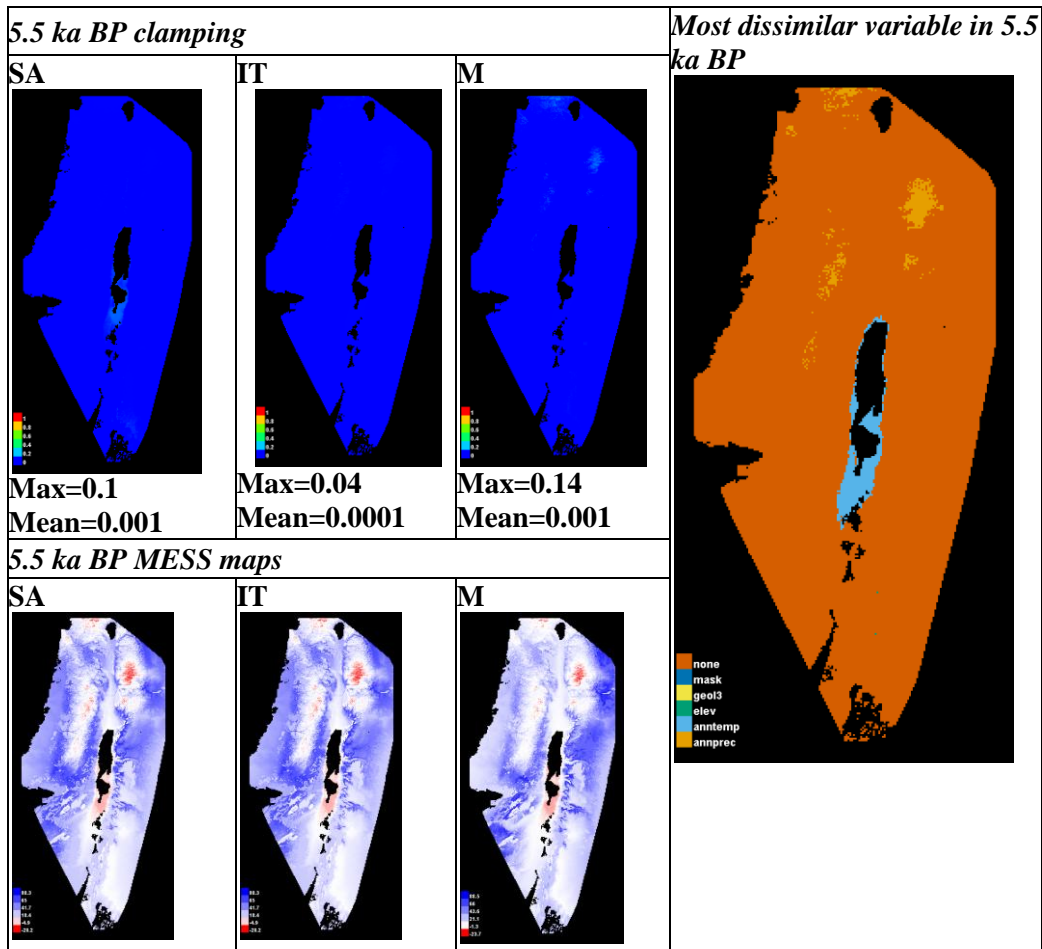


Figure 6.42. Clamping and MESS maps for 5.5 ka BP, taken from Maxent.

The areas where extrapolation occurred (due to higher than present day precipitation values) have shrunk again. As a result, clamping values have become smaller and the area affected by this has been again reduced. At the same time, the area

adjacent to the Dead Sea where average annual temperatures are higher than present day values has also contracted from the previous period. In other words, the climate grids for 5.5 ka BP represent similar climatic conditions to the present.

The following figure (Figure 6.43) shows the area occupied by the different vegetation types in 5.5 ka BP, after the threshold that maximizes the sum of sensitivity plus specificity was applied. These categories were combined to produce the following detailed vegetation map (Map 6.13).

As seen from 6.5 to 6 ka BP, the area occupied by the drier categories continues to expand into areas formerly occupied by the more mesic categories. The most obvious place is the Judean Desert, which almost holds no trace of forest patches as desert scrub and shrub steppe become more abundant. The desert scrub vegetation in this area is also spreading towards the lower elevation slopes of the Samarian Desert which then intersect with grasslands and other species typical of the Mediterranean savannoid category like *Ziziphus spina Christi* and *Ziziphus lotus*. The southern extent of the Judean Mountains is also contracting as shrub steppe and desert scrub continue to expand.

The forests of the southern highlands east of the rift valley are surrounded by semi steppe batha between Wadi Mujib and Wadi Musa. South of Wadi Musa, they are encroached by shrub steppe on the plateau and desert scrub along the Rift Valley, which denotes a more arid environment around this area.

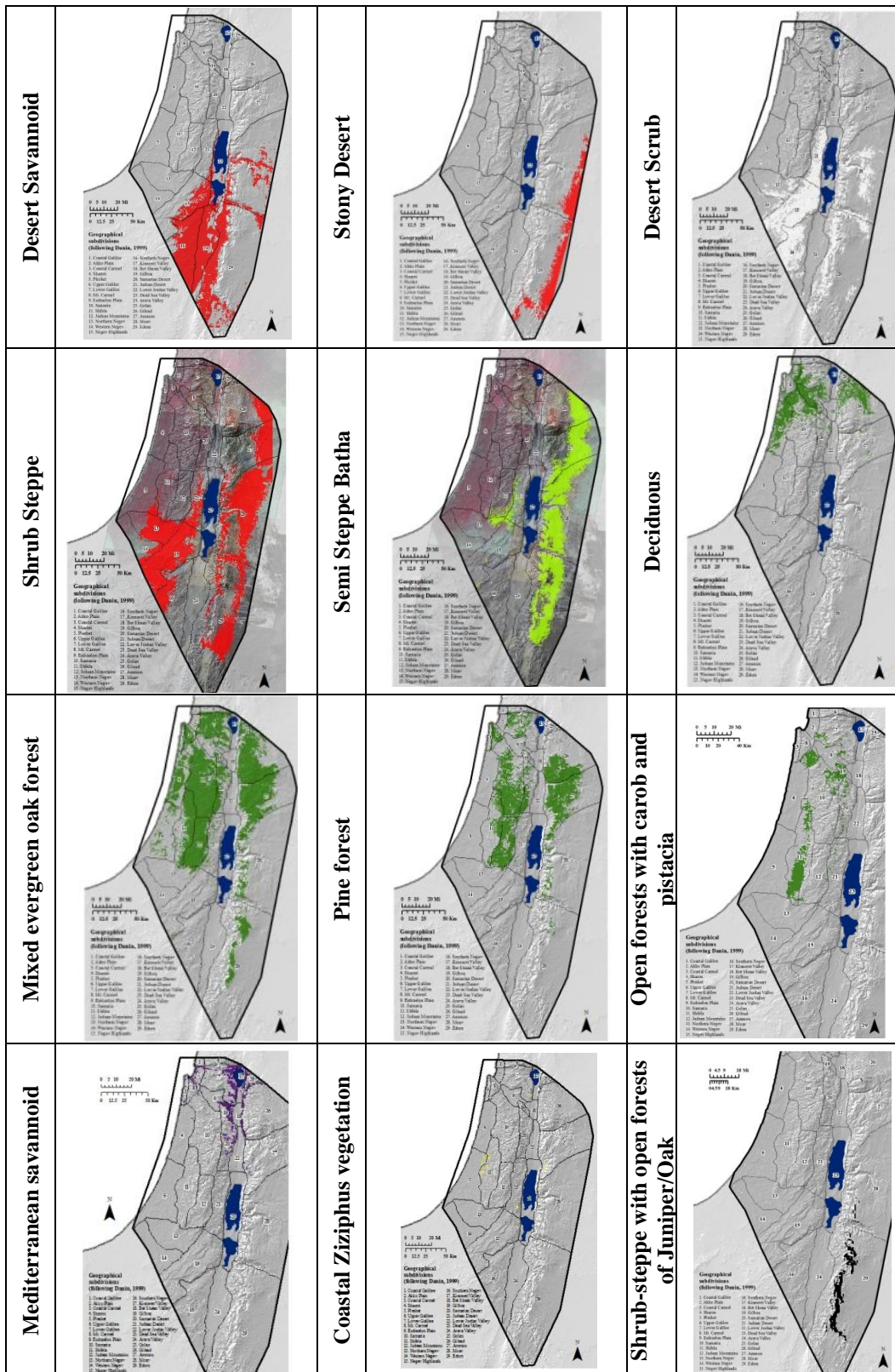
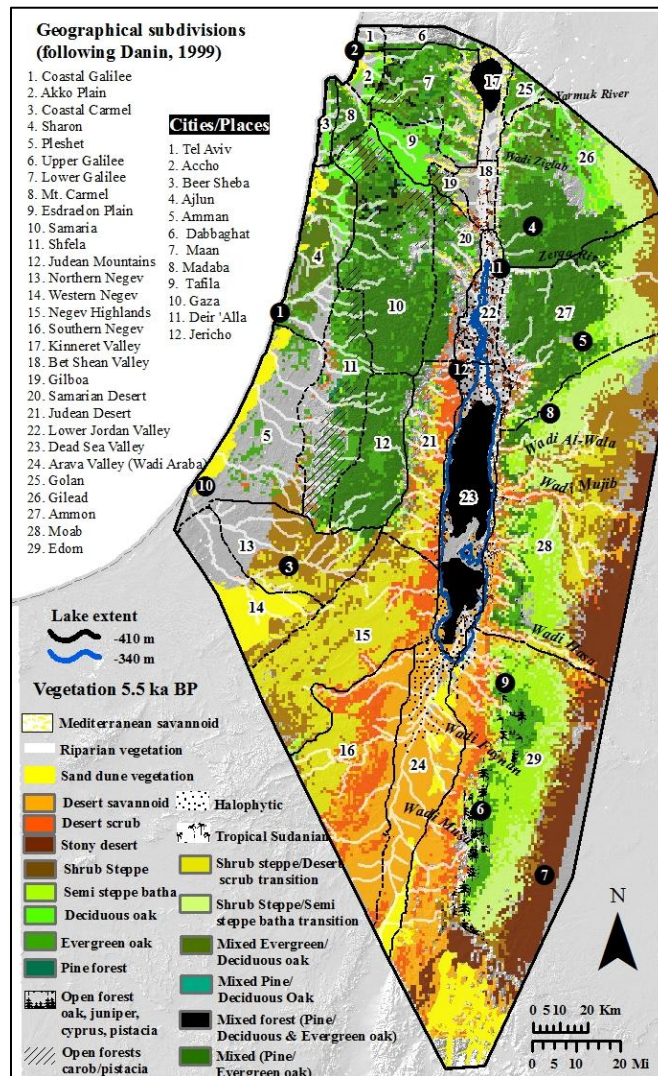


Figure 6.43. Suitable area in 5.5 ka BP per vegetation subcategory.



Map 6.13. Detailed vegetation map for 5.5 ka BP.

From 6 ka BP, forested areas have only minimally contracted along some of their boundaries. Unlike the other forest categories, the open forests of carob and pistacia continue to expand the area they occupy, as does the Mediterranean savannoid vegetation (but to a smaller degree). Also, deciduous oak forests represented by *Quercus ithaburensis* have increased around Golan, Lower Galilee, and the Kinneret Valley. The coastal plains in Sharon continue to be suitable to both oaks. The coastal plains further south find scattered patches suitable to evergreen oak (represented by the *Quercus calliprinos* – *Pistacia palaestina* association).

6.1.15 Model output for 5 ka BP

The results for the modeled plant geographic associations for 5 ka BP are given in Figure 6.44. The column on the left shows the area suitable for each of the main categories. These areas were combined to produce a 5 ka BP map of plant geographic associations (shown on the right).

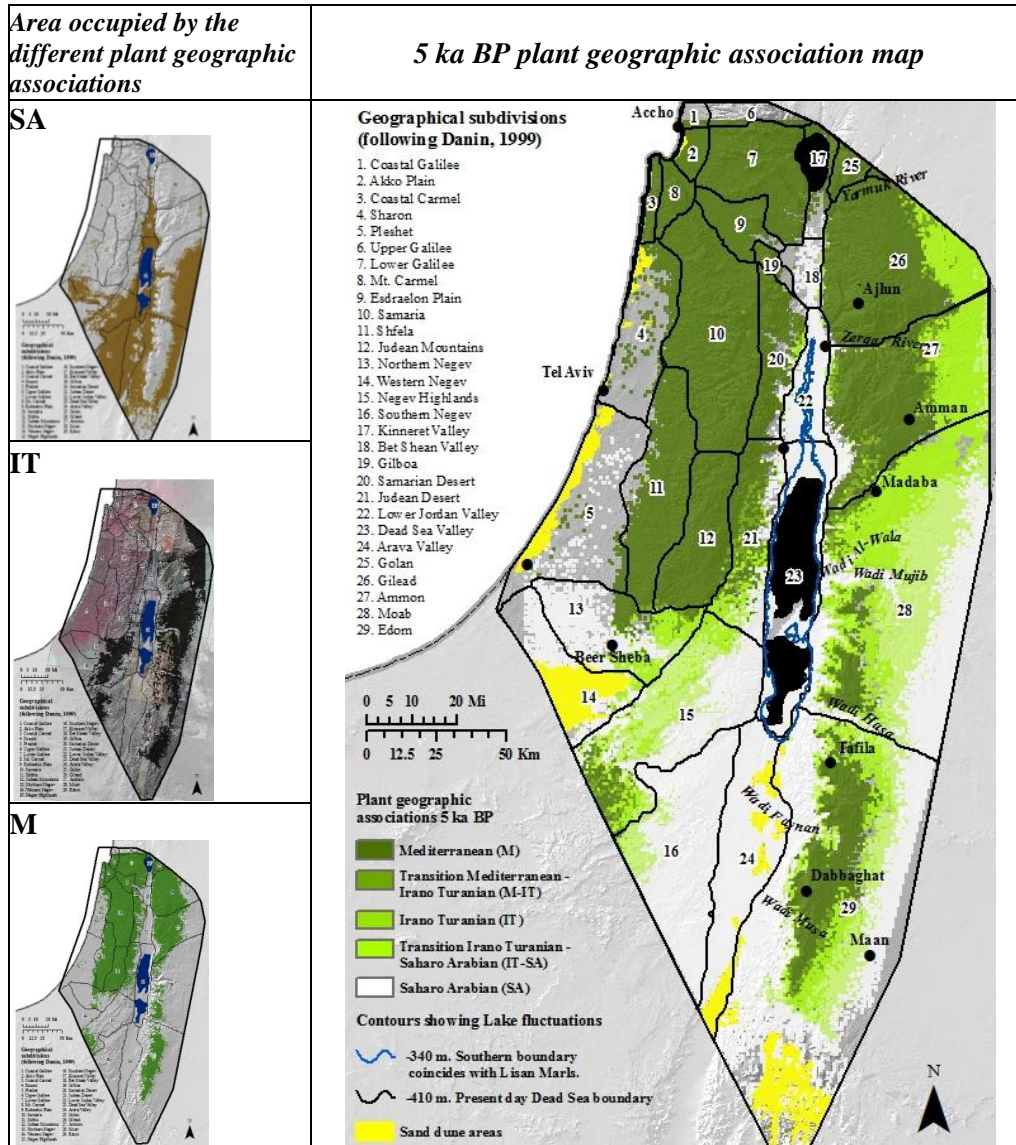


Figure 6.44. Vegetation model for 5 ka BP, by plant geographic association.

The Mediterranean association continues to retreat as the Irano Turanian and Sahara Arabian associations expand. The Northern Negev is an exception, where the area

occupied by the Saharo Arabian category becomes slightly fragmented, the Irano Turanian association remains the same, and the Mediterranean category experiences a slight increase.

The following figure (Figure 6.45) shows how the environmental conditions in 5 ka BP differed to those of the present. The first row shows where clamping has occurred. The second row shows the MESS maps. The figure on the right shows which variables where outside their training region in 5 ka BP (most dissimilar than those of the present), and responsible for extreme values seen in the MESS maps. These show that the high clamping values seen during the Early Holocene due to climatic conditions that were different to the modern analog have stopped, even though slightly warmer temperatures and higher rainfall are still seen in the Dead Sea Valley and Gilead, respectively.

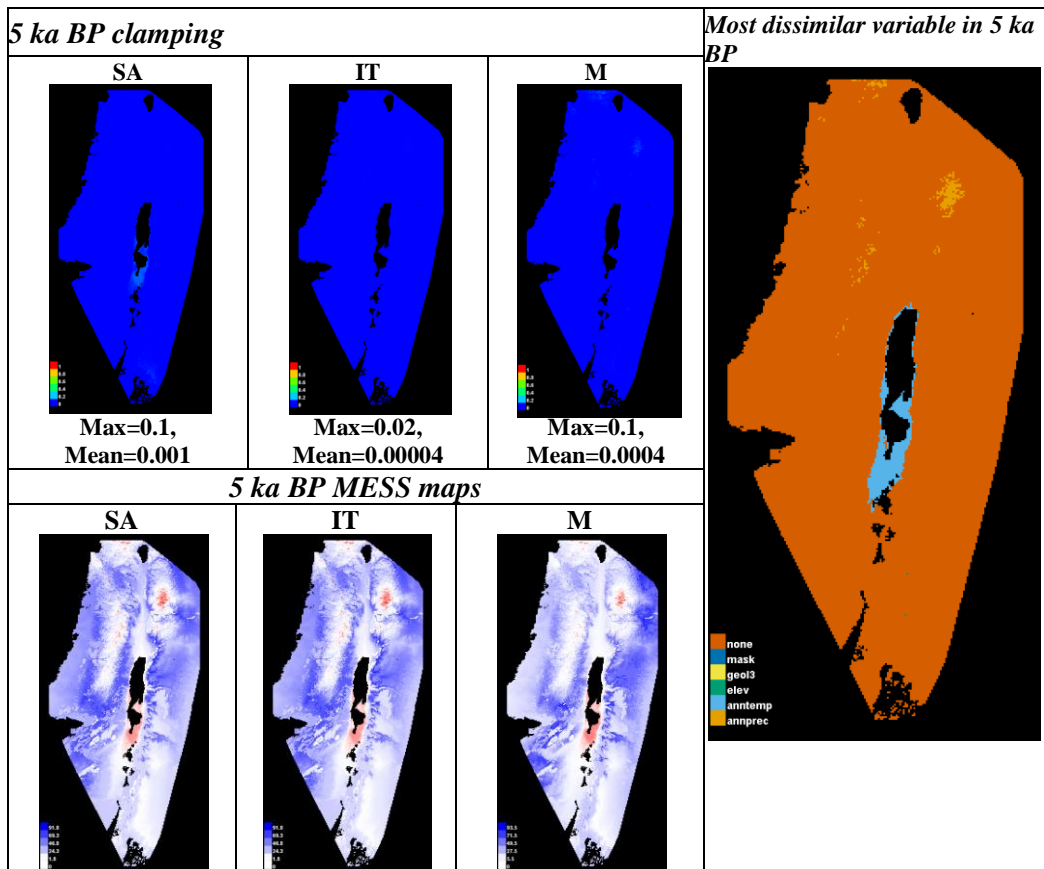


Figure 6.45. Clamping and MESS maps for 5 ka BP, taken from Maxent.

The following figure (Figure 6.46) shows the area occupied by the different vegetation types in 5 ka BP. These categories were combined to produce the following detailed vegetation map (Map 6.14).

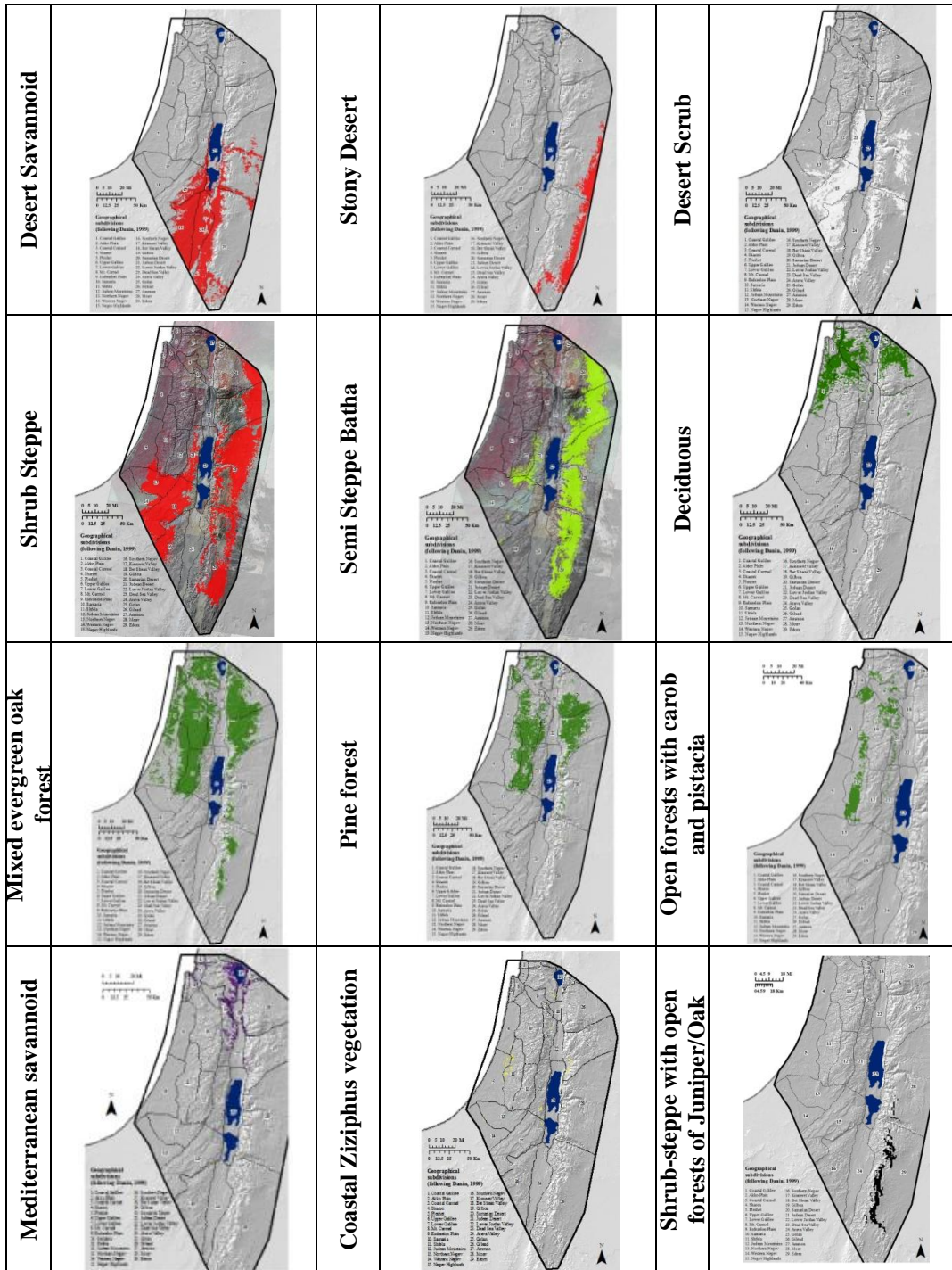
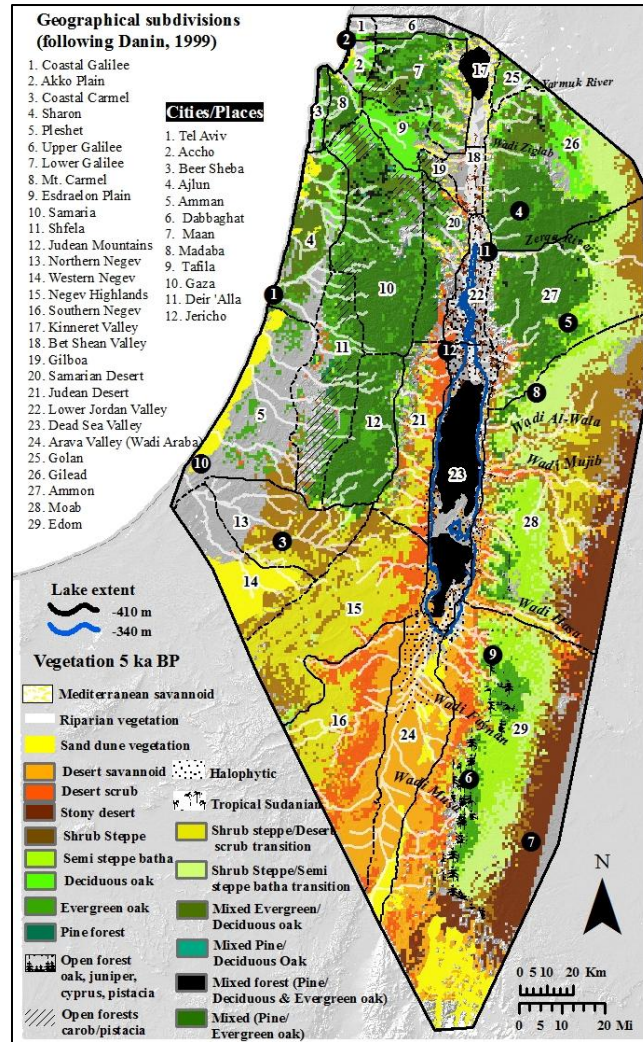


Figure 6.46. Suitable area in 5 ka BP per vegetation subcategory.

Although the area occupied by forests west of the Dead Sea has not changed from 5.5 ka BP, those located on the highlands continue to contract along their eastern boundary. Between the Yarmuk River and Wadi Ziglab in Gilead, deciduous oak forests represented by *Quercus ithaburensis* continue to increase. Another category that keeps expanding is the open forests of carob and pistacia.



6.1.16 Model output for 4.5 ka BP

The results for the modeled plant geographic associations for 4.5 ka BP are given in Figure 6.47. The column on the left shows the area suitable for each of the main

categories. These areas were combined to produce a 4.5 ka BP map of plant geographic associations (shown on the right).

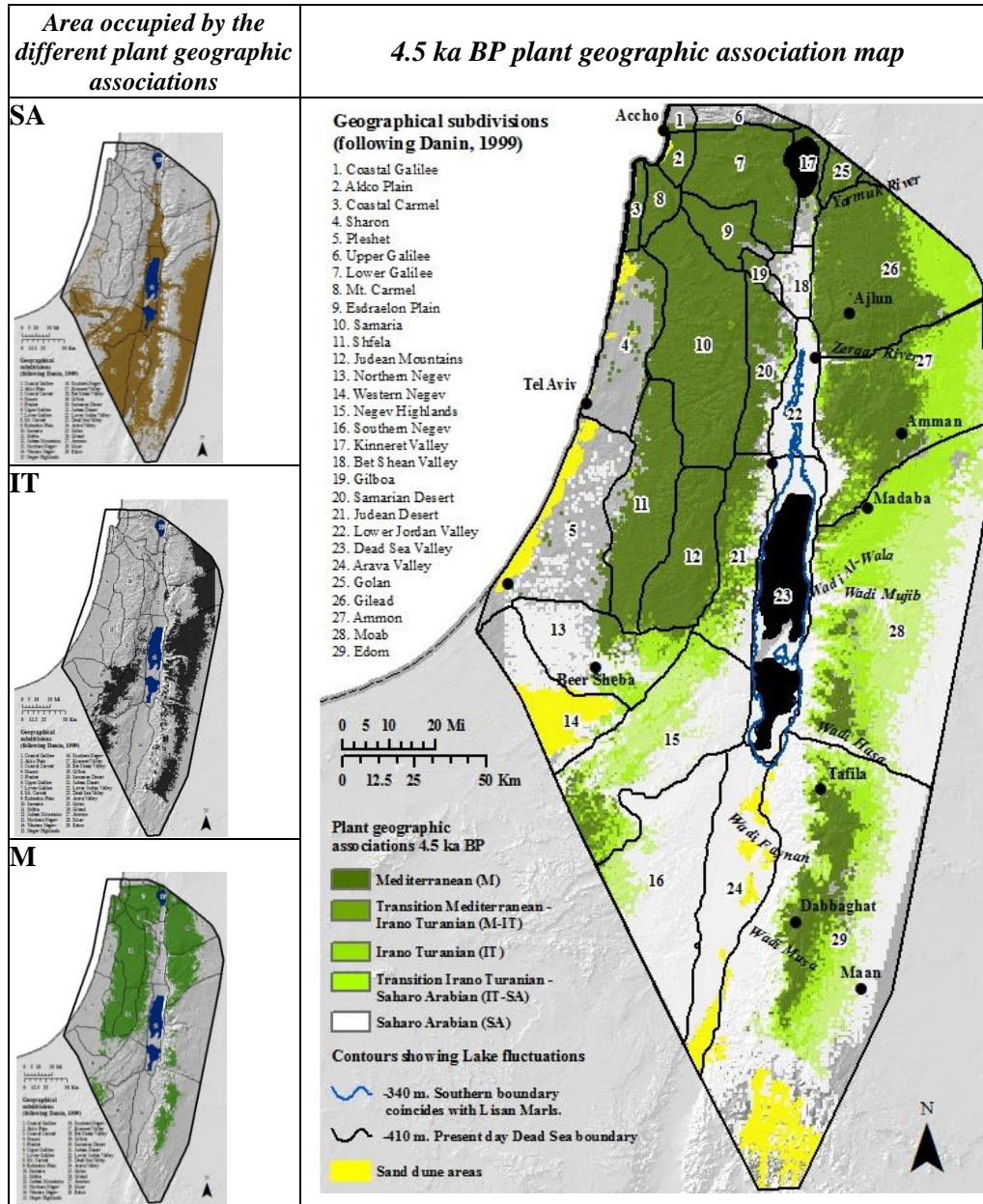


Figure 6.47. Vegetation model for 4.5 ka BP, by plant geographic association.

From 5 to 4.5 ka BP, a reduction of the Mediterranean association is seen throughout the whole study area. The opposite is seen for Saharo Arabian and Irano Turanian categories. The Saharo Arabian association continues its trajectory northward

through the rift valley as well as along the plateau and coastal region. The same occurs to the Irano Turanian category.

Figure 6.48 shows how the environmental conditions in 4.5 ka BP differed to those of the present. The first row shows where clamping has occurred. The second row shows the MESS maps. Increasing negative values show where extrapolation was greatest (darker shades of red). The figure on the right shows which variables were outside their training region in 4.5 ka BP (most dissimilar than those of the present), and responsible for extreme values seen in the MESS maps.

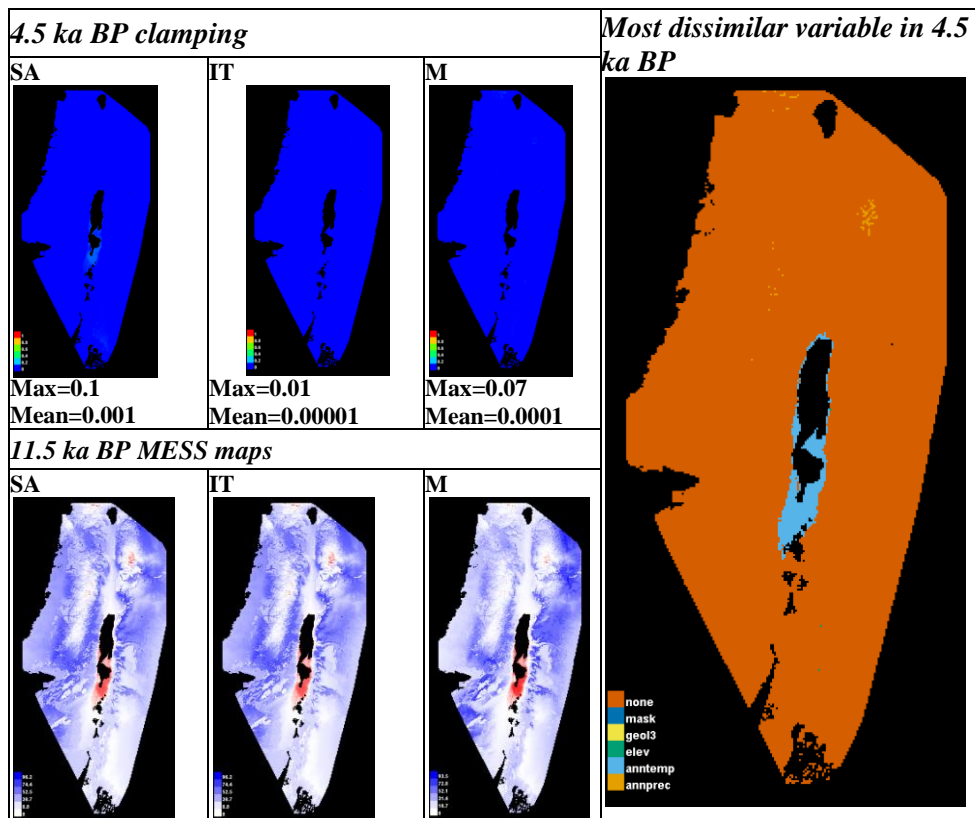
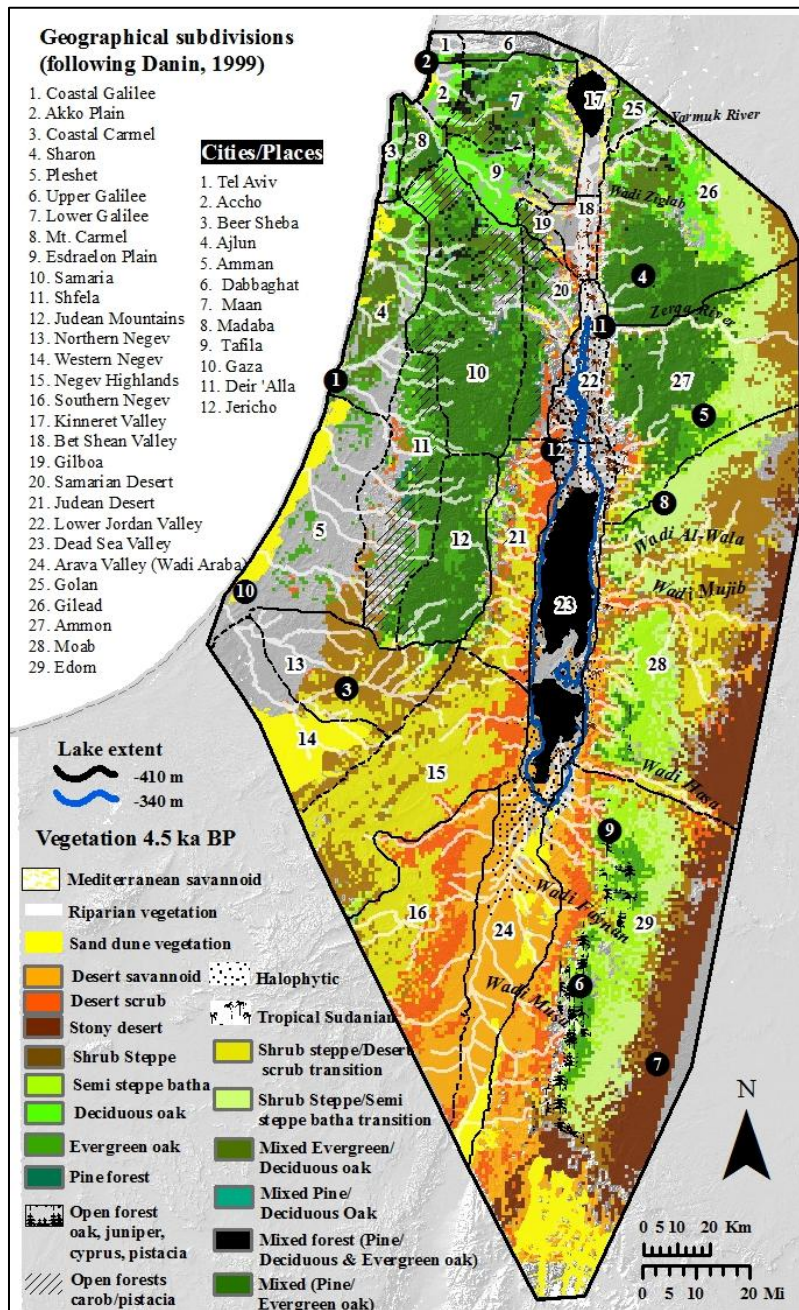


Figure 6.48. Clamping and MESS maps for 4.5 ka BP, taken from Maxent.

Like in 4 ka BP, clamping values for all categories are extremely low. As the MoD shows, there are a few patches where annual temperature is still different to the present, although not by a lot. Temperature around the Dead Sea Valley continues to be slightly higher than today's.



Map 6.15. Detailed vegetation map for 4.5 ka BP.

Except for the open forests of carob and pistacia which have expanded, all the forest areas continue to tighten along their edges. This is most obvious along the eastern boundary of the deciduous, evergreen, and pine forests in Gilead and Ammon. The southern extent of this patch which is around Madaba is also contracting. In the coastal

plains of Pleshet, the fragmented areas still suited to stands represented by *Quercus calliprinos* have also declined. Meanwhile, areas occupied by stony desert vegetation, desert scrub, shrub steppe and desert savannoid vegetation have expanded. In the rift valley, shrub steppe and desert scrub continue their northward latitudinal expansion and from there spread into the lower elevations of adjacent slopes as well as into wadi valleys (i.e., Zerqa River). On the mountains, semi steppe batha also spreads into areas formerly suited to the forest categories. The southern juniper forests remain the same.

6.1.17 Model output for 4 ka BP

The results for the modeled plant geographic associations for 4 ka BP are given in Figure 6.50. The column on the left shows the area suitable for each of the main categories. These areas were combined to produce a 4 ka BP map of plant geographic associations (shown on the right).

This time period shows a reversal to the slow and mostly steady contraction of the Mediterranean association since during earlier time periods. The Saharo Arabian association, which had reached the Bet Shean Valley north of the Dead Sea and also expanded throughout the Negev and plateau region by 4.5 ka BP, retreats considerably in 4 ka BP. Areas that were formerly Saharo Arabian are now suitable to the Irano Turanian plant geographic association. Meanwhile, the Mediterranean category expands significantly.

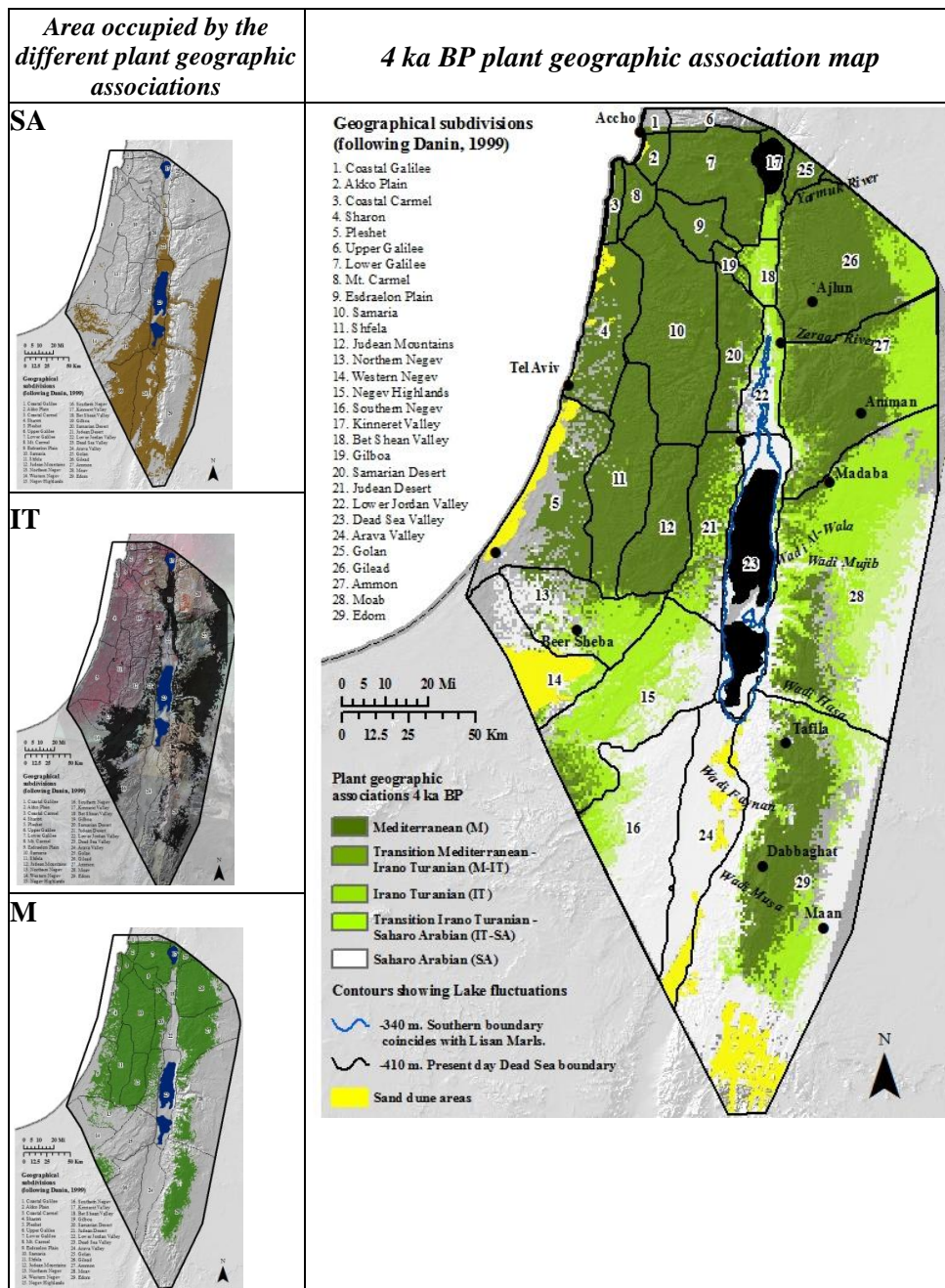


Figure 6.50. Vegetation model for 4 ka BP, by plant geographic association.

The following figure (Figure 6.51) shows how the environmental conditions in 4 ka BP differed to those of the present. The first row shows where clamping has occurred. The second row shows the MESS maps. Increasing negative values show where extrapolation was greatest (darker shades of red). The figure on the right shows which

variables where outside their training region in 4 ka BP (most dissimilar than those of the present), and responsible for extreme values seen in the MESS maps.

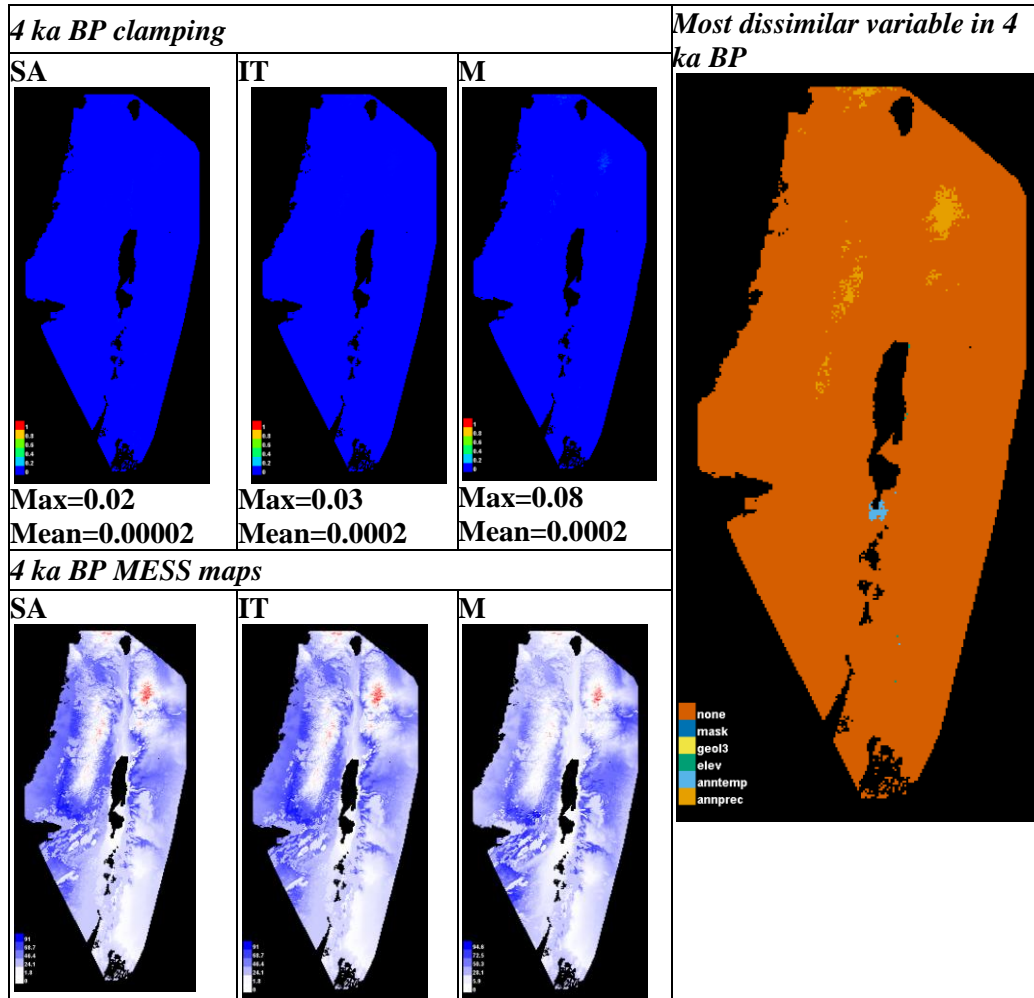


Figure 6.51. Clamping and MESS maps for 4 ka BP, taken from Maxent.

From 12 ka BP until now, the MESS maps indicate that climatic conditions are gradually become more like those of the present. This period presents an exception, as the MoD and MESS maps show. Nevertheless, clamping values are still quite low.

Figure 6.52 shows the area occupied by the different vegetation subcategories in 4 ka BP, after the threshold that maximizes the sum of sensitivity plus specificity was applied. These categories were combined to produce the following detailed vegetation map (Map 6.16).

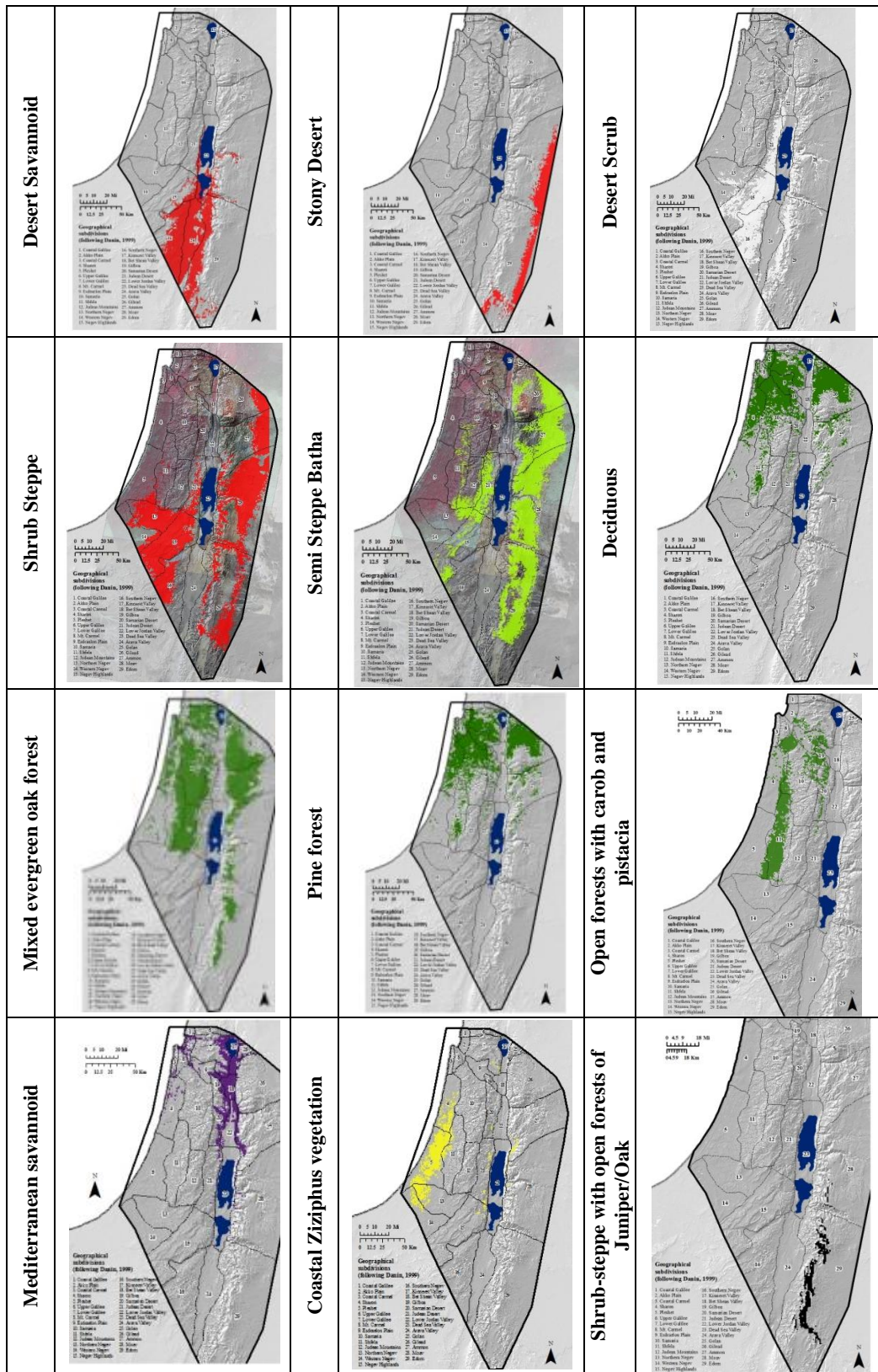
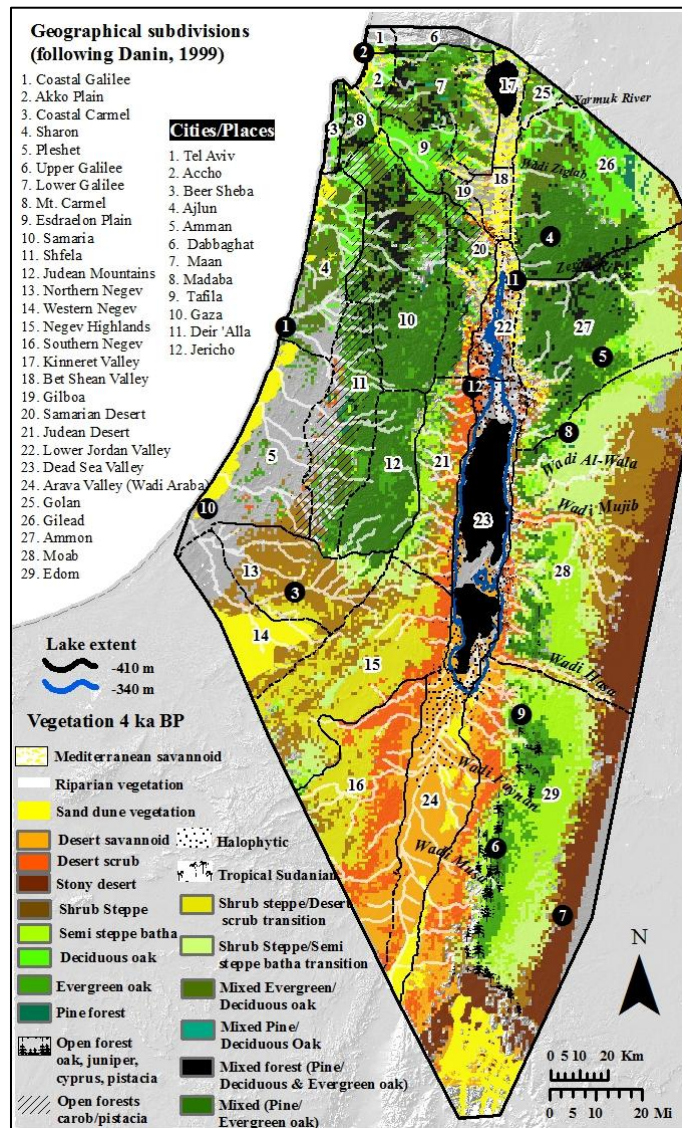


Figure 6.52. Suitable area in 4 ka BP per vegetation subcategory.



Map 6.16. Detailed vegetation map for 4 ka BP.

The trend of forest contraction seen so far stops and is reversed in 4 ka BP, as the area occupied by all of the forest categories expands. All areas formerly occupied by the open forests of carob and pistacia have expanded in all directions in the three locations where it occurs today. The strip that descends into the coastal plain now occupies most of Schfela as well as fragmented patches in the Pleshet coastal plains, which sit surrounded by *Quercus ithaburensis* and *Q. calliprinos* maquis. East of the Rift Valley, all forest

areas also expand in all directions. Gilead once again becomes mostly forested as *Quercus ithaburensis* expands in the north, matched by an increase in the areas occupied by *Pinus halepensis* and *Q. calliprinos* further south. Once again, the Zerqa River is surrounded by these types of forest which stretch south until Madaba. In 4.5 ka BP, the forested areas of Moab had nearly disappeared. However 500 years later, they find suitable conditions between Wadi Mujib and Wada Hasa (according to the modeled outputs). Further south still, the oak and juniper forests also expand. Another category that expands the area it occupies is the Mediterranean savannoid vegetation, which is once again present in the rift valley from the Lower Jordan Valley to the Kinneret Valley. From here, it spreads into adjacent basins.

Shrub steppe and semi steppe batha vegetation, which had been penetrating into the more moist areas during previous dates, now retreat. Instead, they move towards the drier areas. This is evident in the area surrounding Wadi Mujib and in the Negev Highlands. The categories which are indicative of drier areas (e.g., desert savannoid, desert scrub, stony desert), also contract. In the Negev region and the Judean Desert, these are partly replaced by steppe vegetation. It is interesting to note that this is the only time period that indicates an extensive area suitable to coastal ziziphus vegetation.

6.1.18 Model output for 3.5 ka BP

The results for the modeled plant geographic associations for 3.5 ka BP are given in Figure 6.53. The column on the left shows the area suitable for each of the main categories. These areas were combined to produce a 3.5 ka BP map of plant geographic associations (shown on the right).

This time period stands in contrast to the previous one, when the Mediterranean and Irano Turanian associations had expanded. An obvious contraction of the

Mediterranean category and expansion of areas occupied by the Saharo Arabian association suggest a return to the aridification trend seen since throughout the Holocene.

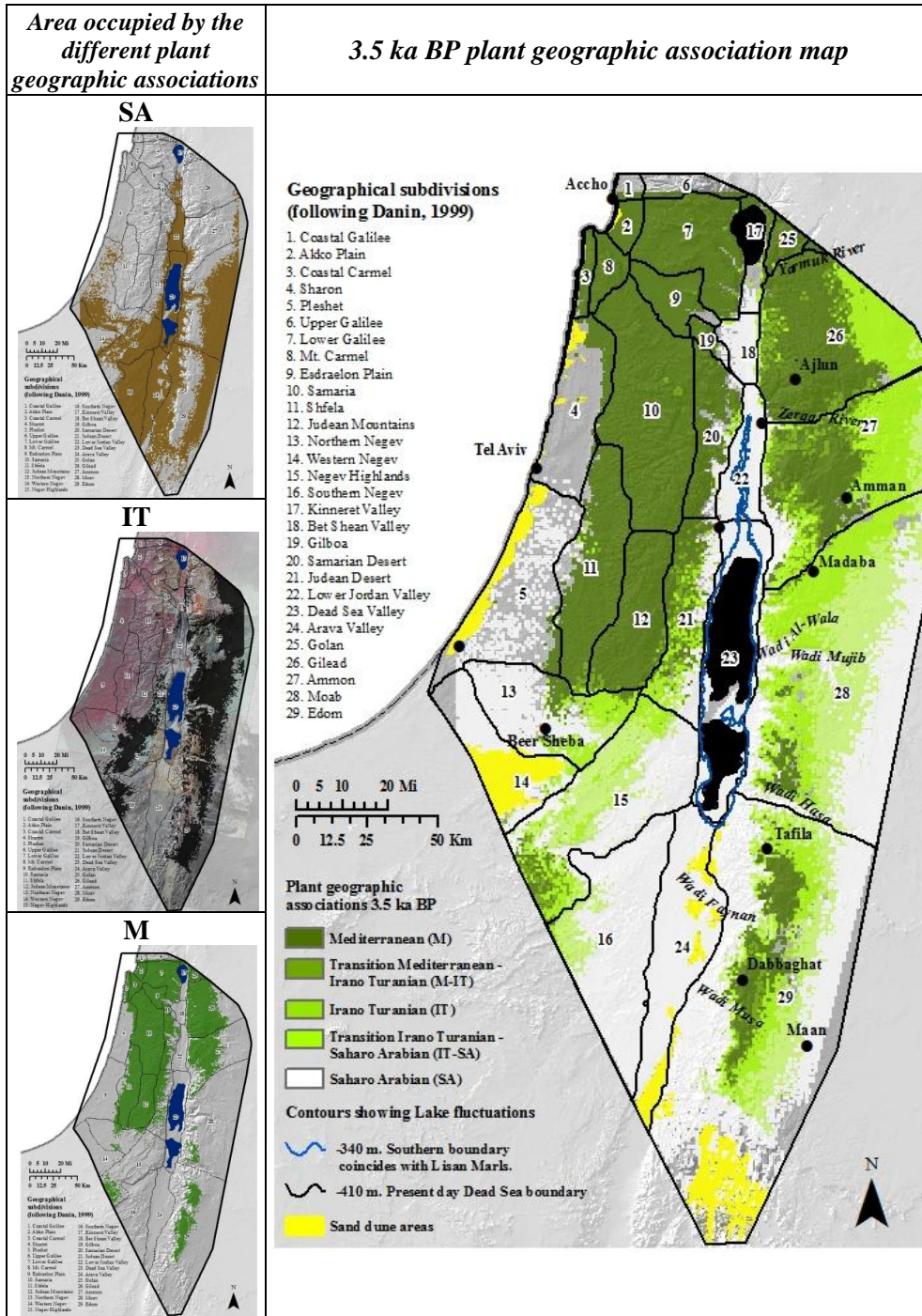


Figure 6.53. Vegetation model for 3.5 ka BP, by plant geographical association.

Figure 6.54 shows how the environmental conditions in 3.5 ka BP differed to those of the present. The first row shows where clamping has occurred. The second row shows the MESS maps. Increasing negative values show where extrapolation was greatest (darker shades of red). The figure on the right shows which variables were outside their training region in 3.5 ka BP (most dissimilar than those of the present), and responsible for extreme values seen in the MESS maps.

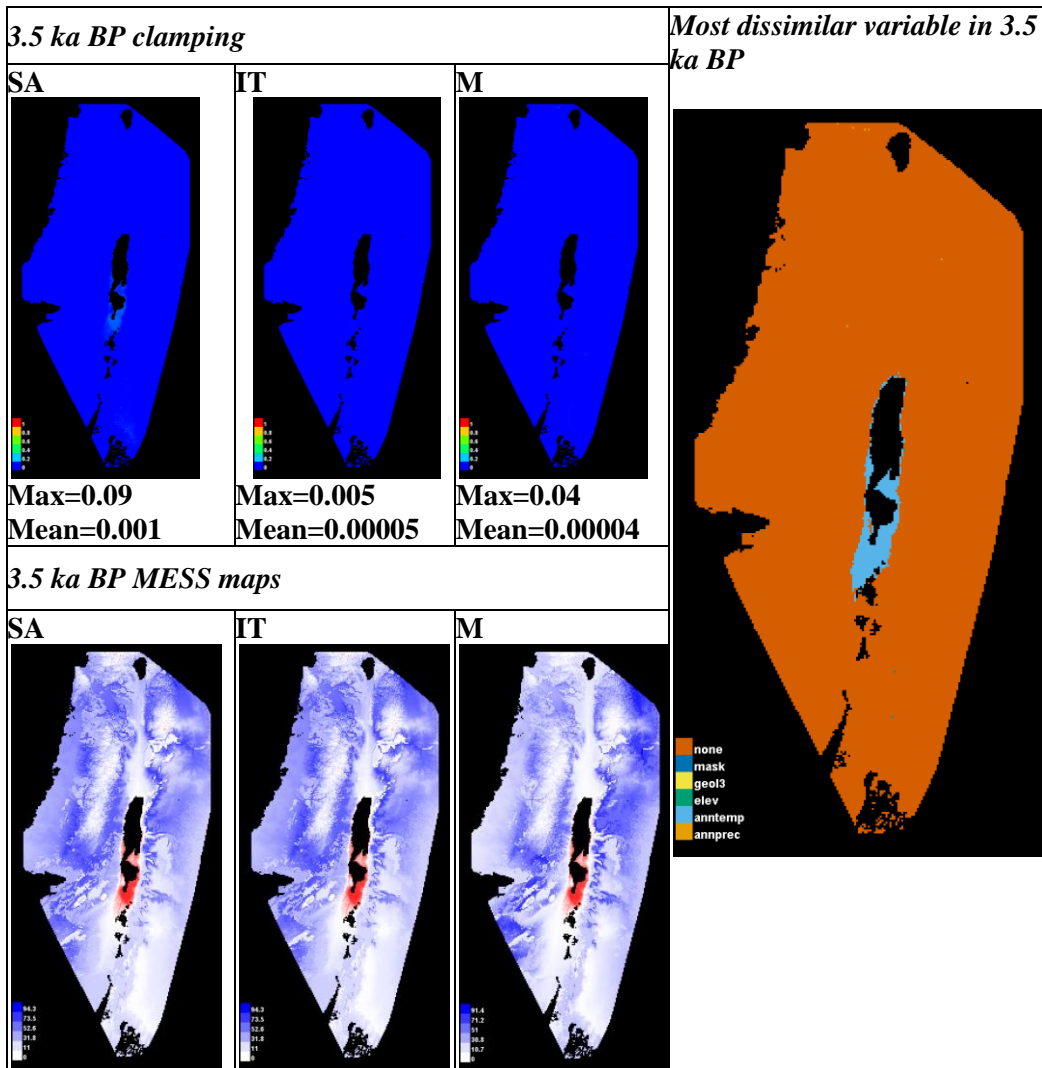


Figure 6.54. Clamping and MESS maps for 3.5 ka BP, taken from Maxent.

These plots indicate that precipitation in 3.5 ka BP is not that different to precipitation levels today. The only variable that is outside its training range is average

yearly temperature (in the immediate vicinity of the Southern Dead Sea basin temperatures are slightly higher than those of the present).

The following figure (Figure 6.55) shows the area occupied by the different vegetation subcategories in 3.5 ka BP, after the threshold that maximizes the sum of sensitivity plus specificity was applied. These categories were combined to produce a detailed vegetation map (Map 6.17), which is quite similar to the one in 4.5 ka BP.

In 3.5 ka BP, all forest categories contract from the areas they had expanded to 500 years earlier. The open forests of carob and pistacia, which had expanded to the coastal plains and valleys in 4 ka BP, now contract and retreat towards the highlands (where it is more wet). The mixed *Quercus calliprinos*, *Pinus halepensis* forested area of the northern highlands retreats across all its boundaries. In the northern portion around Wadi Ziglab, patches dominated by *Quercus ithaburensis* retreat by about 10 km. Forest segments around Wadi Mujib disappear, and those further south around Tafila dramatically contract. In a similar way, the grasslands of the Mediterranean savannoid vegetation noticeably decline as they retreat to the Kinneret Valley. Nevertheless, patches of forests are still present in all of the plateau subdivisions.

Two categories that show obvious expansions from 4 ka BP are shrub steppe and desert scrub. These can be seen encroaching on forest areas and penetrating into river basins (i.e., Zerqa River, Wadi Hasa, Wadi Mujib). In Moab, the mixed shrub steppe-semi steppe batha transition category has virtually replaced semi steppe batha vegetation, indicating a return to more arid conditions. Along the Rift Valley, desert scrub has expanded towards the north.

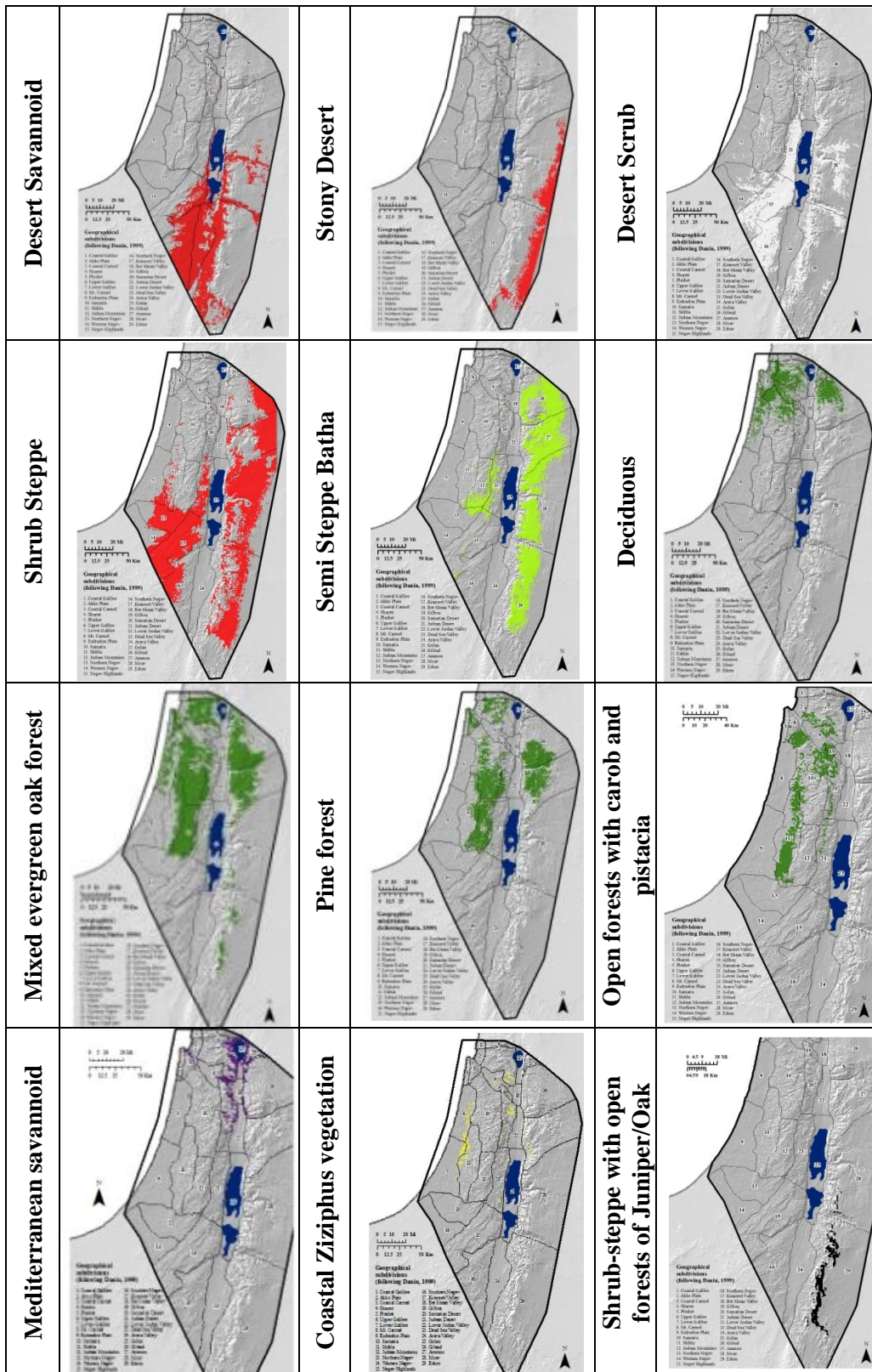
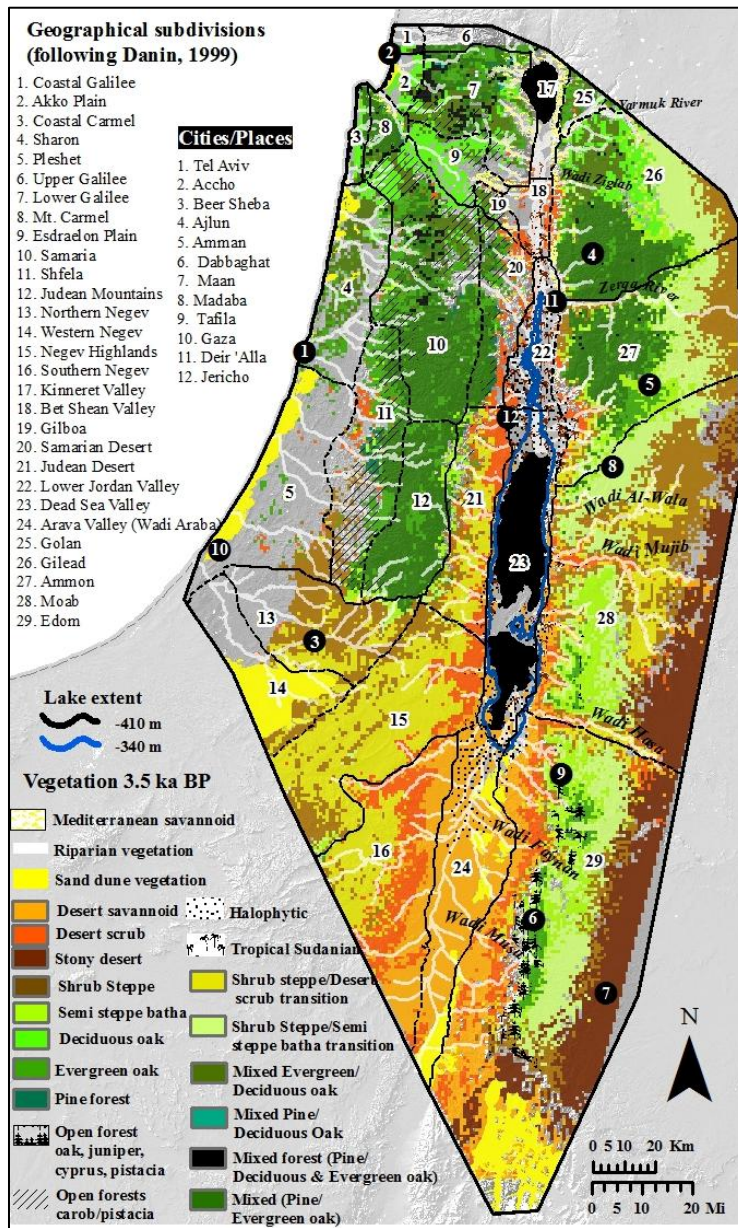


Figure 6.55 Suitable area in 3.5 ka BP per vegetation subcategory.



Map 6.17. Detailed vegetation map for 3.5 ka BP.

6.1.19 Model output for 3 ka BP

The results for the modeled plant geographic associations for 3 ka BP are given in Figure 6.56. The column on the left shows the area suitable for each of the main categories. These areas were combined to produce a 3 ka BP map of plant geographic associations (shown on the right).

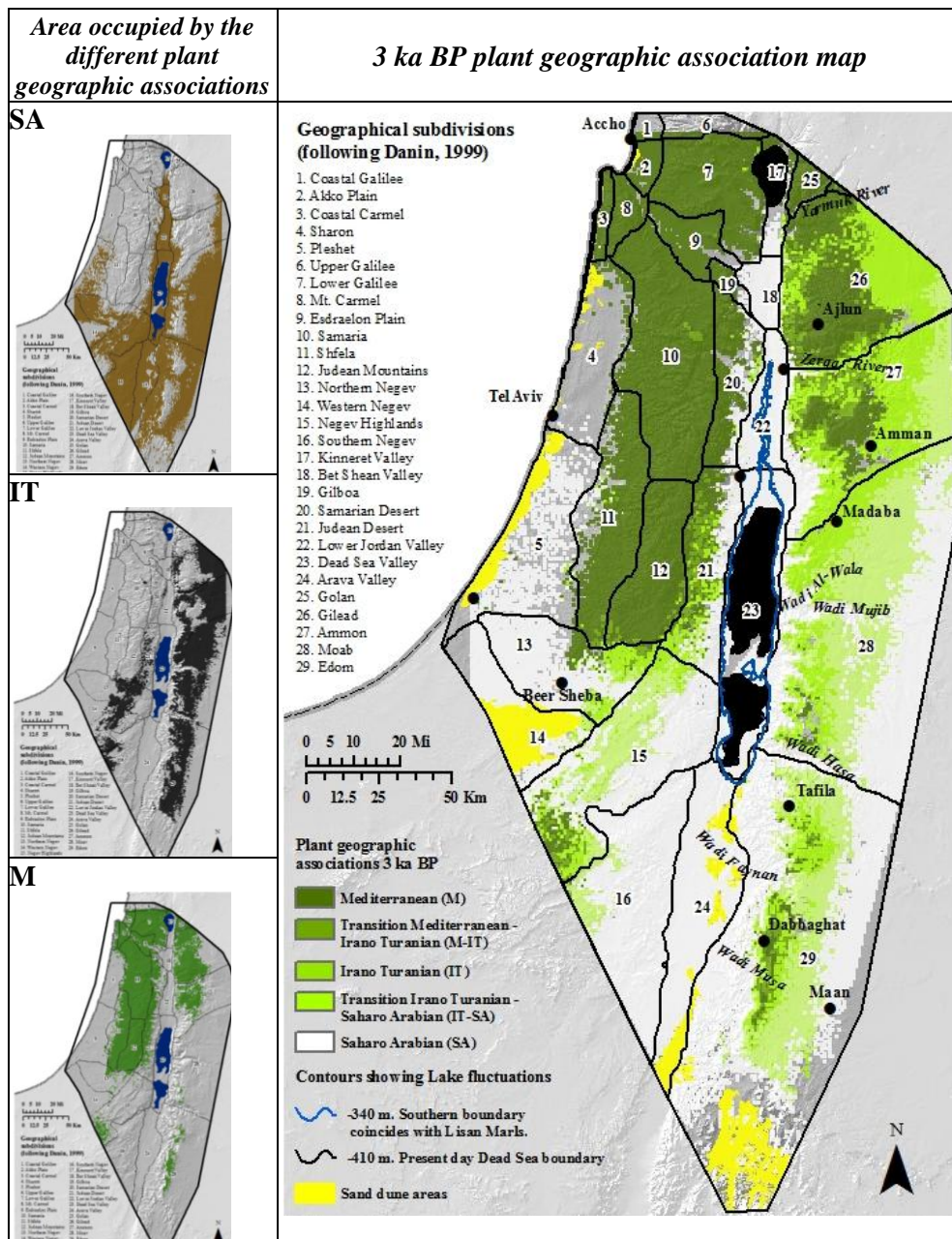


Figure 6.56. Vegetation model for 3 ka BP, by plant geographical association.

This period shows an obvious acceleration of the expansion of Saharo Arabian and retreat of Mediterranean region. The area suitable to Mediterranean in Moab and Edom has shrunk radically to its lowest coverage. The drier Saharo Arabian and IT-SA wrap around Mediterranean and IT areas throughout the whole study region.

The following figure (Figure 6.57) shows how the environmental conditions in 3 ka BP differed to those of the present. The first row shows where clamping has occurred. The second row shows the MESS maps. Increasing negative values show where extrapolation was greatest (darker shades of red). The figure on the right shows which variables were outside their training region in 3 ka BP (most dissimilar than those of the present), and responsible for extreme values seen in the MESS maps.

Only the Saharo Arabian category was slightly affected by clamping in the area immediately south of the Dead Sea. This was caused by temperatures that were slightly higher than those of the present.

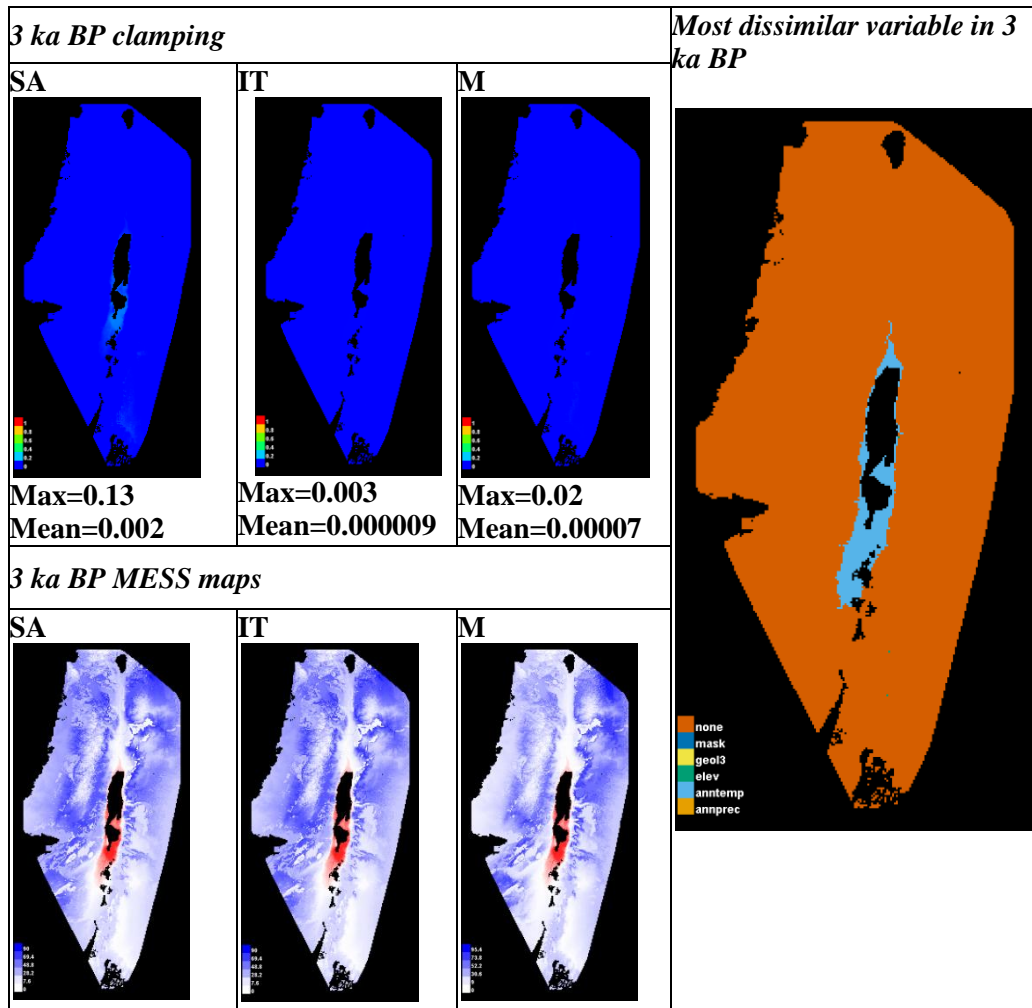


Figure 6.57. Clamping and MESS maps for 3 ka BP, taken from Maxent.

The following Figure 6.58 shows the area occupied by the different vegetation subcategories in 3 ka BP. These categories were combined to produce the following detailed vegetation map (Map 6.18).

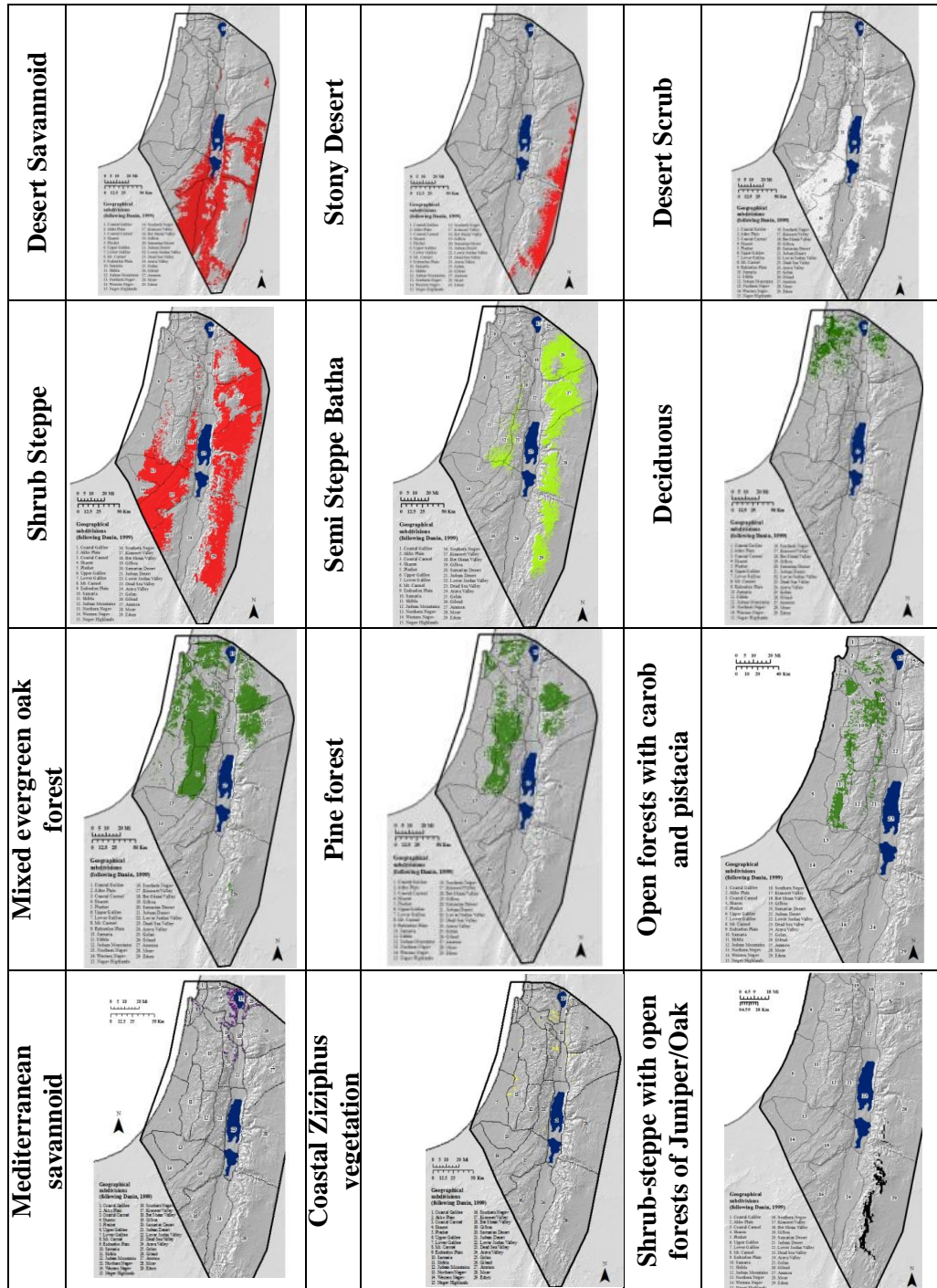
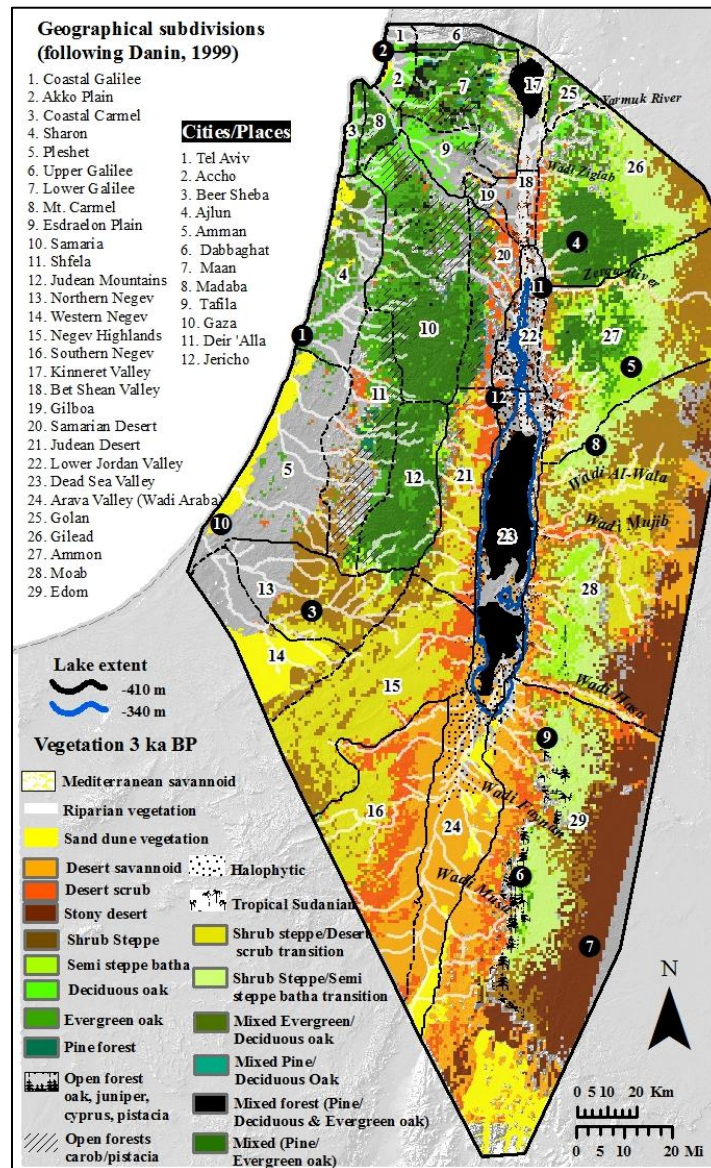


Figure 6.58. Suitable area in 3 ka BP per vegetation subcategory.



Map 6.18 Detailed vegetation map for 3 ka BP.

According to the vegetation models, the landscape was drier in 3 ka BP than it is at present. As a result, forest areas noticeably contracted once again. There are no longer areas suitable to the forest categories in Moab, and those of Edom have reduced substantially. The large forest patch in Gilead and Ammon has been split along the Zerqa River, which is now surrounded BP by steppe vegetation. Further north, the areas formerly occupied by deciduous oak forests represented by *Quercus ithaburensis* have nearly

disappeared. The same has occurred in the Esdraelon Plain, which was entirely represented by this category in previous dates. In a similar way, areas formerly occupied by the Mediterranean Savannoid and semi steppe batha categories have declined. The open forests of carob and pistacia continue to shift towards upland areas where conditions are moister.

At the same time, the drier categories continue to expand across the whole study area. On the southern portion of the plateau, stony desert vegetation expands into areas formerly covered by steppe. Further north, a mixture of this category along with shrub steppe/desert scrub transition vegetation and shrub steppe vegetation advances towards areas populated by semi steppe batha and forest vegetation. To the west of the Rift Valley and throughout the Negev, desert categories also expand and replace the few remaining patches of steppe vegetation that had been present in 4 ka BP.

6.1.20 Model output for 2.5 ka BP

The results for the modeled plant geographic associations for 2.5 ka BP are given in Figure 6.59. The column on the left shows the area suitable for each of the main categories. These areas were combined to produce a 2.5 ka BP map of plant geographic associations (shown on the right).

Out of all the periods modeled in this study, 2.5 ka BP appears to be the driest. Although all the subdistricts south of the Dead Sea including the Negev and plateau have not changed from 3 ka BP, the Mediterranean association throughout the northern portion of the study area has once again slightly contracted.

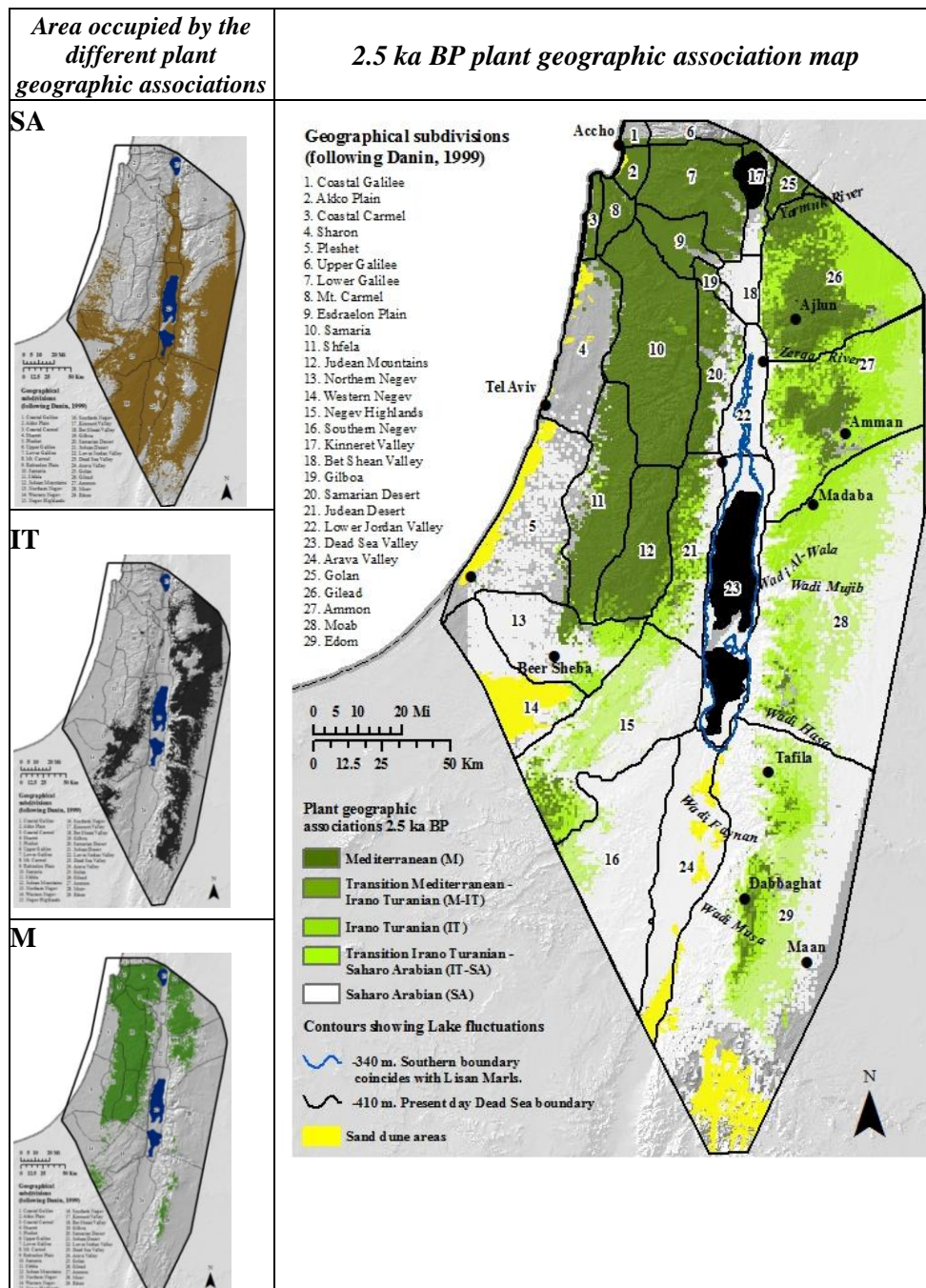


Figure 6.59. Vegetation model for 2.5 ka BP, by plant geographic association.

Figure 6.60 shows how the environmental conditions in 2.5 ka BP differed to those of the present. The first row shows where clamping has occurred. The second row shows the MESS maps. Increasing negative values show where extrapolation was

greatest (darker shades of red). The figure on the right shows which variables were outside their training region in 2.5 ka BP (most dissimilar than those of the present), and responsible for extreme values seen in the MESS maps.

Only the Saharo Arabian category was moderately affected by clamping in the area immediately south of the Dead Sea. This was caused by temperatures which were above those at the present used for training the model.

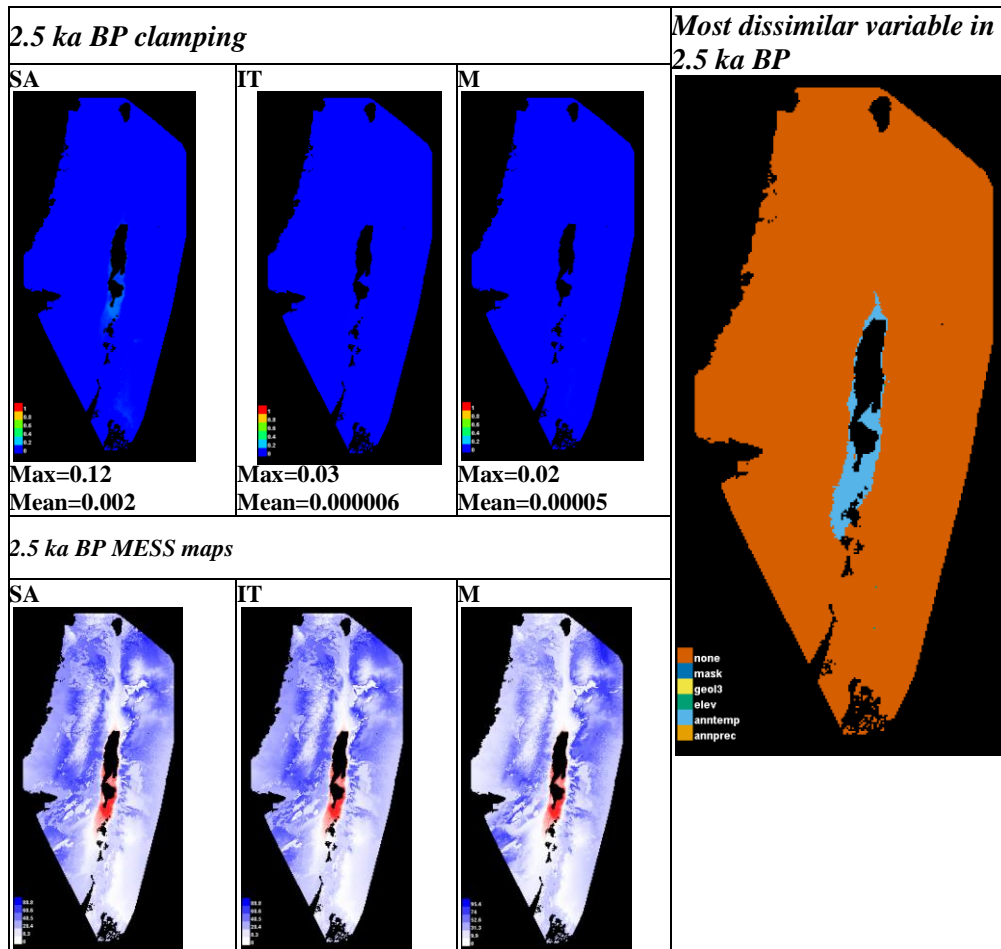


Figure 6.60. Clamping and MESS maps for 2.5 ka BP, taken from Maxent.

Figure 6.61 shows the area occupied by the different vegetation subcategories in 2.5 ka BP, after the threshold that maximizes the sum of sensitivity plus specificity was applied. These categories were combined to produce the following detailed vegetation map (Map 6.19).

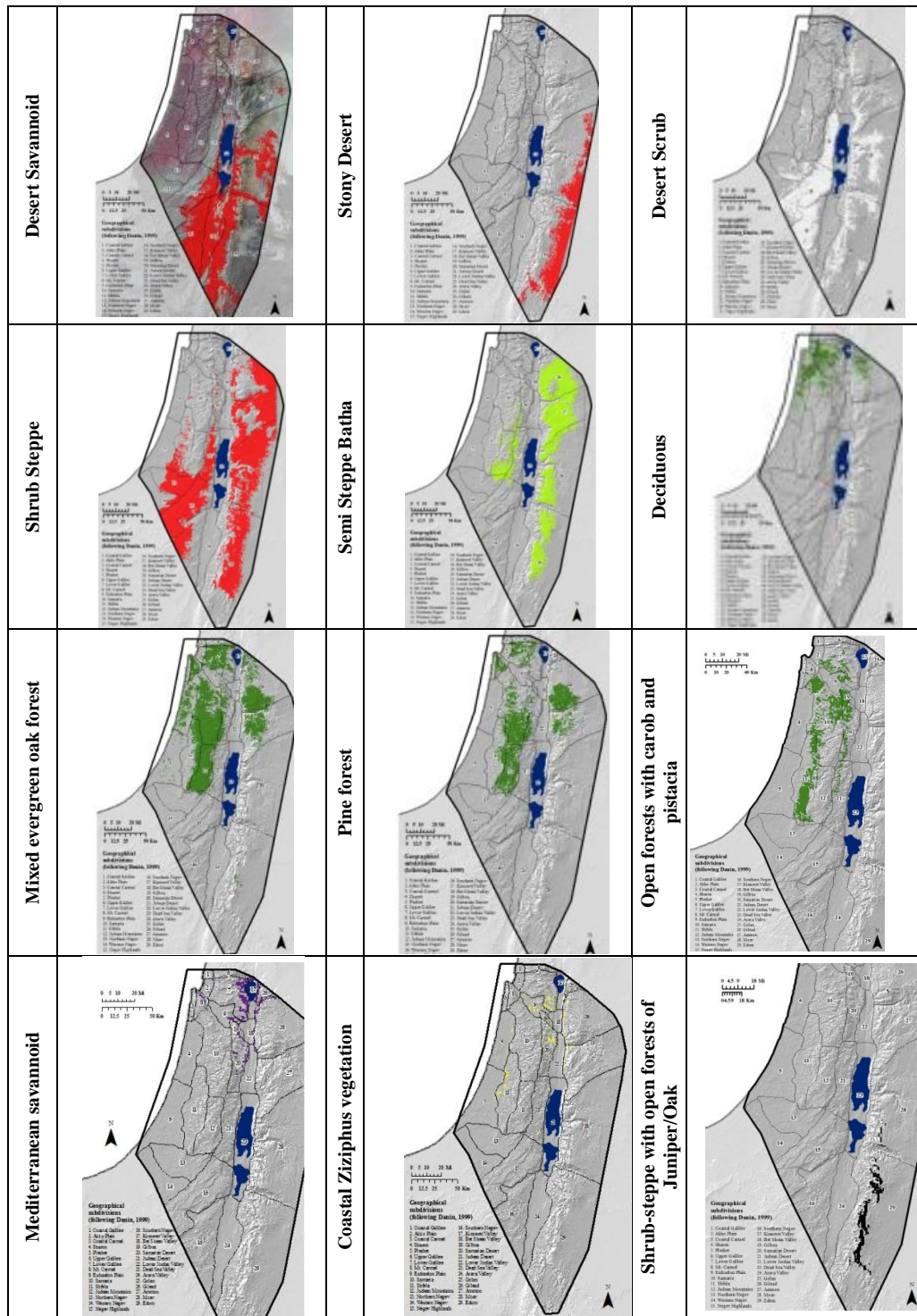
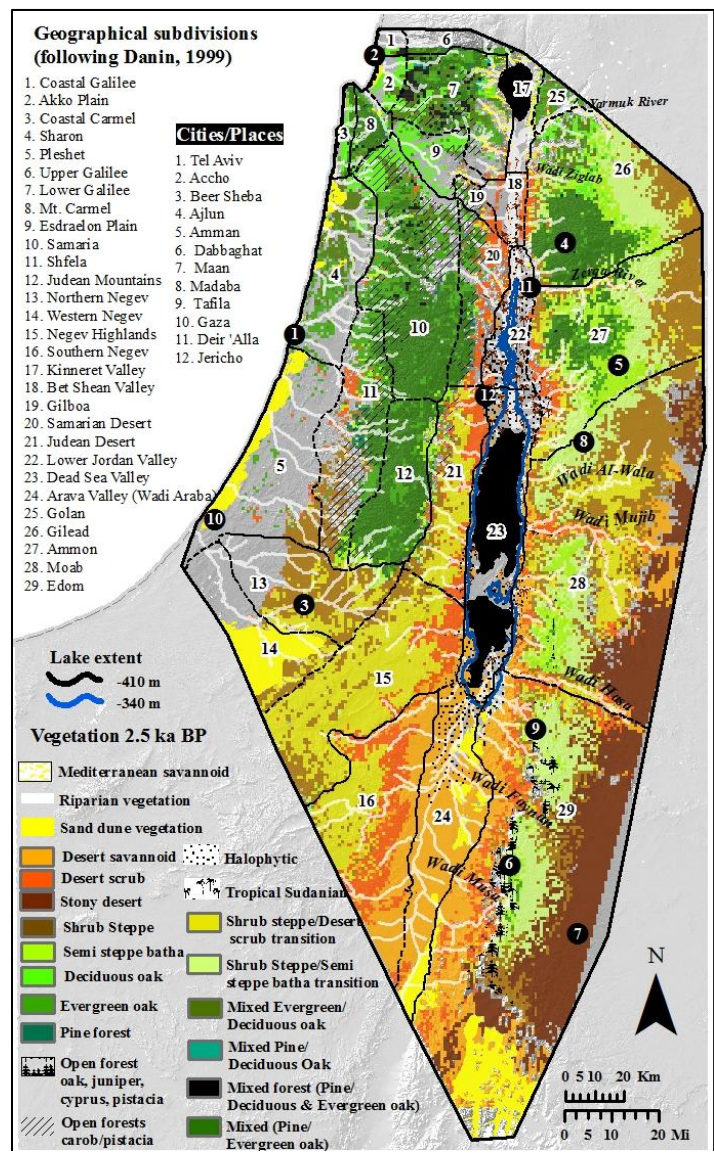


Figure 6.61. Suitable area in 2.5 ka BP per vegetation subcategory.

This map is in agreement with the map by plant geographic associations. It shows a progressive retreat of forests matched by an increase in the area occupied by desert and

steppe. However, the changes seen from 3 to 2.5 ka BP do not appear to be in the same magnitude as the changes observed from 4 to 3 ka BP. In fact, the deciduous forest has once again slightly expanded and shifted southwards. The category of open forests of carob and pistacia also expanded in all directions. The areas suitable to semi steppe batha vegetation have not changed since the previous period. Stony desert vegetation, on the other hand, has continued to expand. The same has happened to the desert scrub and shrub steppe categories.



6.2 Vegetation trends and comparison against proxy records

When looking at the vegetation models from the LatePleistocene-Holocene transition until the Late Holocene, a gradual aridification trend is detected. Gradually, areas suitable to forest categories are contracting while desert vegetation expands. However, this trend has not occurred at a regular pace, since some periods have appeared as stable (from the previous period), others have seen only slight forest contractions, and several have even experienced a reversal to this trend. These patterns are summarized in Table 6.2.1 (they are color coded, to facilitate interpretation).

Period (ka BP)	Change observed from previous period
11.5	Forest contraction
11	Significant forest contraction
10.5	Significant forest expansion
10	Slight forest contraction
9.5	Significant forest contraction
9	Stable period
8.5	Slight forest contraction
8	Slight forest contraction
7.5	Significant forest contraction
7	Slight forest contraction
6.5	Significant forest contraction
6	Slight forest contraction
5.5	Stable period
5	Stable period
4.5	Forest contraction
4	Significant forest expansion
3.5	Significant forest contraction
3	Significant forest contraction
2.5	Slight forest contraction

Table 6.1. Forest trend detected from 12 to 2.5 ka BP.

A comparison between the vegetation models and proxy records is shown in Tables 6.2 and 6.3. Those records that provide information regarding the state of vegetation are compared against the model outputs presented in Table 6.3. For the most part, the models agree with the records although there are a few exceptions. These are discussed in the following chapter.

Table 6.2. Proxy records throughout the study area and model outputs.

Geologic Period	Cultural period	Yr ka BP	POLLEN							OTHER PROXY										Dead Sea Level		Model prediction																																																	
			Hula Basin (1)	E.Medit. Sea (2)	Wadi Faynan, S. Jordan(3)	W Dead Sea (5)	W Dead Sea (6)	Dor Lagoon, Carmel	Soil, coast (8)	Ghab, NW Syria (9)	Wadi Faynan, S. Jordan(10)	SW shore of Dead Sea (11)	Soreq Cave Speleothem (12)	Soreq Cave Speleothem (13)	Cave Speleothem (14)	N.Negev Molluscs (15)	N.Negev Molluscs (16)	Beidha, S Jordan plateau (17)	Stein et al. 2010	Migo ws ki et al. 2004																																																			
Late Epipaleolithic ca. 15.2-10	Natufian (12.5-10.2)	12	<p>Low AP, high Artemisia, Rivers flowing Cold with some precip.</p> <p>Wet & warm. Decid oak peak 8.8. Between 300-1200 m asl, mean ann prec 800-1200. Avg ann T 15°C.</p> <p>Steppe & steppe veg forest with oak, pine, juniper, cypress, olive, elm, hop-hornbeam in vicinity (plateau). Wet.</p> <p>Arid event ~8.1</p> <p>Perennial rivers around area, increase in rainfall</p>	<p>High AP, high Artemisia, Rivers flowing Cold with some precip.</p>	<p>Wet & warm. Decid oak peak 8.8. Between 300-1200 m asl, mean ann prec 800-1200. Avg ann T 15°C.</p>	<p>Steppe & steppe veg forest with oak, pine, juniper, cypress, olive, elm, hop-hornbeam in vicinity (plateau). Wet.</p>	<p>Perennial streams in S. Jordan Wet</p>	<p>Soil, coast (8)</p>	<p>Ghab, NW Syria (9)</p>	<p>Wadi Faynan, S. Jordan(10)</p>	<p>SW shore of Dead Sea (11)</p>	<p>Soreq Cave Speleothem (12)</p>	<p>Soreq Cave Speleothem (13)</p>	<p>Cave Speleothem (14)</p>	<p>N.Negev Molluscs (15)</p>	<p>N.Negev Molluscs (16)</p>	<p>Beidha, S Jordan plateau (17)</p>	<p>Stein et al. 2010</p>	<p>Migo ws ki et al. 2004</p>	<p>Model prediction</p>																																																			
		11.5																			11	10.5	10	9.5	9	8.5	8	7.5	7																																										
Early Holocene (10-7.5 ka)	10.3-9.2 PPNA	10																			<p>Low AP, high Artemisia, Rivers flowing Cold with some precip.</p>	<p>Wet & warm. Decid oak peak 8.8. Between 300-1200 m asl, mean ann prec 800-1200. Avg ann T 15°C.</p>	<p>Steppe & steppe veg forest with oak, pine, juniper, cypress, olive, elm, hop-hornbeam in vicinity (plateau). Wet.</p>	<p>Perennial streams in S. Jordan Wet</p>	<p>Soil, coast (8)</p>	<p>Ghab, NW Syria (9)</p>	<p>Wadi Faynan, S. Jordan(10)</p>	<p>SW shore of Dead Sea (11)</p>	<p>Soreq Cave Speleothem (12)</p>	<p>Soreq Cave Speleothem (13)</p>	<p>Cave Speleothem (14)</p>	<p>N.Negev Molluscs (15)</p>	<p>N.Negev Molluscs (16)</p>	<p>Beidha, S Jordan plateau (17)</p>	<p>Stein et al. 2010</p>	<p>Migo ws ki et al. 2004</p>	<p>Model prediction</p>																																		
		9																																				8.5	8	7.5	7																														
9.3-7.5 PPNB	7.5-6.5 Pottery Neolithic (Ceramic Neolithic)	9																																				<p>Low AP, high Artemisia, Rivers flowing Cold with some precip.</p>	<p>Wet & warm. Decid oak peak 8.8. Between 300-1200 m asl, mean ann prec 800-1200. Avg ann T 15°C.</p>	<p>Steppe & steppe veg forest with oak, pine, juniper, cypress, olive, elm, hop-hornbeam in vicinity (plateau). Wet.</p>	<p>Perennial streams in S. Jordan Wet</p>	<p>Soil, coast (8)</p>	<p>Ghab, NW Syria (9)</p>	<p>Wadi Faynan, S. Jordan(10)</p>	<p>SW shore of Dead Sea (11)</p>	<p>Soreq Cave Speleothem (12)</p>	<p>Soreq Cave Speleothem (13)</p>	<p>Cave Speleothem (14)</p>	<p>N.Negev Molluscs (15)</p>	<p>N.Negev Molluscs (16)</p>	<p>Beidha, S Jordan plateau (17)</p>	<p>Stein et al. 2010</p>	<p>Migo ws ki et al. 2004</p>	<p>Model prediction</p>																	
		8																																																					7.5	7															
7.5-6.5 Pottery Neolithic (Ceramic Neolithic)	7.5-6.5 Pottery Neolithic (Ceramic Neolithic)	7																																																					<p>Low AP, high Artemisia, Rivers flowing Cold with some precip.</p>	<p>Wet & warm. Decid oak peak 8.8. Between 300-1200 m asl, mean ann prec 800-1200. Avg ann T 15°C.</p>	<p>Steppe & steppe veg forest with oak, pine, juniper, cypress, olive, elm, hop-hornbeam in vicinity (plateau). Wet.</p>	<p>Perennial streams in S. Jordan Wet</p>	<p>Soil, coast (8)</p>	<p>Ghab, NW Syria (9)</p>	<p>Wadi Faynan, S. Jordan(10)</p>	<p>SW shore of Dead Sea (11)</p>	<p>Soreq Cave Speleothem (12)</p>	<p>Soreq Cave Speleothem (13)</p>	<p>Cave Speleothem (14)</p>	<p>N.Negev Molluscs (15)</p>	<p>N.Negev Molluscs (16)</p>	<p>Beidha, S Jordan plateau (17)</p>	<p>Stein et al. 2010</p>	<p>Migo ws ki et al. 2004</p>	<p>Model prediction</p>
		6.5																																																																					

Table 6.3. Model Comparison against proxy records.

Geologic Period	Cultural Period	Year BP	Location (Name, lat, long, elev)	Reference	Vegetation inferred from pollen	Model prediction	Model agreement
Pleistocene - Holocene Transition	Natufian	12000	Ghab 240m asl 35°39'N, 36°15'E	Yasuda et al. 2000	High NAP (chenopodiacea and grasses).	Extensive forest.	No
		11500	Ghab 240m asl 35°39'N, 36°15'E	Yasuda et al. 2000	High NAP (chenopodiacea and grasses).	Extensive forest, although forest contracts and steppe expands from last period.	No
		11000	Northern Negev 31°16'N, 34°47'E	Goodfriend 1990	C3 is believed to have occupied considerable parts of the Negev	Forest categories found throughout most of the N.Negev.	Yes
			Hula Basin, 182m asl, 33°10'N, 35°35'E	Van et al. 2009	Low AP, high Artemisia, Rivers flowing.	Extensive forest.	No
		10500	Northern Negev 31°16'N, 34°47'E	Goodfriend 1990	C3 is believed to have occupied considerable parts of the Negev	Forest categories found throughout most of the No. Negev.	Yes
			Hula Basin, 182m asl, 33°10'N, 35°35'E	Van et al. 2009	Low AP, high Artemisia, Rivers flowing.	Extensive forest and Mediterranean Savannoid vegetation.	No
Early Holocene	PPNA	10000	Northern Negev 31°16'N, 34°47'E	Goodfriend 1990	C3 is believed to have occupied considerable parts of the Negev	Forest categories found throughout northern half of the Negev.	Yes
			Eastern Mediterranean Sea	Rossignol-Strick 1995	Pistacia phase. Extensive AP (oak and pistacia)	Extensive forests with <i>Quercus ithaburensis</i> , <i>Q. calliprinos</i> , <i>P. halepensis</i> .	Yes
			Hula Basin, 182m asl, 33°10'N, 35°35'E	Van et al. 2009	Rise in AP (mostly <i>Q. ithaburensis</i> & some <i>Q. calliprinos</i> , olive, pistacia), drop in herb pollen, chenopod & Artemisia. Dense forest.	Extensive forests with <i>Quercus ithaburensis</i> , <i>Q. calliprinos</i> , <i>P. halepensis</i> .	Yes
			Wadi Faynan, ca. 170m asl, 30°37'E, 35°27'E	Hunt et al. 2004	Steppe & riparian veg. forest with oak, pine, juniper, cypress, olive, elm, hop-hornbeam in vicinity (plateau).	Extensive forests with <i>Quercus ithaburensis</i> , <i>Q. calliprinos</i> , <i>P. halepensis</i> , <i>Juniperus phoenicia</i> .	Yes
			Dor Lagoon, Carmel Coast, 1m asl, 32°36'N, 34°55'E	Kadosh et al. 2004	Swampy environment. Extensive <i>Q. calliprinos</i> and some <i>Q. ithaburensis</i> in vicinity.	Coast is mainly represented by <i>Q. calliprinos</i> and <i>Q. ithaburensis</i> .	Yes
	PPNA	9500	Northern Negev 31°16'N, 34°47'E	Goodfriend 1990	C3 is believed to have occupied considerable parts of the Negev	Northward retreat of forest in the N. Negev, although they still occupy parts of this area.	Yes
			Eastern Mediterranean Sea	Rossignol-Strick 1995	Pistacia phase. Extensive AP (oak and pistacia)	Extensive forests with <i>Quercus ithaburensis</i> , <i>Q. calliprinos</i> , <i>P. halepensis</i> .	Yes
			Dor Lagoon, Carmel Coast, 1m asl, 32°36'N, 34°55'E	Kadosh et al. 2004	Swampy environment. Extensive <i>Q. calliprinos</i> and some <i>Q. ithaburensis</i> in vicinity.	Coast is mainly represented by <i>Q. calliprinos</i> and <i>Q. ithaburensis</i> .	Yes
			Hula Basin, 182m asl, 33°10'N, 35°35'E	Van et al. 2009	Rise in AP (mostly <i>Q. ithaburensis</i> & some <i>Q. calliprinos</i> , olive, pistacia), drop in herb pollen, chenopod & Artemisia. Dense forest.	Extensive forests with <i>Quercus ithaburensis</i> , <i>Q. calliprinos</i> , <i>P. halepensis</i> .	Yes
			Wadi Faynan, ca. 170m asl, 30°37'E, 35°27'E	Hunt et al. 2004	Steppe and forest. Wet.	Steppe & riparian veg. forest with oak, pine, juniper, cypress, olive, elm, hop-hornbeam in vicinity (plateau).	Yes

Table 6.3. (continued).

Geologic Period	Cultural Period	Year BP	Location (Name, lat, long, elev)	Reference	Vegetation inferred from pollen	Model prediction	Model agreement
Early Holocene	PPNB	9000	Northern Negev 31°16'N, 34°47'E	Goodfriend 1990	C3 is believed to have occupied considerable parts of the Negev	Forests extend into this region from the Judean Mountains. Mediterranean Region occupies about half this area.	Yes
			Eastern Mediterranean Sea	Rossignol-Strick 1995	Pistacia phase. Extensive AP.	Extensive forests with <i>Quercus ithaburensis</i> , <i>Q. calliprinos</i> , <i>P. halepensis</i> .	Yes
			Hula Basin, 182m asl, 33°10'N, 35°35'E	Van et al. 2009	Rise in AP (mostly <i>Q. ithaburensis</i> & some <i>Q. calliprinos</i> , olive, pistacia), drop in herb pollen, chenopod & <i>Artemisia</i> . Dense forest.	Extensive forests with <i>Quercus ithaburensis</i> , <i>Q. calliprinos</i> , <i>P. halepensis</i> .	Yes
			Wadi Faynan, ca. 170m asl, 30°37'E, 35°27'E	Hunt et al. 2004	Steppe and forest. Wet.	Steppe & riparian veg, forest with oak, pine, juniper, cypress, olive, elm, hop-hornbeam in vicinity (plateau).	Yes
			Dor Lagoon, Carmel Coast, 1m asl, 32°36'N, 34°55'E	Kadosh et al. 2004	Marsh dries up. Chenopodiaceae values increase.	Area still mainly represented by <i>Q. calliprinos</i> , <i>Q. ithaburensis</i> .	No
	PPNB	8500	Northern Negev 31°16'N, 34°47'E	Goodfriend 1990	C3 is believed to have occupied considerable parts of the Negev	Forests extend into this region from the Judean Mountains. Mediterranean Region occupies about half this area.	Yes
			Eastern Mediterranean Sea	Rossignol-Strick 1995	Pistacia phase. Extensive AP. Peak of deciduous oak ca. 8.8 BP.	Extensive forests with <i>Quercus ithaburensis</i> , <i>Q. calliprinos</i> , <i>P. halepensis</i> .	Yes
			Hula Basin, 182m asl, 33°10'N, 35°35'E	Van et al. 2009	Rise in AP (mostly <i>Q. ithaburensis</i> & some <i>Q. calliprinos</i> , olive, pistacia), drop in herb pollen, chenopod & <i>Artemisia</i> .	Extensive forests with <i>Quercus ithaburensis</i> , <i>Q. calliprinos</i> , <i>P. halepensis</i> .	Yes
			Wadi Faynan, ca. 170m asl, 30°37'E, 35°27'E	Hunt et al. 2004	Steppe and forest. Wet.	Steppe & riparian veg, forest with oak, pine, juniper, cypress, olive, elm, hop-hornbeam in vicinity (plateau).	Yes
			Dor Lagoon, Carmel Coast, 1m asl, 32°36'N, 34°55'E	Kadosh et al. 2004	Marsh dries up. Chenopodiaceae values increase.	Area still mainly represented by <i>Q. calliprinos</i> , <i>Q. ithaburensis</i> .	No
	PPNB	8000	Northern Negev 31°16'N, 34°47'E	Goodfriend 1990	C3 is believed to have occupied considerable parts of the Negev	Slight forest contraction and retreat of Mediterranean region.	Yes
			Wadi Faynan, ca. 170m asl, 30°37'E, 35°27'E	Hunt et al. 2004	An arid event is detected around 8.1.	Forests contract around the Wadi Faynan and W. Dana area.	Yes
			Hula Basin, 182m asl, 33°10'N, 35°35'E	Van et al. 2009	Drop in AP, mostly <i>Q. ithaburensis</i> & rise in herb and cereal pollen. Riparian pollen also drops.	Slight forest contraction and retreat of Mediterranean region.	No
			Negev Desert	Horowitz 1992	Significant expansion of the Negev Desert.	Slight forest contraction and retreat of Mediterranean region.	No
			Northern Negev 31°16'N, 34°47'E	Goodfriend 1990	the C3/C4 transition area was about 20 km further south than where it is at present.	The boundary of the Mediterranean region is found around this area.	Yes
Pottery Neolithic	7500	Negev Desert	Horowitz 1992	Significant expansion of the Negev Desert.	A significant contraction of the Mediterranean region and forest categories is observed, whereas the desert categories expand in the Negev Highlands.	Yes	
		Hula Basin, 182m asl, 33°10'N, 35°35'E	Van et al. 2009	AP/NAP ratios show moderate fluctuations. Slight rise of <i>Q. ithab.</i> Forests essentially composed of <i>Q. ithaburensis</i> - <i>P. atlantica</i> and have a more open character than before.	An increase of forests with <i>Q. ithaburensis</i> is detected	Yes	
		Northern Negev 31°16'N, 34°47'E	Goodfriend 1990	the C3/C4 transition area was about 20 km further south than where it is at present.	The boundary of the Mediterranean region is found around this area.	Yes	
Mid Holocene	Pottery Neolithic	7000	Negev Desert	Horowitz 1992	Significant expansion of the Negev Desert.	There is an expansion of shrub steppe into the shrub steppe/desert scrub vegetation of the Northern Highlands.	No

Table 6.3. (continued).

Geologic Period	Cultural Period	Year BP	Location (Name, lat, long, elev)	Reference	Vegetation inferred from pollen	Model prediction	Model agreement
Mid Holocene	Chalcolithic	6500	Ze'elim, Dead Sea 400m bsl 31°21' N 35°23'E	Neumann et al. 2007	Low AP (including olive) and high Chenopodiaceae. Arid.	Significant forest contraction	Yes
			Northern Negev 31°16'N, 34°47'E	Goodfriend 1990	the C3/C4 transition area was about 20 km further south than where it is at present.	The boundary of the Mediterranean region is found around this area.	Yes
	Chalcolithic	6000	Northern Negev 31°16'N, 34°47'E	Goodfriend 1990	the C3/C4 transition area was about 20 km further south than where it is at present.	The boundary of the Mediterranean region is found around this area.	Yes
			Wadi Faynan, ca. 170m asl, 30°37'E, 35°27'E	Hunt et al. 2004	Increase in rainfall detected in pollen record, however forests did not regenerate. Authors attribute this to human causes.	Forests are contracting around this area.	No
	Early Bronze Age	5500	Northern Negev 31°16'N, 34°47'E	Goodfriend 1990	the C3/C4 transition area was about 20 km further south than where it is at present.	The boundary of the Mediterranean region has significantly contracted.	No
			Hula Basin, 182m asl, 33°10'N, 35°35'E	Van et al. 2009	Drop in <i>Q. ithab</i> , steady rise in olive (orchard). Slight increase in <i>Artemisia</i> . The <i>Q.</i> callip curve remains steady during half this period and then drops, recovering towards the end.	Significant forest areas (e.g., Judan and Samarian mountains, Sharon coastal plain, Galilee region and plateau) are still predicted to be populated by the different forest categories.	Yes
	Early Bronze Age	5000	Northern Negev 31°16'N, 34°47'E	Goodfriend 1990	the C3/C4 transition area was about 20 km further south than where it is at present.	The boundary of the Mediterranean region has significantly contracted.	No
			Hula Basin, 182m asl, 33°10'N, 35°35'E	Van et al. 2009	Drop in <i>Q. ithab</i> , steady rise in olive (orchard). Slight increase in <i>Artemisia</i> . The <i>Q.</i> callip curve remains steady during half this period and then drops, recovering towards the end.	Significant forest areas (e.g., Judan and Samarian mountains, Sharon coastal plain, Galilee region and plateau) are still predicted to be populated by the different forest categories.	Yes
	Early Bronze Age	4500	Northern Negev 31°16'N, 34°47'E	Goodfriend 1990	the C3/C4 transition area was about 20 km further south than where it is at present.	The boundary of the Mediterranean region has significantly contracted.	No
			Hula Basin, 182m asl, 33°10'N, 35°35'E	Van et al. 2009	Drop in <i>Q. ithab</i> , steady rise in olive (orchard). Slight increase in <i>Artemisia</i> . The <i>Q.</i> callip curve remains steady during half this period and then drops, recovering towards the end.	Significant forest areas (e.g., Judan and Samarian mountains, Sharon coastal plain, Galilee region and plateau) are still predicted to be populated by the different forest categories.	Yes
	Middle Bronze Age	4000	Northern Negev 31°16'N, 34°47'E	Goodfriend 1990	the C3/C4 transition area was about 20 km further south than where it is at present.	Significant expansion of the Mediterranean region into this area.	Yes
			Hula Basin, 182m asl, 33°10'N, 35°35'E	Van et al. 2009	Drop in olive, notable rise in deciduous and evergreen oak (the last of which is unprecedented in the record). Slight rise in <i>Pistacia</i> , <i>Pinus</i> & <i>Vitis</i> .	Significant forest expansion.	Yes
			Ze'elim, Dead Sea 400m bsl 31°21' N 35°23'E	Neumann et al. 2007	Increase AP (olive), decrease chenopodiacea	Significant forest expansion.	Yes
	Late Holocene	Late Bronze Age	3500	W. Dead Sea. 285m bsl 31°32'N 35°23'E	Neumann et al. 2010	Low AP (e.g., pine, oak & cultivated olive), high herb pollen.	Significant forest contraction
W. Dead Sea 360m bsl 31°7'N 35°22'E.				Neumann et al. 2010	Increased chenopodiacea.	Significant forest contraction	Yes
Northern Negev 31°16'N, 34°47'E				Goodfriend 1990	the C3/C4 transition area was about 20 km further south than where it is at present.	The boundary of the Mediterranean region has significantly contracted.	No
Ein Feshka, Dead Sea 400m bsl 31°43'N 35°27'E				Neumann et al. 2007	Low AP in general, high herb pollen	Significant forest contraction	Yes
Iron Age		2500	Hula Basin, 182m asl, 33°10'N, 35°35'E	Van et al. 2009	Drop in <i>Q. itharubensis</i> (nearly disappears from record) and <i>Q. calliprinos</i> (not as dramatic). Increase in <i>Olea europea</i> .	Significant forest contraction	Yes

This chapter presented the results of the vegetation models according to plant geographic associations and detailed vegetation maps from the Pleistocene-Holocene transition until the Late Holocene, (12 – 2.5 ka BP) at 500 year intervals. From the Pleistocene-Holocene transition until the Early Holocene, the Mediterranean association (which consists of the various forest categories) occupied most of the study area. To the west of the Rift Valley, this category stretched into the Negev and occupied vast areas of the Negev Highlands. On the plateau, it formed a continuous belt from Gilead to Edom. The clamping surfaces and MESS maps indicate that during this time, climatic conditions were quite different to present day ones, with some areas receiving 2.5 times their present day annual average precipitation values (in the highland areas opposite the northern portion of the Rift Valley). Nevertheless, a gradual contraction of the Mediterranean association is seen throughout this time.

As forests continue their retreat throughout the Mid Holocene, the resulting vegetation maps begin to resemble their current distributions. This is confirmed by the clamping and MESS maps, which show increasingly similar climatic conditions with the modern climate surfaces used to train the model.

The most recent maps for 2.5 ka BP show a landscape that is more arid than the present day one (Maps 5.1 and 5.2). This stands in contrast to earlier periods when forests occupied vast areas while the more drought tolerant categories were mainly confined to the Arava Valley and outer edges of the plateau. In 2.5 ka BP, the desert and steppe categories have expanded onto the plateau from the Wadi Araba via drainage basins like Wadi Mujib and Wadi Hasa. These categories have also stretched into the Negev, where they occupy most of the area. The forests that were formerly widespread in the plateau have become extremely fragmented and remain as isolated patches.

Chapter 7

DISCUSSION

This chapter discusses the resulting paleovegetation models, within the context of what is known from the proxy records and ensuing paleoenvironmental history of the region. A comprehensive review of the cultural developments occurring during this time is beyond the scope of this work. Nevertheless, the major cultural developments are also discussed.

7.1 Environmental reconstruction and proxy records

The earliest paleovegetation models coincide with the Pleistocene-Holocene transition and partially overlap with the Younger Dryas (12.7-11.5 cal ka BP), a period that was supposedly much colder and drier than present (e.g., Bar-Mathews et al. 2003; Gvirtzman and Wieder 2001; Robinson et al. 2006; Yasuda et al. 2000). The intensity of this event, however, is debated (i.e., Stein et al. 2010). Counter evidence from raising lake levels (Stein et al. 2010), continuously flowing streams and rivers as suggested by high levels of pollen from riparian vegetation in the Hula (van Zeist et al. 2009), and a predicted mean annual precipitation of 550-750 mm/yr in the Judean Mountains suggests that environmental conditions were not as dry.

The paleovegetation models in 12 ka BP show a radically different vegetated landscape when compared to present. According to these, the Mediterranean plant geographic association and forest categories reach their greatest extent during this time. Through the next two periods (11.5 and 11 ka BP), the models show forest areas retreating, before expanding in 10.5 ka BP.

It should be noted that the clamping surfaces and MESS maps produced by Maxent from 12 to 10 ka BP reflect climatic conditions that are noticeably different to

those of the present (e.g., Figure 6.3). In other words, the values of the precipitation and temperature grids during this time along the mountainous regions (used for projecting the vegetation models) are outside of the range of the present day ones, which were used for training the models. As a result, projected vegetation along these areas should be interpreted with caution since they reflect the greatest uncertainty amongst model outputs.

At the same time, it is important to highlight that environmental conditions during this time (according to proxy records) were indeed supposed to be quite different to those of the present. Even if the Younger Dryas was not as dry and cold as some records suggest, it probably wasn't as forested as the models predict it to be during 12 and 11.5 ka BP. An interesting outcome observed in the models from 12 to 8.5 ka BP in low lying areas that were not impacted by clamping concerns the predicted suitable area of Mediterranean Savannoid vegetation, which reached its greatest extent during this time. This category includes grasses and cereals like wheat, oat, and barley, which were domesticated during this time.

From 11.5 to 10 cal ka BP, Bar-Mathews et al. (1997) detect an increase in precipitation around the Judean Mountains between 680-850 mm/yr. Meanwhile, Stein et al. (2010) found evidence of increasing aridity between 11 to 10 cal ka BP. The vegetation models for this time show a contraction of forest and expansion of steppe between 11.5 and 11 BP. Nevertheless, forests are still extensive, and reach the Northern Negev, which agrees with Goodfriend's findings of this region being occupied by C_3 plants during this time (1990).

Most proxy records agree that the Early Holocene (ca. 10-7.5 cal ka BP) was the warmest/wettest period experienced during the Holocene. Consequently, extensive deciduous forests are believed to have occupied Northern Israel (van Zeist et al. 2009).

The Carmel Coast was supposedly a swampy-forest environment with *Quercus calliprinos* and some *Q. ithaburensis* (Kadosh et al. 2004). In Southern Jordan, rivers were perennial and the plateau was covered by forests with oak, pine, juniper, cypress, and olive (Hunt et al. 2004; McLaren et al. 2004). In the Northern Negev, C₃ vegetation was extensive (Goodfriend 1990). After 10 ka BP (Pre-Pottery Neolithic), large settlements referred to as “proto towns” by Falconer and Fall (1995), appear in places like Jericho, ‘Ain Ghazal, and Basta in the Rift Valley and Plateau (Map 3.1).

The models produced in this study provide continuous coverage every 500 years. Like the proxy records, they suggest the Early Holocene was a wet period when the Mediterranean plant geographic association occupied a considerable portion of the study area. However, they also show fluctuations during this time. The most obvious is a contraction of forests and the Mediterranean region from 10 to 9.5 BP, and a more moderate forest contraction (and significant retreat of Mediterranean savanoid vegetation) from 9 to 8.5 BP. It is interesting to note that in the Dor Lagoon in the Carmel Coast, the record indicates a decrease in arboreal pollen and the drying of the swamp sometime between 9.4-8.5 cal ka BP (Kadosh et al. 2004). Further up on the plateau east of the Rift Valley, a decline in rainfall is detected to have occurred sometime around 8.5 BP. A cold arid event was reported in Spain between 8.6 and 8 ka (Leira and Santos 2002; Santos et al. 2000), and in the Levant during 8.2 (Robinson et al. 2006). This time period coincides with the abandonment of mega sites (Map 3.1) like ‘Ain Ghazal (on the Plateau just north of Amman) and Jericho in the Dead Sea Valley during the PPNB period (Bar-Yosef 2000) as well as settlements further south in the Wadi Araba and Plateau region (Gebel et al. 1988).

From 8 to 7.5 cal ka BP, the vegetation models show a significant contraction of the forest categories and Mediterranean association. After 8.1 cal ka BP, Hunt et al.

(2004) noticed a decline in precipitation. Between 8.4 and 7.9 cal ka BP, arboreal and riparian pollen from the Hula Basin declines (van Zeist et al. 2009). Soil analysis from the central coastal plains indicate a dry period between 7.4 and 7 which peaked around 7.2 cal ka BP (Gvirtzman and Wieder 2001). In southern Jordan, fluvial terrace analysis from Wadi Faynan indicates declining rainfall after 8.1 cal ka BP.

The models indicate that during the next three intervals (7, 6.5, 6), forests continue to retreat and the Mediterranean association continues to contract. The contraction observed from 7 to 6.5 is the most significant. It coincides with the transition from the Pottery Neolithic to the Chalcolithic cultural period. In the analysis of Dead Sea Cores (Neuman et al. 2007), this date also coincides with a decrease of arboreal pollen and an increase in chenopodiacea pollen which suggests increasing aridity. A salt layer believed to have been deposited in the Dead Sea between 7.5 and 5.5 also suggests arid conditions (Neev and Emery 1995). The speleothem record from the Soreq cave shows that after 7 cal ka BP, mean annual precipitation declined from 675-950 mm/yr (between 10-7 cal ka BP) to 450-580 mm/yr (Bar-Mathews et al. 1999). Contrary to these findings which signal a deterioration of environmental conditions, rivers continued to flow continuously in Southern Jordan until 6 cal ka BP. From their soil analysis in the central coastal plains, Gvirtzman and Wieder (2001) also detect a wet phase between 7-6.5 ka BP followed by an arid one which lasted from 6.5-5. According to the archaeological record, towns during ca. 8 to 5.5 ka BP were smaller and less aggregated (Fall et al. 2002). Presumably, people left the area during this time of climatic deterioration.

Between 7.4-3.2, Goodfriend estimates the transition area between C₃/C₄ vegetation to have been 20 km further south than where it presently stands (in other words, the 260 isohyet used to be where the 150 isoyet now is, which is just south of Beer Sheba and then curves towards the northeast encircling the Judean Desert). Besides the

predicted vegetation for 4 ka BP (discussed below), the models agree with this assumption only until 6 ka BP. After this date, the models suggest a northward retreat of the forest and Mediterranean region around this area.

After the moderate retreat of forests and the Mediterranean region from 6.5 to 6, the next two periods (5.5 and 5 ka BP) appear to have been relatively stable. Although increased aridity is detected to have occurred around 5 cal ka BP (Bar-Mathews et al. 2003) and two wet peaks are suggested during 4.8 and 4.7 cal ka BP (Gvirtzman and Wieder 2008 and Bar-Mathews et al. 2003, respectively), the period must have been relatively stable according to various pollen cores which suggest a decline in oak and pine but a steep increase in olive as a result of increased olive orchard cultivation (e.g., McLaren et al. 2004; van Zeist et al. 2009; Yasuda et al. 2000).

From 5 to 4.5 ka BP forests appear to recede once again. This is most obvious in the remaining forest patches in Moab and Edom. Gvirtzman and Wieder (2001) detect a dry phase in the central coastal plains between 4.6 to 4 cal ka BP. Bar-Mathews et al. (2003) report a decline in precipitation after a peak around 4.7 cal ka BP. Isaar and Zohar (2004) believe that the abandonment of settlements between 3300 – 3200 cal ka BP (EBIV) was caused by a long drought. Proxy records indicate that the climate was unfavorable, with signals of a pervasive drought appearing in many proxy records (Neumann et al. 2007, 2010).

From 4.5 to 4 ka BP, a complete reversal of the trend detected so far regarding forest contraction is seen. A significant expansion of forests, Mediterranean savannoid and steppe vegetation (Mediterranean and Irano Turanian regions) occurs throughout the whole study area. This is in agreement with higher lake levels (Migowski et al. 2004) and the Ze'elim Dead Sea core (Neuman et al. 2007), which detects improved climatic conditions. A decrease in chenopodiacea is matched by an increase in olive pollen. This

coincides with the Middle Bronze Age period, an extremely prosperous period that saw the rise of the first cities.

The predicted vegetation for 3.5 ka BP is almost identical to the 4.5 ka BP modeled output. From 4 ka BP, it signals deteriorating climatic conditions, reflected by shrinking forests. Pollen cores from the Dead Sea also record a decrease in forest vegetation and expansion of desert species (low arboreal pollen and high chenopidacea pollen). This model coincides with the beginning of the Late Bronze Age, a period of instability, when many sites were abandoned (Finkelstein 1989).

During the next two periods (3 and 2.5 ka BP), forest patches continue to shrink until they reach the lowest levels recorded in the study from 12 ka BP until 2.5 ka BP. The most dramatic change is seen from 3.5 to 3 ka BP, when the remaining forest patches in Edom and Moab almost disappear.

Chapter 8

CONCLUSION

8.1 Summary and Findings

In this study, robust models of present day vegetation and plant geographic associations have been created and then projected into 500 year intervals throughout the Holocene, to create continuous paleovegetation models. The vegetation models derived in this study suggest that there has been a gradual decline in rainfall that has progressively caused forest areas to retreat.

Although not at the intensity and magnitude of the glacial episodes that marked the Pleistocene, the Holocene has also experienced climatic events at a smaller scale. These appear to be cyclical, but the rate is debated. Dooze-Rolinski and others (2001) interpret from laminated cores in the Indian Ocean a dry phase every 100 to 200 years. Others suggest the occurrence of abrupt cooling events every 1,000 to 2,000 years (de Menocal 2001:668). The proxy records and archaeological evidence suggest that the Southern Levant has been impacted by both sudden and gradual shifts in climate throughout the Holocene. Although abrupt changes in vegetation were detected at some time intervals (significant forest contractions at 11; 9.5; 7.5; 6.5; 3.5; 3 ka BP and significant forest expansion at 10.5 and 4 ka BP), the remaining intervals were either stable or showed slight forest retreat. This observation may well be a result of the temporal resolution of the data. Unfortunately, because models were only generated at 500 year intervals, climatic episodes occurring at finer resolutions such as those detected by Bar-Matthews and Ayalon (2011) could not be assessed. What the models indicate instead is a general trend of increasing aridification which has only paused temporarily during stable periods or brief moments of forest expansion (10.5 and 4 ka BP).

Until 10 ka BP, forests are present throughout most of the study region, including the coastal plains and Negev Highlands. From 10 to 8 ka BP, they slightly contract, although they still spill into the Northern Negev and are found in the Negev Highlands. By 7.5 ka BP, they have significantly contracted from the Negev marginal areas.

A conceptual picture of extensive forests seems hard to imagine given the limited areas they occupy at present and the fact that some of these marginal areas are today desert. Nevertheless, proxy records and macrobotanical information support the view of extensive forests during the Early Holocene. Although extinct today, *Juniperus* was abundant in the Northern Negev region at the end of the Pleistocene (Baruch and Goring-Morris 1997). Furthermore, arboreal pollen from the Negev Highlands of *Quercus*, *Cupressus*, *Olea*, *Pistacia* and *Amygdalus* dated to ca. 11 to 8 ka BP has been found (Horowitz 1976, 1992). At present, this region contains a shrubby Irano Turanian understory with an open forest of *Pistacia atlantica* and *Amygdalus ramonensis*, which Danin considers to be a refugium of relict Mediterranean species. According to the vegetation models, this refugium significantly contracted after the Early Holocene.

Gradually, the forests contracted until they reached their lowest levels in 2.5 ka BP. Since the present day models of vegetation show a greater area that could potentially be occupied by forests, climatic conditions must have improved since 2.5 ka BP. Throughout the whole time period, only two reversals from this trend of forest contraction were detected, from 11 to 10.5 ka BP and from 4.5 to 4 ka BP. During the rest of the intervals, forests either contracted (slightly or significantly) or remained stable.

The places where forest contraction has been most dramatic is in the marginal areas which include the Negev Highlands, Judean Desert and Southern Plateau region. Al-Eisawi (1996) notes an extensive area throughout the Plateau which sits in between steppe and the remaining forest vegetation which is now subdivided into patches in the

north (Gilead and Ammon) and South (Edom), which he calls 'Non forest vegetation'. He also states how some authors believe this vegetation would regenerate into forest, if left undisturbed (Al-Eisawi 1996: 54). In their review of the forests of Jordan, Atkinson and Beaumont (1971) express the difficulty of assessing the potential contribution of climate change in the deterioration and contraction of the forests, given the long history of intensive use and exploitation. While some authors believe climate to have been influential, others disagree (Huntington 1911 and Lowdermilk 1953, respectively). This study shows that climate has played a significant role in the reduction of these forests.

8.2 Paleo vegetation models and how they fit into the cultural context

A departure from the cold and dry conditions of the last glacial period that prevailed for thousands of years to warmer temperatures and increased rainfall during what is known as the Bølling-Allerød interstadial would have allowed plant and animal populations like gazelle, wild goat and sheep to expand. This shift would have been welcome by the local inhabitants of the time, since it opened access into areas that were formerly unsuitable due to the harsh cold and dry conditions that would have made living conditions extremely difficult (Gilead 1998). Even if the climate cooled during the Younger Dryas, it probably wasn't in the same intensity as the last glacial period. Furthermore, rain exceeded modern levels (Bar-Mathews et al. 1996) causing riparian vegetation to thrive and the level of the Dead Sea to rise (Stein et al. 2010; van Zeist et al. 2009).

The expansion of forests and its accompanying resources towards the end of the Pleistocene is believed to have influenced the transition towards more permanent settlements and early farming endeavours with wild cereals during the Natufian (Henry 1997). What is clear from the vegetation models derived in this study is that from 12 to 9

ka BP, the study area is covered by forests and extensive Mediterranean Savannoid vegetation (which includes the cereals that were first farmed).

The agricultural developments and population explosion experienced during the Neolithic are believed by some authors to have been triggered by the climatic events that ensued during the Late Pleistocene and Early Holocene (Rossignol-Strick 1999; Yasuda et al. 2000). While the pervasive arid conditions are hypothesized to have facilitated the establishment of cereal grasses like emmer wheat and two-row barley through natural selection, the increased precipitation of the Early Holocene facilitated sedentary establishments.

From 10 to 8 ka BP, a series of large sites were established throughout the region, probably as a result of the favorable climatic conditions and available resources (water and food). From 10 to 9.5 ka BP, the models detect a significant contraction of forest areas. Nevertheless, the archaeological record indicates that the region was flourishing with large sites. If the models are accurate, they serve as an example of an environmental downturn that was not followed by the abandonment of settlements. It is also possible that this change did not significantly impact the population, since at this time humans were minimally impacting the landscape.

Between 8 and 5 ka BP, a drying trend has been detected in North Africa, the Levant, and Asia. In the eastern desert in Jordan, archaeological and geomorphological evidence suggests the drying phase began between 7-5 ka BP (Allison 1997). The models show significant forest contraction occurring at 7.5 and 6.5 ka BP. Both periods were preceded by slight episodes of forest retreat. By around 8 to 7.5 ka BP, many of the mega sites that had been established after 10 ka BP were abandoned. Evidence from one of these located in the northern Plateau ('Ain Ghazal) indicates the surrounding area was under pressure due to deforestation and grazing activities (Köhler-Rollefson 1988, 1992).

The climate appeared to stabilize and improve around 6 ka BP (Migowski et al. 2006). This coincides with the boom of the Egyptian and Mesopotamian Dynasties. Given the location of the study area between the two, it began to flourish once again during the Early Bronze Age as resources like copper and salt were mined around the Dead Sea region. The Early Bronze Age saw the rise of the first fortified towns. Towards the end of this period (Early Bronze IV) these towns were abandoned as a drought that lasted several centuries began. The models indicate that the period between 6 to 5 ka BP was a stable one. However, it shows a retreat of forests from 5 to 4.5 ka BP (two centuries prior the EBIV drought).

The Middle Bronze Age is known as a period of 'urban florescence' (Fall et al. 2002: 450), during which large towns flourish as population grows. The model shows significant forest expansion from 4.5 to 4 ka BP. This is followed by a reversal from 4 to 3.5, which coincides with the Late Bronze Age, a period of urban decline. During the next two phases (3 and 2.5 ka BP) forests continue to shrink, until they have almost disappeared in marginal areas like the southern Plateau and Negev Highlands.

8.3 Potential areas of improvement and future work

According to the diagnostic statistics, all of the modeled categories performed well. However, when comparing their present day resulting potential distributions against ancillary references, the categories of coastal *Ziziphus* vegetation and open forests of oak, juniper, cyprus and pistachio may not have been correctly characterized and should be further investigated.

One limitation in the detailed vegetation models is the assumption that wetlands have not changed, which is highly unlikely (Levin et al. 2009). Perhaps a way to improve

the model is to determine or establish some rate of wetland expansion and incorporate this into the model.

The next step in this research is to compile information regarding how humans modified the landscape throughout the Holocene. This is a gargantuan task, given the long history and prehistory of the region. Nevertheless, each cultural period can be summarized according to the major sites that were occupied. The activities they performed can be characterized through macrobotanical remains and pollen evidence, for example. This is an exciting avenue that will bring the dimension of human interaction with the landscape into the picture, and allow room for other interesting questions regarding land use change in the ancient Levant to be investigated.

REFERENCES

- Al-Eisawi, D. 1985. Vegetation in Jordan. In *Studies in the History and Archaeology of Jordan, II*, edited by A. Hadidi, pp. 465-473. Amman: Department of Antiquities.
- Al-Eisawi, D. 1996. *Vegetation of Jordan*. Cairo: UNESCO.
- Al-Eisawi, D., El-Oqlah A., Oran S., and Lahham J. 2000. Jordan Country Study on Biological Diversity: Plant Biodiversity and Taxonomy, edited by U. Publication. Amman.
- Allison, R.J. 1997. The Arabian Peninsula. In *Zone Geomorphology*, edited by D. S. G. Thomas. Chichester: Wiley.
- Allouche, O., A. Tsoar, and R. Kadmon. 2006. Assessing the accuracy of species distribution models: prevalence, kappa, and the true skill statistic (TSS). *Journal of Applied Ecology* 43 (6):1223 – 1232.
- Amiran, R. 1986. The fall of the Early Bronze age II city of Arad. *Israel Exploration Journal* 36:74–76.
- Anderson, R.P., M. Gomez-Laverde, and A.T. Peterson. 2002. Geographical distributions of spiny pocket mice in South America: Insights from predictive models. *Global Ecology and Biogeography* 11:131-141.
- Anderson, R.P., D. Lew, and A.T. Peterson. 2003. Evaluating predictive models of species' distributions: criteria for selecting optimal models. *Ecol. Model.* 162: 211–232.
- Araújo, M.B., and P.H. Williams. 2000. Selecting areas for species persistence using occurrence data. *Biological Conservation* 96:331–345.
- Araújo, M.B., P.H. Williams, and R.J. Fuller. 2002. Dynamics of extinction and the selection of nature reserves. *Proceedings of the Royal Society of London* 269:1970–1980.
- Arundel, S.T. 2005. Using spatial models to establish climatic limiters of plant species' distributions. *Ecological Modelling* 182:159-181.
- Arzt, J. 2003. Climate Change in Mesopotamia, 9000-3000 BC. Paper presented at the Annual Meeting of the Society for American Archaeology, Milwaukee, WI.
- Arzt, J. 2005. Climate and Settlement in the Jebel Abd al-Aziz, Syria: a comparison of the Yale Khabur Basin Project Survey and a model of the Holocene climate for Hasseke. Paper presented at the Annual Meeting of the Society for American Archaeology, Salt Lake City, UT.

- Aspinal, R. 1992. An inductive modeling procedure based on Bayes' theorem for analysis of pattern in spatial data. *International Journal of Geographic Information Systems* 6 (2):105-121.
- Atallah, S. 1977. Mammals of the eastern Mediterranean region, their ecology, systematics and zoogeographical relationships. *Saeugetierk Mitteilungen* 25:241-320.
- Atkinson, K., and P. Beaumont. 1971. The forests of Jordan. *Economic Botany* 25 (4):305-311.
- Austin, M.P. 1985. Continuum concept, ordination methods and niche theory. *Annual Review Ecological Systems* 16:39-61.
- Austin, M.P., A.O. Nicholls, M.D. Doherty, and J.A. Meyers. 1994. Determining species response functions to an environmental gradient by means of a beta function. *Journal of Vegetation Science* 5: 215–28.
- Baly, D. 1957. *The Geography of the Bible*. London: Lutteworth Press.
- Barry, S., and J. Elith. 2006. Error and uncertainty in habitat models. *Journal of Applied Ecology* 43:413–423.
- Bartov, Y. 1994. The geology of the Arava Valley. Israeli Geological Survey Report GSI/4/94, 16.
- Bartov, Y., S. Goldstein, M. Stein, and Y. Enzel. 2003. Catastrophic arid episodes in the eastern Mediterranean linked with North Atlantic Heinrich events. *Geology* 31: 439-442.
- Bartov, Y., Y. Enzel, N. Porat, and M. Stein. 2007. Evolution of the Late Pleistocene Holocene Dead Sea Basin from Sequence Stratigraphy of Fan Deltas and Lake-Level Reconstruction. *Journal of Sedimentary Research* 77 (9): 680-692.
- Baruch, U. 1986. The late Holocene vegetational History of Lake Kinneret (Sea of Galilee), Israel. *Paléorient* 12 (2):37–48.
- Baruch, U. 1990. Palynological evidence of human impact on the vegetation as recorded in late Holocene Lake sediments in Israel. In *Man's Role in the Shaping of the Eastern Mediterranean Landscape.*, edited by S. Bottema, G. Entjes-Nieborg and W. Van Zeist. Rotterdam: Balkema.
- Baruch, U. 1999. A new pollen diagram from Lake Hula—vegetational, climatic and anthropogenic implications. In *Ancient Lakes: Their Cultural and Biological Diversity.*, edited by H. Kawanabe, G. W. Coulter and A. C. Roosevelt. Belgium: Kenobi Productions.

- Baruch, U. and N. Goring-Moris. 1997. The arboreal vegetation of the Central Negev Highlands, Israel, at the end of the Pleistocene: evidence from archeological charred wood remains. *Vegetation History and Archeobotany*, 6: 249-259.
- Baruch, U., and S. Bottema. 1991. Palynological Evidence for Climatic Changes in the Levant ca. 17,000-9,000 B.P. In *The Natufian Culture in the Levant* edited by O. Bar-Yosef and F. R. Valla. Ann Arbor, MI: International Monographs in Prehistory.
- Bar-Matthews, M., and A. Ayalon. 2011. Mid-Holocene climate variations revealed by high-resolution speleothem records from Soreq Cave, Israel and their correlation with cultural changes. *The Holocene* 21 (1): 163-171.
- Bar-Matthews, M., A. Ayalon, and A. Kaufman. 1997. Late Quaternary Paleoclimate in the Eastern Mediterranean Region from stable isotope analysis of speleothems at Soreq Cave, Israel. *Quaternary Research* 47: 155–168.
- Bar-Matthews, M., A. Ayalon, M. Gilmour, A. Matthews, and C.J. Hawkesworth. 2003. Sea–land oxygen isotopic relationships from planktonic foraminifera and speleothems in the Eastern Mediterranean region and their implication for paleorainfall during interglacial intervals. *Geochimica et Cosmochimica Acta* 67: 3181–3199.
- Barrows et al. 2008. Using occurrence records to model historic distributions and estimate habitat losses for two psammophilic lizards. *Biological Conservation*. 141: 1885-1893.
- Barry et al. 2002. Modelling potential impacts of climate change on the bioclimatic envelope of species in Britain and Ireland. *Global Ecology and Biogeography* 11, 453-462.
- Barton, C. M., I. I. Ullah, and S. Bergin. 2010. Land use, water and Mediterranean landscapes: modelling long-term dynamics of complex socio-ecological systems. *Philosophical transactions. Series A, Mathematical, physical, and engineering sciences* 368 (1931): 5275-5297.
- Bar-Yosef, O. (1986). The walls of Jericho: An alternative interpretation. *Current Anthropology* 27: 157–162.
- Bar-Yosef, O., and A. Belfer-Cohen. 1992. From foraging to farming in the Mediterranean Levant. In *Transition to Agriculture in Prehistory.*, edited by A. G. Gebauer and T. D. Price. Madison, WI, Prehistory Press.
- Bell, A. 1971. The Dark Ages in Ancient History: I. The first Dark Age in Egypt. *American Journal of Archaeology* 75:1–26.
- Benito Garzón, M., R. Sánchez de Dios, and H. Sáinz Ollero. 2007. Predictive modelling of tree species distributions on the Iberian Peninsula during the Last Glacial Maximum and Mid-Holocene. *Ecography* 30 (1): 120-134.

- Benito, Blas M., M. Montserrat Martínez-Ortega, L. M. Muñoz, J. Lorite, and J. Peñas. 2009. Assessing extinction-risk of endangered plants using species distribution models: a case study of habitat depletion caused by the spread of greenhouses. *Biodiversity and Conservation* 18 (9): 2509-2520.
- BioGIS (Israel Biodiversity Information System Database) [http://habitat.bot.huji.ac.il/biogis/static/en/index.html].
- BioGIS. 2000. A. Danin's grid database. Israel Biodiversity Information System. [http://www.biogis.huji.ac.il] .
- BioGIS. 2002. Israel Nature and Parks Authority database. Israel Biodiversity Information System. [http://www.biogis.huji.ac.il].
- Boyko, H. 1954. A New Plant Geographical Subdivision of Israel, As an Example for Southwest Asia. *Vegetatio* 4/6 (1):309-318.
- Bradley, R.S. 1985. *Quaternary Paleoclimatology, Methods of palaeoclimatic reconstruction*. . Australia: Allen & Unwin Australia.
- Breiman, L. 2001. Random Forests. *Machine Learning* 45 (1): 5–32.
- Bryson, R.A. 1992. A macrophysical model of the Holocene Intertropical Convergence and Jetstream positions and rainfall for the Saharan region. *Meteorology and Atmospheric Physics* 47: 247-258.
- Bryson, R.A. 1997 Proxy Indications of Holocene Winter Rains in Southwest Asia Compared with Simulated Rainfall. In *Third Millenium BC Climate Change and Old World Collapse*, edited by H. N. Dalfes, G. Kukla and H. Weiss, pp. 465-473. vol. I 49. NATO ASI Series, Berlin.
- Bryson, R.A. and K. McEnaney-DeWall (eds) (2007). A Paleoclimatology Workbook: High Resolution, Site-Specific, Macrophysical Climate Modeling & Template CD. Mammoth Site of Hot Springs, SD, Hot Springs, SD. CCR #930.
- Bryson, R.A. and R.U. Bryson. 1997. Macrophysical climate modeling of Africa's Late Quaternary climate: site-specific, high-resolution applications for archaeology. *African Archaeological Reviews* 14(3): 143-160.
- Bryson, R. A., and R. U. Bryson. 1998. An Archaeoclimatology Workbook: High-Resolution, Site-Specific Climate Modeling for Field Scientists. Center for Climatic Research, University of Wisconsin-Madison and Department of Geology and Geophysics, University of Minnesota. University of Wisconsin, Madison.
- Bryson, R.A. and R.U. Bryson. 1999. Holocene climates of Anatolia: as simulated with archaeoclimatic modeling. *Türkyie Bilimer Akademisi Arkeoloji Dergisi* 2: 1-13.

- Bryson 2007. The Volcanic Record and Climatic Cycles. In A Paleoclimatology Workbook: High Resolution, Site-Specific, Macrophysical Climate Modeling, edited by R. A. Bryson and K. M. DeWall, pp. 137-140. The Mammoth Site, Hot Springs, SD.
- Brzeziecki, B., F. Kienast, and O. Wildi. 1993. A simulated map of the potential natural forest vegetation of Switzerland. *Journal of Vegetation Science* 4: 499-508.
- Buermann, S., S. Saatchi, T.B. Smith, Zutta B.R., J.A. Chaves, B. Milá, and C.H. Graham. 2008. Modeling distribution of Amazonian tree species and diversity using remote sensing measurements. *Remote Sensing of Environment* 112 (5):2000-2017.
- Buisson et al. 2010 Uncertainty in ensemble forecasting of species distribution. *Global Change Biology* 16:1145-1157.
- Busby, JR. (1986) Bioclimatic Prediction System (BIOCLIM) User's Manual Version 2.0 Australian Biological Resources Study Leaflet.
- Callaghan, R.T., 2003. Comments on the Mainland Origins of the Preceramic Cultures of the Greater Antilles. *American Archaeology* 14 (3): 323-338.
- Carnaval, A.C., and C. Moritz. 2008. Historical climate modeling predicts patterns of current biodiversity in the Brazilian Atlantic forest. *Journal of Biogeography* 35 (7):1187-1201.
- Carpenter, G., Gillson, A.N., and Winter. J. 1993. DOMAIN: a flexible modeling procedure for mapping potential distributions of plants and animals. *Biodiversity and Conservation* 2:667-680.
- Cibula, W., and M. Nyquist. 1987. Use of topographic and climatological models in a geographical data base to improve Landsat MSS classification for Olympic National Park. *Photogrammetric Engineering and Remote Sensing*, 53: 67-75.
- Cordova, C. 2008. Floodplain degradation and settlement history in Wadi al-Wala and Wadi ash-Shallalah, Jordan. *Geomorphology* 101 (3): 443-457.
- Corsi, F., J. de Leeuw, and A. Skidmore. 2000. Modeling species distributions with GIS. In *Research techniques in animal ecology*, edited by L. Boitani and T. K. Fuller. Columbia University Press, New York.
- Cramer, J.S. 2003. *Logit models from economics and other fields*. Cambridge: Cambridge University Press.
- Danin, A. 1970. A Phytosociological-Ecological study of the Northern Negev of Israel. The Hebrew University (Hebrew). Jerusalem.
- Danin, A. 1983. *Desert vegetation of Israel and Sinai*. Jerusalem: Cana Pub. House.

- Danin, A. 1988. Flora and vegetation of Israel. In *The zoogeography of Israel*, edited by Y. Yom-Tov and E. Tchernov. Dordrecht, Netherlands: Dr. Junk.
- Danin, A. 1991. Synanthropic flora of Israel. *Flora et Vegetatio Mundi* 9: 95–103.
- Danin, A. 1995. Man and the natural environment. In *The Archaeology of Society in the Holy Land*, edited by T. E. Levy. London: Leicester University Press.
- Danin, A. 1996. Plants of desert dunes. In *Adaptations of desert organisms*. Berlin: Springer-Verlag.
- Danin, A. 1999. Desert rocks as plant refugia in the Near East. . *Botanical Review* 65 (2):93-170.
- Danin, A. 2001. Near East ecosystems, plant diversity. In *Encyclopedia of Biodiversity*, ed. S. Levin, Academic, edited by S. Levin. New York: Academic Press.
- Danin, A. 2004. *Distribution Atlas of Plants in the Flora Palaestina Area*: The Israeli Academy of Sciences and Humanities.
- Danin, A. (ed.) 2006. Continuously updated, Flora of Israel online. The Hebrew University of Jerusalem, Jerusalem, Israel. Published at <http://flora.huji.ac.il/browse.asp>, accessed frequently from 2008 to 2011.
- Danin, A., Plitmann, U. 1987. Revision of the plant geographical territories of Israel and Sinai. *Plant Systematics and Evolution* 150:43-53.
- Davies, C.P., and P.L. Fall. 2001. Modern pollen precipitation from an elevational transect in central Jordan and its relationship to vegetation. *Journal of Biogeography* 28:1195-1210.
- Davis, M. 1978. Climatic interpretations of pollen in quaternary sediments. In *Biology and Quaternary Environments*, edited by D. Walker and J. C. Guppy, pp. 35-51. Melbourne: Australian Academy of Sciences.
- Dever, W.G. 1989. The collapse of the urban Early Bronze age in Palestine: toward a systematic analysis. In *L'urbanisation de la Palestine à l'âge du Bronze Ancien*, edited by P. de Miroschedji. Oxford: BAR International Series.
- Dormann, Carsten F, Oliver Purschke, Jaime R García Márquez, Sven Lautenbach, and Boris Schröder. 2008. Components of uncertainty in species distribution analysis: a case study of the Great Grey Shrike. *Ecology* 89 (12): 3371-86.
- Eig, A. 1927. On the Vegetation of Palestine. In *Institute Agricultural Natural History Rehovot*. Tel-Aviv: Zionist Organisation. Institute of Agriculture and Natural History. Division of Biology.

- Eig,A. 1931-1932. Les elements et les groupes phytogeographiques auxiliaires dans la flore Palestinienne. Feddes Repert. *Spec. Nov. Reg. Veg. Beih.* 63(1): 1-201; 63(2) 1-120.
- Eig,A. 1938. On the pytogeographical subdivision of Palestine. *Palestine Journal of Botany* 1:4-12.
- Eig,A. 1946. Synopsis of the phytosociological units of Palestine. *Palestine Journal of Botany* 3:183-284.
- Elith, J. 2008. Species Distribution Modelling for Threatened Species Map Updates - Parts 1 and 2. In *Consultancy report for the Department of Environment, Water, Heritage and the Arts*.
- Elith, J. and M.A. Burgman. 2003. Habitat models for population viability analysis. In *Population viability in plants*, edited by C. A. Brigham and M. W. Schwartz, pp. 203-205. Springer-Verlag, New York.
- Elith J, and C. Graham. 2009. Do they? How do they? WHY do they differ? . . . on finding reasons for differing performances of species distribution models. *Ecography* 32:66–77
- Elith, J, and J Leathwick. 2009. Conservation prioritisation using species distribution models. Ed. Moilanen. *Spatial conservation prioritization: quantitative methods and computational tools*. Oxford University Press.
- Elith, J., C. Graham, R.P. Anderson, M. Dudi'k, S. Ferrier, A. Guisan, R.J. Hijmans, F. Huettmann, J. Leathwick, A. Lehmann, J. Li, L.G. Lohmann, B.A. Loiselle, G. Manion, C. Moritz, M. Nakamura, Y. Nakazawa, J.M. Overton, A.T. Peterson, S.J. Phillips, K. Richardson, R. Scachetti-Pereira, R. Schapire, J. Soberon, S.E. Williams, M.S. Wisz, and N.E. Zimmermann. 2006. Novel methods improve prediction of species' distributions from occurrence data. *Ecography* 29 (2):129-151.
- Elith, Jane, Michael Kearney, and Steven Phillips. 2010. The art of modelling range-shifting species. *Methods in Ecology and Evolution* 1 (4): 330-342
- Elith, Jane, Steven J. Phillips, Trevor Hastie, Miroslav Dudík, Yung En Chee, and Colin J. Yates. 2011. A statistical explanation of MaxEnt for ecologists. *Diversity and Distributions* 17, no. 1 (25): 43-57.
- Elith, J., and J. Leathwick. 2007. Predicting species' distributions from museum and herbarium records using multiresponse models fitted with multivariate adaptive regression splines. *Diversity and Distributions* 13:165-175.
- Elith, J., and J. Leathwick. 2009. Conservation prioritisation using species distribution models. In *Spatial conservation prioritization: quantitative methods and computational tools*, edited by Moilanen, Wilson and Possingham: Oxford University Press.

- Elith, J., and J. Leathwick. 2009. Species Distribution Models: Ecological Explanation and Prediction Across Space and Time. *Annual Review of Ecology, Evolution, and Systematics* 40 (1): 677-697.
- Enzel, Y., L.L. Ely, S. Mishra, R. Ramesh, R. Amit, B. Lazar, S.N. Rajuguru, V.R. Baker, and A. Sandler. 1999. High-resolution Holocene environmental changes in the Thar Desert, northwestern India. *Science* 284:125–128.
- Enzel, Y., R. Bookman (Ken-Tor), D. Sharon, H. Gvirtzman, U. Dayan, B. Ziv, and M. Stein. 2003. Late Holocene climates of the Near East deduced from Dead Sea level variations and modern regional winter rainfall. *Quaternary Research* 60:263–273.
- Falconer, S. E., and P. L. Fall. 1995. Human impacts on the environment during the rise and collapse of civilization in the eastern Mediterranean. In *Late Quaternary Environments and Deep History: A Tribute to Paul S. Martin*, edited by J.I. Mead, and D. Steadman. The Mammoth Site, Hot Spring, AR.
- Fall, P.L., S.E. Falconer, and L. Lines. 2002. Agricultural Intensification and the Secondary Products Revolution Along the Jordan Rift. *Human Ecology* 30 (4):445-482.
- Fall, P.L., L. Lines, and S.E. Falconer. 1998. Seeds of civilization: Bronze Age rural economy and ecology in the Southern Levant. *Annals of the Association of American Geographers* 88:107-125.
- Fielding, A.H., and J.F. Bell. 1997. A review of methods for the assessment of prediction errors in conservation presence/absence models. *Environmental Conservation* 24 (1):38-49.
- Finkelstein, I. 1989. Further observations on the socio-demographic structure of the Intermediate Bronze Age. *Levant* 21:129–140.
- Fish, S.K. 1989. The Beidha pollen record. In *The Natufian encampment at Beidha: late Pleistocene adaptation in the Southern Levant*. Edited by B.F. Byrd. Aarhus University, Denmark: Jutland Archaeological Society Publications, 23: 91-96.
- Fløjgaard, C., S. Normand, F. Skov, and J.-C. Svenning. 2009. Ice age distributions of European small mammals: insights from species distribution modelling. *Journal of Biogeography* 36 (6):1152-1163.
- Franklin, J. 1995. Predictive vegetation mapping: geographic modelling of biospatial patterns in relation to environmental gradients. *Progress in Physical Geography* 19 (4):474-499.
- Franklin, J. 2009. *Mapping Species Distributions, Spatial Inference and Prediction*: Cambridge University Press.

- Freeman, E.A., and G.G. Moisen. 2008. A comparison of the performance of threshold criteria for binary classification in terms of predicted prevalence and kappa. *Ecological Modelling* 217:48-58.
- Frumkin, A. 1997 The Holocene History of Dead Sea Levels. In *The Dead Sea The Lake and its Setting*, edited by T. M. Niemi, Z. Ben-Avraham and J. R. Gat: Oxford University Press, Oxford.
- Frumkin, A. 2009. Stable isotopes of a subfossil Tamarix tree from the Dead Sea region, Israel, and their implications for the Intermediate Bronze Age environmental crisis. *Quaternary Research* 71 (3) 319-328.
- Frumkin, A., I. Carmi, I. Zak, and M. Magaritz. 1991. The Holocene climatic record of the salt caves of Mount Sedom, Israel. *The Holocene* 1 (3):191-200.
- Frumkin, A., G. Kadan, Y. Enzel, and Y. Eyal. 2001. Radiocarbon chronology of the Holocene Dead Sea: attempting a regional correlation. *Radiocarbon* 43 (2C):1179-1190.
- Garrard, A., S. Colledge, and L. Martin. 1996. The Emergence of Crop Cultivation and Caprine Herding in the "Marginal Zone" of the Southern Levant. In *The Origins and Spread of Agriculture and Pastoralism in Eurasia*, edited by D. Harris. London: UCL Press.
- Gasse, F. 2000. Hydrological changes in the African tropics since the Last Glacial Maximum. *Quaternary Science Reviews* 19: 189-211.
- Gebel, H.G., Muheisen, M. S., and Nissen, H. J. (1988). Preliminary report on the first season of excavations at Basta. In *The Prehistory of Jordan*. Edited by A.N. Garrard, and H.G. Gebel. The State of Research in 1986, British Archaeological Reports, International Series 396, Oxford, pp. 101-134.
- Gilead, I. 1998. The Chalcolithic Period in the Levant. *Journal of World Prehistory* 2(4): 397-443.
- Goldberg, P. 1994. Interpreting Late Quaternary continental sequences in Israel. In *Late Quaternary Chronology and Paleoclimates of the Eastern Mediterranean*, edited by O. Bar-Yosef and R. S. Kra: Tucson: Radiocarbon.
- Goodfriend, G. 1990. Rainfall in the Negev Desert during the middle Holocene, based on $\delta^{13}C$ of organic matter in land snail shells. *Quaternary Research* 34 (2): 186-197.
- Goodfriend, G. 1991. Holocene trends in $\delta^{18}O$ in land snail shells from the Negev Desert and their implications for changes in rainfall source areas. *Quaternary Research* 35 (3): 417-426.
- Goodfriend, G. 1999. Terrestrial stable isotope records of Late Quaternary paleoclimates in the eastern Mediterranean region. *Quaternary Science Reviews* 18: 501-513.

- Goring-Morris, N., U. Baruch, A. Belfer-Cohen, and S. Rosen. 1998. Epipalaeolithic occupations in Nahal Neqarot Rockshelter, Negev, Israel: Radiocarbon dating and identification of charred wood remains. *Geoarchaeology* 13 (2): 219-232.
- Graham, C. H., R. Santiago, J.C. Ron, C.J. Santos, C. J. Schneider, and C. Moritz. 2004. Integrating Phylogenetics and Environmental Niche Models To Explore Speciation Mechanisms in Dendrobatid Frogs. *Evolution* 58 (8): 1781-1793.
- Grinnell, J. 1904. The origin and distribution of the chestnut-backed chickadee. *Auk* 21:364-65.
- Grinnell, J. 1924. Geography and evolution. *Ecology* 5: 225-229.
- Guisan, A., and N.E. Zimmermann. 2000. Predictive habitat distributional models in ecology. *Ecological Modeling* 135:147-186.
- Guisan, A., S.B. Weiss, and A.D. Weiss. 1999. GLM versus CCA spatial modeling of plant species distribution. *Plant Ecology* 143: 107-122.
- Gvirtzman, G., and M. Wieder. 2001. Climate of the last 53,000 Years in the eastern Mediterranean, based on soil-sequence Stratigraphy in the coastal plain of Israel. *Quaternary Science Reviews* 20 (18): 1827-1849.
- Haase-Schramm, Alexandra, Steven L. Goldstein, and Mordechai Stein. 2004. U-Th dating of Lake Lisan (late Pleistocene dead sea) aragonite and implications for glacial east Mediterranean climate change. *Geochimica et Cosmochimica Acta* 68 (5): 985-1005.
- Hanley J.A., and B.J. McNeil. 1982. The meaning and use of the area under a receiver operating characteristic (ROC) curve. *Radiology* 143:29-36.
- Hannah, L., G. Midgley, G. Hughes, and B. Bomhard. The view from the Cape: Extinction Risk, Protected Areas, and Climate Change. *BioScience* 55, 231-242
- Henry, D. 1986. The Prehistory and paleoenvironments of Jordan : An overview. *Paléorient* 12 (2): 5-26.
- Henry, D. 1997. Prehistoric human ecology in the Southern Levant east of the Rift from 20 000-6 000 BP. *Paléorient* 23 (2): 107-119.
- Hastie, T., R. Tibshirani, and J.H. Friedman. 2001. The Elements of Statistical Learning: Data Mining, Inference, and Prediction, Springer-Verlag, New York.
- Heim, C., N.R. Nowaczyk, J.F.W. Negendank, S.A.G. Leroy, and L. Ben-Avraham. 1997. Near East desertification: Evidence from the Dead Sea. *Naturwissenschaften* 84:398-401.
- Hernandez, P. A., I. Franke, S. K. Herzog, V. Pacheco, L. Paniagua, H. L. Quintana, A. Soto, J. J. Swenson, C. Tovar, T. H. Valqui, J. Vargas, and B. E. Young. 2008.

- Predicting species distributions in poorly-studied landscapes. *Biodiversity and Conservation* 17 (6):1353-1366.
- Hernandez, P.A., C. Graham, L.L. Master, and D.L. Albert. 2006. The effect of sample size and species characteristics on performance of different species distribution modeling methods. *Ecography* 29:773-785.
- Hijmans, R.J., and C. Graham. 2006. The ability of climate envelope models to predict the effect of climate change on species distributions. *Global Change Biology* 12:2272-2281.
- Hijmans, R. J., S. E. Cameron, J. L. Parra, P. G. Jones, and A. Jarvis. 2005. Very high resolution interpolated climate surfaces for global land areas. *International Journal of Climatology* 25 (15): 1965-1978.
- Hill, J.B., Miller, A.E., Wentz, E., Barton, C.M., 2008. Archaeoclimatology and Ancient Mediterranean Landscape Dynamics. Paper presented at Annual Meetings of the Society for American Archaeology, Vancouver, Canada.
- Hirzel, A.H., V. Helfer, and F. Metral. 2001. Assessing habitat-suitability models with a virtual species. *Ecological Modelling* 145 (2-3): 111-121.
- Hirzel, A.H., J. Hausser, D. Chessel, and N. Perrin. 2002. Ecological-niche factor analysis: How to compute habitat-suitability map without absence data. *Ecology* 83:2027-2036.
- Hirzel, A.H., G. Le Lay, V. Helfer, C. Randin, and A. Guisan. 2006. Evaluating the ability of habitat suitability models to predict species presences. *Ecological Modelling* 199:142–152.
- Horowitz, A. 1971. Climatic And Vegetational Developments in Northeastern Israel during Upper Pleistocene-Holocene Times. *Pollen et Spores* 13 (2):255-278.
- Horowitz, A. 1979. *The Quaternary of Israel*. New York: Academic Press Inc.
- Horowitz, A. 1992. *Palynology of Arid Lands*: Elsevier Science Publishers B.V.
- Hunt, C.O., H.A. Elrishi, D.D. Gilbertson, J. Grattan, S. McLaren, F.B. Pyatt, G. Rushworth, and G.W. Barker. 2004. Early-Holocene environments in the Wadi Faynan, Jordan. *The Holocene* 14 (6): 921-930.
- Huntington, E. 1911. *Palestine and its Transformation*, London.
- Issar, A.S., and M. Zohar. 2004. *Climate Change - Environment and Civilization in the Middle East*. New York: Springer, Berlin–Heidelberg.
- Iverson, L.R., A.M. Prasad, S.N. Matthews, and M.P. Peters. 2010. Merger of three modeling approaches to assess potential effects of climate change on trees in the eastern United States. *Landscape Ecology*: 135-141.

- Jaynes, E.T., 1957. Information theory and statistical mechanics. *Physical Review* 106: 620–630.
- Kadosh, D., D. Sivan, H. Kutiel, and M. Weinstein-evron. 2004. A Late Quaternary Paleoenvironmental Sequence from a Late Quaternary Paleoenvironmental Sequence from Dor, Carmel Coastal Plain, Israel. *Palynology* 28 (1): 143-157.
- Kaplan, S. W., K. A. McEnaney and R. A. Bryson. 2005. The Testing of a Macrophysical Climate Model with Field Data in Wisconsin and the Upper Midwest. Paper presented at the Annual Meeting, Geological Society of America, Salt Lake City, UT.
- Kasapligil, B. 1956. Report to the Government of the Hashemite Kingdom of Jordan on an ecological survey of the vegetation in relation to forestry and grazing. Rome: UNESCO/FAO.
- Kohavi, R. (1995) In Proceedings of the Fourteenth International Joint Conference on Artificial Intelligence. Morgan Kaufmann, San Mateo, CA: 1137-1143.
- Kremen, C., A. Cameron, A. Moilanen, S.J. Phillips, C.D. Thomas, H. Beentje, J. Dransfield, B.L. Fisher, F. Glaw, T.C. Good, G.J. Harper, R.J. Hijmans, D.C. Lees, E. Jr. Louis, R.A. Nussbaum, C.J. Raxworthy, A. Razafimpahanana, G.E. Schatz, M. Vences, D.R. Vieites, P.C. Wright, and M.L. Zjhra. 2007. Aligning conservation priorities across taxa in Madagascar with high-resolution planning tools. *Science* 320:222-226.
- Kurtzman, D. and R. Kadmon. 1999. Mapping of temperature variables in Israel: a comparison of different interpolation methods. *Climate Research*, 13: 33–43.
- Lawler, A. 2007. Climate spurred later Indus decline, Society for American Archaeology Meeting. *Science* 316 (5827):978-979.
- Leathwick, J. R., J. Elith, M. P. Francis, T. Hastie, and P. Taylor. 2006. Variation in demersal fish species richness in the oceans surrounding New Zealand: an analysis using boosted regression trees. *Marine Ecology Progress Series* 321: 267–281.
- Lehmann, A., J.M. Overton, and J. Leathwick. 2002. GRASP: generalized regression analysis and spatial prediction. *Ecological Modelling* 157:189-207.
- Leira, M., and L. Santos. 2002. An early Holocene short climatic event in the northwest Iberian Peninsula inferred from pollen and diatoms. *Quaternary International* 93–94: 3–12.
- Leroy, S. A. G. 2010 Pollen analysis of core DS7-1SC (Dead Sea) showing intertwined effects of climatic change and human activities in the Late Holocene. *Journal of Archaeological Science* 37: 306–316.

- Levin, N., E. Elron, and A. Gasith. 2009. Decline of wetland ecosystems in the coastal plain of Israel during the 20th century: Implications for wetland conservation and management. *Landscape and Urban Planning* 92 (3-4): 220-232.
- Lioubimsteva, E.U. 1995. Landscape changes in the Saharo-Arabian area during the last glacial cycle. *Journal of Arid Environments* 30:1– 17.
- Liphschitz, N., and G. Biger. 1990. Ancient Dominance of the *Quercus calliprinos* - *Pistacia palaestina* Association in Mediterranean Israel. *Journal of Vegetation Science* 1 (1):67-70.
- Liphschitz, N., and T. Noy. 1991. Vegetational Landscape and the Macroclimate of the Gilgal Region during the Natufian and Pre-Pottery Neolithic A *Journal of the Israel Prehistoric Society* 24:59-63.
- Liu, C., P.M. Bery, T.P. Dawson, and R.G. Pearson. 2005. Selecting thresholds of occurrence in the prediction of species distributions. *Ecography* 28:385-393.
- Liverman, D. 1999. Geography and the Global Environment. *The Annals of the Association of American Geographers* 89 (1):107-120.
- Lowdermilk, W. C. 1953. Conquest of the Land Through Seven Thousand Years, Agric. Bull. 99, Soil Conservation Service, U. S. Dept. of Agric., Washington.
- Lozier, J.D., P. Aniello, and M. J. Hickerson. 2009. Predicting the distribution of Sasquatch in western North America: anything goes with ecological niche modelling. *Journal of Biogeography* 36:1623-1627.
- Magaritz, M., S. Rahner, Y. Yechieli, R.V. Krishnamurthy. 1991. $^{13}\text{C}/^{12}\text{C}$ ratio in organic matter from the Dead Sea area: palaeoclimatic interpretation. *Naturwissenschaften* 78: 453–455.
- Mahiny, A. S. and B.J. Turner. 2003. Modeling past vegetation change through remote sensing and G.I.S.: A comparison of neural networks and logistic regression methods. University of Southampton: 1-23.
- Malanson, G. P., D.R. Butler, D.M. Cairns, T. E. Welsh, and L. M. Resler. 2002. Variability in an edaphic indicator in alpine tundra. *Catena* 49 (3): 203–15.
- Manel, S., H.C. Williams, and S.J. Ormerod. 2001. Evaluating presence-absence models in ecology: the need to account for prevalence. *Journal of Applied Ecology* 38:921-931.
- McCarthy, M.A. (2007). *Bayesian Methods for Ecology*, Cambridge University Press, Cambridge.
- McDonald, G. H., and R. A. Bryson. 2010. Modeling Pleistocene local climatic parameters using macrophysical climate modeling and the paleoecology of Pleistocene megafauna. *Quaternary International* 217 (1-2): 131-137.

- McEnaney, K. A., A. H. Ruter and R. A. Bryson. 2006 The Modeled Discharge of the Mississippi during the Holocene [Poster]. Paper presented at the International Conference on Rivers and Civilization, June 25-28, La Crosse, WI.
- McGarry, S.F. and C. Caseldine. 2004. Speleothem palynology: an undervalued tool in Quaternary studies. *Quaternary Science Reviews*, 23: 2389-2404.
- McLaren, S.J., D.D. Gilbertson, J.P. Grattan, C.O. Hunt, G.A.T. Duller, and G. Barker. 2004. Quaternary palaeogeomorphologic evolution of the Wadi Faynan area, southern Jordan. *Palaeogeography, Palaeoclimatology, Palaeoecology* 205:131–154.
- Meadows, J., 2005. The Younger Dryas episode and the radiocarbon chronologies of the Lake Huleh and Ghab Valley pollen diagrams, Israel and Syria. *Holocene* 15(4), 631–636.
- Migowski, C., A. Agnon, R. Bookman, J.F.W. Negendank, M. Stein. 2004. Recurrence pattern of Holocene earthquakes along the Dead Sea Transform revealed by varve-counting and radiocarbon dating of lacustrine sediments. *Earth and Planetary Science Letters* 222: 301–314.
- Migowski, C., M. Stein, S. Prasad, J.F.W. Negendank, and A. Agnon. 2006. Holocene climate variability and cultural evolution in the Near East from the Dead Sea sedimentary record. . *Quaternary Research* 66 (3):421–431.
- Miller, N. 1998. The Macrobotanical Evidence for Vegetation in the Near East, c. 18 000/16 000 to 4 000 BC. *Paléorient* 23 (2):197-207.
- Mueller-Dombois, D. and Ellenberg, H. 1974. *Aims and methods of vegetation ecology*. John Wiley and Sons. New York. 547 p.
- Murray, A. 1866. *The Geographical Distribution of Mammals*. London: Day & Son.
- Neef, R. 1990. Introduction, development and environmental implications of olive culture: The evidence from Jordan. In *Man's Role in the Shaping of the Eastern Mediterranean Landscape*, edited by S. Bottema, G. Entjes, and W. van Zeist, pp. 295–306. Balkema, Rotterdam, Netherlands.
- Neev, D., and K.O. Emery. 1995. *The destruction of Sodom, Gomorrah, and Jericho*. Oxford: Oxford University Press.
- Neumann, F.H., E. J. Kagan, M. J. Schwab, and M. Stein. 2007. Palynology, sedimentology and palaeoecology of the late Holocene Dead Sea. *Quaternary Science Reviews* 26.
- Neumann, F.H., E.J. Kagan, S.a.G. Leroy, and U. Baruch. 2010. Vegetation history and climate fluctuations on a transect along the Dead Sea west shore and their impact on past societies over the last 3500 years. *Journal of Arid Environments* 74 (7): 756-764.

- Ng, A. Y. and M.I. Jordan. 2001. On discriminative vs. generative classifiers: a comparison of logistic regression and naive Bayes. *Adv. Neural Inform. Process. Syst.* 14: 605-610.
- Nicolson, M. 1987. Alexander von Humboldt, Humboldtian Science and the Origins of the Study of Vegetation. *History of Science* 25 (2):167 – 194.
- Niemi, T.M. 1997 Fluctuations of Late Pleistocene Lake Lisan in the Dead Sea Rift. In *The Dead Sea The Lake and its Setting*, edited by T. M. Niemi, Z. Ben-Avraham and J. R. Gat: Oxford University Press, Oxford.
- Niklewski, J. and W. van Zeist. 1970. A Late Quaternary pollen diagram from northwestern Syria. *Acta Botanica Neerlandica* 19: 737 - 754.
- Nix, H. 1986. A biogeographic analysis of Australian elapid snakes. *Atlas of Elapid Snakes of Australia*, edited by R. Longmore: 4–15. Australian Government Publishing Service, Canberra.
- Nogués-Bravo D, Rodríguez J, Hortal J, Batra P, Araújo MB (2008) Climate change, humans, and the extinction of the woolly mammoth. *PLoS Biol* 6(4): 685-692.
- Palmer, A. R., and J. M. Staden. 1992. Predicting the distribution of plant communities using annual rainfall and elevation: an example from southern Africa. *Journal of Vegetation Science* 3 (2): 261-266.
- Parolo, G., G. Rossi, and A. Ferrari. 2008. Toward improved species niche modelling: *Arnica montana* in the Alps as a case study. *Journal of Applied Ecology* 45:1410–1418.
- Pearce, J., and S. Ferrier. 2000. Evaluating the predictive performance of habitat models developed using logistic regression. *Ecological Modelling* 133:225-245.
- Pearson, R.G. (2007). Species' distribution modeling for conservation educators and practitioners. Synthesis. American Museum of Natural History. <http://ncep/amnh.org>.
- Pearson, R.G., T.P. Dawson, P.M. Berry, and P.A. Harrison. 2002. Species: A spatial evaluation of climate impact on the envelope of species. *Ecological Modelling* 154: 289-300.
- Pearson, R. G., and T. P. Dawson. 2003. Predicting the impacts of climate change on the distribution of species: are bioclimate envelope models useful? *Global Ecology and Biogeography* 12 (5): 361-371.
- Pearson, R. G., W. Thuiller, M. B. Araújo, E. Martinez-Meyer, L. Brotons, C. McClean, L. Miles, P. Segurado, T. P. Dawson, and D. C. Lees. 2006. Model-based uncertainty in species range prediction. *Journal of Biogeography* 33, (10): 1704-1711.

- Penman, T. D., D.A. Pike, J.K. Webb, and R. Shine, R., 2010. Predicting the impact of climate change on Australia's most endangered snake, *Hoplocephalus bungaroides*. *Diversity & Distributions* 16 (1): 109-118.
- Peterson, A.T. 2003. Predicting the geography of species' invasions via ecological niche modeling. *The Quarterly review of biology* 78 (4): 419-433.
- Peterson, A.T. and Cohoon K.P. 1999 Sensitivity of distributional prediction algorithms to geographic data completeness. *Ecological Modeling* 117: 159–164.
- Peterson, A.T., M.A. Ortega-Huerta, J. Bartley, V. Sanchez-Cordero, J. Soberon, R.W. Buddemeier, and D.R.B. Stockwell. 2002. Future projections for mexican faunas under global climate change Scenarios. *Nature* 416:626-629.
- Peterson, A.T., and C.R. Robins. 2003. Using Ecological-Niche Modeling to Predict Barred Owl Invasions with Implications for Spotted Owl Conservation. *Conservation Biology* 17 (4): 1161-1165.
- Peterson, A.T., and J.J. Shaw. 2003. *Lutzomyia* vectors for cutaneous leishmaniasis in southern brazil: Ecological niche models, predicted geographic distributions, and climate change effects. *International Journal of Parasitology* 33:919-931.
- Peterson, A.T., J. Soberón, and V. Sánchez-Cordero. 1999. Conservatism of ecological niches in evolutionary time. *Science* 285:1265-1267.
- Peterson, A. Townsend, Monica Papes, and Daniel A. Kluza. 2003. Predicting the Potential Invasive Distributions of Four Alien Plant Species in North America. *Weed Science* 51: 863-868.
- Philip, G. 2001. The Early Bronze I–III Ages. In *The Archaeology of Jordan*, edited by B. MacDonald, R. Adams, and P. Bienkowski: Sheffield Academic Press, Sheffield: 163–232.
- Phillips, S., Phillips@research.att.com “Clamping and V3.3.0,” 25 January 2011, Personal email (25 January 2011).
- Phillips, S.J. 2010. MaxEnt tutorial - from <http://www.cs.princeton.edu/~schapire/maxent/>
- Phillips, S.J. and Dudík, M. 2008 Modeling of species distributions with Maxent: new extensions and a comprehensive evaluation. *Ecography*, 31: 161–175.
- Phillips, S.J., M. Dudík, R.E. Schapire. 2004. A maximum entropy approach to species distribution modeling. In: *Proceedings of the 21st International Conference on Machine Learning*, ACM Press, New York, pp. 655–662.
- Phillips, S. J., M. Dudík, J. Elith, C. H Graham, A. Lehmann, J. Leathwick, and S. Ferrier. 2009. Sample selection bias and presence-only distribution models: implications

for background and pseudo-absence data. *Ecological applications : a publication of the Ecological Society of America* 19 (1): 181-97.

- Phillips, S.J., R.P. Anderson, and R. Schapire. 2006. Maximum entropy modeling of species geographic distributions. *Ecological Modelling* 190:231-259.
- Pollastro, P.M., A.S. Karshbaum, and R.J. Viger. 1998. Maps Showing Geology, Oil and Gas Fields, and Geologic Provinces of the Arabian Peninsula, edited by USGS: USGS.
- Por, F.D. 1985. The Levantine Landbridge: Historical and present patterns. Paper read at Proceedings of the Symposium on the Fauna and Zoogeography of the Middle East, at Mainz.
- Post, G. E. 1888. Narrative of a Scientific Expedition in the Transjordanic Region in the Spring of 1886. *Palestine Exploration Quarterly* 20: 175-237.
- Prentice I.C., W. Cramer, S.P. Harrison, R. Leemans, R.A. Monserud, A.M. Solomon. 1992. A global biome model based on plant physiology and dominance, soil properties and climate. *Journal of Biogeography* 19:117-13.
- Qishawi. M, L. El-Moghrabi, G, Taqsh, A. Hammad, and M. Bdour. 1999. Flora Baseline Survey, Wadi Rum Protected Area. Unpublished report. Available at RSCN, [<http://www.wadirum.jo/library/rum%20reports/floramenu.htm>]
- Rambeau, C.M.C. 2011. Palaeoenvironmental reconstruction in the Southern Levant: synthesis, challenges, recent developments and perspectives. *Philosophical transactions of the Royal Society. Series A, Mathematical, physical, and engineering sciences* 368 (1931): 5225-48.
- Rambeau, C. M. C., B. Finlayson, S.J. Smith, S. Black, R. Inglis, and S. Robinson, S. In press. Palaeoenvironmental reconstruction at Beidha, Southern Jordan (ca 18 000–8500 BP): implications for human occupation during the Natufian and Pre-Pottery Neolithic. In *Water, life and civilisation: climate, environment and society in the Jordan Valley*, edited by S. Mithen and E. Black. Cambridge, UK: Cambridge University Press.
- Randin, C. F., T. Dirnbock, S. Dullinger, N. E. Zimmermann, M. Zappa, and A. Guisan. 2006. Are niche-based species distribution models transferable in space? *Journal of Biogeography* 33:1689–1703.
- Richards, S. 1980. Toward a consensus of opinion on the end of the Early Bronze age in Palestine-Transjordan. *Bulletin of the American Schools of Oriental Research* 237:5–34.
- Robertson, E.A., M.H. Zweig, and M.D. Van Steirteghem. 1983. Evaluating the clinical accuracy of laboratory tests. *American Journal of Clinical Pathology* 79:78–86.

- Robinson, S., S. Black, B. Sellwood, and P. Valdes. 2006. A review of palaeoclimates and palaeoenvironments in the Levant and Eastern Mediterranean from 25,000 to 5000 years BP: setting the environmental background for the evolution of human civilisation. *Quaternary Science Reviews* 25 (13-14): 1517-1541.
- Rossignol-Strick, M. 1993. Late Quaternary climate in the Eastern Mediterranean Region. *Paleorient*, 19(1): 135-152.
- Rossignol-Strick, M. 1995. Sea-land correlation of pollen records in the Eastern Mediterranean for the glacial–interglacial transition: biostratigraphy versus radiometric time-scale. *Quaternary Science Reviews* 14: 893–915.
- Rossignol-Strick, M. 1999. The Holocene climatic optimum and pollen records of sapropel 1 in the eastern Mediterranean, 9000–6000BP. *Quaternary Science Reviews* 18: 515-530.
- Rudel, T., and J. Roper. 1997. The Paths to Rain Forest Destruction: Crossnational Patterns of Tropical Deforestation, 1975 – 90. *World Development* 25 (1):53 – 65.
- Ruter, A. H., J. Arzt, S. Vavrus, R. A. Bryson and J. E. Kutzbach. 2004. Climate and environment of the subtropical and tropical Americas (NH) in the mid-Holocene: comparison of observations with climate model simulations. *Quaternary Science Reviews* 23:663-679.
- Santos, L., J.R. Vidal Romani, and G. Jalut. 2000. History of vegetation during the Holocene in the Courel and Queixa Sierras, Galicia, northwest Iberian Peninsula. *Journal of Quaternary Science* 15:621–632.
- Scheingross, J.S., S.D. Schoville, and G.K. Roderick. 2007. The use of species distribution models in determining areas of conservation and measuring the effects of climate change on alpine butterflies. Presented at 92nd annual meeting of Ecological Society of America, August 5 - 10, 2007, San Jose, CA, USA. (AbstractESA2007).
- Schimper, A. F. W. 1903. *Plant-geography upon a physiological basis*. Clarendon Press, Oxford, UK.
- Schwab, M.J., F. Neumann, T. Litt, J.F.W. Negendank, and M. Stein. 2004. Holocene palaeoecology of the Golan Heights (Near East): investigation of lacustrine sediments from Birkat Ram crater lake. *Quaternary Science Reviews* 23:1723-1731.
- Scott, J. M., T.H. Tear, and F.W. Davis (Eds). 1996. *Gap analysis: a landscape approach to biodiversity planning*. Bethesda, MD: American Society for Photogrammetry and Remote Sensing.
- Sneh, A., Y. Bartov, T. Weissbrod, and M. Rosensaft. 1998. Geological map of Israel. Geological Survey of Israel, scale 1:200,000.

- Stein, M. 2001. The sedimentary and geochemical record of Neogene- Quaternary water bodies in the Dead Sea Basin – inferences for the regional paleoclimatic history. *Journal of Paleolimnology* 26: 271-282.
- Stein, M., A. Torfstein, I. Gavrieli, and Y. Yechieli. 2010. Abrupt aridities and salt deposition in the post-glacial Dead Sea and their North Atlantic connection. *Quaternary Science Reviews* 29 (3-4): 567-575.
- Stockwell, D.R.B. and I.R. Noble 1992. Induction of sets of rules from animal distribution data: a robust and informative method of data analysis. *Math. Comp. Simul.* 32: 249–254.
- Stockwell, D.R.B., and D.P. Peters. 1999. The GARP modelling system: Problems and solutions to automated spatial prediction. *International Journal of Geographical Information Systems* 13:143-158.
- Swenson 2006. GisBased Niche Models Reveal Unifying Climatic Mechanisms That Maintain the Location of Avian Hybrid Zones in a North American Suture Zone. *Journal of Evolutionary Biology* 19:717-25.
- Svenning, Jens-Christian, Signe Normand, and Masa Kageyama. 2008. Glacial refugia of temperate trees in Europe: insights from species distribution modelling. *Journal of Ecology* 96, (6): 1117-1127.
- Swets, J.A. 1988. Measuring the accuracy of diagnostic systems. *Science* 240:1285–1293.
- Thuiller, W. . 2003. Biomod - optimizing predictions of species distributions and projecting potential future shifts under global change. *Global Change Biology* 9:1353-1362.
- Thuiller, W., D.M. Richardson, P. Pysek, G.F. Midgley, G.O. Hughes, and M. Rouget. 2005. Niche-based modeling as a tool for predicting the risk of alien plant invasions at a global scale. *Global Change Biology* 11:2234–2250.
- Tittensor, D.P., A.R. Baco, P.E. Brewin, M.R. Clark, M. Consalvey, J. Hall-Spencer, A.A. Rowden, T. Schlacher, K.I. Stocks and A.D. Rogers 2009. Predicting global habitat suitability for stony corals on seamounts. *Journal of Biogeography* 36: 1111–1128.
- Turner, B.L. II. 1997. Spirals, Bridges and Tunnels: Engaging Human-Environment Perspectives in Geography. *Ecumene*. *Ecumene* 4:196-217.
- Turner, B.L. II, R.H. Moss, and D.L. Skole. 1993. Relating Land Use and Global Land-Cover Change: A Proposal for an IGBM-HDP Core Project. International Geosphere-Biosphere Program. Stockholm, Sweden.
- Tüxen,R. 1956. Die heutige potentielle natürliche Vegetation als Gegenstand der Vegetationskartierung. *Angewandte Pflanzensoziologie*, 13: 5-42.

- VanDerWal, J., L.P. Shoo, and S.E. Williams. 2009. New approaches to understanding late Quaternary climate fluctuations and refugial dynamics in Australian wet tropical rain forests. *Journal of Biogeography* 36:291-301.
- van Zeist, W., and Bottema, S. 1982. Vegetational history of the Eastern Mediterranean and the Near East during the last 20,000 years. In: Bintliff, J.L., van Zeist, W. (Eds.), *Palaeoclimates, Palaeoenvironments and Human Communities in the Eastern Mediterranean Region in Later Prehistory*, BAR International Series, vol. 133, pp. 277–321.
- van Zeist, W., and S. Bottema. 1991. Late Quaternary Vegetation of the Near East, Beihefte zum Tu" binger Atlas des vorderen orientis. Reihe A (Naturwissenschaften) 18.
- van Zeist, W., and H. Woldring. 1980. Holocene vegetation and climate of Northwestern Syria. *Palaeohistoria* 22, 111–125.
- van Zeist, W., U. Baruch, and S. Bottema. 2009. Holocene Palaeoecology of the Hula Area, Northeastern Israel. In *A Timeless Vale*, ed. E. Kaptijn and L.P. Petit, 29-64. Leiden: Leiden University Press.
- von Humboldt, A. 1807. *Essai sur la Géographie des Plantes*: Paris, France.
- Walker, M.J., A.K. Stockman, P. E. Marek, and J. E. Bond. 2009. Pleistocene glacial refugia across the Appalachian Mountains and coastal plain in the millipede genus *Narceus*: Evidence from population genetic, phylogeographic, and paleoclimatic data. *BMC Evolutionary Biology* 9 (25):1-11.
- Welk E., K. Schubert, and M.H. Hoffmann. 2002. Present and potential distribution of invasive garlic mustard (*Alliaria petiolata*) in North America. *Diversity and Distributions* 8:219–233.
- Wheeler, D.J. 1993 Commentary: Linking environmental models with Geographic Information System for global change research. *Photogrammetric Engineering and Remote Sensing* 59 (10): 1497-1501.
- Whittaker, R.H. 1956. Vegetation of the Great Smoky Mountains. *Ecol. Monogr.*26: 1-80.
- Whittaker, R.H. 1962. Classification of Natural Communities. *Botanical Review* 28 (1):1 – 239.
- Whyte, R.O. 1950. The Phytogeographical Zones of Palestine. *Geographical Review* 40 (4):600 – 614.
- Willcox, G. 1991. Exploitation des espèces ligneuses au proche-Orient: données anthracologiques. *Paléorient* 17 (2): 117-126.

- Willcox, G. 1996. Evidence for plant exploitation and vegetation history from three Early Neolithic pre-pottery sites on the Euphrates (Syria). *Archaeobotany and Vegetation History*, 5: 143-152.
- Wilkinson, T.J. 2003. *Archaeological Landscapes of the Near East*. University of Arizona Press, Tucson.
- Woodward, F.I., and L. Rochefort L.1991. Sensitivity analysis of vegetation diversity to environmental change. *Global Ecology and Biogeography Letters* 1: 7–23.
- Yasuda, Y., H. Kitagawa, and T. Nakagawa. 2000. The earliest record of major anthropogenic deforestation in the Ghab Valley, northwest Syria: a palynological study. *Quaternary International* 73-74 (1): 127-136.
- Zimmerer, K. 1996. Ecology as Cornerstone and Chimera in Human Geography. In *Concepts in Human Geography*, edited by E. Carville, K. Mathewson and M. Kenzer. Boston Way, Maryland Rowman & Littlefield Publishers.
- Zohary, M. 1944. Vegetational Transects in Sinai Peninsula. *Palestine Journal of Botany Jerusalem Series* 3: 57-78.
- Zohary, M. 1947a. A vegetation map of Western Palestine. *Journal of Ecology* 34(1): 1-19.
- Zohary, M. 1947b. A geobotanical soil map of Western Palestine. *Palestine Journal of Botany Jerusalem Series* 4: 24-35.
- Zohary, M. 1962. *Plant Life of Palestine (Israel and Jordan)*. New York: The Ronald Press Company.
- Zohary, M. 1966. *Flora Palaestina, part i.* . Jerusalem: Israel Academy of Sciences and Humanities.
- Zohary, M. and G. Orshan. 1959. The Maquis of *Ceratonia Siliqua* in Israel. *Vegetatio* 8(5/6): 285-297.
- Zohary, M. 1962. *Plant Life of Palestine (Israel and Jordan)*. New York: The Ronald Press Company.
- Zohary, M. 1973. 1973. Geobotanical foundations of the Middle East. *Geobotanica Selecta*, vol. 3. Gustav Fischer, Stuttgart.
- Zohary, M., and N. Feinbrun-Dothan. 1966. *Flora Palestina (Volume 1)*. Jerusalem: The Israel Academy of Sciences and Humanities, Jerusalem.